# CHAPTER 4

# ION TRANSPORT IN SOLUTIONS

## 4.1. INTRODUCTION

The interaction of an ion in solution with its environment of solvent molecules and other ions has been the subject of the previous two chapters. Now, attention will be focused on the motion of ions through their environment. The treatment is restricted to solutions of true electrolytes.

There are two aspects to these ionic motions. First, there is the *individual* aspect. This concerns the dynamic behavior of ions as individuals—the trajectories they trace out in the electrolyte, and the speeds with which they dart around. These ionic movements are basically random in direction and speed. Second, ionic motions have a *group* aspect that is of particular significance when more ions move in certain directions than in others and produce a drift, or flux,[1] of ions. This drift has important consequences because an ion has a mass and bears a charge. Consequently, the flux of ions in a preferred direction results in the transport of matter and a flow of charge.

If the directional drift of ions did not occur, the interfaces between the electrodes and electrolyte of an electrochemical system would run out of ions to fuel the charge-transfer reactions that occur at such interfaces. Hence, the movements and drift of ions is of vital significance to the continued functioning of an electrochemical system.

A flux of ions can come about in three ways. If there is a difference in the concentration of ions in different regions of the electrolyte, the resulting concentration gradient produces a flow of ions. This phenomenon is termed *diffusion* (Fig. 4.1). If there are differences in electrostatic potential at various points in the electrolyte, then

[1]The word *flux* occurs frequently in the treatment of transport phenomena. The flux of any species $i$ is the number of moles of that species crossing a unit area of a reference plane in 1 s; hence, *flux is the rate of transport.*

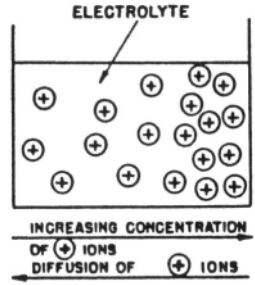


**Fig. 4.1.** The diffusion of positive ions resulting from a concentration gradient of these ions in an electrolytic solution. The directions of increasing ionic concentration and of ionic diffusion are shown below the diagram.

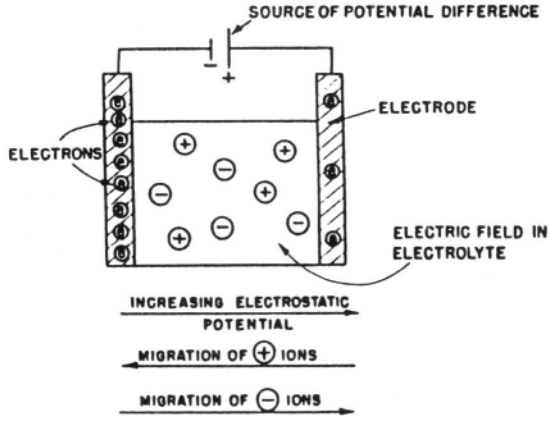


**Fig. 4.2.** The migration of ions resulting from a gradient of electrostatic potential (i.e., an electric field) in an electrolyte. The electric field is produced by the application of a potential difference between two electrodes immersed in the electrolyte. The directions of increasing electrostatic potentials and of ionic migration are shown below the diagram.

the resulting electric field produces a flow of charge in the direction of the field. This is termed *migration* or *conduction* (Fig. 4.2). Finally, if a difference in pressure or density or temperature exists in various parts of the electrolyte, then the liquid begins to move as a whole or parts of it move relative to other parts. This is *hydrodynamic* flow.

It is intended to restrict the present discussion to the transport processes of diffusion and conduction and their interconnection. (The laws of hydrodynamic flow will not be described, mainly because they are not particular to the flow of electrolytes; they are characteristic of the flow of all gases and liquids, i.e., of fluids.) The initial treatment of diffusion and conduction will be in phenomenological terms; then the molecular events underlying these transport processes will be explored.

In looking at ion–solvent and ion–ion interactions, it has been possible to present the phenomenological or nonstructural treatment in the framework of equilibrium thermodynamics, which excludes time and therefore fluxes, from its analyses. Such a straightforward application of thermodynamics cannot be made, however, to transport processes. The drift of ions occurs precisely because the system is not at equilibrium; rather, the system is seeking to attain equilibrium. In other words, the system undergoes change (there cannot be transport without temporal change!) because the free energy is not uniform and tends to reach a minimum. It is the existence of such gradients of free energy that sets up the process of ionic drift and makes the system strive to attain equilibrium by the dissipation of free energy.

## 4.2. IONIC DRIFT UNDER A CHEMICAL-POTENTIAL GRADIENT: DIFFUSION

### 4.2.1. The Driving Force for Diffusion

It has been remarked in the previous section that diffusion occurs when a concentration gradient exists. The theoretical basis of this observation will now be examined.

Consider that in an electrolytic solution, the concentration of an ionic species $i$ varies in the $x$ direction but is constant in the $y$ and $z$ directions. If desired, one can map equiconcentration surfaces (they will be parallel to the $yz$ plane) (Fig. 4.3).

The situation pictured in Fig. 4.3 can also be considered in terms of the partial molar free energy, or chemical potential, of the particular species $i$. This is achieved through the use of the defining equation for the chemical potential [Eq. (3.61)]

$$\mu_i = \mu_i^0 + RT \ln c_i$$

(The use of concentration rather than activity implies that the solution is assumed to behave ideally.) Since $c_i$ is a function of $x$, the chemical potential also is a function of $x$. Thus, the chemical potential varies along the $x$ coordinate, and, if desired, equi-$\mu$ surfaces can be drawn. Once again, these surfaces will be parallel to the $yz$ plane.

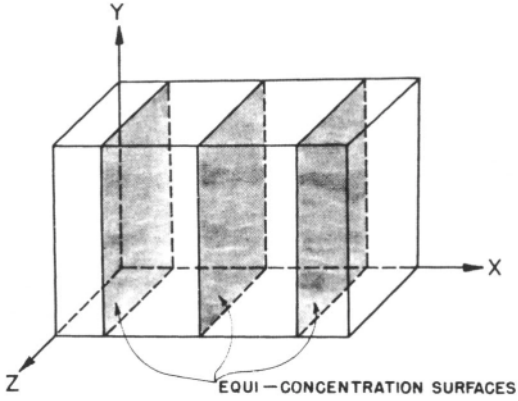


**Fig. 4.3.** A schematic representation of a slice of electrolytic solution in which the concentration of a species *i* is constant on the shaded equiconcentration surfaces parallel to the *yz* plane.

Now, if one transfers a mole of the species *i* from an initial concentration $c_I$ at $x_I$ to a final concentration $c_F$ at $x_F$, then the change in free energy, or chemical potential, of the system is (Fig. 4.4):

$$\Delta\mu = \mu_F - \mu_I = RT \ln \frac{c_F}{c_I} \tag{4.1}$$

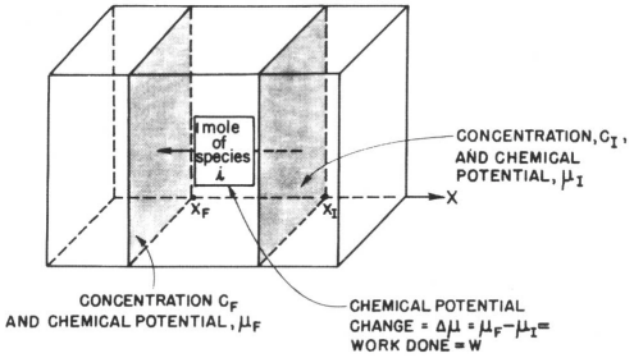


**Fig. 4.4.** A schematic representation of the work *W* done in transporting a mole of species *i* from an equiconcentration surface where its concentration and chemical potential are $c_I$ and $\mu_I$ to a surface where its concentration and chemical potential are $c_F$ and $\mu_F$.

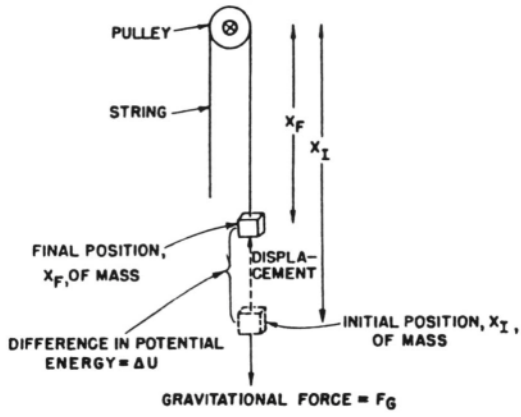


**Fig. 4.5.** Schematic diagram to illustrate that the mechanical work $W$ done in lifting a mass from an initial height $x_I$ to a final height $x_F$ is $W = \Delta U = -F_G(x_I - x_F)$.

However, the change in free energy is equal to the net work done *on* the system in an isothermal, constant-pressure reversible process. Thus, the work done to transport a mole of species $i$ from $x_I$ to $x_F$ is

$$W = \Delta\mu \tag{4.2}$$

Think of the analogous situation in mechanics. The work done to lift a mass from an initial height $x_I$ to a final height $x_F$ is equal to the difference in gravitational potential (energies) $\Delta U$ at the two positions (Fig. 4.5):

$$W = \Delta U \tag{4.3}$$

One may go further and say that this work has to be done because a gravitational force $F_G$ acts on the body and that[2]

$$W = -F_G(x_I - x_F) = -F_G\Delta x = \Delta U \tag{4.4}$$

[2]The minus sign arises from the following argument: The displacement $x_I - x_F$ of the mass is *upward* and the force acts *downward*; hence, the product of the displacement and force vectors is negative. If a minus sign is not introduced, the work done $W$ will turn out to be negative. It is desirable to have $W$ as a positive quantity because of the convention that work done on a system is taken to be positive; hence, a minus sign must be inserted.

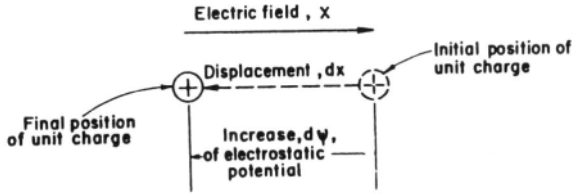


**Fig. 4.6.** Schematic diagram to illustrate the electrostatic work $W = d\psi = -X\,dx$ done in moving a unit positive charge through a distance $dx$ against an electric field $X$.

In other words, the gravitational force can be defined thus:

$$F_G = -\frac{\Delta U}{\Delta x} \tag{4.5}$$

The potential energy, however, may not vary linearly with distance, and thus the ratio $\Delta U/\Delta x$ may not be a constant. So it is better to consider infinitesimal changes in energy and distance and write

$$F_G = -\frac{dU}{dx} \tag{4.6}$$

Thus, the gravitational force is given by the *gradient* of the gravitational potential energy, and the region of space in which it operates is said to be a *gravitational field.*

A similar situation exists in electrostatics. The electrostatic work done in moving a unit charge from $x$ to $x + dx$ defines the difference $d\psi$ in electrostatic potential between the two points (Fig. 4.6)

$$W = d\psi \tag{4.7}$$

Further, the electrostatic work is the product of the electric field, or force per unit charge, $X$ and the distance $dx$

$$-X\,dx = d\psi \tag{4.8}$$

or

$$X = -\frac{d\psi}{dx} \tag{4.9}$$

The electric force per unit charge is therefore given by the negative of the gradient of the electrostatic potentials, and the region of space in which the force operates is known as the *electric field.*

**TABLE 4.1**

**Certain Forces in the Phenomenological Treatment of Transport**

| Force | Acting On | Results In |
|---|---|---|
| $-\frac{dU}{dx}$ | Mass | Movement of mass |
| $-\frac{d\psi}{dx}$ | Charge | Movement of charge (current) |
| $-\frac{d\mu}{dx}$ | Species $i$ | Movement of species $i$, i.e., diffusional flux of species $i$ |

Since the negative of the gradient of gravitational potential energy defines the gravitational force, and the negative of the gradient of electrostatic potential defines the electric force, one would expect that the negative of the gradient of the chemical potential would act formally like a force. Furthermore, just as the gravitational force results in the motion of a mass and the electric force results in the motion of a charge, the chemical-potential gradient results in the net motion, or transfer, of the species $i$ from a region of high chemical potential to a region of low chemical potential. This net flow of the species $i$ down the chemical-potential gradient is diffusion, and therefore the gradient of chemical potential may be looked upon[3] as the diffusional force $F_D$. Thus, one can write

$$F_D = -\frac{d\mu_i}{dx} \tag{4.10}$$

by analogy with the gravitational and electric forces [Eqs. (4.6) and (4.9)] and consider that the diffusional force produces a diffusional flux $J$, the number of moles of species $i$ crossing per second per unit area of a plane normal to the flow direction (Table 4.1).

### 4.2.2. The "Deduction" of an Empirical Law: Fick's First Law of Steady-State Diffusion

Qualitatively speaking, the macroscopic description of the transport process of diffusion is simple. The gradient of chemical potential resulting from a nonuniform concentration is equivalent to a driving force for diffusion and produces a diffusion

[3]It will be shown later on (Section 4.2.6) that for the phenomenon of diffusion to occur, all that is necessary is an inequality of the net number of diffusing particles in different regions; there is, in fact, no directed force on the individual particles. Thus, $-d\mu/dx$ is only a *pseudo*force like the centrifugal force; it is *formally* equivalent to a force.

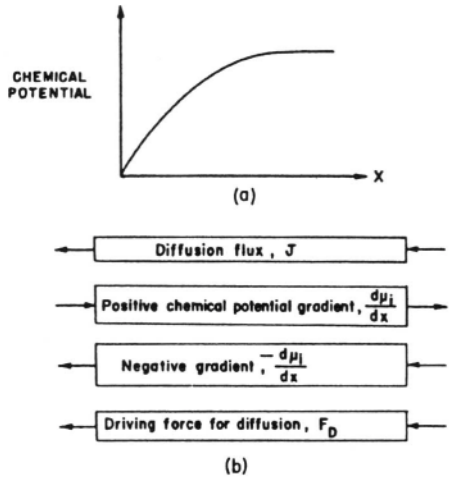


**Fig. 4.7.** Schematic diagram to show (a) the distance variation of the chemical potential of a species *i* and (b) the relative directions of the diffusion flux, driving force for diffusion, etc.

flux (Fig. 4.7). What is the quantitative cause-and-effect relation between the driving force $d\mu_i/dx$ and the flux $J$? This question must now be considered.

Suppose that when diffusion is occurring, the driving force $F_D$ and the flux $J$ reach values that do not change with time. The system can be said to have attained a *steady state*. Then the as-yet-unknown relation between the diffusion flux $J$ and the diffusional force $F_D$ can be represented quite generally by a power series

$$J = A + BF_D + CF_D^2 + DF_D^3 + \ldots \tag{4.11}$$

where $A$, $B$, $C$, etc., are constants. If, however, $F_D$ is less than unity and sufficiently small,[4] the terms containing the powers (of $F_D$) greater than unity can be neglected.

Thus, one is left with

$$J = A + BF_D \tag{4.12}$$

but the constant $A$ must be equal to zero; otherwise, it will mean that one would have the impossible situation of having diffusion even though there is no driving force for diffusion.

---

[4]Caution should be exercised in applying the criterion. The value of $F_D$ that will give rise to unity will depend on the units chosen to express $F_D$. Thus, the extent to which $F_D$ is less than unity will depend on the units, but one can always restrict $F_D$ to an appropriately small value.

Hence, the assumption of a sufficiently small driving force leads to the result

$$J = BF_D \tag{4.13}$$

i.e., the flux is linearly related to the driving force. The value of $F_D = 0$ (zero driving force) corresponds to an equilibrium situation; therefore, the assumption of a small value of $F_D$ required to ensure the linear relation (4.13) between flux and force is tantamount to saying that the system is *near equilibrium, but not at equilibrium.*

The driving force on 1 mole of ions has been stated to be $-d\mu_i/dx$ [Eq. (4.10)]. If, therefore, the concentration of the diffusing species adjacent to the transit plane (Fig. 4.8), across which the flux is reckoned, is $c_i$ moles per unit volume, the driving force $F_D$ at this plane is $-c_i(d\mu_i/dx)$. Thus, from relation (4.13), one obtains

$$J_i = -Bc_i \frac{d\mu_i}{dx} \tag{4.14}$$

Writing

$$\mu = \mu^0 + RT \ln c_i$$

which is tantamount to assuming ideal behavior, Eq. (4.14) becomes

$$J_i = -Bc_i \frac{RT}{c_i} \frac{dc_i}{dx} = -BRT \frac{dc_i}{dx} \tag{4.15}$$

Thus, *the steady-state diffusion flux has been theoretically shown to be proportional to the gradient of concentration.* That such a proportionality existed has been

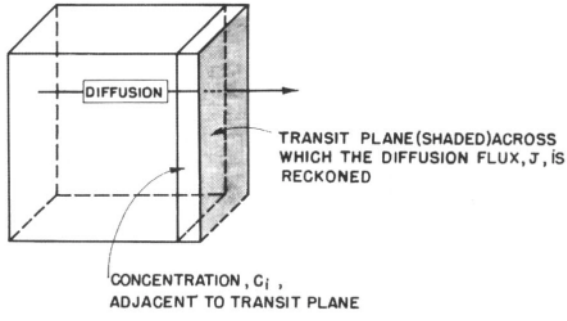


**Fig. 4.8.** Diagram for the derivation of the linear relation between the diffusion flux $J_i$ and the concentration gradient $dc_i/dx$.

**TABLE 4.2**
**Diffusion Coefficient *D* of Ions in Aqueous Solutions**

| Ion | Diffusion Coefficient, ($cm^2\ s^{-1}$) |
|---|---|
| $Li^+$ | $1.028 \times 10^{-5}$ |
| $Na^+$ | $1.334 \times 10^{-5}$ |
| $K^+$ | $1.569 \times 10^{-5}$ |
| $Cl^-$ | $2.032 \times 10^{-5}$ |
| $Br^-$ | $2.080 \times 10^{-5}$ |

known *empirically* since 1855 through the statement of Fick's first law of steady-state diffusion, which reads

$$J_i = -D\frac{dc_i}{dx} \tag{4.16}$$

where $D$ is termed the *diffusion coefficient* (Table 4.2).

### 4.2.3. The Diffusion Coefficient *D*

It is important to stress that, in the empirical Fick's first law, the concentration $c$ is expressed in moles per cubic centimeter, and not in moles per liter. The flux is expressed in moles of diffusing material crossing a unit area of a transit plane per unit of time, i.e., in moles per square centimeter per second, and therefore the diffusion coefficient $D$ has the dimensions of centimeters squared per second. The negative sign is usually inserted in the right-hand side of the empirical Fick's law for the following reason: The flux $\boldsymbol{J}_i$ and the concentration gradient $\mathbf{dc_i/dx}$ are vectors, or quantities which have both magnitude and direction. However, the vector $\mathbf{J}$ is in an opposite sense to the vector representing a positive gradient $\mathbf{dc_i/dx}$.Matter flows downhill (Fig. 4.9). Hence, if $\boldsymbol{J}_i$ is taken as positive, $\mathbf{dc_i/dx}$ must be negative, and, if there is no negative sign in Fick's first law, the diffusion coefficient will appear as a negative quantity—perhaps an undesirable state of affairs. Hence, to make $D$ come out a positive quantity, a negative sign is added to the right-hand side of the equation that states the empirical law of Fick.

Equating the coefficients of $\mathbf{dc_i/dx}$ in the phenomenological equation (4.15) with that in Fick's law [Eq. (4.16)], is seen that

$$BRT = D \tag{4.17}$$

Now, is the diffusion coefficient a concentration-independent constant? A naive answer would run thus: $B$ is a constant and therefore it *appears* that $D$ also is a constant.

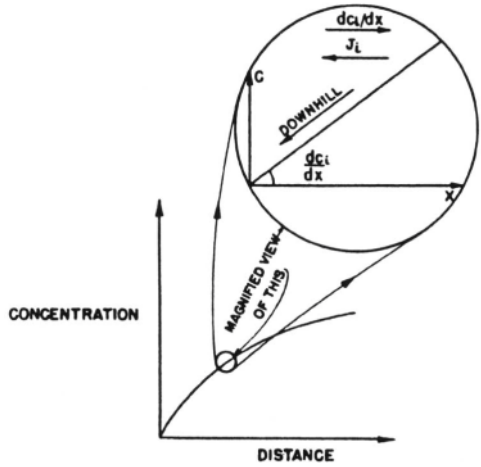


**Fig. 4.9.** Diagram to show that diffusion flow $J_i$ is in a direction opposite to the direction of positive concentration gradient $dc_i/dx$. Matter flows downhill, i.e., down the concentration gradient.

However, expression (4.17) was obtained only because an ideal solution was considered, and activity coefficients $f_i$ were ignored in Eq. (3.61). Activity coefficients, however, are concentration dependent. So, if the solution does not behave ideally, one has, starting from Eq. (4.14), and using Eq. (3.63),

$$J_i = -Bc_i \frac{d\mu_i}{dx}$$

$$= -Bc_i \frac{d}{dx}(\mu_i^0 + RT \ln f_i c_i)$$

$$= -Bc_i \frac{RT}{f_i c_i} \frac{d}{dx} f_i c_i$$

$$= -BRT \frac{dc_i}{dx} - \frac{BRTc_i}{f_i} \frac{df_i}{dx}$$

$$= -BRT \frac{dc_i}{dx} - \frac{BRTc_i}{f_i} \frac{df_i}{dc_i} \frac{dc_i}{dx}$$

$$= -BRT \frac{dc_i}{dx} \left(1 + \frac{c_i}{f_i} \frac{df_i}{dc_i}\right)$$

**TABLE 4.3**
**Variation of the Diffusion Coefficient *D* with Concentration**

| | Diffusion Coefficient $D$ in Units of $10^{-5}$ cm$^2$ s$^{-1}$ at Concentration (in molarity) | | | |
|---|---|---|---|---|
| Electrolyte | 0.05 | 0.1 | 0.2 | 0.5 |
| HCl | 3.07 | 3.05 | 3.06 | 3.18 |
| LiCl | 1.28 | 1.27 | 1.27 | 1.28 |
| NaCl | 1.51 | 1.48 | 1.48 | 1.47 |

$$= -BRT\frac{dc_i}{dx}\left(1+\frac{d\ln f_i}{d\ln c_i}\right) \tag{4.18}$$

and therefore

$$D = BRT\left(1+\frac{d\ln f_i}{d\ln c_i}\right) \tag{4.19}$$

Rigorously speaking, the diffusion coefficient is not a constant (Table 4.3). If, however, the variation of the activity coefficient is not significant over *the concentration difference that produces diffusion*, then $(c_i/f_i)(\partial f_i/\partial c_i) \ll 1$ and for all practical purposes $D$ is a constant.[5] *This effective constancy of D with concentration will be assumed in most of the discussions presented here.*

The treatment so far has been phenomenological and therefore the dependence of the diffusion coefficient on factors such as temperature and type of ion can be theoretically understood only by an atomistic analysis. The quantity $D$ can be understood in a fundamental way only by probing into the ionic movements, the results of which show up in the macroscopic world as the phenomenon of diffusion. What are these ionic movements, and how do they produce diffusion? The answering of these two questions will constitute the next topic.

### 4.2.4. Ionic Movements: A Case of the Random Walk

Long before the movements of ions in solution were analyzed, the kinetic theory of gases was developed and it involved the movements of gas molecules. The *overall*

[5]For example, in diffusion between solutions that have a large concentration difference, such as 0.1 to 0.01 mol dm$^{-3}$, a rough calculation suggests that the activity-coefficient correction is on the order of a few percent.

pattern of ionic movements is quite similar to that of gas molecules and therefore the latter will be recalled first.

Imagine a hypothetical situation in which all the gas molecules except one are at rest. According to Newton's first law of motion, the moving molecule will travel with a uniform velocity until it collides with a stationary molecule. During the collision, there is a transfer of momentum (mass $m$ times velocity $v$). So, the moving molecule loses some speed in the collision, but the stationary molecule is set in motion. Now both molecules are moving, and they will undergo further collisions. The number of collisions will increase with time, and soon all the molecules of the gas will be continually moving, colliding, and changing their directions of motion and their velocities—a scene of hectic activity.

It would be of interest to have an idea of the path of such a gas molecule in the course of time. One might think that the detailed paths of all the particles could be predicted by applying Newton's laws to the motions of molecules. The problem, however, is obviously too complex for a practical solution. To use the laws of motion requires a knowledge of the position and velocity of each particle and even in 1 mole there are $6.023 \times 10^{23}$ (the Avogadro number) particles.

One can, however, try another approach. Is the ceaseless jostling of molecules manifested in any gross (macroscopic) phenomenon? Consider a frictionless piston in mechanical equilibrium with a mass of gas enclosed in a cylinder. Owing to its weight, the piston exerts a force on the gas. What force balances the piston's weight? One says that the gas exerts a pressure (force per unit area) on the piston owing to the continual buffeting that the piston receives from the gas molecules. Despite this fact, the bombardment by the gas molecules does not produce any *visible* motion of the piston. Evidently the mass of the piston is so large compared with that, of the gas molecules that the movements of the piston are too small to be detected.

Now let the mass of the piston be reduced. Then the jiggling of the extremely light piston as a result of being struck by gas molecules should make itself apparent to an observer. This is what happens if one tries to make a mirror galvanometer more and more sensitive. The essential part of this instrument is a thin quartz fiber that supports a light coil of wire seated in a magnetic field (Fig. 4.10). The deflections of the coil are made visible by fixing a mirror onto the quartz fiber and bouncing a beam of light off the mirror onto a scale. To increase the sensitivity of the instrument, one tries lighter coils, lighter mirrors, and thinner fibers. There comes a stage, however, when the "kicks" which the fiber-mirror-coil assembly receives from the air molecules are sufficient to make the assembly jiggle about. The reflected light beam then jumps about on the scale (Fig. 4.11). The movements of the spot about a mean position on the scale represent *noise*. (It is as if each collision produced a sound, in which case the irregular bombardment of the mirror assembly would result in a nonstop noise.) Signals (coil deflections) that are of this same order of magnitude obviously cannot be separated from the noise.

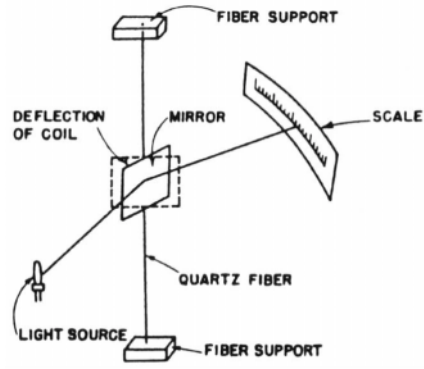


**Fig. 4.10.** Schematic representation of the essential parts of a mirror galvanometer, used for detecting Brownian motion.

Instead of mirrors, one could equally consider pistons of a microscopic size, large enough to be seen with the aid of a microscope but small enough to display motions due to collisions with molecules. Such small "pistons" are present in nature. A colloidal particle in a liquid medium behaves as such a piston if it is observed in a microscope. It shows a haphazard, zigzag motion as shown in Fig. 4.12. The irregular path of the particle must be a slow-motion version of the *random-walk* motion of the molecules in the liquid.

One has therefore a picture of the solvated ions (in an electrolytic solution) in ceaseless motion, perpetually colliding, changing direction, staggering hither and thither from site to site. This is the qualitative picture of ionic *movements.*

### 4.2.5. The Mean Square Distance Traveled in a Time *t* by a Random-Walking Particle

The movements executed by an ion in solution are a three-dimensional affair because the ion has a three-dimensional space available for roaming around. So one

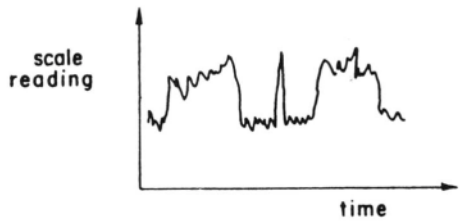


**Fig. 4.11.** The time variation of the reading on the scale of a mirror galvanometer.

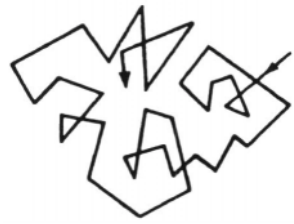

**Fig. 4.12.** The haphazard zigzag motion of a colloidal particle.

must really call the movements a "random flight" because the ion *flies* in three dimensions and *walks* in two dimensions. This fine difference, however, will be ignored and the term *random walk* will be retained.

The aim now is to seek a quantitative description of ionic random-walk movements. There are many exotic ways of stating the random-walk problem. It is said, for example, that a drunken sailor emerges from a bar. He intends to get back to his ship, but he is in no state to control the direction in which he takes a step. In other words, the direction of each step is completely random, all directions being equally likely. The question is: On the average, how far does the drunken sailor progress in a time $t$?

For the sake of simplicity, the special case of a one-dimensional random walk will be considered. The sailor starts off from $x = 0$ on the $x$ axis. He tosses a coin: heads—he moves forward in the positive $x$ direction, tails—he moves backward. Since, for an "honest" coin, heads are as likely as tails, the sailor is equally as likely to take a forward step as a backward step. Of course, each step is decided on a fresh toss and is uninfluenced by the results of the previous tosses. After allowing him $N$ steps, the distance $x$ from the origin is noted[6] (Fig. 4.13). Then the sailor is brought back to the bar ($x = 0$) and started off on another try of $N$ steps.

The process of starting the sailor off from $x = 0$, allowing him $N$ steps, and measuring the distance $x$ traversed is repeated many times, and it is found that the distances traversed from the origin are $x(1)$, $x(2)$, $x(3)$, . . . , $x(i)$, where $x(i)$ is the distance from the origin traversed in the $i$th try. The *average distance* $\langle x \rangle$ from the origin is

$$\langle x \rangle = \frac{\sum_i x(i)}{\sum_i i} = \frac{\text{Sum of distances from origin}}{\text{Number of tries}} \tag{4.20}$$

[6]It will be zero only if an equal number $N/2$ of heads and tails turns up. For a small number of trials, this will not happen every time. So, after each small number of tosses, the sailor is not certain to be back where he started (i.e., in the bar).

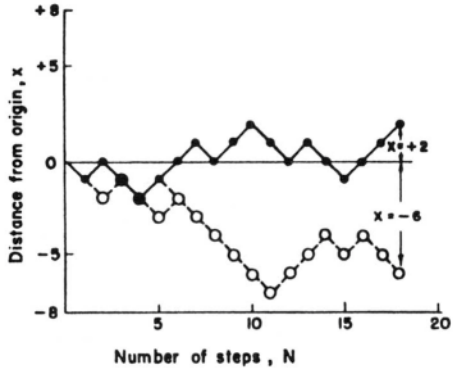


**Fig. 4.13.** The distance $x$ (from the origin) traversed by the drunken sailor in two tries, each of $N = 18$ steps.

Since the distance $x$ traversed by the sailor in $N$ steps is as likely for a large number of trials to be in the plus-$x$ direction as in the minus-$x$ direction, it is obvious from the canceling out of the positive and negative values of $x$ that the *mean* progress from the origin is given by

$$\langle x \rangle = 0 \tag{4.21}$$

Hence, it is not very fruitful to compute the mean distance $\langle x \rangle$ traversed by the sailor in $N$ steps. To avoid such an unenlightening result, which arises because $x(i)$ can take either positive or negative values, it is best to consider the square of $x(i)$, which is always a positive quantity whether $x(i)$ itself is negative or positive. Hence, if $x(1)$, $x(2)$, $x(3)$,..., $x(i)$ are all squared and the mean of these quantities is taken, then one can obtain the *mean square distance* $\langle x^2 \rangle$, i.e.,

$$\langle x^2 \rangle = \frac{\sum_i [x(i)]^2}{\sum i} = \frac{\text{Sum of distances } x \text{ squared}}{\text{Number of tries}} \tag{4.22}$$

Since the square of $x(i)$, i.e., $[x(i)]^2$, is always a positive quantity, the mean square distance traversed by the sailor is always a positive nonzero quantity (Table 4.4).[7]

---

[7] That $\Sigma x/n = 0$ but $\Sigma x^2/n$ is finite at first seems difficult to comprehend. One can get to it by recalling that the drunken sailor may not make *net* progress ($\Sigma x/n = 0$), but the range of his lurching to the right or to the left is also interesting and this is obtained if one eliminates the sign of $x$ (which causes the mean of the sum of the $x$s to be zero) and deals in $\sqrt{\langle x^2 \rangle}$, the square root of the mean of the sum of $x^2$. Then this root-mean-square value of $x$ indicates the range of the drunk's wandering, no matter in what direction (Section 4.2.14).

**TABLE 4.4**

**One-Dimensional Random Walk of the Sailor[a]**

| Trial | $N_F$[b] | $N_B$[c] | $x$[d] | $x^2$ |
|---|---|---|---|---|
| 1 | 11 | 19 | −8 | 64 |
| 2 | 16 | 14 | +2 | 4 |
| 3 | 17 | 13 | +4 | 16 |
| 4 | 15 | 15 | 0 | 0 |
| 5 | 17 | 13 | +4 | 16 |
| 6 | 16 | 14 | +2 | 4 |
| 7 | 19 | 11 | +8 | 64 |
| 8 | 18 | 12 | +6 | 36 |
| 9 | 15 | 15 | 0 | 0 |
| 10 | 13 | 17 | −4 | 16 |
| 11 | 11 | 19 | −8 | 64 |
| 12 | 17 | 13 | +4 | 16 |
| 13 | 17 | 13 | +4 | 16 |
| 14 | 12 | 18 | −6 | 36 |
| 15 | 20 | 10 | +10 | 100 |
| 16 | 23 | 7 | +16 | 256 |
| 17 | 11 | 19 | −8 | 64 |
| 18 | 16 | 14 | +2 | 4 |
| 19 | 17 | 13 | +4 | 16 |
| 20 | 14 | 16 | −2 | 4 |
| 21 | 16 | 14 | +2 | 4 |
| 22 | 12 | 18 | −6 | 36 |
| 23 | 15 | 15 | 0 | 0 |
| 24 | 10 | 20 | −10 | 100 |
| 25 | 7 | 23 | −16 | 256 |
| 26 | 15 | 15 | 0 | 0 |
| | $\langle x \rangle = 0$ | $\langle x^2 \rangle = 47.67$ | | $\sqrt{\langle x^2 \rangle} = 6.90$ |

[a] Total number of steps in each trial = $N = 30$.
[b] Number of forward steps = $N_F$.
[c] Number of backwards steps = $N_B$.
[d] Distance from the origin = $x$.

Furthermore, it can easily be shown (Appendix 4.1) that the magnitude of $\langle x^2 \rangle$ is proportional to $N$, the number of steps and since $N$ itself increases linearly with time, it follows that the mean square distance traversed by the random-walking sailor is proportional to time

$$\langle x^2 \rangle \propto t \tag{4.23}$$

It is to be noted that it is the *mean square distance*—and not the *mean distance*—that is proportional to time. If the mean distance were proportional to time, then the

drunken sailor (or the ion) would be proceeding at a uniform velocity. This is not the case because the mean distance $<x>$ traveled is zero. The only type of progress that the ion is making from the origin is such that the mean *square* distance is proportional to time. This is the characteristic of a random walk.

### 4.2.6. Random-Walking Ions and Diffusion: The Einstein–Smoluchowski Equation

Consider a situation in an electrolytic solution where the concentration of the ionic species of interest is constant in the $yz$ plane but varies in the $x$ direction. To analyze the diffusion of ions, imagine a *unit area* of a reference plane normal to the $x$ direction. This reference plane will be termed the *transit plane* of unit area (Fig. 4.14). There is a random walk of ions across this plane both from left to right and from right to left. On either side of the transit plane, one can imagine two planes $L$ and $R$ that are parallel to the transit plane and situated at a distance $\sqrt{<x^2>}$ from it. In other words, the region under consideration has been divided into left and right compartments in which the concentrations of ions are different and designated by $c_L$ and $c_R$, respectively.

In a time of $t$ s, a random-walking ion covers a mean square distance of $<x^2>$, or a mean distance of $\sqrt{<x^2>}$. Thus, by choosing the plane $L$ to be at a distance $\sqrt{<x^2>}$ from the transit plane, one has ensured that all the ions in the left compartment will cross the transit plane in a time $t$ *provided* they are moving in a left-to-right direction.

The number of moles of ions in the left compartment is equal to the volume $\sqrt{<x^2>}$ of this compartment times the concentration $c_L$ of ions. It follows that the number of moles of ions that make the $L \rightarrow T$ crossing in $t$ s is $\sqrt{<x^2>}c_L$ times the fraction of ions making left-to-right movements. Since the ions are random-walking,

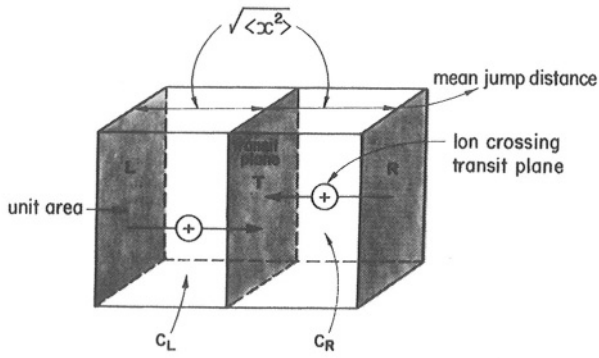


**Fig. 4.14.** Schematic diagram for the derivation of the Einstein–Smoluchowski relation, showing the transit plane $T$ in between and at a distance $\sqrt{<x^2>}$ from the left $L$ and right $R$ planes. The concentrations in the left and right compartments are $c_L$ and $c_R$, respectively.

right-to-left movements are as likely as left-to-right movements, i.e., only half the ions in the left compartment are moving toward the right compartment. Thus, in $t$ s the number of moles of ions making the $L \rightarrow T$ crossing is $1/2\sqrt{<x^2>}c_L$ and therefore the number of moles of ions making the $L \rightarrow T$ crossing in 1 s is $1/2(\sqrt{<x^2>}/t)c_L$. Similarly, the number of moles of ions making the $R \rightarrow T$ crossing in 1 s is $1/2(\sqrt{<x^2>}/t)c_R$.

Hence, the diffusion flux of ions across the transit plane (i.e., the net number of moles of ions crossing unit area of the transit plane per second from left to right) is given by

$$J = \frac{1}{2}\frac{\sqrt{<x^2>}}{t}(c_L - c_R) \tag{4.24}$$

This equation reveals that all that is required to have diffusion is *a difference in the numbers* per unit volume of particles in two regions. The important point is that no special diffusive force acts *on the particles* in the direction of the flux.

If no forces are pushing particles in the direction of the flow, then what about the driving force for diffusion, i.e., the gradient of chemical potential (Section 4.2.1)? The latter is only *formally equivalent* to a force in a macroscopic treatment; it is a sort of pseudoforce like a centrifugal force. The chemical-potential gradient is not a true force that acts on the individual diffusing particles and from this point of view is quite unlike, for example, the Coulombic force, which acts on individual charges.

Now, the concentration gradient $dc/dx$ in the left-to-right direction can be written

$$\frac{dc}{dx} = \frac{c_R - c_L}{\sqrt{<x^2>}} = -\frac{c_L - c_R}{\sqrt{<x^2>}}$$

or

$$c_L - c_R = -\sqrt{<x^2>}\frac{dc}{dx} \tag{4.25}$$

This result for $c_L - c_R$ can be substituted in Eq. (4.24) to give

$$J = -\frac{1}{2}\frac{<x^2>}{t}\frac{dc}{dx} \tag{4.26}$$

and, by equating the coefficients of this equation with that of Fick's first law [Eq. (4.16)], one has

$$\frac{<x^2>}{2t} = D$$

or

$$<x^2> = 2Dt \tag{4.27}$$

This is the Einstein–Smoluchowski equation; it provides a bridge between the microscopic view of random-walking ions and the coefficient $D$ of the macroscopic Fick's law.

A coefficient of 2 is intimately connected with the approximate nature of the derivation, i.e., a *one-dimensional* random walk with ions being permitted to jump forward and backward only. More rigorous arguments may yield other values for the numerical coefficient, e.g., 6.

The characteristic of a random walk in the Einstein–Smoluchowski equation is the appearance of the mean square distance (i.e., square centimeters), and since this mean square distance is proportional to time (seconds), the proportionality constant $D$ in Eq. (4.27) must have the dimensions of centimeters squared per second. It must not be taken to mean that every ion that starts off on a random walk travels in time $t$ a mean square distance $<x^2>$ given by the Einstein-Smoluchowski relation (4.27). If a certain number of ions are, in an imaginary or thought experiment, suddenly introduced on the $yz$ plane at $x = 0$, then, in $t$ s, some ions would progress a distance $x_1$; others, $x_2$; still others, $x_3$; etc. The Einstein–Smoluchowski relation only says that [*cf.* Eqs. (4.22) and (4.27)]

$$\frac{x_1^2 + x_2^2 + \cdots + x_n^2}{n} = <x^2> = 2Dt \tag{4.28}$$

How many ions travel a distance $x_1$; how many, $x_2$; etc.? In other words, how are the ions *spatially distributed* after a time $t$, and how does the spatial distribution vary with time? This spatial distribution of ions will be analyzed, but only after a phenomenological treatment of *non*steady-state diffusion is presented.

### 4.2.7. The Gross View of Nonsteady-State Diffusion

What has been done so far is to consider steady-state diffusion in which neither the flux nor the concentration of diffusing particles in various regions changes with time. In other words, the whole transport process is time independent. What happens if a concentration gradient is suddenly produced in an electrolyte initially in a time-invariant equilibrium condition? Diffusion starts of course, but it will not immediately reach a steady state that does not change with time. For example, the distance variation of concentration, which is zero at equilibrium, will not instantaneously hit the final steady-state pattern. How does the concentration vary with time?

Consider a parallelepiped (Fig. 4.15) of unit area and length $dx$. Ions are diffusing in through the left face of the parallelepiped and *out* through the right face. Let the concentration of the diffusing ions be a continuous function of $x$. If $c$ is the concentration of ions at the left face, the concentration at the right force is

$$c + \frac{dc}{dx}\,dx$$

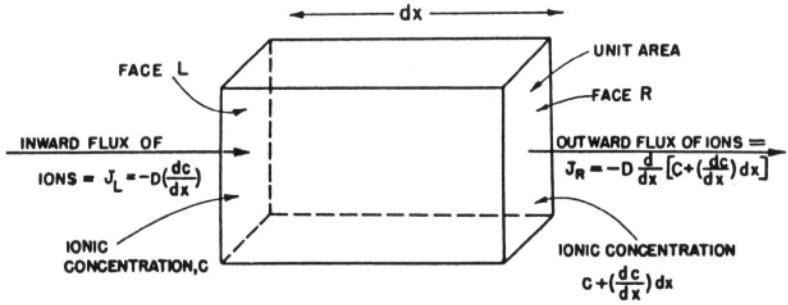


**Fig. 4.15.** The parallelepiped of electrolyte used in the derivation of Fick's second law.

Fick's law [Eq. (4.16)] is used to express the flux into and out of the parallelepiped. Thus the flux into the left face $J_L$ is

$$J_L = -D\frac{dc}{dx} \tag{4.29}$$

and the flux out of the right face is

$$J_R = -D\frac{d}{dx}\left(c + \frac{dc}{dx}dx\right)$$

$$= -D\frac{dc}{dx} - D\frac{d^2c}{dx^2}dx \tag{4.30}$$

The net *out*flow of material from the parallelepiped of volume $dx$ is

$$J_L - J_R = D\frac{d^2c}{dx^2}dx \tag{4.31}$$

Hence, the net outflow of ions *per unit volume* per unit time is $D\,(d^2c/dx^2)$. But this net outflow of ions per unit volume per unit time from the parallepiped is in fact the sought-for variation of concentration with time, i.e., $dc/dt$. One obtains partial differentials because the concentration depends both on time and distance, but the subscripts $x$ and $t$ are generally omitted because it is, for example, obvious that the time variation is at a fixed region of space, i.e., constant $x$. Hence,

$$\frac{\partial c}{\partial t} = D\frac{\partial^2 c}{\partial x^2} \tag{4.32}$$

This partial differential equation is known as *Fick's second law.* It is the basis for the treatment of most time-dependent diffusion problems in electrochemistry.

That Fick's second law is in the form of a differential equation implies that it describes what is common to *all* diffusion problems and it has "squeezed out" what is characteristic of any *particular* diffusion problem.[8] Thus, one always has to calculate the precise functional relationship

$$c = f(x, t)$$

for a particular situation. The process of calculating the functional relationship consists in solving the partial differential equation, which is Fick's second law, i.e., Eq. (4.32).

### 4.2.8. An Often-Used Device for Solving Electrochemical Diffusion Problems: The Laplace Transformation

*Partial* differential equations, such as Fick's second law (in which the concentration is a function of both time and space), are generally more difficult to solve than *total* differential equations, in which the dependent variable is a function of only one independent variable. An example of a total differential equation (of second order[9]) is the linearized Poisson–Boltzmann equation

$$\frac{1}{r^2}\frac{d}{dr}\left(r^2\frac{d\psi}{dr}\right) = \kappa^2\psi$$

It has been shown (Section 3.3.7) that the solution of this equation (with $\psi$ dependent on $r$ only) was easily accomplished.

One may conclude therefore that the solution of Fick's second law (a partial differential equation) would proceed smoothly if some mathematical device could be utilized to convert it into the form of a total differential equation. The Laplace transformation method is often used as such a device.

Since the method is based on the operation[10] of the Laplace transformation, a digression on the nature of this operation is given before using it to solve the partial differential equation involved in nonsteady-state electrochemical diffusion problems, namely, Fick's second law.

Consider a function $y$ of the variable $z$, i.e., $y = f(z)$, represented by the plot of $y$ against $z$. The familiar operation of differentiation performed on the function $y$ consists in finding the slope of the curve representing $y = f(z)$ for various values of $z$, i.e., the

---

[8]This point is dealt with at greater length in Section 4.2.9.

[9]The order of a differential equation is the order of its highest derivatives, which in the example quoted is a second-order derivative, $d^2\psi/dr^2$.

[10]A mathematical operation is a rule for converting one function into another.

differentiation operation consists in evaluating $dy/dz$. The integration operation consists in finding the area under the curve, i.e., it consists in evaluating $\int_{z_1}^{z_2} f(z)\,dz$.

The operation of Laplace transformation performed on the function $y = f(z)$ consists of two steps:

1. Multiplying $y = f(z)$ by $e^{-pz}$, where $p$ is a positive quantity that is independent of $z$
2. Integrating the resulting product $ye^{-pz}$ $[= f(z)e^{-pz}]$ with respect to $z$ between the limits $z = 0$ and $z = \infty$

In short, the Laplace transform $y = f(z)$ is

$$\int_0^\infty e^{-pz} y\,dz \quad \text{or} \quad \int_0^\infty e^{-pz} f(z)\,dz$$

Just as one often symbolizes the result of the differentiation of $y$ by $y'$, the result of the operation of Laplace transformation performed on $y$ is often represented by a symbol $\bar{y}$. Thus,

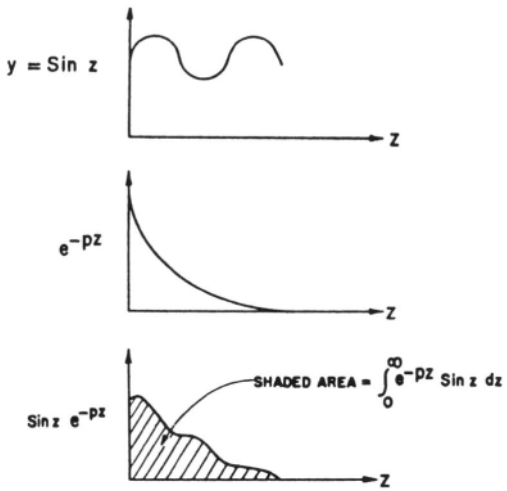


**Fig. 4.16.** Steps in the operation of the Laplace transformation of (a) the function of $y = \sin z$, showing (b) $e^{-pz}$ and (c) the product $e^{-pz}$ sin $z$ integrated between the limits 0 and $\infty$.

**TABLE 4.5**
**Laplace Transforms**

| Function | Transform |
|---|---|
| $f(t)$ | $\bar{f} = \int_0^\infty e^{-pt} f(t)\, dt$ |
| 1 | $\frac{1}{p}$ |
| $\lambda$ (a constant) | $\frac{\lambda}{p}$ |
| $\frac{1}{\sqrt{\pi t}}$ | $\frac{1}{\sqrt{p}}$ |
| $2\sqrt{\frac{1}{\pi}}$ | $p^{-3/2}$ |
| $e^{\omega t}$ | $\frac{1}{p-\omega}$ |
| $\frac{1}{\sqrt{\pi t}} \exp\left(-\frac{k^2}{4t}\right)$ | $\frac{1}{\sqrt{p}} e^{-k\sqrt{p}}$ $[k \geq 0]$ |
| $2\sqrt{\frac{t}{\pi}} \exp\left(-\frac{k^2}{4t}\right) - k \operatorname{erfc}\left(\frac{k}{2\sqrt{t}}\right)$ | $p^{-3/2} e^{-k\sqrt{p}}$ $[k \geq 0]$ |
| $\cos \omega t$ | $\frac{p}{p^2 + \omega^2}$ |

$$\bar{y} = \text{Laplace transform of } y = \int_0^\infty e^{-pz} y\, dz \tag{4.33}$$

What happens during Laplace transformation can be easily visualized by choosing a function, say, $y = \sin z$, and representing the operation in a figure (Fig. 4.16). It can be seen[11] that the operation consists in finding the area under the curve $ye^{-pz}$ between

[11]From Fig. 4.16, it can also be seen that apart from having to make the integral converge, the exact value of $p$ is not significant because $p$ disappears after the operation of inverse transformation (see Section 4.2.11).

the limits $z = 0$ and $z = \infty$. The Laplace transforms of some functions encountered in diffusion problems are collected in Table 4.5.

### 4.2.9. Laplace Transformation Converts the Partial Differential Equation into a Total Differential Equation

It will now be shown that by using the operation of Laplace transformation, Fick's second law—a partial differential equation—is converted into a total differential equation that can be readily solved. Since whatever operation is carried out on the left-hand side of an equation must be repeated on the right-hand side, both sides of Fick's second law will be subject to the operation of Laplace transformation (*cf.* Eq. (4.33)]

$$\int_0^\infty e^{-pt} \frac{\partial c}{\partial t}\, dt = \int_0^\infty e^{-pt} D \frac{\partial^2 c}{\partial x^2}\, dt \tag{4.34}$$

which, by using the symbol for a Laplace-transformed function, can be written

$$\overline{\frac{\partial c}{\partial t}} = D \overline{\frac{\partial^2 c}{\partial x^2}} \tag{4.35}$$

To proceed further, one must evaluate the integrals of Eq. (4.34). Consider the Laplace transform

$$\overline{\frac{\partial c}{\partial t}} = \int_0^\infty e^{-pt} \frac{\partial c}{\partial t}\, dt \tag{4.36}$$

The integral can be evaluated by the rule for integration by parts as follows:

$$\int_0^\infty e^{-pt} \frac{\partial c}{\partial t}\, dt = e^{-pt} \int_0^\infty \partial c - \int_0^\infty \left[ \int_0^\infty \partial c \right] de^{-pt}$$

$$u \quad dv \qquad u \quad v \qquad\qquad v \quad du$$

$$= \left[ e^{-pt} c \right]_0^\infty + p \int_0^\infty e^{-pt} c\, dt \tag{4.37}$$

Since $\int_0^\infty e^{-pt} c\, dt$ is in fact the Laplace transform of $c$ [*cf.* the defining equation (4.33)], and for conciseness is represented by the symbol $\bar{c}$, and since $e^{-pt}$ is zero when $t \to \infty$ and unity when $t = 0$, Eq. (4.36) reduces to

$$\overline{\frac{\partial c}{\partial t}} = \int_0^\infty e^{-pt} \frac{\partial c}{\partial t}\, dt = -c[t=0] + p\bar{c} \tag{4.38}$$

where $c[t = 0]$ is the value of the concentration $c$ at $t = 0$.

Next, one must evaluate the integral on the right-hand side of Eq. (4.34), i.e.,

$$D\,\overline{\frac{\partial^2 c}{\partial x^2}} = \int_0^\infty e^{-pt} D \frac{\partial^2 c}{\partial x^2}\, dt \tag{4.39}$$

Since the integration is with respect to the variable $t$ and the differentiation is with respect to $x$, their order can be interchanged. Furthermore, one can move the constant $D$ outside the integral sign. Hence, one can write

$$D\,\overline{\frac{\partial^2 c}{\partial x^2}} = D \frac{\partial^2}{\partial x^2} \int_0^\infty e^{-pt} c\, dt \tag{4.40}$$

Once again, it is clear from Eq. (4.33) that $\int_0^\infty e^{-pt} c\, dt$ is the Laplace transform of $c$, i.e., $\bar{c}$, and therefore

$$D\,\overline{\frac{\partial^2 c}{\partial x^2}} = D \frac{\partial^2}{\partial x^2} \bar{c} \tag{4.41}$$

From Eqs. (4.32), (4.38), and (4.41), it follows that after Laplace transformation, Fick's second law takes the form

$$p\bar{c} - c[t=0] = D \frac{d^2\bar{c}}{dx^2} \tag{4.42}$$

This, however, is a total differential equation because it contains only the variable $x$. Thus, by using the operation of Laplace transformation, Fick's second law has been converted into a more easily solvable total differential equation involving $\bar{c}$, the Laplace transform of the concentration.

### 4.2.10. Initial and Boundary Conditions for the Diffusion Process Stimulated by a Constant Current (or Flux)

A differential equation can be arrived at by differentiating an original equation, or *primitive*, as it is called. In the case of Fick's second law, the primitive is the equation that gives the precise nature of the functional dependence of concentration on space and time; i.e., the primitive is an elaboration on

$$c = f(x, t)$$

Since, in the process of differentiation, constants are eliminated and since three differentiations (two with respect to $x$ and one with respect to time) are necessary to arrive at Fick's second law, three constants have been eliminated in the process of going from the precise concentration dependence that characterizes a particular problem to the general relation between the time and space derivatives of concentration that describes any nonstationary diffusion situation.

The three characteristics, or *conditions*, as they are called, of a particular diffusion process cannot be rediscovered by mathematical argument applied to the differential equation. To get at the three conditions, one has to resort to a physical understanding of the diffusion process. Only then can one proceed with the solution of the (now) total differential equation (4.42) and get the precise functional relationship between concentration, distance, and time.

Instead of attempting a general discussion of the three conditions characterizing a particular diffusion problem, it is best to treat a typical electrochemical diffusion problem. Consider that in an electrochemical system a constant current is switched on at a time arbitrarily designated $t = 0$ (Fig. 4.17). The current is due to charge-transfer reactions at the electrode–solution interfaces, and these reactions consume a species. Since the concentration of this species at the interface falls below the bulk concentration, a concentration gradient for the species is set up and it diffuses toward the interface. Thus, the externally controlled current sets up[12] a diffusion flux within the solution.

The diffusion is described by Fick's second law

$$\frac{\partial c}{\partial t} = D \frac{\partial^2 c}{\partial x^2} \tag{4.32}$$

or, after Laplace transformation, by

$$p\bar{c} - c[t = 0] = D \frac{d^2\bar{c}}{dx^2} \tag{4.42}$$

To analyze the diffusion problem, one must solve the differential equation, i.e., describe how the concentration of the diffusing species varies with distance $x$ from the electrode and with the time that has elapsed since the constant current was switched

[12]When the externally imposed current sets up charge-transfer reactions that provoke the diffusion of ions, there is a very simple relation between the current density and the diffusion flux. The diffusion flux is a mole flux (number of moles crossing 1 $cm^2$ in 1 s), and the current density is a charge flux (Table 4.1). Hence, the current density $j$, or charge flux, is equal to the charge $zF$ per mole of ions ($z$ is the valence of the diffusing ion and $F$ is the Faraday constant) times the diffusion flux $J$, i.e., $j = zFJ$.

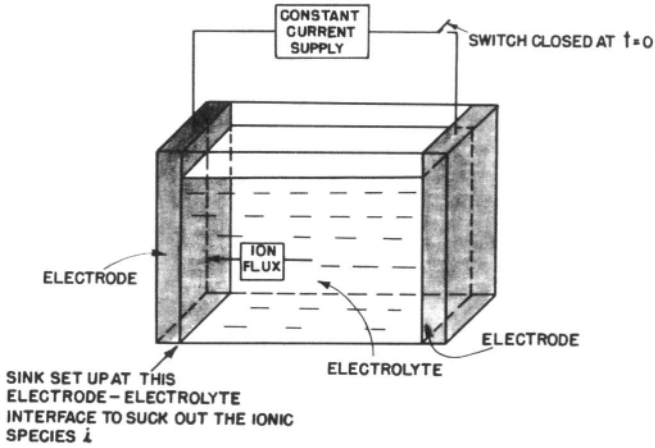


**Fig. 4.17.** Schematic representation of an electrochemical system connected to a constant current supply that is switched on at $t = 0$. The current promotes a charge-transfer reaction at the electrode–electrolyte interfaces, which results in the diffusion flux of the species $i$ toward the interface.

on. First one must think out the three characteristics, or conditions, of the diffusion process described above.

The nature of one of the conditions becomes clear from the term $c[t = 0]$ in the Laplace-transformed version [see Eq. (4.42)] of Fick's second law. The term $c[t = 0]$ refers to the concentration before the start of diffusion; i.e., it describes the initial condition of the electrolytic solution in which diffusion is made to occur by the passage of a constant current. Since before the constant current is switched on and diffusion starts, one has an unperturbed system, the concentration $c$ of the species that subsequently diffuses must be the same throughout the system and equal to the bulk concentration $c^0$. Thus, the initial condition of the electrolytic solution is

$$c[t = 0] = c^0 \tag{4.43}$$

The other two conditions pertain to the situation after the diffusion begins, e.g., after the diffusion-causing current is switched on. Since these two conditions often pertain to what is happening to the boundaries of the system (in which diffusion is occurring), they are usually known as *boundary conditions.*

The first boundary condition is the expression of an obvious point, namely, that very far from the boundary at which the diffusion source or sink is set up, the concentration of the diffusing species is unperturbed and remains the same as in the initial condition

$$c[x \to \infty] = c[t = 0] = c^0 \tag{4.44}$$

Thus, the concentration of the diffusing species has the same value $c^0$ at any $x$ at $t = 0$ or for any $t > 0$ at $x \to \infty$. This is true for almost all electrochemical diffusion problems in which one switches on (at $t = 0$) the appropriate current or potential difference across the interface and thus sets up interfacial charge-transfer reactions which, by consuming or producing a species, provoke a diffusion flux of that species.

What is characteristic of one particular electrochemical diffusion process and distinguishes it from all others is the nature of the diffusion flux that is started off at $t = 0$. Thus, the essential characteristic of the diffusion problem under discussion is the switching on of the constant current, which means that the diffusing species is consumed at a constant rate at the interface and the species diffuses across the interface at a constant rate. In other words, the flux of the diffusing species at the $x = 0$ boundary of the solution is a constant.

It is convenient from many points of view to assume that the constant value of the flux is unity, i.e., 1 mole of the diffusing species crossing $1\ \text{cm}^2$ of the electrode–solution interface per second. This unit flux corresponds to a constant current density of $1\ \text{A cm}^{-2}$. This normalization of the flux scarcely affects the generality of the treatment because it will later be seen that the concentration response to an arbitrary flux can easily be obtained from the concentration response to a unit flux.

If one looks at the time variation of current or the flux across the solution boundary, it is seen that for $t < 0$, $J = 0$ and for $t > 0$, there is a constant flux $J = 1$ (Fig. 4.18) corresponding to the constant current switched on at $t = 0$. In other words, the time variation of the flux is like a step; that is why the flux produced in this setup is often known as a *step function* (of time).

At any instant of time, the constant flux across the boundary is related to the concentration gradient there through Fick's first law, i.e.,

$$J_{x=0} = 1 = -D\left(\frac{\partial c}{\partial x}\right)_{x=0} \tag{4.45}$$

The above initial and boundary conditions can be summarized thus:

$$c[t = 0] = c^0 \tag{4.43}$$

$$c[x \to \infty] = c^0 \tag{4.44}$$

$$\left(\frac{\partial c}{\partial x}\right)_{x=0} = -\frac{1}{D} \tag{4.45}$$

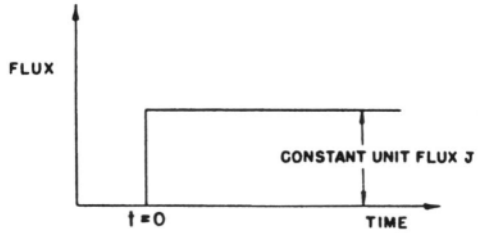


**Fig. 4.18.** When a constant unit flux of 1 mol $cm^{-2}$ $s^{-1}$ is switched on at $t = 0$, the variation of flux with time resembles a step. (It is only an ideal switch that makes the current and therefore the flux instantaneously rise from zero to its constant value; this problem of technique is ignored in the diagram.)

The three conditions just listed describe the special features of the constant (unit)-flux diffusion problem. They will now be used to solve Fick's second law.

### 4.2.11. Concentration Response to a Constant Flux Switched On at $t = 0$

It has been shown (Section 4.2.9) that after Laplace transformation, Fick's second law takes the form

$$p\bar{c} - c[t = 0] = D\frac{d^2\bar{c}}{dx^2} \tag{4.42}$$

The solution of an equation of this type is facilitated if the second term is zero. This objective can be attained by introducing a new variable $c_1$ defined as

$$c_1 = c^0 - c \tag{4.46}$$

The variable $c_1$ can be recognized as the departure $c^0 - c$ of the concentration from its initial value $c^0$. In other words, $c_1$ represents the *perturbation* from the initial concentration (Fig. 4.19).

The partial differential equation [Eq. (4.32)] and the initial and boundary conditions now have to be restated in terms of the new variable $c_1$. This is easily done by using Eq. (4.46) in Eqs. (4.32), (4.43), (4.44), and (4.45). One obtains

$$\frac{\partial c_1}{\partial t} = D\frac{\partial^2 c_1}{\partial x^2} \tag{4.47}$$

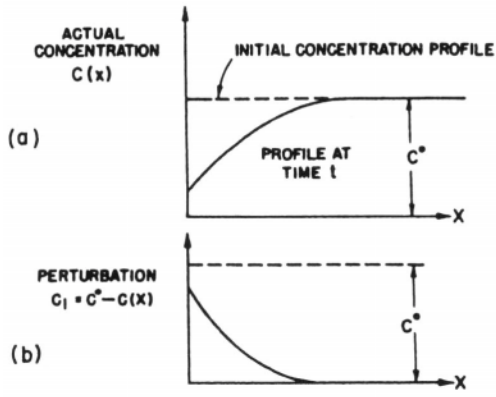


**Fig. 4.19.** Schematic representation of (a) the variation of concentration with distance $x$ from the electrode at $t = 0$ and $t = t$ and (b) the variation of the perturbation $c_1 = c^0 - c_x$ in concentrations.

$$c_1[t = 0] = 0 \tag{4.48}$$

$$c_1[x \to \infty] = 0 \tag{4.49}$$

$$\left(\frac{\partial c_1}{\partial x}\right)_{x=0} = -\frac{1}{D} \tag{4.50}$$

After Laplace transformation of Eq. (4.47), the differential equation becomes

$$p\bar{c}_1 - c_1[t = 0] = D\frac{d^2\bar{c}_1}{dx^2} \tag{4.51}$$

Since, however, $c_1[t = 0] = 0$ [*cf.* Eq. (4.48)], it is clear that

$$\frac{d^2\bar{c}_1}{dx^2} = \frac{p}{D}\bar{c}_1 \tag{4.52}$$

This equation is identical in form to the linearized P–B equation [*cf.* Eq. (3.21)] and therefore must have the same general solution, i.e.,

$$\bar{c}_1 = Ae^{-(p/D)^{1/2}x} + Be^{(p/D)^{1/2}x} \tag{4.53}$$

where $A$ and $B$ are the arbitrary integration constants to be evaluated by the use of the boundary conditions. If the Laplace transformation method had not been used, the solution of Eq. (4.47) would not have been so simple.

The constant $B$ must be zero by virtue of the following argument. From the boundary condition $c_1[x \to \infty] = 0$, i.e., Eq. (4.49), it is clear that after Laplace transformation,

$$\bar{c}_1[x \to \infty] = 0 \tag{4.54}$$

Hence, as $x \to \infty$, $\bar{c}_1 \to 0$, but this will be true only if $B = 0$ because otherwise $\bar{c}_1$ in Eq. (4.53) will go to infinity instead of zero.

One is left with

$$\bar{c}_1 = Ae^{-(p/D)^{1/2}x} \tag{4.55}$$

Differentiating this equation with respect to $x$, one obtains

$$\frac{d\bar{c}_1}{dx} = -\sqrt{\frac{p}{D}}\,Ae^{-(p/D)^{1/2}x} \tag{4.56}$$

which at $x = 0$ leads to

$$\left(\frac{d\bar{c}_1}{dx}\right)_{x=0} = -\sqrt{\frac{p}{D}}\,A \tag{4.57}$$

Another expression for $(d\bar{c}_1/dx)_{x=0}$ can be obtained by applying the operation of Laplace transformation to the constant-flux boundary condition (4.50). Laplace transformation on the left-hand side of the boundary condition leads to $(d\bar{c}_1/dx)_{x=0}$; and the same operation performed on the right-hand side, to $-1/Dp$ (Appendix 4.2). Thus, from the boundary condition (4.50) one gets

$$\left(\frac{d\bar{c}_1}{dx}\right)_{x=0} = -\frac{1}{Dp} \tag{4.58}$$

Hence, from Eqs. (4.57) and (4.58), it is found that

$$A = \frac{1}{p^{3/2}D^{1/2}} \tag{4.59}$$

Upon inserting this expression for $A$ into Eq. (4.55), it follows that

$$\bar{c}_1 = \frac{1}{D^{1/2}p^{3/2}}\,e^{-(p/D)^{1/2}x} \tag{4.60}$$

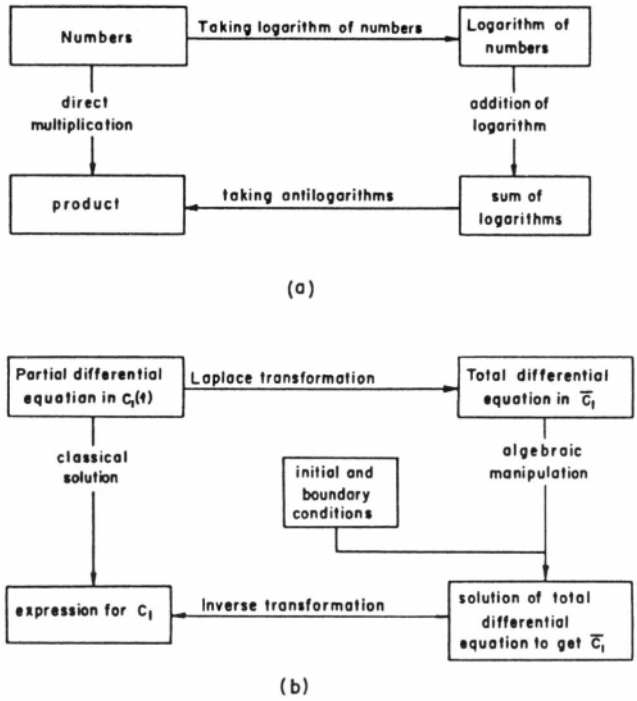


**Fig. 4.20.** Comparison of the use of (a) logarithms and (b) Laplace transformation.

The ultimate aim, however, is not to get an expression for $\bar{c}_1$, the Laplace transform of $c_1$, but to get an expression for $c_1$ (or c) as a function of distance $x$ and time $t$. The expression $\bar{c}_1$ has been obtained by a Laplace transformation of $c_1$; hence, to go from $\bar{c}_1$ to $c_1$, one must do an inverse transformation. The situation is analogous to using logarithms to facilitate the working-out of a problem (Fig. 4.20). In order to get $c_1$ from $\bar{c}_1$, one asks the question: Under Laplace transformation, what function $c_1$ would give the Laplace transform $\bar{c}_1$ of Eq. (4.60)? In other words, one has to find $c_1$ in the equation

$$\int_0^\infty e^{-pt} c_1 \, dt = \bar{c}_1 = \frac{1}{D^{1/2} p^{3/2}} e^{-(p/D)^{1/2} x} \tag{4.61}$$

A mathematician would find the function $c_1$ (i.e., do the inverse transformation) by making use of the theory of functions of variables which are complex. Since, however, there are extensive tables of functions $y$ and their transforms $\bar{y}$, it is only

necessary to look up the column of Laplace transforms in the tables (Table 4.5). It is seen that corresponding to the transform of the equation arising from Eq. (4.60)

$$p^{-3/2} \exp\left(-\frac{x}{\sqrt{D}} p^{1/2}\right)$$

is the function

$$2\pi^{-1/2} t^{1/2} \exp\left(-\frac{x^2}{4Dt}\right) - xD^{-1/2} \operatorname{erfc}\left(\frac{x^2}{4Dt}\right)^{1/2}$$

where erfc is the *error function complement* defined thus:

$$\operatorname{erfc}(y) = 1 - \operatorname{erf}(y) \tag{4.62}$$

erf($y$) being the *error function* given by (Fig. 4.21)

$$\operatorname{erf}(y) = \frac{2}{\sqrt{\pi}} \int_0^y e^{-u^2}\, du \tag{4.63}$$

Hence, the expression for the concentration perturbation $c_1$ in Eq. (4.61) must be

$$c_1 = \frac{1}{D^{1/2}} \left[ \frac{2t^{1/2}}{\pi^{1/2}} \exp\left(-\frac{x^2}{4Dt}\right) - xD^{-1/2} \operatorname{erfc}\left(\frac{x^2}{4Dt}\right)^{1/2} \right] \tag{4.64}$$

If one is interested in the true concentration $c$, rather than the deviation $c_1$ in the concentration from the initial value $c^0$, one must use the defining equation for $c_1$

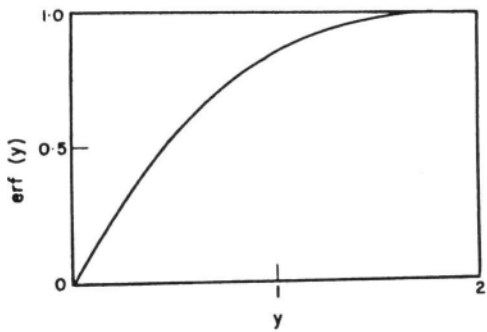


**Fig. 4.21.** Variation of the error function erf($y$) with argument $y$.

$$c_1 = c^0 - c \tag{4.46}$$

The result is

$$c = c^0 - \frac{1}{D^{1/2}}\left[\frac{2t^{1/2}}{\pi^{1/2}}\exp\left(-\frac{x^2}{4Dt}\right) - \frac{x}{D^{1/2}}\operatorname{erfc}\left(\frac{x^2}{4Dt}\right)^{1/2}\right] \tag{4.65}$$

This then is the fundamental equation showing how the concentration of the diffusing species varies with distance $x$ from the electrode–solution interface and with

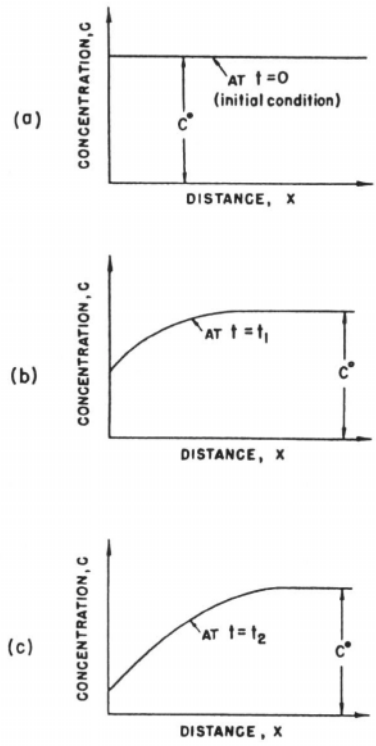


**Fig. 4.22.** Graphical representation of the variation of the concentration $c$ with distance $x$ from the electrode or diffusion sink. (a) The initial condition at $t = 0$; (b) and (c) the conditions at $t_1$ and $t_2$, where $t_2 > t_1 > t = 0$. Note that, at $t > 0$, $(dc/dx)_{x=0}$ is a constant, as it should be in the constant-flux diffusion problem.

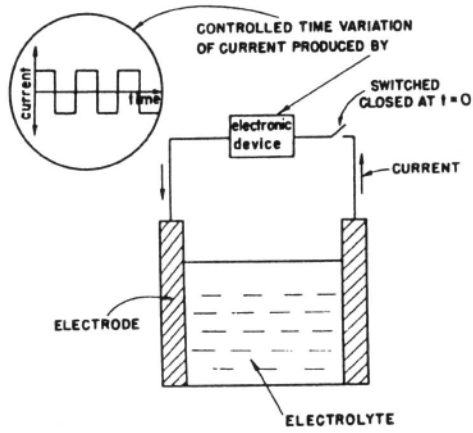


**Fig. 4.23.** Use of an electronic device to vary the current passing through an electrochemical system in a controlled way.

the time $t$ that has elapsed since a constant unit flux was switched on. In other words, Eq. (4.65) describes the diffusional response of an electrolytic solution to the stimulus of a flux which is in the form of a step function of time. The nature of the response is best appreciated by seeing how the concentration profile of the species diffusing varies as a function of time [Fig. 4.22(a), (b), and (c)]. Equation (4.65) is also of fundamental importance in describing the response of an electrochemical system to a current density that varies as a step function, i.e., to a constant current density switched on at $t = 0$.

### 4.2.12. How the Solution of the Constant-Flux Diffusion Problem Leads to the Solution of Other Problems

The space and time variation of a concentration in response to the switching on of a constant flux has been analyzed. Suppose, however, that, instead of a constant flux, one switches on a sinusoidally varying flux.[13] What is the resultant space and time variation of the concentration of the diffusing species?

One approach to this question is to set up the new diffusion problem with the initial and boundary conditions characteristic of the sinusoidally varying flux and to obtain a solution. There is, however, a simpler approach. Using the property of Laplace transforms, one can use the solution (4.65) of the constant-flux diffusion problem to generate solutions for other problems.

---

[13]If one feels that *current* is a more familiar word than flux, one can substitute the word current because these diffusion fluxes are often, but not always, provoked by controlling the current across an electrode-solution interface.

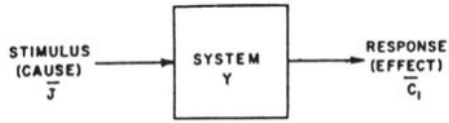


**Fig. 4.24.** Schematic representation of the response $\bar{c}_1$ of a system $Y$ to a stimulus $\bar{J}$.

An electronic device is connected to an electrochemical system so that it switches on a current (Fig. 4.23) that is made to vary with time in a controllable way. The current provokes charge-transfer reactions that lead to a diffusion flux of the species involved in the reactions. This diffusion flux varies with time in the same way as the current. The time variation of the flux will be represented thus

$$J = g(t) \tag{4.66}$$

The imposition of this time-varying flux stimulates the electrolytic solution to respond with a space and time variation in the concentration $c$ or a perturbation in concentration, $c_1$. The response depends on the stimulus, and the mathematical relationship between the cause $J(t)$ and the effect $c_1$ can be represented (Fig. 4.24) quite generally thus[14]:

$$\bar{c}_1 = y\bar{J} \tag{4.67}$$

where $\bar{c}_1$ and $\bar{J}$ are the Laplace transforms of the perturbation in concentration and the flux, and $y$ is the to-be-determined function that links the cause and effect and is characteristic of the system.

The relationship (4.67) has been defined for a flux that has an arbitrary variation with time; hence, it must also be true for the constant unit flux described in Section 4.2.10. The Laplace transform of this constant unit flux $J = 1$ is $1/p$ according to Appendix 4.2; and the Laplace transform of the concentration response to the constant unit flux is given by Eq. (4.60), i.e.,

$$\bar{c}_1 = D^{-1/2} p^{-3/2} \exp\left(-\sqrt{\frac{p}{D}}\, x\right) \tag{4.60}$$

Hence, by substituting $1/p$ for $\bar{J}$ and $D^{-1/2} p^{-3/2} e^{-(p/D)^{1/2} x}$ for $\bar{c}_1$ in Eq. (4.67), one has

[14]It will be seen further on that one uses a relationship between the Laplace transforms of the concentration perturbation and the flux rather than the quantities $c_1$ and $J$ themselves, because the treatment in Laplace transforms is not only elegant but fruitful.

$$y = D^{-1/2} p^{-1/2} \exp\left(-\sqrt{\frac{p}{D}}\, x\right) \tag{4.68}$$

On introducing this expression for $y$ into the general relationship (4.67), the result is

$$\bar{c}_1 = \left[D^{-1/2} p^{-1/2} \exp\left(-\sqrt{\frac{p}{D}}\, x\right)\right] \bar{J} \tag{4.69}$$

This is an important result: Through the evaluation of $y$, it contains the concentration response to a constant unit flux switched on at $t = 0$. In addition, it shows how to obtain the concentration response to a flux $J(t)$ that is varying in a known way. All one has to do is to take the Laplace transform $\bar{J}$ of this flux $J(t)$ switched on at time $t = 0$, substitute this $\bar{J}$ in Eq. (4.69), and get $\bar{c}_1$. If one inverse-transforms the resulting expression for $\bar{c}_1$, one will obtain $c_1$, the perturbation in concentration as a function of $x$ and $t$.

Consider a few examples. Suppose that instead of switching on a constant unit flux at $t = 0$ (see Section 4.2.10), one imposes a flux that is a constant but now has a magnitude of $\lambda$ mol cm$^{-2}$ s$^{-1}$, i.e., $J = \lambda$. Since the transform of a constant is $1/p$ times the constant (Appendix 4.2), one obtains

$$\bar{J} = \frac{\lambda}{p} \tag{4.70}$$

which when introduced into Eq. (4.69) gives

$$\bar{c}_1 = \frac{\lambda}{D^{1/2} p^{3/2}} e^{-(x/D^{1/2}) p^{1/2}} \tag{4.71}$$

The inverse transform of the right-hand side of Eq. (4.71) is identical to that for the unit step function [*cf.* Eq. (4.60)] except that it is multiplied by $\lambda$. That is,

$$c_1 = \frac{\lambda}{D^{1/2}}\left[\frac{2t^{1/2}}{\pi^{1/2}} \exp\left(-\frac{x^2}{4Dt}\right) - \frac{x}{D^{1/2}} \operatorname{erfc}\left(\frac{x^2}{4Dt}\right)^{1/2}\right] \tag{4.72}$$

In other words, the concentration response of the system to a $J = \lambda$ flux is a magnified-$\lambda$-times version of the response to a constant unit flux.

One can also understand what happens if instead of sucking ions out of the system, the flux acts as a source and pumps in ions. This condition can be brought about by changing the direction of the constant current going through the interface and thus changing the direction of the charge-transfer reactions so that the diffusing species is produced rather than consumed. Thus, diffusion from the interface into the solution occurs. Because the direction of the flux vector is reversed, one has

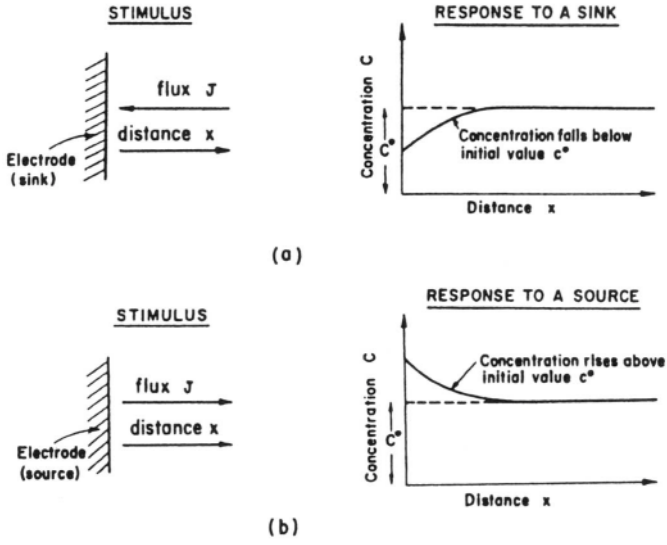


**Fig. 4.25.** The difference in the concentration response to the stimulus of (a) a sink and (b) a source at the electrode–electrolyte interface.

$$J = -\lambda \quad \text{or} \quad \bar{J} = -\frac{\lambda}{p} \tag{4.73}$$

and thus

$$c_1 = \frac{-\lambda}{D^{1/2}}\left[\frac{2t^{1/2}}{\pi^{1/2}}\exp\left(-\frac{x^2}{4Dt}\right) - \frac{x}{D^{1/2}}\operatorname{erfc}\left(\frac{x^2}{4Dt}\right)^{1/2}\right] \tag{4.74}$$

or, in view of Eq. (4.46),

$$c = c^0 + \frac{\lambda}{D^{1/2}}\left[\frac{2t^{1/2}}{\pi^{1/2}}\exp\left(-\frac{x^2}{4Dt}\right) - \frac{x}{D^{1/2}}\operatorname{erfc}\left(\frac{x^2}{4Dt}\right)^{1/2}\right] \tag{4.75}$$

Note the plus sign; it indicates that the concentration $c$ rises above the initial value $c^0$ (Fig. 4.25).

Consider now a more interesting type of stimulus involving a periodically varying flux (Fig. 4.26). After representing the imposed flux by a cosine function

$$J = J_{\max} \cos \omega t \tag{4.76}$$

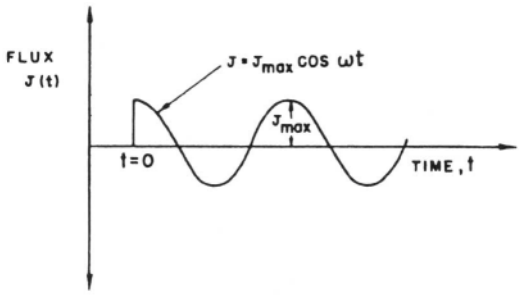


**Fig. 4.26.** A sinusoidally varying flux at an electrode–electrolyte interface, produced by passing a sinusoidally varying flux through the electrochemical system.

its Laplace transform is (see Table 4.5)

$$\bar{J} = J_{\max} \frac{p}{p^2 + \omega^2} \tag{4.77}$$

When this is combined with Eq. (4.69), one gets

$$\bar{c}_1 = \frac{p}{p^2 + \omega^2} \left[ \frac{1}{D^{1/2} p^{1/2}} e^{-(x/D^{1/2}) p^{1/2}} \right] J_{\max} \tag{4.78}$$

To simplify matters, the response of the system will only be considered at the boundary, i.e., at $x = 0$. Hence, one can set $x = 0$ in Eq. (4.78), in which case,

$$\bar{c}_1[x=0] = \frac{p}{p^2 + \omega^2} \frac{1}{D^{1/2} p^{1/2}} J_{\max} \tag{4.79}$$

The inverse transform reads

$$c_1[x=0] = \frac{J_{\max}}{(D\omega)^{1/2}} \cos\left(\omega t - \frac{\pi}{4}\right) \tag{4.80}$$

which shows that, corresponding to a periodically varying flux (or current), the concentration perturbation also varies periodically, but there is a $\pi/4$ phase difference between the flux and the concentration response (Fig. 4.27).

This is an extremely important result because an alternating flux can be produced by an alternating current density at the electrode–electrolyte interface, and in the case of sufficiently fast charge-transfer reactions, the concentration at the boundary is related to the potential difference across the interface. Thus, the current density and

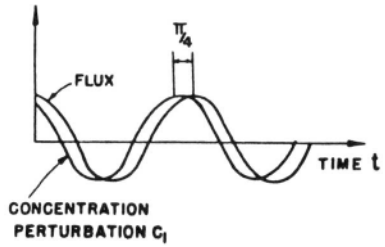


**Fig. 4.27.** When a sinusoidally varying diffusion flux is produced in an electrochemical system by passing a sinusoidally varying current through it, the perturbation in the concentration of the diffusing species also varies sinusoidally with time, but with a phase difference of $\pi/4$.

the potential difference both vary periodically with time, and it turns out that the phase relationship between them provides information on the rate of the charge-transfer reaction.

### 4.2.13. Diffusion Resulting from an Instantaneous Current Pulse

There is another important diffusion problem, the solution of which can be generated from the concentration response to a constant current (or a flux). Consider that in an electrochemical system there is a plane electrode at the boundary of the electrolyte. Now, suppose that with the aid of an electronic pulse generator, an extremely short time current pulse is sent through the system (Fig. 4.28). The current is directed so as to dissolve the metal of the electrode; hence, the effect of the pulse is to produce a burst of metal dissolution in which a layer of metal ions is piled up at the interface (Fig. 4.29).

Because the concentration of metal ions at the interface is far in excess of that in the bulk of the solution, diffusion into the solution begins. Since the source of the diffusing ions is an ion layer parallel to the plane electrode, it is known as a *plane source*; and since the diffusing ions are produced in an instantaneous pulse, a fuller description of the source is contained in the term *instantaneous plane source.*

As the ions from the instantaneous plane source diffuse into the solution, their concentration at various distances will change with time. The problem is to calculate the distance and time variation of this concentration.

The starting point for this calculation is the general relation between the Laplace transforms of the concentration perturbation $c_1$ and the time-varying flux $J(t)$

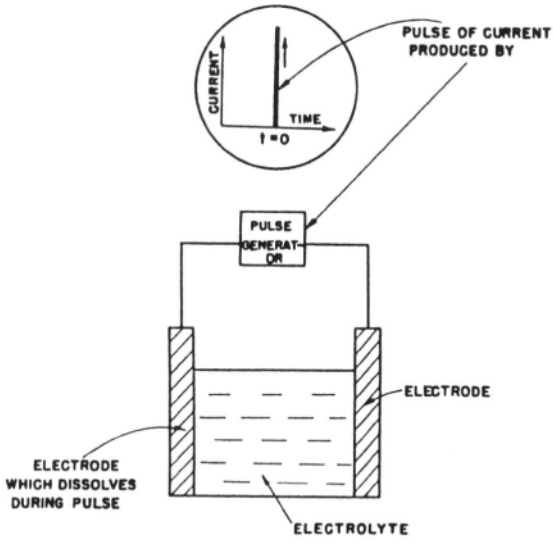


**Fig. 4.28.** The use of an electronic pulse generator to send an extremely short time current pulse through an electrochemical system so that there is dissolution at one electrode during the pulse.

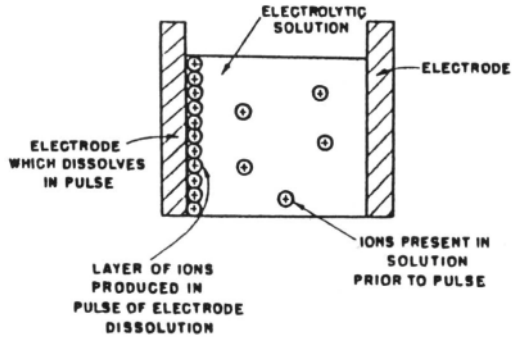


**Fig. 4.29.** The burst of electrode dissolution during the current pulse produces a layer of ions adjacent to the dissolving electrode (negative ions are not shown in the diagram).

$$\bar{c}_1 = D^{-1/2} p^{-1/2} \exp\left(-\sqrt{\frac{p}{D}}x\right)\bar{J} \tag{4.69}$$

One has to substitute for $\bar{J}$ the Laplace transform of a flux that is an instantaneous pulse. This is done with the help of the following interesting observation.

If one takes any quantity that varies with time as a step, then the differential of that quantity with respect to time varies with time as an instantaneous pulse (Fig. 4.30). In other words, the time derivative of a step function is an instantaneous pulse. Suppose therefore one considers a constant flux (or current) switched on at $t = 0$ (i.e., the flux is a step function of time and will be designated $\boldsymbol{J}_{\text{step}}$); then the time derivative of that constant flux is a pulse of flux (or current) at $t = 0$, referred to by the symbol $\boldsymbol{J}_{\text{pulse}}$, i.e.,

$$\boldsymbol{J}_{\text{pulse}} = \frac{d}{dt}\boldsymbol{J}_{\text{step}} \tag{4.81}$$

If, now, one takes Laplace transforms of both sides and uses Eq. (4.38) to evaluate the right-hand side, one has

$$\bar{J}_{\text{pulse}} = p\bar{J}_{\text{step}} - \bar{J}_{\text{step}}\,[t = 0] \tag{4.82}$$

But at $t = 0$, the magnitude of a flux that is a step function of time is zero. Hence,

$$\bar{J}_{\text{pulse}} = p\bar{J}_{\text{step}} \tag{4.83}$$

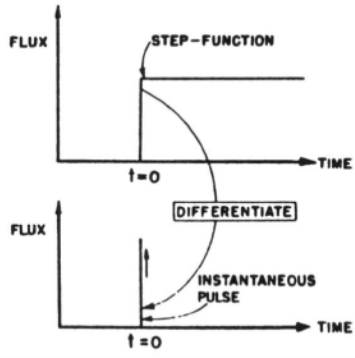


**Fig. 4.30.** The time derivative of a flux that is a step function of time is an instantaneous pulse of flux.

If the pumping of diffusing particles into the system by the step-function flux consists in switching on, at $t = 0$, a flux of $-\lambda$ mol cm$^{-2}$ s$^{-1}$, then

$$J_{\text{step}} = -\lambda \tag{4.84}$$

and

$$\bar{J}_{\text{step}} = -\frac{\lambda}{p} \tag{4.85}$$

Using this relation in Eq. (4.83), one has

$$\bar{J}_{\text{pulse}} = -\lambda \tag{4.86}$$

and, by substitution in Eq. (4.69),

$$\bar{c}_1 = -\lambda D^{-1/2} p^{-1/2} \exp\left(-\sqrt{\frac{p}{D}}\, x\right) \tag{4.87}$$

By inverse transformation (Table 4.5),

$$c_1 = -\lambda (\pi D t)^{-1/2} \exp\left(-\frac{x^2}{4Dt}\right) \tag{4.88}$$

or by referring to the actual concentration $c$ instead of the perturbation $c_1$ in concentration, the result is

$$c = c^0 + \lambda (\pi D t)^{-1/2} \exp\left(-\frac{x^2}{4Dt}\right) \tag{4.89}$$

If, prior to the current pulse, there is a zero concentration of the species produced by metal dissolution, i.e.,

$$c[t = 0] = c^0 = 0 \tag{4.90}$$

then Eq. (4.89) reduces to

$$c = \frac{\lambda}{(\pi D t)^{1/2}} e^{-x^2/4Dt} \tag{4.91}$$

It can be seen from Eq. (4.86) that $\lambda$ is the Laplace transform of the pulse of flux. However, a Laplace transform is an integral with respect to time. Hence, $\lambda$, which is a flux (of moles per square centimeter per second) in the constant-flux problem (see Section 4.2.12), is in fact the total concentration (moles per square centimeter) of the

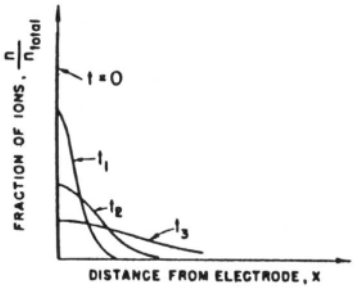


**Fig. 4.31.** Plots of the fraction $n/n_{total}$ of ions (produced in the pulse of electrode dissolution) against the distance $x$ from the electrode. At $t = 0$, all the ions are on the $x = 0$ plane, and at $t > 0$, they are distributed in the solution as a result of dissolution and diffusion. In the diagram, $t_3 > t_2 > t_1 > 0$, and the distribution curve becomes flatter and flatter.

diffusing ions produced on the $x = 0$ plane in the burst of metal dissolution. If, instead of dealing with concentrations, one deals with *numbers* of ions, the result is

$$n = \frac{n_{total}}{(\pi Dt)^{1/2}} e^{-x^2/4Dt} \tag{4.92}$$

where $n$ is the number of ions at a distance $x$ and a time $t$, and $n_{total}$ is the number of ions set up on the $x = 0$ plane at $t = 0$; i.e., $n_{total}$ is the total number of diffusing ions.

This is the solution to the instantaneous-plane-source problem. When $n/n_{total}$ is plotted against $x$ for various times, one obtains curves (Fig. 4.31) that show how the ions injected into the $x = 0$ plane at $t = 0$ (e.g., ions produced at the electrode in an impulse of metal dissolution) are distributed in space at various times. At any particular time $t$, a semi-bell-shaped distribution curve is obtained that shows that the ions are mainly clustered near the $x = 0$ plane, but there is a "spread." With increasing time, the spread of ions increases. This is the result of diffusion, and after an infinitely long time, there are equal numbers of ions at any distance.

### 4.2.14. Fraction of Ions Traveling the Mean Square Distance $\langle x^2 \rangle$ in the Einstein–Smoluchowski Equation

In the previous section, an experiment was described in which a pulse of current dissolves out of the electrode a certain number $n_{total}$ of ions, which then start diffusing

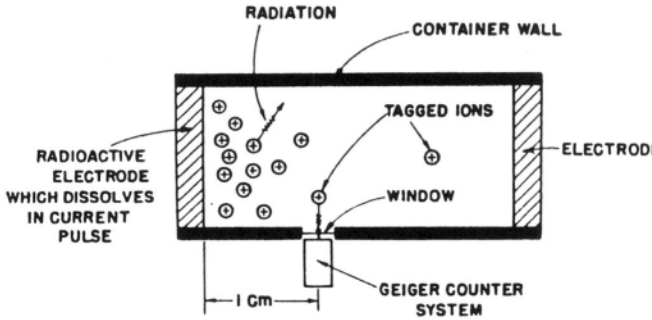


**Fig. 4.32.** Schematic of experiment to note the time interval between the pulse of electrode dissolution (at $t = 0$) and the arrival of radioactive ions at the window where they are registered in the Geiger-counter system.

into the solution. Now suppose that the electrode material is made radioactive so that the ions produced by dissolution are detectable by a counter (Fig. 4.32). The counter head is then placed near a window in the cell at a distance of 1 cm from the dissolving electrode, so that as soon as the tagged ions pass the window, they are registered by the counter. How long after the current pulse at $t = 0$ does the counter note the arrival of the ions?

It is experimentally observed that the counter begins to register within a few seconds of the termination of the instantaneous current pulse. Suppose, however, that one attempted a theoretical calculation based on the Einstein–Smoluchowski equation (4.27), i.e.,

$$\langle x^2 \rangle = 2Dt \tag{4.27}$$

using, for the diffusion coefficient of ions, the experimental value of $10^{-5}$ cm$^2$ s$^{-1}$. Then, the estimated time for the radioactive ions to reach the counter is

$$t = \frac{1}{2 \times 10^{-5} \times 60} \text{ min}$$

or

$$t \approx 10^3 \text{ min}$$

This is several orders of magnitude larger than is indicated by experience.

The dilemma may be resolved as follows. If $\langle x^2 \rangle$ in the Einstein–Smoluchowski relation pertains to the mean square distance traversed by a majority of the radioactive particles and if Geiger counters can—as is the case—detect a very small number of

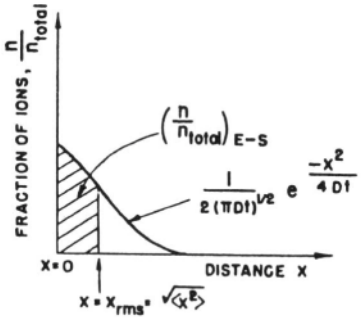


**Fig. 4.33.** The Einstein–Smoluchowski equation, $\langle x^2 \rangle = 2\,Dt$, pertains to the fraction $(n/n_{total})_{ES}$, of ions between $x = 0$ and $x = x_{rms} = \sqrt{\langle x^2 \rangle}$. This fraction is found by integrating the distribution curve between $x = 0$ and $x = x_{rms}$.

particles, then one can qualitatively see that there is no contradiction between the observed time and that estimated from Eq. (4.27). The time of $10^3$ min estimated by the Einstein–Smoluchowski equation is far too large because it pertains to a number of radioactive ions far greater than the number needed to register in the counting apparatus. The way in which the diffusing particles spread out with time, i.e., the distribution curve for the diffusing species (Fig. 4.31), shows that even after very short times, some particles have diffused to very large distances, and these are the particles registered by the counter in a time far less than that predicted by the Einstein–Smoluchowski equation.

The qualitative argument just presented can now be quantified. The central question is: To what fraction $n/n_{total}$ of the ions (released at the instantaneous-plane source) does $\langle x^2 \rangle = 2Dt$ apply?[15] This question can be answered easily by integrating the $n$ versus $x$ distribution curve (Fig. 4.33) between the lower limit $x = 0$ (the location of the plane source) and the value of $x$ corresponding to the square root of $\langle x^2 \rangle$. This upper limit of $\sqrt{\langle x^2 \rangle}$—the root-mean-square distance—is, for conciseness, represented by the symbol $x_{rms}$, i.e.,

$$x_{rms} = \sqrt{\langle x^2 \rangle} \tag{4.93}$$

Thus, the Einstein–Smoluchowski fraction $(n/n_{total})_{ES}$ is given by [*cf.* Eq. (4.92)]

[15]This fraction will be termed the *Einstein–Smoluchowski fraction.*

$$\left(\frac{n}{n_{\text{total}}}\right)_{\text{ES}} = \int_0^{x_{\text{rms}}} \frac{1}{(\pi Dt)^{1/2}} e^{-x^2/4Dt}\, dx$$

$$= \frac{\sqrt{2}}{\pi^{1/2}(2Dt)^{1/2}} \int_0^{x_{\text{rms}}} e^{-x^2/2(2Dt)}\, dx \tag{4.94}$$

According to the Einstein–Smoluchowski relation,

$$2Dt = \langle x^2 \rangle$$

Hence,

$$(2Dt)^{1/2} = \sqrt{\langle x^2 \rangle} = x_{\text{rms}} \tag{4.95}$$

By using this relation, Eq. (4.94) becomes

$$\left(\frac{n}{n_{\text{total}}}\right)_{\text{ES}} = \frac{\sqrt{2}}{\pi^{1/2} x_{\text{rms}}} \int_0^{x_{\text{rms}}} e^{-\frac{1}{2}(x/x_{\text{rms}})^2} dx \tag{4.96}$$

To facilitate the integration, substitute

$$\frac{x}{x_{\text{rms}}} = \sqrt{2}\, u \tag{4.97}$$

in which case several relations follow

$$\left(\frac{x}{x_{\text{rms}}}\right)^2 = 2u^2 \tag{4.98}$$

$$dx = \sqrt{2}\, x_{\text{rms}}\, du \tag{4.99}$$

$$u = \frac{1}{\sqrt{2}} \quad \text{when} \quad x = x_{\text{rms}} \tag{4.100}$$

and

$$u = 0 \quad \text{when} \quad x = 0 \tag{4.101}$$

With the use of these relations, Eq. (4.96) becomes

$$\left(\frac{n}{n_{\text{total}}}\right)_{\text{ES}} = \frac{2}{\pi^{1/2}} \int_0^{1/\sqrt{2}} e^{-u^2}\, du \tag{4.102}$$

The integral on the right-hand side is the error function of $1/\sqrt{2}$ [*cf.* Eq. (4.63)].

Values of the error function have been tabulated in detail (Table 4.6). The value of the error function of $1/\sqrt{2}$, i.e.,

$$\frac{2}{\pi^{1/2}} \int_0^{1/\sqrt{2}} e^{-u^2} du$$

is 0.68. Hence,

$$\left(\frac{n}{n_{\text{total}}}\right)_{\text{ES}} = 0.68 \tag{4.103}$$

and therefore about two-thirds (68%) of the diffusing species are within the region from $x = 0$ to $x_{\text{rms}} = \sqrt{2Dt}$. This means, however, that the remaining fraction, namely one-third, have crossed beyond this distance. Of course, the radioactive ions that are sensed by the counter almost immediately after the pulse of metal dissolution belong to this one-third group (Fig. 4.34).

**TABLE 4.6**
**The Value of the Integral $\frac{2}{\sqrt{\pi}} \int_0^{1/\sqrt{2}} e^{-u^2}\, du$**

| $y$ | Value |
|---|---|
| 0.00 | 0.00000 |
| 0.01 | 0.01128 |
| 0.02 | 0.02256 |
| 0.10 | 0.11246 |
| 0.20 | 0.22270 |
| 0.30 | 0.32863 |
| 0.40 | 0.42839 |
| 0.50 | 0.52050 |
| 0.60 | 0.60386 |
| 0.70 | 0.67780 |
| 0.80 | 0.74210 |
| 0.90 | 0.79691 |
| 1.00 | 0.84270 |
| 2.00 | 1.00000 |

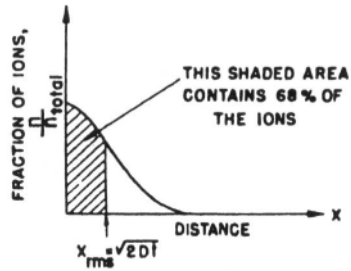


**Fig. 4.34.** When diffusion occurs from an instantaneous plane source (set up, e.g., by a pulse of electrode dissolution), then 68% of the ions produced in the pulse lie between $x = 0$ and $x = x_{rms}$, after the time $t$.

In the above experiment, diffusion toward the $x \to -\infty$ direction is prevented by the presence of a physical boundary (i.e., the electrode). If no such boundary exists and diffusion in both the $+x$ and $-x$ directions is possible, then 68% of the particles will distribute themselves in the region from $x = -x_{rms} = -\sqrt{2Dt}$ to $x = +x_{rms} = +\sqrt{2Dt}$. From symmetry considerations, one would expect 34% to be within $x = 0$ and $x = +x_{rms}$ and an equal amount to be on the other side (Fig. 4.35).

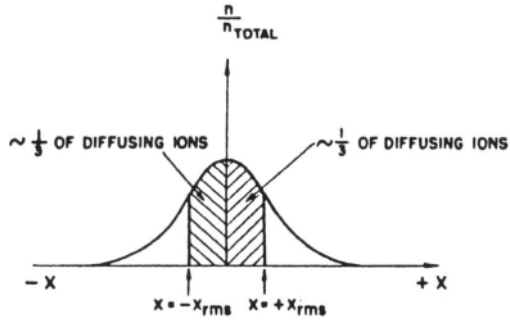


**Fig. 4.35.** If it were possible for diffusion to occur in the $+x$ and $-x$ directions from an instantaneous plane source at $x = 0$, then one-third of the diffusing species would lie between $x = 0$ and $x = +x_{rms}$ and a similar number would lie between $x = 0$ and $x = -x_{rms}$.

From the above discussion, the advantages and limitations of using the Einstein–Smoluchowski relation become clear. If one is considering phenomena involving a few particles, then one can be misled by making Einstein–Smoluchowski calculations. If, however, one wants to know about the diffusion of a sizable fraction of the total number of particles, then the relation provides easily obtained, although rough, answers without having to go through the labor of obtaining the exact solution for the diffusion problem (see, e.g., Section 4.6.8).

### 4.2.15. How Can the Diffusion Coefficient Be Related to Molecular Quantities?

The diffusion coefficient $D$ has appeared in both the macroscopic (Section 4.2.2) and the atomistic (Section 4.2.6) views of diffusion. How does the diffusion coefficient depend on the structure of the medium and the interatomic forces that operate? To answer this question, one should have a deeper understanding of this coefficient than that provided by the empirical first law of Fick, in which $D$ appeared simply as the proportionality constant relating the flux $J$ and the concentration gradient $dc/dx$. Even the random-walk interpretation of the diffusion coefficient as embodied in the Einstein–Smoluchowski equation (4.27) is not fundamental enough because it is based on the mean square distance traversed by the ion after $N$ steps taken in a time $t$ and does not probe into the laws governing each step taken by the random-walking ion.

This search for the atomistic basis of the diffusion coefficient will commence from the picture of random-walking ions (see Sections 4.2.4 to 4.2.6). It will be recalled that a net diffusive transport of ions occurs in spite of the completely random zigzag dance of individual ions, because of unequal numbers of ions in different regions.

Consider one of these random-walking ions. It can be proved (see Appendix 4.1) that the mean square distance $\langle x^2 \rangle$ traveled by an ion depends on the number $N$ of jumps the ion takes and the mean jump distance $l$ in the following manner (Fig. 4.36):

$$\langle x^2 \rangle = Nl^2 \tag{4.104}$$

It has further been shown (Section 4.2.6) that in the case of a one-dimensional random walk, $\langle x^2 \rangle$ depends on time according to the Einstein–Smoluchowski equation

$$\langle x^2 \rangle = 2Dt \tag{4.27}$$

By combining Eqs. (4.104) and (4.27), one obtains the equation

$$Nl^2 = 2Dt \tag{4.105}$$

which relates the number of jumps and the time. If now only one jump of the ion is considered, i.e., $N = 1$, Eq. (4.105) reduces to

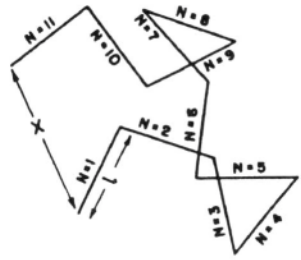


**Fig. 4.36.** Schematic representation of $N = 11$ steps (each of mean length $l$) in the random walk of an ion. After 11 steps, the ion is at a distance x from the starting point.

$$D = \frac{1}{2}\frac{l^2}{\tau} \tag{4.106}$$

where $\tau$ is the *mean jump time* to cover the mean jump distance $l$. This mean jump time is the number of seconds per jump,[16] and therefore $1/\tau$ is the jump frequency, i.e., the number of jumps per second. Putting

$$k = \frac{1}{\tau} \tag{4.107}$$

one can write Eq. (4.106) thus:

$$D = \frac{1}{2} l^2 k \tag{4.108}$$

Equation (4.108) shows that the diffusion depends on how far, on average, an ion jumps and how frequently these jumps occur.

### 4.2.16. The Mean Jump Distance *l*, a Structural Question

To go further than Eq. (4.108), one has to examine the factors that govern the mean jump distance $l$ and the jump frequency $k$. For this, the picture of a liquid (in which diffusion is occurring) as a structureless continuum is inadequate. In reality, the liquid has a structure—ions and molecules in definite arrangements at any one instant

[16]This mean jump time will include any waiting time between two successive jumps.

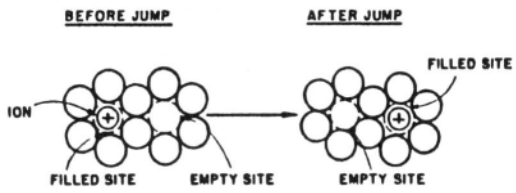


**Fig. 4.37.** Diagram to illustrate one step in the random walk of an ion.

of time. This arrangement in a liquid (unlike that in a solid) is local in extent, transitory in time, and mobile in space. The details of the structure are not necessary to continue the present discussion. What counts is that ions zigzag in a random walk, and for any particular step, the ion has to *maneuver out of* one site in the liquid structure into another site (Fig. 4.37). This maneuvering process can be symbolically represented thus:

$$\boxed{\text{Ion}} + \square \rightarrow \square + \boxed{\text{Ion}} \tag{4.109}$$

where $\boxed{\text{Ion}}$ is a site occupied by an ion and $\square$ is an empty acceptor site waiting to receive a jumping ion. The mean jump distance $l$ is seen to be the mean distance between sites, and its numerical value depends upon the details of the structure of the liquid, i.e., upon the instantaneous and local atomic arrangement.

### 4.2.17. The Jump Frequency, a Rate-Process Question

The process of diffusion always occurs at a finite rate; it is a *rate process.* Chemical reactions, e.g., three-atom reactions of the type

$$AB + C \rightarrow A + BC \tag{4.110}$$

are also rate processes. Further, a three-atom reaction can be formally described as the jump of the particle $B$ from a site in $A$ to a site in C (Fig. 4.38). With this description, it can be seen that the notation (4.109) used to represent the jump of an ion has in fact established an analogy between the two rate processes, i.e., diffusion and chemical reaction. Thus, the basic theory of rate processes should be applicable to the processes of both diffusion and chemical reactions.

The basis of this theory is that the potential energy (and standard free energy) of the system of particles involved in the rate processes varies as the particles move to accomplish the process. Very often, the movements crucial to the process are those of a single particle, as is the case with the diffusive jump of an ion from site to site. If the free energy of the system is plotted as a function of the position of the crucial particle,

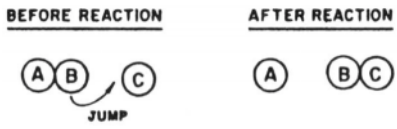


**Fig. 4.38.** A three-atom chemical reaction $AB + C \rightarrow A + BC$ viewed as the jump of atom $B$ from atom $A$ to atom $C$.

e.g., the jumping ion, then the standard free energy of the system has to attain a critical value (Fig. 4.39)—the activation free energy $\Delta G^\circ$—for the process to be accomplished. One says that the system has to cross an *energy barrier* for the rate process to occur. The number of times per second that the rate process occurs, $k$, i.e., the jump frequency in the case of diffusion, can be shown to be given by[17]

$$\vec{k} = \frac{kT}{h} e^{-\Delta G^{\circ\ddagger}/RT} \tag{4.111}$$

### 4.2.18. The Rate-Process Expression for the Diffusion Coefficient

To obtain the diffusion coefficient in terms of atomistic quantities, one has to insert the expression for the jump frequency (4.111) into that for the diffusion coefficient [Eq. (4.108)]. The result is

$$D = \frac{1}{2} l^2 \vec{k}$$

$$= \frac{1}{2} l^2 \frac{kT}{h} e^{-\Delta G^{\circ\ddagger}/RT} \tag{4.112}$$

The numerical coefficient $\frac{1}{2}$ has entered here only because the Einstein–Smoluchowski equation $\langle x^2 \rangle = 2Dt$ for a *one*-dimensional random walk was considered. In general, it is related to the probability of the ion's jumping in various directions, not just forward and backward. For convenience, therefore, the coefficient will be taken to be unity, in which case

$$D \approx l^2 \vec{k} \tag{4.113}$$

$$\approx l^2 \frac{kT}{h} e^{-\Delta G^{\circ\ddagger}/RT} \tag{4.114}$$

[17] The $\vec{k}$ on the left-hand side is the jump frequency; the $k$ in the term $kT/h$ is the Boltzmann constant.

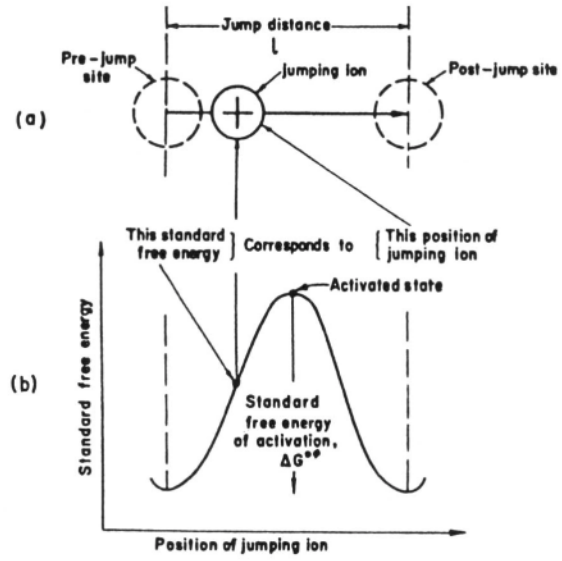


**Fig. 4.39.** (a) The jump of an ion from a prejump site to a postjump site through a jump distance *l*. (b) Corresponding to each position of the jumping ion, the system (sites + jumping ion) has a standard free energy. Thus, the standard free-energy changes corresponding to the ionic jump can be represented by the passage of a point (representing the standard free energy of the system) over the barrier by the acquisition of the standard free energy of activation.

As to the value of *l*, this depends on the model process seen as the mechanism for diffusion. This is discussed for liquid electrolytes rather fully in Section 5.7. In one mechanism ("shuffling along"), the diffusing particles are seen to be analogues of persons pushing through a crowd. Each microstep is less than the distance between two sites. In another, the ion moves by jumps, taking the opportunity when a void or vacancy turns up beside it to move in to fill the void. Then the value of *l* would be equal to the intersite distance. Thus, in the shuffle-along model, the range of *l*s would be as little as 0.01 nm, and in the jump-into-a-hole model, perhaps 0.2–0.3 nm.

### 4.2.19. Ions and Autocorrelation Functions

Autocorrelation functions involve concepts that one sometimes reads about in analyses of transport in liquids and are therefore concepts with which the student should be familiar. These are mathematical devices used in some discussions of the theory of transport in liquids, e.g., in treatment of viscous flow and diffusion. It is

possible, for example, to represent the diffusion coefficient $D$ in terms of the autocorrelation function of a particle's velocity. When a particle in solution collides with another (say, an ion colliding with a solvent molecule), the collision is tantamount to a force operating for a very short time on the particle. This time is much shorter than the time needed for the normal so-called "Stokes' resistance" (see Section 4.4.7), which slows down the particle that has "received a knock" to the average velocity (e.g., in flow). Now consider dealing with diffusion coefficients in terms of molecular dynamics (see a description of this technique in Section 2.3.2). This method is used to determine how the dynamics of motion of a given particle will be affected by its collision with other particles. Thus, it is important to know the relation between the velocity of a particle at the beginning ($t = 0$), that is, just after collision, and that at some later time $t$.

This is where one brings in the concept of the *velocity autocorrelation function.* This indeed concerns the velocity at $t=0$, $v_0$, and the velocity at some subsequent time, $v_t$. To what extent does the subsequent velocity depend upon the velocity at time $t = 0$? That is the sort of information given by the autocorrelation function.

There are several technical details in a rigorous definition of the autocorrelation function for velocity. First, one has to remember the vectorial character of velocity, because clearly the direction in which the particle is knocked is important to its subsequent dynamic history. Then, according to the way it is defined, one has to take the product of the velocity at $t = 0$, $v_0$, and that at the later chosen time, $v_t$. However, it is not as simple as just multiplying together the two vectors, $v_0$ and $v_t$. One has to allow for the distribution of positions and momenta of the particle in the system at the beginning, that is, at $t = 0$. To allow for this, one can introduce symbolically a probability distribution coefficient, $g_0$. Therefore, the expression for the autocorrelation function will involve the product $g_0 v_0 v_t$.

Thereafter, there is only one step left, but it is a vital one. One has to carry out an averaging process for the entire liquid (or solution) concerned. Such averaging processes can be carried out in more than one way. One of these involves an integration with respect to time. One ends up by writing down the full-blown expression for the autocorrelation function as a function of an expression dependent on time, $A(t)$. Then, in a general way, an autocorrelation function would run

$$C(\tau) = \langle A(t)A(t + \tau)\rangle \tag{4.115}$$

where the brackets represent "the average value of," as defined in Eq. (4.20).

How can this concept be used to calculate diffusion coefficients in ionic solutions? First one has to remember that for diffusion in one direction,

$$\langle x^2\rangle = 2Dt \tag{4.116}$$

However, the displacement of the particle $x$ is in reality a function of time and therefore can also be expressed in terms of an autocorrelation function similar to that presented

in Eq. (4.115). One advantage of this procedure is that the autocorrelation function will depend only on a time interval, $\tau - t$, and not on the time itself. Through the use of Eq. (4.116) and some mechanics produced earlier in the century by Langevin, one finds that the diffusion coefficient D can be expressed by the *time integral of the velocity autocorrelation function* and eventually obtains the useful equation

$$D = \int_0^\infty \langle v(0)v(\tau)\rangle \, d\tau = \frac{kT}{f_c} \tag{4.117}$$

where $f_c$ is the frictional coefficient.

Does this concern ions in solution and electrochemistry? It does indeed concern some approaches to diffusion and hence the related properties of conduction and viscous flow. It has been found that the autocorrelation function for the velocity of an ion diffusing in solution decays to zero very quickly, i.e., in about the same time as that of the random force due to collisions between the ion and the solvent. This is awkward because it is not consistent with one of the approximations used to derive analytical expressions for the autocorrelation function.[18] The result of this is that instead of an analytical expression, one has to deal with molecular dynamics simulations.

One of the simplest examples of this type of calculation involves the study of a system of rare-gas atoms, as in, e.g., calculations carried out on liquid argon. The relaxation time after a collision was found to be on the order of $10^{-13}$ s, which is about the same time as that for rather large ions (e.g., of 500 pm). Thus, much of what one learns from the MD study of molecular motion in liquid argon should be applicable to ionic diffusion.

Figure 4.40 shows the velocity autocorrelation function for liquid argon as calculated by Levesque et al. Looking now at this figure, one can see at first the fast exponential decay of the autocorrelation function. The function then becomes negative (reversal of velocity), indicating a scattering collision with another molecule. At longer times it trails off to zero, as expected, for eventually the argon atom's motion becomes unconnected to the original collision. The time for this to happen is relatively long, about $10^{-12}$ s.

In summary, then, autocorrelation functions are useful mathematical devices which, when applied to velocities, tell us to what degree the motion of a particle at a given instant is related to the impelling force of the last collision. Their usefulness is mainly in molecular dynamics, the principal computer-oriented method by which systems are increasingly being analyzed (Section 2.17).

---

[18]Here it is assumed that the influence of the collision lasts a lot longer than the force due to the collision itself.

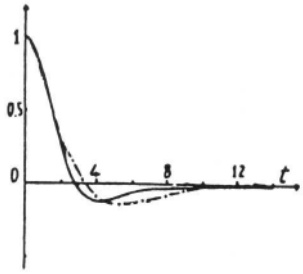


**Fig. 4.40.** Autocorrelation function of the velocity (time units $10^{-13}$ s) obtained by Levesque et al. (dash-dot curve). The solid curve is the molecular dynamics results (D. Levesque, L Verlet, and J. Kurkijarvi, *Phys. Rev. A 7:* 1690,1973.)

### 4.2.20. Diffusion: An Overall View

An electrochemical system runs on the basis of charge-transfer reactions at the electrode–electrolyte interfaces. These reactions involve ions or molecules that are constituents of the electrolyte. Thus, the transport of particles to or away from the interface becomes an essential condition for the continued electrochemical transformation of reactants at the interface.

One of the basic mechanisms of ionic transport is diffusion. This type of transport occurs when the concentration of the diffusing species is different in different parts of the electrolyte. What makes diffusion occur? This question can be answered on a macroscopic and on a microscopic level.

The macroscopic view is based on the fact that when the concentration varies with distance, so does the chemical potential. However, a nonuniformity of chemical potential implies that the free energy is not the same everywhere and therefore the system is not at equilibrium. How can the system attain equilibrium? By equalizing the chemical potential, i.e., by transferring the species from the high-concentration regions to the low-concentration regions. Thus, the negative gradient of the chemical potential, $d\mu/dx$, behaves like a driving force (see Section 4.2.1) that produces a net flow, or flux, of the species.

When the driving force is small, it may be taken to be linearly related to the flux. On this basis, an equation can be derived for the rate of steady-state diffusion, which is identical in form to the empirical first law of Fick,

$$J = -D\frac{dc}{dx}$$

The microscopic view of diffusion starts with the movements of individual ions. Ions dart about haphazardly, executing a random walk. By an analysis of one-dimensional random walk, a simple law can be derived (see Section 4.2.6) for the mean square distance $\langle x^2 \rangle$ traversed by an ion in a time $t$. This is the Einstein–Smoluchowski equation

$$\langle x^2 \rangle = 2Dt \tag{4.27}$$

It also turns out that the random walk of individual ions is able to give rise to a flux, or flow, on the level of the group. Diffusion is simply the result of there being more random-walking particles in one region than in another (see Section 4.2.6). The gradient of chemical potential is therefore only a pseudoforce that can be regarded as operating on a society of ions but not on individual ions.

The first law of Fick tells one how the concentration gradient is related to the flux under steady-state conditions; it says nothing about how the system goes from nonequilibrium to steady state when a diffusion source or sink is set up inside or at the boundary of the system. Thus, it says nothing about how the concentration changes with time at different distances from the source or sink. In other words, Fick's first law is inapplicable to nonsteady-state diffusion. For this, one has to go to Fick's second law

$$\frac{\partial c}{\partial t} = D \frac{\partial^2 c}{\partial x^2} \tag{4.32}$$

which relates the time and space variations of the concentration during diffusion.

Fick's second law is a partial differential equation. Thus, it describes the general characteristics of all diffusion problems but not the details of any one particular diffusion process. Hence, the second law must be solved with the aid of the initial and boundary conditions that characterize the particular problem.

The solution of Fick's second law is facilitated by the use of Laplace transforms, which convert the partial differential equation into an easily integrable total differential equation. By utilizing Laplace transforms, the concentration of diffusing species as a function of time and distance from the diffusion sink when a constant normalized current, or flux, is switched on at $t = 0$ was shown to be

$$c = c^0 - \frac{1}{D^{1/2}} \left[ \frac{2t^{1/2}}{\pi^{1/2}} \exp\left( -\frac{x^2}{4Dt} \right) - \frac{x}{D^{1/2}} \operatorname{erfc}\left( \frac{x^2}{4Dt} \right)^{1/2} \right] \tag{4.65}$$

With the solution of this problem (in which the flux varies as a unit-step function with time), one can easily generate the solution of other problems in which the current, or flux, varies with time in other ways, e.g., as a periodic function or as a single pulse.

When the current, or flux, is a single impulse, an instantaneous-plane source for diffusion is set up and the concentration variation is given by

$$c(x, t) = \frac{\lambda}{(\pi Dt)^{1/2}} e^{-x^2/4Dt} \tag{4.91}$$

in the presence of a boundary. From this expression, it turns out that in a time $t$, only a certain fraction (two-thirds) of the particles travel the distance given by the Einstein–Smoluchowski equation. Actually, the spatial distribution of the particles at a given time is given by a semi-bell-shaped distribution curve.

The final step involves the relation of the diffusion coefficient to the structure of the medium and the forces operating there. It is all a matter of the mean distance $l$ through which ions jump during the course of their random walk and of the mean jump frequency $k$. The latter can be expressed in terms of the theory of rate processes, so that one ends up with an expression for the rate of diffusion that is in principle derivable from the local structure of the medium.

There is more than one way of calculating diffusion coefficients, and a method being used increasingly involves molecular dynamics. Some description of this technique is given in Sections 2.3.2 and 2.17. One aspect of it is the velocity autocorrelation function as explained in Section 4.2.19.

This then is an elementary picture of diffusion. The next task is to consider the phenomenon of conduction, i.e., the migration of ions in an electric field.

## Further Reading

### *Seminal*

1. M. Smoluchowski, "Diffusive Movements in Liquids," Ann. *Physik (Paris)* **25**:205 (1908).
2. A. Einstein, *Investigations on the Theory of Brownian Movement,* Methuen & Co., London (1926).
3. Lin Yong and M. T. Simned, "Measurement of Diffusivity in Liquid Systems," in *Physicochemical Measurements at High Temperatures,* J. O'M. Bockris, J. L. White, and J. W. Tomlinson, eds., Butterworth, London (1959).

### *Review*

1. J. G. Wijmans and R. W. Baker, "The Solution-Diffusion Model: A Review," *J. Membr. Sci.* **107:** 1 (1995).

### *Papers*

1. T. Munakata and Y. Kaneko, *Phys. Rev. E.: Stat. Phys. Plasmas, Fluids, Relat. Interdiscip. Top.* **47**: 4076 (1993).
2. J. P. Simmon, P. Turq, and A. Calado, *J. Phys. Chem.* **97**: 5019 (1993).
3. S. Rondot, J. Cazaux, and O. Aaboubi, *Science* **263**: 1739 (1994).
4. E. Hawlichka, *Chem. Soc. Rev.* **24**: 367 (1994).
5. Z. A. Metaxiotou and S. G. Nychas, *AIChE J* **41**: 812 (1995).
6. R. Biswas, S. Roy, and B. Bagchi, *Phys. Rev. Lett.* **75**: 1098 (1995).

## 4.3. IONIC DRIFT UNDER AN ELECTRIC FIELD: CONDUCTION

### 4.3.1. Creation of an Electric Field in an Electrolyte

Assume that two plane-parallel electrodes are introduced into an electrolytic solution so as to cover the end walls of the rectangular insulating container (Fig. 4.41). With the aid of an external source, let a potential difference be applied across the electrodes. How does this applied potential difference affect the ions in the solution?

The potential in the solution has to vary from the value at one electrode, $\psi_{\mathrm{I}}$, to that at the other electrode, $\psi_{\mathrm{II}}$. The major portion of this potential drop $\psi_{\mathrm{I}} - \psi_{\mathrm{II}}$ occurs across the two electrode-solution interfaces (see Chapter 6); i.e., if the potentials on the solution side of the two interfaces are $\psi'_{\mathrm{I}}$ and $\psi'_{\mathrm{II}}$, then the interfacial potential differences are $\psi_{\mathrm{I}} - \psi'_{\mathrm{I}}$ and $\psi'_{\mathrm{II}} - \psi_{\mathrm{II}}$ (Fig. 4.42). The remaining potential drop, $\psi'_{\mathrm{I}} - \psi'_{\mathrm{II}}$, occurs in the electrolytic solution. The electrolytic solution is therefore a region of space in which the potential at a point is a function of the distance of that point from the electrodes.

Let the test ion in the solution be at the point $x_1$, where the potential is $\psi_1$ (Fig. 4.43). This potential is by definition the work done to bring a unit of positive charge from infinity up to the particular point. [In the course of this journey of the test charge from infinity to the particular point, it may have to cross phase boundaries, for example, the electrolyte-air boundary, and thereby do extra work (see Chapter 6). Such surface work terms cancel out, however, in discussions of the differences in potential between two points in the same medium.] If another point $x_2$ is chosen on the normal from $x$ to the electrodes, then the potential at $x_2$ is different from that at $x_1$ because of the variation

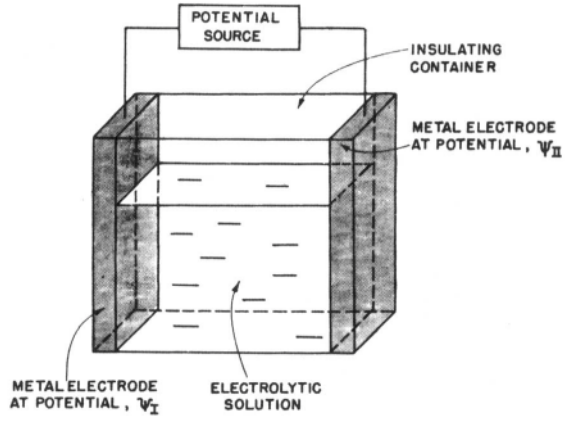


**Fig. 4.41.** An electrochemical system consisting of two plane-parallel electrodes immersed in an electrolytic solution is connected to a source of potential difference.

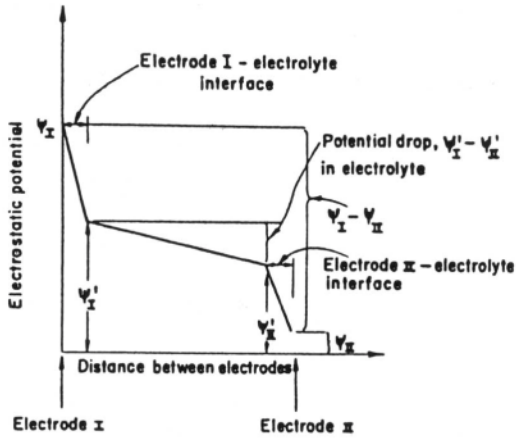


**Fig. 4.42.** Diagram to illustrate how the total potential difference $\psi_I - \psi_{II}$ is distributed in the region between the two electrodes.

of the potential along the distance coordinate between the electrodes. Let the potential at $x_2$ be $\psi_2$. Then $\psi_1 - \psi_2$, the difference in potential between the two points, is the work done to take a unit of charge from $x_1$ to $x_2$.

When this work $\psi_1 - \psi_2$ is divided by the distance over which the test charge is transferred, i.e., $x_1 - x_2$, one obtains the *force per unit charge*, or the electric field $X$

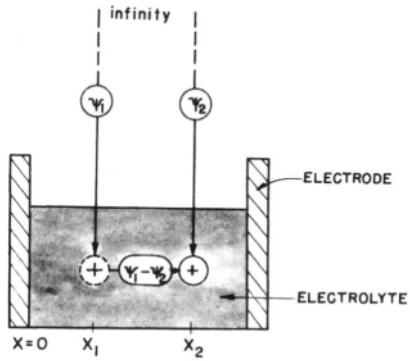


**Fig. 4.43.** The work done to transport a unit of positive charge from $x_1$ to $x_2$ in the solution is equal to the difference $\psi_1 - \psi_2$ in electrostatic potential at the two points.

$$X = -\frac{\psi_1 - \psi_2}{x_1 - x_2} \tag{4.118}$$

where the minus sign indicates that the force acts on a positive charge in a direction opposite to the direction of the positive gradient of the potential. In the particular case under discussion, i.e., parallel electrodes covering the end walls of a rectangular container, the potential drop in the electrolyte is linear (as in the case of a parallel-plate condenser), and one can write

$$X = -\frac{\text{Potential difference across the solution}}{\text{Distance across the solution}} \tag{4.119}$$

In general, however, it is best to be in a position to treat nonlinear potential drops. This is done by writing (Fig. 4.44)

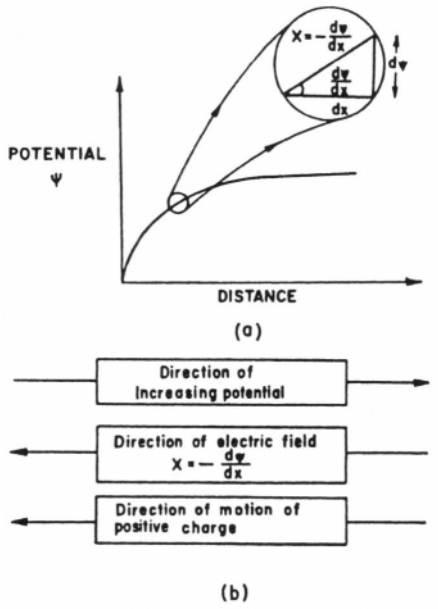


**Fig. 4.44.** (a) In the case of a nonlinear potential variation in the solution, the electric field at a point is the negative gradient of the electrostatic potential at that point. (b) The relative directions of increasing potential, field, and motion of *a* positive charge.

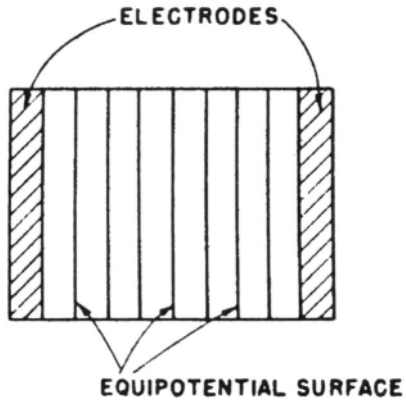


**Fig. 4.45.** A geometric representation of the electric field in an electrochemical system in which plane-parallel electrodes are immersed in an electrolyte so that they extend up to the walls of the rectangular insulating container. The equipotential surfaces are parallel to the electrodes.

$$X = -\frac{d\psi}{dx} \tag{4.120}$$

where now the electric field may be a function of $x$.

The imposition of a potential difference between two electrodes thus makes an electrolytic solution the scene of operation of an electric field (i.e., an electric force) acting upon the charges present. This field can be mapped by drawing equipotential surfaces (all points associated with the same potential lie on the same surface). The potential map yields a geometric representation of the field. In the case of plane-parallel electrodes extending to the walls of a rectangular cell, the equipotential surfaces are parallel to the electrodes (Fig. 4.45).

### 4.3.2. How Do Ions Respond to the Electric Field?

In the absence of an electric field, ions are in ceaseless random motion. This random walk of ions has been shown to have an important characteristic: The mean distance traversed by the ions as a whole is zero because while some are displaced in one direction, an equal number are displaced in the opposite direction. From a phenomenological view, therefore, the random walk of ions can be ignored because it does not lead to any net transport of matter (as long as there is no difference in

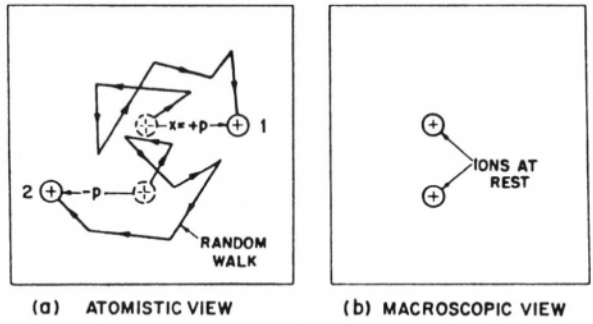


**Fig. 4.46.** (a) Schematic representation of the random walk of two ions showing that ion 1 is displaced a distance $x = +p$ and ion 2, a distance $x = -p$ and hence the mean distance traversed is zero. (b) Since the mean distance traversed by the ions is zero, there is no net flux of the ions and from a macroscopic point of view, they can legitimately be considered at rest.

concentration in various parts of the solution so that net diffusion down the concentration gradient occurs). The net result is as if the ions were at rest (Fig. 4.46).

Under the influence of an electric field, however, the net result of the zigzag jumping of ions is not zero. Ions feel the electric field; i.e., they experience a force directing them toward the electrode that is charged oppositely to the charge on the ion.

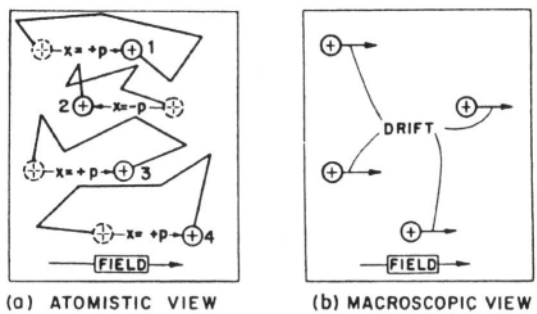


**Fig. 4.47.** (a) Schematic representation of the movements of four ions which random walk in the presence of a field. Their displacements are $+p$, $-p$, $+p$, and $+p$, i.e., the mean displacement is finite. (b) From a macroscopic point of view, one can ignore the random walk and consider that each ion drifts in the direction of the field.

This directed force is equal to the charge on the ion, $z_i e_0$, times the field at the point where the ion is situated. The driving force of the electric field produces in all ions of a particular species a velocity component in the direction $p$ of the potential gradient. Thus, the establishment of a potential difference between the electrodes produces a drift, or flux, of ions (Fig. 4.47). This drift is the migration (or conduction) of ions in response to an electric field.

As in diffusion, the relationship between the steady-state flux $J$ of ions and the driving force of the electric field will be represented by the expression

$$J = A + BX + CX^2 + \ldots \tag{4.121}$$

For small fields, the terms higher than $BX$ will tend to zero. Further, the constant $A$ must be zero because the flux of ions must vanish when the field is zero. Hence, for small fields, the flux of ions is proportional to the field (see Section 4.2.2)

$$J = BX \tag{4.122}$$

### 4.3.3. The Tendency for a Conflict between Electroneutrality and Conduction

When a potential gradient, i.e., electric field, exists in an electrolytic solution, the positive ions drift toward the negative electrode and the negative ions drift in the opposite direction. What is the effect of this ionic drift on the state of charge of an electrolytic solution?

Prior to the application of an external field, there is a time-averaged electroneutrality in the electrolyte over a distance that is large compared with $\kappa^{-1}$ (see Section 3.3.8); i.e., the net charge in any macroscopic volume of solution is zero because the total charge due to the positive ions is equal to the total charge due to the negative ions. Owing to the electric field, however, ionic drift tends to produce a spatial separation of charge. Positive ions will try to segregate near the negatively charged electrode, and negative ions near the positively charged electrode.

This tendency for gross charge separation has an important implication: electroneutrality tends to be upset. Furthermore, the separated charge causing the lack of electroneutrality tends to set up its own field, which would run counter to the externally applied field. If the two fields were to become equal in magnitude, the net field in the solution would become zero. (Thus, the driving force on an ion would vanish and ion migration would stop.)

It appears from this argument that an electrolytic solution would sustain only a transient migration of ions and then the tendency to conform to the principle of electroneutrality would result in a halt in the drift of ions after a short time. A persistent flow of charge, an electric current, appears to be impossible. In practice, however, an electrolytic solution can act as a conductor of electricity and is able to pass a current, i.e., maintain a continuous flow of ions. Is there a paradox here?

### 4.3.4. Resolution of the Electroneutrality-versus-Conduction Dilemma: Electron-Transfer Reactions

The solution to the dilemma just posed can be found by comparing an electrolytic solution with a metallic conductor. In a metallic conductor, there is a lattice of positive ions that hold their equilibrium positions during the conduction process. In addition, there are the free conduction electrons which assume responsibility for the transport of charge. Contact is made to and from the metallic conductor by means of other metallic conductors [Fig. 4.48(a)]. Hence, electrons act as charge carriers *throughout the entire circuit*.

In the case of an electrolytic conductor, however, it is necessary to make electrical contact to and from the electrolyte by metallic conductors (wires). Thus, here one has the interesting situation in which electrons transport charge in the external circuit and

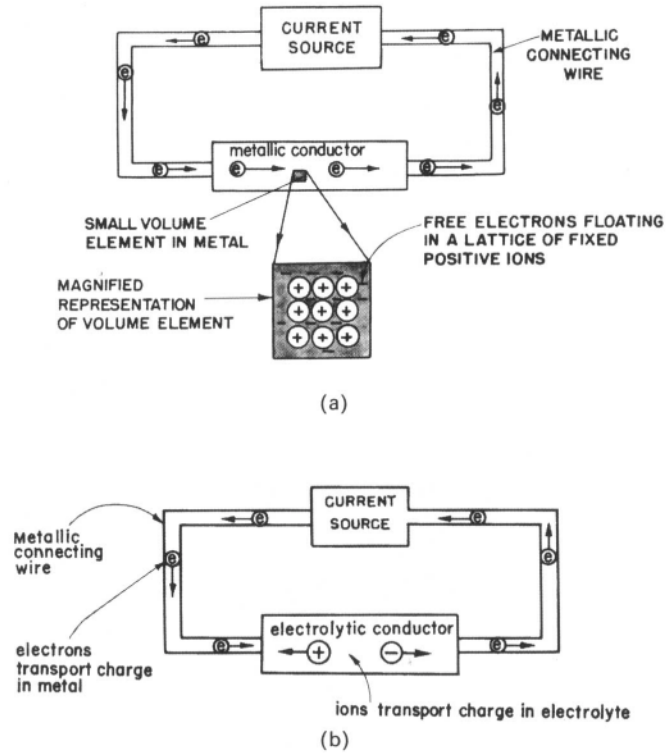


**Fig. 4.48.** Comparison of electric circuits that consist of (a) a metallic conductor only and (b) an electrolytic conductor as well as a metallic one.

ions carry the charge in the electrolytic solution [Fig. 4.48(b)]. Obviously, one can maintain a steady flow of charge (current) in the entire circuit only if there is a change of charge carrier at the electrode–electrolyte interface. In other words, for a current to flow in the circuit, ions have to hand over or take electrons from the electrodes.

Such electron transfers between ions and electrodes result in chemical changes (changes in the valence or oxidation state of the ions), i.e., in electrodic reactions. When ions receive electrons from the electrode, they are said to be "electronated," or *to undergo reduction*; when ions donate electrons to the electrodes, they are said to be "deelectronated," or *to undergo oxidation.*

The occurrence of a reaction at each electrode is tantamount to removal of equal amounts of positive and negative charge from the solution. Hence, when electron-transfer reactions occur at the electrodes, ionic drift does *not* lead to segregation of charges and the building up of an electroneutrality field (opposite to the applied field). Thus, the flow of charge can continue; i.e., the solution conducts. It is an ionic conductor.

### 4.3.5. Quantitative Link between Electron Flow in the Electrodes and Ion Flow in the Electrolyte: Faraday's Law

Charge transfer is the essence of an electrodic reaction. It constitutes the bridge between the current $I_e$ of electrons in the electrode part of the electrical circuit and the current $I_i$ of ions in the electrolytic part of the circuit (Fig 4.49). When a steady-state

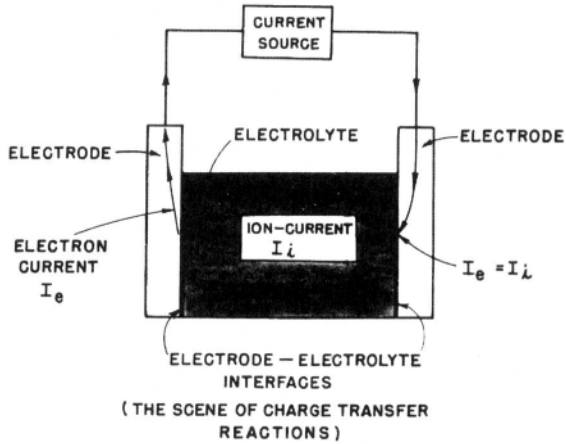


**Fig. 4.49.** Diagram for the derivation of Faraday's laws. The electron current $I_e$ in the metallic part of the circuit must be equal to the ion current $I_i$ in the electrolytic part of the circuit.

current is passing through the circuit, there must be a continuity in the currents at the electrode–electrolyte interfaces, i.e.,

$$I_e = I_i \tag{4.123}$$

(This is in fact an example of Kirchhoff's law, which says that the *algebraic* sum of the currents at any junction must be zero.) Further, if one multiplies both sides of Eq. (4.123) by the time $t$, one obtains

$$I_e t = I_i t \tag{4.124}$$

which indicates[19] that the quantity $Q_e$ of electricity carried by the electrons is equal to that carried by the ions

$$Q_e = Q_i \tag{4.125}$$

Let the quantity of electricity due to electron flow be the charge borne by an Avogadro number of electrons, i.e., $Q_e = N_A e_0 = F$. If the charge on each ion participating in the electrodic reaction is $z_i e_0$, it is easily seen that the number of ions required to preserve equality of currents [Eq. (4.123)] and equality of charge transported across the interface in time $t$ [Eq. (4.125)] is

$$\frac{Q_e}{z_i e_0} = \frac{N_A e_0}{z_i e_0} = \frac{N_A}{z_i} \text{ ions} = \frac{1}{z_i} \text{ mole of ions}$$

$$= 1 \text{ g-eq} \tag{4.126}$$

Thus, the requirement of steady-state continuity of current at the interface leads to the following law: The passage of 1 faraday (F) of charge results in the electrodic reaction of one equivalent ($1/z_i$ moles) of ions, each of charge $z_i e_0$. This is Faraday's law.[20] Conversely, if $1/z_i$ moles of ions undergo charge transfer, then 1 F of electricity passes through the circuit, or $zF$ faradays per mole of ions transformed.

### 4.3.6. The Proportionality Constant Relating Electric Field and Current Density: Specific Conductivity

In the case of small fields, the steady-state flux of ions can be considered proportional to the driving force of an electric field (see Section 4.3.2), i.e.,

---

[19]The product of the current and time is the quantity of electricity.

[20]Alternatively, Faraday's law states that if a current of $I$ amp passes for a time $t$ s, then $It/zF$ moles of reactants in the electronic reaction are produced or consumed.

$$J = BX \tag{4.122}$$

The quantity $J$ is the number of moles of ions crossing a unit area per second. When $J$ is multiplied by the charge borne by 1 mole of ions $zF$, one obtains the current density $i$, or *charge flux*, i.e., the quantity of charge crossing a unit area per second. Because $i$ has direction, it will be written as a vector quantity, $\vec{j}$.

$$\vec{j} = JzF = zFBX \tag{4.127}$$

The constant $zFB$ can be set equal to a new constant $\sigma$, which is known as the *specific conductivity* (Table 4.7). The relation between the current density $i$ and the electric field $X$ is therefore

$$X = \frac{1}{\sigma} j \tag{4.128}$$

The electric field is very simply related (Fig. 4.50) to the potential difference across the electrolyte, $\psi'_I - \psi'_{II}$ [see Eq. (4.119)],

$$X = \frac{\Delta\psi}{l} \tag{4.129}$$

where $l$ is the distance across the electrolyte. Furthermore, the total current $I$ is equal to the area $A$ of the electrodes times the current density $i$

$$I = jA \tag{4.130}$$

Substituting these relations [Eqs. (4.129) and (4.130)] in the field-current-density relation [Eq. (4.128)], one has

**TABLE 4.7**

**Representative Values of Specific Conductivity**

| Substance | Type of Conductor | Specific Conductivity ($S\ cm^{-1}$) | $T$ (K) |
|---|---|---|---|
| Copper | Metallic | $5.8 \times 10^{5}$ | 293 |
| Lead | Metallic | $4.9 \times 10^{5}$ | 273 |
| Iron | Metallic | $1.1 \times 10^{5}$ | 273 |
| 4 $M$ $H_2SO_4$ | Electrolytic | $7.5 \times 10^{-1}$ | 291 |
| 0.1 $M$ KCl | Electrolytic | $1.3 \times 10^{-2}$ | 298 |
| Xylene | Nonelectrolyte | $1 \times 10^{-19}$ | 298 |
| Water | Nonelectrolyte | $4 \times 10^{-8}$ | 291 |

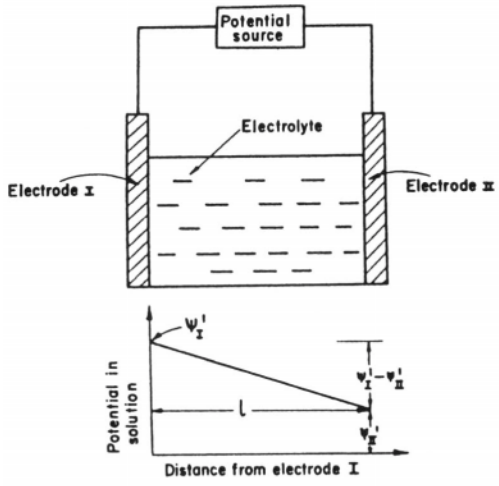


**Fig. 4.50.** Schematic representation of the variation of the potential in the electrolytic conductor of length *l*.

$$\frac{\Delta\psi}{l} = \frac{1}{\sigma}\frac{I}{A}$$

or

$$\Delta\psi = \frac{l}{\sigma A} I \tag{4.131}$$

The constants $\sigma$, $l$, and $A$ determine the resistance $R$ of the solution

$$R = \frac{l}{\sigma A} \tag{4.132}$$

and therefore one has the equation

$$\Delta\psi = RI \tag{4.133}$$

which reexpresses in the conventional Ohm's law form the assumption Eq. of (4.122) concerning flux and driving force.

Thus, an electrolytic conductor obeys Ohm's law for all except very high fields and, *under steady-state conditions*, it can be represented in an electrical circuit (in which there is only a dc source) by a resistor. (An analogue must obey the same equation as the system it represents or simulates.)

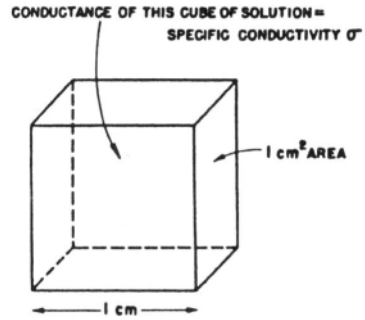


**Fig. 4.51.** Diagram to illustrate the meaning of the specific conductivity of an electrolyte.

As in the case of a resistor, the dc resistance of an electrolytic cell increases with the length of the conductor (distance between the electrodes) and decreases with the area [*cf*. Eq. (4.132)]. It can also be seen by rearranging this equation into the form

$$\sigma = \frac{1}{R}\frac{l}{A} \tag{4.134}$$

that the specific conductivity $\sigma$ is the conductance $1/R$ of a cube of electrolytic solution 1 cm long and $1\ \text{cm}^2$ in area (Fig. 4.51).

### 4.3.7. Molar Conductivity and Equivalent Conductivity

In the case of metallic conductors, once the specific conductivity is defined, the macroscopic description of the conductor is complete. In the case of electrolytic

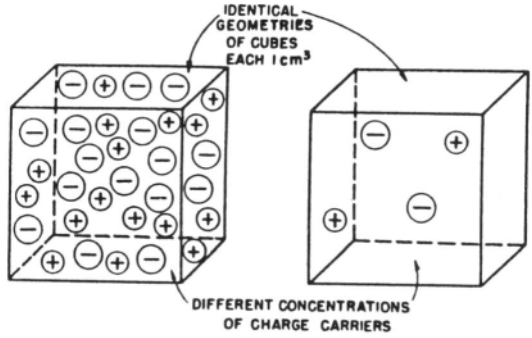


**Fig. 4.52.** A schematic explanation of the variation of the specific conductivity with electrolyte concentration.

**TABLE 4.8**
**Specific Conductivities of KCl Solutions**

| KCl (g $kg^{-1}$ of solution) | Specific Conductivity (S $cm^{-1}$) | | |
|---|---|---|---|
| | 273 K | 281 K | 298 K |
| 1.0 | 0.065144 | 0.097790 | 0.11187 |
| 0.1 | 0.0071344 | 0.0111612 | 0.012896 |
| 0.01 | 0.00077326 | 0.00121992 | 0.001427 |

conductors, further characterization is imperative because not only can the concentration of charge carriers vary but also the charge per charge carrier.

Thus, even though two electrolytic conductors have the same geometry, they need not necessarily have the same specific conductivity (Fig. 4.52 and Table 4.8); the number of charge carriers in that normalized geometry may be different, in which case their fluxes under an applied electric field will be different. Since *the specific conductivity of an electrolytic solution varies as the concentration*, one can write

$$\sigma = f(c) \tag{4.135}$$

where $c$ is the concentration of the solution in gram-moles of solute dissolved in $1\ cm^3$ of solution.[21] The specific conductivities of two solutions can be compared only if they contain the same concentration of ions. The conclusion is that in order to compare the conductances of electrolytic conductors, one has to normalize (set the variable quantities equal to unity) not only the *geometry* but also the *concentration* of ions.

The normalization of the geometry (taking electrodes of $1\ cm^2$ in area and 1 cm apart) defines the specific conductivity; the additional normalization of the concentration (taking 1 mole of ions) defines a new quantity, the molar conductivity (Table 4.9),

$$\Lambda_m = \frac{\sigma}{c} = \sigma V \tag{4.136}$$

where $V$ is the volume of solution containing 1 g-mole of solute (Fig. 4.53). Defined thus, it can be seen that the molar conductivity is the specific conductivity of a solution times the volume of that solution in which is dissolved 1 g-mole of solute; the molar conductivity is a kind of conductivity per particle.

[21] As in the case of diffusion fluxes, the concentrations used in the definition of conduction currents (or fluxes) and conductances are not in the usual moles per liter but in moles per cubic centimeter.

**TABLE 4.9**
**Molar Conductivities of Electrolytes**

| Electrolyte | Molar Conductivity ($S\ cm^2\ mol^{-1}$ at 0.01 mol $dm^{-3}$) |
|---|---|
| KCl | 141.3 |
| NaCl | 118.5 |
| $MgCl_2$ | 229.2 |
| $Na_2SO_4$ | 224.8 |

One can usefully compare the molar conductivities of two electrolytic solutions only if the charges borne by the charge carriers in the two solutions are the same. If there are singly charged ions in one electrolyte (e.g., NaCl) and doubly charged ions in the other (e.g., $CuSO_4$), then the two solutions will contain different amounts of charge even though the same quantity of the two electrolytes is dissolved. In such a case, the specific conductivities of the two solutions can be compared only if they contain equivalent amounts of charge. This can be arranged by taking 1 mole of charge in each case, i.e., 1 mole of ions divided by $z$, or 1 g-eq of the substance. Thus, the *equivalent conductivity* $\Lambda$ of a solution is the specific conductivity of a solution times the volume $V$ of that solution containing 1 g-eq of solute dissolved in it (Fig. 4.54 and Table 4.10). Hence, the equivalent conductivity is given by[22]

$$\Lambda = \frac{\sigma}{cz} \tag{4.137}$$

where $cz$ is the number of gram-equivalents per cubic centimeter of solution (see Fig. 4.55 for units of these quantities).

There is a simple relation between the molar and equivalent conductivities. It is [*cf.* Eqs. (4.136) and (4.137)]

$$\Lambda_m = z\Lambda \tag{4.138}$$

The equivalent conductivity $\Lambda$ is in the region (±25%) of 100 S $cm^2\ mol^{-1}\ eq^{-1}$ for most dilute electrolytes of 1:1 salts.

## 4.3.8. Equivalent Conductivity Varies with Concentration

At first sight, the title of this section may appear surprising. The equivalent conductivity has been defined by normalizing the geometry of the system *and* the

[22]Since $1/z$ mole of ions is 1 g-eq, $c$ moles is $cz$ g-eq.

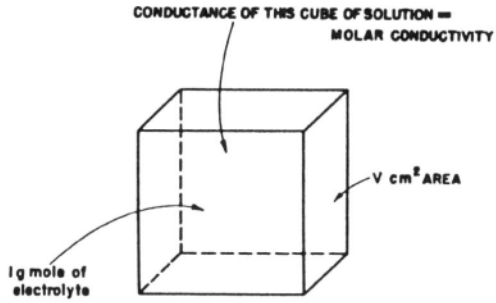


**Fig. 4.53.** Diagram to illustrate the meaning of the molar conductivity of an electrolyte.

charge of the ions; why then should it vary with concentration? Experiment, however, gives an unexpected answer. The equivalent conductivity varies significantly with the concentration of ions (Table 4.11). The direction of the variation may also surprise some, for the equivalent conductivity *increases* as the ionic concentration decreases (Fig. 4.56).

It would be awkward to have to refer to the concentration every time one wished to state the value of the equivalent conductivity of an electrolyte. One should be able to define some reference value for the equivalent conductivity. Here, the facts of the experimental variation of equivalent conductivity with concentration come to one's aid; as the electrolytic solution is made more dilute, the equivalent conductivity approaches a limiting value (Fig. 4.57). This limiting value should form an excellent basis for comparing the conducting powers of different electrolytes, for it is the only value in which the effects of ionic concentration are removed. The limiting value will be called the *equivalent conductivity at infinite dilution*, designated by the symbol $\Lambda^0$ (Table 4.12).

**TABLE 4.10**

**Equivalent Conductivities of True Electrolytes in Dilute Aqueous Solutions at 298 K**

| Electrolyte | Equivalent Conductivity ($S\ cm^2\ mol^{-1}\ eq^{-1}$ at 0.005 g-eq $dm^{-3}$) |
|---|---|
| KCl | 143.55 |
| NaOH | 240.00 |
| $AgNO_3$ | 127.20 |
| $\frac{1}{2}\ BaCl_2$ | 128.02 |
| $\frac{1}{2}\ NiSO_4$ | 93.20 |

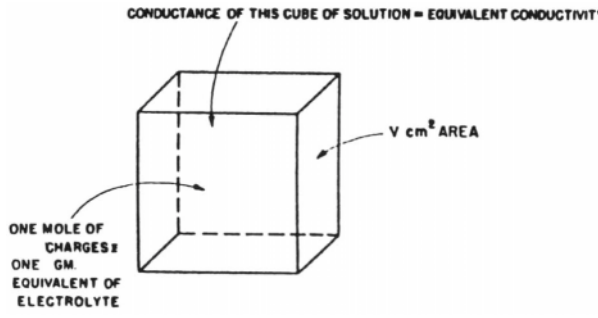


**Fig. 4.54.** Diagram to illustrate the meaning of the equivalent conductivity of an electrolyte.

It may be argued that if at infinite dilution there are no ions of the solute, how can the solution conduct? The procedure for determining the equivalent conductivity of an electrolyte at infinite dilution will clarify this problem. One takes solutions of a substance of various concentrations, determines the $\sigma$, and then normalizes each to the equivalent conductivity of particular solutions. If these values of $\Lambda$ are then plotted against the logarithms of the concentration and this $\Lambda$ versus log $c$ curve is extrapo-

| | | | |
|---|---|---|---|
| G | CONDUCTANCE | $\frac{1}{R}$ | S or $\Omega^{-1}$ |
| $\rho$ | RESISTIVITY | $\frac{RA}{\ell}$ | $S^{-1}$ cm |
| $\sigma$ | SPECIFIC CONDUCTIVITY | $\frac{\ell}{RA}$ | S $cm^{-1}$ |
| $\Lambda_m$ | MOLAR CONDUCTIVITY | $\frac{\sigma}{C}$ | S $cm^2$ $mol^{-1}$ |
| $\Lambda$ | EQUIVALENT CONDUCTIVITY | $\frac{\sigma}{CZ}$ | S $cm^2$ $mol^{-1}$ $eq^{-1}$ |

**Fig. 4.55.** Definitions and units of the conductivity of electrolyte solutions.

**TABLE 4.11**

**Equivalent Conductivity Varies with Concentration**

| Concentration (mol $dm^{-3}$) (KCl solutions) | $\Lambda$ (S $cm^2$ $mol^{-1}$ $eq^{-1}$) |
|---|---|
| 0.001 | 146.9 |
| 0.005 | 143.5 |
| 0.01 | 141.2 |
| 0.02 | 138.2 |
| 0.05 | 133.3 |
| 0.10 | 128.9 |

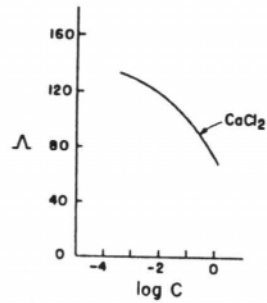


**Fig. 4.56.** The observed variation of the equivalent conductivity of $CaCl_2$ with concentration.

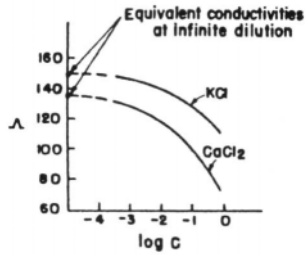


**Fig. 4.57.** The equivalent conductivity of an electrolyte at infinite dilution is obtained by extrapolating the $\Lambda$ versus log $c$ curve to zero concentration.

**TABLE 4.12**
**Equivalent Conductivities at Infinite Dilution of Electrolytes in Aqueous Solution at 298 K**

| Electrolyte | $\Lambda^0$ (S cm$^2$ mol$^{-1}$ eq$^{-1}$) |
|---|---|
| HCl | 426.0 |
| NaOH | 247.9 |
| NaCl | 126.4 |
| KCl | 149.8 |
| $K_4Fe(CN)_6$ | 183.9 |
| $CaCl_2$ | 135.7 |

lated, it approaches a limiting value (Fig. 4.57). It is this extrapolated value at zero concentration that is known as the equivalent conductivity at infinite dilution.

Anticipating the atomistic treatment of conduction that follows, it may be mentioned that at very low ionic concentrations, the ions are too far apart to exert appreciable interionic forces on each other. Only under these conditions does one obtain the pristine version of equivalent conductivity, i.e., values unperturbed by ion–ion interactions, which have been shown in Chapter 3 to be concentration dependent. The state of infinite dilution therefore is not only the reference state for the study of equilibrium properties (Section 3.3), it is also the reference state for the study of the nonequilibrium (irreversible) process, which is called *ionic conduction*, or *migration* (see Section 4.1).

### 4.3.9. How Equivalent Conductivity Changes with Concentration: Kohlrausch's Law

The experimental relationship between equivalent conductivity and the concentration of an electrolytic solution is found to be best brought out by plotting $\Lambda$ against $c^{1/2}$. When this is done (Fig. 4.58), it can be seen that up to concentrations of about 0.01 $N$ there is a linear relationship between $\Lambda$ and $c^{1/2}$; thus,

$$\Lambda = \Lambda^0 - A c^{1/2} \tag{4.139}$$

where the intercept is the equivalent conductivity at infinite dilution $\Lambda^0$ and the slope of the straight line is a positive constant $A$.

This empirical relationship between the equivalent conductivity and the square root of concentration is a law named after Kohlrausch. His extremely careful measurements of the conductance of electrolytic solutions can be considered to have played a leading role in the initiation of ionics, the physical chemistry of ionic solutions.

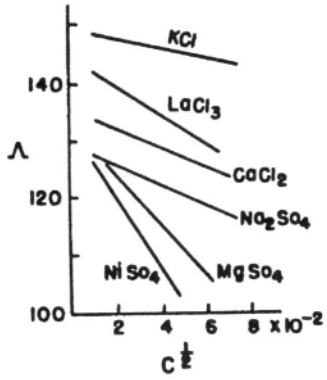


**Fig. 4.58.** The experimental basis for Kohlrausch's law: $\Lambda$ versus $c^{1/2}$ plots consist of straight lines.

However, Kohlrausch's law [Eq. (4.139)] had to remain nearly 40 years without a theoretical basis.

The justification of Kohlrausch's law on theoretical grounds cannot be obtained within the framework of a macroscopic description of conduction. It requires an intimate view of ions in motion. A clue to the type of theory required emerges from the empirical findings by Kohlrausch: (1) the $c^{1/2}$ dependence and (2) the intercepts $\Lambda^0$ and slopes $A$ of the $\Lambda$ versus $c^{1/2}$ curves depend not so much on the particular electrolyte (whether it is KCl or NaCl) as on the type of electrolyte (whether it is a 1:1 or 2:2 electrolyte) (Fig. 4.59). All this is reminiscent of the dependence of the activity coefficient on $c^{1/2}$ (Chapter 3), to explain which the subtleties of ion–ion interactions had to be explored. Such interactions between positive and negative ions would determine to what extent they would influence each other when they move, and this would in turn bring about a fall in conductivity.

Kohlrausch's law will therefore be left now with only the sanction of experiment. Its incorporation into a theoretical scheme will be postponed until the section on the atomistic view of conduction is reached (see Section 4.6.12).

### 4.3.10. Vectorial Character of Current: Kohlrausch's Law of the Independent Migration of Ions

The driving force for ionic drift, i.e., the electric field $X$, not only has a particular magnitude, it also acts in a particular direction. It is a *vector*. Since the ionic current density $j$, i.e., the flow of electric charge, is proportional to the electric field operating in a solution [Eq. (4.128)],

$$j = \sigma X \qquad (4.128)$$

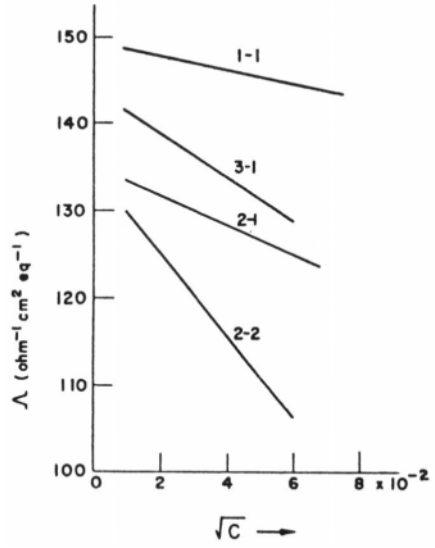


**Fig. 4.59.** The experimental $\Lambda$ versus $c^{1/2}$ plots depend largely on the type of electrolyte.

the ionic current density must also be a vector. Vectorial quantities are often designated by arrows placed over the quantities (unless their directed character is obvious) or are indicated by bold type. Hence, Eq. (4.128) can be written

$$\vec{j} = \sigma \vec{X} \tag{4.140}$$

How is this current density constituted? What are its components? What is the structure of this ionic current density?

The imposition of an electric field on the electrolyte (Fig. 4.60) makes the positive ions drift toward the negative electrode and the negative ions drift in the opposite direction. The flux of positive ions $\vec{J}_+$ gives rise to a positive-ion current density $\vec{j}_+$, and the flux of negative ions in the opposite direction $*_-$ results in a negative-ion current density $\vec{j}_-$. By convention, the direction of current flow is taken to be either the direction in which positive charge flows or the direction opposite to that in which the negative charge flows. Hence, the positive-ion flux $\vec{J}_+$ corresponds to a current toward the negative electrode $\vec{j}_+$ and the negative-ion flux $*_-$ also corresponds to a current $\vec{j}_-$ *in the same direction* as that due to the positive ions.

It can be concluded therefore that the total current density $\vec{j}$ is made up of two contributions, one due to a flux of positive ions and the other due to a flux of negative ions. Furthermore, assuming for the moment that the drift of positive ions toward the

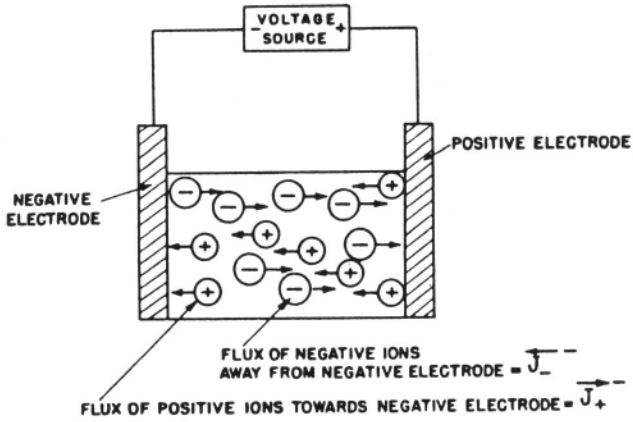


**Fig. 4.60.** Schematic representation of the direction of the drifts (and fluxes) of positive and negative ions acted on by an electric field.

negative electrode does not interfere with the drift of negative ions in the opposite direction, it follows that the component current densities are additive, i.e.,

$$\vec{j} = \vec{j}_+ + \vec{j}_- \tag{4.141}$$

Do ions migrate independently? Is the drift of the positive ions in one direction uninfluenced by the drift of the negative ions in the opposite direction? This is so if, and only if, the force fields of the ions do not overlap significantly, i.e., if there is negligible interaction or coupling between the ions. Coulombic ion–ion interactions usually establish such coupling. The only conditions under which the absence of ion–ion interactions can be assumed occur when the ions are infinitely far apart. Strictly speaking, therefore, ions migrate independently only at infinite dilution. Under these conditions, one can proceed from Eq. (4.141) to write

$$\frac{\vec{j}}{\vec{X}} = \frac{\vec{j}_+}{\vec{X}} + \frac{\vec{j}_-}{\vec{X}} \tag{4.142}$$

or [from Eq. (4.128)],

$$\sigma = \sigma_+ + \sigma_- \tag{4.143}$$

whence

$$\Lambda^0 = \lambda_+^0 + \lambda_-^0 \tag{4.144}$$

**TABLE 4.13**
**Equivalent Conductances (S $cm^2$ $mol^{-1}$ $eq^{-1}$) of Individual Ions at Infinite Dilution at 298 K**

| Cation | $\lambda_+^0$ | Anion | $\lambda_-^0$ |
|---|---|---|---|
| $H^+$ | 349.82 | $OH^-$ | 198.5 |
| $K^+$ | 73.52 | $Br^-$ | 78.4 |
| $Na^+$ | 50.11 | $I^-$ | 76.8 |
| $Li^+$ | 38.69 | $Cl^-$ | 76.34 |
| $\frac{1}{2}Ba^{2+}$ | 63.64 | $CH_3CO_2^-$ | 40.9 |

This is Kohlrausch's law of the independent migration of ions: The equivalent conductivity (at infinite dilution) of an electrolytic solution is the sum of the equivalent conductivities (at infinite dilution) of the ions constituting the electrolyte (Table 4.13).

At appreciable concentrations, the ions can be regarded as coupled or interacting with each other (see the ion-atmosphere model of Chapter 3). This results in the drift of positive ions toward the negative electrode, hindering the drift of negative ions toward the positive electrode; i.e., the interionic interaction results in the positive ions' equivalent conductivity reducing the magnitude of the negative ions' equivalent conductivity to below the infinite dilution value, and vice versa. To make quantitative estimates of these effects, however, one must calculate the influence of ionic-cloud effects on the phenomenon of conduction, a task that will be taken up further on.

## 4.4. A SIMPLE ATOMISTIC PICTURE OF IONIC MIGRATION

### 4.4.1. Ionic Movements under the Influence of an Applied Electric Field

In seeking an atomic view of the process of conduction, one approach is to begin with the picture of ionic movements as described in the treatment of diffusion (Section 4.2.4) and then to consider how these movements are perturbed by an electric field. In the treatment of ionic movements, it was stated that the ions in solution perform a random walk in which all possible directions are equally likely for any particular step. The analysis of such a random walk indicated that the mean displacement of ions is zero (Section 4.2.4), diffusion being the result of the statistical bias in the movement of ions, due to inequalities in their numbers in different regions.

When, however, the ions are situated in an electric field, their movements are affected by the fact that they are charged. Hence, the imposition of an electric field singles out one direction in space (the direction parallel to the field) for preferential ionic movement. Positively charged particles will prefer to move toward the negative electrode, and negatively charged particles, in the opposite direction. The walk is no longer quite random. The ions drift.

Another way of looking at ionic drift is to consider the fate of any particular ion under the field. The electric force field would impart to it an acceleration according to Newton's second law. Were the ion completely isolated (e.g., in vacuum), it would accelerate indefinitely until it collided with the electrode. In an electrolytic solution, however, the ion very soon collides with some other ion or solvent molecule that crosses its path. This collision introduces a discontinuity in its speed and direction. The motion of the ion is not smooth; it is as if the medium offers resistance to the motion of the ion. Thus, the ion stops and starts and zigzags. However, the applied electric field imparts to the ion a direction (that of the oppositely charged electrode), and the ion gradually works its way, though erratically, in the direction of this electrode. The ion drifts in a preferred direction.

### 4.4.2. Average Value of the Drift Velocity

Any particular ion starts off after a collision with a velocity that may be in any direction; this is the randomness in its walk. The initial velocity can be ignored precisely because it can take place in any direction and therefore does not contribute to the drift (preferred motion) of the ion. But the ion is all the time under the influence of the applied-force field.[23] This force imparts a component to the velocity of the ion, an extra velocity component in the same direction as the force vector $\vec{F}$. It is this additional velocity component due to the force $\vec{F}$ that is called the *drift velocity* $v_d$. What is its average value?

From Newton's second law, it is known that the force divided by the mass of the particle is equal to the acceleration. Thus,

$$\frac{\vec{F}}{m} = \frac{dv}{dt} \tag{4.145}$$

Now the time between collisions is a random quantity. Sometimes the collisions may occur in rapid succession; at others, there may be fairly long intervals. It is possible, however, to talk of a mean time between collisions, $\tau$. In Section 4.2.5, it was shown that the number of collisions (steps) is proportional to the time. If $N$ collisions occur in a time $t$, then the average time between collisions is $t/N$. Hence,

$$\tau = \frac{t}{N} \tag{4.146}$$

The average value of that component of the velocity of an ion picked up from the externally applied force is the product of the acceleration due to this force and the average time between collisions. Hence, the drift velocity $v_d$ is given by

[23]The argument is developed in general for any force, not necessarily an electric force.

$$v_d = \frac{dv}{dt}\tau$$

$$= \frac{\vec{F}}{m}\tau \qquad (4.147)$$

*This is an important relation.* It opens up many vistas. For example, through the mean time $\tau$, one can relate the drift velocity to the details of ionic jumps between sites, as was done in the case of diffusion (Section 4.2.15).

Furthermore, the relation (4.147) shows that the drift velocity is proportional to the driving force of the electric field. The flux of ions will be shown (Section 4.4.4) to be related to the drift velocity[24] in the following way:

$$\text{Flux} = \text{Concentration of ions} \times \text{drift velocity} \qquad (4.148)$$

Thus, if the $\vec{F}$ in Eq. (4.147) is the electric force that stimulates conduction, then this equation is the molecular basis of the fundamental relation used in the macroscopic view of conduction [see Eq. (4.122)], i.e.,

$$\text{flux} \propto \text{electric field}$$

The derivation of the basic relation (4.147) reveals the conditions under which the proportionality between drift velocity (or flux) and electric field breaks down. It is essential to the derivation that in a collision, an ion does not preserve any part of its extra velocity component arising from the force field. If it did, then the actual drift velocity would be greater than that calculated by Eq. (4.147) because there would be a cumulative carryover of the extra velocity from collision to collision. In other words, every collision must wipe out all traces of the force-derived extra velocity, and the ion must start afresh to acquire the additional velocity. This condition can be satisfied only if the drift velocity, and therefore the field, is small (see the autocorrelation function, Section 4.2.19).

### 4.4.3. Mobility of Ions

It has been shown that when random-walking ions are subjected to a directed force $\vec{F}$, they acquire a nonrandom, directed component of velocity—the drift velocity $v_d$. This drift velocity is in the direction of the force $\vec{F}$ and is proportional to it

$$v_d = \frac{\tau}{m}\vec{F} \qquad (4.147)$$

[24]The dimensions of flux are moles per square centimeter per second, and they are equal to the product of the dimensions of concentration expressed in moles per cubic centimeter and velocity expressed in centimeters per second.

Since the proportionality constant $\tau/m$ is of considerable importance in discussions of ionic transport, it is useful to refer to it with a special name. It is called *the absolute mobility* because it is an index of how mobile the ions are. The absolute mobility, designated by the symbol $\bar{u}_{abs}$, is a measure of the drift velocity $v_d$ acquired by an ionic species when it is subjected to a force $\vec{F}$, i.e.,

$$\bar{u}_{abs} = \frac{\tau}{m} = \frac{v_d}{\vec{F}} \tag{4.149}$$

which means that the absolute mobility is the drift velocity developed under unit applied force ($\vec{F} = 1$ dyne) and the units in which it is available in the literature are centimeters per second per dyne.

For example, one might have an electric field $X$ of $0.05\ \text{V cm}^{-1}$ in the electrolyte solution and observe a drift velocity of $2 \times 10^{-5}\ \text{cm s}^{-1}$. The electric force $\vec{F}$ operating on the ion is equal to the electric force per unit charge, i.e., the electric field $X$, times the charge $z_i e_0$ on each ion

$$\begin{aligned} \vec{F} &= z_i e_0 X \\ &= 1.60 \times 10^{-19} \times 0.05\ 10^2 \times 10^5 \\ &= 8 \times 10^{-14}\ \text{dynes} \end{aligned} \tag{4.150}$$

($10^5$ dynes = 1 Newton) for univalent ions. Hence, the absolute mobility is

$$\begin{aligned} \bar{u}_{abs} &= \frac{2 \times 10^{-5}}{8 \times 10^{-14}} \\ &= 2.5 \times 10^8\ \text{cm s}^{-1}\ \text{dyn}^{-1} \end{aligned}$$

In electrochemical literature, however, mobilities of ions are not usually expressed in the absolute form defined in Eq. (4.149). Instead, they are more normally recorded as the drift velocities in *unit electric field* ($1\ \text{V cm}^{-1}$) and will be referred to here as *conventional (electrochemical) mobilities* with the symbol $u_{conv}$.

The relation between the absolute and conventional mobilities follows from Eq. (4.149)

$$(V_{Drift})_{1\ \text{volt cm}^{-1}} = u_{conv} = \bar{u}_{ABS}\, z_i e_0 x \tag{4.151}$$

$$x = 1\ \text{volt}$$

i.e.,

$$u_{conv} = \bar{u}_{abs} z_i e_0 \tag{4.152}$$

Thus, the conventional and absolute mobilities are proportional to each other, the proportionality constant being an integral multiple $z_i$ of the electronic charge. In the example cited earlier,

$$u_{conv} = \frac{2 \times 10^{-5}}{0.05}$$

$$= 4 \times 10^{-4} \text{ cm}^2 \text{ V}^{-1} \text{ s}^{-1}$$

Though the two types of mobilities are closely related, it must be stressed that the concept of absolute mobility is more general because it can be used for *any* force that determines the drift velocity of ions and not only the electric force used in the definition of conventional mobilities.

### 4.4.4. Current Density Associated with the Directed Movement of Ions in Solution, in Terms of Ionic Drift Velocities

It is the aim now to show how the concept of drift velocity can be used to obtain an expression for the ionic current density flowing through an electrolyte in response to an externally applied electric field. Consider a transit plane of unit area normal to the direction of drift (Fig. 4.61). Both the positive and the negative ions will drift across this plane. Consider the positive ions first, and let their drift velocity be $(v_d)_+$ or simply $v_+$. Then, in 1 s, all positive ions within a distance $v_+$ cm of the transit plane will cross it. The flux $J_+$ of positive ions (i.e., the number of moles of these ions arriving in 1 second at the plane of unit area) is equal to the number of moles of positive ions in a volume of 1 $\text{cm}^2$ in area and $v$ cm in length (with $t$ = 1 s). Hence, $J_+$ is equal to the volume $v_+$ in cubic centimeters times the concentration $c_+$ expressed in moles per cubic centimeter

$$J_+ = c_+ v_+ \tag{4.153}$$

The flow of charge across the plane due to this flux of positive ions (i.e., the current density $\vec{j}_+$) is obtained by multiplying the flux $J_+$ by the charge $z_+F$ borne by 1 mole of ions

$$j_+ = z_+ F c_+ v_+ \tag{4.154}$$

This, however, is only the contribution of the positive ions. Other ionic species will make their own contributions of current density. In general, therefore, the current density due to the $i$th species will be

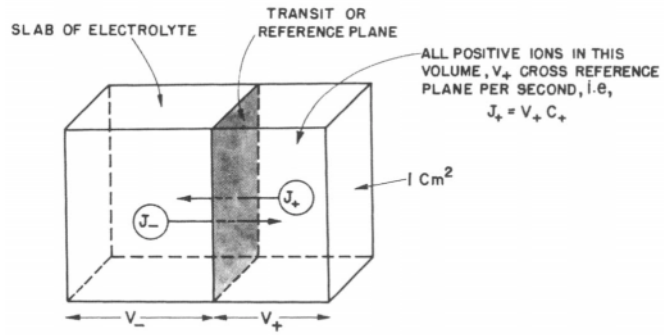


**Fig. 4.61.** Diagram for the derivation of a relation between the current density and the drift velocity.

$$\vec{j}_i = z_i F c_i v_i \tag{4.155}$$

The total current density due to the contribution of all the ionic species will therefore be

$$\vec{j} = \Sigma_i \vec{j}_i \tag{4.156}$$

$$= \Sigma_i z_i F c_i v_i \tag{4.157}$$

If a $z$:$z$-valent electrolyte is taken, then $z_+ = z_- = z$ and $c = c_+ = c_-$ and one has

$$\vec{j} = zFc(v_+ + v_-) \tag{4.158}$$

By recalling that the ionic drift velocities are related through the force operating on the ions to the ionic mobilities [Eq. (4.151)], it will be realized that Eq. (4.157) is the basic expression from which may be derived the expressions for conductance, equivalent conductivity, specific conductivity, etc.

### 4.4.5. Specific and Equivalent Conductivities in Terms of Ionic Mobilities

Let the fundamental expression for the drift velocity of ions [Eq. (4.151)] be substituted in Eq. (4.157) for current density. One obtains

$$\vec{j} = \Sigma z_i F c_i (u_{\text{conv}})_i X \tag{4.159}$$

or, from Eq. (4.128)

$$\sigma = \frac{\vec{j}}{X} = \Sigma z_i F c_i (u_{\text{conv}})_i \tag{4.160}$$

which reduces in the special case of a $z{:}z$-valent electrolyte to

$$\sigma = zFc[(u_{\text{conv}})_- + (u_{\text{conv}})_-] \tag{4.161}$$

Several conclusions follow from this atomistic expression for specific conductivity. First, it is obvious from this equation that the specific conductivity $\sigma$ of an electrolyte cannot be a concentration-independent constant (as it is in the case of metals). It will vary because the number of moles of ions per unit volume $c$ can be varied in an electrolytic solution.

Second, the specific conductivity can easily be related to the molar $\Lambda_m$ and equivalent $\Lambda$ conductivities. Take the case of a $z{:}z$-valent electrolyte. With Eqs. (4.161), (4.136), and (4.138), it is found that

$$\Lambda_m = \frac{\sigma}{c}$$

$$= zF[(u_{\text{conv}})_+ + (u_{\text{conv}})_-] \tag{4.162}$$

and

$$\Lambda = \frac{\Lambda_m}{z}$$

$$= F[(u_{\text{conv}})_+ + (u_{conv})_-] \tag{4.163}$$

What does Eq. (4.163) reveal? It shows that the equivalent conductivity will be a constant independent of concentration only if the electrical mobility does not vary with concentration. It will be seen, however, that ion–ion interactions (which have been shown in Section 3.3.8 to depend on concentration) prevent the electrical mobility from being a constant. Hence, the equivalent conductivity must be a function of concentration.

### 4.4.6. The Einstein Relation between the Absolute Mobility and the Diffusion Coefficient

The process of diffusion results from the random walk of ions; the process of migration (i.e., conduction) results from the drift velocity acquired by ions when they experience a force. The drift of ions does not obviate their random walk; in fact, it is superimposed on their random walk. Hence, the drift and the random walk must be

intimately linked. Einstein† realized this and deduced a vital relation between the absolute mobility $\bar{u}_{abs}$, which is a quantitative characteristic of the drift, and the diffusion coefficient $D$, which is a quantitative characteristic of the random walk.

Both diffusion and conduction are nonequilibrium (irreversible) processes and are therefore not amenable to the methods of equilibrium thermodynamics or equilibrium statistical mechanics. In these latter disciplines, the concepts of time and change are absent. It is possible, however, to imagine a situation where the two processes oppose and balance each other and a "pseudoequilibrium" obtains. This is done as follows (Fig. 4.62).

Consider a solution of an electrolyte MX to which a certain amount of radioactive $M^+$ ions are added in the form of the salt MX. Further, suppose that the tracer ions are not dispersed uniformly throughout the solution; instead, let there be a concentration gradient of the tagged species so that its diffusion flux $J_D$ is given by Fick's first law

$$J_D = -D\frac{dc}{dx} \tag{4.16}$$

Now let an electric field be applied. Each tagged ion feels the field, and the drift velocity is

$$v_d = \bar{u}_{abs}\vec{F} \tag{4.149}$$

This drift velocity produces a current density given by [*cf.* Eq. (4.154)][25]

$$\vec{j} = z_+ F c v_d \tag{4.164}$$

i.e., a conduction flux $J_c$ that is arrived at by dividing the conduction current density $\vec{j}$ by the charge per mole of ions

---

†Albert Einstein's name remains firmly as that of the most well know scientist in the world, and his name gives rise to the image students have of what it is like to be a scientist. This is because he produced two theories which few other scientists understand but seem to show that, in extreme situations of mass and/or velocity, the world is not what it seems at all. But the fertility of Einstein's thought extended in several other directions and most of them are presented in this chapter. Thus, he produced a theory of Brownian motion (and related it to the net movement in one direction of a diffusing particle); he joined the ancient law of Stokes to diffusion and showed how knowledge of viscosity and the radius of a particle allowed one to know the corresponding diffusion coefficient; and he gave rise to a most unexpected connection of the coefficient of diffusion to the rate of the vectorial drift of ions under an electric field (later taken up by Nernst and connected to conductivity). If Relativity is Einstein's most famous work, that which has been most immediately useful lies in electrochemistry.

Many books have described Einstein's life, particularly after he came to Princeton. He was a stickler for time keeping and rode a bike to the office, 9:00 arrival, riding home again at 1:00 p.m. to work with his assistant in mathematics. But he sometimes caused embarrassment in the social scene—arriving, say, at a formal banquet in dinner jacketed and black tie, but wearing casual grey pants and sandals (no socks). To questions about this, his rejoinder was logical: "The invitation said "Dinner jacket and black tie."

[25]In Eq. (4.154), one will find $v_+$; the reason is that, in Section 4.4.4, the drift velocity of a positive ion, $(v_d)_+$, had been concisely written as $v_+$.

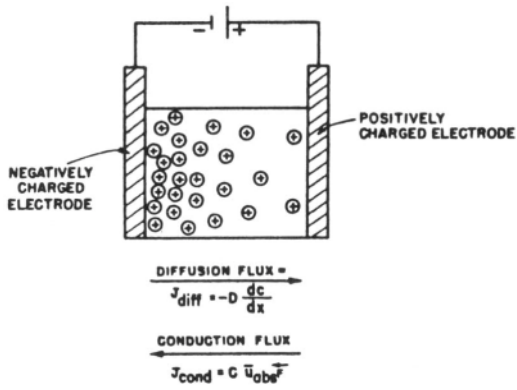


**Fig. 4.62.** An imaginary situation in which the applied field is adjusted so that the conduction flux of tagged ions (the only ones shown in the diagram) is exactly equal and opposite to the diffusion flux.

$$J_c = \frac{\vec{j}}{zF} = cv_d \tag{4.165}$$

By introducing the expression (4.149) for the drift velocity into (4.165), the conduction flux becomes

$$J_c = c\bar{u}_{abs}\vec{F}$$

The applied field is adjusted so that the conduction flux exactly compensates for the diffusion flux. In other words, if the tracer ions (which are positively charged) are diffusing toward the positive electrode, then the magnitude of the applied field is such that the positively charged electrode repels the positive tracer ions to an extent that their net flux is zero. Thus

$$J_D + J_c = 0 \tag{4.166}$$

or

$$-D\frac{dc}{dx} + c\bar{u}_{abs}\vec{F} = 0$$

i.e.,

$$\frac{dc}{dx} = \frac{c\bar{u}_{abs}\vec{F}}{D} \tag{4.167}$$

Under these "balanced" conditions, the situation may be regarded as tantamount to equilibrium because there is no net flux or transport of ions. Hence, the Boltzmann law can be used. The argument is that since the potential varies along the $x$ direction, the concentration of ions at any distance $x$ is given by

$$c = c^0 e^{-U/kT} \tag{4.168}$$

where $U$ is the potential energy of an ion in the applied field and $c^0$ is the concentration in a region where the potential energy is zero. Differentiating this expression, one obtains

$$\frac{dc}{dx} = -c^0 e^{-U/kT} \frac{1}{kT} \frac{dU}{dx}$$

$$= -\frac{c}{kT} \frac{dU}{dx} \tag{4.169}$$

But, by the definition of force,

$$\vec{F} = -\frac{dU}{dx} \tag{4.170}$$

Hence, from Eqs. (4.169) and (4.170), one obtains

$$\frac{dc}{dx} = \frac{c}{kT} \vec{F} \tag{4.171}$$

If, now, Eqs. (4.167) and (4.171) are compared, it is obvious that

$$\frac{\bar{u}_{abs}}{D} = \frac{1}{kT}$$

or

$$D = \bar{u}_{abs} kT \tag{4.172}$$

This is the Einstein relation. It is probably the most important relation in the theory of the movements and drift of ions, atoms, molecules, and other submicroscopic particles. It has been derived here in an atomistic way. It will be recalled that in the phenomenological treatment of the diffusion coefficient (Section 4.2.3), it was shown that

$$BRT = D \tag{4.17}$$

where $B$ was an undetermined phenomenological coefficient. If one combines Eqs. (4.172) and (4.17), it is clear that

$$BRT = \bar{u}_{abs} kT$$

or

$$B = \frac{\bar{u}_{abs} kT}{RT} = \frac{\bar{u}_{abs}}{N_A} \tag{4.173}$$

Thus, one has provided a fundamental basis for the phenomenological coefficient $B$; it is the absolute mobility $\bar{u}_{abs}$ divided by the Avogadro number.

The Einstein relation also permits experiments on diffusion to be linked up with other phenomena involving the mobility of ions, i.e., phenomena in which there are forces that produce drift velocities. Two such forces are the force experienced by an ion when it overcomes the viscous drag of a solution and the force arising from an applied electric field. Thus, the diffusion coefficient may be linked up to the viscosity (the Stokes–Einstein relation) and to the equivalent conductivity (the Nernst–Einstein relation).

### 4.4.7. Drag (or Viscous) Force Acting on an Ion in Solution

Striking advances in science sometimes arise from seeing the common factors in two apparently dissimilar situations. One such advance was made by Einstein when he intuitively asserted the similarity between a macroscopic sphere moving in an incompressible fluid and a particle (e.g., an ion) moving in a solution (Fig. 4.63).

The macroscopic sphere experiences a viscous, or drag, force that opposes its motion. The value of the drag force depends on several factors—the velocity $v$ and diameter $d$ of the sphere and the viscosity $\eta$ and density $\rho$ of the medium. These factors can all be combined and used to define a dimensionless quantity known as the *Reynolds number* (Re) defined thus:

$$\mathrm{Re} = vd\frac{\rho}{\eta} \tag{4.174}$$

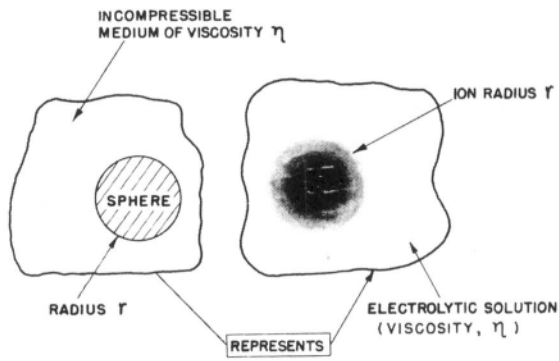


**Fig. 4.63.** An ion drifting in an electrolytic solution is like a sphere (of the same radius as the ion) moving in an incompressible medium (of the same viscosity as the electrolyte).

When the hydrodynamic conditions are such that this Reynolds number is much smaller than unity, Stokes showed that the drag force $F$ opposing the sphere is given by the following relation

$$F = 6\pi r\eta v \tag{4.175}$$

where $v$ is the velocity of the macroscopic body. The relation is known as Stokes' law. Its derivation is lengthy and awkward because the most convenient coordinates to describe the sphere and its environment are spherical coordinates and those to describe the flow are rectangular coordinates.

The real question, of course, centers around the applicability of Stokes' law to microscopic ions moving in a structured medium in which the surrounding particles are roughly the same size as the ions. Initially, one can easily check on whether the Reynolds number *is* smaller than unity for ions drifting through an electrolyte. With the use of the values $d_{ion} \approx 10^{-8}$ cm, $v_{ion} = v_d \approx 10^{-4}$ cm s$^{-1}$, $\eta \approx 10^{-2}$ poise, and $\rho \simeq 1$, it turns out that the Reynolds number for an ion moving through an electrolyte is about $10^{-10}$. Thus, the hydrodynamic condition Re $<<$ 1 required for the validity of Stokes' law is easily satisfied by an ion in solution.

However, the hydrodynamic problem that Stokes solved to get $F = 6\pi r\eta v$ pertains to a sphere moving in an incompressible *continuum* fluid. This is a far cry indeed from the actuality of an ion drifting inside a discontinuous electrolyte containing particles (solvent molecules, other ions, etc.) of about the same size as the ion. Furthermore, the ions considered may not be spherical.

From this point of view, the use of Stokes' law for the viscous force experienced by ions is a bold step. Several attempts have been made over a long time to theorize about the viscous drag on tenths of nanometer-sized particles in terms of a more realistic model than that used by Stokes. It has been shown, for example, that if the moving particle is cylindrical and not spherical, the factor $6\pi$ should be replaced by $4\pi$. While refraining from the none-too-easy analysis of the degree of applicability of Stokes' law to ions in electrolytes, one point must be stressed. For sufficiently small ions, Stokes' law does not have a numerical significance[26] greater than about ±50%. Attempts to tackle the problem of the flow of ions in solution without resorting to Stokes' law do not give much better results.

---

[26]Stokes' law is often used in electrochemical problems, but its approximate nature is not always brought out. Apart from the validity of extrapolating from the macroscopic–sphere-continuum-fluid model of Stokes to atomic near-spheres in a molecular liquid, another reason for the limited validity of Stokes' law arises from questions concerning the radii which should be substituted in any application of the law. These should not be the crystallographic radii, and an appraisal of the correct value implies a rather detailed knowledge of the structure of the solvation sheath (see Section 2.4). Furthermore, the viscosity used in Stokes' law is the bulk average viscosity of the whole solution, whereas it is the local viscosity in the neighborhood of the ion that should be taken. The two may not be the same, because the ion's field may affect the solvent structure and hence its viscosity.

### 4.4.8. The Stokes–Einstein Relation

During the course of diffusion, the individual particles are executing the complicated starts, accelerations, collisions, stops, and zigzags that have come to be known as random walk. When a particle is engaged in its random walk, it is of course subject to the viscous drag force exerted by its environment. The application of Stokes' law to these detailed random motions is no easy matter because of the haphazard variation in the speed and direction of the particles. Instead, one can apply Stokes' law to the diffusional movements of ions by adopting the following artifice suggested by Einstein.

When diffusion is occurring, it can be considered that there is a driving force $-d\mu/dx$ operating on the particles. This driving force produces a steady-state diffusion flux $J$, corresponding to which [*cf.* Eq. (4.14)] one can imagine a drift velocity $v_d$ for the diffusing particles.[27] Since this velocity $v_d$ is a steady-state velocity, the diffusional driving force $-d\mu/dx$ must be opposed by an equal resistive force, which will be taken to be the Stokes viscous force $6\pi r\eta v_d$. Hence,

$$-\frac{d\mu}{dx} = 6\pi r\eta v_d \tag{4.176}$$

The existence of a charge on a moving body has the following effect on a polar solvent: It tends to produce an orientation of solvent dipoles in the vicinity of the ion. Since, however, the charge is moving, once oriented, the dipoles take some finite relaxation time $\tau$ to disorient. During this relaxation time, a relaxation force operates on the ion; this relaxation force is equivalent to an additional frictional force on the ion and results in an expression for the drag force of the form

$$F = 6\pi\eta vr - 6\pi\eta v\frac{s}{\varepsilon}$$

where $s$ is $(4/9)(\tau/6\pi\eta)e_0^2/r^3$ and $\varepsilon$ is the dielectric constant of the medium. The correction may be as much as 25% but will be neglected here in the interest of deriving the classical Stokes–Einstein relation.

One can therefore define the absolute mobility $\bar{u}_{\text{abs}}$ for the diffusing particles by dividing the drift velocity by either the diffusional driving force or the equal and opposite Stokes viscous force

$$\bar{u}_{\text{abs}} = \frac{v_d}{-d\mu/dx} = \frac{v_d}{6\pi r\eta v_d} = \frac{1}{6\pi r\eta} \tag{4.177}$$

[27] The hypothetical nature of the argument lies in the fact that in diffusion, there is no actual force exerted on the particles. Consequently, there is not the actual force-derived component of the velocity; i.e., there is no actual drift velocity (see Section 4.2.1). Thus, the drift velocity enters the argument only as a device.

The fundamental expression (4.172) relating the diffusion coefficient and the absolute mobility can be written thus:

$$\bar{u}_{abs} = \frac{D}{kT} \tag{4.178}$$

By equating Eqs. (4.177) and (4.178), the Stokes–Einstein relation is obtained.

$$D = \frac{kT}{6\pi r\eta} \tag{4.179}$$

It links the processes of diffusion and viscous flow.

The Stokes–Einstein relation proved extremely useful in the classical work of Perrin. Using an ultramicroscope, he watched the random walk of a colloidal particle, and from the mean square distance $\langle x^2 \rangle$ traveled in a time $t$, he obtained the diffusion coefficient $D$ from the relation (4.27)

$$D = \frac{\langle x^2 \rangle}{2t} \tag{4.27}$$

The weight of the colloidal particles and their density being known, their radius $r$ was then obtained. Then the viscosity $\eta$ of the medium could be used to obtain the Boltzmann constant

$$k = \frac{6\pi r\eta D}{T} \tag{4.180}$$

But

$$k = \frac{R}{N_A} \tag{4.181}$$

or

$$N_A = \frac{R}{k} \tag{4.182}$$

and thus the Avogadro number could be determined.

The use of Stokes' law also permits the derivation of a very simple relation between the viscosity of a medium and the conventional electrochemical mobility $u_{conv}$. Starting from the earlier derived equation (4.177)

$$\bar{u}_{abs} = \frac{1}{6\pi r\eta} \tag{4.177}$$

one substitutes for the absolute mobility the expression from Eq. (4.152)

$$u_{conv} = \bar{u}_{abs} z_i e_0 \tag{4.152}$$

and gets the result

$$u_{conv} = \frac{z_i e_0}{6\pi r \eta} \tag{4.183}$$

This relation shows that, owing to the Stokes viscous force, the conventional mobility of an ion depends on the charge and radius[28] of the solvated ion and the viscosity of the medium. The mobility given by Eq. (4.183) is often called the *Stokes mobility.* It will be seen later that the Stokes mobility is a highly simplified expression for mobility, and ion–ion interaction effects introduce a concentration dependence that is not seen in Eq. (4.183).

### 4.4.9. The Nernst–Einstein Equation

Now the Einstein relation (4.172) will be used to connect the transport processes of diffusion and conduction. The starting point is the basic equation relating the equivalent conductivity of a *z*:*z*-valent electrolyte to the conventional mobilities of the ions, i.e., to the drift velocities under a potential gradient of 1 V $cm^{-1}$,

$$\Lambda = F[(u_{conv})_+ + (u_{conv})_-] \tag{4.163}$$

By using the relation between the conventional and absolute mobilities, Eq. (4.163) can be written

$$\Lambda = z_i e_0 F[(\bar{u}_{abs})_+ + (\bar{u}_{abs})_-] \tag{4.184}$$

With the aid of the Einstein relation (4.172),

$$(\bar{u}_{abs})_+ = \frac{D_+}{kT} \quad \text{and} \quad (\bar{u}_{abs})_- = \frac{D_-}{kT} \tag{4.185}$$

one can transform Eq. (4.184) into the form

$$\Lambda = \frac{z e_0 F}{kT}(D_+ + D_-) \tag{4.186}$$

[28]Earlier, the radius dependence of the conventional mobility was used to obtain information on the solvation number (see Section 2.8).

This is one form of the Nernst–Einstein equation; from a knowledge of the diffusion coefficients of the individual ions, it permits a calculation of the equivalent conductivity. A more usual form of the Nernst–Einstein equation is obtained by multiplying numerator and denominator by the Avogadro number, in which case it is obvious that

$$\Lambda = \frac{zF^2}{RT}(D_+ + D_-) \tag{4.187}$$

## 4.4.10. Some Limitations of the Nernst–Einstein Relation

There were several aspects of the Stokes–Einstein relation that reduced it to being only an approximate relation between the diffusion coefficient of an ionic species and the viscosity of the medium. In addition, there were fundamental questions regarding the extrapolation of a law derived for macroscopic spheres moving in an incompressible medium to a situation involving the movement of ions in an environment of solvent molecules and other ions. In the case of the Nernst–Einstein relation, the factors that limit its validity are more subtle.

An implicit but principal requirement for the Nernst–Einstein equation to hold is that the species involved in diffusion must also be the species responsible for conduction. Suppose now that the species M exists not only as ions $M^{z+}$ but also as ion pairs $M^{z+}A^{z-}$ of the type described in Section 3.8.1.

The diffusive transport of M proceeds through both ions and ion pairs. In the conduction process, however, the situation is different (Fig. 4.64). The applied electric field exerts a driving force on only the charged particles. An ion pair as a whole is electrically neutral; it does not feel the electric field. Thus, ion pairs are not participants in the conduction process. This point is of considerable importance in conduction in nonaqueous media (see Section 4.7.12).

In systems where ion-pair formation is possible, the mobility calculated from the diffusion coefficient $\bar{u}_{abs} = D/kT$ is not equal to the mobility calculated from the equivalent conductivity $\bar{u}_{abs} = u_{conv}/z_i e_0 = (\Lambda/z_i e_0)F$ and therefore the Nernst–Einstein equation, which is based on equating these two mobilities, may not be completely valid. In practice, one finds a degree of nonapplicability of up to 25%.

Another important limitation on the Nernst–Einstein equation in electrolytic solutions may be approached through the following considerations. The diffusion coefficient is in general not a constant. This has been pointed out in Section 4.2.3, where the following expression was derived,

$$D = BRT\left(1 + \frac{d \ln f}{d \ln c}\right) \tag{4.19}$$

It is clear that $BRT$ is the value of the diffusion coefficient when the solution behaves ideally, i.e., $f = 1$; this ideal value of the diffusion coefficient will be called $D^0$. Hence,

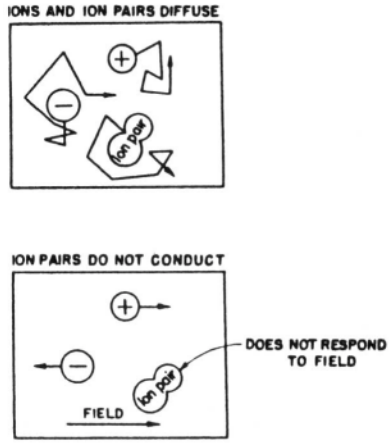


**Fig. 4.64.** The difference in the behavior of neutral ion pairs during diffusion and conduction.

$$D = D^0\left(1 + \frac{d\ln f}{d\ln c}\right)$$

$$= D^0\left(1 + c\,\frac{d\log f}{dc}\right) \qquad (4.188)$$

and making use of the Debye–Hückel limiting law for the activity coefficient (see Section 3.5),

$$\log f = -A c^{1/2}$$

one has

$$D = D^0(1 - \tfrac{1}{2} A c^{1/2}) \qquad (4.189)$$

an expression which shows how the diffusion coefficient varies with concentration. In addition, there is Kohlrausch's law

$$\Lambda = \Lambda^0 - A c^{1/2} \qquad (4.139)$$

where $\Lambda^0$ is the equivalent conductivity at infinite dilution, i.e., the ideal value.

From Eqs. (4.189) and (4.139), it is obvious that the diffusion coefficient $D$ and the equivalent conductivity $\Lambda$ have different dependencies on concentration (Fig. 4.65). This experimentally observed fact has an important implication as far as the

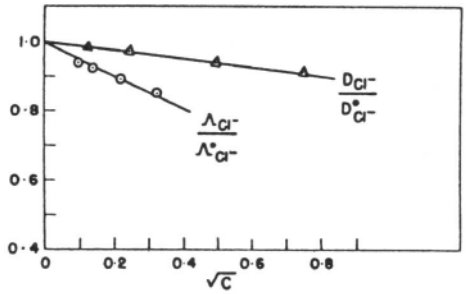


**Fig. 4.65.** The variation of the diffusion coefficient and the equivalent conductivity with concentration.

applicability of the Nernst–Einstein equation in electrolytic solutions is concerned. If the equation is true at one concentration, it cannot be true at another because the diffusion coefficient and the equivalent conductivity have varied to different extents in going from one concentration to the other.

The above argument brings out an important point about the limitations of the Nernst–Einstein equation. It does not matter whether the diffusion coefficient and the equivalent conductivity vary with concentration; to introduce deviations into the Nernst–Einstein equation, $D$ and $\Lambda$ must have different concentration dependencies. The concentration dependence of the diffusion coefficient has been shown to be due to nonideality ($f \neq 1$), i.e., due to ion–ion interactions, and it will be shown later that the concentration dependence of the equivalent conductivity is also due to ion–ion interactions. It is not the existence of interactions *per se* that underlies deviations from the Nernst–Einstein equation; otherwise, molten salts and ionic crystals, in which there are strong interionic forces, would show far more than the observed few percent deviation of experimental data from values calculated by the Nernst–Einstein equation. The essential point is that the interactions must affect the diffusion coefficient and the equivalent conductivity by *different mechanisms* and thus to different extents. How this comes about for diffusion and conduction in solution will be seen later.

In solutions of electrolytes, the $c^{1/2}$ terms in the expressions for $D$ and $\Lambda$ tend to zero as the concentration of the electrolytic solution decreases, and the differences in the concentration variation of $D$ and $\Lambda$ become more and more negligible; in other words, the Nernst–Einstein equation becomes increasingly valid for electrolytic solutions with increasing dilution.

## 4.4.11. The Apparent Ionic Charge

In Eqs. (4.172) and (4.186), two relations between the random movement of particles and directed drift (mobility under an electric field gradient) have been

deduced. In Eq. (4.172), $D$ is related to ionic mobility (Einstein equation) and in Eq. (4.186), it is related to the equivalent conductivity (Nernst–Einstein equation).

The relations derived were based upon very acceptable concepts, such as the random movement of particles in fluids, or their drift in the direction of an applied electric field. These ideas are so general that they cannot be doubted—they do not involve models later found to be wrong and to be displaced by other models, etc. For this reason, equations such as those named above are called *phenomenological*, meaning that they involve phenomena (drift and random movement) that cannot be doubted by the greatest skeptic. They happen.

One gets a mild shock therefore when one looks into the experimental tests of these equations, for only under extremely simple conditions (in fact, very dilute solutions) do they work out to be correct. Although the results never hint that the equations are wrong, there is sufficient discrepancy (e.g., between the diffusion coefficient calculated by using an experimental mobility substituted in the Einstein equation and that determined by direct experiment) for one to take notice and form some idea of a puzzle. How can simple mathematical reasoning based on the existence of movements undeniably present give rise to error?

There are two kinds of response to this challenge. In the first, one can invent special models to explain the observed discrepancy. One such model is displayed on several pages of Chapter 5—it deals with the deviations from the Einstein equations in high–temperature ionic liquids. It is suggested that the discrepancies arise because there are some kinds of molecular movements that contribute to diffusion but not to conduction. One kind of diffusive mode involves pairs of oppositely charged ions moving together. This would contribute to $D$, but because a pair of oppositely charged ions carries no net charge, its movement would not contribute to the mobility $u_i$ or to the equivalent conductivity $\Lambda$, which reflects only the movement of individual charged particles moving under an applied field. This kind of movement—*individual* ionic movement—contributes to $D_{\text{exptl}}$ also. Therefore, $D_{\text{exptl}}$ receives two kinds of contributions (uncharged pairs and charged individuals), but the $u_i$ receives only one (that of the individual charges). Clearly then, the $D_{\text{exptl}}$ determined from radiotracer experiments would be greater than the $D$ calculated from the Einstein or Nernst–Einstein equations because in their deduction only individual ions count—those that drift in one direction under the applied field, and not pairs of ions, which the field cannot affect.

This explanation is all very well for the liquid sodium chloride type of case, but deviations from the predictions of the Nernst–Einstein equation occur in dilute aqueous solutions also, and here the + and – ions are separated by stretches of water, and ion pairs do not form significantly until about 0.1 *M*.

Because deviations from the Nernst–Einstein equation are so widespread, and because the reasoning that gives rise to the equation is phenomenological, it is better to work out a general kind of noncommittal response—one that is free of a specific model such as that suggested in the molten salt case (see Section 5.2). The response

is to suggest that it is useful to imagine that ions carry (effectively), not the charge we would normally associate with them (e.g., 2 for $SO_4^{2-}$), but a slightly different charge—one which, when used in the Nernst–Einstein equation in the form (4.186) will make the $D$ to which it gives rise have the same value as the experimental one. It is clear that this way of describing a discrepancy from what is expected from reasoning that is evidently too simple bears some resemblance to the use of activity coefficients to describe why the use of concentrations (and not "activities") does not work well when describing the equilibrium properties of true electrolytes (Section 3.4.2).

The original Einstein equation is

$$D_{\text{calc}} = \bar{u}_{\text{abs}} kT \tag{4.190}$$

Now $z$ is the formal charge on the ion (e.g., 3 for $La^{3+}$). One finds experimentally, however, that the $D_{\text{calc}}$ obtained in this way is smaller than the one that is determined experimentally by means of radiotracers. It might be reasonable then to write

$$D_{\text{real}} = \frac{u_{\text{conv}}}{z_{\text{apparent}}} \frac{kT}{e_0} \tag{4.191}$$

The $z_{\text{apparent}}$ is chosen so the equation comes out to fit the experiment. In this second response to the challenge of the deviant values from the Einstein equation, one draws picture or suggest a model for why $z_{\text{apparent}}$ is not equal to $z$. The apparent charge is just a coverup for the deviation.

Now from Eq. (4.187), and for a symmetrical electrolyte

$$z_{\text{apparent}} = \frac{RT}{F^2} \frac{\Lambda}{(D_+ + D_-)} \tag{4.192}$$

At infinite dilution the ions are truly independent of each other (no interionic attraction) and there would be no reason for any difference between $z_{\text{apparent}}$ and $z$.

In Section 5.6.6, one will see the details of the modeling treatment of the deviations for the Nernst–Einstein equation outlined here. Of course, a modeling explanation is more enlightening than a general-explanation type of approach. However, the difficulty is that the model of paired ions jumping together applies primarily to a pure liquid electrolyte, or alloy, where the existence of paired vacancies is a fact. Other models would have to be devised for other kinds of systems where deviations do occur (Fig. 4.66).

### 4.4.12. A Very Approximate Relation between Equivalent Conductivity and Viscosity: Walden's Rule

The Stokes–Einstein equation (4.179) connects the diffusion coefficient and the viscosity of the medium; the Nernst–Einstein equation (4.187) relates the diffusion coefficient to the equivalent conductivity. Hence, by eliminating the diffusion coeffi-

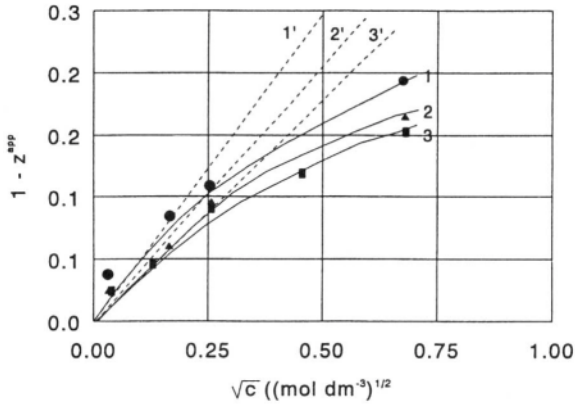


**Fig. 4.66.** Apparent charge of alkali halides as a function of concentration. Aqueous solutions of NaF (I), NaCl (2), and KCl (3) at 25 °C. Broken lines: limiting law of Debye and Hückel. (Reprinted from P. Turq, J. Barthel, and M. Chemla, in *Transport Relaxation and Kinetic Processes in Electrolyte Solutions*, Springer-Verlag, Berlin, 1992.)

cient in these two equations, it is possible to obtain a relation between the equivalent conductivity and the viscosity of the electrolyte. The algebra is as follows:

$$D = \frac{kT}{6\pi r\eta} = \frac{RT}{zF^2}\Lambda \tag{4.193}$$

and therefore

$$\Lambda = \frac{zF^2k}{6\pi R}\frac{1}{r\eta} \tag{4.194}$$

Since $F = N_A e_0$ and $k/R = 1/N_A$, one obtains

$$\Lambda = \frac{ze_0F}{6\pi}\frac{1}{r\eta}$$

$$\Lambda\eta = \frac{\text{constant}}{r} \tag{4.195}$$

Hence, if the radius of the moving (kinetic) entity in conduction, i.e., the solvated ion, can be considered the same in solvents of various viscosities, the following relation is obtained:

**TABLE 4.14**

**Tests of Walden's Rule. The Product $\Lambda\eta$ for Potassium Iodide in Various Solvents at 298 K**

| Solvent | $\Lambda$ | $\eta$ | $\Lambda\eta$ |
|---|---|---|---|
| Sulfur dioxide[a] | 265 | 0.00394 | 1.044 |
| Acetonitrile | 198.2 | 0.00345 | 0.684 |
| Acetone | 185.5 | 0.00316 | 0.586 |
| Nitromethane | 124.0 | 0.00611 | 0.758 |
| Methyl alcohol | 114.8 | 0.00546 | 0.627 |
| Pyridine[b] | 71.3 | 0.00958 | 0.682 |
| Ethyl alcohol | 50.9 | 0.01096 | 0.560 |
| Furfural | 43.1 | 0.01490 | 0.642 |
| Acetophenone | 39.8 | 0.01620 | 0.644 |

[a] 273 K.
[b] 293 K.

$$\Lambda\eta = \text{constant} = \frac{ze_0F}{6\pi r} \tag{4.196}$$

This means that the product of the equivalent conductivity and the viscosity of the solvent for a particular electrolyte at a given temperature should be a constant (at one temperature). This is indeed what the empirical Walden's rule states.

Some experimental data on the product $\Lambda\eta$ are presented in Table 4.14 for solutions of potassium iodide in various solvents. Walden's rule has some rough applicability in organic solvents. When, however, the $\Lambda\eta$ products for a solute dissolved on the one hand in water and on the other in organic solvents are compared, it is found that there is considerable discrepancy (Table 4.15). This should hardly come as a surprise; one should expect differences in the solvation of ions in water and in organic solvents (Section 2.20) and the resulting differences in radii of the moving ions.

**TABLE 4.15**

**The Product $\Lambda\eta$ for Sodium Chloride in Various Solvents at 298 K**

| Solvent | $\Lambda$ | $\eta$ | $\Lambda\eta$ |
|---|---|---|---|
| Water | 126.39 | 0.00895 | 1.131 |
| Methyl alcohol | 96.9 | 0.00546 | 0.529 |
| Ethyl alcohol | 42.5 | 0.01096 | 0.466 |

### 4.4.13. The Rate-Process Approach to Ionic Migration

The fundamental equation for the current density (flux of charge) as a function of the drift velocity has been shown to be

$$\vec{j} = zFcv_d \tag{4.164}$$

Hitherto, the drift velocity has been related to macroscopic forces (e.g., the Stokes viscous force $\vec{F} = 6\pi r\eta$ or the electric force $\vec{F} = ze_0X$) through the relation

$$v_d = \frac{\vec{F}}{m}\tau \tag{4.147}$$

Another approach to the drift velocity is by molecular models. The drift velocity $v_d$ is considered the net velocity, i.e., the difference of the velocity $\vec{v}$ of ions in the direction of the force field and the velocity $\overleftarrow{v}$ of ions in a direction opposite to the field (Fig. 4.67). In symbols, one writes

$$v_d = \vec{v} - \overleftarrow{v} \tag{4.197}$$

Any velocity is given by the distance traveled divided by the time taken to travel that distance. In the present case, the distance is the jump distance $l$, i.e., the mean distance that an ion jumps in hopping from site to site in the course of its directed random walk, and the time is the mean time $\tau$ between successive jumps. This mean time includes the time the ion may wait in a "cell" of surrounding particles as well as the actual time involved in jumping. Thus,

$$\vec{v} = \frac{\text{Mean jump distance } l}{\text{Mean time between jumps } \tau} \tag{4.198}$$

The reciprocal of the mean time between jumps is the net jump frequency $k$, which is the number of jumps per unit of time. Hence,

$$\text{Velocity} = \text{Jump distance} \times \text{net jump frequency}$$

or

$$\vec{v} = l\vec{k} \tag{4.199}$$

and

$$\overleftarrow{v} = l\overleftarrow{k} \tag{4.200}$$

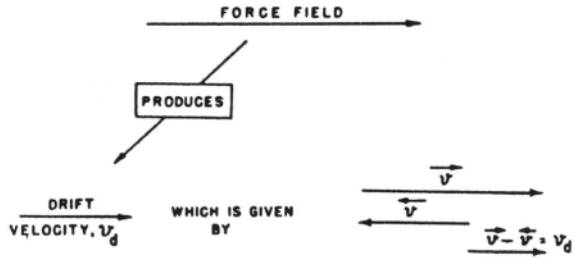


**Fig. 4.67.** The drift velocity $v_d$ can be considered to be made up of a velocity $\vec{v}$ in the direction of the force field and a velocity* in a direction opposite to the force field.

For diffusion, the net jump frequency $k$ was related to molecular quantities by viewing the ionic jumps as a rate process (Equation 4.111). In this view, for an ion to jump, it must possess a certain free energy of activation to surmount the free-energy barrier. It was shown that the net jump frequency is given by

$$\vec{k} = \frac{kT}{h} e^{-\Delta G^{\circ\ddagger}/RT} \tag{4.111}$$

To emphasize that this is the jump frequency for a pure diffusion process, in which case the ions are not subjected to an externally applied field, a subscript $D$ will be appended to the net jump frequency and to the standard free energy of activation, i.e.,

$$\vec{k}_D = \frac{kT}{h} e^{-\Delta G_D^{\circ\ddagger}/RT} \tag{4.201}$$

Now, suppose an electric field is applied so that it *hinders* the movement of a positive ion from right to left. Then the work that is done on the ion in moving it from the equilibrium position to the top of the barrier (Fig. 4.68) is the product of the charge on the ion, $z_+e_0$, and the potential difference between the equilibrium position and the activated state, i.e., the position at the top of the barrier. Let this potential difference be a fraction $\beta$ of the total potential difference (i.e., the applied electric field $X$ times the distance $l$) between two equilibrium sites. Then the electrical work done on one positive ion in making it climb to the top of the barrier, i.e., in activating it, is equal to the charge on the ion $z_+e_0$ times the potential difference $\beta Xl$ through which it is transported. Thus the electrical work is $z_+e_0\beta Xl$ per ion, or $z_+F\beta Xl$ per mole of ions.

The electrical work of activation corresponds to a free-energy change. It appears therefore that there is a contribution to the total free energy of activation due to the electrical work done on the ion in making it climb the barrier. This electrical contribution to the free energy of activation is

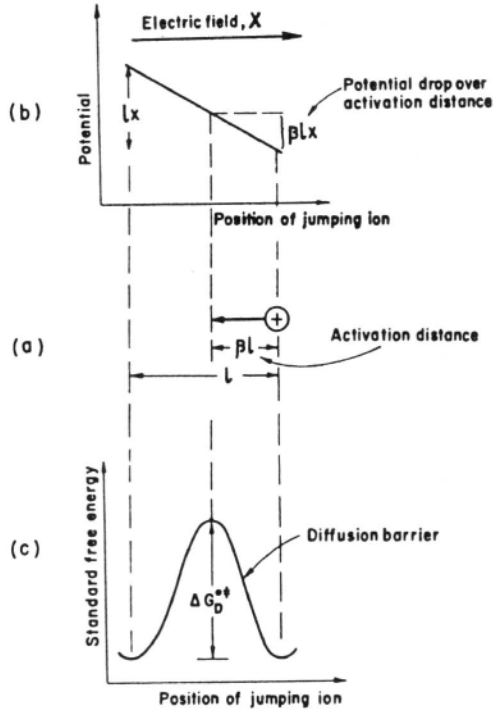


**Fig. 4.68.** (a) As the ion moves for the jump, it has to climb (b) the potential gradient arising from the electric field in the electrolyte, in addition to (c) the free-energy barrier for diffusion. To be activated, the ion has to climb the fraction $\beta Xl$ of the total potential difference $Xl$ between the initial and final positions for the jump.

$$\Delta G_e^{\circ\ddagger} = z_+ F\beta Xl \tag{4.202}$$

Hence, the *total* free energy of activation (for positive ions moving from right to left) is

$$\Delta G_{\text{total}}^{\circ\ddagger} = \Delta G_D^{\circ\ddagger} + \Delta G_e^{\circ\ddagger} \tag{4.203}$$

Thus, in the presence of the field, the frequency of right → left jumps is

$$\overleftarrow{k} = \frac{kT}{h} e^{-(\Delta G_D^{\circ\ddagger} + z_+ F\beta Xl)/RT} \tag{4.204}$$

or

$$\overleftarrow{k} = k_D e^{-z_+ F\beta Xl/RT} \tag{4.205}$$

By a similar argument, the left → right jump frequency $\vec{k}$, or the number of jumps per second from left to right, may be obtained. There are, however, two differences: When positive ions move from left to right, (1) they are moving with the field and therefore are *helped*, not *hindered*, by the field, and (2) they have to climb through only a fraction $1 - \beta$ of the barrier. Hence, the electrical work of activation is $-[z_+F(1-\beta)Xl]$, the minus sign indicating that the field assists the ion. Thus,

$$\vec{k} = k_D e^{z_+ F(1-\beta)Xl/RT} \tag{4.206}$$

If the factor $\beta$ is assumed to be $\frac{1}{2}$,[29] then $\beta = 1 - \beta = \frac{1}{2}$ and Eqs. (4.205) and (4.206) can be written

$$\overleftarrow{k} = k_D e^{-pX} \tag{4.207}$$

and

$$\vec{k} = k_D e^{+pX} \tag{4.208}$$

where for conciseness $p$ is written instead of $z_+Fl/2RT$. It follows from these equations that $\overleftarrow{k} < k_D$ and $\vec{k} > k_D$, or $\vec{k} > \overleftarrow{k}$.

In the presence of the field therefore, the jumping frequency is anisotropic, i.e., it varies with direction. The jumping frequency $\vec{k}$ of an ion in the direction of the field is greater the jumping frequency that $\overleftarrow{k}$ against the field. When, however, there is no field, the jump frequency $k_D$ is the same in all directions, and therefore jumps in all directions are equally likely. This is the characteristic of a random walk. The application of the field destroys the equivalence of all directions. The walk is not quite random. The field makes the ions more likely to move with it than against it. There is drift. In Eqs. (4.207) and (4.208), the $k_D$ is a random-walk term, the exponential factors are the perturbations due to the field, and the result is a drift. The equations are therefore a quantitative expression of the qualitative statement made in Section 4.4.1.

Drift due to field = Random walk in absence of field × perturbation due to field (4.209)

### 4.4.14. The Rate-Process Expression for Equivalent Conductivity

Introducing the expressions (4.207) and (4.208) for $\vec{k}$ and $\overleftarrow{k}$ into the equations for the component forward and backward velocities $\vec{v}$ and $\overleftarrow{v}$ [i.e., into Eqs. (4.199) and (4.200)], one obtains

[29] This implies (Fig. 4.68) that the energy barrier is symmetrical.

$$\overleftarrow{v} = lk_D e^{-pX} \tag{4.210}$$

and

$$\overrightarrow{v} = lk_D e^{+pX} \tag{4.211}$$

where, as stated earlier,

$$p = \frac{z_+ Fl}{2RT}$$

The drift velocity $v_d$ is obtained [*cf.* Eq. (4.197)] by subtracting Eq. (4.210) from Eq. (4.211), thus,

$$\begin{aligned} v_d = \overrightarrow{v} - \overleftarrow{v} &= lk_D e^{+pX} - lk_D e^{-pX} \\ &= lk_D(e^{+pX} - e^{-pX}) \\ &= 2lk_D \sinh pX \end{aligned} \tag{4.212}$$

The net charge transported per second across a unit area (i.e., the current density $j$) is given by Eq. (4.164),

$$\overrightarrow{j} = z_+ Fcv_d \tag{4.164}$$

Upon inserting the expression (4.212) for the drift velocity into Eq. (4.164), it is clear that

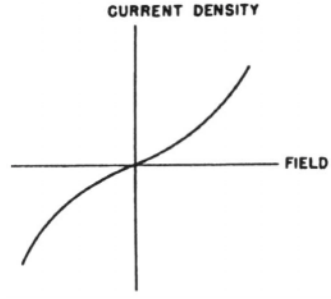


**Fig. 4.69.** The hyperbolic sine relation between the ionic current density and the electric field according to Eq. (4.213).

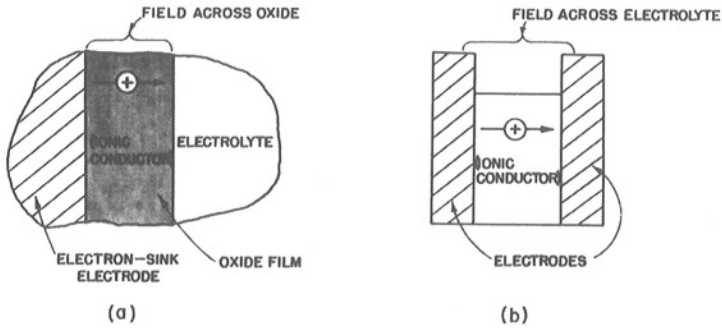


**Fig. 4.70.** The similarity between the ionic current flowing (a) through an oxide film between an electrode and an electrolyte and (b) through an electrolyte between two electrodes.

$$\vec{j} = z_+ Fc(2lk_D \sinh pX) \tag{4.213}$$

A picture of the hyperbolic sine relation between the ionic current density and the electric field that would result from Eq. (4.213) is shown in Fig. 4.69.

The fundamental thinking used in the derivation of Eq. (4.213) has wide applicability. Take the case of an oxide film that grows on an electron-sink electrode (anode). All one has to do is to consider an ionic crystal (the oxide) instead of an electrolytic solution, and all the arguments used to derive the hyperbolic sine relation (4.213) become immediately applicable to the ionic current flowing through the oxide in response to the potential gradient in the solid (Fig. 4.70). In fact, Eq. (4.213) is the basic equation describing the field-induced migration of ions in any ionic conductor. Equation (4.213) is also formally similar to the expression for the current density due to a charge-transfer electrodic reaction occurring under the electric field present at an electrode–electrolyte interface (Chapter 7).

In all these cases, two significant approximations can be made. One is the *high-field Tafel type* (see Chapter 7) of approximation, in which the absolute magnitude of the exponents $|pX|$ in Eq. (4.213) [i.e., the argument $pX$ of the hyperbolic sine in Eq. (4.213)] is much greater than unity. Under this condition of $pX >> 1$, one obtains $\sinh pX \approx e^{pX}/2$ because one can neglect $e^{-pX}$ in comparison with $e^{pX}$. Thus (Fig. 4.71)

$$j = z_+ Fclk_D e^{pX} \tag{4.214}$$

i.e., the current density bears an exponential relation to the field. Such an exponential dependence of current on field is commonly observed in oxide growth, at electrode–electrolyte interfaces, but not in electrolyte solutions.

In electrolytic solutions, however, the conditions for the high-field approximation are not often observed. The applied field $X$ is generally relatively small, in which case $pX << 1$ and the following approximation can be used:

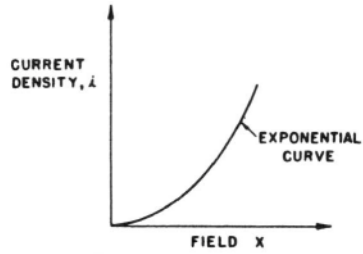


**Fig. 4.71.** Under high-field conditons, there is an exponential relation between ionic current density and the field across an oxide.

$$\sinh pX \approx pX = \frac{z_+ FlX}{2RT} \tag{4.215}$$

and the current density in Eq. (4.213) is approximately given (Fig. 4.72) by

$$\vec{j}_+ = z_+ Fc2lk_D \frac{z_+ FlX}{2RT}$$

$$= \left( z_+^2 F^2 c \frac{l^2 k_D}{RT} \right) X \tag{4.216}$$

All the quantities within the parentheses are constants in a particular electrolyte and therefore

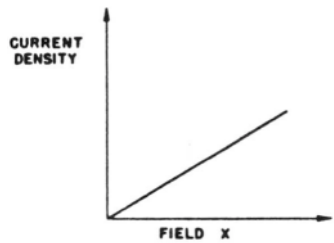


**Fig. 4.72.** Under low-field conditions, there is a linear relation between the ionic current density and the field in the electrolyte.

$$\vec{j}_+ = \text{constant} \times X \tag{4.217}$$

and according to Eq. (4.160), the value of the constant is equal to $\sigma$. This is the *low-field* approximation. It is in fact the rate-process version of Ohm's law. An important point, however, has emerged: *Ohm's law is valid only for sufficiently small fields.* Of course, this was accounted for in the phenomenological treatment of conduction where the general flux–force relation

$$J = A + BX + CX^2 + \ldots \tag{4.121}$$

reduced to the linear relation

$$J = BX \tag{4.122}$$

only for "small" fields.

However, words such as "small" and "large" are relative. If one proceeds to substitute numerical values in the conditions for a linear relation between current and field, one starts with $pX << 1$. For example, $zFlX/2RT < 0.1$; then, with $F/RT = 39.0$ $\mathbf{V}^{-1}$ at 25 °C, $z = 1$, and $l = 3 \times 10^{-8}$ cm, one obtains $X < 10^5$ V cm$^{-1}$ as the condition for the linearization of Eq. (4.213). This condition also implies a proportionality of the current to the applied field in the electrolyte and hence [*cf.* Eq. (4.213)] independence of the conductivity on the potential applied to the cell.

Since one often works in the laboratory with $0 < X < 10$ V cm$^{-1}$, when one says that $X$ has to be "small" for the conductivity to be independent of field strength, this becomes a very relative matter. It is better to say that the conductivity remains independent of the value of the applied field so long as it is not very high. Indeed, it has been found that the conductivity finally does increase with the applied field but only at $10^6$ V cm$^{-1}$.

### 4.4.15. The Total Driving Force for Ionic Transport: The Gradient of the Electrochemical Potential

In the rate-process view of conduction that has just been presented, it has been assumed that the concentration is the same throughout the electrolyte. Suppose, however, that there is a concentration gradient of a particular ionic species, say, positively charged radiotracer ions. Further, let the concentration vary continuously in the $x$ direction (see Fig. 4.73), so that if the concentration of positive ions at $x$ on the left of the barrier is $(c_+)_x$, the concentration on the right (i.e., at $x + l$) is given by

$$\begin{matrix}\text{Concentration} \\ \text{on the right}\end{matrix} = \begin{matrix}\text{Concentration} \\ \text{on the left}\end{matrix} + \begin{matrix}\text{rate of change of} \\ c_+ \text{ with distance}\end{matrix} \times \text{distance}$$

i.e.,

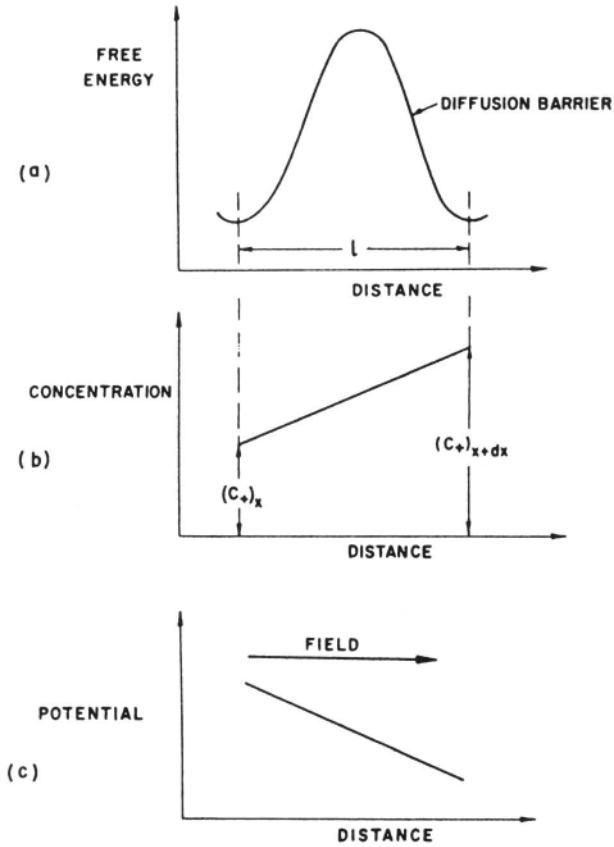


**Fig. 4.73.** Measurement of ions under both a concentration gradient and a potential gradient: (a) the free-energy barrier for the diffusive jump of an ion, (b) the concentration variation over the jump distance, and (c) the potential variation over the jump distance.

$$(c_+)_{x+l} = (c_+)_x + \frac{dc_+}{dx} l \tag{4.218}$$

In this case, there will be diffusion of the tracer ions and therefore the current density $j_+$ is not given by a conduction law, i.e., by Eq. (4.159), which governs the situation in the absence of a concentration gradient. Instead, the expression for the current density has to be written [the subscript $x$ in $(c_+)_x$ has been dropped for the sake of convenience]

$$j_+ = z_+ F c_+ \vec{v} - z_+ F \left( c_+ + \frac{dc_+}{dx} l \right) \overleftarrow{v} \tag{4.219}$$

However, $\vec{v}$ and $\overleftarrow{v}$ have been evaluated as

$$\vec{v} = lk_D e^{pX} \tag{4.211}$$

and

$$\overleftarrow{v} = lk_D e^{-pX} \tag{4.210}$$

Under low-field conditions $pX << 1$, the exponentials can be expanded and linearized to give

$$\vec{v} \approx lk_D(1 + pX) \tag{4.220}$$

and

$$\overleftarrow{v} \approx lk_D(1 - pX) \tag{4.221}$$

Combining Eqs. (4.219), (4.220), and (4.221), one gets

$$\begin{aligned} j_+ &= z_+Fc_+\vec{v} - z_+Fc_+\overleftarrow{v} - z_+F\frac{dc_+}{dx}\,l\,\overleftarrow{v} \\ &= z_+Fc_+lk_D(1 + pX) - z_+Fc_+lk_D(1 - pX) \\ &\quad - z_+Fl^2k_D(1 - pX)\frac{dc_+}{dx} \\ &= 2z_+Fc_+lk_DpX - z_+Fl^2k_D(1 - pX)\frac{dc_+}{dx} \end{aligned} \tag{4.222}$$

This expression can be simplified further, first, by applying the low-field condition $pX << 1$. It becomes

$$j_+ = 2z_+Fc_+lk_D\,pX - z_+Fl^2k_D\frac{dc_+}{dx} \tag{4.223}$$

Second, by substituting $z_+Fl/(2RT)$ for $p$, one has

$$j_+ = z_+^2F^2c_+\frac{l^2k_D}{RT}X - z_+Fl^2k_D\frac{dc_+}{dx} \tag{4.224}$$

and finally by replacing $l^2k_D$ with $D_+$ [*cf.* Eq. (4.113)], the result is

$$j_+ = \frac{z_+^2 F^2 c_+ D_+ X}{RT} - z_+ F D_+ \frac{dc_+}{dx} \tag{4.225}$$

To go from the current density $j_+$ to the flux $J_+$ of positive tracer ions is straightforward. Thus,

$$J_+ = \frac{j_+}{z_+ F} = \frac{D_+ c_+}{RT}(z_+ F X) - D_+ \frac{dc_+}{dx} \tag{4.226}$$

The second term on the right-hand side can be rewritten as

$$\begin{aligned} D_+ \frac{dc_+}{dx} &= \frac{D_+ c_+}{RT} \frac{RT}{c_+} \frac{dc_+}{dx} \\ &= \frac{D_+ c_+}{RT} \frac{d(RT \ln c_+)}{dx} \\ &= \frac{D_+ c_+}{RT} \frac{d(\mu_+^0 + RT \ln c_+)}{dx} \\ &= \frac{D_+ c_+}{RT} \frac{d\mu_+}{dx} \end{aligned} \tag{4.227}$$

since, according to the definition of the chemical potential for ideal solutions [*cf.* Eq. (3.54)],

$$\mu_+ = \mu_+^0 + RT \ln c_+$$

In addition, from Eq. (4.9), the electric field $X$ is equal to minus the gradient of the electrostatic potential, i.e.,

$$X = -\frac{d\psi}{dx} \tag{4.9}$$

Hence,

$$\begin{aligned} J_+ = \frac{j_+}{z_+ F} &= -\frac{D_+ c_+}{RT}\left(z_+ F \frac{d\psi}{dx} + \frac{d\mu_+}{dx}\right) \\ &= -\frac{D_+ c_+}{RT} \frac{d}{dx}(z_+ F \psi + \mu_+) \end{aligned} \tag{4.228}$$

This is an interesting result. The negative gradient of the chemical potential $d\mu_+/dx$ is known to be the driving force for pure diffusion and $-z_+F(d\psi/dx) = z_+FX$, the driving force for pure conduction. However, when there is both a chemical potential (or concentration) gradient and an electric field $(-d\psi/dx)$, then the total driving force for ionic transport is the negative gradient of

$$\underset{\text{Electrostatic potential}}{z_+F\psi} + \underset{\text{Chemical potential}}{\mu_+}$$

This quantity $z_+F\psi + \mu_+$ could be called the *electrostatic-chemical* potential, or simply the *electrochemical potential*, of the positive ions and is denoted by the symbol $\bar{\mu}_+$. Thus,

$$\bar{\mu}_+ = \mu_+ + z_+F\psi \tag{4.229}$$

and the total driving force for the drift of ions is the gradient of the electrochemical potential. Thus, one can write the flux $J_+$ of Eq. (4.228) in the form

$$J_+ = \frac{j_+}{z_+F} = -\frac{D_+c_+}{RT}\frac{d\bar{\mu}_+}{dx} \tag{4.230}$$

Or, by making use of the Einstein relation,

$$D_+ = (\bar{u}_{abs})_+kT \tag{4.172}$$

and the relation between absolute and conventional mobilities, i.e.,

$$(u_{conv})_+ = (\bar{u}_{abs})_+z_+e_0 \tag{4.152}$$

one can rewrite Eq. (4.230) in the form

$$\begin{aligned} J_+ = -\frac{D_+}{RT}c_+\frac{d\bar{\mu}_+}{dx} &= -\frac{(\bar{u}_{abs})_+kT}{RT}c_+\frac{d\bar{\mu}_+}{dx} \\ &= -\frac{(u_{conv})_+}{z_+e_0}\frac{kT}{RT}c_+\frac{d\bar{\mu}_+}{dx} \\ &= -\frac{(u_{conv})_+}{z_+F}c_+\frac{d\bar{\mu}_+}{dx} \end{aligned} \tag{4.231}$$

Expression (4.231) is known as the *Nernst–Planck flux equation.* It is an important equation for the description of the flux or flow of a species under the total driving force

of an electrochemical potential. The Nernst–Planck flux expression is useful in explaining, for example, the electrodeposition of silver from silver cyanide ions. In this process, the negatively charged $[Ag(CN)_2]^-$ ions travel to the negatively charged electron source or cathode, a fact that cannot be explained by considering that the only driving force on the $[Ag(CN)_2]^-$ ions is the electric field because the electric field drives these ions *away from* the negatively charged electrode. If, however, the concentration gradient of these ions in a direction normal to the electron source is such that in the expanded form of the Nernst–Planck equation, i.e.,

$$J = \frac{Dc}{RT} zFX - D\frac{dc}{dx} \tag{4.226}$$

the second term is larger than the first, then the flux of the $[Ag(CN)_2]^-$ ions is opposite to the direction of the electric field, i.e., toward the negatively charged electrode.

## Further Reading

### *Seminal*

1. A. Einstein, *Investigations on the Theory of Brownian Movement*, Methuen & Co., London (1926).
2. R. W. Gurney, *Ionic Processes in Solution*, Dover, New York (1953).
3. R. A. Robinson and R. H. Stokes, *Electrolyte Solutions*, Butterworth, London (1955).

### *Review*

1. P. Turq, J. Barthel, and M. Chemla, *Transport, Relaxation and Kinetic Processes in Electrolyte Solutions*, Springer-Verlag, Berlin (1992).

### *Papers*

1. J. Horno, J. Castilla, and C. F. Gonzalez-Fernandez, *J. Phys. Chem.* **96**: 854 (1992).
2. G. E. Spangler, *Anal. Chem.* **65**: 3010 (1993).
3. C. A. Lucy and T. L. McDonald, *Anal. Chem.* **67**: 1074 (1995).
4. R. Bausch, *J. Chem. Ed.* **72**: 713 (1995).
5. A. A. Moya, J. Castilla, and J. Horno, *J. Phys. Chem.* **99**: 1292 (1995).

## 4.5. THE INTERDEPENDENCE OF IONIC DRIFTS

### 4.5.1. The Drift of One Ionic Species May Influence the Drift of Another

The processes of diffusion and conduction have been treated so far with the assumption that each ionic species drifts independently of every other one. In general, however, the assumption is not realistic for electrolytic solutions because it presupposes the absence of ionic atmospheres resulting from ion–ion interactions. One has

been talking therefore of ideal laws of ionic transport and expressed them in the Nernst–Planck equation for the independent flux of a species *i*.

$$J_i = -\frac{(u_{\text{conv}})_i}{z_i F} c_i \frac{d\bar{\mu}_i}{dx} \tag{4.232}$$

The time has come to free the treatment of ionic transport from the assumption of the independence of the various ionic fluxes and to consider some phenomena which depend on the fact that the drift of a species *i* is affected by the flows of other species present in the solution. It is the whole society of ions that displays a transport process, and each individual ionic species takes into account what all the other species are doing. Ions interact with each other through their Coulombic fields and thus it will be seen that the law of electroneutrality that seeks zero excess charge in any macroscopic volume element plays a fundamental role in phenomena where ionic flows influence each other.

A stimulating approach to the problem of the interdependence of ionic drifts can be developed as follows. Since different ions have different radii, their Stokes mobilities, given by

$$(u_{\text{conv}})_i = \frac{z_i e_0}{6\pi r \eta} \tag{4.183}$$

must be different. What are the consequences that result from the fact that different ionic species have unequal mobilities?

### 4.5.2. A Consequence of the Unequal Mobilities of Cations and Anions, the Transport Numbers

The current density $\vec{j}_i$ due to an ionic species *i* is related to the mobility $u_{\text{conv},i}$ in the following manner [*cf.* Eq. (4.159)]

$$\vec{j}_i = z_i F c_i (u_{\text{conv}})_i X \tag{4.159}$$

If therefore one considers a unit field $X = 1$ in an electrolyte solution containing a *z*:*z*-valent electrolyte (i.e., $z_+ = z_- = z$ and $c'_+ = c'_- = c$), then since $(u_{\text{conv}})_+ \neq (u_{\text{conv}})_-$, it follows that

$$j_+ \neq j_- \tag{4.233}$$

This is a thought-provoking result. It shows that although all ions feel the externally applied electric field to the extent of their charges, some respond by migrating more than others. It also shows that though the burden of carrying the current through the electrolytic solution falls on the whole community of ions, the burden is not shared equally among the various species of ions. Even if there are equal numbers

**TABLE 4.16**
**Transport Numbers of Cations in Aqueous Solutions at 298 K in 0.1 *N* Solutions**

| Electrolyte | HCl | LiCl | NaCl | KCl | $KNO_3$ | $AgNO_3$ | $BaCl_2$ |
|---|---|---|---|---|---|---|---|
| Transport number of cation, $t_+$ | 0.83 | 0.32 | 0.39 | 0.49 | 0.51 | 0.47 | 0.43 |

of the various ions, those that have higher mobility contribute more to the communal task of transporting the current through the electrolytic solution than the ions handicapped by lower mobilities.

It is logical under these circumstances to seek a quantitative measure of the extent to which each ionic species is taxed with the job of carrying current. This quantitative measure, known as the *transport number* (Table 4.16), should obviously be defined by the *fraction* of the total current carried by the particular ionic species, i.e.,

$$t_i = \frac{j_i}{j_T} = \frac{j_i}{\sum j_i} \tag{4.234}$$

This definition requires that the sum of the transport numbers of all the ionic species be unity for

$$\sum t_i = \sum \frac{j_i}{\sum j_i} = 1 \tag{4.235}$$

Thus, the conduction current carried by the species $i$ (e.g., $Na^+$ ions in a solution containing NaCl and KCl) depends upon the current transported by all the other species. Here then is a clear and simple indication that the drift of the $i$th species depends on the drift of the other species.

For example, consider a 1:1-valent electrolyte (e.g., HCl) dissolved in water. The transport numbers will be given by[30]

$$t_{H^+} = \frac{j_{H^+}}{j_{H^+} + j_{Cl^-}} = \frac{z_{H^+} F c_{H^+} u_{H^+} X}{z_{H^+} F c_{H^+} u_{H^+} X + z_{Cl^-} F c_{Cl^-} u_{Cl^-} X}$$

However, $z_{H^+} = z_{Cl^-} = 1$ and $c_{H^+} = c_{Cl^-} = c$, and therefore

[30]To avoid cumbersome notation, the symbol $u_{conv}$ for the conventional mobilities has been contracted to $u$. The absence of a bar above the $u$ stresses that it is not the absolute mobility $\bar{u}_{abs}$.

$$t_{H^+} = \frac{u_{H^+}}{u_{H^+} + u_{Cl^-}} \tag{4.236}$$

Similarly,

$$t_{Cl^-} = \frac{u_{Cl^-}}{u_{H^+} + u_{Cl^-}} \tag{4.237}$$

The mobilities of the $H^+$ and $Cl^-$ ions in 0.1 *N* HCl at 25 °C are $33.71 \times 10^{-4}$ and $6.84 \times 10^{-4}$ cm$^2$ s$^{-1}$ V$^{-1}$, respectively, from which it turns out the transport numbers of the $H^+$ and $Cl^-$ ions are 0.83 and 0.17, respectively. Thus, in this case, the positive ions carry a major fraction (~83%) of the current.

Now suppose that an excess of KCl is added to the HCl solution so that the concentration of $H^+$ is about $10^{-3}$ *M* in comparison with a $K^+$ concentration of 1 *M*. The transport numbers in the mixture of electrolytes will be

$$\frac{t_{K^+}}{t_{H^+}} = \frac{c_{K^+}u_{K^+}/\Sigma c_i u_i}{c_{H^+}u_{H^+}/\Sigma c_i u_i} \tag{4.238}$$

$$= \frac{c_{K^+}}{c_{H^+}} \frac{u_{K^+}}{u_{H^+}} \tag{4.239}$$

The ratio $c_{K^+}/c_{H^+}$ is $10^3$, and the ratio of mobilities is

$$\frac{u_{K^+}}{u_{H^+}} = \frac{6 \times 10^{-4}}{30 \times 10^{-4}} = \frac{1}{5}$$

Hence,

$$\frac{t_{K^+}}{t_{H^+}} = 200$$

which means that although the $H^+$ is about 5 times more mobile than the $K^+$ ion, it carries 200 times less current. Thus, the addition of the excess of KCl has reduced to a negligible value the fraction of the current carried by the $H^+$ ions.

In fact, the transport number of the $H^+$ ions under such circumstances is virtually zero, as shown from the following approximate calculation.

$$t_{H^+} = \frac{c_{H^+}u_{H^+}}{c_{H^+}u_{H^+} + c_{K^+}u_{K^+} + c_{Cl^-}u_{Cl^-}}$$

$$= \frac{10^{-6}u_{H^+}}{10^{-6}u_{H^+} + 10^{-3}u_{K^+} + 10^{-3}u_{Cl^-}} = 10^{-3} \qquad (4.240)$$

Thus the conduction current carried by an ion depends very much on the concentration in which the other ions are present.

### 4.5.3. The Significance of a Transport Number of Zero

In the previous section, it was shown that the addition of an excess of KCl makes the fraction of the migration (i.e., conduction) current carried by the $H^+$ ions tend to zero. What happens if this mixture of HCl and KCl is placed between two electrodes and a potential difference is applied across the cell (Fig. 4.74)?

In response to the electric field developed in the electrolyte, a migration of ions occurs and there is a conduction current in the solution. Since this conduction current is almost completely borne by $K^+$ and $Cl^-$ ions ($t_{H^+} \to 0$), there is a tendency for the

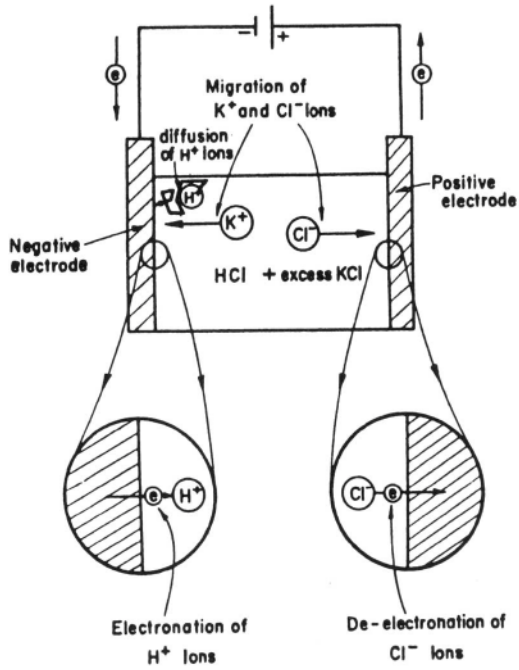


**Fig. 4.74.** A schematic diagram of the transport processes in an electrolyte (of HCl – KCl, with an excess of KCl) and of the reactions at the interfaces.

$Cl^-$ ions to accumulate near the positive electrode, and the $K^+$ ions near the negative electrode. If the excess negative charge near the positive electrode and vice versa were to build up, then the resulting field due to lack of electroneutrality (see Section 4.3.3) would tend to bring the conduction current to a halt. It has been argued (Section 4.3.4), however, that conduction (i.e., migration) currents are sustained in an electrolyte because of charge-transfer reactions (at the electrode–electrolyte interfaces), which remove the excess charge that tends to build up near the electrodes.

In the case of the HCl + KCl electrolyte, the reaction at the positive electrode may be considered the deelectronation of the $Cl^-$ ions. Furthermore, according to Faraday's law (see Section 4.3.5), 1 g-eq of $Cl^-$ ions must be deelectronated at the positive electrode for the passage of 1 F of charge in the external circuit. This means, however, that at the other electrode, 1 g-eq of positive ions must be involved in a reaction. Thus, either the $K^+$ or the $H^+$ ions must react, but by keeping the potential difference within certain limits one can ensure that only the $H^+$ ions react.

There is no difficulty in effecting the reaction of the layer of $H^+$ near the negative electrode, but to keep the reaction going, there must be a flux of $H^+$ ions from the bulk of the solution toward the negative electrode. By what process does this flux occur? It cannot be by migration because the presence of the excess of $K^+$ ions makes the transport number of $H^+$ tend to zero. It is here that diffusion comes into the picture; the removal of $H^+$ ions by the charge-transfer reactions causes a depletion of these ions near the electrode, and the resulting concentration gradient provokes a diffusion of $H^+$ ions toward the electrode.

To provide a quantitative expression for the diffusion flux $J_{H^+}$, one cannot use the Nernst–Planck flux equation (4.231) because the latter describes the independent flow of one ionic species and in the case under discussion it has been shown that the migration current of the $H^+$ ions is profoundly affected by the concentration of the $K^+$ ions. A simple modification of the Nernst–Planck equation can be argued as follows.

Since conduction (i.e., migration) and diffusion are the two possible[31] modes of transport for an ionic species, the total flux $J_i$ must be the sum of the conduction flux $(J_C)_i$ and the diffusion flux $(J_D)_i$. Thus,

$$J_i = (J_C)_i + (J_D)_i \tag{4.241}$$

The conduction flux is equal to $1/z_iF$ times the conduction current $j_i$ borne by the particular species

$$(J_C)_i = \frac{j_i}{z_iF} \tag{4.242}$$

[31] Another possible mode of transport, hydrodynamic flow, is not considered in this chapter.

and the conduction current carried by the species $i$ is related to the total conduction current $j_T = \sum j_i$ through the transport number of the species $i$ [*cf.* Eq. (4.234)]

$$j_i = t_i \sum j_i = t_i j_T \tag{4.243}$$

Hence,

$$(J_C)_i = \frac{t_i j_T}{z_i F} \tag{4.244}$$

Furthermore, the diffusion flux $(J_D)_i$ is given by[32]

$$(J_D)_i = -Bc_i \frac{d\mu_i}{dx} \tag{4.14}$$

or approximately by Fick's first law

$$(J_D)_i = -D_i \frac{dc_i}{dx} \tag{4.16}$$

so that the total flux of species $i$ is

$$J_i = \frac{t_i j_T}{z_i F} - Bc_i \frac{d\mu_i}{dx} \tag{4.245}$$

or approximately

$$J_i = \frac{t_i j_T}{z_i F} - D_i \frac{dc_i}{dx} \tag{4.246}$$

From these modified forms of the Nernst–Planck flux equation (4.231), one can see that even if $t_i \to 0$, it is still possible to have a flux of a species provided there is a concentration gradient, which is often brought into existence by interfacial charge-transfer reactions at the electrode–electrolyte interfaces consuming or generating the species.

From the modified Nernst–Planck flux equation (4.245), one can give a more precise definition of the transport number. If $d\mu_j/dx = 0$, in which case $dc_j/dx = 0$, then

---

[32]The constant $B$ has been shown in Section 4.4.6 to be equal to $\bar{u}_{abs}/N_A$.

$$t_j = \left(\frac{z_j F J_j}{j_T}\right)_{d\mu_j/dx=0}$$

$$= \left(\frac{j_j}{j_T}\right)_{d\mu_j/dx=0} \tag{4.247}$$

It should be emphasized therefore that the transport number only pertains to the conduction flux (i.e., to that portion of the flux produced by an *electric field*) and any flux of an ionic species arising from a chemical potential gradient (i.e., any diffusion flux) is *not* counted in its transport number. From this definition, the transport number of a particular species can tend to zero, $t_i \to 0$, and at the same time its diffusion flux can be finite.

This is an important point in electroanalytical chemistry, where the general procedure is to arrange for the ions that are being analyzed to move to the electrode-electrolyte interface by diffusion only. Then if the experimental conditions correspond to clearly defined boundary conditions (e.g., constant flux), the partial differential equation (Fick's second law) can be solved exactly to give a theoretical expression for the bulk concentration of the substance to be analyzed. In other words, the transport number of the substance being analyzed must be made to tend to zero if the solution of Fick's second law is to be applicable. This is ensured by adding some other electrolyte in such excess that it takes on virtually the entire burden of the conduction current. The added electrolyte is known as the *indifferent* electrolyte. It is indifferent only to the electrodic reaction at the interface; it is far from indifferent to the conduction current.

### 4.5.4. The Diffusion Potential, Another Consequence of the Unequal Mobilities of Ions

Consider that a solution of a $z$:$z$-valent electrolyte (of concentration $c$ moles $\mathrm{dm}^{-3}$) is instantaneously brought into contact with water at the plane $x = 0$ (Fig. 4.75). A concentration gradient exists both for the positive ions and for the negative ions. They therefore start diffusing into the water.

Since, in general,[33] $\bar{u}_+ \neq \bar{u}_-$, let it be assumed that $\bar{u}_+ > \bar{u}_-$. With the use of the Einstein relation (4.172), it is clear that

$$D_+ = \bar{u}_+ kT \quad \text{and} \quad D_- = \bar{u}_- kT$$

or that

[33] Though the subscript "abs" has been dropped, it is clear from the presence of a bar over the *us* that one is referring to absolute mobilities.

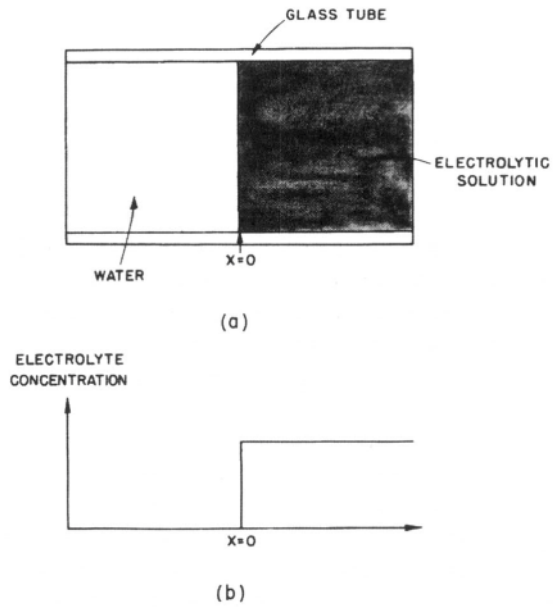


**Fig. 4.75.** (a) An electrolytic solution is instantaneously brought into contact with water at a plane $x = 0$; (b) the variation of the electrolyte concentration in the container at the instant of contact.

$$D_- < D_+$$

This means that the positive ions try to lead the negative ions in the diffusion into the water. But when an ionic species of one charge moves faster than a species of the opposite charge, any unit volume in the water phase will receive more ions of the faster-moving variety.

Compare two unit volumes (Fig. 4.76), one situated at $x_2$ and the other at $x_1$, where $x_2 > x_1$; i.e., $x_2$ is farther from the plane of contact ($x = 0$) of the two solutions. The positive ions are random-walking faster than the negative ions, and therefore the greater the value of $x$, the greater is the ratio $c_{+x}/c_{-x}$.

All this is another way of saying that the center of the positive charge tends to separate from the center of the negative charge (Fig. 4.76). Hence, there is a tendency for the segregation of charge and the breakdown of the law of electroneutrality.

When charges of opposite sign are spatially separated, a potential difference develops. This potential difference between two unit volumes at $x_2$ and $x_1$ *opposes* the attempt at charge segregation. The faster-moving positive ions face strong opposition from the electroneutrality field and they are slowed down. In contrast, the slower-

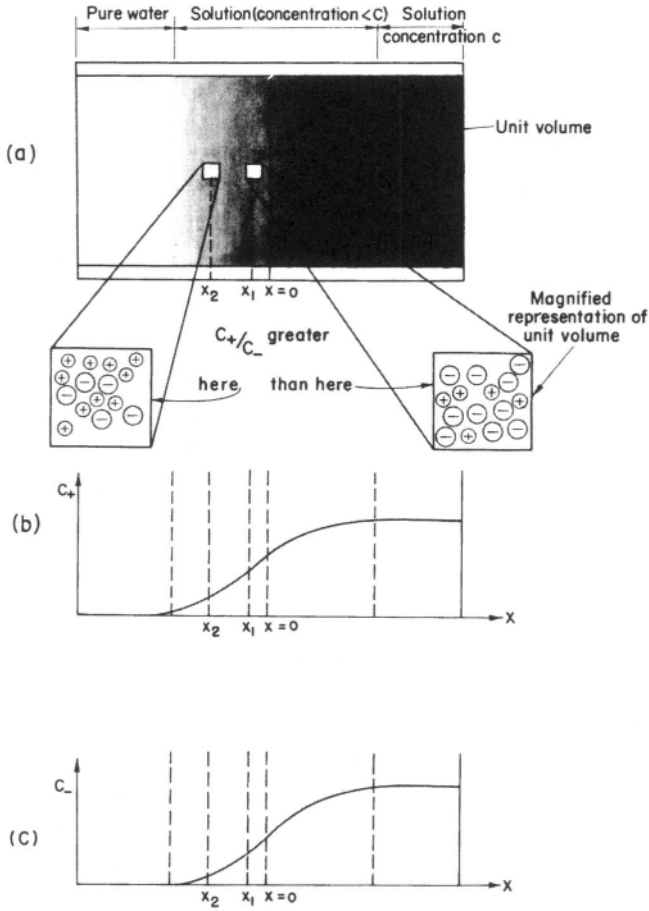


**Fig. 4.76.** (a) At a time $t > 0$ after the electrolyte and water are brought into contact, pure water and the electrolyte are separated by a region of mixing. In this mixing region, the $c_+/c_-$ ratio increases from right to left because of the higher mobility of the positive ions, (b) and (c) The distance variations of the concentrations of positive and negative ions.

moving negative ions are assisted by the potential difference (arising from the incipient charge separation) and they are speeded up. When a steady state is reached, the acceleration of the slow negative ions and the deceleration of the initially fast, positive ions resulting from the electroneutrality field that develops exactly compensate for the inherent differences in mobilities. The electroneutrality field is the leveler of ionic mobilities, helping and retarding ions according to their need so as to keep the situation as electroneutral as possible.

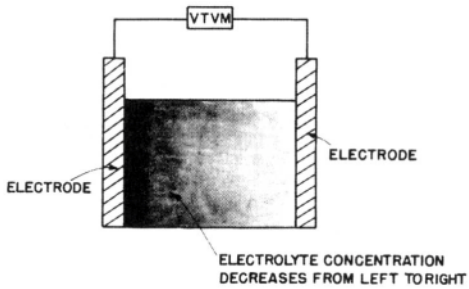


**Fig. 4.77.** A potential difference is registered by *a* vacuum-tube voltmeter (VTVM) connected to a concentration cell, i.e., to electrodes dipped in an electrolyte, the concentration of which varies from electrode to electrode.

The conclusion that may be drawn from this analysis has quite profound ramifications. The basic phenomenon is that whenever solutions of differing concentration are allowed to come into contact, diffusion occurs; there is a tendency for charge separation due to differences between ionic mobilities; and a potential difference develops across the interphase region in which there is a transition from the concentration of one solution to the concentration of the other.

This potential is known by the generic term *diffusion potential.* The precise name given to the potential varies with the situation, i.e., with the nature of the interphase region. If one ignores the interphase region and simply sticks two electrodes, one into each solution, in order to "tap" the potential difference, then the whole assembly is known as a *concentration cell* (Fig. 4.77). On the other hand, if one constrains or restricts the interphase region by interposing a sintered-glass disk or any uncharged membrane between the two solutions so that the concentrations of the two solutions are uniform up to the porous material, then one has a *liquid-junction potential* [34] (Fig. 4.78). A *membrane potential* is a more complicated affair for two main reasons: (1) There may be a pressure difference across the membrane, producing hydrodynamic flow of the solution, and (2) the membrane itself may consist of charged groups, some fixed and others exchangeable with the electrolytic solution, a situation equivalent to having sources of ions within the membrane.

[34]Now that the origin of a liquid-junction potential is understood, the method of minimizing it becomes clear. One chooses positive and negative ions with a negligible difference in mobilities; $K^+$ and $Cl^-$ ions are the usual pair. This is the basis of the so-called "KCI salt bridge."

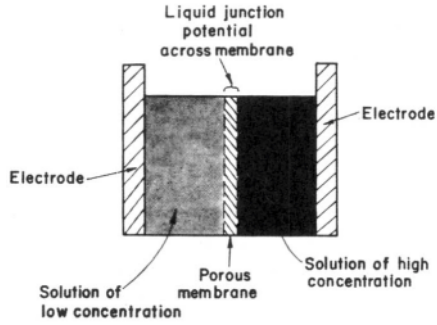


**Fig. 4.78.** A potential difference, the liquid-junction potential, is developed across a porous membrane introduced between two solutions of differing concentration.

### 4.5.5. Electroneutrallty Coupling between the Drifts of Different Ionic Species

The picture of the development of the electroneutrality field raises a general question concerning the flow or drift of ions in an electrolytic solution. Is the flux of one ionic species dependent on the fluxes of the other species? In the diffusion experiment just discussed, is the diffusion of positive ions affected by the diffusion of negative ions? The answer to both these questions is in the affirmative.

Without doubt, the ionic flows start off as if they were completely independent, but it is this attempt to assert their freedom that leads to an incipient charge separation and the generation of an electroneutrality field. This field, which is dependent on the flows of all ionic species, curtails the independence of any one particular species. In this way, the flow of one ionic species is "coupled" to the flows of the other species.

In the absence of any interaction or coupling between flows, i.e., when the drift of any particular ionic species $i$ is completely independent, the flow of that species $i$ (i.e., the number of moles of $i$ crossing per square centimeter per second) is described as follows.

The total driving force on an ionic species that is drifting independently of any other ionic species is the gradient of the electrochemical potential, $d\bar{\mu}_i/dx$. In terms of this total driving force, the expression for the total independent flux is given by the Nernst–Planck flux equation

$$J_i = \frac{j_i}{z_i F} = -\frac{u_i}{z_i F} c_i \frac{d\bar{\mu}_i}{dx} \tag{4.231}$$

When, however, the flux of the species $i$ is affected by the flux of the species $j$ through the electroneutrality field, then another modification (see Section 4.5.3) of the

Nernst–Planck flux equations has to be made. The modification that will now be described is a more detailed version which will lead us back to transport numbers.

### 4.5.6. How to Determine Transport Number

Before introducing the reader to the ways in which these transport numbers can be experimentally measured, it may be helpful to think again about just what they mean. The bare definition is given in Eq. (4.234) but this often only arouses puzzlement. For how, asks the thoughtful reader, can unequal amounts of negative and positive charges pass across a solution without doing injury to the electroneutrality condition that (understood over a time average) must always apply to the bulk of a solution?[35] The trouble seems at first a deep one because in some systems (an extreme case would be the liquid silicates) the alkali metal cation (a relatively small entity) has a $t_+$ near unity, whereas the anion (the giant silicate polyanion, in the case cited) hardly moves at all.

Looked at in terms of an analogy, the difficulty is seen to be less than real. Consider the ions as black (negative) and white (positive) balls. There are just two lines of black balls and white balls, an equal number of each, and both lines are at first stationary. Obviously, with an equal number of (oppositely charged) black and white balls, electroneutrality is preserved.

Now let the white balls all roll steadily off to the left while the black balls retain their stations. Let there be a machine that produces any required number of new white balls and inserts them into the beginning of this line on the right. Correspondingly, on the left, a consumer of white balls acts to bring about their disappearance. Consider then the middle part. The white balls move along while the black balls remain immovable. Then, framing a certain element of the bulk, the number of white and black balls remains always equal in number. As one white ball comes into the frame, one white ball also goes out of it. The blacks remain constant. Clearly, electroneutrality in the volume element considered is preserved. The same would be found for any piece of the bulk of the solution. The only reservation is the presence of the two machines, one of which produces the white balls on the right while another annihilates them on the left. In the real case, these functions would be supplied by the electrodes, the positive anode dissolving ions into the solution while the negative cathode destroys the ions by depositing them as atoms. So one can have $t_+$ and $t_-$ of any value, with the proviso that for a 1:1 electrolyte, $t_+ + t_- = 1$. Now let three entirely different approaches for determining $t$'s be described.

4.5.6.1. *Approximate Method for Sufficiently Dilute Solutions.* In order to use the method, one has to use the Einstein equation

[35] To the bulk only? Yes. For near the interfaces there is an electrode reaction (an exchange of charge of ions with the electrode) and the positive ions (the cations) will tend to exceed the negative ones (the anions) near the negative electrode (and obviously vice versa at the positive electrode).

$$kT\bar{u}_i = D_i \tag{4.172}$$

From this equation and from the definition of transport number, i.e., Eq. (4.236),

$$t_i = \frac{D_i}{D_i + D_j} \tag{4.248}$$

and then $t_i$ can be determined experimentally so long as the diffusion coefficients of the relevant ions can be measured (e.g., by means of radiotracers). However, there are a few reservations necessary before this method can be utilized.

1. The Einstein equation is exact only at very low concentrations in aqueous solution. As explained in a general way in Section 4.4.6, and in a detailed way for a given system in Section 5.6.6.2, there is usually some deviation—perhaps as much as 20%—between the results of Einstein's equation and experimental fact. Thus, outside very dilute solutions, using the Einstein equation to determine transport numbers is a rough-and-ready method and the results carry a burden of ±10%.

2. The method is clearly limited to ions that have suitable ($\beta$- or $\alpha$-emitting) radiotracers. Those ions having radioactive isotopes that emit $\gamma$ radiation are more difficult to measure because the long range and penetrating power of the $\gamma$ radiation make it difficult precisely to determine the position of the radiotracer ions as they spread through a solution.

Another approximate approach to determining transport number is to use the zeroth approximation equation for ionic mobility, i.e., Eq. (4.183)

$$u_{\text{conv}} = \frac{z_i e_0}{6\pi r_S \eta} \tag{4.183}$$

where $r_S$ is the Stokes radius of the ion concerned, $\eta$ is the viscosity of the solution, and $u_{\text{conv}}$ is the mobility or ionic velocity under a field gradient of 1 $\mathrm{V\ cm^{-1}}$.

All one has to know here is the viscosity (for dilute solutions this is roughly equal to that of water) and the radius $r_S$ of a hydrated ion. The principal approximation lies in the nature of the Stokes equation (4.175) (see Section 4.4.7). This may introduce an error of up to 25%.

4.5.6.2. *Hittorf's Method.* This method of determining transport numbers was devised as long ago as 1901 and has been described in innumerable papers and many books. Nevertheless, it is not all that simple to understand and contains a number of assumptions not always stated.

To start with, let an overall description of the method be given. The essentials of the apparatus (Fig. 4.79) are two clearly separated compartments joined by a substantial middle compartment. There is an aqueous electrolyte, say, silver nitrate, and if this

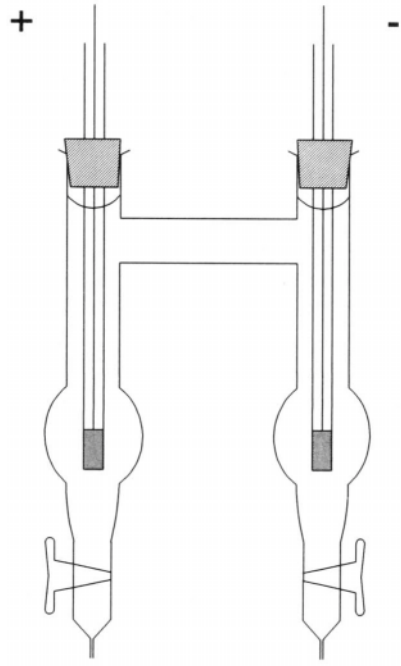


**Fig. 4.79.** Hittorf's cell. (After E. A. Muelwhyn Hughes, 1968)

is the case, the electrodes will each be made of silver. Before the experiment begins, the concentration of $AgNO_3$ is the same throughout the cell. The experiment involves passage of a direct electric current (from some power source not shown in the figure) through the cell.

At the left-hand electrode, Ag dissolves and increases the $AgNO_3$ concentration in this compartment. In the right-hand compartment, $Ag^+$ ions deposit so the $AgNO_3$ concentration decreases in the solution in the right-hand compartment. Measurement of the changes in concentration in each compartment after a 2–3 hr passage of current yields the transport number of the anion (since $t_+ + t_- = 1$, it also gives that of the cation). Now, let the analysis of what happens be written out.

The current gets passed for the requisite time. Thereafter, the anolyte (see Fig. 4.80) has an increased concentration $c_1$ and the catholyte a decreased concentration $c_3$. The middle compartment does not change its concentration of silver nitrate, which will be designated $c_2$.

After $t$ seconds (s) at current $I$, the number of g-ions of Ag introduced into the anolyte is

$$N = \frac{It}{\mathrm{F}} \tag{4.249}$$

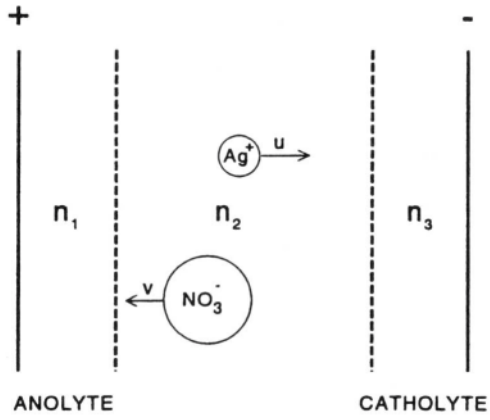


**Fig. 4.80.** The principle of Hittorf's experiment. (After E. A. Moelwhyn-Hughes, 1968)

where F is the faraday or electrical charge on one g-ion of $Ag^+$.

In the central compartment, in which the concentration is shown by experiment to remain constant, one can write for the current:

$$I = Ac_2F(u_2 + v_2) \tag{4.250}$$

where $A$ is the cross-sectional area of the central compartment and $u_2$ and $v_2$ are the ionic mobilities, respectively, of $Ag^+$ and $NO_3^-$, under a unit applied field. Therefore, from Eqs. (4.249) and (4.250)

$$N = Ac_2(u_2 + v_2)t \tag{4.251}$$

In the *left-hand* compartment, $Ag^+$ ions are not only produced, they also get moved out. Hence,

$$\frac{dN_1}{dt} = \frac{I}{F} - Ac_1u_1 \tag{4.252}$$

The principle of electroneutrality demands that the concentration of both positive and negative ions in the left-hand compartment be the same. Therefore,

$$\frac{dN_1}{dt} = Ac_2v_2 \tag{4.253}$$

which represents the rate at which anions introduced by dissolution from the silver electrode move into the left-hand compartment to partner the cation. Integrating (4.253) gives

$$N_1 - N_1^0 = A c_2 v_2 t \tag{4.254}$$

where $N_1^0$ is the number of moles of $AgNO_3$ in the compartment before the current $I$ was switched on.

Turning attention now to the catholyte, it follows that with the $Ag^+$ being removed by deposition and being augmented by transport from the middle compartment,

$$\frac{dN_3}{dt} = A c_2 u_2 - \frac{I}{F} \tag{4.255}$$

However, diffusion of $Ag^+$ and its removal by deposition is not the only thing happening in the right-hand compartment. $NO_3^-$ clearly moves out to allow electroneutrality to be maintained. It must move out at the same rate as $Ag^+$ disappears. Thus

$$\frac{dN_3}{dt} = -A c_3 v_3 \tag{4.256}$$

Integration of (4.256) gives

$$N_3^0 - N_3 = A c_3 v_3 t \tag{4.257}$$

It has been assumed all along (but it needs an experiment to verify it) that the central compartment keeps a constant concentration while the $AgNO_3$ is increasing on the anolyte and decreasing in the catholyte. Hence,

$$N_1 - N_1^0 = N_3^0 - N_3 \tag{4.258}$$

Now from Eqs. (4.251) and (4.254)

$$t_- = \frac{v_2}{u_2 + v_2} = \frac{N_1 - N_1^0}{N} = \frac{\text{Gain in weight in anolyte}}{\text{Loss of weight in anode}} \tag{4.259}$$

and from Eqs. (4.251) and (4.257),

$$\frac{N_3^0 - N_3}{N} = \frac{\text{Loss of weight of silver in catholyte}}{\text{Gain in weight of cathode}} \tag{4.260}$$

Is this all there is to be said about Dr. Hittorf 's classic method? The reader may have noticed a weak point in the argument. Where does the middle compartment begin and end? This is not a silly question if by "the middle compartment" one does not mean that section of the apparatus shown in the figure to divide the two compartments, but that section of the electrolyte between the two compartments which maintains its concentration constant. Thus, the method does have an Achilles heel: one has to be

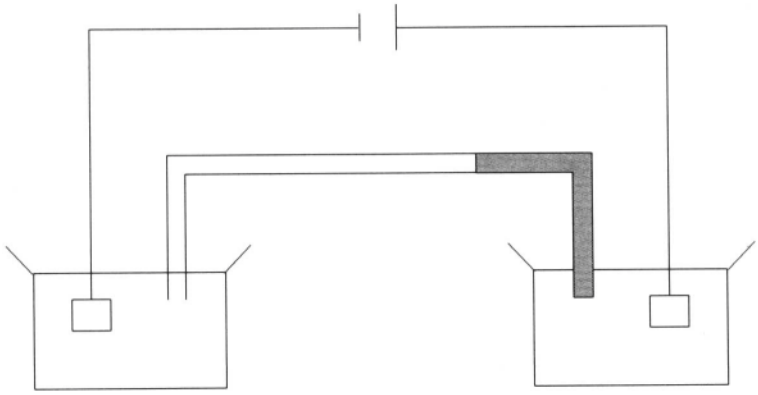

**Fig. 4.81**. Lodge's moving-boundary apparatus.

careful that the concentration changes that occur in anolyte and catholyte do not spread to the central compartment. This in turn means that the current must not flow for too long at a time and the downside of that is that the concentration changes in the cathode and anode compartments may not then be large enough to be accurately measurable.[36]

4.5.6.3. *Oliver Lodge's Experiment.* An experiment first done by the English physicist Oliver Lodge is the origin of a third method by which transport numbers can be obtained. Here also there is a limitation: one must be able to observe a boundary between two electrolytes, for knowledge of the boundary's movement is the observation upon which the method is based. This implies that the ions concerned must differ in color (not always an easy condition to fulfill) or at least in refractive index (but then the observation of the boundary may not always be easy).

To understand how this method works, let us have a look at Fig. 4.81. It involves a tube and in this tube there are two solutions and a boundary between them. Let the electrolyte in the upper compartment be named *MR* and be at a concentration *c*. The second (bottom) solution is ***M′R***, containing the same anion *R*, but a different cation, ***M′***.

Now a current is passed. The boundary moves and the velocity of that movement *u* is given by

$$u = \frac{x}{t} \tag{4.261}$$

with *x* being the distance the boundary moves in *t* s.

[36]However, this objection is much lessened by the improvement in differential analysis made in the last quarter-century.

Now from Eq. (4.250)

$$\mathrm{I} = AcF(u_+ + v_-) \tag{4.250}$$

where $A$ is the cross section of the solution. Hence, from Eqs. (4.250) and (4.261)

$$t_+ = \frac{u_+}{u_+ + u_-} = \frac{xAcF}{It} \tag{4.262}$$

One can see that the method would work best with a colored cation, e.g., a cation that is chromophoric, such as $Cr^{2+}$ ions.

### 4.5.7. The Onsager Phenomenological Equations

The development of an electroneutrality field introduces an interaction between flows and makes the flux of one species dependent on the fluxes of all the other species. To treat situations in which there is a coupling between the drift of one species and that of another, a general formalism will be developed. It is only when there is zero coupling or zero interaction that one can accurately write the Nernst–Planck flux equation

$$J_i = -\frac{u_i}{z_i F} c_i \frac{d\bar{\mu}_i}{dx} \tag{4.231}$$

Once the interaction (due to the electroneutrality field) develops, a correction term is required, i.e.,

$$J_i = -\frac{u_i}{z_i F} c_i \frac{d\bar{\mu}_i}{dx} + \text{Coupling correction} \tag{4.263}$$

It is in the treatment of such interacting transport processes, or coupled flows, that the methods of near-equilibrium thermodynamics yield a clear understanding of such phenomena, but only from a macroscopic or phenomenological point of view. These methods, as relevant to the present discussion, can be summarized with the following series of statements:

1. As long as the system remains close to equilibrium and the fluxes are independent, the fluxes are treated as proportional to the driving forces. Experience (Table 4.17) commends this view for diffusion [Fick's law, Eq. (4.16)], conduction [Ohm's law, Eq. (4.130)], and heat flow (Fourier's law). Thus, the *independent* flux of an ionic species 1 given by the Nernst–Planck equation (4.231) is written

$$J_1 = L_{11}\vec{F}_1 \tag{4.264}$$

where $L_{11}$ is the proportionality or phenomenological constant and $\vec{F}_1$ is the driving force.

**TABLE 4.17**
**Some Linear Flux–Force Laws**

| Phenomenon | Flux of | Driving Force | Law |
|---|---|---|---|
| Diffusion | Matter $J$ | Concentration gradient $dc/dx$ | Fick $J = -D\,dc/dx$ |
| Migration (conduction) | Charge $i$ | Potential gradient $X = -d\psi/dx$ | Ohm $i = \sigma X$ |
| Heat conduction | Heat $J_{heat}$ | Temperature gradient | Fourier $J_{heat} = K\,dT/dx$ |

2. When there is coupling, the flux of one species (e.g., $J_1$) is not simply proportional to its own (or as it is called, *conjugate*) driving force (i.e., $\vec{F}_1$), but receives contributions from the driving forces on all the other particles. In symbols,

$$J_1 = L_{11}\vec{F}_1 + \text{Coupling correction}$$

$$= L_{11}\vec{F}_1 + \begin{matrix}\text{Flux of 1 due}\\ \text{to driving force}\\ \text{on species 2}\end{matrix} + \begin{matrix}\text{Flux of 1 due}\\ \text{to driving force}\\ \text{on species 3}\end{matrix} + \text{etc.} \qquad (4.265)$$

3. The linearity or proportionality between fluxes and conjugate driving force is also valid for the contributions to the flux of one species from the forces on the *other* species. Hence, with this assumption, one can write Eq. (4.265) in the form

$$J_1 = L_{11}\vec{F}_1 + [L_{12}\vec{F}_2 + L_{13}\vec{F}_3 + \cdots] \qquad (4.266)$$

4. Similar expressions are used for the fluxes of all the species in the system. If the system consists of an electrolyte dissolved in water, one has three species: positive ions, negative ions, and water. By using the symbol + for the positive ions, – for the negative ions, and 0 for the water, the fluxes are

$$J_+ = L_{++}\vec{F}_+ + L_{+-}\vec{F}_- + L_{+0}\vec{F}_0$$

$$J_- = L_{-+}\vec{F}_+ + L_{--}\vec{F}_- + L_{-0}\vec{F}_0$$

$$J_0 = L_{0+}\vec{F}_+ + L_{0-}\vec{F}_- + L_{00}\vec{F}_0 \qquad (4.267)$$

These equations are known as the *Onsager phenomenological equations.* They represent a complete macroscopic description of the interacting flows when the system is near equilibrium.[37] It is clear that all the "straight" coefficients $L_{ij}$, where the indices

[37]If the system is not near equilibrium, the flows are no longer proportional to the driving forces [*cf.* Eq. (4.265)].

are equal, $i = j$, pertain to the independent, uncoupled fluxes. Thus $L_{++}X_+$ and $L_{--}X_-$ are the fluxes of the positive and negative ions, respectively, when there are no interactions. All other cross terms represent interactions between fluxes; e.g., $L_{+-}X_-$ represents the contribution to the flux of positive ions from the driving force on the negative ions.

5. What are the various coefficients $L_{ij}$? Onsager put forward the helpful *reciprocity relation.* According to this, all symmetrical coefficients are equal, i.e.,

$$L_{ij} = L_{ji} \tag{4.268}$$

This principle has the same status in nonequilibrium thermodynamics as the law of conservation of energy has in classical thermodynamics; it has not been disproved by experience.

### 4.5.8. An Expression for the Diffusion Potential

The expression for the diffusion potential can be obtained in a straightforward though hardly brief manner by using the Onsager phenomenological equations to describe the interaction flows. Consider an electrolytic solution consisting of the ionic species $\mathbf{M}^{z+}$ and $\mathbf{A}^{z-}$ and the solvent. When a transport process involves the ions in the system, there are two ionic fluxes, $J_+$ and $J_-$. Since, however, the ions are solvated, the solvent also participates in the motion of ions and hence there is also a solvent flux $J_0$.

If, however, the solvent is considered fixed, i.e., the solvent is taken as the coordinate system or the frame of reference,[38] then one can consider ionic fluxes *relative* to the solvent. Under this condition, $J_0 = 0$, and one has only two ionic fluxes. Thus, one can describe the interacting and independent ionic drifts by the following equations

$$J_+ = L_{++}\vec{F}_+ + L_{+-}\vec{F}_- \tag{4.269}$$

$$J_- = L_{-+}\vec{F}_+ + L_{--}\vec{F}_- \tag{4.270}$$

The straight coefficients $L_{++}$ and $L_{--}$ represent the independent flows, and the cross coefficients $L_{+-}$ and $L_{-+}$, the coupling between the flows.

The important step in the derivation of the diffusion potential is the statement that under conditions of steady state, the electroneutrality field sees to it that the quantity of positive charge flowing into a volume element is equal in magnitude but opposite in sign to the quantity of negative charge flowing in (Fig. 4.82). That is,

[38] Coordinate systems are chosen for convenience.

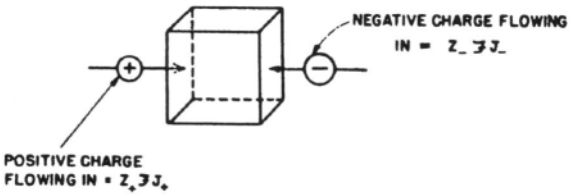


**Fig. 4.82.** According to the principle of electroneutrality as applied to the fluxes, the flux of positive ions into a volume element must be equal to the flux of negative ions into the volume element, so that the total negative charge is equal to the total positive charge.

$$z_+FJ_+ + z_-FJ_- = 0 \tag{4.271}$$

For convenience, $z_+F$ and $z_-F$ are written as $q_+$ and $q_-$, respectively. Now the expressions (4.269) and (4.270) for $J_+$ and $J_-$ are substituted in Eq. (4.271)

$$q_+L_{++}\vec{F}_+ + q_+L_{+-}\vec{F}_- + q_-L_{-+}\vec{F}_+ + q_-L_{--}\vec{F}_- = 0$$

or

$$\vec{F}_+(q_+L_{++} + q_-L_{-+}) + \vec{F}_-(q_+L_{+-} + q_-L_{--}) = 0 \tag{4.272}$$

Using the symbols

$$p_+ = q_+L_{++} + q_-L_{-+} \tag{4.273}$$

and

$$p_- = q_+L_{+-} + q_-L_{--} \tag{4.274}$$

one has

$$p_+\vec{F}_+ + p_-\vec{F}_- = 0 \tag{4.275}$$

What are the driving forces $\vec{F}_+$ and $\vec{F}_-$ for the independent flows of the positive and negative ions? They are the gradients of electrochemical potential (see Section 4.4.15)

$$\vec{F}_+ = \frac{d\mu_+}{dx} + q_+\frac{d\varphi}{dx} \tag{4.276}$$

and

$$\vec{F}_- = \frac{d\mu_-}{dx} + q_- \frac{d\varphi}{dx} \tag{4.277}$$

With these expressions, Eq. (4.275) becomes

$$p_+ \frac{d\mu_+}{dx} + p_+ q_+ \frac{d\varphi}{dx} + p_- \frac{d\mu_-}{dx} + p_- q_- \frac{d\varphi}{dx} = 0$$

or

$$-\frac{d\psi}{dx} = \frac{p_+}{p_+ q_+ + p_- q_-} \frac{d\mu_+}{dx} + \frac{p_-}{p_+ q_+ + p_- q_-} \frac{d\mu_-}{dx} \tag{4.278}$$

It can be shown, however, that (Appendix 4.3)

$$\frac{p_+}{p_+ q_+ + p_- q_-} = \frac{t_+}{z_+ F} \tag{4.279}$$

and

$$\frac{p_-}{p_+ q_+ + p_- q_-} = \frac{t_-}{z_- F} \tag{4.280}$$

where $t_+$ and $t_-$ are the transport numbers of the positive and negative ions. By making use of these relations, Eq (4.278) becomes

$$-\frac{d\psi}{dx} = \frac{t_+}{z_+ F} \frac{d\mu_+}{dx} + \frac{t_-}{z_- F} \frac{d\mu_-}{dx}$$

$$= \sum \frac{t_i}{z_i F} \frac{d\mu_i}{dx} \tag{4.281}$$

The negative sign before the electric field shows that it is opposite in direction to the chemical potential gradients of all the diffusing ions.

If one considers (Fig. 4.83) an infinitesimal length $dx$ parallel to the direction of the electric- and chemical-potential fields, one can obtain the electric-potential difference $d\psi$ and the chemical-potential difference $d\mu$ across the length $dx$

$$-\frac{d\psi}{dx} dx = \sum \frac{t_i}{z_i F} \frac{d\mu_i}{dx} dx \tag{4.282}$$

or

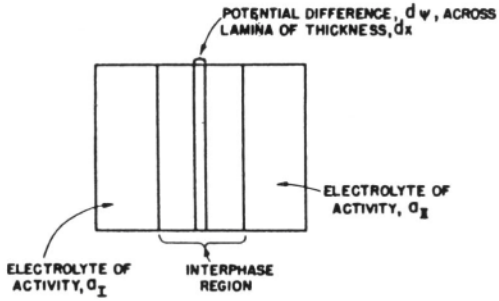


**Fig. 4.83.** Schematic representation of a *dx*-thick lamina in the interphase region between two electrolytes of activities $a_I$ and $a_{II}$.

$$-d\psi = \frac{1}{F}\sum \frac{t_i}{z_i} d\mu_i \tag{4.283}$$

$$= \frac{RT}{F}\sum \frac{t_i}{z_i} d\ln a_i \tag{4.284}$$

This is the basic equation for the diffusion potential. It has been derived here on the basis of a realistic point of view, namely, that the diffusion potential arises from the *nonequilibrium* process of diffusion.

There is, however, another method[39] of deriving the diffusion potential. One takes note of the fact that when a steady-state electroneutrality field has developed, the system relevant to a study of the diffusion potential hangs together in a delicate balance. The diffusion flux is exactly balanced by the electric flux; the concentrations and the electrostatic potential throughout the interphase region *do not vary with time.* (Remember the derivation of the Einstein relation in Section 4.4.) In fact, one may turn a blind eye to the drift and pretend that the whole system is in equilibrium.

On this basis, one can equate to zero the sum of the electrical and diffusional work of transporting ions across a lamina *dx* of the interphase region (Fig. 4.84). If one equivalent of charge (both positive and negative ions) is taken across this lamina, the electrical work is $F\,d\psi$. But this one equivalent of charge consists of $t_+/z_+$ moles of positive ions and $t_-/z_-$ moles of negative ions. Hence, the diffusional work is $d\mu_+$ per mole, or $(t_+/z_+)\,d\mu_+$ per $t_+/z_+$ moles, of positive ions and $(t_-/z_-)\,d\mu_-$ per $t_-/z_-$ moles of negative ions. Thus,

[39]This method is based on Thomson's hypothesis, according to which it is legitimate to apply equilibrium thermodynamics to the reversible parts of a steady-state, nonequilibrium process.

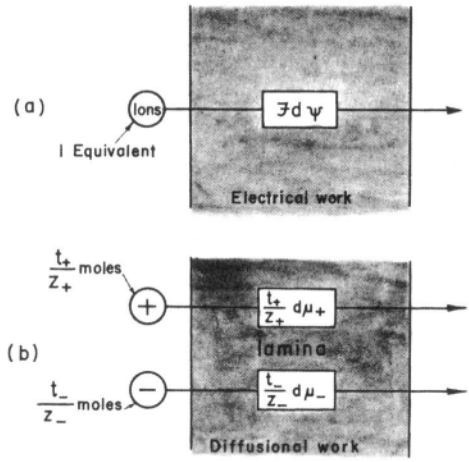


**Fig. 4.84.** The sum of (a) the electrical work $F\,d\psi$ and (b) the diffusional work $(t_+/z_+)d\mu_+ + (t_-/z_-)d\mu_-$ of transporting one equivalent of ions across a $dx$-thick lamina in the interphase region is equal to zero.

$$F\,d\psi + \frac{t_+}{z_+}d\mu_+ + \frac{t_-}{z_-}d\mu_- = 0 \tag{4.285}$$

or

$$-d\psi = \frac{1}{F}\sum \frac{t_i}{z_i}\,d\mu_i \tag{4.283}$$

$$= \frac{RT}{F}\sum \frac{t_i}{z_i}\,d\ln a_i \tag{4.284}$$

### 4.5.9. The Integration of the Differential Equation for Diffusion Potentials: The Planck–Henderson Equation

An equation has been derived for the diffusion potential [*cf.* Eq. (4.283)], but it is a *differential* equation relating the infinitesimal potential difference $d\psi$ developed across an infinitesimally thick lamina $dx$ in the interphase region. What one measures experimentally, however, is the total potential difference $\Delta\psi = \psi^0 - \psi^l$ across a transition region extending from $x = 0$ to $x = l$ (Fig. 4.85). Hence, to theorize about the

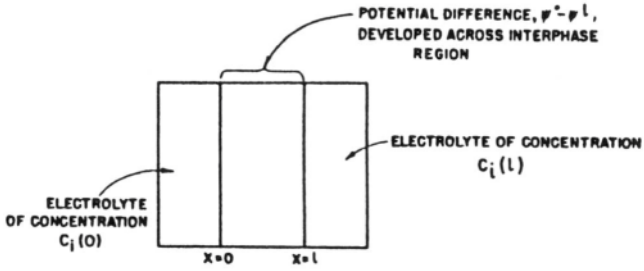


**Fig. 4.85.** The measured quantity is the total potential difference $\psi^0 - \psi^l$ across the whole interphase region between electrolytes of differing concentration $c_i(0)$ and $c_i(l)$.

measured potential differences, one has to integrate the differential equation (4.283); i.e.,

$$-\Delta\psi = \psi^0 - \psi^l = \frac{1}{F}\sum_i \int_{x=0}^{x=l} \frac{t_i}{z_i}\frac{d\mu_i}{dx}\,dx$$

$$= \frac{RT}{F}\sum_i \int_{x=0}^{x=l} \frac{t_i}{z_i}\frac{d\ln a_i}{dx}\,dx$$

$$= \frac{RT}{F}\sum_i \int_{x=0}^{x=l} \frac{t_i}{z_i}\frac{1}{f_i c_i}\frac{d(f_i c_i)}{dx}\,dx \qquad (4.286)$$

Here lies the problem. To carry out the integration, one must know:

1. How the concentrations of all the species vary in the transition region.
2. How the activity coefficients $f_i$ vary with $c_i$.
3. How the transport number varies with $c_i$.

The general case is too difficult to solve analytically, but several special cases can be solved. For example (Fig. 4.86), the activity coefficients can be taken as unity, $f_i = 1$—ideal conditions; the transport numbers $t_i$ can be assumed to be constant; and a linear variation of concentrations with distance can be assumed. The last assumption implies that the concentration $c_i(x)$ of the $i$th species at $x$ is related to its concentration $c_i(0)$ at $x = 0$ in the following way

$$c_i(x) = c_i(0) + k_i x \qquad (4.287)$$

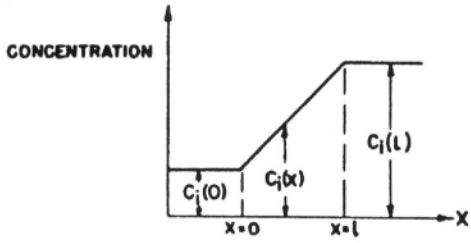


**Fig. 4.86.** In the derivation of the Planck–Henderson equation, a linear variation of concentration is assumed in the interphase region, which commences at $x = 0$ and ends at $x = l$.

and

$$\frac{dc_i}{dx} = \text{Constant} = k_i = \frac{c_i(l) - c_i(0)}{l} \tag{4.288}$$

With the aid of these assumptions, the integration becomes simple. Thus, with $t_i \neq f(x), f_i = 1$, and Eqs. (4.287) and (4.288), one has in (4.286)

$$-\Delta\psi = \frac{RT}{F} \sum_i \int_{x=0}^{x=l} \frac{t_i}{z_i} \frac{k_1\, dx}{c_i(0) + k_1 x}$$

$$= \frac{RT}{F} \sum_i \frac{t_i}{z_i} \int_{x=0}^{x=l} \frac{d[c_i(0) + k_1 x]}{c_i(0) + k_1 x}$$

$$= \frac{RT}{F} \sum_i \frac{t_i}{z_i} \left\{ \ln \left[ c_i(0) + k_1 x \right] \right\}_{x=0}^{x=l}$$

$$= \frac{RT}{F} \sum_i \frac{t_i}{z_i} \ln \frac{c_i(l)}{c_i(0)} \tag{4.289}$$

This is known as the Planck–Henderson equation for diffusion or liquid-junction potentials.

In the special case of a $z{:}z$-valent electrolyte, $z_+ = z_- = z$ and $c_+ = c_- = c$, Eq. (4.289) reduces to

$$-\Delta\psi = \frac{RT}{zF} (t_+ - t_-) \ln \frac{c(l)}{c(0)} \tag{4.290}$$

and since $t_+ + t_- = 1$,

$$-\Delta\psi = (2t_+ - 1)\frac{RT}{zF}\ln\frac{c(l)}{c(0)} \tag{4.291}$$

In the highly simplified treatment of the diffusion potential that has just been presented, several drastic assumptions have been made. The one regarding the concentration variation within the transition region can be avoided. One may choose a more realistic concentration versus distance relationship either by thinking about it in more detail or by using experimental knowledge on the matter. Similarly, instead of assuming the activity coefficients to be unity, one can feed in the theoretical or experimental concentration dependence of the activity coefficients. Of course, the introduction of nonideality $(f_i \neq 1)$ makes the mathematics awkward; in principle, however, the problem is understandable.

What about the assumption of the constancy of the transport number? Is this reasonable? In the case of a *z*:*z*-valent electrolyte, the transport number depends on the mobilities

$$t_+ = \frac{u_+}{u_+ + u_-} \quad \text{and} \quad t_- = \frac{u_-}{u_+ + u_-}$$

Thus, the constancy of the transport numbers with concentration depends on the degree to which the mobilities vary with concentration. That is something to be dealt with in the model-oriented arguments of the next section.

### 4.5.10. A Bird's Eye View of Ionic Transport

In the section on diffusion (Section 4.2), we were concerned with the random walk, but we learned that because this type of movement is purposeless in direction, it causes particles to spread out in all available directions. To bring about a diffusional flux in a given direction, all one has to do is to introduce a concentration gradient into the system and, although the movement of each particle is random, the fact that there are fewer ions in one direction than in others means that the random walk gradually raises the concentration in the dilute parts of the solution until all is uniform. In this sense, there is a directed diffusion flux down the concentration gradient.

Then we discussed the idea that this randomness can have superimposed upon it an electrical field that does indeed have a direction, so that there are still random motions by cations and the anions, but a little less randomness for the positive ion in the direction of the negative electrode and for the negative ion in the direction of the positive electrode. There thus arises a net drift of ions in the direction of the field.

In the phenomenological treatment of the directed drift that the field brings, we take the attitude that there is a stream of cations going toward the negative electrode and anions going toward the positive one. We now neglect the random diffusive movements; they do not contribute to the vectorial flow that produces an electrical current.

This discussion then follows on to give rise to the idea of a *transport number*. This is a term that describes the fact that when we talk about the drift velocity, cations and anions of equal but opposite charge do not have the same speed although the applied field is the same. On the whole, cations tend to be smaller than anions and we show that the drift velocity is inversely proportional to the radius of the solvated ion, so that transport numbers tend to be larger for the cation and smaller for the anion in an electrolyte.

This brings us to an apparent dilemma because, according to laws first laid down by Faraday himself, when one passes a certain amount of electricity through a solution for a certain time, the number of cations and anions carrying the same numerical charge put on the cathode and anode, respectively, is the same.

Because there is a difference in the cationic and anionic transport number and hence mobilities, this is at first difficult to understand. One would expect more of the ions with the higher transport number to be preferentially deposited.

The dilemma is solved by taking into account the fact that the lack of an equal supply rate for cations and anions carried toward the electrodes by the electric current will create a concentration gradient near the interface for the slower ions, and this concentration gradient will speed up the motion of the slower ions to compensate for their poorer performance. It is this diffusional component that makes Faraday's laws come true. The diffusional gradient pitches in to help the slower ions to the electrode at the same rate as the faster ones.

Several famous equations (Einstein, Stokes–Einstein, Nernst–Einstein, Nernst–Planck) are presented in this chapter. They derive from the heyday of phenomenological physical chemistry, when physical chemists were moving from the predominantly thermodynamic approach current at the end of the nineteenth century to the molecular approach that has characterized electrochemistry in this century. The equations were originated by Stokes and Nernst but the names of Einstein and Planck have been added, presumably because these scientists had examined and discussed the equations first suggested by the other men.

As stated earlier, these phenomenological relationships existed after physical chemistry had passed through its predominantly thermodynamic stage. However, Onsager produced a late bloom in the 1930s by applying *nonequilibrium thermodynamics* to transport in ionic solutions. In this subdiscipline, *transport coefficients* are described and their relation to ionic drift in terms of the interaction between the ions (sodium–sodium, chloride–chloride, and sodium–chloride) is represented mathematically. Accordingly, the potential difference between two liquid phases differing in ionic concentrations or even in ionic species is treated in terms of Onsager's theory, and the equation for the electrical potential across a liquid–liquid junction is derived and presented as the Planck–Henderson equation. All this then is a phenomenological prelude to applying ionic-atmosphere concepts (see Chapter 3) to ionic migration in order to provide the physical explanation of a famous empirical law due originally to

Kohlrausch—that equivalent conductivity decreases linearly with the increase of the square root of the concentration.

## Further Reading

### *Seminal*

1. M. Planck, "Diffusion and Potential at Liquid–Liquid Boundaries," *Ann. Physik* **40**: 561 (1890).
2. P. Henderson, "An Equation for the Calculation of Potential Difference at any Liquid Junction Boundary," *Z. Phys. Chem. (Leipzig)* **59**: 118 (1907).
3. C. A. Angell and J. O'M. Bockris, "The Measurement of Diffusion Coefficients," *J. Sci. Instrum.* **29**: 180(1958).

### *Review*

1. P. Turq, J. Barthel, and M. Chemla, *Transport, Relaxation and Kinetic Processes in Electrolyte Solutions,* Springer-Verlag, Berlin (1992).

### *Papers*

1. O. J. Riveros, *J. Phys. Chem.* **96**: 6001 (1992).
2. T. F. Fuller and J. Newman, *J. Electrochem. Soc.* **139**: 1332 (1992).
3. P. Vanysek, *Adv. Chem. Ser.* **235**: 55 (1994).
4. M. Olejnik, A. Blahut, and A. B. Szymanski, *Appl. Opt.* **24**: 83 (1994).
5. M. Suzuki, *J. Electroanal. Chem.* **384**: 77 (1995).
6. K. Aoki, *J. Electroanal. Chem.* **386**: 17 (1995).

## 4.6. INFLUENCE OF IONIC ATMOSPHERES ON IONIC MIGRATION

### 4.6.1. Concentration Dependence of the Mobility of Ions

In the phenomenological treatment of conduction (Section 4.2.12), it was stated that the equivalent conductivity $A$ varies with the concentration $c$ of the electrolyte according to the empirical law of Kohlrausch [Eq. (4.139)]

$$\Lambda = \Lambda^0 - A c^{1/2} \tag{4.139}$$

where $A$ is a constant and $\Lambda^0$ is the pristine or ungarbled value of equivalent conductivity, i.e., the value at infinite dilution.

The equivalent conductivity, however, has been related to the conventional electrochemical mobilities[40] $u_+$ and $u_-$ of the current-carrying ions by the following expression

[40]To avoid cumbersome notation, the conventional mobilities are written in this section without the subscript "conv"; i.e., one writes $u_+$ instead of $(u_{conv})_+$.

$$\Lambda = F(u_+ + u_-) \tag{4.163}$$

from which it follows that

$$\Lambda^0 = F(u_+^0 + u_-^0) \tag{4.292}$$

where the $u^0$s are the conventional mobilities (i.e., drift velocities under a field of 1 V $cm^{-1}$) at infinite dilution. Thus, Eq. (4.163) can be written as

$$(u_+ + u_-) = (u_+^0 + u_-^0) - \left(\frac{A}{F}\frac{1}{2}\right)(c_+^{1/2} + c_-^{1/2}) \tag{4.293}$$

or it can be split up into two equations

$$u_+ = u_+^0 - A'c_+^{1/2} \tag{4.294}$$

and

$$u_- = u_-^0 - A'c_-^{1/2} \tag{4.295}$$

What is the origin of this experimentally observed dependence of ionic mobilities on concentration? Equations (4.294) and (4.295) indicate that the more ions there are per unit volume, the more they diminish each other's mobility. In other words, at appreciable concentrations, the movement of any particular ion does not seem to be independent of the existence and motions of the other ions, and there appear to be forces of interaction between ions. This coupling between the individual drifts of ions has already been recognized, but now the discussion is intended to be on an atomistic rather than phenomenological level. The interactions between ions can be succinctly expressed through the concept of the ionic cloud (Chapter 3). It is thus necessary to analyze and incorporate ion-atmosphere effects into the zero-approximation atomistic picture of conduction (Section 4.4) and in this way understand how the mobilities of ions depend on the concentration of the electrolyte.

Attention should be drawn to the fact that there has been a degree of inconsistency in the treatments of ionic clouds (Chapter 3) and the elementary theory of ionic drift (Section 4.4.2). When the ion atmosphere was described, the central ion was considered—from a time-averaged point of view—at rest. To the extent that one seeks to interpret the equilibrium properties of electrolytic solutions, this picture of a static central ion is quite reasonable. This is because in the absence of a spatially directed field acting on the ions, the only ionic motion to be considered is random walk, the characteristic of which is that the mean distance traveled by an ion (not the mean square distance; see Section 4.2.5) is zero. The central ion can therefore be considered to remain where it is, i.e., to be at rest.

When, however, the elementary picture of ionic drift (Section 4.4.2) was sketched, the ionic cloud around the central ion was ignored. This approximation is justified only when the ion atmosphere is so tenuous that its effects on the movement of ions can be neglected. This condition of extreme tenuosity (in which there is a negligible coupling between ions) obtains increasingly as the solution tends to infinite dilution. Hence, the simple, unclouded picture of conduction (Section 4.4) is valid only at infinite dilution.

To summarize the duality of the treatment so far: When the ion atmosphere was treated in Chapter 3, the motion of the central ion was ignored and only equilibrium properties fell within the scope of analysis; when the motion of the central ion under an applied electric field was considered, the ionic cloud (which is a convenient description of the interactions between an ion and its environment) was neglected and only the infinite-dilution conduction could be analyzed. Thus, a unified treatment of *ionic atmospheres around moving ions* is required. The central problem is: How does the interaction between an ion and its cloud affect the motion of the ion?

### 4.6.2. Ionic Clouds Attempt to Catch Up with Moving Ions

In the absence of a driving force (e.g., an externally applied electric field), no direction in space from the central ion is privileged. The Coulombic field of the central ion has spherical symmetry and therefore the probability of finding, say, a negative ion at a distance $r$ from the reference ion is the same irrespective of the direction in which the point $r$ lies. On this basis, it was shown that the ionic cloud was spherically symmetrical (see Section 3.8.2).

When, however, the ions are subject to a driving force (be it an electric field, a velocity field due to the flow of an electrolyte, or a chemical-potential field producing diffusion), one direction in space becomes privileged. The distribution function (which is a measure of the probability of finding an ion of a certain charge in a particular volume element) has to be lopsided, or asymmetrical. The probability depends not only on the distance of the volume element from the central ion but also on the direction in which the volume element lies in relation to the direction of ionic motion. The procedure of Chapter 3 no longer applies. One cannot simply assume a Boltzmann distribution and, for the work done to bring an ion (of charge $z_i e_0$) to the volume element under consideration, use the electrostatic work $z_i e_0 \psi$ because the electrostatic potential $\psi$ was, in the context of Chapter 3, a function of $r$ only and one would then infer a symmetrical distribution function.

The rigorous but unfortunately mathematically difficult approach to the problem of ionic clouds around moving ions is to seek the asymmetrical distribution functions and then work out the implications of such functions for the electric fields developed among moving ions. A simpler approach will be followed here. This is the relaxation approach. The essence of relaxation analysis is to consider a system in one state, then perturb it slightly with a stimulus and analyze the *time dependence* of the system's response to the stimulus. (It will be seen later that relaxation techniques are much used in modern studies of the mechanism of electrode reactions.)

Consider therefore the spherically symmetrical ionic cloud around a stationary central ion. Now let the stimulus of a driving force displace the reference ion in the $x$ direction. The erstwhile spherical symmetry of the ion atmosphere can be restored only if its contents (the ions and the solvent molecules) *immediately* readjust to the new position of the central ion. This is possible only if the movements involved in restoring spherical symmetry are instantaneous, i.e., if no frictional resistances are experienced in the course of these movements. But the readjustment of the ionic cloud involves ionic movements which are rate processes. Hence, a finite time is required to reestablish spherical symmetry.

Even if this time were available, spherical symmetry would obtain only if the central ion did not move still farther away while the ionic cloud was trying to readjust. Under the influence of the externally applied field, the central ion just keeps moving on, and its ionic atmosphere never quite catches up. It is as though the part of the cloud behind the central ion is left standing. This is because its reason for existence (the field of the central ion) has deserted it and thermal motions try to disperse this part of the ionic cloud. In front of the central ion, the cloud is being continually built up. When ions move therefore, one has a picture of the ions losing the part of the cloud behind them and building up the cloud in front of them.

### 4.6.3. An Egg-Shaped Ionic Cloud and the "Portable" Field on the Central Ion

The constant lead which the central ion has on its atmosphere means that the center of charge of the central ion is displaced from the center of charge of its cloud. The first implication of this argument is that the ionic cloud is no longer spherically symmetrical around the *moving* central ion. It is egg-shaped (see Fig. 4.87).

A more serious implication is that since the center of charge on a drifting central ion does not coincide with the center of charge of its oppositely charged (egg-shaped) ionic cloud, an electrical force develops between the ion and its cloud. The development of an electrical force between a moving ion and its lagging atmosphere means that the ion is then subject to an electric field. Since this field arises from the continual relaxation (or decay) of the cloud behind the ion and its buildup in front of the ion, it is known as a *relaxation field.* Notice, however, that the centers of charge of the ion and of the cloud lie on the path traced out by the moving ion (Fig. 4.88). Consequently, the relaxation field generated by this charge separation acts in a direction precisely opposite to that of the driving force on the ion (e.g., the externally applied field). Hence, a moving ion, by having an egg-shaped ionic cloud, carries along its own "portable" field of force, the relaxation field, which acts to retard the central ion and decrease its mobility compared with that which it would have were it only pulled on by the externally applied field and retarded by the Stokes force [the zeroth-order theory of conductance; see Eq. (4.183)].

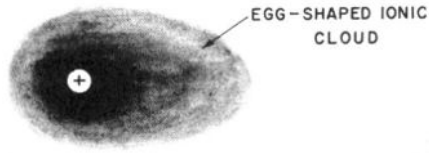


**Fig. 4.87.** The egg-shaped ionic cloud around a moving central ion.

### 4.6.4. A Second Braking Effect of the Ionic Cloud on the Central Ion: The Electrophoretic Effect

The externally applied electric field acts not only on the central ion but also on its oppositely charged cloud. Consequently, the ion and its atmosphere tend to move in *opposite directions.*

This poses an interesting problem. The ionic atmosphere can be considered a charge sphere of radius $\kappa^{-1}$ (Fig. 4.89). The charged sphere moves under the action of an electric field. The thickness of the ionic cloud in a millimolar solution of a 1:1 -valent electrolyte is about 10 nm (see Table 3.2). One is concerned therefore with the migration of a fairly large "particle" under the influence of the electric field. The term *electrophoresis* is generally used to describe the migration of particles of colloidal dimensions (1 to 1000 nm) in an electric field. It is appropriate therefore to describe the migration of the ionic cloud as an *electrophoretic effect.*

The interesting point is that when the ionic cloud moves, it tries to carry along its entire baggage: the ions and the solvent molecules constituting the cloud *plus* the central ion. Thus, not only does the moving central ion attract and try to keep its cloud (the *relaxation effect*), but the moving cloud also attracts and tries to keep its central ion by means of a force which is then termed the *electrophoretic force* $\vec{F}_E$.

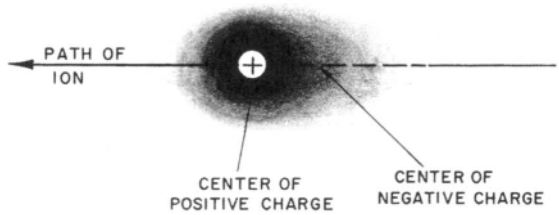


**Fig. 4.88.** The centers of charge of the ion and of the cloud lie on the path of the drifting ion.

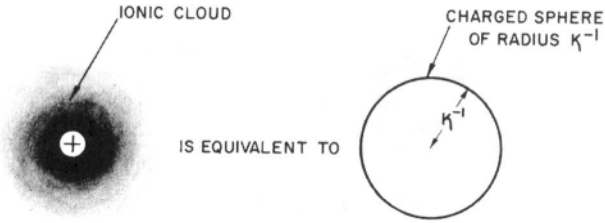


**Fig. 4.89.** The ionic atmosphere can be considered a charged sphere of radius $\kappa^{-1}$.

### 4.6.5. The Net Drift Velocity of an Ion Interacting with Its Atmosphere

In the elementary treatment of the migration of ions, it was assumed that the drift velocity of an ion was determined solely by the *electric force* $\vec{F}$ arising from the externally applied field. When, however, the mutual interactions between an ion and its cloud were considered, it turned out (Sections 4.6.3 and 4.6.4) that there were two other forces operating on an ion. These extra forces consisted of (1) the *relaxation force* $\vec{F}_R$ resulting from the distortion of the cloud around a moving ion and (2) the *electrophoretic force* $\vec{F}_E$ arising from the fact that the ion shares in the electrophoretic motion of its ionic cloud. Thus, in a rigorous treatment of the migrational drift velocity of ions, one must consider a *total force* $\vec{F}_{\text{total}}$, which is the resultant of force due to the applied electric field together with the relaxation and electrophoretic forces (Fig. 4.90)

$$\vec{F}_{\text{total}} = \vec{F} - (\vec{F}_E + \vec{F}_R) \tag{4.296}$$

The minus sign is used because both the electrophoretic and relaxation forces act in a direction opposite to that of the externally applied field.

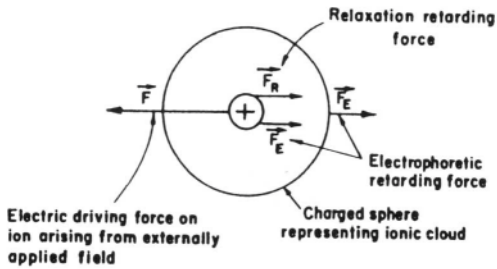


**Fig. 4.90.** The ion drift due to a net force which is a resultant of the electric driving force and two retarding forces, the relaxation and electrophoretic forces.

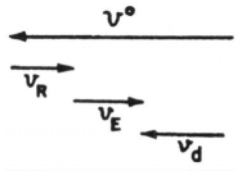


**Fig. 4.91.** The components of the overall drift velocity.

Since an ion is subject to a resultant or net force, its drift velocity also must be a *net* drift velocity resolvable into components. Furthermore, since each component force should produce a component of the overall drift velocity, there must be three components of the net drift velocity. The first component, which will be designated $v^0$, is the direct result of the externally applied field only and excludes the influence of interactions between the ion and the ionic cloud; the second is the electrophoretic component $v_E$ and arises from the participation of the ion in the electrophoretic motion of its cloud; finally, the third component is the relaxation field component $v_R$ originating from the relaxation force that retards the drift of the ion. Since the electrophoretic and relaxation forces act in a sense opposite to the externally applied electric field, it follows that the electrophoretic and relaxation components must diminish the overall drift velocity (Fig. 4.91), i.e.,

$$v_d = v^0 - (v_E + v_R) \tag{4.297}$$

The next step is to evaluate the electrophoretic and relaxation components of the net drift velocity of an ion.

### 4.6.6. Electrophoretic Component of the Drift Velocity

The electrophoretic component $v_E$ of the drift velocity of an ion is equal to the electrophoretic velocity of its ionic cloud because the central ion shares in the motion of its cloud. If one ignores the asymmetry of the ionic cloud, a simple calculation of the electrophoretic velocity $v_E$ can be made.

The ionic atmosphere is accelerated by the externally applied electric force $ze_0X$ but is retarded by a Stokes viscous force. When the cloud attains a steady-state electrophoretic velocity $v_E$, then the viscous force is exactly equal and opposite to the electric force driving the cloud

$$ze_0X = \text{Stokes' force on cloud} \tag{4.298}$$

The general formula for Stokes' viscous force is $6\pi r\eta v$, where $r$ and $v$ are the radius and velocity of the moving sphere. In computing the viscous force on the cloud, one can substitute $\kappa^{-1}$ for $r$ and $v_E$ for $v$ in Stokes' formula. Thus,

$$ze_0X = 6\pi\kappa^{-1}\eta v_E \tag{4.299}$$

from which it follows that

$$v_E = \frac{ze_0}{6\pi\kappa^{-1}\eta} X \tag{4.300}$$

This is the expression for the electrophoretic contribution to the drift velocity of an ion.

### 4.6.7. Procedure for Calculating the Relaxation Component of the Drift Velocity

From the familiar relation [*cf.* Eq. (4.149)],

$$\text{Velocity} = \text{Absolute mobility} \times \text{force}$$

it is clear that the relaxation component $v_R$ of the drift velocity of an ion can be obtained by substituting for the relaxation force $\vec{F}_R$ in

$$v_R = \bar{u}^0_{\text{abs}} \vec{F}_R \tag{4.301}$$

The problem therefore is to evaluate the relaxation force.

Since the latter arises from the distortion of the ionic cloud, one must derive a relation between the relaxation force and a quantity characterizing the distortion. It will be seen that the straightforward measure of the asymmetry of the cloud is the distance $d$ through which the center of charge of the ion and the center of charge of the cloud are displaced.

However, the distortion $d$ of the cloud itself depends on a relaxation process in which the part of the cloud in front of the moving ion is being built up and the part at the back is decaying. Hence, the distortion $d$ and the relaxation force $\vec{F}_R$ must depend on the time taken by a cloud to relax, or decay.

Thus, it is necessary first to calculate how long an atmosphere would take to decay, then to compute the distortion parameter $d$, and finally to obtain an expression for the relaxation force $\vec{F}_R$. Once this force is evaluated, it can be introduced into Eq. (4.30) for the relaxation component $v_R$ of the drift velocity.

### 4.6.8. Decay Time of an Ion Atmosphere

An idea of the time involved in the readjustment of the ionic cloud around the moving central ion can be obtained by a thought experiment suggested by Debye (Fig. 4.92). Consider a static central ion with an equilibrium, spherical ionic cloud around it. Let the central ion suddenly be discharged. This perturbation of the ion–ionic cloud system sets up a relaxation process. The ionic cloud is now at the mercy of the thermal

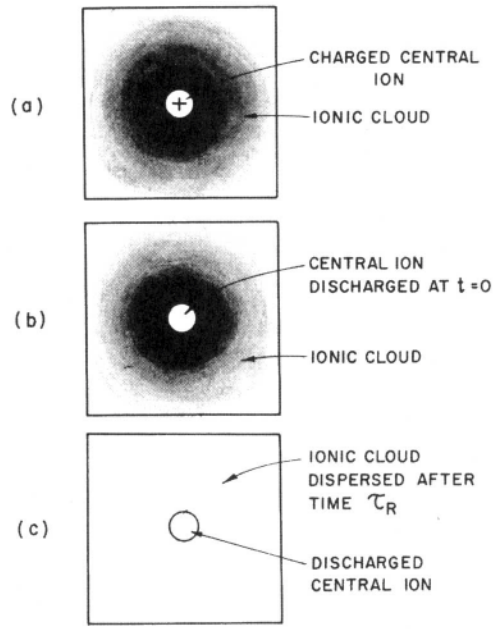


**Fig. 4.92.** Debye's thought experiment to calculate the time for the ion atmosphere to relax: (a) the ionic cloud around a central ion; (b) at $t = 0$, the central ion is discharged; and (c) after time $\tau_R$, the ion atmosphere has relaxed or dispersed.

forces, which try to destroy the ordering effect previously maintained by the central ion and responsible for the creation of the cloud.

The actual mechanism by which the ions constituting the ionic atmosphere are dispersed is none other than the random-walk process described in Section 4.2. Hence, the time taken by the ionic cloud to relax or disperse may be estimated by the use of the Einstein–Smoluchowski relation (Section 4.2.6)

$$t = \frac{\langle x^2 \rangle}{2D} \tag{4.27}$$

What distance $x$ is to be used? In other words, when can the ionic cloud be declared to have dispersed or relaxed? These questions may be answered by recalling the description of the ionic atmosphere where it was stated that the charge density in a $dr$-thick spherical shell in the cloud declines rapidly at distances greater than the Debye–Hückel length $\kappa^{-1}$. Hence, if the ions diffuse to a distance $\kappa^{-1}$, the central ion

can be stated to have lost its cloud, and the time taken for this diffusion provides an estimate of the relaxation time $\tau_R$. One has, by substituting $\kappa^{-1}$ in the Einstein–Smoluchowski relation [Eq. (4.27)]

$$\tau_R = \frac{(\kappa^{-1})^2}{2D} \tag{4.302}$$

which, with the aid of the Einstein relation $D = \bar{u}_{abs} kT$ [Eq. (4.172)], can be transformed into the expression

$$\tau_R = \frac{(\kappa^{-1})^2}{2\bar{u}_{abs} kT} \tag{4.303}$$

### 4.6.9. The Quantitative Measure of the Asymmetry of the Ionic Cloud around a Moving Ion

To know how asymmetric the ionic cloud has become owing to the relaxation effect, one must calculate the distance $d$ through which the central ion has moved in the relaxation time $\tau_R$. This is easily done by multiplying the relaxation time $\tau_R$ by the velocity $v^0$ which the central ion acquires from the externally applied electric force, i.e.,

$$d = \tau_R v^0 \tag{4.304}$$

By substituting the expression (4.303) for the relaxation time $\tau_R$, Eq. (4.304) becomes

$$d = \frac{v^0 (\kappa^{-1})^2}{2\bar{u}^0_{abs} kT} \tag{4.305}$$

The center of charge of the relaxing ionic cloud coincides with the original location of the central ion; in the meantime, however, the central ion and its center of charge move through a distance $d$. The centers of charge of the central ion and its ionic cloud are displaced through the distance $d$, which is a quantitative measure of the egg-shapedness of the ion atmosphere around a moving ion.

### 4.6.10. Magnitude of the Relaxation Force and the Relaxation Component of the Drift Velocity

Consider first a *static* central ion. The ion may exert an electric force on the cloud and vice versa, but at first the net force is zero because of the spherical symmetry of the cloud around the static central ion.

When the central ion moves, it can be considered to be at a distance $d$ from the center of its cloud. The net force due to the asymmetry of the cloud is nonzero. A rough calculation of the force can be made as follows.

The relaxation force is zero when the centers of charge of the ion and its cloud coincide, and it is nonzero when they are separated. So let it be assumed in this approximate treatment that the relaxation force is proportional to $d$, i.e., proportional to the distance through which the ion has moved from the original center of charge of the cloud. On this basis, the relaxation force $\vec{F}_R$ will be given by the maximum total force of the atmosphere on the central ion, i.e., $z^2e_0^2/[\varepsilon(\kappa^{-1})^2]$,[41] multiplied by the fraction of the radius of the cloud through which the central ion is displaced during its motion under the external field, i.e., $d/\kappa^{-1}$. Hence, the relaxation force is

$$\vec{F}_R = \frac{z^2e_0^2}{\varepsilon(\kappa^{-1})^2}\frac{d}{\kappa^{-1}} \tag{4.306}$$

and using Eq. (4.305) for $d$, one has

$$\vec{F}_R = \frac{z^2e_0^2}{\varepsilon(\kappa^{-1})^2}\frac{1}{\kappa^{-1}}\frac{v^0(\kappa^{-1})^2}{2\bar{u}^0_{\text{abs}}kT}$$

$$= \frac{z^2e_0^2\kappa}{2\varepsilon kT}\frac{v^0}{\bar{u}^0_{\text{abs}}} \tag{4.307}$$

Since, however, the velocity $v^0$ arises solely from the externally applied field and excludes the influence of ion–ion interactions, the ratio $v^0/\bar{u}^0_{\text{abs}}$ is equal to the applied electric force

$$\frac{v^0}{\bar{u}^0_{\text{abs}}} = \vec{F} = ze_0X \tag{4.308}$$

On inserting this into Eq. (4.307), it turns out that

$$\vec{F}_R = \frac{z^3e_0^3\kappa X}{2\varepsilon kT} \tag{4.309}$$

In the above treatment of the relaxation field, it has been assumed that the only motion of the central ion destroying the spherical symmetry of the ionic cloud is motion

[41] This total force is obtained by considering the ionic cloud equivalent to an equal and opposite charge placed at a distance $\kappa^{-1}$ from the central ion. Then, Coulomb's law for the force between these two charges gives the result $z^2e_0^2/[\varepsilon(\kappa^{-1})^2]$.

in the direction of the applied external field. This latter directed motion is in fact a drift superimposed on a random walk. The random walk is itself a series of motions, and these motions are random in direction. Thus, the central ion exercises an erratic, rather than a consistent, leadership on its atmosphere.

Onsager considered the effect that this erratic character of the leadership would have on the time-averaged shape of the ionic cloud and therefore on the relaxation field. His final result differs from Eq. (4.309) in two respects: (1) Instead of the numerical factor $\frac{1}{2}$, there is a factor $\frac{1}{3}$; and (2) a correction factor $\omega/2z^2$ has to be introduced, the quantity $\omega$ being given by

$$\omega = z_+ z_- \frac{2q}{1+\sqrt{q}} \tag{4.310}$$

in which

$$q = \frac{z_+ z_-}{z_+ + z_-} \frac{\lambda_+ + \lambda_-}{z_+\lambda_+ + z_-\lambda_-} \tag{4.311}$$

where $\lambda_+$ and $\lambda_-$ are related to mobilities of cation and anion, respectively. For symmetrical or $z$:$z$-valent electrolytes, the expression for $q$ reduces to $\frac{1}{2}$, and that for $\omega$ becomes (Table 4.18)

$$\omega = z^2 \frac{1}{1+(1/\sqrt{2})} \tag{4.312}$$

Thus, a more rigorous expression for the relaxation force is

$$\vec{F}_R = \frac{z^3 e_0^3 \kappa}{3\varepsilon kT} \frac{\omega}{2z^2} X$$

$$= \frac{z e_0^3 \kappa \omega}{6\varepsilon kT} X \tag{4.313}$$

**TABLE 4.18**

**Values of $\omega$ for Different Types of Electrolytes**

| Type of Electrolyte | $\omega$ |
|---|---|
| 1:1 | 0.5859 |
| 2:2 | 2.3436 |

Substituting the expression (4.313) for the relaxation force in Eq. (4.301) for the relaxation component of the drift velocity, one gets

$$v_R = \bar{u}^0_{\text{abs}} \frac{z e_0^3 \kappa \omega}{6\varepsilon k T} X \tag{4.314}$$

Furthermore, from the definition (4.152) of the conventional mobility,

$$u^0 = u^0_{\text{conv}} = \bar{u}^0_{\text{abs}} z e_0$$

Eq. (4.314) becomes

$$v_R = \frac{u^0}{z e_0} \frac{z e_0^3 \kappa \omega}{6\varepsilon k T} X = \frac{u^0 e_0^2 \kappa \omega}{6\varepsilon k T} X \tag{4.315}$$

### 4.6.11. Net Drift Velocity and Mobility of an Ion Subject to Ion–Ion Interactions

Now that the electrophoretic and relaxation components in the drift velocity of an ion have been evaluated, they can be introduced into Eq. (4.297) to give

$$\begin{aligned} v_d &= v^0 - (v_E + v_R) \\ &= v^0 - \left( \frac{z e_0 \kappa}{6\pi\eta} X + \frac{u^0 e_0^2 \kappa \omega}{6\varepsilon k T} X \right) \\ &= v^0 - \left( \frac{z e_0}{6\pi\eta} + \frac{u^0 e_0^2 \omega}{6\varepsilon k T} \right) \kappa X \end{aligned}$$

If one divides throughout by $X$, then according to the definition of the conventional mobility $u_{\text{conv}} = u = v/X$, one has

$$u = u^0 - \left( \frac{z e_0}{6\pi\eta} + \frac{u^0 e_0^2 \omega}{6\varepsilon k T} \right) \kappa \tag{4.316}$$

An intelligent inspection of expression (4.316) shows that the mobility $u$ of ions is not a constant independent of concentration. It depends on the Debye–Hückel reciprocal length $\kappa$. But this parameter $\kappa$ is a function of concentration (see Eq. 3.84). Hence, Eq. (4.316) shows that the mobility of ions is a function of concentration, as was suspected (Section 4.6.1) on the basis of the empirical law of Kohlrausch.

As the concentration decreases, $\kappa^{-1}$ increases and $\kappa$ decreases, as can be seen from Eq. (3.84). In the limit of infinite dilution $(c \to 0)$, $\kappa^{-1} \to \infty$ or $\kappa \to 0$. Under these conditions, the second and third terms in Eq. (4.316) drop out, which leaves

$$u_{\text{limit},c\to 0} = u^0 \tag{4.317}$$

The quantity $u^0$ is therefore the mobility at infinite dilution and can be considered to be given by the expression for the Stokes mobility (Section 4.4.8), i.e.,

$$u^0 = \frac{ze_0}{6\pi r\eta} \tag{4.183}$$

To go back to the question that concluded the previous section, it is clear that since transport numbers depend on ionic mobilities, which have been shown to vary with concentration, the transport number must itself be a concentration-dependent quantity (Table 4.19). However, it is seen that this variation is a small one.

### 4.6.12. The Debye–Hückel–Onsager Equation

The equivalent conductivity $\Lambda$ of an electrolytic solution is simply related to the mobilities of the constituent ions [Eq. (4.163)]

$$\Lambda = F(u_+ + u_-)$$

Thus, to obtain the equivalent conductivity, one has only to write down the expression for the mobilities of the positive and negative ions, multiply both the expressions by the Faraday constant $F$, and then add up the two expressions. The result is

$$\Lambda = F(u_+ + u_-)$$

**TABLE 4.19**

**Transport Numbers of Cations in Aqueous Solutions at 298 K**

| Concentration | HCl | LiCl | NaCl | KCl |
|---|---|---|---|---|
| 0.01 *N* | 0.8251 | 0.3289 | 0.3918 | 0.4902 |
| 0.02 | 0.8266 | 0.3261 | 0.3902 | 0.4901 |
| 0.05 | 0.8292 | 0.3211 | 0.3876 | 0.4899 |
| 0.1 | 0.8314 | 0.3168 | 0.3854 | 0.4898 |
| 0.2 | 0.8337 | 0.3112 | 0.3821 | 0.4894 |
| 0.5 | — | 0.300 | — | 0.4888 |
| 1.0 | — | 0.287 | — | 0.4882 |

$$= F\left[u_+^0 - \kappa\left(\frac{z_+ e_0}{6\pi\eta} + \frac{e_0^2\omega}{6\varepsilon kT}u_+^0\right)\right] \tag{4.318}$$

$$+ F\left[u_-^0 - \kappa\left(\frac{z_- e_0}{6\pi\eta} + \frac{e_0^2\omega}{6\varepsilon kT}u_-^0\right)\right]$$

For a symmetrical electrolyte, $z_+ = z_- = z$ or $z_+ + z_- = 2z$, and Eq. (4.318) reduces to

$$\Lambda = F(u_+^0 + u_-^0) - \left[\frac{ze_0F\kappa}{3\pi\eta} + \frac{e_0^2\omega\kappa}{6\varepsilon kT}F(u_+^0 + u_-^0)\right] \tag{4.319}$$

However, according to Eq. (4.292)

$$\Lambda^0 = F(u_+^0 + u_-^0) \tag{4.292}$$

Hence,

$$\Lambda = \Lambda^0 - \left(\frac{ze_0F\kappa}{3\pi\eta} + \frac{e_0^2\omega\kappa}{6\varepsilon kT}\Lambda^0\right) \tag{4.320}$$

Replacing $\kappa$ by the familiar expression (3.84), i.e.,

$$\kappa = \left(\frac{8\pi z^2 e_0^2 c}{\varepsilon kT}\right)^{1/2}\left(\frac{N_A}{1000}\right)^{1/2} \tag{3.84}$$

one has

$$\Lambda = \Lambda^0 - \left[\frac{ze_0F}{3\pi\eta}\left(\frac{8\pi z^2 e_0^2 N_A}{1000\varepsilon kT}\right)^{1/2} + \frac{e_0^2\omega}{6\varepsilon kT}\left(\frac{8\pi z^2 e_0^2 N_A}{1000\varepsilon kT}\right)^{1/2}\Lambda^0\right]c^{1/2} \tag{4.321}$$

This is the well-known Debye–Hückel–Onsager equation for a symmetrical electrolyte. By defining the following constants

$$A = \frac{ze_0F}{3\pi\eta}\left(\frac{8\pi z^2 e_0^2 N_A}{1000\varepsilon kT}\right)^{1/2} \quad \text{and} \quad B = \frac{e_0^2\omega}{6\varepsilon kT}\left(\frac{8\pi z^2 e_0^2 N_A}{1000\varepsilon kT}\right)^{1/2}$$

it can also be written

$$\Lambda = \Lambda^0 - (A + B\Lambda^0)c^{1/2}$$

$$= \Lambda^0 - \text{constant } c^{1/2} \tag{4.322}$$

Thus, the theory of ionic clouds has been able to give rise to an equation that has the same form as the empirical law of Kohlrausch (Section 4.3.9).

### 4.6.13. Theoretical Predictions of the Debye–Hückel–Onsager Equation versus the Observed Conductance Curves

The two constants

$$A = \frac{ze_0F}{3\pi\eta}\left(\frac{8\pi z^2 e_0^2 N_A}{1000\varepsilon kT}\right)^{1/2} \tag{4.323}$$

and

$$B = \frac{e_0^2\omega}{6\varepsilon kT}\left(\frac{8\pi z^2 e_0^2 N_A}{1000\varepsilon kT}\right)^{1/2} \tag{4.324}$$

in the Debye–Hückel–Onsager equation are completely determined (Table 4.20) by the valence type of the electrolyte $z$, the temperature $T$, the dielectric constant $\varepsilon$, and the viscosity $\eta$ of the solution, and universal constants.

The Debye–Hückel–Onsager equation has been tested against a large body of accurate experimental data. A comparison of theory and experiment is shown in Fig. 4.93 and Table 4.21 for aqueous solutions of true electrolytes, i.e., substances that consisted of ions in their crystal lattices before they were dissolved in water. At very low concentrations ($< 0.003\ N$), the agreement between theory and experiment is very good. There is no doubt that the theoretical equation is a satisfactory expression for the *limiting tangent* to the experimentally obtained $\Lambda$ versus $c^{1/2}$ curves.

One cannot, however, expect the Debye–Hückel–Onsager theory of the non-equilibrium conduction properties of ionic solutions to fare better at high concentration than the corresponding Debye–Hückel theory of the equilibrium properties (e.g.,

**TABLE 4.20**

**Values of the Onsager Constants for Uni-Univalent Electrolytes at 298 K**

| Solvent | $A$ | $B$ |
|---|---|---|
| Water | 60.20 | 0.229 |
| Methyl alcohol | 156.1 | 0.923 |
| Ethyl alcohol | 89.7 | 1.83 |
| Acetone | 32.8 | 1.63 |
| Acetonitrile | 22.9 | 0.716 |
| Nitromethane | 125.1 | 0.708 |
| Nitrobenzene | 44.2 | 0.776 |

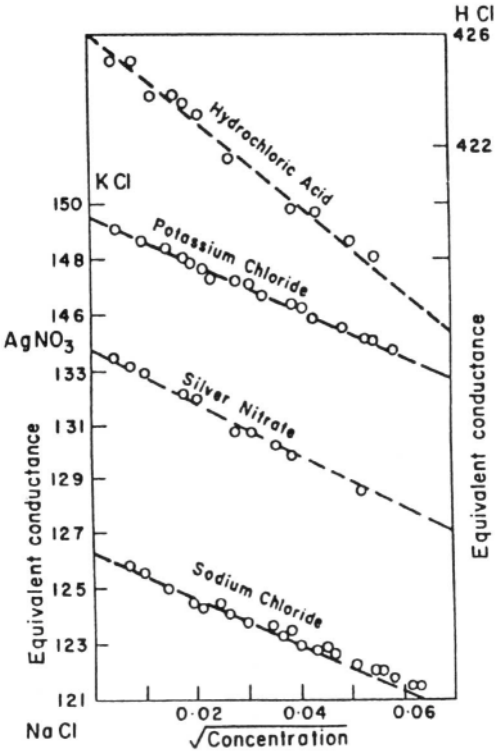


**Fig. 4.93.** Comparison of the equivalent conductivities of HCl and some salts predicted by the Debye–Hückel–Onsager equation (4.321) with those observed experimentally.

**TABLE 4.21**

**Observed and Calculated Onsager Slopes in Aqueous Solutions at 298 K**

| Electrolyte | Observed Slope | Calculated Slope |
|---|---|---|
| LiCl | 81.1 | 72.7 |
| $NaNO_3$ | 82.4 | 74.3 |
| KBr | 87.9 | 80.2 |
| KCNS | 76.5 | 77.8 |
| CsCl | 76.0 | 80.5 |
| $MgCl_2$ | 144.1 | 145.6 |
| $Ba(NO_3)_2$ | 160.7 | 150.5 |
| $K_2SO_4$ | 140.3 | 159.5 |

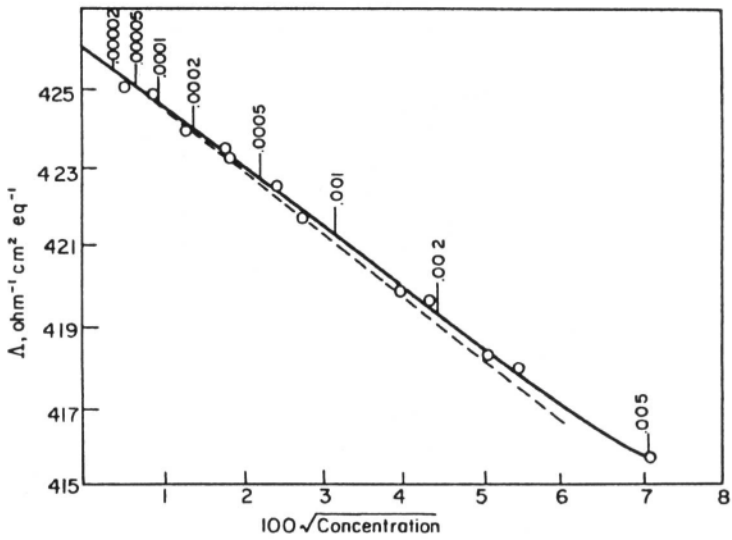


**Fig. 4.94.** Deviation of the predicted equivalent conductivities from those observed for HCl.

activity coefficients of electrolytic solutions); both theories are based on the ionic-cloud concept. In the case of the Debye–Hückel–Onsager equation, it is seen from Fig. 4.94 that as the concentration increases (particularly above 0.003 *N*), the disparity between the theoretical and experimental curves widens.

### 4.6.14. Changes to the Debye–Hückel–Onsager Theory of Conductance

The original Debye–Hückel–Onsager theory of conductance of ions in solution takes into account the two ionic atmosphere effects in reducing the mobility and therefore the lessening of the conductivity of the ions that occurs as their concentration is increased (see Section 4.6.12). The original theory formed a peak in the physical chemistry of the first half of the twentieth century, but it was first published some three-quarters of a century ago. Moreover, as indicated in Fig. 4.94, the original theory showed deviations from experiments even at really low aqueous concentrations. In nonaqueous solutions, where the dielectric constants are usually lower than the 80 one finds for water, the interionic attractions are higher (interionic forces are inversely proportional to the dielectric constant of the solution), and hence the deviations from the zeroeth approximation of no interionic interactions are greater. For this reason the deviation between theory and experiment begins at even lower concentrations than it does in aqueous solutions. Of course, if one removes some of the primitivities of the

early theory (e.g., neglecting the fact that ions have finite size), then the concentration range for the applicability of the theory widens.

Apart from improvements made by taking into account the fact that ions do indeed take up some of the space in electrolytic solutions, one has to consider also that *ion association* occurs in true electrolytes,

$$Na^+ + Cl^- \rightleftharpoons [Na^+Cl^-]^0 \tag{4.325}$$

and the associated ionic molecule is a dipole, not an ion, and therefore is no longer in the running as far as contributing to the conductance is concerned. This was allowed for in an empirical equation due to Justice,

$$\frac{\Lambda_m}{\alpha} = \Lambda_m^0 - S\sqrt{\alpha c} + E\alpha c \ln(\alpha c) + J_1 \alpha c - J_2(\alpha c)^{3/2} \tag{4.326}$$

where $\alpha$ is the degree of association of the electrolyte, $S$ is the Onsager limiting-law coefficient, $c$ is the electrolyte concentration, and $E$, $J_1$, and $J_2$ are constants. The parameter $\alpha$ is related to an association constant $K_A$ by

$$\frac{(1-\alpha)f_A}{\alpha^2 c f_\pm^2} = K_A \tag{4.327}$$

where $f_A$ is the activity coefficient of the dipole. The $f_\pm$ is given by the relevant expression found in the activity coefficient of the Debye–Hückel theory (see Section 3.4.4).

What is the use of an empirical equation such as Eq. (4.326)? It acts as a hanger for the facts. One fits experimental data of $\Lambda_m$ as a function of $c$ to the equation and determines by a least-squares fitting procedure the values of $\Lambda_m^0$ and $K_A$.[42]

These empirical modifications of the Debye–Hückel–Onsager theory of electrolytes do not yet give much *physical* insight into what changes in the elderly (but still famous) theory might improve the theory of ionic conductance. A more relevant improvement can be attributed to Fuoss and to Lee and Wheaton. Instead of thinking about bare ions traveling in a structureless dielectric medium, these authors have taken the ion to have three regions, as shown in Fig. 4.95. In the first of these regions, that nearest to the ion, the water molecules are regarded as being "totally oriented" to the ion, so that their effective dielectric constant would be that of water dielectrically

[42]In his derivation, Justice suggested that the distance of closest approach $a$ involved in the determination of $f_\pm$ [*cf.* Eq. (3.120)] be replaced by the Bjerrum parameter $q$. While $q$ is the distance of closest approach of the unpaired ions that contribute to the conductance of the solution, ions separated by distances between $q$ and $a$ are ion-paired and do not contribute to the conductance. The advantage of this approximation is that $a$ is not known *a priori*, whereas $q$ is defined by Eq. (3.144).

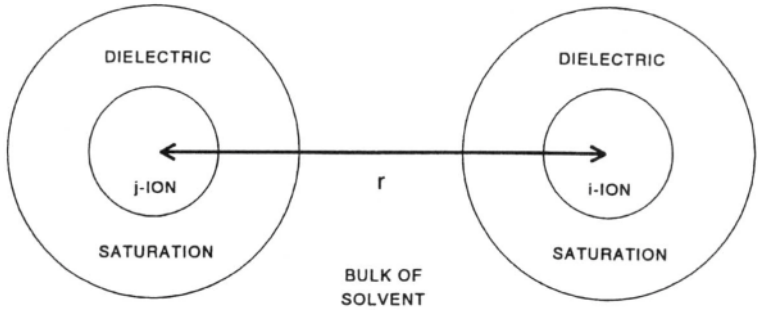


**Fig. 4.95.** Regions of dielectric saturation about *i*- and *j*-ions according to Lee and Wheaton (W. H. Lee and R. J. Wheaton, *J. Chem. Soc. Faraday Trans. // **75***:1128, 1979).

saturated, i.e., having all its orientation polarization used up by the electric field of the ion itself. In the second region, there is only partial dielectric saturation. This region is part of the secondary hydration. Outside these first two regions, the influence of the ion's field is taken to be only the long-range Coulomb forces generally used in arguments about the properties of ionic solutions.[43]

On the basis of this model, Lee and Wheaton arrived at an equation for $\Lambda_m$ in terms of $q$, the Bjerrum distance. The equation is several lines long and clearly only fit for use in appropriate software. The application of experimental data of $\Lambda_m$ to the equation allows one to find values of $\Lambda_m^0$, $K_A$, and the co-sphere radius $R$. These values are then taken as if they had been experimentally determined, an assumption that is true only in a secondary way because they depend on the validity of Lee and Wheaton's equation.

Another approach to the conductance of electrolytes, which is less complex than that of Lee and Wheaton, is due to Blum and his co-workers. This theory goes back to the original Debye–Hückel–Onsager concepts, for it does not embrace the ideas of Lee and Wheaton about the detailed structure around the ion. Instead, it uses the concept of mean spherical approximation of statistical mechanics. This is the rather portentous phrase used for a simple idea, which was fully described in Section 3.12. It is easy to see that this is an approximation because in reality an ionic collision with another ion will be softer than the brick-wall sort of idea used in an MSA approach. However, using MSA, the resulting mathematical treatment turns out to be relatively simple. The principal equation from the theory of Blum et al. is correspondingly simple and can be quoted. It runs

[43]These regions have been met before (Section 3.6.2) in discussions of recent models for finding activity and osmotic coefficients. They correspond to the 1949 models for primary and secondary hydration of Bockris [*cf.* the Gurney co-sphere (1971)].

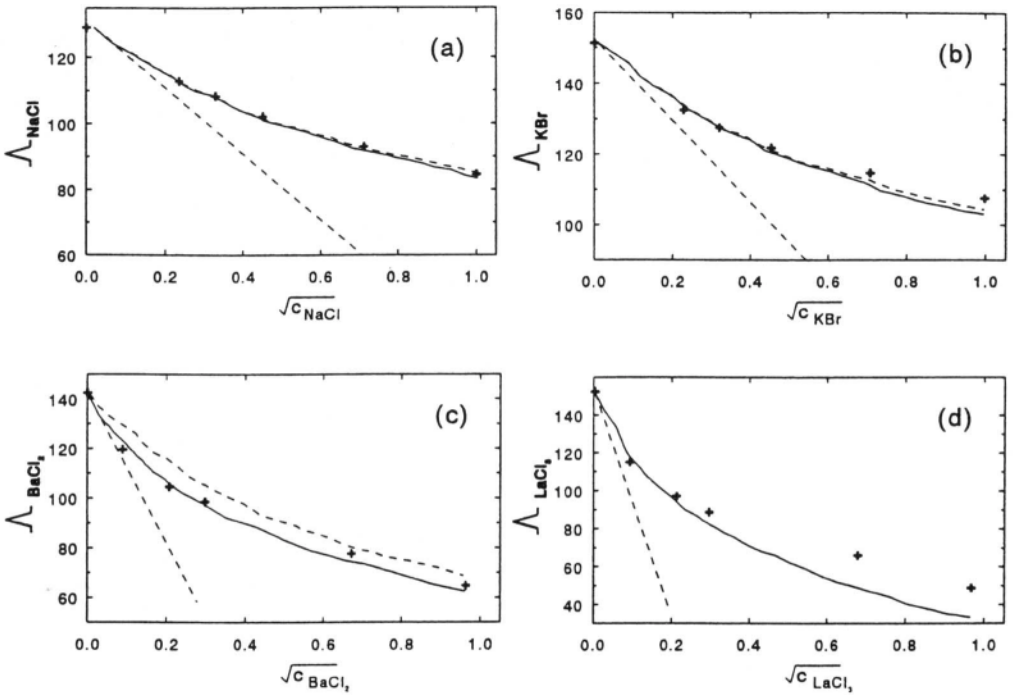


**Fig. 4.96.** Equivalent conductivity of aqueous electrolyte solutions as a function of the square root molarity: (+), experimental values; (—•—•—), Debye–Hückel–Onsager limiting law; (- - -) and (—), theoretical values predicted by Blum's approach. (a) Aqueous NaCl solutions. (b) Aqueous KBr solutions. (c) Aqueous $BaCl_2$ solutions. (d) Aqueous $LaCl_3$ solutions. (Reprinted from O. Bernard, W. Kunz, P. Turq, and L. Blum, *J. Phys. Chem.***96**: 3833, 1992.)

$$\Lambda_m = \sum_i \lambda_i^0 \left(1 + \frac{v_i^E}{v_i^0}\right)\left(1 + \frac{\Delta E}{E}\right) \tag{4.328}$$

with $v_i^E$, the drift velocity under a field $E$, defined as

$$v_i^E = \frac{z_i e_0 E D_i^0}{kT} \tag{4.329}$$

where $E$ is the electric field applied across the solution, $D_i^0$ is the diffusion coefficient of the ion $i$, and $\lambda_i^0$ is the individual conductance of the ion $i$ at infinite dilution.

The application of Blum's theory to experiment is unexpectedly impressive: it can even represent conductance up to 1 mol $\mathbf{dm}^{-3}$. Figure 4.96 shows experimental data and both theories—Blum's theory and the Debye–Hückel–Onsager first approximation. What is so remarkable is that the Blum equations are able to show excellent agreement with experiment without taking into account the solvated state of the ion, as in Lee and Wheaton's model. However, it is noteworthy that Blum stops his comparison with experimental data at 1.0 *M*.

Blum's use of the MSA represents a significant advance, but it does not take into account either ionic association or Bjerrum's very reasonable idea (Section 3.8) about the removal of free water in the solution by means of hydration. Furthermore, Blum's equations do not explain the relation between conductance and concentration noted for many electrolytes, particularly at high concentrations, that is,

$$\Lambda_m = \Lambda_m^0 - Ac^{1/3} \tag{4.330}$$

There are some who see this equation as indicative that a whole different approach to conductance theory might be waiting in the wings, as it were. As the concentration increases, the idea of an ionic atmosphere becomes less useful and one might start at the other end, with ideas used to treat molten salts (Chapter 5), but in a diluted form. This would repeat the history of the theory of liquids which, in the early part of this century, was derived from the treatment of very compressed gases but later seemed to be more developable from modifications of how solids are treated.

## 4.7. DIVERSE RELAXATION PROCESSES IN ELECTROLYTIC SOLUTIONS

### 4.7.1. Definition of Relaxation Processes

The term *relaxation*, as applied in physical chemistry (*cf.* Section 4.6.8), refers to molecular processes occurring after the imposition of a stress on a system. Thus, one can have a system at equilibrium to which a new constraint is applied (e.g., an electric field switched on suddenly onto a dipole-containing liquid). The system is then

constrained to a new position of equilibrium. The time it takes to change position is called the *relaxation time.*

To understand better what is meant by relaxation time, consider a system under the following equilibrium

$$A \underset{\overleftarrow{k'}}{\overset{\vec{k'}}{\rightleftharpoons}} B \tag{4.331}$$

The rate of change of $A$ is given by

$$\frac{dc_A}{dt} = -\vec{k}'c'_A + \overleftarrow{k}'c'_B = 0 \tag{4.332}$$

Upon the imposition of a constraint, the system reaches a new equilibrium. Moreover, the constraint changes the rate constants that control the interconversion of states $A$ and $B$. During the first equilibrium, these were $\vec{k}'$ and $\overleftarrow{k}'$, and they become $\vec{k}$ and $\overleftarrow{k}$ under the new conditions. While $A$ is adjusting (relaxing) to its new equilibrium value, its concentration changes from $c'_A$ to $c_A + x$ until it reaches its new equilibrium state, $c_A$. In the same way, under the constraint, the concentration of $B$ changes to the new value $c_B$, but during the relaxation it is $c_B - x$. The concentration of $A$ then changes as follows

$$\frac{dc_A}{dt} = -\vec{k}(c_A + x) + \overleftarrow{k}(c_B - x) \tag{4.333}$$

and after reaching the new equilibrium state,

$$\frac{dc_A}{dt} = -\vec{k}c_A + \overleftarrow{k}c_B = 0 \tag{4.334}$$

Therefore, Eq. (4.333) becomes

$$\frac{dc_A}{dt} = \frac{dx}{dt} = -(\vec{k} + \overleftarrow{k})x \tag{4.335}$$

Integrating from a time 0 when $x = x_0$, to a time $t$ when $x = x_t$,

$$x_t = x_0 e^{-(\vec{k}+\overleftarrow{k})t} \tag{4.336}$$

The change of the concentration of $A$ as it goes from the preconstraint equilibrium value $x_0$ to the after-constraint equilibrium value $x_t$ follows the exponential change indicated by Eq. (4.336) and shown in Fig. (4.97).

What is called the relaxation time $\tau$ is a somewhat arbitrary quantity: it is taken to be the time that makes the exponential in Eq. (4.336) unity, i.e.,

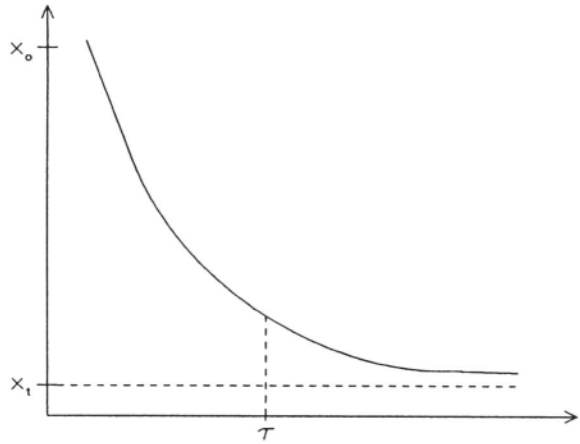


**Fig. 4.97.** Concentration change of species *A* from its preconstraint equilibrium value $x_0$ to the after-constraint equilibrium value $x_f$.

$$\tau = \frac{1}{\vec{k} + \overleftarrow{k}} \tag{4.337}$$

Hence, at the relaxation time,

$$\frac{x_\tau}{x_0} = e^{-1} = 0.368 \tag{4.338}$$

A trivial calculation shows that Eq. (4.338) implies that $x$ at time $\tau$ changed some 63% of the way from the initial value of $x_0$ to the final value of $x_f$. Thus, $\tau$ is some *measure* of the time to complete the change caused by the constraint just as the half-life of a radioactive element is a measure of the lifetime of a radioactive element.[44] In the next subsections, the relaxation times of certain systems will be presented.

### 4.7.2. Dissymmetry of the Ionic Atmosphere

One kind of relaxation time has already been discussed in Section 4.6.8, namely, the time of adjustment to dissymmetry of the ionic atmosphere around an ion when an applied electric field is switched on. Its understanding is basic to our picture of ionic

[44] And for the same sort of reason. The change in both cases follows an exponential law and the rate of change slows down toward completion of the change so that formally the change is never quite finished.

solutions. Thus, in the absence of an electric field, the ions randomly jump about (or shuffle around) in all directions. When an electric field forces them to move preferentially in one direction, the ionic atmosphere around the ions becomes dissymmetric—egg-shaped—so that the longer part of the egg is behind the ion and, having more counter charge behind it than in front, retards the ion's forward motion.

An interesting effect in the conductivity of ions is related to the relaxation time of their ionic atmosphere. Imagine that the electrical conductance of ionic solutions is measured by using alternating currents of a certain frequency, let's say 1000 counts per second.[45] Imagine also the ions moving in the solution and following the dictates of the oscillating electric field. Since this is constantly altering its direction, for a millisecond it pulls the cations to the right and then for a millisecond pulls them to the left, with analogous movements but in opposite directions being forced upon the anions.

The frequency of $1000\ s^{-1}$ has been mentioned because it is typical for measurement of electrical conductivity. To perform the measurement, the researcher varies the frequency $(\nu)$ and plots the corresponding measured resistance values against $1/\nu$, extrapolating the measured resistance in the ordinate to "infinite frequency."

Suppose, however, that instead of making conductance measurements at, say, 10, 100, 1000, and $10{,}000\ s^{-1}$, and performing the said extrapolation to infinite frequency, one goes on increasing the frequency past $100{,}000\ s^{-1}$. Think again now of a given ion and its atmosphere in the system. As the frequency increases, the ionic atmosphere has a harder time keeping the changes in its dissymmetry in tune with the changes in direction of drift of the ions—moving now to the right and now to the left. Below about $10^7\ s^{-1}$, the ionic atmosphere manages to adjust its shape every time the ion changes direction and present the appropriate asymmetric stance, slowing down the ionic movements.

Eventually there is a critical frequency above $10^7\ s^{-1}$ at which the ionic cloud cannot adjust anymore to the ion's movements in the right way because there is too much inertia to execute the rapid changes required by the oscillating applied field. The reciprocal of this critical frequency is called the *relaxation time of the asymmetry of the ionic cloud.* As a consequence, an increase in conductivity occurs at this frequency because there is no longer more charge behind the ion than in front. This increase in conductance at the critical frequency is called the *Debye effect.* It is part of the evidence that shows that the ionic atmosphere is indeed present and functioning according to the way first calculated by Debye.

---

[45]The reason for this is that with a direct current, an unwanted ionic layer forms at the interfaces with the solution of the electrodes used to make contact with the outside power source. These nonequilibrium structures at the surface–solution boundaries create a new resistance that interferes with the solution resistance one is trying to measure. This is wiped out if an alternating current, which keeps on reversing the structure at the interface, is applied.

### 4.7.3. Dielectric Relaxation in Liquid Water

Water is not only the most abundant of all liquids on this planet but also one of the most complex (see Section 2.4). The dielectric constant (permittivity) at frequencies below about $10^{11}\ s^{-1}$ is about 78 at room temperature, and this is about one whole order of magnitude higher than the dielectric constant of simple liquids such as carbon tetrachloride. Kirkwood was the first to develop a model to explain why the dielectric constant of water is so high. He pictured groups of $H_2O$'s coupled together by means of H bonding. His idea was that the dielectric constant of water consists of three parts.

First, there would be the part based on the distortion of the electronic shells of the atoms making up water molecules. Because their inertia is so small, electrons have no difficulty in keeping up with an applied field as its frequency increases. Such a contribution is part of the permittivity of any liquid.

The second part can be viewed as the distortion of the nuclei of the atoms making up water—how much the applied field disturbs the positions of the nuclei in the O and H atoms of molecular water. This part is also present in all liquids.

The third contribution involves the dipole moment of the individual molecules. In water and associated liquids, the dipoles should be taken in groups as a result of the intermolecular H bonding (Fig. 4.98). It is this coupling of the molecules that provides the huge permittivity of water.

Were water a simple unassociated dipolar liquid, the effect of an applied field would be simply to orient it, to inhibit its random libration and bend the average

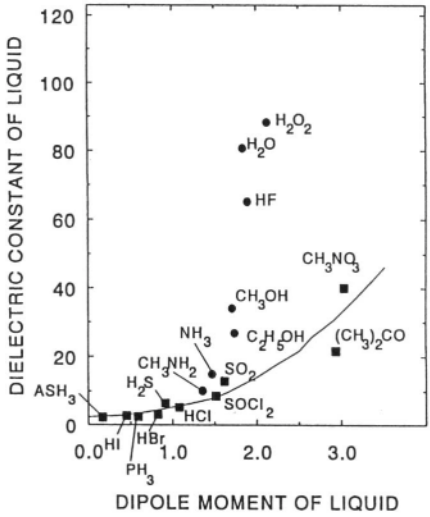


**Fig. 4.98.** The dielectric constants of liquids as a function of their dipole moments (■ = unassociated liquids, and ● = H-bonded liquids).

direction of the molecules to lie more along the lines of the field. With water, the molecular dipoles also feel the force of the field. The special feature is that each of the water molecules, being bound together with H bonds, pulls other waters with it as it bonds to the field. When one water molecule goes to obey the field and align with it, the ones to which it is bound get a pull from the waters to which they are bound and this helps them turn also. Thus, in an associated liquid one gets a double whammy from the oscillating applied field. It pulls each dipolar molecule around. This is an effect on the individual dipoles that one would find with any dipolar liquid, but there is also a correlated additive effect due to the orienting effect of one dipole on another.

Now, what of relaxation? According to the picture drawn here (Fig. 4.99), there should be two relaxation times. The first will be that corresponding to the state in which the dipoles can no longer react in consonance with the applied field. At some critical high frequency, the permittivity falls (loss of the biggest contributor—the netted dipolar groups), and the dielectric constant falls from 78 to ~5 at 298 K. The value of the associated time, that is, the reciprocal of the critical frequency of the applied ac field at which the permittivity falls, is $8.32 \times 10^{-12}$ s, which corresponds to a frequency of $1.2 \times 10^{11}$ $s^{-1}$.

At frequencies above $10^{11}$ $s^{-1}$, the next thing to be exceeded is the speed at which the nuclei in the molecules can react to changes in the direction of the field. The protons in the nuclei have an inertia approximately 2000 times greater than that of the electrons in the outer shell and accordingly a relaxation time much less than that of the electron shells. This value for water is $1.02 \times 10^{-12}$ s, and the critical frequency is $9.8 \times 10^{11}$ $s^{-1}$. The remaining permittivity at frequencies higher than this is due to distortion of the electron shell of the atoms. This last and most fundamental permittivity is often called the *optical* permittivity because it pertains to movements in the liquid (distortion of the electron shells), which occur near the speed of light).

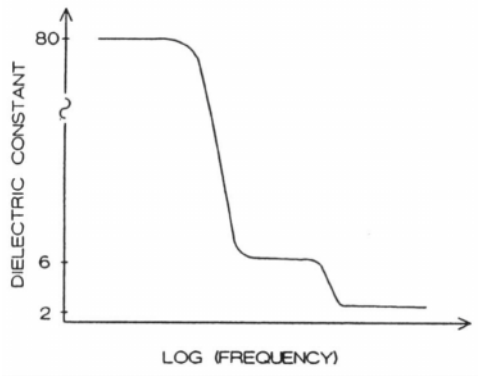


**Fig. 4.99.** Variation of the dielectric constant as a function of the frequency of an applied ac electric field.

**TABLE 4.22**

**Dielectric Parameters of Several Polar Solvents Showing Discontinuous Relaxation Time Distributions**

| Solvent | $\varepsilon_s$ | $\varepsilon_\infty$ | $n_D^2$ | $(\tau_1/ps)$ | $(\tau_2/ps)$ | $(\tau_3/ps)$ |
|---|---|---|---|---|---|---|
| Water | 78.36 | 4.49 | 1.7765 | 8.32 | | 1.02 |
| Methanol | 32.63 | 2.79 | 1.7596 | 51.15 | 7.09 | 1.12 |
| Ethanol | 24.35 | 2.69 | 1.8473 | 163 | 8.97 | 1.81 |
| Formamide | 109.5 | 4.48 | 2.096 | 37.3 | | 1.16 |
| *N*-Methylformamide | 185.98 | 3.20 | 2.0449 | 128 | 7.93 | 0.78 |
| *N,N*-Dimethylformamide | 37.24 | 2.94 | 2.0400 | — | 10.4 | (0.76) |
| Acetonitrile | 35.92 | 2.26 | 1.7800 | — | 3.21 | — |
| Propylene carbonate | 64.96 | 4.14 | 2.0153 | — | 43.1 | — |

Source: Reprinted from P. Turq, J. Barthel, and M. Chemla, *Transport, Relaxation and Kinetic Processes in Electrolyte Solutions*, Springer-Verlag, Heidelberg, 1992, p. 81.

Much information can be obtained from the study of dielectric relaxation times in liquids, for example, the extent to which the waters are netted together (Table 4.22).

### 4.7.4. Effects of Ions on the Relaxation Times of the Solvents in Their Solutions

There are three new "effects" related to the properties of relaxation time that arise when ions are added to water.

First, the solution's relaxation time appears to change. If solvent molecules are far away, say more than 1000 pm distant from an ion, the ion's effect on the relaxation time will be negligible. Conversely, water molecules bound to ions will be what is called *dielectrically saturated*; they will be so tightly held in the ion's local electric field that they will not be affected by the applied electric field used to measure the dielectric constant of the solution. The average relaxation time of all the waters will be increased, because the water molecules attached to the ions now have, in effect, an infinite relaxation time.

The second effect is related to the formation of ion pairs. If ion pairs or other ionic aggregates are present, they will introduce a new relaxation time above that exhibited by the pure solvent.

Figure 4.100 shows the Argand **diagram**[†] of water (curve 1) and the permittivity for 0.8 *M* KC1 (curve 2) in water. The "structural" part of the spectrum is represented by curve 3. The difference of curves 2 and 3 is the result of electrolytic conductance.

[†]An Argand diagram (also called a Cole-Cole plot) is a diagram of the real $\varepsilon'$ and imaginary $\varepsilon''$ components of the dielectric constant of the system.

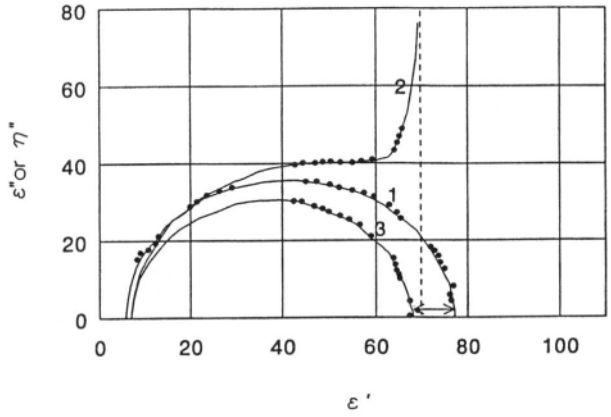


**Fig. 4.100.** Argand diagrams of a completely dissociated electrolyte and its pure solvent. Full circles: experimental data from frequency domain measurements on aqueous potassium chloride solutions at 25 °C. Curve 1: Argand diagram of pure water. Curve 2: Argand diagram, $\theta'' = f(\varepsilon')$, of an 0.8 *M* aqueous KCl solution, Curve 3: Argand diagram, $\varepsilon'' = f(\varepsilon')$, obtained from curve 2. (Reprinted from P. Turq, J. Barthel, and M. Chemla, in *Transport, Relaxation and Kinetic Processes in Electrolyte Solutions*, Springer-Verlag, Berlin, 1992, p. 78).

The permittivity of ionic solutions, is less than that of the pure solvent and decreases linearly with an increase in concentration. The reason for this has already been discussed (Section 2.12.1): water dipoles held by the very strong local field of an ion cannot orient against the weak applied field used in measuring the dielectric constant. The average is therefore decreased.

The linear relation found between dielectric constant and concentration can be interpreted in a first approximation as the result of a number of "irrotationally bound" waters. Such waters would constitute the primary hydration water referred to in Section 2.4.

## Further Reading

### *Seminal*

1. P. Debye and E. Hückel, "The Interionic Attraction Theory of Deviations from Ideal Behavior in Solution," Z. *Phys.* **24**: 185 (1923).
2. L. Onsager, "Interionic Attraction Theory of Conductance," Z. *Phys.* **28**: 277 (1927).
3. R. M. Fuoss, "Conductance in Aqueous Solutions," *Proc. Natl. Acad. Sci. U.S.A.* **75**: 16 (1928).

4. R. M Fuoss and C. A. Krauss, "Dimer and Trimer Formation in Ionic Solution," *J. Am. Chem. Soc.* **55**: 476 (1933).

### *Review*

1. M. Chabanel, "Ionic Aggregates of 1-1 Salts in Non-aqueous Solutions: Structure, Thermodynamic and Solvations," *Pure Appl. Chem.* **62**: 35 (1990).

### *Papers*

1. J. Barthel, H. Hetzenauer, and R. Buchner, *Ber. Bunsenges. Phys. Chem.* **96**: 988 (1992).
2. D. D. K. Chingakule, P. Gans, J. B. Gill, and P. L. Longdon, *Monatsh. Chem.* **123**: 521 (1992).
3. H. Ohshma, *J. Colloid Interface Sci.* **168**: 269 (1994).
4. M. Bachelin, P. Gans, and J. B. Gill, in *Chemistry of Nonaqueous Solutions: Current Progress*, G. Mamantov and A. I. Popov, eds., pp. 1–148, VCH Publishers, New York (1994).
5. M. R. Gittings and D. A. Saville, *Langmuir* **11:** 798 (1995).
6. A. R. Volkel and J. Noolandi, *J. Chem. Phys.* **102**: 5506 (1995).

## 4.8. NONAQUEOUS SOLUTIONS: A NEW FRONTIER IN IONICS

### 4.8.1. Water Is the Most Plentiful Solvent

Not only is water the most plentiful solvent, it is also a most successful and useful solvent. There are several facts that support this description. First, the dissolution of true electrolytes occurs by solvation (Chapter 2) and therefore depends on the free energy of solvation. A sizable fraction of this free energy depends on electrostatic forces. It follows that the greater the dielectric constant of the solvent, the greater is its ability to dissolve true electrolytes. Since water has a particularly high dielectric constant (Table 4.23), it is a successful solvent for true electrolytes.

A second advantage of water is that in addition to being able to dissolve electrolytes by the physical forces involved in solvation, it is also able to undergo *chemical* proton-transfer reactions with potential electrolytes and produce ionic solutions. Water is able to donate protons to, and to receive protons from, molecules of potential electrolytes. Thus, water can function as both a source and a sink for protons and consequently can enter into ion-forming reactions with a particularly large range of substances. This is why potential electrolytes often react best with water as a partner in the proton-transfer reactions. Finally, water is stable both chemically and physically at ambient temperature, unlike many organic solvents which tend to evaporate (Table 4.24) or decompose slowly with time.

On the whole, therefore, ionics is best practiced in water. Nevertheless, there are also good reasons why nonaqueous solutions of electrolytes are often of interest.

**TABLE 4.23**

**Dielectric Constants of Some Solvents (Temperature 298 K unless Otherwise Noted)**

| Solvent | Dielectric Constant |
|---|---|
| Water | 78.30 |
| Acetone | 20.70 |
| Acetonitrile | 36.70 |
| Ammonia (239 K) | 22.00 |
| Benzene | 2.27 |
| Dimethylacetamide | 37.78 |
| Dimethyl sulfoxide | 46.70 |
| Dioxane | 2.21 |
| Ethanol | 24.30 |
| Ethylenediamine | 12.90 |
| Hydrogen cyanide (289 K) | 118.30 |
| Pyridine | 12.00 |
| Sulfuric acid | 101.00 |

### 4.8.2. Water Is Often Not an Ideal Solvent

If water were the ideal solvent, there would be no need to consider other solvents. However, in many situations, water is hardly the ideal solvent. Take the electrolytic production of sodium metal, for example. If an aqueous solution of a sodium salt is taken in an electrolytic cell and a current is passed between two electrodes, then all that will happen at the cathode is the liberation of hydrogen gas; there will be no electrodeposition of sodium (see Chapter 7). Hence, sodium cannot be electrowon from aqueous solutions. This is why the electrolytic extraction of sodium has taken place from molten sodium hydroxide, i.e., from a medium free of hydrogen. This process requires the system to be kept molten (~ 600 °C) and therefore requires the

**TABLE 4.24**

**Boiling Points of Some Solvents**

| Solvent | Boiling point (K) |
|---|---|
| Water | 373.15 |
| Acetone | 329.35 |
| Benzene | 353.25 |
| 1,1-Dichloroethane | 330.15 |
| Methanol | 338.11 |

use of high-temperature technology with its associated materials problems. It would be a boon to industry if one could use a low-temperature conducting solution having the capacity to maintain sodium ions in a nonaqueous solvent free of ionizing hydrogen. This argument is valid for many other metals which are extracted today by electrodic reactions in fused salts at high temperatures, with the attendant difficulties of corrosion and heat losses.

Another field attracting the development of nonaqueous electrochemistry is that of energy storage for automobiles. Many reasons (e.g., the growing danger of pollution from automobile exhausts; the increasing concentration of $CO_2$, with its consequences of planetary warming; and the accelerating consumption of oil reserves) make the search for an alternative to the internal combustion engine a necessity. Nuclear reactors with their attendant shielding problems will always be too heavy for the relatively small power needed in road vehicles. There would be attractive advantages to a zero-emission, vibration-free electric power source. However, the currently available cheap electrochemical storage device—the lead–acid battery—is too heavy for the electric energy it needs to store to offer a convenient distance range between recharging. The electrochemical energy storers available today that do have a sufficiently high energy capacity per unit weight are expensive. The highest energy density theoretically conceivable is in a storage device that utilizes the dissolution of lithium or beryllium. However, aqueous electrolytes are debarred because in them, these metals corrode wastefully rather than dissolving with useful power production. So one answer to the need for an electrochemically powered transport system is the development of a nonaqueous electrochemical energy storage system that incorporates alkali metal (in particular lithium) electrodes. Many other examples could be cited in which the use of water as a solvent is a nuisance. In all these cases, there may be an important future for applications using nonaqueous solutions.

A nonaqueous solution must be able to conduct electricity if it is going to be useful. What determines the conductivity of a nonaqueous solution? Here, the theoretical principles involved in the conductance behavior of *true* electrolytes in nonaqueous solvents will be sketched. However, before that, let the pluses and minuses of working with nonaqueous solutions (particularly those involving organic solvents) be laid out.

### 4.8.3. More Advantages and Disadvantages of Nonaqueous Electrolyte Solutions

First, compared with aqueous electrolytes, nonaqueous solutions generally are liquid over a larger temperature range; this may include temperatures below 273 K, which is useful for applications in cold climates. They allow the electroplating of substances that would be unstable in aqueous solutions, such as aluminum, beryllium, silicon, titanium, and tungsten. One can even plate high-temperature superconductors and oxidize and reduce many organic and inorganic materials in electrosyntheses as long as one uses organic solvents. (The reason for the preference for nonaqueous

solutions here is the absence of protons and $OH^-$ ions. These tend to undergo preferential electrode reactions, evolving, respectively, hydrogen and oxygen. Such reactions compete with the intended organic reaction and often dominate it. In a nonaqueous solutions, the "window of opportunity," the potential range in which something useful may be done, is as much as 6 V.) Nonaqueous solutions are useful in the electromachining of metals and, as mentioned earlier, in high-energy-density batteries, which eventually could allow the use of these batteries in automobiles.

On the other hand, the drawbacks of nonaqueous solutions include their lower conductivities and their toxicity and flammability. They need extreme purification and handling under a highly purified inert-gas atmosphere. They may not be exposed to the atmosphere because they will pick up water, which may give rise to the undesired co-deposition of hydrogen.

The most important concentration range of conductivity studies for these electrolytes is below $10^{-3}$ mol $dm^{-3}$. Their most determined enemy is water, which acts as a contaminant. If one considers that 20 ppm of water is equivalent to a $10^{-3}$ mol $dm^{-3}$ solution of water in a nonaqueous solvent, it is no surprise that electrochemical quantities recorded in the literature are much less precise than those for aqueous solutions. Conductivities that are said to be as precise as $\pm 1\%$ are often $\pm 10\%$ in the nonaqueous literature. With materials that react with water (e.g., Li and Na) the water level has to be cut to less than 0.05 ppm and kept there; otherwise a monolayer of oxide forms on the metals' surfaces.

Drying of nonaqueous solutions can be carried out by various methods which include the addition of sodium, in the form of wires, or powdered solids such as barium oxide; alternatively, a high potential difference between auxciliary electrodes can be used to getter the $H^+$ and $OH^-$ ions. The quality of the nonaqueous work in electrochemistry is increasing rapidly.

### 4.8.4. The Debye–Hückel–Onsager Theory for Nonaqueous Solutions

An examination of the Debye–Hückel–Onsager theory in Section 4.6.12 together with the recent developments described in Section 4.6.14 shows that the developments are in no way wedded to water as a solvent. Does experiment support the predicted $\Lambda$ versus $c^{1/2}$ curve in nonaqueous solutions also?

Figure 4.101 shows the variation of the equivalent conductivity versus concentration for a number of alkali sulfocyanates in a methanol solvent. The agreement with the theoretical predictions demonstrates the applicability of the Debye–Hückel–Onsager equation up to at least $2 \times 10^{-3}$ mol $dm^{-3}$.

When one switches from water to some nonaqueous solvent, the magnitudes of several quantities in the Debye–Hückel–Onsager equation alter, sometimes drastically, even if one considers the same true electrolyte in all these solvents. These quantities are the viscosity and the dielectric constant of the medium, and the distance of closest approach of the solvated ions (i.e., the sum of the radii of the solvated ions). As a result, the mobilities of the ions at infinite dilution, the slope of the $\Lambda$ versus

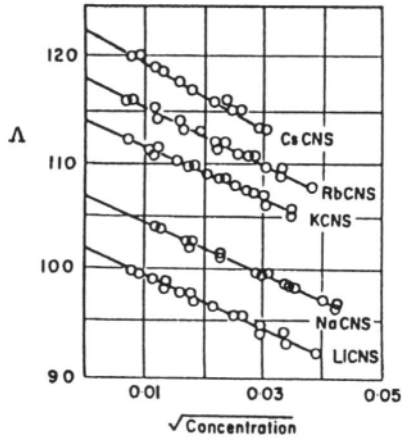


**Fig. 4.101.** Change in the equivalent conductivity of some alkali sulfocyanates with concentration in methyl alcohol.

$c^{1/2}$ curve, and finally, the concentration of *free* ions cause the conductance behavior of an electrolyte to vary when one goes from water to nonaqueous solvent. Before we get into equations which will deal with such effects to some degree, it is useful to look at the data available for nonaqueous solutions.

Among the goals of this brief survey is overcoming a common prejudice—that nonaqueous solutions are always less conductive than aqueous ones. A clear example is that of highly concentrated electrolyte solutions such as 5 *M* $LiBF_4$ in 1,2-dimethoxyethane (DME), which has a conductivity comparable to that in aqueous solutions at the same temperature.

## 4.8.5. What Type of Empirical Data Are Available for Nonaqueous Electrolytes?

4.8.5.1. *Effect of Electrolyte Concentration on Solution Conductivity.* It has been seen that reliable conductivity values are known only at low electrolyte concentrations. Under these conditions, even conductance equations for models such as the McMillan–Mayer theory (Sections 3.12 and 3.16) are known. However, the empirical extension of these equations to high concentration ranges has not been successful. One of the reasons is that conductivity measurements in nonaqueous solutions are still quite crude and literature values for a given system may vary by as much as 50% (doubtless due to purification problems).

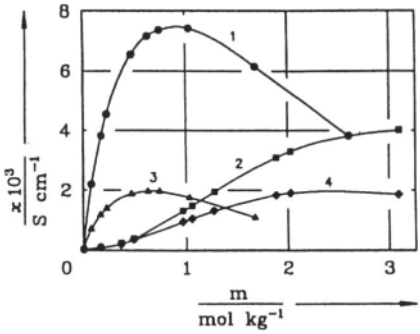


**Fig. 4.102.** Conductivity of $LiBF_4$ in $\gamma$-butyrolactone at (1) 298 K and (3) 238 K, and in tetrahydrofuran at (2) 298 K and (4) 238 K (M. Kindler, Dissertation, Regensburg, 1985).

One characteristic of conductivity curves when studied in a wide concentration range is the appearance of maxima, as shown in Fig. 4.102. These maxima are always observed when the solubility of the electrolyte in the given solvent is sufficiently high. They are the result of the competition between the increase of conductivity due to the

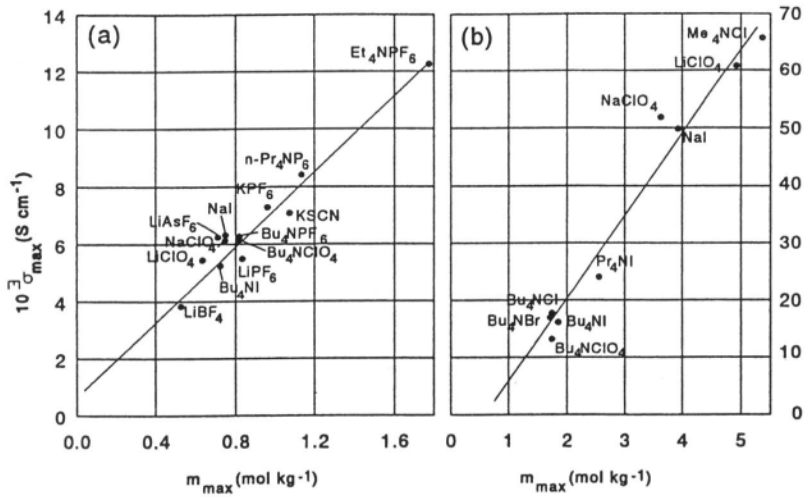


**Fig. 4.103.** Dependence of $\sigma_{max}$ vs. $c_{max}$ for various salts in (a) propylene carbonate and (b) methanol at 298 K (J. Barthel and H.-J. Gores, *Pure Appl. Chem.* **57**:1071,1985).

increase of free ions and the decrease of conductivity due to the decrease of ionic mobility as the electrolyte concentration increases. A linear relation has been found (Fig. 4.103) between the maxima plotted for specific conductivity and the concentration at which the maxima are observed.

Another type of behavior observed when plotting conductivities versus $c^{1/2}$ is the presence of temperature-dependent minima and maxima, as shown in Fig. 4.104. This unusual behavior has been attributed to triplet-ion formation (see Section 4.8.11). In this case Walden's rule (Section 4.4.12) has been used to calculate the values of equivalent conductivities at infinite dilution $\Lambda^0$.

4.8.5.2. *Ionic Equilibria and Their Effect on the Permittivity of Electrolyte Solutions.* Most of the commonly used solvents exhibit several relaxation processes that show up in the change of dielectric constant with frequency (see Section 2.12). These relaxation processes include rotation and libration of the molecules of the solvents, aggregates of ionic species, and H-bonding dynamics.

Relaxation times and dispersion amplitudes[46] change when ions are added. If ion pairs are formed, a new relaxation region appears on the solvent relaxation spectrum on the low-frequency side. Figure 4.105 shows the dielectric absorption spectrum of LiBr in acetonitrile, and how a maximum is developed in the low-frequency region as the concentration of solute increases and ion pairs are formed. Association constants can be determined from these data and contribute to the identification of the ion pair present.

4.8.5.3. *Ion–Ion Interactions in Nonaqueous Solutions Studied by Vibrational Spectroscopy.* Conventional methods to determine ion association measure a single property of the bulk solution, that is, an average of the interactions occurring over the time of the measurement. Microwave absorption studies exemplify such methods to determine solvation and ion association by studying, e.g., dielectric relaxation phenomena (see Section 2.12).

On the other hand, techniques that give information on the particular ion–ion and ion–solvent interactions would be of great help in the electrochemistry of nonaqueous solutions. Such help can be obtained from the various vibrational spectroscopic techniques, which are able to probe specific species in solution.

Raman spectra are related to the concentration of the species that give rise to them and offer a tool by which one may perform quantitative evaluations of ion-pair equilibria. For example, the ion association constant for ion pairing between $Ag^+$ and

[46]The dielectric constant (or relative permittivity) is an important property in the study of electrolyte conductivity of solutions and their solvents. However, the measurable quantity is the frequency-dependent complex permittivity, $\varepsilon(\omega)$. The static permittivity (dielectric constant) is obtained by extrapolation to zero frequency of the frequency-dependent complex permittivity $\varepsilon(\omega) = \varepsilon'(\omega) - i\varepsilon''(\omega)$, and both relaxation times and dispersion amplitudes can be obtained from these variables. The real part $\varepsilon'(\omega)$ yields the dispersion curve, and the imaginary part $\varepsilon''(\omega)$ the absorption curve of the dielectric spectrum.

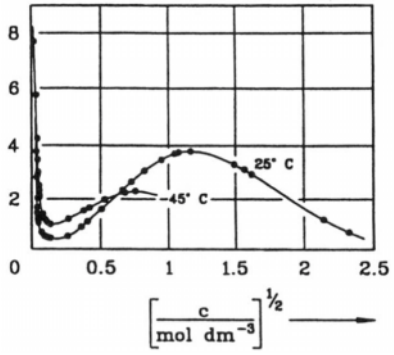


**Fig. 4.104.** Molar conductivity of $LiBF_4$ solutions in 1,2-dimethoxyethane at –45 and 25 °C, showing negative temperature coefficients at moderate concentrations (J. Barthel and H.-J. Gores, "Solution Chemistry: A Cutting Edge in Modern Electrochemical Technology," in *Chemistry of Nonaqueous Solutions: Current Progress*, G. Mamantov and A. I. Popov, eds., VCH Publishers, New York, 1994).

$NO_3^-$ in acetonitrile has been obtained by Janz and Müller. Associated structures of ions have been studied in nonaqueous solvents over a wide range of dielectric constants. LiCNS in solvents of low dielectric constant, such as ethers and thioethers, gives rise to several different types of ion aggregates. Many different types of contact ion pairs or agglomerates have been identified, and the role the solvent has in this association—whether the solvent separates the ions or not—has been determined. The Bjerrum critical distance, that is, the distance at which the ion is able to interact with other ions to form ion-pair structures (see Section 4.8.8), is of great use in these types of studies. Table 4.25 shows some values for 1:1, 2:2, and 3:3 electrolytes in different solvents.

It might be expected that NMR would be the ultimate technique for the identification of ion pairs in nonaqueous solutions because of its specificity for differentiating resonances of nuclei in ions in different environments. Several studies that involve $^7Li$, $^{13}C$, and $^{17}O$ among others, have been examined satisfactorily. Nevertheless, NMR also has drawbacks, such as a lack of well-defined spectra, which make interpretation difficult. The main reason seems to be the short lifetimes of the complexes (the ion pair lasts probably less than the data acquisition time, which is on the order of $10^{-6}$ s), which allow only small chemical shifts to be detected.

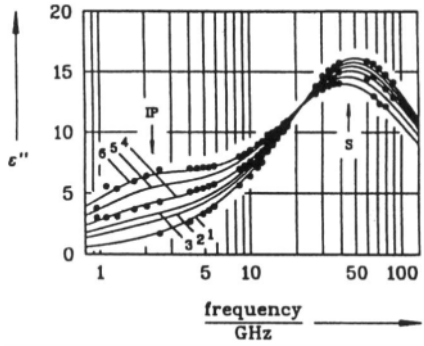


**Fig. 4.105.** Dielectric absorption spectrum (imaginary part of the complex permittivity, $\varepsilon''$) of LiBr solutions in acetonitrile at 25 °C. 1, Pure solvent; 2, 0.107 *M*; 3,0.194 *M*; 4,0.303 *M*; 5,0.479 *M*; 6, 0.657 *M*. *S* and IP indicate the frequency regions of the relaxation processes of solvent and solute. For the sake of clarity, experimental data (•) are added only for curves 1, 4, and 6 (J. Barthel, H. Hetzenauer, and R. Buchner, *Ber. Bunsenges. Phys. Chem.* **96**: 988, 1992).

**TABLE 4.25**

**Bjerrum Critical Distances for Three Solvents**

| | Temperature (K) | Permittivity ($\varepsilon$) | Bjerrum Critical Distances (pm) 1:1 | 2:2 | 3:3 |
|---|---|---|---|---|---|
| Water | 298 | 78.3 | 357 | 1428 | 3,213 |
| Acetonitrile | 298 | 36.7 | 3044 | 6849 | |
| Liquid ammonia | 203 | 26.3 | 1062 | 4248 | 9,558 |
| | 230 | 22.4 | 1248 | 4992 | 11,232 |
| | 298 | 16.9 | 1654 | 6616 | 14,886 |
| | 350 | 13.5 | 2071 | 8284 | 18,640 |

Source: Reprinted from J. B. Gill, "The Study of Ion–Ion Interactions in Electrolyte Solutions by Vibrational Spectroscopy," in *Chemistry of Nonaqueous Solutions: Current Progress*, G. Mamantov and A. I. Popov, eds., VCH Publishers, New York, 1994, p. 203.

It seems likely that improvements in the technology of the various spectroscopic techniques will make it possible to increase our knowledge of ion association in nonaqueous solutions. Knowledge of parameters such as $\Delta H_{\text{association}}$ and $\Delta S_{\text{association}}$ is becoming indispensable for understanding ionic association processes. For example, it is possible that the driving force to form ion pairs is a reorganizational one; that is, it is entropic and not enthalpic in nature, as might have been expected at first.

4.8.5.4. *Liquid Ammonia as a Preferred Nonaqueous Solvent.* Liquid ammonia has been widely used as a nonaqueous solvent in the study of ion-pair association. One of its advantages is the large range of dielectric constants—from 12 to 26—when the temperature is changed over 200 degrees. In contrast, the dielectric constant of water does not change throughout its normal liquid temperature range enough to move it out of the high dielectric constant range.

Furthermore, many salts are highly soluble in $NH_3$ because of the high solvation energies it makes possible. Finally, from the spectroscopic point of view, the small ammonia molecule has few molecular vibrations, which eases the interpretation of spectra observed in it—a characteristic difficult to find in other (more complex) solvents.

The first evidence of ion pairing in liquid ammonia came from a study of nitrate solutions by means of Raman spectroscopy. A number of bands larger than the ones expected for "free" nitrate ions were observed. A full understanding of these bands

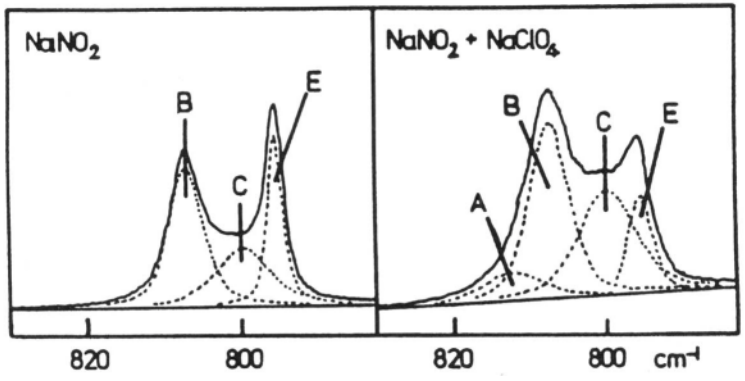


**Fig. 4.106.** The $\nu_2(NO_2)$ stretching region of the Raman spectra of sodium nitrite solutions at about 1.0 *M* in liquid ammonia at 293 K. The second spectrum is one of a solution in which $[NaClO_4]/[NaNO_2] = 4$. Band A, either ion triplet $[Na^+ \cdot NO_2^- \cdot Na^+]^+$ or contact ion pair containing bidentate $NO_2^-$; bands B and C, contact ion pairs $[Na^+ \cdot NO_2^-]^0$ and $[Na^+ \cdot ONO^-]^0$; band E, "free" solvated anion $[NO_2(NH_3)_x]^-$ (P. Gans and J. B. Gill, J. Chem. Soc. *Faraday Discuss.* **64**:150, 1978).

has not been accomplished yet, but researchers agree that the observed changes in symmetry are due to ion association. Figure 4.106 illustrates these Raman spectra.

4.8.5.5. *Other Protonic Solvents and Ion Pairs.* Apart from information for the solvent liquid ammonia, little spectroscopic data are available on this topic. The reason seems to be the great complexity of spectra when solvents like methanol or ethanol are used.

## 4.8.6. The Solvent Effect on Mobility at Infinite Dilution

At infinite dilution, neither relaxation nor electrophoretic effects are operative on the drift of ions; both these effects depend for their existence on a finite-sized ionic cloud. Under these special conditions, the infinite-dilution mobility can be considered to be given by the Stokes mobility

$$u^0_{\text{conv}} = \frac{ze_0}{6\pi r\eta} \tag{4.183}$$

Considering the same ionic species in several solvents, one has

$$u^0_{\text{conv}} r\eta = \text{constant} \tag{4.339}$$

If the radius $r$ of the solvated ion is independent of the solvent, then one can approximate Eq. (4.339) to[47]

$$u^0\eta = \text{constant} \tag{4.340}$$

Hence, an increase in the viscosity of the medium leads to a decrease in the infinite-dilution mobility and vice versa.

Tables 4.14 and 4.15 contains data on the equivalent conductivity, the viscosity, and the Walden constant $\Lambda^0\eta$ for two electrolytes and several solvents. It is seen that (1) Eq. (4.340) is a fair approximation for many solvents and (2) its validity is better for solvents other than water.

In fact, the radius of the kinetic entity may change in going from one solvent to another because of changes in the structure of the solvation sheath. Sometimes these solvation effects on the radius may be as much as 100%. Hence, it is only to a rough degree that one can use the approximate equation (4.340).

In some cases, the changes in the radii of the solvated ions are mainly due to the changes in the sizes of the solvent molecules in the solvation sheath. Thus, in the case of water, methanol, and ethanol, the size of the three solvent molecules increases in the order

[47] Actually, Eq. (4.340) containing the mobility is a form of Walden's rule [*cf.* Eq. (4.196)], which contains the equivalent conductivity. Since $\Lambda^0 = F[(u_{\text{conv}})^0_+ + (u_{\text{conv}})^0_-]$—*cf.* Eq. (4.292)—it is easy to transform Eq. (4.340) into the usual form of Walden's rule.

$$\text{Water} \rightarrow \text{methanol} \rightarrow \text{ethanol}$$

Since the radius of the solvated ions should also increase in the same order, it follows from Eq. (4.339) that the mobility or equivalent conductivity at infinite dilution should increase from ethanol to methanol to water. This is indeed what is observed (see Table 4.15).

One should be careful in using a simple Walden's rule $\Lambda\eta$ = constant, which assumes that the radii of the moving ions are independent of the solvent. Rather, one should use a generalized Walden's rule, namely,

$$u^0 r\eta = \text{constant} \tag{4.339}$$

where $r$ is the radius of the ionic entity concerned in a given solvent.

### 4.8.7. Slope of the $\Lambda$ versus $c^{1/2}$ Curve as a Function of the Solvent

If one takes the generalized Walden's rule (4.339) and calculates (from $\Lambda^0 = Fu^0$) the equivalent conductivity at *infinite dilution* for a number of nonaqueous solutions, it turns out that the values of $\Lambda^0$ in such solutions are relatively high. They are near those of water and are in some cases greater than those of water.

One might naively conclude from this fact that in using nonaqueous solutions instead of aqueous solutions in an electrochemical system, the conductivity presents no problem. Unfortunately, this is not the case. The crucial quantity that often determines the feasibility of using nonaqueous solutions in practical electrochemical systems is the *specific conductivity* $\sigma$ *at a finite concentration*, not the equivalent conductivity $\Lambda^0$ at infinite dilution. The point is that it is the specific conductivity which, in conjunction with the electrode geometry, determines the electrolyte resistance $R$ in an electrochemical system. This electrolyte resistance is an important factor in the operation of an electrochemical system because the extent to which useful power is diverted into the wasteful heating of the solution depends on $I^2R$, where $I$ is the current passing through the electrolyte; hence, $R$ must be reduced or the $\sigma$ increased.

Now, $\sigma$ is related to the equivalent conductivity $\Lambda$ at the same concentration

$$\sigma = \Lambda zc \tag{4.341}$$

but $\Lambda$ varies with concentration; this is what the Debye–Hückel–Onsager equation (4.321) was all about. To understand the specific conductivity $\sigma$ at a concentration $c$, it is not enough to know the equivalent conductivity under a hypothetical condition of infinite dilution. One must be able to calculate,[48] for the nonaqueous solution, the

[48]Of course, the validity of the calculation depends upon whether the theoretical expression for the equivalent conductivity (e.g., the Debye–Hückel–Onsager equation) is valid in the given concentration range.

equivalent conductivity at finite concentrations, utilizing the $\Lambda^0$ value and the theoretical slope of the $\Lambda$ versus $c^{1/2}$ curve. This will be possible if one knows the values of the constants $A$ and $B$ in the Debye–Hückel–Onsager equation

$$\Lambda = \Lambda^0 - (A + B\Lambda^0)c^{1/2}$$

where

$$A = \frac{ze_0F}{3\pi\eta}\left(\frac{8\pi z^2 e_0^2}{\varepsilon kT}\right)^{1/2}\left(\frac{N_A}{1000}\right)^{1/2}$$

and

$$B = \frac{e_0^2\omega}{6\varepsilon kT}\left(\frac{8\pi z^2 e_0^2}{\varepsilon kT}\right)^{1/2}\left(\frac{N_A}{1000}\right)^{1/2}$$

When one looks at the above expressions for $A$ and $B$, it becomes obvious that as $\varepsilon$ decreases, $A$ and $B$ increase; the result is that $\Lambda$ and therefore $\sigma$ decrease. Physically, this corresponds to the stronger interionic interactions arising as $\varepsilon$ is reduced.

So the question of the specific conductivity of nonaqueous solutions *vis-à-vis* aqueous solutions hinges on whether the dielectric constant of nonaqueous solvents is lower or higher than that of water. Table 4.23 shows that many nonaqueous solvents have $\varepsilon$'s considerably lower than that of water. There are some notable exceptions, namely, the hydrogen-bonded liquids.

Thus, because of the lower dielectric constant values, the effect of an increase of electrolyte concentration on lowering the equivalent conductance is much greater in nonaqueous than in aqueous solutions. The result is that the specific conductivity of nonaqueous solutions containing practical electrolyte concentrations is far less than the specific conductivity of aqueous solutions at the same electrolyte concentration (Table 4.26 and Fig. 4.107).

In summary, it is the lower dielectric constants of the typical nonaqueous solvent that cause a far greater decrease in equivalent conductivity with an increase of concentration than that which takes place in typical aqueous solutions over a similar concentration range. Even if the infinite-dilution value $\Lambda^0$ makes a nonaqueous electrochemical system look hopeful, the practically important values of the specific conductivity (i.e., the ones at real concentrations) are nearly always much less than those in the corresponding aqueous solution. That is another unfortunate aspect of nonaqueous solutions, to be added to the difficulty of keeping them free of water in ambient air.

**TABLE 4.26**

**Specific Conductivities of Electrolytes in Aqueous and Nonaqueous Solvents at the Same Concentration**

| Electrolyte | Concentration (mol dm$^{-3}$) | Specific Conductivity, ohm$^{-1}$ cm$^{-1}$ at 298 K | | |
|---|---|---|---|---|
| | | Water | Nonaqueous Solvent | |
| HCl | 0.1 | $391.32 \times 10^{-4}$ | (methanol) | $122.5 \times 10^{-4}$ |
| | | | (ethanol) | $35.43 \times 10^{-4}$ |
| NaCl | 0.01 | $11.85 \times 10^{-4}$ | (methanol) | $7.671 \times 10^{-4}$ |
| KCl | 0.01 | $14.127 \times 10^{-4}$ | (methanol) | $8.232 \times 10^{-4}$ |

## 4.8.8. Effect of the Solvent on the Concentration of Free Ions: Ion Association

The concentration $c$ that appears in the Debye–Hückel–Onsager equation pertains only to the free ions. This concentration becomes equal to the analytical concentration (which is designated here as $c_a$) only if every ion from the ionic lattice from which the electrolyte was produced is stabilized in solution as an independent mobile charge carrier; i.e., $c \neq c_a$ if there is ion-pair formation. Whether ion-pair formation occurs depends on the relative values of $a$, the distance of closest approach of oppositely charged ions, and the Bjerrum parameter $q = (z_+ z_- e_0^2/2kT)\,1/\varepsilon$. When $a < q$, the condition for ion-pair formation is satisfied and when $a > q$, the ions remain free.

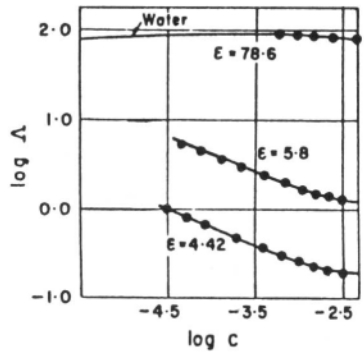


**Fig. 4.107.** Comparison of the concentration dependence of the equivalent conductivity of tetraisoamylammonium nitrate dissolved in water and in water–dioxane mixtures.

From the expression for $q$, it is clear that the lower the dielectric constant of the solvent, the larger is the magnitude of $q$. Hence, when one replaces water with a nonaqueous solvent, the likelihood of ion-pair formation increases because of the increasing $q$ (assuming that $a$ does not increase in proportion to $q$).

It has already been emphasized that, taken as a whole, an ion pair is electrically neutral and ceases to play its role in the ionic cloud (Section 3.8). For the same reason (i.e., that the ion pair is uncharged), the ion pair does not respond to an externally applied electric field. Hence, ion pairs do not participate in the conduction of current. A quantitative analysis of the extent to which ion-pair formation affects the conductivity of an electrolyte must now be considered.

### 4.8.9. Effect of Ion Association on Conductivity

In treating the thermodynamic consequences of ion-pair formation (Section 3.8.4), it was shown that the association constant $K_A$ for the equilibrium between free ions and ion pairs is given by

$$K_A = \frac{\theta}{(1-\theta)^2}\frac{1}{c_a}\frac{f_{IP}}{f_{\pm}^2} \tag{3.154}$$

where $\theta$ is the fraction of ions that are associated, $c_a$ is the analytical concentration of the electrolyte, $f_{\pm}$ is the mean activity coefficient, and $f_{IP}$ is the activity coefficient for the ion pairs. Since neutral ion pairs are not involved in the ion–ion interactions responsible for activity coefficients deviating from unity, it is reasonable to assume that $f_{IP} \approx 1$, in which case,

$$K_A(1-\theta)^2 c_a f_{\pm}^2 = \theta \tag{4.342}$$

A relation between $\theta$ and the conductivity of the electrolyte will now be developed. The specific conductivity has been shown [*cf.* Eq. (4.161)] to be related to the concentration of mobile charge carriers (i.e., of free ions) in the following way:

$$\sigma = zF(u_+ + u_-)c_{\text{free ions}} \tag{4.343}$$

One can rewrite this equation in the form

$$\sigma = zF(u_+ + u_-)\frac{c_{\text{free ions}}}{c_a}c_a \tag{4.344}$$

Since $c_{\text{free ions}}/c_a$ is the fraction of ions that are *not* associated (i.e., are free), it is equal to unity minus the fraction of ions that *are* associated. Hence,

$$\frac{c_{\text{free ions}}}{c_a} = 1 - \theta \tag{4.345}$$

and using this result in Eq. (4.344)

$$\sigma = zF(u_+ + u_-)(1 - \theta)c_a \tag{4.346}$$

or, from the definition of equivalent conductivity, i.e.,

$$\Lambda = \frac{\sigma}{zc_a} \tag{4.341}$$

one can write

$$\Lambda = F(u_+ + u_-)(1 - \theta) \tag{4.347}$$

If there is no ion association, i.e., $\theta = 0$, then one can define a quantity $\Lambda_{\theta=0}$, which is given by [*cf.* Eq. (4.163)]

$$\Lambda_{\theta=0} = F(u_+ + u_-) \tag{4.348}$$

By dividing Eq. (4.347) by Eq. (4.348), the result is

$$1 - \theta = \frac{\Lambda}{\Lambda_{\theta=0}} \tag{4.349}$$

and

$$\theta = 1 - \frac{\Lambda}{\Lambda_{\theta=0}} \tag{4.350}$$

Introducing these expressions for $\theta$ and $1 - \theta$ into Eq. (4.342), one finds that

$$K_A \frac{\Lambda^2}{\Lambda_{\theta=0}^2} c_a f_\pm^2 = 1 - \frac{\Lambda}{\Lambda_{\theta=0}}$$

or

$$\frac{1}{\Lambda} = \frac{1}{\Lambda_{\theta=0}} + \frac{K_A f_\pm^2}{\Lambda_{\theta=0}^2} \Lambda c_a \tag{4.351}$$

Though Eq. (4.351) relates the equivalent conductivity to the electrolyte concentration, it contains the unevaluated quantity $\Lambda_{\theta=0}$. By combining Eqs. (4.346) and (4.348), one gets

$$\Lambda_{\theta=0} = F(u_+ + u_-) = \frac{\sigma}{z[(1-\theta)c_a]} \tag{4.352}$$

from which it is clear that $\Lambda_{\theta=0}$ is the equivalent conductivity of a solution in which there is no ion association but in which the concentration is $(1-\theta)c_a$. Thus, for small concentrations (see Section 4.6.12), one can express $\Lambda_{\theta=0}$ by the Debye–Hückel–Onsager equation (4.321), taking care to use the concentration $(1-\theta)c_a$. Thus,

$$\Lambda_{\theta=0} = \Lambda^0 - (A + B\Lambda^0)(1-\theta)^{1/2}c_a^{1/2} \tag{4.353}$$

which can be written in the form (see Appendix 4.4)

$$\Lambda_{\theta=0} = \Lambda^0 - (A + B\Lambda^0)(1-\theta)^{1/2}c_a^{1/2} = \Lambda^0 Z \tag{4.354}$$

where Z is the continued fraction

$$Z = 1 - z\{1 - z[1 - z(\cdots)^{-1/2}]^{-1/2}\}^{-1/2} \tag{4.355}$$

with

$$z = \frac{(A + B\Lambda^0)c_a^{1/2}\Lambda^{1/2}}{\Lambda^{0\,3/2}} \tag{4.356}$$

Introducing expression (4.354) for $\Lambda_{\theta=0}$ into Eq. (4.351), one has

$$\frac{1}{\Lambda} = \frac{1}{\Lambda^0 Z} + \frac{K_A f_\pm^2}{(\Lambda^0)^2 Z^2}\Lambda c_a$$

or

$$\frac{Z}{\Lambda} = \frac{1}{\Lambda^0} + \frac{K_A}{(\Lambda^0)^2}\frac{\Lambda c_a f_\pm^2}{Z} \tag{4.357}$$

This is an interesting result. It can be seen from Eq. (4.357) that the association of ions into ion pairs has entirely changed the form of the equivalent conductivity versus concentration curve. In the absence of significant association, $\Lambda$ was linearly dependent on $c^{1/2}$, as empirically shown by Kohlrausch. When, however, there is

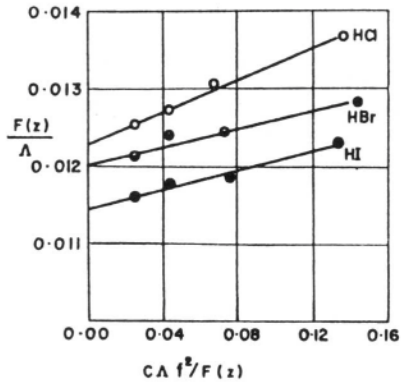


**Fig. 4.108.** Plots of Eq. (4.357) for the hydrogen halides in ethyl alcohol.

considerable ion-pair formation (as would be the case in nonaqueous solvents of low dielectric constant), instead of the Kohlrausch law, one finds that when $Z/\Lambda$ is plotted against $\Lambda f_{\pm}^2 c_a/Z$, a straight line is obtained with slope $K_A/(\Lambda^0)^2$ and intercept $1/\Lambda^0$. Figure 4.108 shows the experimental demonstration of this conductance behavior.

### 4.8.10. Ion-Pair Formation and Non-Coulombic Forces

The theory of ion-pair formation in nonaqueous solutions has been substantially advanced by the work of Barthel, who demonstrated how important it is to take into account the non-Coulombic forces at small ionic distances in addition to the Coulombic ones used by Bjerrum. These non-Coulombic forces are represented by the mean force potential $W_{+-}^*(r)$ in the region $a \le r \le R$,[49]

$$K_A = 4\pi N_A \int_a^R r^2 \exp\left[\frac{2q'}{r} - \frac{W_{+-}^*}{kT}\right] dr \tag{4.358}$$

where $q'$ is related to Bjerrum's parameter $q$ (*cf.* Eq. 3.144).

Non-Coulombic forces are those that are responsible for different degrees of association of electrolytes in isodielectric solvents. For example, one can see the importance of non-Coulombic forces in respect to ion-pair formation when one compares the temperature dependence of the association constants of alkali metal salts and the tetraalkylammonium salts in protic solvents. The association constants of alkali metal halides show a monotonically increasing $K_A$ when plotted against $(\varepsilon T)^{-1}$,

[49] In this region, the ion pair suppresses long-range interactions with other ions in solution.

**TABLE 4.27**

**Association Constants, Gibbs Energies, Enthalpies, and Entropies of Ion-Pair Formation of Alkali Metal and Tetraalkylammonium Iodides in 1-Propanol from Temperature-Dependent Conductivity Measurements**

| Electrolyte | $K_A$ ($dm^3$/mol) | $\Delta G_A$ (kJ/mol) | $\Delta H_A$ (kJ/mol) | $\Delta S_A$ (J $K^{-1}$ $mol^{-1}$) |
|---|---|---|---|---|
| NaI | 205 | −13.19 | 15.60 | 96.57 |
| KI | 336 | −14.41 | 17.56 | 107.21 |
| RbI | 433 | −15.04 | 16.28 | 105.03 |
| $Et_4NI$ | 543 | −15.60 | 5.29 | 70.05 |
| $Pr_4NI$ | 515 | −15.47 | 4.57 | 67.21 |
| $Bu_4NI$ | 517 | −15.48 | 4.33 | 66.44 |
| $Pent_4NI$ | 537 | −15.57 | 3.87 | 65.21 |

Source: Reprinted from J. Barthel, R. Wachter, G. Schmeer, and H. Hilbinger, *J. Sol. Chem.* **15:** 531, 1986.

whereas the tetraalkylammonium halide plot passes through a minimum at a temperature that is characteristic of the anion and solvent studied. Cation exchange has no effect on the position of this minimum.

In Table 4.27, one can see the $K_A$, free energies, enthalpies, and entropies of ion-pair formation. The enthalpies and entropies of the alkali metal salts are on the order of $16\ kJ\ mol^{-1}$ and $100\ J\ K^{-1}\ mol^{-1}$, respectively. In contrast, the small enthalpies and entropies of the tetraalkylammonium ions reflect lesser solvation of the cations in the protic solvents.

### 4.8.11. Triple Ions and Higher Aggregates Formed in Nonaqueous Solutions

When the dielectric constant of the nonaqueous solvent goes below about 15, ions can associate not only in ion pairs but also in ion triplets. This comes about by one of the ions (e.g., $M^+$) of an ion pair $M^+ \cdot\cdot A^-$ Coulombically attracting a free ion $A^-$ strongly enough to overcome the thermal forces of dissociation

$$A^- + M^+ \cdot\cdot A^- \rightleftharpoons A^- \cdot\cdot M^+ \cdot\cdot A^-$$

From the conductance point of view, ion pairs and triple ions behave quite differently. The former, being uncharged, do not respond to an external field; the latter are charged and respond to the external field by drifting and contributing to the conductance.

The extent of ion-pair formation is governed by the equilibrium between free ions and ion pairs. In like fashion, the extent of triple-ion formation depends on the equilibrium between ion pairs and triple ions.

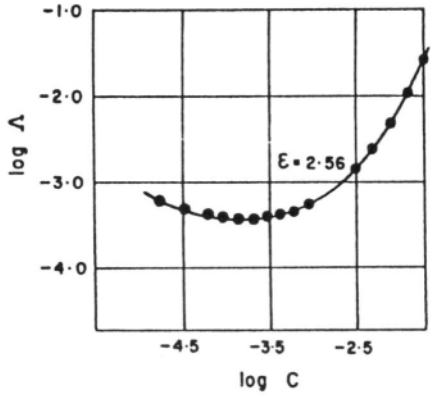


**Fig. 4.109.** Minimum in the curve for equivalent conductivity vs. concentration in the case of tetraisoamylammonium nitrate in a water–dioxane mixture of dielectric constant $\varepsilon = 2.56$.

$$M^+ + A^- \rightleftharpoons M^+ \cdot\cdot A^- \overset{A^-}{\rightleftharpoons} A^- \cdot\cdot M^+ \cdot\cdot A^-$$

Thus, the greater the stoichiometric concentration, the greater is the ion-pair formation and triple-ion formation.

With increasing concentration, therefore, ion-pair formation dominates the equivalent conductivity, which decreases with increasing concentration faster than if there had been no formation. At still higher concentrations, when triple-ion formation starts becoming significant, the equivalent conductivity starts increasing after passing through a minimum. This behavior has been experimentally demonstrated (Fig. 4.109).

Nevertheless, minima in plots of $\Lambda$ vs. $\sqrt{c}$ do not unambiguously prove the existence of triple ions. Grigo showed that it is also possible to reproduce the $\Lambda$ data for sodium iodide in butanol in terms of dielectric constant variation without the assumption of ion triplets. In summary, doubts still exist in relation to the formation of triple ions. Such doubts are most likely to be relieved by information that may become available through Raman and other kinds of spectroscopy.

### 4.8.12. Some Conclusions about the Conductance of Nonaqueous Solutions of True Electrolytes

The change from aqueous to nonaqueous solutions of *true* electrolytes results in characteristic effects on the conductance. The order of magnitude of the equivalent conductivity at infinite dilution is approximately the same in both types of solutions and is largely dependent on the viscosity of the solvent. However, the slope

of the equivalent-conductivity versus concentration curve is considerably more negative in nonaqueous solutions than in the corresponding aqueous solutions. This means that the actual specific conductivity σ, which is the significant quantity as far as the conducting power of an actual solution is concerned, is much lower for nonaqueous solutions. Ion-pair formation worsens the conductance situation; triple-ion formation may be a slight help.

Thus, nonaqueous solutions of true electrolytes are not to be regarded with unrestrained optimism for applications in which there is a premium on high specific conductivity and minimum power losses through resistance heating. One may have to think of solutions of *potential* electrolytes where there is an ion-forming reaction between the electrolyte and the solvent (Section 2.4).

## Further Reading

### *Seminal*

1. R. M. Fuoss and F. Ascania, *Electrolytic Conductance*, Interscience, New York (1959).
2. H. J. Gores and J. M. C. Barthel, "Nonaqueous Solutions: New Materials for Devices and Processes Based on Recent Applied Research," *Pure Appl. Chem.* **67**: 919 (1995).

### *Review*

1. J. Barthel and H. J. Gores, *Nonaqueous Solutions: Ionic Conductors with Widely Varying Properties,* in *Chemistry of Nonaqueous Solutions,* G. Mamantov and A. Popov, eds., p. 36, VCH Publishers, New York (1994).

### *Papers*

1. A. N. Ogude and J. D. Bradley, *J. Chem. Ed.* **71**: 29 (1994).
2. Z. H. Wang and D. Scherson, *J. Electrochem. Soc.* **142**: 4225 (1995).
3. Y. Koga, V. J. Loo, and K. T. Puhacz, *Can. J. Chem.* **73**: 1294 (1995).
4. Y. C. Wu and P. A. Berezansky, *J. Res. Natl. Inst. Standards Technol.* **100**: 521 (1995).
5. A. A. Chialvo, P. T. Cummings, H. D. Cochran, J. M. Simonson, and R. E. Mesmer, *J. Chem. Phys.* **103**: 9379 (1995).
6. G. H. Zimmerman, M. S. Gruszkiewicz, and R. H. Wood, *J. Phys. Chem.* **99**: 11612 (1995).
7. M. G. Lee and J. Jorne, *J. Membr. Sci.* **99**: 39 (1995).
8. J. Barthel, H. J. Gores, and L. Kraml, *J. Phys. Chem.* **100**: 3671 (1996).

## 4.9. ELECTRONICALLY CONDUCTING ORGANIC COMPOUNDS IN ELECTROCHEMISTRY

### 4.9.1. Why Some Polymers Become Electronically Conducting

Although organic compounds by and large have very poor electronic conductivity with values of specific conductivity $\sigma$ that are as much as $10^{12}$ times lower than those

**TABLE 4.28**

**Conductivity Values for Conducting Polymers and Other Materials**

| | $\sigma$ (S cm$^{-1}$) |
|---|---|
| I-Polyacetylene[a] | $1 \times 10^4$ |
| Polysulfur nitride (film) | $3 \times 10^3$ |
| Polypyrrole[b] | 40.7 |
| Poly-3-methylthiophene (foil)[c] | 16.7 |
| PPy-p7MB/$ClO_4$[d] | 13.74 |
| Polythiophene (PTh) 95%[e] | 0.6 |
| P3TASH[f] | 0.01 |
| Cu | $6 \times 10^5$ |
| KCl (aq. 1 *M*) | 0.1 |
| CuO | $1 \times 10^{-5}$ |
| Glass | $1 \times 10^{-14}$ |

[a] R. Menon, *Synthetic Metals* **80:** 223, 1996.
[b] 0.1 *M* $Fe_2(SO_4)_3$ oxidant; 0.022 sodium alkyl sufonate additive; Y. Kudoh, *Synthetic Metals* **79:** 17, 1996.
[c] U. Barsch and F. Beck, *Electrochim. Acta* **41:** 1761, 1996.
[d] PPy-p7MB/$ClO_4$ = Polypyrrole-poly(heptamethylene *p,p′*-bibenzoate); M. A. de la Plaza, M. J. Gonzalez-Tejera, E.S. de la Blanca, J. R. Jurado, and I. Hernandez-Fuentes, *Polymer Int.* **38:** 395, 1995.
[e] S. Yigit, J. Hacaloglu, U. Akbulut, and L. Toppare, *Synthetic Metals* **79:** 11, 1996.
[f] P3TASH = Poly[2-(3′-thienyl)ethanesulfonic acid]; S-A. Chen and M.-Y. Hua, *Macromolecules* **29:** 4919, 1996.

of a metal, certain organic polymers (conjugated compounds such as polyaniline and polypyrrole) conduct relatively well (see Table 4.28). The actual range of $\sigma$ at room temperature observed among organic polymers is large, but some organic polymers have values of $\sigma$ around unity. A few have specific conductivities that are even comparable with those of metals.

The degree of conductivity of organic polymers arises from their states of relative oxidation or reduction. In such states the polymer itself loses (for oxidation) or gains (for reduction) electrons in its structure. The number of monomer units that gain or lose an electron is variable but may be, e.g., 1 unit in 4. Once the polymer is electronically charged, counterions from solution enter the polymer fibrils to guard electrostatic neutrality. These neutralizing ions are often referred to as *dopants.* However, this is not doping in the sense of semiconductor doping (see Chapter 6), where the dopant itself ionizes to provide the charge carriers. In conducting polymers, the charge carriers are generated within the polymer chain. On the other hand, it is convenient to refer to the counterions in the charged polymers as dopants, so this term is widely used.

One model used to explain conductivity in polymeric structures is that of *polaron formation.*[50] Upon oxidation, double bonds along the chain are broken, leaving a

[50] A polaron is the term given to the quantum of electrostatic energy.

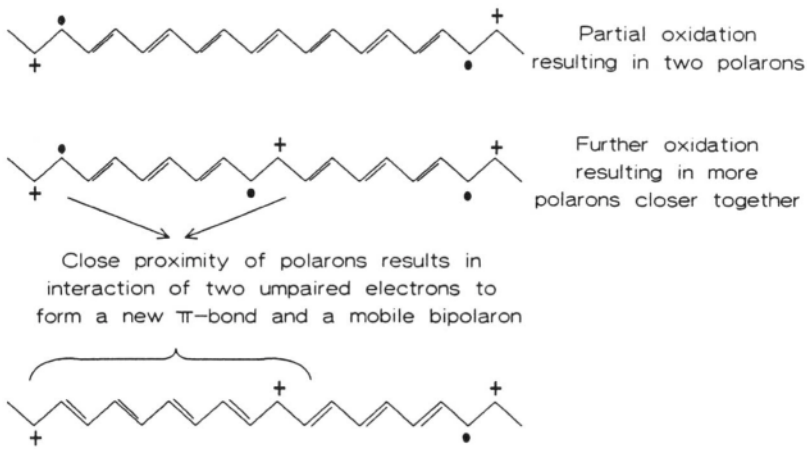


**Fig. 4.110.** Conductivity in polymeric structures by polaron formation. (After Lyons, 1996.)

radical and a positive charge unit on the polymer chain—and this positive charge is called a *polaron* (see Fig 4.110). After further oxidation, more polarons are formed along the chain. When the polaron concentration gets high enough, the radical cations spread out through adjacent $\pi$ structures across approximately eight bond lengths. At this distance the polarons are able to "feel" each other, making contact between them. The combination of two radicals—one from each polaron—forms a new $\pi$ bond. This $\pi$ bond is more stable than the two radical-cation bonds; that is, the $\Delta G$ of the $\pi$ bond is greater than the $\Delta G$ of dissociation of the two polarons. The result is a *bipolaron* that is more stable than two polarons the same distance apart. The bipolarons are then free to move along the polymer chain, which gives rise to electronic conductivity. It is at this point in the oxidation process that the conductivity undergoes a marked

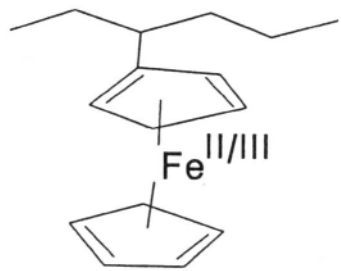


POLY(VINYLFERROCENE)

**Fig. 4.111.** An example of a redox polymer.

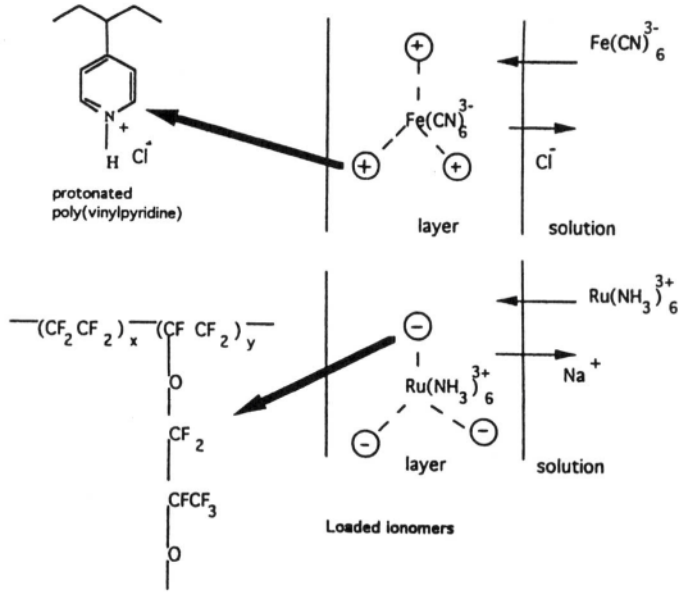


**Fig. 4.112.** Mechanism of conduction of loaded ionomers. (After Lyons, 1996.)

increase. Once the radical components of the polarons have combined to form $\pi$ bonds, the remaining positive charges achieve high mobility along the chain.

Organic materials that conduct electricity are grouped into three classes. These are called, respectively (see Figs. 4.111–4.113),

1. redox polymers
2. loaded ionomer materials
3. electronically conducting polymers

The redox polymers contain, as the name indeed suggests, redox-active groups that are in turn bound to the polymer's spine, as shown in Fig. 4.111. Electrons travel macroscopic distances by hopping along using the redox groups attached to the spine at points between which the hops occur.

For electrodes at which redox processes occur (Chapter 7), the redox potential $E$ is given by the expression

$$E = E^0 + \frac{RT}{nF} \ln \frac{c_{ox}}{c_{red}} \tag{4.359}$$

At the *standard redox potential* $E^0$ it is found that the conductivity passes through a maximum. This maximum of conduction occurs when $c_{ox} = c_{red}$. Hence, highly oxidized or highly reduced polymers do not conduct well at all.

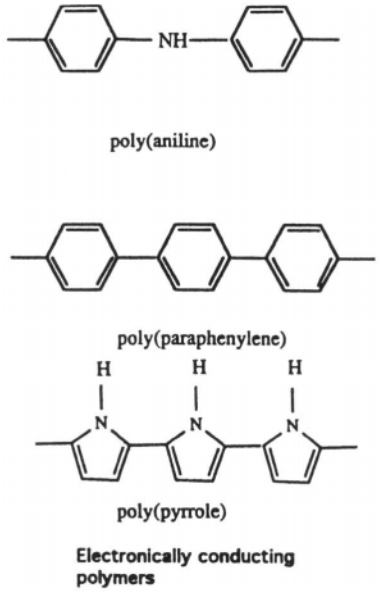


**Fig. 4.113.** Examples of electronically conducting polymers.

A second type of conducting electroactive organic substance is called a *loaded ionomer* (Fig. 4.112). Here the redox-active groups are mixed into the matrix of the ion-containing substance or *ionomer.* It can be seen in Fig. 4.112 what happens when an ionomer is placed in solution. As with the redox polymers, ionomers have charged sites attached to the polymer spine. Each of these charged sites has a partner or counterion of opposite sign. Once placed in a solution which itself contains ions that can take part in redox processes, the ionomer takes part in an ion-exchange process. The counterions originally belonging to the ionomer transport themselves into the surrounding solution, and the redox-active ions which were in the solution to begin with enter the ionomer and become electrostatically attached to the opposite charges in the polymer that makes up the ionomer material (usually a film). The conduction has the same mechanism as that for the redox polymer: electrons hop along between charged sites.

It is when one reaches the electronically conducting polymers that the really high conductances are found. There is a clear reason for this: for these substances (Fig. 4.113) the spine contains many conjugated structures and in these electrons are delocalized. Along such conjugated structures, charge transport is very fast and the rate-determining act is crossing from chain to chain.

Such materials also vary greatly in conductivity, depending on the state of oxidation. However, the conductance does not maximize at the standard redox poten-

tial—as with redox polymers—but when the polymer is in the highly oxidized state, so that many electrons are set free (i.e., $Fe^{2+} \rightarrow Fe^{3+} + e^-$). In the reduced state, electrons are withdrawn and the electronically conducting polymers become insulating polymers; the loss in conductivity is dramatically sudden and tends to disrupt the happiness of the experimenter. Thus, to keep the electronically conducting polymers conducting, they always have to be oxidized.[51]

### 4.9.2. Applications of Electronically Conducting Polymers in Electrochemical Science

*4.9.2.1. Electrocatalysis.* New materials that may act as electrocatalysts, that is, that may improve the desired path in a given reaction, are always needed if they are inexpensive and/or more easily handled than conventional materials. The development of conducting polymers to act as electrocatalysts is an area of research that began in the 1990s. It is relatively easy for organic compounds to be "adjusted," that is, the surface groups in the polymer can be varied to a great degree, which is just what is needed to give catalysts a variety and power corresponding to those of enzymes.

Corresponding to this is the idea of biosensors that could be implanted in the body for the electroanalysis of conceivably any chemical in the body. Thus, it may become possible to adsorb enzymes on the surface of electrodes and then tune these enzymes to react with appropriate biomolecules, as represented in Fig. 4.114. How would conducting polymers figure in such devices? They might be useful as the biosensor itself, since, being organic, they are more likely to interact positively with enzymes and biochemicals than metal electrodes would.

4.9.2.2. *Bioelectrochemistry.* A potential area of application of conducting polymers is in prosthetic devices. One of the difficulties in this area of research is blood clotting, which occurs when the electrical potential of the implanted device is negative insufficiently in potential. Blood clotting is common when metals are used as prosthetics, but given the great variety of materials that could become suitable through the use of electronically conducting organic polymers, the range of possible materials is much increased. The further possibility of organically conducting materials being able to be made into artificial organs[52]—replacing the difficult-to-find transplants—is an enticing one, particularly in the future development of electrochemistry in concepts such as the "cyborg" (Chapter 1).

---

[51] There are other factors that also affect the degree of conduction of electronically conducting polymers when they are in the oxidized state; one is alignment of the polymer chains. Thus, a rate-determining step in conduction may be the transfer of electrons from one unit in the spine to another: here linearity in the chain would help and junctions out of alignment would impede the continued passage of electrons along the chain.

[52] Although this goal is enticing, and perhaps not more than a decade away, a prerequisite to its achievement is much more knowledge of the surface properties of electronically conducting polymers.

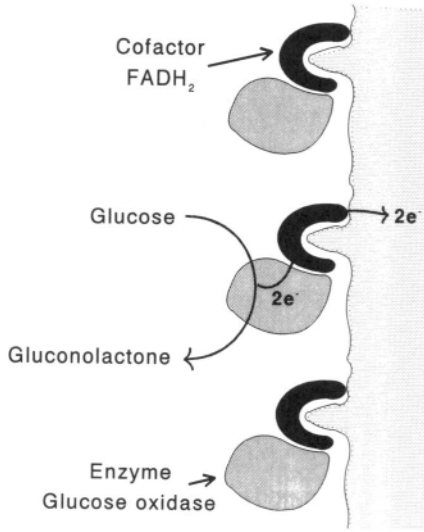


**Fig. 4.114.** Glucose sensor in which the enzyme (containing *a* reduced cofactor) is oxidized directly at an electrode.

4.9.2.3. *Batteries and Fuel Cells.* The work that directed commercial attention toward the use of electronically conducting polymers was initiated by Alien MacDiarmid at the University of Pennsylvania, who reported in 1980 on a battery using polyacetylene in propylene carbonate. The original battery is shown in Fig. 4.115. The conductivity of the polymer is adjusted by varying the content of lithium perchlorate, which acted as doping material in the polyacetylene. The maximum conductivity of the polyacetylene is on the order of $10^3$ S $cm^{-1}$. The energy density obtained by this battery, which discharges with an initial current of 25 mA $cm^{-2}$, was about 170 W-hr per kilogram, compared with about 30 for the lead acid-battery. Since MacDiarmid's pioneer work, many other batteries involving conducting polymers have been studied. They are attractive, particularly for their potential as extremely cheap electricity storers, perhaps for widespread use in electrically powered bicycles.

An attraction of conducting organic materials as batteries is their low densities of about 1 g $cm^{-3}$ compared with 10 g $cm^{-3}$ for metals. Their use in aircraft might be cost effective. Such prospects must be balanced against the relatively small potential range in which the present electronically conducting polymers are stable.

4.9.2.4. *Other Applications of Electronically Conducting Polymers.* Future applications of electrochemistry in clean energy systems (based on solar light or chemically stimulated nuclear changes) seem possible. A major difficulty so far has been the expense of the materials. In this area, one of the initial studies involving

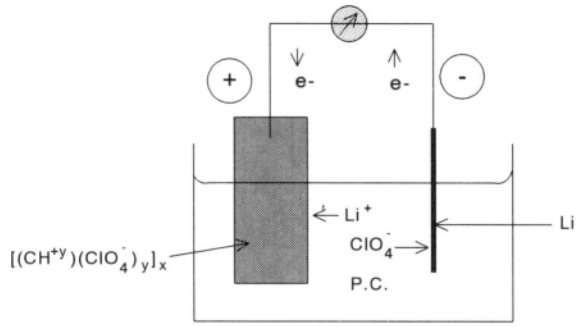


**Fig. 4.115.** Schematic representation of the discharge process in a $(CH)_x/LiClO_4/Li$ rechargeable storage battery celt (A. J. Heeger and A. G. MacDiarmid, in *The Physics and Chemistry of Low Dimensional Solids*, L. Alcacer, ed., D. Reidel, Boston, 1980, p.45).

conducting polymers was carried out by Shirakawa et al. in the early 1990s. Their cell is shown in Fig. 4.116.

One of the fields in which conducting polymers may have a great potential for development is the one broadly classified as *molecular electronics.* The fabrication of reliable electronic devices based on organic molecules or biological macromolecules offers formidable challenges. Is there a possibility of utilizing conducting organic compounds in miniaturizing electronic devices so that eventually molecules take the place of wires, transistors, and memory devices? Electronically conducting polymers should be useful in such advanced developments.

Another area of potential applicability of conducting polymers is monitoring the composition of gaseous ambients. Although solid-state gas sensors are available, they present a disadvantage: the high temperatures needed for the sensor elements to operate. Here is where research may find conducting organic polymers useful. For example, it has been shown by Miasik et al. that the resistance of a polypyrrole deposited on a filter paper is sensitive to the presence of ammonia at room temperature. Thus, the resistance increases in the presence of a reducing gas, such as ammonia, and decreases in the presence of an oxidizing gas, such as nitrogen dioxide. The response of such an electrode is depicted in Fig. 4.117.

### 4.9.3. Summary

The major difficulty in the 1990s for the development of electronically conducting polymers lies in the limited understanding we have about the relation between the molecular structure of the organic material and the resulting electronic conductance.

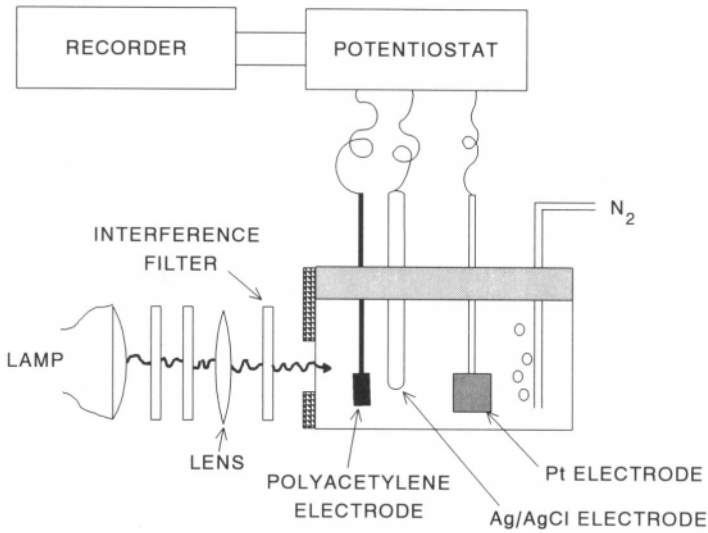


**Fig. 4.116.** Experimental apparatus used by Shirakawa et al. for photoelectrochemical measurements of a polyacetylene electrode (H. Shirakawa, S. Ikeda, M. Aizawa, J. Yoshitake, and

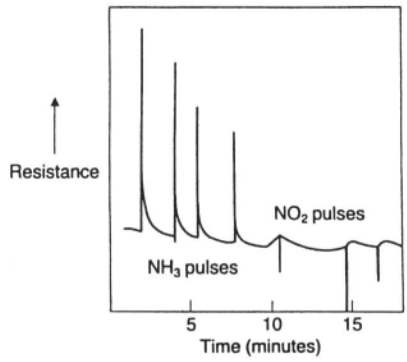


**Fig. 4.117.** Qualitative dc resistance response characteristic at room temperature of a conductive polypyrrole sensor to pulses of ammonia and nitrogen dioxide (J. J. Miasik, A. Hooper, P. T. Mosely, and B. C. Tofield, "Electronically Conducting Polymer Gas Sensors," in *Conducting Polymers,* Luis Alcacer, ed., Reidel, Dordrecht, The Netherlands, 1987).

However, the field is ripe for development, particularly in electrocatalysis for obtaining cheap, light, electrochemical storage and in molecular electronics coupled with prosthetics.

## 4.10. A BRIEF RERUN THROUGH THE CONDUCTION SECTIONS

We learned early on that equivalent conductivity and specific conductivity differed in that the former was not directly proportional to concentration but only secondarily so. However, it turned out that this secondary dependence was considerable and arose because the mobility of the ion itself decreased with an increase in concentration. Thus, as ions get near enough to feel each other through the interaction of their electric fields, they slow down.

At a molecular level, this slowdown is described in terms of two effects. One of these effects is called *electrophoretic* and the other, *relaxational.* The electrophoretic effect is easy to understand because it is a kind of electrical friction: as one ion passes the other within electrical hailing distance, both ions slow down in recognition of the electrical existence of the other.

The relaxation effect is a bit more difficult to explain. It has to do with the fact that when an ion moves in a given direction, inertia causes the ionic cloud around it to become egg shaped, and this dissymmetric ionic cloud has more counter charge toward its rear than toward its front. The dissymmetry of charges acts to counteract the effect of the directional electric field applied through the solution, and so this also slows the ion down. Both these effects combine to explain why mobility falls with increasing concentration, for the two effects increase in strength with the square root of the concentration.

Then, having broached the subject of the relaxation of the ion's atmosphere—its taking up a dissymmetric shape when the ion moves—we went on to tackle the subject of relaxation quite generally. For example, if an electric field is suddenly applied to a solution, it would orient the solvent dipoles therein. A new equilibrium would then be set up. The relaxation time is a measure of the time it takes to set up this new equilibrium. At first it seems peculiar that one should call it "a measure of" and not the time itself. However, the situation is similar to that of radioactive decay because in changing from state 1 to state 2, the concentration of a radioactive nucleus decreases exponentially with time, taking an infinite time to disappear completely. Since this is not a practical measure, we agree to use another measure of the rate of decay—the time to decline by 63%.

These ideas about relaxation times are applied to several phenomena, including the changes in asymmetry of the ionic atmosphere and the unusual behavior of the dielectric constant of water, which has three values according to the frequency with which it is measured. They are 78, 5, and 2.

Nonaqueous solutions are one of two final topics in this section. They form a subfield in which there has been immense progress since 1970. Nonaqueous solutions

allow a much greater electrochemical window than do the aqueous solutions because of course in the latter, one is subject to hydrogen evolution if one goes too negative and evolution of oxygen if one goes too positive. In practice, in aqueous solutions, there is only about 1.5 V of practical working potential—a relatively short range when one recalls that the electrochemical series extends over about 4.5 V. This is one of the reasons why the study of nonaqueous solutions has increased in intensity so much in recent years. It opens up several new areas, and one of them concerns the strange new ions that are formed there. This is because the dielectric constant is so much lower in nonaqueous than in aqueous solutions and therefore the Coulombic attraction between ions of opposite sign is higher in the former solutions, so that there is a greater tendency to "stick together." Dimers, trimers, and even larger aggregates occur.

Last of all, we discussed the conductivity of certain polymers. This is a fairly new area and very promising for electrochemical devices, the breadth of application of which may be greatly extended. We started off by pointing out why it is that only certain types of organic materials produce relatively high concentrations of mobile electrons that can leave the tiny prescribed molecular area in which they usually have their being and become mobile along a whole polymer chain, by hopping along charged sites in the polymer spine. In this way organic materials (that normally would be considered insulators) may become significantly conducting (e.g., $10^3$ S $cm^{-1}$).

Electronically conducting polymers form so new a field that it exists more in hope than in reality. As with the progress of much scientific research, it depends on the amount of funding available. Nonaqueous solutions offer tremendous scope because they allow one to introduce so much variety in properties. Among the applications already mentioned is the possibility of making cheap electricity energy storers (or batteries) utilizing, e.g., polyacetylene or polypyrrole. A really exciting suggestion for the future is the possibility that we might be able to manufacture artificial organs for the body by using conducting organics and hence avoid the wait for transplants.

## Further Reading

### *Seminal*

1. H. Kallmann and M. Pope, "Conductivity of Insulators in Contact with Ionic Solutions," *J. Chem.Phys.* **32**: 300(1960).
2. H. Mehl, J. M. Hale, and F. Lohmaan, "Electrode Made out of Insulators," *J. Electrochem. Soc.* **113**: 1166 (1966).
3. R. Pethig and G. Szent-Györgyi, "Redox Properties in Biomolecules," *Proc. Natl. Acad. Sci. U.S.A.* **74**: 226 (1978).
4. J. Heeger and A. G. MacDiarmid, "Electronically Conducting Polyacetylene," in *The Physics and Chemistry of Low Dimensional Solids*, L. Alcacer, ed., p. 73, D. Reidel, Boston (1980).

### *Reviews*

1. J. O'M. Bockris and D. Miller, "An Introduction to Conducting Polymers," in *Conducting Polymers*, Luis Alcacer, ed., Reidel, Dordrecht, The Netherlands (1987).

2. W. H. Smyrl and M. Lien, "Conductivity in Electronically Conducting Polymers," in *Applications of Electroactive Polymers*, B. Scrosati, ed., Chapman and Hall, London (1993).
3. M. E. G. Lyons, in *Electroactive Polymer Chemistry*, Part I. *Fundamentals*, M. E. G. Lyons, ed., Chapter I, Plenum Press, New York (1994).

### *Papers*

1. D. L. Miller and J. O'M. Bockris, *J. Electrochem. Soc.* **139**: 967 (1992).
2. A. Szucs, G. D. Hitchens, and J. O'M. Bockris, *Electrochim. Acta* **37**: 277 (1992).
3. S. Li, C. W. Macosko, and H. S. White, *Science* **259**: 957 (1993).
4. G. Shi, S. Jin, and G. Xue, *Science* **267**: 994 (1995).
5. M. S. Walaszlowski, J. Orlikowski, and R. Juchniewicz, *Corros. Sci.* **37**: 645 (1995).
6. M. S. Freund and N. S. Lewis, *Proc. Natl. Acad. Sci. U.S.A.* **92**: 2652 (1995).
7. X. B. Chen, J. Devaux, J. P. Issi, and D. Billaud, *Polym. Eng. Sci.* **35**: 637 (1995).
8. B. Coffey, P. V. Madson, T. O. Poehler, and P. C. Searson, *J. Electrochem. Soc.* **142**: 321 (1995).

## 4.11. THE NONCONFORMING ION: THE PROTON

### 4.11.1. The Proton as a Different Sort of Ion

The reason for having a whole section in this book on proton conduction is that this particle exhibits characteristics quite different from those of other ions; moreover, the particle itself is *tiny* in dimension. Instead of carrying with it the electron shell normal to all other ions—hence having its radius expressed in nanometers—the proton is a nucleus only, and its radius is only about 1 fermi (F) ($10^{-13}$ cm). This makes it the smallest ion and the lightest, giving it the property of being able to approach much closer to a neighboring ion or atom than any other ion or atom can. The tiny proton is, however, also a mighty proton: it attracts electrons much more powerfully than, say, Li. This particular property is shown by the magnitude of the ionization energy: 1309 kJ $mol^{-1}$ for hydrogen vs. 519 kJ $mol^{-1}$ for lithium. Apart from this display of power, protons have a unique characteristic—they form H bonds. Partly for this reason, the time a proton remains bare in water is small indeed; it spends less than 1% of its time alone. The remaining 99% of its time, a proton in solution is closely attached to an $H_2O$ molecule, forming $H_3O^+$, a hydronium ion.

Being such a famous performer, the shape and size of the hydronium ion have been determined by NMR and other methods. The $H_3O^+$ ion has a rather flat trigonal-pyramidal structure with the hydrogen at the corners of the pyramid and the oxygen in the middle, as shown in Fig. 4.118. Its structure resembles that of the ammonia molecule.

A great deal can be learned about the proton simply by reviewing some energy quantities assigned to it. The energy change associated with the interaction between a

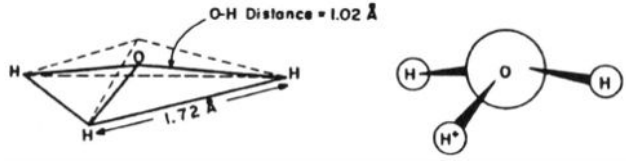


**Fig. 4.118.** The trigonal-pyramid structure of the hydronium ion $H_3O^+$.

proton and a single water molecule, the *proton affinity of water*, is $-711\ kJ\ mol^{-1}$. This value corresponds to the interaction of $H^+$ and $H_2O$ in the *gas phase*, not in solution. The corresponding value of the enthalpy or heat of hydration of the proton is $-1112\ kJ\ mol^{-1}$. How are these two values related? If the *proton affinity* is subtracted from the *total hydration heat* of a proton, one gets then the *heat of hydration* of an $H_3O^+$ ion! This value is $-401\ kJ\ mol^{-1}$, a reasonable value when one compares it with the heat of hydration of a $K^+$ ion $(-344\ kJ\ mol^{-1})$, which has approximately the same radius as the $H_3O^+$ ion.

The value of $-401\ kJ\ mol^{-1}$ for the hydration energy of the hydronium ion indicates that it itself is hydrated. How many molecules of water hydrate it? A look at Fig. 4.119 shows that approximately three water molecules are associated to the hydronium ion, giving a structure of $(H_9O_4)^+$.[53]

How is the $H^+$ a nonconforming ion? For one thing, because of its special association with water; it is nearly always tightly bound to *one* water. This structure seems to exist as an entity which itself is being solvated by other waters.

This is not the only nor the main differentiating property of the nonconforming ion. Having seen that $H^+$ is usually to be found tightly attached to $H_2O$, one would expect that $H_3O^+$ would be the transporting entity. It is not! $H_3O^+$ movement contributes only about 10% of the transport of $H^+$ in aqueous solution, and the main mode of transport is, indeed, entirely different from that of other ions.

Why is it that one regards the proton as different from all other ions? There are three reasons, all connected with its tiny size and small mass: (1) The tiny size means that such an ion can go anywhere (e.g., diffusing in Pd). (2) Its small mass turns out to give rise to a mechanism of motion in solution quite different from that of any other ion (except its isotope, the deuteron). (3) In quantum mechanical tunneling (see also Chapter 9), low mass is a vital factor. The electron, the mass of which is nearly 2000 times less than that of a proton, can easily tunnel through barriers more than 2000 pm in thickness. The ability of the proton to tunnel is much less than that of the electron,

[53] In the coordination shell of an $H_3O^+$ ion, $n$ water molecules are compressed owing to the electric field of the ion, and thus the molar volume is decreased compared to what one would expect from the volume of water. By measuring molar volumes or densities as a function of temperature and comparing them with curves calculated for an assumed value of $n$, the number of coordinating water molecules can be predicted.

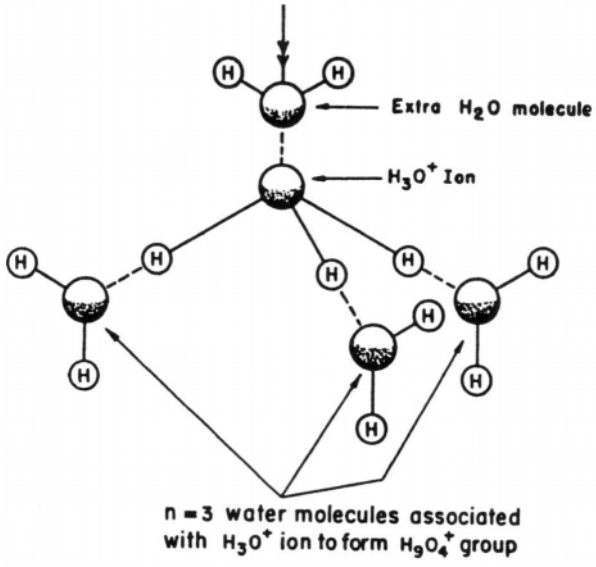


**Fig. 4.119.** Schematic configuration of $H_9O_4^+$ group shown with an extra $H_2O$ molecule electrostatically bound.

but its quantum properties are still significant—and that is something that sets it apart from heavier ions, even $He^+$ and certainly $Li^+$. So this ion's properties deserve a special section of which this is the introduction.

### 4.11.2. Protons Transport Differently

The starting point to elucidate the way the proton moves in solution is to consider its movement through the solvent at a steady state—constant velocity—and at a concentration so low that there is no interionic interaction (zeroth approximation). This occurs when the electric driving force $ze_0X$ balances the Stokes viscous force, $6\pi r\eta v$. Thus, the Stokes mobility is

$$u_0 = \frac{ze_0}{6\pi r\eta} \tag{4.183}$$

What radius should one use? Suppose one takes a rough-and-ready measure to consider the hydronium ion. Since it has approximately the same radius as that of a $K^+$ ion, one would expect its mobility to be approximately the same, i.e., about $5 \times 10^{-4}\ cm^2\ V^{-1}\ s^{-1}$. It is here that one encounters the great anomaly—the nonconforming ion—for the mobility of the proton is in reality $36 \times 10^{-4}\ cm^2\ V^{-1}s^{-1}$, a sevenfold excess.

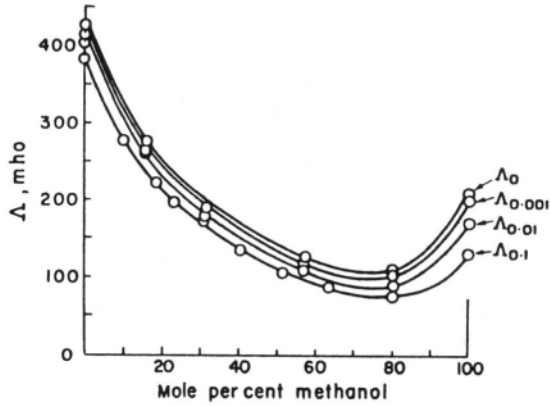


**Fig. 4.120.** The equivalent conductivity of HCl in methanol-water mixtures decreases with increasing alcohol content and reaches a minimum at about 80 mol % of alcohol. At this concentration, the abnormal mobility, i.e., the mobility of the $H_3O^+$ ion compared with that of the $K^+$ ion (which is of similar size), is reduced almost to zero.

One can pick up a clue as to the reason for this anomaly in mobility if one asks: What is the proton's mobility in other, related solvents? This rather vital question was addressed and solved in a Ph.D. thesis by an Austrian student, Hanna Rosenberg, more than 40 years ago. She found that if, for example, methanol was added to water, the anomalous mobility of the proton was decreased (Fig. 4.120). When methanol was replaced by other, larger alcohols (no water present), she was astounded to find that the anomalous mobility was greatly reduced until by the time *n*-propanol was reached, the difference between HCl and LiCl was greatly reduced (Table 4.29).

**TABLE 4.29**

**Equivalent Conductivities (S $cm^2$ $eq^{-1}$) at Infinite Dilution of HCl and LiCl at 293 K**

| | Solvent | | | |
|---|---|---|---|---|
| | Water | Methanol | Ethanol | *n*-Propanol |
| $\Lambda_{HCl}$ | 426.2 | 192.0 | 84.3 | 22 |
| $\Lambda_{LiCl}$ | 115.0 | 90.9 | 38.0 | 18 |
| $\frac{\Lambda_{HCl}}{\Lambda_{LiCl}}$ | 3.71 | 2.11 | 2.22 | 1.22 |

Another fact came up in further work stimulated by Ms. Rosenberg: the ratio of the proton and deuterium mobilities in water had been found to be 1.4 at 25 °C, an unexpectedly large value. If the proton mobility was to be understood in terms of movements of $H_3O^+$ or $D_3O^+$ in a viscous fluid (i.e., if it were determined by Stokes' law), the two values should be about the same, because the actual difference in size of the two ions ($H_3O^+$ and $D_3O^+$) would be negligible. Finally, when one looks into the conductance of protons in water at various temperatures, one expects that as with the other ions, there will be a constant energy of activation over an appreciable range of temperatures. The truth is, the $\log \Lambda$ vs. $1/T$ plot shows curvature, suggesting that as the temperature increases, the entity contributing to the transport is changing.

The proton is indeed anomalous in its conductance and mobility. These properties do not vary with temperature in the expected, regular way. There is not the expected near-sameness for hydronium and deuterium ion mobilities. The conductance of protons in aqueous-non-aqueous media is wholly dependent on the mole-fraction of water present.

### 4.11.3. The Grotthuss Mechanism

The use of Stokes' law to calculate the mobility of an ion implies a mechanism for the way an ion goes through a solution. When Stokes derived his famous equation (the one that gives the resistive force to flow as $6\pi r\eta v$; (Section 4.4.7)), ions had not been thought of, and the movement that Stokes imagined was much more like a brass ball being pulled through molasses. As the decades passed, Stokes' law turned out to perform remarkably well, not only for brass balls in molasses, but also right down to particles of angstrom size, the size of normal, regular ions. So it is not unreasonable to conclude that ions, too, have a slow, viscous kind of movement through a solvent. The molecular-level picture is that of the ion—in the absence of an applied field—lurching hither and staggering thither, the direction of each lurch being randomly determined. When an electric field is applied, there is still this lurching all over the place, as in diffusion (Section 4.2), but now there is a slightly preferred component to the random movement—that of the ion's movement in the direction of the electric field. It is to this drift movement—movement in the direction of the electric field—that Stokes' law applies.

It was demonstrated earlier in several ways that although it may well apply to $K^+$ and $Na^+$, Stokes' law certainly *does not* apply to the proton, the nonconforming ion. There may be a slow, viscous drifting of $H_3O^+$ through the solvent. However, it does not explain the proton's movement.

A Swedish worker, Grotthus, had noticed that in a row of marbles in contact, the collision of the marble at one end of the row with a new marble caused a marble at the far end to detach itself and go off alone (Fig. 4.121). This sort of movement would provide a rapid way for an ion to appear to travel through a solution. There would then be no need for a whole $H_3O^+$ to lumber along, taking the proton with it. Could a proton

**Fig. 4.121.** Effect of marbles colliding in a row: the Grotthuss mechanism.

attach itself to one end of a chain of water molecules in solution and push one off at the other end of the chain?

Stokes and Grotthuss both worked during the Victorian age. It appeared that Stokes' drift of whole ions though solutions had won out as far as most ions are concerned, and Grotthuss's concept found no resonance until in 1933 Bernal and Fowler, in the first issue of the famous *Journal of Chemical Physics*, suggested a mechanism that borrowed some things from it. In Fig. 4.122 one sees a suggestion for the mechanism of a proton jumping from one water molecule to the next, which is vaguely what Grotthuss had suggested. Thus, when a proton arrives at one water, making it temporarily $H_3O^+$, another different proton from the same $H_3O^+$ detaches itself from the $H_3O^+$ for the next hop. It is at once clear that this "relay-like" mechanism provides an exciting possibility for more rapid transport than Stokes' law would allow. There is no need for the relatively heavy $H_3O^+$ to lumber along; the tiny proton itself hops from $H_3O^+$ to $H_2O$ (making it $H_3O^+$), and new $H_3O^+$s are rapidly formed across the solution.

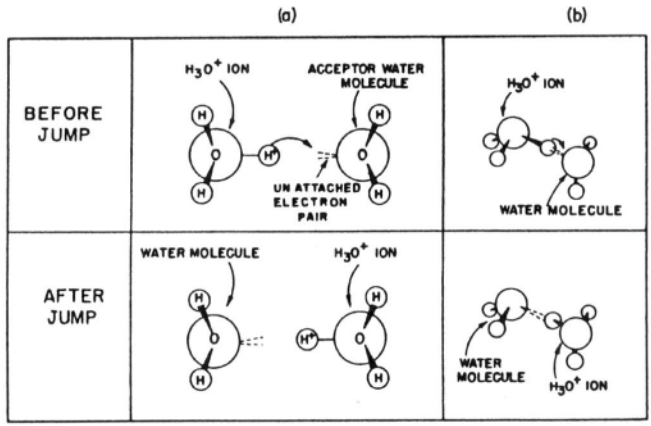


**Fig. 4.122.** Two schematic views (a) and (b) of a water molecule adjacent to an $H_3O^+$ ion. The free electron pair (orbital) of the O of the water molecule is oriented along the O (of $H_3O^+$)–$H^+$–O (of $H_2O$) line. The jump of the proton $H^+$ from the $H_3O^+$ ion to the water molecule converts the water molecule into an $H_3O^+$ ion and the $H_3O^+$ ion into a water molecule.

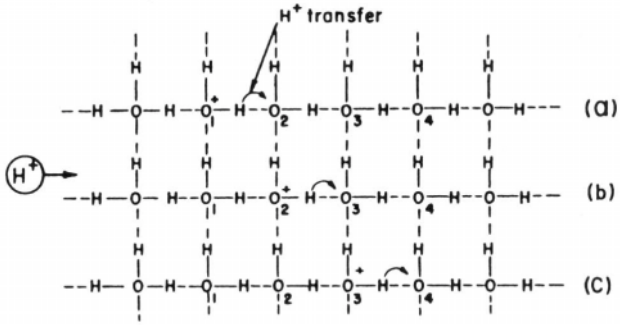


**Fig. 4.123.** If there are a series of proton jumps down a line of water molecules, the net result is equivalent to the migration of an $H_3O^+$ ion (indicated by a charge on the oxygen) along the line.

This latter impression is better seen by looking at Fig. 4.123 because there one sees that although in reality it is always a proton that does the jumping, the positions *a, b, c* represent an ensemble of waters netted together by means of H bonding, with a proton swinging away from one water to the next, making each *stationary* water[54] become momentarily a hydronium ion, and causing the casual onlooker to get the impression that $H_3O^+$ itself is moving through the solution.

### 4.11.4. The Machinery of Nonconformity: A Closer Look at How the Proton Moves

If one is going to consider protons actually jumping from one quasi-stationary water molecule to the next, the classical view would be to ask what fraction of them would be sufficiently activated to get over the top of the corresponding energy barrier. Another possibility was discussed not long after the introduction of quantum mechanics in 1928 by Bernal and Fowler. In a famous paper of 1933, they applied quantum mechanics to the possibility of tunneling through a barrier.

It is not reasonable just to say "the proton transfers to a water molecule," because that is a fairly vague statement. One starts asking questions like: Can it transfer to a water molecule when it arrives from *any* direction? Hardly, for it has to find an orbital on O to form a bond with—and orbitals have direction. Considering that water molecules librate and sometimes break H bonds and rotate, the next question which will have to be researched is: Does a water get into a proton-receiving posture all by

[54]Not quite stationary! Every time a water molecule is blessed by the arrival of a proton, it momentarily become an $H_3O^+$ and lumbers off a bit down the electric field gradient. But, as the proton detaches itself again, it jumps off to the next $H_2O$, and so each $H_3O^+$ undergoes a Stokeslike movement only to a small degree that corresponds to the short time an $H^+$ is attached to it.

itself, spontaneously, or does it have to be pushed by the powerful electric field of the approaching proton to turn around and offer an orbital to which the proton can jump?

To start finding out what happens to the energy of a proton when it leaps from one water molecule to the next, let the $H_3O^+$ system be simplified to be treated as though it were a diatomic entity, $W{-}H^+$, where W is the water molecule. Then the potential energy of any diatomic system can be represented accurately in the gas phase and roughly in solution by a Morse-type equation,

$$U_r = D_0\{1 - e^{[-a(r-r_{eq})]}\}^2 \tag{4.360}$$

where $U_r$ is the energy of the diatomic system as a function of the actual distance $r$ at any degree of stretching or compressing around the equilibrium distance $r_{eq}$ of the two "atoms"; $D_0$ is the dissociation energy of $W{-}H^+$ and a is a constant as a function of the frequency of vibration. For $D_0$, the overall hydration energy of the proton is used, i.e., $1112\ \text{kJ mol}^{-1}$, and for $r_{eq}$, the distance is 98 pm.

Knowing these parameters, one can plot the $U_r$ vs. $r$ curve for the stretch of a proton along one of the $p$ orbitals of oxygen. This plot is known as a *Morse curve* and is shown in Fig. 4.124 for our system. The energy trajectory under study here pertains to the reaction shown in Fig. 4.125. Because of the symmetry of the system, one has an identical curve for the approach of the proton to the second water molecule. Thus,

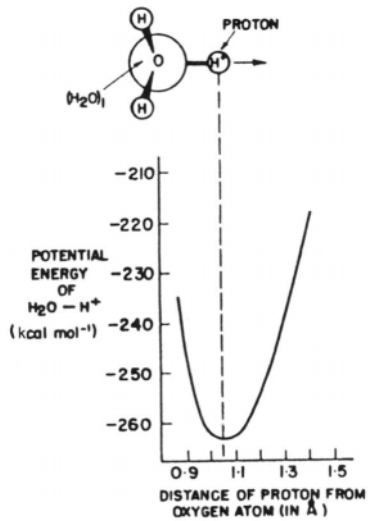


**Fig. 4.124.** Variation of the potential energy of the $W_1{-}H^+$ system with the stretching of the $W_1{-}H^+$ bond (Morse curve).

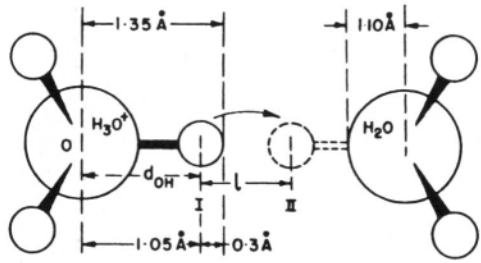


**Fig. 4.125.** Model for proton transfer between an $H_3O^+$ ion and a favorably oriented $H_2O$ molecule.

the two Morse curves, one for $W_1-H^+$ and the other for $H^+-W_2$, are put together (Fig. 4.126) and form the potential-energy barrier for proton transfer.

This then is the energy barrier for the jump of a proton from one water molecule to another *over* a potential-energy barrier. From this barrier, one can calculate the energy of activation and thus the rate of proton transfer. How can one create and locate the curves with respect to each other?

Eyring and Stearn made the first study of the probability that the proton would have enough energy to climb over the potential-energy barrier. The basic application of the theory of absolute reaction rates made by Eyring begins with the equation for the frequency at which the proton crosses the barrier, i.e., the rate constant $\vec{k}$

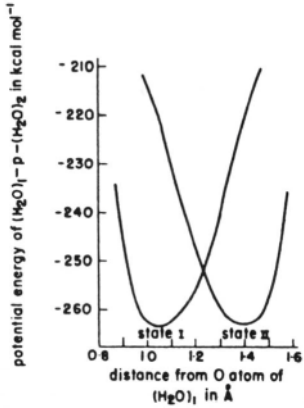


**Fig. 4.126.** Potential-energy barrier for proton transfer from $H_3O^+$ to $H_2O$.

$$\vec{k} = \frac{kT}{h} \exp\left[-\frac{\Delta G^{\neq} - XF\delta \cos\theta}{RT}\right] \tag{4.361}$$

where $\Delta G^{\neq}$ denotes the free energy of activation at zero local field $X$. Equation (4.361) is derived from the basic equation for all rate constants in Eyring's famous theory. However, the free energy of activation is modified (reduced from the proton's forward movement toward the negative pole) by the term $XF\delta \cos\theta$. Thus, $X$ is the electric field applied to the solution at an angle $\theta$ to the proton's movement, $F$ is the charge per g-ion on the proton, and $\delta$ is the activation or half-jump distance, i.e., half the distance the proton must travel in crossing a symmetrical barrier. This second electrical term in the exponent represents the change in energy which acts to reduce $\Delta G^{\neq}$ for a forward direction jump.

If we average over all angles $\theta$ of orientation of the jumping direction to the field, from 0 to $\pi$ (180°), then the rate constant becomes

$$\vec{k} = \frac{kT}{h} \exp\left[-\frac{\Delta G^{\neq}}{RT}\right] \left[\frac{\int_0^{\pi} \exp\left(\frac{XF\delta \cos\theta}{RT}\right) \cos\theta \sin\theta \, d\theta}{\int_0^{\pi} \sin\theta \, d\theta}\right] \tag{4.362}$$

If one substitutes $1\ \mathrm{V\ cm^{-1}}$ for $X$, $3 \times 10^{-8}$ cm for $\delta$, and the usual values of $F$ and $R$ at room temperature, the exponential in the integral can become less than $10^{-6}$, a rather small number, and the exponential can be linearized as approximately $1 + x$.

We can use this model to fix the relative positions of the minima of the Morse curves. When the two minima are fixed, we can see from Fig. 4.127 that the two Morse

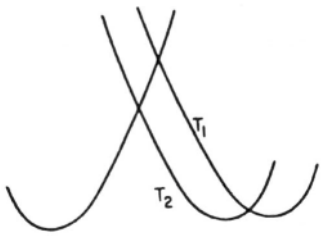


**Fig. 4.127.** Schematic diagram to show that the activation energy for proton transfer depends upon the distance between the minima of the Morse curves.

curves intersect and a potential-energy barrier is fabricated. To obtain the height of the energy barrier, the resonance energy of the activated complex is required. In an O–H···O hydrogen bond, resonance energy would account for half the hydrogen bond energy if the hydrogen were symmetrically distributed between the two oxygen atoms. The hydrogen bond energy has been established as $-24.7\ \text{kJ mol}^{-1}$, and so the resonance energy of the activated state can be taken as $-12.35\ \text{kJ mol}^{-1}$. This value must be subtracted from the energy of activation calculated from the point of intersection of the Morse curves. A microscopic look at Figure 4.126 shows that the intersection point occurs at about $28.45\ \text{kJ mol}^{-1}$ above the zero-point energy for the proton, and so the energy of activation is about $16.1\ \text{kJ mol}^{-1}$. An important feature to note is that the barrier height is reasonably low and that the width (the transfer distance) is of atomic dimensions, about 35 pm.

Is Eyring's theory on proton mobility in water successful in predicting the experimental values of mobility? The unfortunate answer is that this classical calculation is not acceptable at all, partly because it gives mobilities that are much smaller than those observed and it does not fit the demanding criterion of $u_{H^+}/u_{D^+} = 1.41$. It is necessary to turn to another view.

### 4.11.5. Penetrating Energy Barriers by Means of Proton Tunneling

A third approach to understanding the anomalous behavior of the nonconforming ion was provided by Bernal and Fowler in the paper mentioned earlier. Their suggestion was that when the proton jumped from an

$$\begin{matrix} H \\ H \end{matrix}\!\!>\!O\!-\!H^+ \text{ to an } \quad O\!<\!\begin{matrix} H \\ H \end{matrix}$$

converting the water on the right to an $H_3O^+$ and leaving a water behind, the crossing of the space between the two waters was accomplished, not by crossing above the energy barrier, but by going *through* it. This is quantum mechanical tunneling. The initial application of this type of novel idea—the earliest application of quantum mechanics to chemistry—had been made by Gurney and Condon to the escape of electrons (then called $\beta$-particles) from nuclei in radioactivity. To think of protons penetrating a barrier in this way was a big step, because a proton is 1840 times heavier than an electron. However, in the Gamow probability function for the penetration of barriers, the probability $P_r$ is proportional to the exponential of the energies of the jumping particle, that is

$$P_r \propto \exp\left[-\frac{4\pi\ell}{h}\sqrt{m(E-U)}\right] \tag{4.363}$$

where $m$ is the mass of the particle penetrating, $\ell$ is the length of the jump, and $E$ and $U$ are the total and potential energies of the jumping particle, respectively. There are

three factors that could compensate for the great decrease of the tunneling probability obtained by increasing the mass of the particle in the expression. To begin with, the probability of tunneling found for electrons penetrating barriers of 1 to 10 eV (the magnitudes of barriers generally found in chemical problems) is approximately 1 up to a distance of 2000 pm. Nevertheless, the very large increase in mass of the proton compared with the electron—which would seem to greatly decrease the tunneling probability—is reduced in effect by being taken as $\sqrt{1840} = 42.8$. Furthermore, the energy quantities in penetrating the barrier between

$$\begin{matrix} H \\ H \end{matrix}\!\!>\!O\!-\!H^+ \text{ and } \quad O\!<\!\begin{matrix} H \\ H \end{matrix}$$

are small—around 0.1 eV, compared with the 1 to 10 eV often observed in electron penetration problems. Putting this all together gives $P_{H^+}/P_{e^-} = 1/66$. This is the result of a very rough calculation, but it suggests that even if the path lengths $\ell$ for jumping were the same for an electron tunneling out of an electrode to a neighboring ion (see Chapter 7) and for a proton passing from one water to another, the proton tunneling probability would be at least 0.01. It is likely[55] to be much more.

This is somewhat the way Bernal and Fowler conjectured the proton to behave more than half a century ago in one of the earliest applications of quantum mechanics to chemistry. However, their conjecture was by no means satisfactory in a numerical sense. It was, as it were, too much of a good thing. The resulting values suggested a velocity for the proton *far greater* than the high rate observed, and also a quite wrong value for $u_{H^+}/u_{D^+}$. Something was still very much amiss.

### 4.11.6. One More Step in Understanding Proton Mobility: The Conway, Bockris, and Linton (CBL) Theory

Rosenberg, whose work on proton conduction in the alcohols led to insights into proton conduction, was also a coauthor of a paper that laid the foundation for the development of the theory of proton conduction in solutions. The theory utilized the idea of proton tunneling as outlined earlier, but added an essential limitation to its rate. Thus, in the Eyring theory, the only prerequisite for a proton to pass from an

$$\begin{matrix} H \\ H \end{matrix}\!\!>\!O\!-\!H^+ \text{ to an } \quad O\!<\!\begin{matrix} H \\ H \end{matrix}$$

in water was a certain degree of activation from the ground state, which is governed by Maxwell's law. The answer was far too small. In the quantum mechanical theory of Bernal and Fowler, the fraction of proton neighbors of a given water which had

[55]The proton's passage turns out from model building to be about 30 pm whereas electrons jumping from an electrode to a neighboring ion tend to jump several thousand picometers.

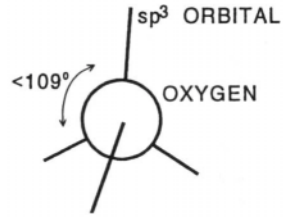


**Fig . 4.128.** The hybrid orbitals of an oxygen atom. (After Lyons, 1996.)

attained a certain activation energy was multiplied by the Gamow probability equation using the energy value corresponding to that of the activated proton [see Eq. (4.363)], and this product was taken as the probability of protons penetrating the energy barrier at a given height. The probabilities for all the heights were added to obtain the total barrier penetration probability. Now the answer was far too large.

A new group of researchers, Conway, Bockris, and Linton, however, asked and answered an important question: Does it not also matter whether the orbitals of the oxygen of the water molecule to which the proton is tunneling are correctly oriented to receive it? The oxygen atom has four orbitals (Fig. 4.128), two of them occupied by H atoms. It would be reasonable to consider it a nonevent if a proton attempted to tunnel to a water that was incorrectly oriented, as depicted in Fig. 4.129, and a successful event if the orientation was adequate, as in Fig. 4.130.

There are two processes that must cooperate for a successful proton transfer, the basis of proton mobility. The first is *water reorientation* and then the second is *proton tunneling*. Hence the rate of proton transfer will be limited by whichever of the two processes is slower. One must therefore suspect that the water reorientation is the *rate-determining step* in the process of proton transfer (because the tunneling through the barrier has already been shown to be too fast to be consistent with the mobility observed).

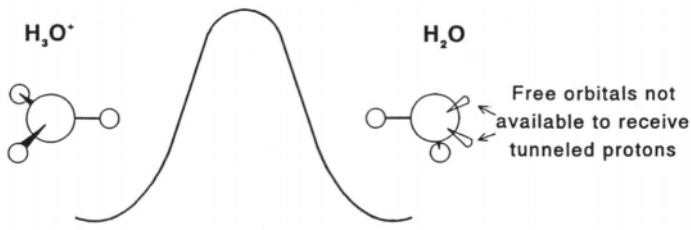


**Fig. 4.129.** None of the free orbitals of the water molecule are correctly aligned and therefore no proton transfer occurs. (After Lyons, 1996.)

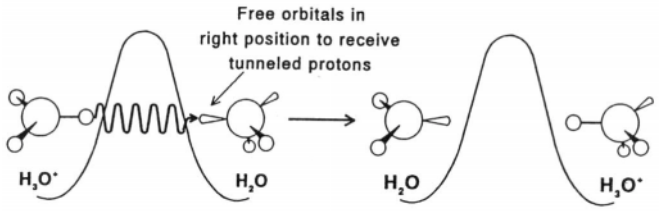


**Fig. 4.130.** One of the free orbitals of a water molecule is properly oriented and the proton is able to tunnel to the water molecule. (After Lyons, 1996.)

Thus, in the new theory by CBL, a model was formulated in which the librational properties of water played an important part. Even that was not the whole story. The calculation of the specific rate of water reorientation is a complex task. One cannot consider the reorienting water molecule as an isolated entity. If that were so, then one could work on the only basis of the rate of rotation of a *gas molecule* and calculate the rate. However, the water molecule is hydrogen bonded to other water molecules within the 3D lattice and therefore the reorientation involves the torsional stretching and breaking of the hydrogen bonds—an attempt that seldom succeeds.

To summarize, in order for the proton to tunnel successfully, it has to wait for the adjacent water molecules to turn so that they provide a properly oriented orbital. If the tunneling protons have to wait for the water molecules to turn around spontaneously and get into the right position every time a proton arrives on the scene,[56] the predicted mobility will be low compared with experiment. Figure 4.131 shows one of the CBL calculations for the variation of energy in this turning process. However, as is hinted by the figure, the energy of turning and finally breaking the H bonds that hold water down is sufficiently large that it will happen seldom and the excessive speedup due to tunneling will be slowed so much that the reduction in rate caused by the proton having to bide its time will lead to an overcorrection.

Therefore there must be another factor, one that helps turn the water molecule around in the "ready" position. The force to do this is readily found; it is provided by the field of the approaching proton itself.[57] The equation for the energy of a proton–water (ion–dipole) interaction is [see Eq. (A2.2.11)],

$$U_{H^+-W} = -\frac{z_{H^+} e_0 \mu_W \cos\theta}{\varepsilon r^2} \tag{4.364}$$

[56]This spontaneous turning of the water molecules by random motions corresponds to the acceptor water molecule's reorientation by the thermal motions without help from surrounding electric fields.

[57]This process is called the *field-induced reorientation* of the water molecules.

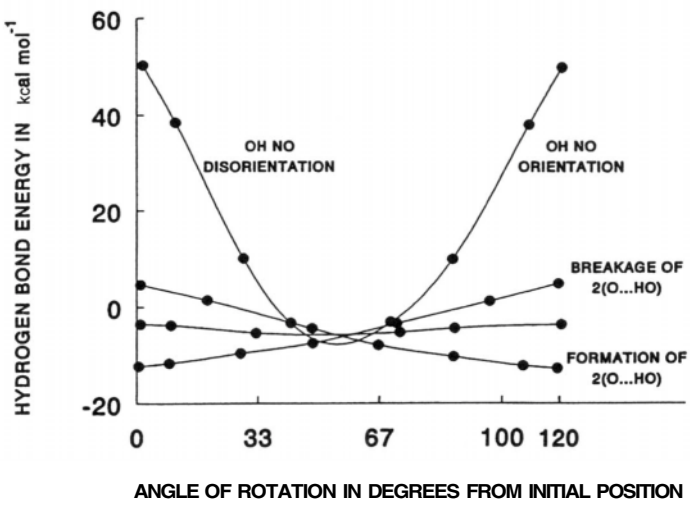


**Fig. 4.131.** Angular electrostatic potential-energy curves for rotation of $H_2O$ near the $H_3O^+$ ion (ion dipole contribution not included) (B. E. Conway, J. O'M. Bockris and H. Linton, *J. Chem. Phys.* **24**: 834,1956).

where $\theta$ is the angle between the water dipole and the line between the proton and the dipole center (Fig. 4.132), $r$ is the ion–dipole distance, $\varepsilon$ is the dielectric constant of the medium, and $\mu_W$ is the dipole moment of water. As $\theta$ is reduced to zero, $U_{H^+-W}$

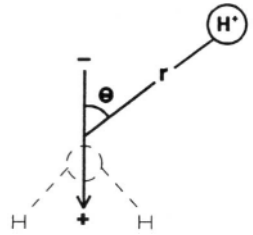


**Fig. 4.132.** Angle of interaction between a proton (positive charge) and a water molecule (dipole). Maximum interaction occurs when $\theta = 0$, and therefore $\cos\theta = 1$. (After Lyons, 1996.)

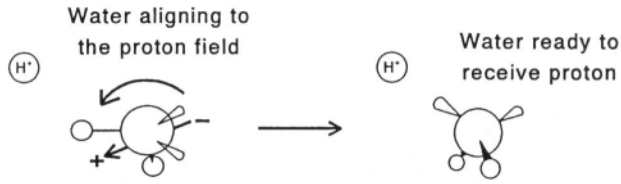


**Fig. 4.133.** Proton field-induced reorientation of a water molecule. (After Lyons, 1996.)

goes to a maximum numerical value. Hence, as the proton approaches a water turned away from it, it swings it around and with it, its appropriately oriented orbital, as shown in Fig. 4.133.

One last matter remains. What has been said could be a description for the self-diffusion of the proton, where the movements are random. In conduction, there has to be a *preferential* movement in the direction of the electric field applied to the cell. CBL calculated this motion also; it is a small correction, but causes a preferential drift toward the negative electrode.

### 4.11.7. How Well Does the Field-Induced Water Reorientation Theory Conform with the Experimental Facts?

Can the CBL theory predict experimental values? The answer is a resounding yes, and the results justify printing the lengthy story of an advance made in 1956. The rate of this field-induced water reorientation was faster than the rate of the spontaneous thermal rotation, but turned out to be much slower than the proton tunneling rate. Thus, it is the *field-induced rotation* of water that determines the overall rate of proton transfer and the rate of proton migration through aqueous solutions. According to the theory, the estimated value of the proton mobility is $28 \times 10^{-4}$ and that observed experimentally is $36 \times 10^{-4}\ \mathrm{cm^2\ s^{-1}\ V^{-1}}$!

The anomalous decrease in the heat of activation with an increase in temperature also follows from the model. An increase in temperature causes increased disorder in the water structure, and consequently there are on average, fewer H bonds to break when water molecules reorient. Since the water reorientation increases, the heat of activation becomes smaller.

The decrease in anomalous mobility of the proton in the presence of added alcohol solvents (see Section 4.11.2) could also be explained: the larger size of the alcohol makes its reorientation more difficult than that for water and causes a fall in proton mobility by the tunneling and solvent-oriented method.

Finally, the stringent test for the CBL model was given by the 1.4 ratio of the mobilities of hydrogen and deuterium. Therefore, the correct calculation of this ratio—as the model indeed makes possible—is strong evidence in favor of a mecha-

nism involving field-assisted water reorientation as the rate-determining step in proton tunneling.[58]

### 4.11.8. Proton Mobility in Ice

If extra confirmation of the CBL model is needed, it is given by interpretation of the fact that in pure ice the proton's *mobility* (not its *conductance*) is approximately 100 times greater than it is in water at the same temperature. Does this means that water molecules turn faster in ice than in water? Intuitively, the reverse might be expected.

However, the CBL model provides the answer. In ice, the concentration of the proton is much less than that in water. Eventually, water molecules in ice do rotate into the correct position, even without the help of an oncoming proton, so that they offer an inviting orbital to any oncoming proton. With so few protons in ice, the waters rotate spontaneously in time for the occasional oncoming proton. Every time a proton is ready to jump, the waiting orbital is there. It is like an all-green traffic light on a main thoroughfare, early in the morning when traffic is light. The former need for water rotation to be spurred by proton attraction is no longer the rate-determining step, and tunneling alone calls the shots. This tunneling is a much faster process than that of water rotation, so that it leads to higher mobilities of protons in ice than in the water or aqueous solutions in which the water rotation is rate determining.

## Further Reading

### *Seminal*

1. J. Bernal and R. E. Fowler, "The Structure of Water and Proton Conduction," *J. Chem. Phys.* **1**: 515 (1933).
2. B. E. Conway, J. O'M. Bockris, and H. Lynton, "Solvent Orientation Model for Proton Transfer," *J. Chem. Phys.* **24**: 834 (1956).
3. B. E. Conway and J. O'M. Bockris, "Proton Conduction in Ice," *J. Chem. Phys.* **28**: 354 (1958).
4. T. Erdey Gruz and S. Langyel, "Proton Transfer in Solution," in *Modern Aspects of Electrochemistry, No. 12*, J. O'M Bockris and B. E. Conway, eds., p. 349, Plenum, New York (1978).

### *Review*

1. K. D. Krener, "Proton Conductivity," *Chem. Mat.* **8**: 610 (1996).

---

[58] Any proton-conduction mechanism in which the rate-determining step involves the breaking of hydrogen bonds would succeed equally well in explaining the heat of activation and alcohol anomalies, but not the $u_{H^+}/u_{D^+}$.

### *Papers*

1. V. Barone, L. Orlandini, and C. Adams, *Int. J. Quantum Chem.* **56**: 697 (1995).
2. S. Consta and R. Kapral, *J. Chem. Phys.* **104**: 4581 (1996).
3. R. Pommes and B. Roux, *J. Phys. Chem.* **100**: 2519 (1996).
4. J. T. Hynes and D. Borgis, *J. Phys. Chem.* **100**: 1118 (1996).

## APPENDIX 4.1. THE MEAN SQUARE DISTANCE TRAVELED BY A RANDOM-WALKING PARTICLE

In the one-dimensional random-walk problem, the expression for $\langle x^2 \rangle$ is found by mathematical induction as follows. Consider that after $N - 1$ steps, the sailor has progressed a distance $x_{N-1}$. If he takes one more step, the distance $x_N$ from the origin will be either

$$x_N = x_{N-1} + l \tag{A4.1.1}$$

or

$$x_N = x_{N-1} - l \tag{A4.1.2}$$

Squaring both sides of Eqs. (A4.1.1) and (A4.1.2), one obtains

$$x_N^2 = x_{N-1}^2 + l^2 + 2x_{N-1}l \tag{A4.1.3}$$

and

$$x_N^2 = x_{N-1}^2 + l^2 - 2x_{N-1}l \tag{A4.1.4}$$

The average of these two possibilities must be

$$x_N^2 = x_{N-1}^2 + l^2 \tag{A4.1.5}$$

This is the result for $x_N^2$ when the distance traveled after $N - 1$ steps is exactly $x_{N-1}$. In general, however, one can only expect, for the value of the square of the distance at the $(N - 1)$th step, an averaged value $\langle x_{N-1}^2 \rangle$, in which case one must write

$$\langle x_N^2 \rangle = \langle x_{N-1}^2 \rangle + l^2 \tag{A4.1.6}$$

At the start of the random walk, i.e., after zero steps, progress is given by

$$\langle x_0^2 \rangle = 0 \tag{A4.1.7}$$

After one step it is

$$\langle x_1^2 \rangle = 1l^2 = l^2 \tag{A4.1.8}$$

After two steps, from Eq. (A4.1.6), one has

$$\langle x_2^2 \rangle = \langle x_1^2 \rangle + l^2 \tag{A4.1.9}$$

and, using Eq. (A4.1.8),

$$\langle x_2^2 \rangle = l^2 + l^2 = 2l^2 \tag{A4.1.10}$$

Similarly,

$$\begin{aligned} \langle x_3^2 \rangle &= \langle x_2^2 \rangle + l^2 \\ &= 2l^2 + l^2 \\ &= 3l^2 \end{aligned} \tag{A4.1.11}$$

Hence, in general,

$$\langle x_N^2 \rangle = Nl^2 \tag{A4.1.12}$$

This equation has been derived for a one-dimensional random walk, but it can be shown to be valid for three-dimensional random flights, too.

The mean square distance $\langle x^2 \rangle$ that a particle travels depends upon the time of travel in the following manner. The number of steps $N$ obviously increases with time and is proportional to it, i.e.,

$$N = kt \tag{A4.1.13}$$

where $k$ is the constant of proportionality. Hence, by combining Eqs. (A4.1.12) and (A4.1.13),

$$\langle x^2 \rangle = ktl^2 \tag{A4.1.14}$$

which may be written

$$\langle x^2 \rangle = \alpha t \tag{A4.1.15}$$

where $\alpha$ is a proportionality constant to be evaluated in the Einstein–Smoluchowski equation.

## APPENDIX 4.2. THE LAPLACE TRANSFORM OF A CONSTANT

The Laplace transform $\bar{\alpha}$ of a constant $\alpha$ is by definition (4.33) given by

$$\bar{\alpha} = \int_0^\infty e^{-pz}\alpha \, dz$$

$$\begin{aligned}\bar{\alpha} &= \alpha\left[\frac{e^{-pz}}{-p}\right]_0^\infty \\ &= \alpha\left[\frac{1}{e^{pz}(-p)}\right]_{z=\infty} - \alpha\left[\frac{1}{e^{pz}(-p)}\right]_{z=0} \\ &= 0 - \left(\frac{\alpha}{-p}\right) \\ &= \frac{\alpha}{p}\end{aligned}$$

Hence, the Laplace transform of a constant is equal to that same constant divided by $p$.

## APPENDIX 4.3. THE DERIVATION OF EQUATIONS (4.279) AND (4.280)

According to notation [*cf.* Eqs. (4.273) and (4.274)],

$$p_+ = q_+L_{++} + q_-L_{-+} \tag{A4.3.1}$$

and

$$p_- = q_+L_{+-} + q_-L_{--} \tag{A4.3.2}$$

Hence, one can carry out the following expansions

$$\frac{p_+}{p_+q_+ + p_-q_-} = \frac{q_+L_{++} + q_-L_{-+}}{q_+(q_+L_{++} + q_-L_{-+}) + q_-(q_+L_{+-} + q_-L_{--})}$$

$$= \frac{q_+L_{++} + q_-L_{-+}}{q_+(q_+L_{++} + q_-L_{+-}) + q_-(q_+L_{-+} + q_-L_{--})}$$

$$= \frac{q_+L_{++}\dfrac{d\varphi}{dx} + q_-L_{-+}\dfrac{d\varphi}{dx}}{q_+\left(q_+L_{++}\dfrac{d\varphi}{dx} + q_-L_{+-}\dfrac{d\varphi}{dx}\right) + q_-\left(q_+L_{-+}\dfrac{d\varphi}{dx} + q_-L_{--}\dfrac{d\varphi}{dx}\right)} \tag{A4.3.3}$$

It has been stated [*cf.* Eq. (4.269)] that

$$J_+ = L_{++}\vec{F}_+ + L_{+-}\vec{F}_- \tag{A4.3.4}$$

and that [*cf.* Eqs. (4.276) and (4.277)]

$$\vec{F}_+ = \frac{d\mu_+}{dx} + q_+\frac{d\psi}{dx} \tag{A4.3.5}$$

and

$$\vec{F}_- = \frac{d\mu_-}{dx} + q_-\frac{d\varphi}{dx} \tag{A4.3.6}$$

Hence, substituting for $\vec{F}_+$ and $\vec{F}_-$ in Eq. (A4.3.4) and setting $d\mu/dx = 0$, one has

$$(J_+)_{d\mu/dx=0} = q_+L_{++}\frac{d\varphi}{dx} + q_-L_{+-}\frac{d\varphi}{dx} \tag{A4.3.7}$$

Similarly,

$$(J_-)_{d\mu/dx=0} = q_+L_{-+}\frac{d\varphi}{dx} + q_-L_{--}\frac{d\varphi}{dx} \tag{A4.3.8}$$

In terms of these expressions, Eq. (A4.3.3) becomes

$$\frac{p_+}{p_+q_+ + p_-q_-} = \left(\frac{J_+}{q_+J_+ + q_-J_-}\right)_{d\mu/dx=0}$$

$$= \frac{1}{q_+}\left(\frac{q_+J_+}{q_+J_+ + q_-J_-}\right)_{d\mu/dx=0} \tag{A4.3.9}$$

By notation,

$$q_+ = z_+F \quad \text{and} \quad q_- = z_-F \tag{A4.3.10}$$

and therefore Eq. (A4.3.9) can be rewritten as

$$\frac{p_+}{p_+q_+ + p_-q_-} = \frac{1}{z_+F}\left(\frac{z_+FJ_+}{z_+FJ_+ + z_-FJ_-}\right)_{d\mu/dx=0} \tag{A4.3.11}$$

Furthermore, according to the relation between current density and flux,

$$i_+ = z_+FJ_+ \tag{A4.3.12}$$

and

$$i_- = z_-FJ_- \tag{A4.3.13}$$

Using these relations in Eq. (A4.3.11), one has

$$\frac{p_+}{p_+q_+ + p_-q_-} = \frac{1}{z_+F}\left(\frac{i_+}{i_+ + i_-}\right)_{d\mu/dx=0} \tag{A4.3.14}$$

By definition, however [*cf.* Eq. (4.247)],

$$t_+ = \left(\frac{i_+}{i_+ + i_-}\right)_{d\mu/dx=0} \tag{A4.3.15}$$

By combining Eqs. (A4.3.14) and (A4.3.15), the result is

$$\frac{p_+}{p_+q_+ + p_-q_-} = \frac{t_+}{z_+F} \tag{A4.3.16}$$

Similarly, it can be shown that

$$\frac{p_-}{p_+q_+ + p_-q_-} = \frac{t_-}{z_-F} \tag{A4.3.17}$$

## APPENDIX 4.4. THE DERIVATION OF EQUATION (4.354)

One can rewrite Eq. (4.353), namely,

$$\Lambda_{\theta=0} = \Lambda^0 - (A + B\Lambda^0)(1-\theta)^{1/2}c_a^{1/2} \tag{A4.4.1}$$

in the form

$$\Lambda_{\theta=0} = \Lambda^0\left[1 - \frac{1}{\Lambda^0} mc_a^{1/2}(1-\theta)^{1/2}\right] \tag{A4.4.2}$$

where for conciseness the symbol $m$ is used instead of $(A + B\Lambda^0)$.

It has been shown, however [*cf.* Eq. (4.349)], that

$$1 - \theta = \frac{\Lambda}{\Lambda_{\theta=0}} \tag{A4.4.3}$$

If this relation is used in Eq. (A4.4.2), one gets

$$\Lambda_{\theta=0} = \Lambda^0\left[1 - \frac{mc_a^{1/2}}{\Lambda^0}\left(\frac{\Lambda}{\Lambda_{\theta=0}}\right)^{1/2}\right] \tag{A.4.4.4}$$

and substituting for $\Lambda_{\theta=0}$ in the right-hand side of Eq (A4.4.2), the result is

$$\Lambda_{\theta=0} = \Lambda^0\left\{1 - \frac{m(\Lambda c_a)^{1/2}}{\Lambda^{0\,3/2}} \frac{1}{[1 - (mc_a^{1/2}/\Lambda^0)(1-\theta)^{1/2}]^{1/2}}\right\} \tag{A4.4.5}$$

One has again been left with $(1-\theta)^{1/2}$ on the right-hand side and thus one again substitutes from Eq. (A4.4.2). This process of substitution can be repeated *ad infinitum* to give the result

$$\Lambda_{\theta=0} = \Lambda^0(1 - z\{1 - z[1 - z(\cdots)^{-1/2}]^{-1/2}\}^{-1/2}) \tag{A4.4.6}$$

$$= \Lambda^0 Z \tag{A4.4.7}$$

where

$$z = 1 - z\{1 - z[1 - z(\cdots)^{-1/2}]^{-1/2}\}^{-1/2} \tag{A4.4.8}$$

with

$$z = \frac{m(\Lambda c_a)^{1/2}}{\Lambda^{0\,3/2}} = \frac{(A + B\Lambda^0)c_a^{1/2}\Lambda^{1/2}}{\Lambda^{0\,3/2}} \tag{A4.4.9}$$

## EXERCISES

1. The unit flux has been used in an attempt to simplify the solution of the partial-derivative equation of Fick's second law. (a) Calculate, for a univalent ion, what current density this flux will cause. Is this current density achievable

in a real experiment? (b) 1 $mA/cm^2$ is a current density typically used in electrochemistry laboratories. What is the flux in this case? (Xu)

2. Calculate the concentration gradient of a univalent ion in 0.1 *M* solution at 25 °C when the electric field is $10^5$ V $cm^{-1}$ and the current density at the electrode is 1 mA $cm^{-2}$. (Kim)

3. Estimate the electrophoretic velocity of a sodium ion in 0.01 *M* NaCl solution under an electric field of 0.1 V $cm^{-1}$. The viscosity of the solution is 0.00895 poise. (Kim).

4. Ohm's law is generally applicable to electrolytes in solution. A theory suggests that the observed current depends on the difference of two exponential terms, i.e., $(e^{AX} - e^{-AX})$, where *A* is *zFU2RT*. The term / is the distance between "sites" in diffusion, *z* is the charge on the ion, and *X* is the applied field. Calculate the applied field in V $cm^{-1}$ at which Ohm's law breaks down.

5. If a current of 10 A is passed between two electrodes, each of 10 $cm^2$, and one is depositing Cu metal from a $CuSO_4$ solution, calculate the thickness of this deposit after 6 h.

6. In an instantaneous-pulse experiment, the electrode material is radioactive and hence detectable by a Geiger counter. As the pulse is realized with an electronic device generating a current of 10 A on a 0.1-$cm^2$ electrode for 0.1 s, with a Geiger counter placed 1 cm from the electrode, register the trace of the radioactive univalent ion at 450 *s* after the pulse. Calculate the limiting sensitivity of the instrument. Suppose the diffusion coefficient of the ion is the typical value of $10^{-9}$ $m^2$ $s^{-1}$. (Xu)

7. Estimate the diffusion coefficient of $Na^+$ and $Cl^-$ in water at 298 K from the equivalent conductivity at infinite dilution, $\Lambda^0$ (NaCl) = 126.46 S $cm^2$ $eq^{-1}$ and the cation transport number $t^0$ ($Na^+$) = 0.396. (Herbert)

8. In experiments involving radiotracer measurements of diffusion in molten salt, the Stokes–Einstein equation has been found to be roughly applicable. For a series of ions, in molten salts it was found that the product $D\eta T^{-1} = 10^{-9}$ dyn $mol^{-1}$. From this information, find whether the best form of the coefficient in this expression for this case is nearer to 6 or 4.

9. For aqueous solutions at room temperature, the order of magnitude of the diffusion coefficient of most of the common simple ions ($Na^+$, $K^+$, $Mg^{2+}$, $ClO_4^-$) is $10^{-5}$ $cm^2$ $s^{-1}$. Suppose now that a capillary tube containing a solution of an electrolyte is brought into contact vertically and very gently with a capillary of pure water; about how far would the electrolyte diffuse into the capillary of water in 24 hr?

10. It is easy to understand that protons must have an abnormal mechanism of transport through the solution. Thus, protons in aqueous solution exist almost entirely as $H_3O^+$ ions yet their conductivity is several times higher than one would expect if they transported primarily by rolling along as $H_3O^+$. Imaginatively discuss the alternatives. Explore what is meant by "transfer to a neighboring water molecule." Can the proton come into this neighbor from any direction? Why does it prefer to drift, particularly in one direction?

11. Write equations representing each of Pick's laws. Exemplify the type of situation in which each law applies. A glucose solution ($D_{glucose} = 0.67 \times 10^{-5}$ cm$^2$ s$^{-1}$) diffuses across a region of 0.2 cm in length and 4.8 cm$^2$ in area. On one side, the concentration is 4 g dm$^{-3}$ and on the other, effectively zero. Calculate the rate of diffusion of the sugar across the boundary in g s$^{-1}$.

12. At first the results arising from the Einstein–Smoluchowski equation ($\langle x^2 \rangle = 2Dt$) may seem difficult to understand. Thus, the diffusion considered in the equation is random. Nevertheless, the equation tells us that there is net movement in one direction arising from this random motion. Furthermore, it allows us to calculate how far the diffusion front has traveled. Is there something curious about randomly moving particles covering distances in one direction? Comment constructively on this apparently anomalous situation.

13. Show that the diffusion coefficient ($D$) is independent of the concentration for dilute (ideal) solutions, using the example of planar steady-state diffusion. Explain the meaning of the negative sign that is usually inserted into Fick's first law of steady-state diffusion. (Bock)

14. A definition for specific ion conductivity frequently cited in electrochemical literature is $\sigma = E_i n_i u_i z_i e_0$, where $i$ is ionic species, $n_i$ the number of the ion in a unit volume, $u_i$ the conventional mobility, $z_i$ the valence state, $e_0$ the elemental charge, and $E$ the electric field. Derive this definition. (Xu)

15. When it comes to practical application, the actual conductance (the inverse of resistance $R$) instead of specific conductivity is the important variable. This is the reason why polymer electrolytes have drawn so much attention as a potential component of alkali-metal batteries although their specific conductivities are usually low ($\sim 10^{-5}$ S cm$^{-1}$) compared with those at nonaqueous electrolytes ($\sim 10^{-2}$ S cm$^{-1}$). Calculate the conductance of 1.0 $M$ $LiSO_3CF_3$ in poly(ethylene oxide) and propylene carbonate, respectively. The former is fabricated into a film of 10 Tm thickness and the latter is soaked with porous separator of 1 mm thickness. (Xu)

16. A conductance cell containing 0.01 potassium chloride was found to have a resistance of 2573 Ohms at 25 °C. The same cell when filled with a solution of 0.2 $N$ acetic acid had a resistance of 5085 Ohms. Calculate (a) the cell constant, (b) the specific resistances of the potassium chloride and acetic acid solutions,

(c) the conductance ratio of 0.2 *N* acetic acid, utilizing the following data at 25 °C: $\lambda^0_{H^+} = 349.82\ \Omega^{-1}\ cm^2\ eq^{-1}$; $\lambda^0_{CH_3COO^-} = 40.9\ \Omega^{-1}\ cm^2\ eq^{-1}$; specific conductivity of 0.01 *N* KCl = $0.0014\ \Omega^{-1}\ cm^{-1}$. (Constantinescu)

17. A 0.2 *N* solution of sodium chloride was found to have a specific conductivity of $1.75 \times 10^{-2}\ \Omega^{-1}\ cm^{-1}$ at 18 °C; the transport number of the cation in this solution is 0.385. Calculate the equivalent conductance of the sodium and chloride ions. (Constantinescu)

18. A conductance cell having a constant $k$ of $2.485\ cm^{-1}$ is filled with 0.01 *N* potassium chloride solution at 25°C; the value of $\Lambda$ for this solution is $141.2\ S\ cm^2\ eq^{-1}$. If the specific conductance, $\sigma$, of the water employed as solvent is $1.0 \times 10^{-6}\ S\ cm^{-1}$, what is the measured resistance of the cell containing the solution? (Constantinescu)

19. The ionic conductivity at infinite dilution of a divalent copper ion is $\lambda^0\ (Cu^{2+}) = 55\ S\ cm^2\ eq^{-1}$ and its ionic radius, $r_i = 72$ pm. Calculate the primary solvation number of $Cu^{2+}$ taking $r_W = 138$ pm for the radius of the water molecule. (Herbert)

20. Calculate the equivalent conductivity of a 0.1 *M* NaCl solution. The diffusion coefficient of $Na^+$ is $1.334 \times 10^{-5}\ cm^2\ s^{-1}$ and that of $Cl^{-1}$ is $2.032 \times 10^{-5}\ cm^2\ s^{-1}$. (Kim)

21. Calculate the conductivity of NaI in acetone ($\eta = 0.00316$ poise) when the radii for $Na^+$ and $I^-$ are 260 and 300 pm, respectively. (Kirn)

22. Calculate the conventional mobility of a sodium ion in 0.01 *M* NaCl. The viscosity of the solution is 0.00895 poise and the Stokes radius of a sodium ion is 260 pm. (Kim)

23. In acetonitrile ($\eta = 0.00345$ poise), the equivalent conductivity for very dilute solutions of KI is 198.2 at 25 °C. Calculate the equivalent conductance of KI in a similar concentration range in acetophenone. ($\eta = 0.0028$ poise)

24. Calculate the specific and equivalent conductivity of LiBr using the data in the text.

25. A student has to determine the equivalent conductivity at infinite dilution for KC1, NaCl, $KNO_3$, and $NaNO_3$ solutions and the transport numbers of the ions in these solutions. He managed to determine only $\lambda^0\ (KNO_3)$, $\lambda^0(NaNO_3)$, $t^0_+\ (Na^+/NaCl)$ and $t^0_+\ (K^+/KCl)$ and wrote them in a table:

| | $NaNO_3$ | $KNO_3$ | NaCl | KCl |
|---|---|---|---|---|
| $\lambda^0$/S cm$^2$ eq$^{-1}$ | 121.4 | 144.9 | — | — |
| $t^0_+$ | — | — | 0.396 | 0.490 |
| $t^0_-$ | — | — | — | — |

Assuming that the determined values are correct, help him fill in the blanks in the table without doing any further experiments. (Herbert)

26. Given the transport number of $Ca^{2+}$ in $CaCl_2$, $t(Ca^{2+}/CaCl_2) = 0.438$ and of $K^+$ in KC1, $t(K^+/KCl) = 0.490$, calculate the transport number of $Ca^{2+}$ in a solution containing both 0.001 *M* $CaCl_2$ and 0.01 *M* KC1, neglecting the variation of $t$ and $\lambda^0$ with concentration. (Herbert)

27. A current of 5 mA flows through a 2-mm inner-diameter glass tube filled with 1 *N* $CuSO_4$ solution in the anode compartment and with a $Cu(CH_3COO)_2$ solution in the cathode compartment. The interface created between the two solutions moves 6.05 mm toward the anode in 10 min. Calculate the transport number of the sulfate ion in this solution. (Herbert)

28. In a 1:1 electrolyte, measurements showed diffusion coefficients of $5.1 \times 10^{-5}$ $cm^2\ s^{-1}$ for the cation and $2.8 \times 10^{-5}\ cm^2\ s^{-1}$ for the anion. Calculate the transport number of the anion.

29. Calculate the absolute mobility of a sodium ion when the drift velocity is $5.2 \times 10^{-5}\ cm\ s^{-1}$ under an electrical field of $0.1\ V\ cm^{-1}$. (Kim)

30. Calculate the conventional mobility of a sodium ion in aqueous solution using the diffusion coefficient of $1.334 \times 10^{-5}\ cm^2\ s^{-1}$ at 25 °C. (Kim)

31. Calculate the radius of the solvated sodium ion in aqueous solution when the absolute mobility of the ion is $3.24 \times 10^8\ cm\ s^{-1}\ dyn^{-1}$. The viscosity of the solution is 0.01 poise. (Kim)

32. The mobility of a cation is $5 \times 10^{-4}\ cm^2\ V^{-1}\ s^{-1}$ and that of the accompanying anion is $2 \times 10^{-4}\ cm^2\ V^{-1}\ s^{-1}$. Calculate the specific conductivity of a $2 \times 10^{-3}$ *M* solution.

33. A tube of glass 60 cm high is closed at one end, blue copper sulfate hydrate crystals are placed at the bottom, and water is introduced. Calculate how far a blue color will have spread upward after 1 min, 1 day, 1 week, and 1 month.

34. Ions are pumped into a system electrochemically. At $t = 0$, a short burst of dissolution of an electrode is caused, giving rise to $n_{total}$ ions, which then begin to diffuse away from the source. Seek in the text the appropriate equation by which one may know the number of ions at a distance $x$ and time $t$. This is a plane-source problem. Thus, Cu ions could be dissolved from a Cu plate filling the end of a tube of solution. The question is how many ions would have diffused 11 cm in 300 s? $D_{CuSO_4} = 0.82 \times 10^{-5}\ cm^2\ s^{-1}$.

35. Imagine, now, a horizontal tube of dilute KC1 solution. Exactly in the middle is a thin slab of smooth, solid copper sulfate covered with an insoluble protective plastic layer, suddenly removed at $t = 0$. At $x$ (which can be positive for the

right-hand side of the $CuSO_4$ slab and negative for the left) equals zero, the $CuSO_4$ begins to dissolve and diffuse in both directions. Draw a qualitative schematic diagram, the concentration of $CuSO_4$ (taken to be unity at $x = 0$) on the ordinate and the distance $x$ in either direction on the abscissa. On the diagram, plot the $CuSO_4$ concentration (a) for a very long time, (b) for a day, and (c) for an hour.

36. The ionic mobilities given in tables are around $10^{-4}$ $cm^2$ $V^{-1}$ $s^{-1}$. What would be the corresponding order of magnitude for the absolute mobility (the velocity under an accelerating force of 1 dyn $s^{-1}$).

37. A saturated solution of silver chloride, when placed in a conductance cell with a constant $k = 0.180$ $cm^{-1}$, has a resistance of 67.953 k$\Omega$ at 25 °C. The resistance of the water used as solvent was found to be 212.180 k$\Omega$ in the same cell. Calculate the solubility $S$ of the salt at 25 °C assuming it to be completely dissociated in its saturated solution in water. (Constantinescu)

38. Utilize the calculated values of the thickness of the ionic atmosphere $R^{-1}$ in 0.1 $N$ solutions of a univalent electrolyte in (a) nitrobenzene, (b) ethyl alcohol, and (c) ethylene dichloride to calculate the relaxation times of the ionic atmospheres. (Constantinescu)

39. Estimate the time for an ionic cloud to relax around a sodium ion in 0.1 $M$ NaCl when the drift velocity is $5.2 \times 10^{-5}$ cm $s^{-1}$ under an electrical field of 0.1 V $cm^{-1}$. (Kim)

40. In the text, a discussion of what happens to an ionic atmosphere when the ion at its center is discharged gives rise to an equation for the relaxation time of the ion atmosphere (as it disperses). Find such an expression. Apply it to find the time the ionic atmosphere takes to relax around $Na^+$ ions in a 0.01 $M$ NaCl solution when the diffusion coefficient of $Na^+$ is $1.93 \times 10^{-5}$ $cm^2$ $s^{-1}$.

41. The diffusion coefficient of an ion in water is $1.5 \times 10^{-5}$ $cm^2$ $s^{-1}$. It seems reasonable to take the distance between two steps in diffusion as roughly the diameter of a water molecule (320 pm). With this assumption, calculate the rate constant in $s^{-2}$ for the ion's diffusion.

42. Assume that a solution (100 ml) containing $Fe^{3+}$ is reduced at a constant current density, ($j$), of 100 mA $cm^{-2}$ employing planar electrodes of 10-$cm^2$ area. Calculate the time after which the concentration of $Fe^{3+}$ ($c_{initial} = 10^{-2}$ $M$) would have decreased by 10%. (Bock)

43. An investigator wants to study the Debye effect of diluted NaCl solution at room temperature but has no clue about what frequency range he should look at. Please help him. The diffusion coefficient of 0.001 $M$ NaCl solution is $1.5 \times 10^{-9}$ $m^2$ $s^{-1}$. (Xu)

44. Calculate the junction potentials for the following situations, (a) 0.1 *M* HC1/0.01 *M* HC1, $t_+ = 0.83$, (b) 0.1 *M* KC1/0.01 *M* KCl, $t_+ = 0.49$. (Kim)

45. From data in the text, calculate the degree of association in NaCl in a 2 *M* solution.

## PROBLEMS

1. In the experiment described in Exercise 6 it was found that at a certain time the Geiger counter registered a maximum ion flux, i.e., the intensity of the radiation has a maximum with respect to time. It was also found that by placing the Geiger counter farther away from the electrode, the time at which the maximum occurs becomes longer, and the peak intensity of the maximum decreases rapidly. Justify this observation and evaluate its usefulness in experimentally measuring diffusion coefficients of ions. (Xu)

2. Does the ion valence affect the statement that the ion diffusion coefficient can be considered a constant? Take electrolytes of the *z*:*z* type, for example, 1:1 and 2:2, and compare their diffusion coefficient variation over the concentration range of 0.1 to 0.01 mol $dm^{-3}$. (Xu)

3. The Einstein–Smoluchowski equation, $\langle x^2 \rangle = 2Dt$, gives a measure of the mean-square displacements of a diffusing particle in a time *t*. There $\langle x^2 \rangle$ is the mean-square distance traveled by most of the ions. Common observation using dyes or scents shows that diffusion of some particles occurs far ahead of the diffusion front represented by the $\langle x^2 \rangle = 2Dt$ equation. Determine the distance of this Einstein–Smoluchowski diffusion front for a colored ion diffusing into a solution for 24 hr ($D = 3.8 \times 10^{-5}$ $cm^2$ $s^{-1}$). Determine for the same solution how far the farthest 1% of the total diffused material diffused in the same time. Discuss how it is possible that one detects perfume across the space of a room in (say) 30 s.

4. In a molten salt solution of $CdCl_2$ in KC1, radiotracer measurements of the diffusion coefficient of Cd at 470 °C showed the heat of activation to be 23.0 kJ $mol^{-1}$. A rough calculation of the entropy of activation showed this to be small, about 41.8 J $mol^{-1}$ $K^{-1}$. When the composition of the melt is 66% KC1, the diffusion coefficient is $1.3 \times 10^{-5}$ $cm^2$ $s^{-1}$. Use these data to examine which of the two models for transport in liquids—jumping from site to site or shuffling along—is favored.

5. There are several ways of expressing ionic mobility. According to one of them, the absolute mobility, $u_{abs}$, is the velocity of an ion under an applied force of 1 dyne. The conventional mobility, $u_{conv}$, on the other hand, is the velocity under the force exerted on an ion by its interaction with an electric field of 1 V $cm^{-1}$. Deduce the relation between $u_{conv}$ and $u_{abs}$.

6. The self-diffusion coefficients of $Cl^-$ and $Na^+$ in molten sodium chloride are, respectively, $33 \times 10^{-4}$ exp(–8500/*RT*) and $8 \times 10^{-4}$ exp(–4000/*RT*) $cm^2\ s^{-1}$. (a) Use the Nernst–Einstein equation to calculate the equivalent conductivity of the molten liquid at 935°C. (b) Compare the value obtained with the value actually measured, 40% less. Insofar as the two values are significantly different, explain this by some kind of structural hypothesis.

7. It is normal to think that positive cations are reduced and deposited at negative cathodes in electrolysis and negative anions react at anodes to be oxidized. Although this is indeed the norm, there are a number of cases where negative anions undergo reaction at negative cathodes. A well-known example is that of the chromate anion, which is the entity from which chromium metal plates out. Consider the phenomenon in terms of the Nernst–Planck equation. Using a 2:2 electrolyte, $D = 5 \times 10^{-5}\ cm^2\ s^{-1}$, $c = 1.5 \times 10^{-3}\ mol\ cm^{-3}$, and $X = 1 \times 10^4\ V\ cm^{-1}$, calculate the needed $\frac{dc}{dx}$ to make anion deposition at a cathode possible.

8. Blum has developed an MSA approach to conductance (Equation 4.328). It applies well in representing conductance as a function of concentration. Conversely, it neglects established characteristics of electrolytes, such as their hydration (which changes with concentration and hence affects the ionic mobility) and association (which has been measured spectroscopically and calculated theoretically to be substantial in the concentration region worked on by Blum). Examine Blum's equation in this text. Compare his treatment with that of Lee and Cheaton. Does parametrization play a part in explaining why Blum gets the right results with a model that neglects established aspects of the structure of the moving particles?

9. The equivalent conductivities of KC1 and $MgCl_2$ aqueous solutions at 25 °C were estimated as 146.95 and 124.11 $(S^{-1}\ cm^2\ eq^{-1})$, respectively. Calculate the molar and the specific conductivities when the concentrations of both solutions were $10^{-3}$ g-eq per $1000\ cm^3$. What would be the measured resistance of these two solutions when two planar Pt electrodes of $2\text{-}cm^2$ area and 0.5 cm apart are employed? Measurements of the specific conductivity and hence of the solution resistance are usually carried out under a small ac field. Explain why a small ac field is used. (Bock)

10. Walden's empirical rule states that the product of the equivalent conductivity and the viscosity of the solvent should be constant at a given temperature. Explain the data in Table P.1, which were obtained for NaI solutions in several different solvents at 25 °C. Calculate the radius of the moving entity in acetone, applying Walden's rule. (Bock)

11. (a) Estimate the concentration of the supporting electrolyte (i.e., KC1) which must be added to a $10^{-6}$ *M* HC1 solution in order to study the diffusion of protons using the data in Table P.2. (Bock)

**TABLE P.1**

| Solvent | 4O (esu C $cm^{-1}$ $eq^{-1}$) |
|---|---|
| Ethanol | 0.754 |
| Acetone | 0.820 |
| Isobutanol | 0.725 |

(b) Explain the differences between the cation transference numbers listed in Table P.3.

12. According to Faraday's laws of electrolysis, an amount of electricity (i.e., number of electrons) will cause the equivalent weight of an ion in solution to react at the electrode. In a very simple case, one might envisage the deposition of $Ag^+$ (needing 1 mole of electrons per mole of Ag) to deposit at the negative electrode or cathode of an electrolytic cell. Correspondingly, at the other electrode, one might imagine an anodic oxidation to be occurring so that 1 mole of $Fe^{2+}$ (say) would be oxidized to 1 mole of $Fe^{3+}$. At each electrode, the same number of electrons would be transferred, and the same number of moles of reactant affected. This sounds simple and expected. However, there is an apparent problem. To react at the electrodes, ions have to be transported through the solution to the interface at the electrode at a sufficient rate. This rate is a fraction of the current given by the transport number. All would be well if each transport number were exactly 0.5. However, this is not the case because transport numbers vary greatly. In extreme cases, for very large ions, they tend to be zero. Explain, with equations and diagrams, how Faraday's laws can still be obeyed.

13. It is desired to know the transport number of protons in trifluoromethanesulfonic acid. The actual measurements made were of tritium self-diffusion and the result

**TABLE P.2**

**Cation Mobilities ($u$) Estimated at 25 °C for 0.1 *M* Solutions**

| Species | $u$ [$cm^2$ $V^{-1}$ $S^{-1}$] |
|---|---|
| $H^+$ | $33.71 \times ^{-4}$ |
| $K^+$ | $6 \times 10^{-4}$ |

**TABLE P.3**

**$t_+^0$ Measured at 25 °C, in Aqueous Solution**

| Salt | $t_+^0$ |
|---|---|
| KCl | 0.4905 |
| KBr | 0.4847 |
| KI | 0.4887 |

obtained for 5 $M$ $CF_3SO_2OH$ at 80 °C was $2.13 \times 10^{-5}$ $cm^2$ $s^{-1}$. The relative values of the mobilities of $u_H$ and $u_T$ are (according to a modeling hypothesis) $\sqrt{3} = 1.73$. As far as $D_{CF_3SO_3^-}$ is concerned, this can be obtained from the Stokes–Einstein equation. The necessary viscosity data are shown in Figure P4.1. Calculate the transport number of $H^+$ in $CF_3SO_2OH$ at 80 °C. (The radius of $CF_3SO_2O^-$ can be obtained from models.)

14. Ohm's law implies that the equivalent conductivity is independent of the strength of the applied electric field. This is certainly so for a very wide variety of applied fields, 1 to $10^5$ V $cm^{-1}$, in fact. However, Wien showed that (with appropriate precaution taken against heating of the solution, etc.), the equivalent conductivity of electrolytes undergoes a substantial increase at about $10^6$ V $cm^{-1}$. By appropriate consideration of the ionic atmosphere and its time of relaxation, show that a credible model to explain the above is that the high applied field

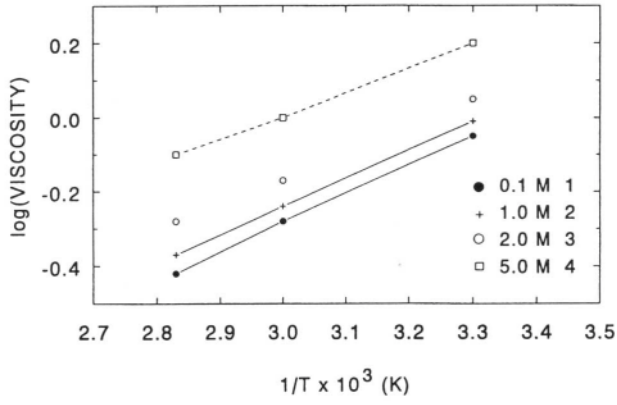


**Fig. P.4.1.** Plot of log $\eta$ vs. $1/T \times 10^3$ K for $CF_3SO_3H$ at different concentrations.

**TABLE P.4**

| Ion | $u_{conv}$ ($cm^2\ V^{-1}\ s^{-1}$) |
|---|---|
| $H^+$ | $3.625 \times 10^{-3}$ |
| $K^+$ | $7.619 \times 10^{-4}$ |
| $Cl^-$ | $7.912 \times 10^{-4}$ |
| $NO_3^-$ | $7.404 \times 10^{-4}$ |

causes the central ion to travel so fast that in fact the ionic atmosphere does not have time to form around the ion as it travels through the solution.

15. (a) Derive and plot the relations for variation in ion concentration at the surface of the electrode, under conditions of constant flux and instantaneous pulse, respectively, (b) In the constant flux-induced diffusion, the time when the ion concentration at the electrode surface reduces to zero is called the *transition time,* and is designated as $\tau$. Derive an expression of $\tau$ and comment on its physical significance. (Assume that in the constant flux experiment the concentration change is only caused by diffusion; i.e., the contribution of ion migration to concentration change is suppressed and therefore negligible.) (Xu)

16. Calculate the junction potentials for the following situations, (a) 0.1 *M* HC1/0.1 *M* KC1, (b) 0.1 *M* HC1/0.01 *M* $KNO_3$. Refer to Table P.4. (Kim)

17. A two-compartment electrochemical cell contains NaCl in one compartment and KC1 in the other. The compartments are separated by a porous partition. Concentrations of both the electrolytes are equal. If $\Lambda_{NaCl}$ and $\Lambda_{KCl}$ are the equivalent conductivities of the two solutions, show that the liquid junction potential $E_L$ is given by

$$E_L = \frac{RT}{F} \ln \frac{\Lambda_{NaCl}}{\Lambda_{KCl}}$$

**TABLE P.5**

**Transference Numbers ($t_+$) Measured at 25 °C for 0.1 *M* Solutions**

| Salt | $t_+$ |
|---|---|
| HCl | 0.83 |
| KCl | 0.49 |

18. (a) What are the liquid–liquid junction potentials for a cell consisting of HC1 (0.1 *M*) in contact with KC1 when (a) the concentration of KC1 is 0.1 *M* and (b) a saturated KC1 solution (i.e., 4.2 *M*) is employed? Refer to Table P.5.

    (b) Discuss any practical advantages of selecting KC1 and/or changing the concentration of the electrolyte in one half-cell. Also consider the factors that could introduce deviations between the calculated and measured values of $E_j$. (Bock)

19. In the study of nonaqueous electrolytes, the ion-pair effect is a severe factor affecting ion conduction. The degree of association of salts in nonaqueous solvents (or the solubilizing ability of the different solvents toward the salt) is often estimated by comparing the Walden product, that is, $\Lambda\eta$. Justify this method and explain what hypothesis is included and how it holds. (Xu)

20. The Einstein–Smoluchowski equation, $\langle x^2 \rangle = 2Dt$, is a phenomenological equation derived for diffusion along one coordinate. (For example, after the release of a barrier, along a tube containing a liquid.) However, it also applies to any medium. Suppose, now, that metal ions, (e.g., Pt) are deposited on a Pd substrate. Calculate how far the Pt would diffuse into the Pd in 6 weeks. (The diffusion coefficient of Pt into Pd can be estimated from other data as $9 \times 10^{-14}$ at 295 K.)

## MICRO RESEARCH PROBLEMS

1. (a) In an electrochemical analysis experiment, a univalent ion in a $10^{-3}$ *M* solution with a large amount of indifferent electrolyte is constantly oxidized at the electrode with a current density of $1.0\ \text{mA cm}^{-2}$. Calculate at 0.05 s after the constant current is switched on, the ion's concentration at $10^{-9}$ m, $5\ 10^{-9}$ m, and $20\ 10^{-9}$ m from the electrode, respectively. The diffusion coefficient of the ion is $10^{-9}\ \text{m}^2\ \text{s}^{-1}$ at 250°C. Use the error function table in the text if necessary, (b) Calculate the concentration at $25\ 10^{-9}$ m, $40\ 10^{-9}$ m, and $100\ 10^{-9}$ m, at 0.5 s after the constant flux is switched on. Compare the results obtained at 0.05 s. (c) Based on the above results and results of Problem 15, qualitatively draw the three-dimensional distribution of the ion with respect to both time *t* and distance *x*. (Xu)

2. From several points of view (for example, in battery technology), it is extremely important to have solutions of maximum specific conductivity. Basically, the specific conductivity increases proportionally to the concentration of ions. On this simplistic ground, it would seem important to have as high a concentration as possible up to the solubility limits. However (see the work of Haymet described in Chapter 3), increasing concentration leads to an increase of ionic association which decreases the concentration of conducting entities. Also, as

the concentration increases, the mobility decreases. By investigating the material in the text and in books of data, propose a solution (aqueous or nonaqueous, including a room-temperature molten salt) that would have a maximum conductivity at 25°C. Estimate its value. Do not omit considering the effect of viscosity and the insights of the Stokes–Einstein equation on the diffusion coefficient and hence (through the Nernst–Einstein equation) on mobility and conductivity.

*This page intentionally left blank*

# CHAPTER 5

# IONIC LIQUIDS

## 5.1. INTRODUCTION

### 5.1.1. The Limiting Case of Zero Solvent: Pure Electrolytes

Modern electrochemistry is concerned not only with systems based on aqueous solutions but also with solvent-free systems. Indeed, it is in such systems that many important electrochemical processes are carried out, such as the production of metals (aluminum, sodium, and magnesium) and the development of high-energy-density batteries.

The rationale behind the use of (and the search for) media other than water will be restated (see also Section 4.8). In aqueous media, electrode reactions involving hydrogen ions and hydroxyl ions may compete with and even supplant the desired electrochemical process (as in the deposition of magnesium from aqueous solutions). Furthermore, in technologies based on the conversion of chemical energy into electrical energy and vice versa, the desired rate of conversion may be limited by the conductivity of the solution: when working with pure electrolytes (as in eutectics such as those formed by LiCl-KCl), conductivity is never limiting.

Some of the difficulties associated with carrying out processes in aqueous solutions, particularly the undesired competition from hydrogen and oxygen evolution, can be sometimes overcome by using nonaqueous solvents consisting usually of organic substances (e.g., acetonitrile) to which are added a solute that dissociates in that solvent. However, often this is not a good approach just because of the low specific conductivities of such solutions (see Section 4.8.5) and their tendencies to absorb water from the surroundings.

So the question arises: Why have a solvent at all? This limiting case of an aqueous or a nonaqueous ionic solution from which all the solvent is removed is a *pure liquid electrolyte.* Conceptually, this definition is accurate. Operationally, however, if one

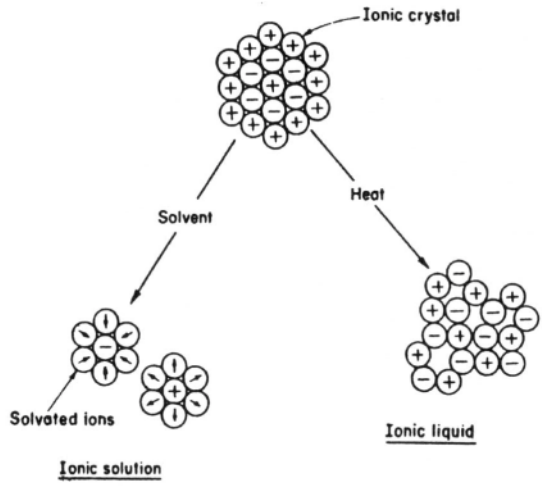


**Fig. 5.1**. An ionic crystal can be dismantled either by the action of a solvent or by the action of heat.

removes solvent molecules from a solution by evaporation, for example, one is left with ionic crystals, pure *solid* electrolyte. A further step in conversion from this solid to the pure liquid form is necessary.

### 5.1.2. Thermal Loosening of an Ionic Lattice

The process of dissolution of a true electrolyte was described in Chapter 2. The basic picture is that the ions in an erstwhile-rigid ionic lattice succumb to the strong attraction[1] of the solvent molecules and follow them into solution, executing a random walk there as free, stable solvated ions. The result is an ionic solution that has the ability to conduct electricity by means of the preferential drift of ions in the direction determined by the applied electric field and the charge on the ion. The disassembly of the ionic lattice was achieved by the solvent overcoming the Coulombic cohesive forces holding together the ions in the regular arrangement called a *lattice* (Fig. 5.1).

A solvent, however, is not the only agency that can cause an ionic lattice to fall to pieces. Heat energy also can overcome the cohesive forces and disrupt the ordered arrangement of ions in a crystal (Fig. 5.1). This process of melting results in a pure liquid electrolyte, a system having a conductance several orders of magnitude larger than that of the corresponding solid (Table 5.1).

[1]In the case of aqueous solutions, the forces are essentially ion–dipole and ion–quadrupole in character.

**TABLE 5.1**
**Specific Conductivities of Solid and Molten NaCl**

| | Specific conductivity (s $cm^{-1}$) |
|---|---|
| Solid NaCl | $1 \times 10^{-3}$ at 1073 K |
| Molten NaCl[a] | 3.9 at 1173 K |

[a]Melting point of NaCl is 1074 K.

### 5.1.3. Some Differentiating Features of Ionic Liquids (Pure Liquid Electrolytes)

A common type of ionic lattice is that of a crystalline salt. One such ionic lattice encountered in everyday life is sodium chloride. Molten sodium chloride is a typical liquid electrolyte and displays the characteristics of many liquid electrolytes.[2]

An appreciation of the properties of liquid electrolytes can be gained by a comparison between molten ice (water) and molten sodium chloride (Table 5.2). Both liquids are clear and colorless. Their viscosities, thermal conductivities, and surface tensions near their melting points are not very different.

In fact, one can go further and make the following statement: Molten salts look like water and not far above their melting points have viscosities, thermal conductivities, and surface tensions on the same orders of magnitude as those of water. In general, however, and with the important exception of some $AlCl_3$–complex organic systems, most fused salts are stable as liquids only at relatively high temperatures (500 to 1300 K) (Table 5.3).

One can quote exceptions to these generalizations. The tetraalkylammonium salts as a class are liquid at temperatures below 300 K. There are liquid electrolytes—produced from dissolving $AlCl_3$ into some complex organics—which are liquid at room temperature (Tables 5.3 and 5.4). Above the normal range of 300–1300 K is another set of molten electrolytes, the molten silicates, borates, and phosphates, for which the characteristic temperature range is 1300–2300 K (Tables 5.5 and 5.6).

### 5.1.4. Liquid Electrolytes Are Ionic Liquids

The crucial difference between molten salts and molten ice lies in the values of the specific conductivity (Table 5.7). Fused salts have about $10^8$ times greater specific conductivity than fused ice.

The temptation to ascribe the high conductance of fused salts to conduction by electrons must be rejected. The conductivity of a molten salt is high compared to that of water; but it is ten thousand times lower than that of a liquid metal, such as mercury (Table 5.8).

[2]The terms *pure liquid electrolyte, ionic liquid, fused salt,* and *molten salt* are used synonymously.

**TABLE 5.2**

**Comparison of Some Properties of Water and Molten NaCl**

| | Water 298 K | Molten NaCl 1123 K |
|---|---|---|
| Viscosity (millipoise) | 8.95 | 2.5 |
| Refractive index | 1.332 | 1.408 |
| Diffusion coefficient ions ($cm^2\ s^{-1}$) | $Na^+\ 3 \times 10^{-5}$ | $Na^+\ 1.53 \times 10^{-4}$<br>$Cl^-\ 0.83 \times 10^{-4}$ |
| Surface tension ($dyn\ cm^{-1}$) | 72 | 111.8 |
| Density | 1.00 | 1.539 |

**TABLE 5.3**

**Melting Points of Some Inorganic Salts**

| Salt | Melting Point (K) | Salt | Melting Point (K) |
|---|---|---|---|
| $LiClO_4$ | 400 | | |
| $LiAlCl_4$ | 418 | | |
| $AgNO_3$ | 483 | $PbCl_2$ | 774 |
| $HgBr_2$ | 511 | $CdCl_2$ | 841 |
| $LiNO_3$ | 527 | LiCl | 883 |
| $ZnCl_2$ | 548 | CaCl | 919 |
| $HgCl_2$ | 550 | NaI | 924 |
| $NaNO_3$ | 583 | $MgCl_2$ | 987 |
| $KNO_3$ | 610 | KCl | 1049 |
| $PbBr_2$ | 646 | NaCl | 1081 |
| AgBr | 707 | $Na_2CO_3$ | 1131 |
| $AlCl_3$-1-methyl-3-ethyl imidazalonium and similar systems | | | room temperature |

**TABLE 5.4**

**Melting Points of Some Tetraalkylammonium Salts**

| Salt | Melting Point (K) |
|---|---|
| Tetramethylammonium bromide | 503 |
| Tetrabutylammonium iodide | 417 |
| Tetrapropylammonium iodide | 553 |
| ($AlCl_3$-1-butyl-pyridinium chloride | < 303 (according to composition)) |

**TABLE 5.5**

**Some Properties of Molten Oxides near the Melting Point**

| Molten oxide | Temp. (K) | Density ($g\ cm^{-3}$) | Surface Tension ($dyn\ cm^{-1}$) | Viscosity (cP) | Specific Conductivity ($s\ cm^{-1}$) |
|---|---|---|---|---|---|
| $Li_2O$-$SiO_2$ | 1523 | 2.07 | 354 | $2.88 \times 10^2$ | 5.5 (2023 K) |
| $Li_2O$-$1\frac{1}{2}SiO_2$ | 1373 | 2.13 | 331 | $5.02 \times 10^3$ | |
| $Li_2O$-$2SiO_2$ | 1373 | 2.16 | 319 | $1.78 \times 10^4$ | 2.5 (2023 K) |
| $Na_2O$-$SiO_2$ | 1373 | 2.23 | 300 | $1.19 \times 10^3$ | 4.8 (2023 K) |
| $Na_2O$-$2SiO_2$ | 1173 | 2.28 | 289 | $3.33 \times 10^5$ | 2.1 (2023 K) |
| $Na_2O$-$3SiO_2$ | 1173 | 2.23 | 282 | $1.99 \times 10^6$ | |
| $K_2O$-$2SiO_2$ | 1373 | 2.20 | 220 | $1.08 \times 10^5$ | 1.5 (2023 K) |
| $CaO$-$SiO_2$ | 1823 | — | 400 | $2.73 \times 10^2$ | 0.8 (2023 K) |

Fused salts conduct by means of the preferential drift of ions in the direction of applied electric fields. They are in fact ionic liquids, that is, liquids containing only ions, the ions being free or associated (see Section 5.4).

Another class of ionic liquids consists of the *molten oxides.* These are highly conducting liquids formed by the addition of a *metal* oxide (e.g., $Li_2O$) to a *non-metal oxide* (e.g., $SiO_2$). These systems melt at much higher temperatures than the molten salts. Some properties of the molten oxides are shown in Table 5.5. To develop a perspective on the properties of liquid electrolytes, some properties of water, liquid sodium, an aqueous solution of NaCl, fused NaCl, and a mixture of fused $Na_2O$ and $SiO_2$ are shown in Table 5.6.

### 5.1.5. Fundamental Problems in Pure Liquid Electrolytes

In dealing with aqueous and nonaqueous solutions of electrolytes, the procedure was first to seek a picture of the time-averaged structure of the electrolytic solution and second to understand the basic laws of ionic movements. The picture that emerged was of ions and solvent molecules interacting together to form solvated ions; of ions interacting with each other to form ionic clouds and associated ion pairs or complexes; and of all these entities executing an aimless random walk at equilibrium, which becomes a directed drift under a concentration gradient or an external electric field. The problems in pure liquid electrolytes are analogous, though more difficult to treat mathematically because of the increased energy of interactions between the ions (compared with those in aqueous solution) arising from the short distance between them.

The first problem can be defined as follows: What idealized model could best replicate a solvent-free system of charged particles forming a highly conducting ionic liquid? In the case of the aqueous solution, it was easy to understand the drift of ions at the behest of the applied electric field. Positive and negative ions separated by large

**TABLE 5.6**

**Comparison of the Properties of Various Liquids**

| Properties | Water at 298 K | Liquid Sodium at m.p. | 1 *M* Sodium Chloride Soln. at 298 K | Liquid Sodium Chloride at m.p. | Liquid Sodium Silicate near the m.p. |
|---|---|---|---|---|---|
| Melting point (K) | 273.15 | 370.9 | 269.8 | 1074.1 | 1361.1 |
| Vapor pressure (Pa) | 3125.8 | $1.295 \times 10^{-5}$ | 2210.5 (293 K) 4052.6 (303 K) | 45.4 | |
| Molar volume ($cm^3$) | 18.07 | 24.76 | 17.80 | 30.47 | 55.36 |
| Density (g $cm^{-3}$) | 0.997 | 0.927 | 1.0369 | 1.5555 | 2.250, 1473 K |
| Compressibility ($10^6$ $cm^2$ $atm^{-1}$) | 46.3055 isoth. | 18.88 isoth. | 40.08 isoth. | 29.08 isoth. | 59.579 adiabatic, 1473 K |
| Diffusion coefficient ($cm^2$ $s^{-1}$) | $3.0 \times 10^{-5}$ | $2.344 \times 10^{-7}$ | $D_{Na^+} = 1.25 \times 10^{-5}$ $D_{Cl^-} = 1.77 \times 10^{-5}$ | $D_{Na^+} = 1.53 \times 10^{-4}$ $D_{Cl^-} = 0.83 \times 10^{-4}$ 1123 K | |
| Surface tension (dyn $cm^{-1}$) | 71.97 | 192.2 | 74.3 | 113.3 | 294, 1473 K |
| Viscosity (cP) | 0.895 | 0.690 | 1.0582 | 1.67 | 980, 1373 K |
| Specific electric conductance (s $cm^{-1}$) | $4.0 \times 10^{-8}$ | $1.04 \times 10^{5}$ | 0.101 mol $cm^{-3}$ | 3.58 | 4.8, 2023 K |
| Refractive index | 1.333 | 1.04 | 1.3426 | 1.408, 1123 K | 1.52, solid, room temp. |

**TABLE 5.7**

**Conductivities of Molten Salts and Water**

| Substance | Temperature (K) | Specific Conductivity ($s\ cm^{-1}$) |
|---|---|---|
| $H_2O$ | 291 | $4 \times 10^{-8}$ |
| LiCl melt | 983 | 6.221 |
| NaCl melt | 1181 | 3.903 |
| KCl melt | 1145 | 2.407 |

**TABLE 5.8**

**Conductivities of Molten NaCl and Mercury**

| Substance | Temperature (K) | Specific Conductivity ($s\ cm^{-1}$) |
|---|---|---|
| Hg | 293 | $1.1 \times 10^{4}$ |
| NaCl melt | 1181 | 3.903 |

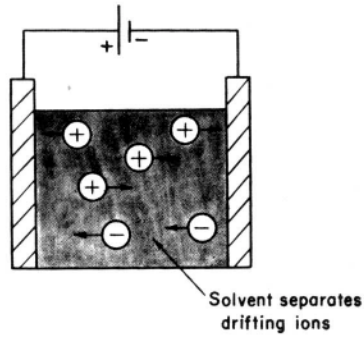


**Fig. 5.2.** In an aqueous solution, the solvent separates the drifting ions.

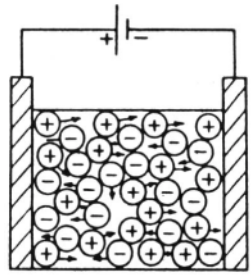

**Fig. 5.3.** In an ionic liquid, there is no solvent separating the drifting ions.

stretches of water drift in opposite directions (Fig. 5.2). In a pure ionic liquid, however, there is no water for the ions to swim in; the ions move about rather aimlessly among themselves (Fig. 5.3). When an external field is switched on, how is it that the ions are able to move past each other? Will not the large interionic force make them stick together, forming a poorly conducting ionic lattice? The situation appears puzzling.

What is the essential difference between the solid form and the liquid form of an ensemble of particles? This is a question that is relevant to all processes of fusion, e.g., the process of solid argon[3] melting to form a liquid. In the case of ionic liquids, the problem is more acute. One must explain the great fluidity and corresponding high conductivity in a liquid that contains only charged particles in contact.

The second problem concerns an understanding of the sharing of transport duties (e.g., the carrying of current) in pure liquid electrolytes. In aqueous solutions, it was possible to comprehend the relative movements of ions in the sense that one ionic species could drift under an electric field with greater agility and therefore transport more electricity than the other until a concentration gradient was set up and the resulting diffusion flux equalized the movements when the electrodes were reached. In fused salts, this comprehension of the transport situation is less easy to acquire. At first, it is even difficult to see how one can retain the concept of transport numbers at all when there is no reference medium (such as the water in aqueous solutions) in which ions can drift.

Third, there exists another problem, that of complex ions. In aqueous and nonaqueous solutions, it is possible to regard the ionic atmosphere as a type of incipient complex in which the mean distance between oppositely charged ions becomes smaller with increasing electrolyte concentration. Eventually the ions come sufficiently close so that the thermal forces that tend to separate them are overcome on an increasingly frequent basis by the Coulombic attraction forces so that cation and anion pairs arise, some of which remain stuck together (see Section 3.8).

[3]This is a relatively simple solid from the point of view of the forces between the uncharged particles.

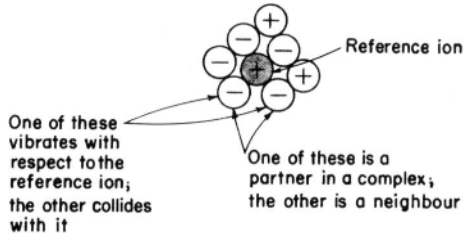


**Fig. 5.4.** The problem of distinguishing a neighboring ion colliding with the reference ion from a ligand (i.e., a partner in complex formation) vibrating in relation to the reference ion.

For the ionic liquids, however, without a separating solvent, the situation is different for the ions are always in contact. This absence of solvent causes conceptual problems regarding the existence of complex ions in ionic liquids. Consider a particular ion associated with another to form a vibrating complex. The ion is also in contact with, and continually jostled by, neighboring ions that are exactly like its partner in the complex (Fig. 5.4). Which is the partner and which the neighbor? Which is the vibration and which the collision? A distinction between these two types of contacts constitutes one of the problems in this field.

In aqueous solutions, the situation is clarified by the solvent. This solvent keeps the complex ions apart at mean distances, defines them as independent stable entities, and permits probing radiation (e.g., visible light) to pick them out from the surroundings (Fig. 5.5).

The concept of complex ions is therefore more subtle in ionic liquids than in aqueous solutions. There is not only the question of an objective means for identifying

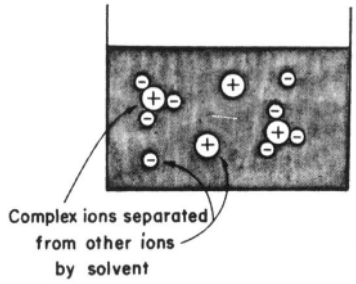


**Fig. 5.5.** In an aqueous solution, the complex ion is spatially separated from the other ions.

ions that can be said to be joined in some way to other ions so that the aggregate is distinctly an individual but also questions of distortion of ions in contact and the introduction of covalent bonds between them.

## Further Reading


### *Seminal*

1. W. Klemm and W. Biltz, "The Distribution of Ionic Conductivity among Molten Chlorides of the Periodic Table," *Z. Anorg. Allg. Chem.* **152**: 255, 267 (1926).
2. J. O'M. Bockris and N. E. Richards, "Free Volumes and Equations of State for Molten Electrolytes," *Proc. Roy. Soc. Lond.* **A241**: 44 (1957).
3. C. Solomons, J. H. P. Clarke, and J. O'M. Bockris, "Identification of Complex Ions in Molten Liquids," *J. Chem. Phys.* **49**: 445 (1968).
4. A. R. Ubbelohde, "Research on Molten Salts: Introduction" in *Ionic Liquids,* D. Inman and D. G. Lovering, eds., Plenum Press, New York (1981).

### *Review*

1. J. E. Enderby, "The Structure of Molten Salts," in *Molten Salt Chemistry,* G. Mamantov and N. R. Marassi, eds., p. 115, NATO ASI Series, Reidel, Dordrecht, The Netherlands (1987).

### *Papers*

1. I. Farnon and J. F. Stebbins, *J. Am. Chem. Soc.* **112**: 32 (1990).
2. I. Strubinizer, W. Sun, W. E. Cleland, and C. L. Hussey, *Inorg. Chem.* **29**: 993 (1990).
3. R. L. McGreevy and M. A. Howe, *Proc. Roy. Soc. Lond.* **430**: 241 (1990).
4. R. L. McGreevy and L. Pusztai, *Proc. Roy. Soc. Lond.* **241A**: 261 (1990).
5. M. L. Saboungi, D. L. Price, C. Scamehorn, and M. P. Tosi, *Europhys. Lett.* **15**: 281 (1991).
6. M. L. Saboungi, D. L. Price, C. Scamehorn, and M. P. Tosi, *Europhys. Lett.* **15**: 283 (1991).
7. Y. Toda, S. Hiroeka, Y. Katsumura, and I. Yemada, *Ind. Eng. Chem. Res.* **31**: 2010 (1992).
8. Z. Ardeniz and M. P. Tosi, *Proc. Roy. Soc. Lond.* **A437**: 85 (1992).
9. M. Oki, K. Fujishima, Y. Iwadate, and J. Mochinaga, in *Molten Salt Chemistry and Technology,* Proceedings of the Electrochemical Society, p. 9 (1993).
10. M. Mahr and K. G. Weil, in *Molten Salt Chemistry and Technology,* Proceedings of the Electrochemical Society, p. 147 (1993).
11. A. N. Yolshin and M. Yu Bryakotin, in *Molten Salt Chemistry and Technology,* Proceedings of the Electrochemical Society, p. 338 (1993).
12. M. Matsunaga, S. Hara, and K. Ogino, in *Molten Salt Chemistry and Technology,* Proceedings of the Electrochemical Society, p. 507 (1993).
13. Y. G. Boshuev and N. L. Kolesnikov, *Industrial Laboratory* **61**: 98 (1995).
14. S. Ohno, A. C. Barnes, and J. E. Enderby, *J. Phys. Cond. Matt.* **20**: 3785 (1996).
15. U. Matenaar, J. Richter, and M. D. Zeidler, *J. Magn. Reson, Series A* **122**: 72 (1996).
16. M. Abraham, M. C. Abraham, and I. Ziogas, *Electrochim. Acta* **41**: 903 (1996).

## 5.2. MODELS OF SIMPLE IONIC LIQUIDS

### 5.2.1. Experimental Basis for Model Building

One's first impression of a liquid (its fluidity, conformity to the shape of the containing vessel, etc.), would suggest that its structure has nothing to do with that of the crystal from which it was obtained by melting. If, however, a beam of monochromatic X-rays is made incident on the liquid electrolyte, the scattered beam has an interesting story to tell, as have corresponding studies on concentrated electrolytes and on molten salts carried out by means of neutron diffraction. The ions are almost at the same internuclear distances in a fused salt as in the ionic crystal, actually at a slightly lesser distance (Table 5.9). The X-ray patterns (Fig. 5.6) also indicate that in the liquid state the local order extends over a very short distance (tens of nanometers). It is as if the fused salt forgets how to continue the ordered arrangements of ions of the parent lattice, *although, curiously, the distance between individual ions becomes smaller rather than greater.*

### 5.2.2. The Need to Pour Empty Space into a Fused Salt

There is another important fact about the melting process. When many ion lattices are melted, *there is a 10 to 25% increase in the volume of the system* (Table 5.10). This volume increase is of fundamental importance to someone who wishes to conceptualize models for ionic liquids because one is faced with an apparent contradiction. From the increase in volume, one would think that the mean distance apart of the ions in a liquid electrolyte would be greater than in its parent crystal. On the other hand, from the fact that the ions in a fused salt are slightly closer together than in the solid lattice,

**TABLE 5.9**

**Internuclear Distances in an Ionic Crystal and the Corresponding Fused Salt**

| | Distance between Oppositely Charged Ions (pm) | |
|---|---|---|
| Salt | Crystal, m.p. | Molten Salt |
| LiCl | 266 | 247 |
| LiBr | 285 | 268 |
| LiI | 312 | 285 |
| NaI | 335 | 315 |
| KCI | 326 | 310 |
| CsCl | 357 | 353 |
| CsBr | 372 | 355 |
| CsI | 394 | 385 |

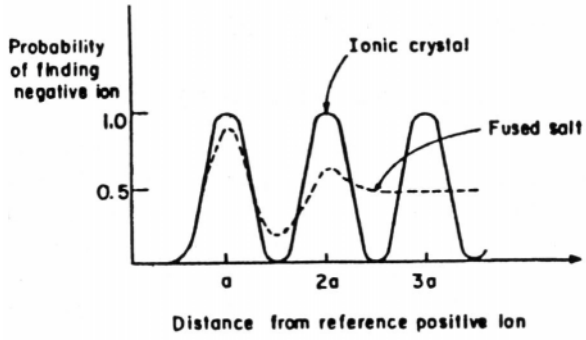


**Fig. 5.6.** Schematic diagram to show short-range and long-range order in an ionic crystal as opposed to only short-range order in a fused salt. In an ideal ionic crystal, if one takes a reference positive ion, there is a certainty of finding a negative ion at the lattice distance or a multiple of this distance; in a fused salt, there is a high probability of finding a negative ion one distance away; but within two or three lattice distances away, the probability becomes half, i.e., a negative ion is as likely as a positive ion. Thus, in a fused salt, there is no long-range order.

one would think that there should be a small volume decrease upon fusion.[4] How is this emptiness—which evidently gets introduced into the solid lattice on melting—to be conceptualized?

Before an answer is given to this central question, it is necessary to retrace the steps that have been taken in respect to Fig. 5.6. One examines how it was obtained because quantitative knowledge of the short-range order which does exist (dotted line in Fig. 5.6) is vital to understanding the liquidity of molten salts.

### 5.2.3. How to Derive Short-Range Structure in Molten Salts from Measurements Using X-ray and Neutron Diffraction

5.2.3.1. *Preliminary.* Before World War I, little was known either about the nature of X-rays (were they like waves or more like particles?) or about the

[4]In the case of some salts, the volume changes on fusion are smaller than are indicated in Table 5.10. Thus, calcium, strontium, and barium halides have volume changes that are about a fifth of the changes for the corresponding alkali halides. This is because such salts crystallize in a form that already contains plenty of open space in the solid lattice. When these open-lattice salts are melted, a smaller volume increase is needed than is the case for the space-filled lattices of the solid alkali halides.

**TABLE 5.10**
**Volume Change on Fusion**

| Substance | % Increase of Volume on Fusion |
|---|---|
| NaCl | 25 |
| NaF | 24 |
| NaI | 19 |
| KCl | 17 |
| KBr | 17 |
| KI | 16 |
| RbCl | 14 |
| $CdCl_2$ | 20 |
| $CdBr_2$ | 28 |
| $NaNO_3$ | 11 |

arrangement of atoms in crystals. Much light was thrown on the latter question as a result of a thought experiment suggested by von Laue. He considered an apparatus known as a *diffraction grating.* This consists of a great number of parallel slits. It can be shown that if light of a specific monochromatic wavelength is incident upon a grating on which the parallel slits are a distance $d$ apart at a certain specific angle $\theta$, then "interference" occurs among the light waves, so that for the Bragg condition, $\lambda = 2d \sin \theta$ and no rays emerge—they have been knocked out by destructive interference with other rays.

The merit in von Laue's thought was to see that the regular rows of atoms which, in 1913 when he did his thinking, were only tentatively thought to be there, could be regarded as a diffraction grating of atomic dimensions.[5] For the diffraction experiment to work with reasonable values of the incident angle, $\theta$, the wavelength $\lambda$ must have the same order of magnitude as the width of the slits in a grating or the interatomic

[5]Von Laue's flash of insight in recognizing that a crystal lattice equals a diffraction grating is a beautiful example of the birth of a scientific idea. Since it gave rise to X-ray diffraction as a technique for obtaining knowledge of the structure of solids, it can be regarded as having great historical significance. It was the beginning of the effective study of the structure of the solid state. This creative thought is analogous to von Helmholtz's suggestion that an electrode in solution charged with excess negative or positive charges would attract to itself a monolayer of ions of opposite charge; the ensemble could be thought of as if it were the two plates of a parallel-plate condenser.

Such flashes, inspirations if you like, do not happen while one is thinking in one's study or talking with a student. They turn up like a photograph in the mind at some odd time later (Leo Szilard, for example, got some of his best ideas while soaking in the bathtub). But they don't turn up at all unless one has thought a great deal about the matter.

distance ($d$) in the crystals. However, X-rays can have wavelengths around 0.1 nm, which is just the right wavelength to react to a grating in which the distance the "slits" are apart is in fact the distance between ions. Von Laue boldly predicted that if a beam of X-rays were incident upon a solid crystal lattice, destructive interference and constructive augmentation would occur and a diffraction pattern[6] would result. Trial experiments succeeded and the method of X-ray diffraction for investigating structure in solids, and solid-state structural chemistry, was born.

Shortly after von Laue's suggestion and its validation, Bragg produced his equation. He showed that conditions for interference would be reached when

$$n\lambda = 2d \sin \theta \tag{5.1}$$

The terms in Bragg's law have been defined above except for $n$, which represents the number of the crystal planes (in succession, going downward from the surface) from which the reflected beam arises and therefore runs 1, 2, 3,.... The condition for interference is that the difference in path length of two rays of light, reflected from neighboring planes, should be an integral multiple of $\lambda$. Finding maxima and minima (non-interfered and interfered conditions) coupled with the strength of the reflection ("intensity") and the corresponding angle values of the reflected X-rays gives $d$ [from Eq. (5.1)], the internuclear distance.

For an ordered solid, as $\theta$ is changed, the peaks representing no constructive interference repeat themselves for values of sin $\theta$ corresponding to $n$ = 1, 2, 3, with a constant $d$; i.e., the arrangement is of long-range order. On the other hand, as has been seen, for liquids (see Fig. 5.6), the peaks fade rapidly with increasing distance from the reference plane, representing a short-range order.

5.2.3.2. *Radial Distribution Functions.* What happens when X-ray diffraction occurs in liquids? To understand this (see also Section 3.11), it is best at first to consider only a single-species liquid; one could have in mind not a binary molten salt such as liquid sodium chloride, but, say, liquid sodium.

Then one defines a quantity called a *pair correlation function*, represented by $g_{A,B}(r)$. Consider a reference particle, $A$. The number of particles called $B$ that occupy a spherical shell having a radius $r$ is

$$dn_r = 4\pi\rho_B g_{A,B}(r) r^2 \, dr \tag{5.2}$$

where $\rho_B$ is the number of $B$'s per unit volume.

---

[6]A diffraction pattern is a series of bright spots alternating with dark areas that results from a plot of the intensity of the reflected beam after it passes through the object examined, as a function of the incident angle of the X-ray beam.

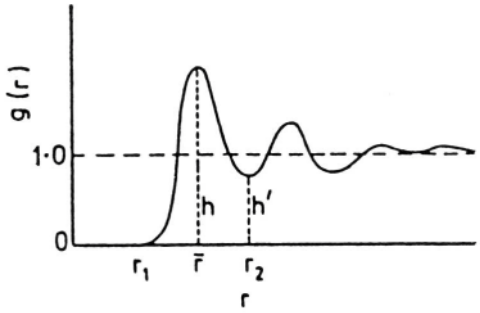


**Fig. 5.7.** A hypothetical radial distribution function $g(r)$ for a liquid that contains just one chemical species. (Reprinted from J. E. Enderby, in *Molten Salts*, *NATO ASI Science Series, Series C* **202:** 2, 1988.)

Enderby has illustrated an idealized "radial distribution function" [see Eq. (5.3)], shown in Fig. 5.7. The figure suggests that starting from the center of $A$, nothing is seen until a distance $r_1$ away, and the most probable distance to the center of the next nearest particle is $\bar{r}$. What does the distance $r_2$ mean? At distances greater than this, as far as $A$ is concerned, nearest-neighbor interactions can be neglected.

From these statements, one can begin to appreciate the significance of the *radial distribution function* shown in the figure. This quantity is obtained by integrating Eq. (5.2).

$$4\pi\rho\int_0^{r_s} g_{A,B}(r)r^2\,dr \tag{5.3}$$

If one takes $g_{A,B}(r)$ as the pair correlation function defined in Eq. (5.2), the radial distribution function represents the number of particles of $B$ in a shell up to $r_2$ around $A$. If $r_s$ is then $r_2$ (see Fig. 5.7), one can regard Eq. (5.2) as giving the *coordination number* of $A$ in the liquid. In the example chosen for simplicity, species $A$ is the same as species $B$ but this of course is only true for radial distributions of monatomics, e.g., sodium. It is found in practice that in a liquid, $g_{A,B}(r)$ settles to unity by the third or fourth atom away from the reference atom $A$.

Radial distribution functions can be determined experimentally using diffraction (i.e., interference) experiments. X-rays or neutrons can be used. If one knows the pair correlation function $g_{A,B}(r)$ for each atom, one can work out the short-range structure in a liquid. The question is then how does one find $g_{A,B}(r)$?

### 5.2.4. Applying Diffraction Theory to Obtain the Pair Correlation Functions in Molten Salts

The mathematical theory of diffraction[7] is heavy stuff, and a very simplified version takes several book pages to deduce. Here, some equations from this theory will be presented to show their shape and size, and their significance to the task on hand will be explained.

The amplitude of waves scattered by nuclei is given by an equation of the form

$$\text{Amplitude} = \sum_{\alpha} f_{\alpha} \sum_{i(\alpha)} \exp[i\mathbf{k} - r_i(\alpha)] \tag{5.4}$$

where $f_\alpha$ is the X-ray form factor and defines the central atom, $\alpha$. In the second summation, $\mathbf{k}$ is the wave vector $2\pi/\lambda$ of the X-rays used, and $r_i(\alpha)$ is the distance from the $i$th nucleus of the species $i$. This second part deals with the phase relationships[8] of the scattered radiation as a function of distance from the given atom, $\alpha$.

The intensity of the scattered light is given by the equation

$$I(\mathbf{k}) = N\left[\sum x_\alpha b_\alpha^2 + F(\mathbf{k})\right] \tag{5.5}$$

In this expression, $x_\alpha$ is the atom fraction of the atomic species $\alpha$; $b_\alpha$, the same as $f_\alpha$, is the X-ray form factor; and $F(\mathbf{k})$ is the average of the quantities called *partial structural factors* and is given by

$$F(\mathbf{k}) = \sum_{\alpha} \sum_{\beta} x_\alpha x_\beta b_\alpha b_\beta [S_{\alpha\beta}(\mathbf{k}) - 1] \tag{5.6}$$

---

[7] Diffraction is sometimes described as "the bending of light around an obstacle." When light is interrupted by an object, the shadow formed is bordered by alternating white and dark bands. To observe such effects, one needs to use a point source and monochromatic light; hence diffraction effects are not observed in everyday life.

Diffraction—and the alternating dark and light bands to which it gives rise—is based on the interference of light waves that occurs when two light beams meet and annihilate or augment each other. Diffraction should not be confused with the primary phenomenon of *refraction*, which refers to the bending of light as it passes from a more dense to a less dense medium. When this occurs (and depending on the angle at which the beam from the dense medium is incident upon the less dense one), the light may pass through from one medium to the next or it may be reflected (or some of both). The change in direction of the light beam on entering the new medium can be regarded as a result of the exchange of kinetic and potential energy at the interface. Refraction is expressed in terms of the refractive index of the dense medium.

[8] In electricity theory, phase relationships refer to the relation of current to potential in an ac circuit. If the current and potential vary together in time, i.e., they reach maximum and minimum together, then they are "in phase." If the current and potential are "out of step," by, say, a quarter of a phase, they are "out of phase." In diffraction theory, the phase refers to the variation of the amplitude of the light wave with time at a given point. Two beams of radiation out of phase by a half cycle will annihilate.

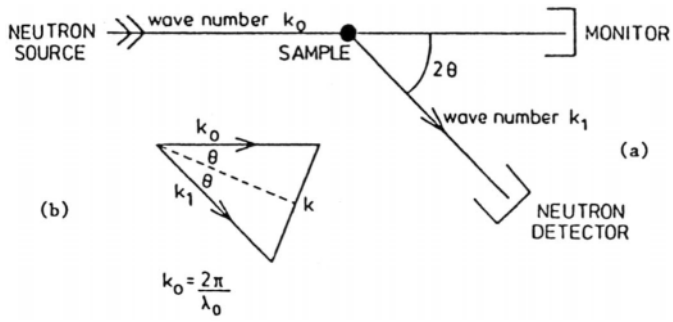


**Fig. 5.8.** The conventional arrangement for neutron diffraction. (Reprinted from J. E. Enderby, in *Physics and Chemistry of Aqueous Ionic Solutions*, M. C. Bellisent-Fund and G. W. Nielson, eds., *NATO ASI Series C* **207**: 131, 1987.)

The quantity symbolized by $S_{\alpha,\beta}$ is called the *structural factor.*

How would pair correlation functions and partial structural factors be written for a binary molten salt, e.g., sodium chloride? The corresponding correlation function would be given by

$$g_{\alpha,\beta} = 1 + \frac{1}{2\pi^2 \rho r} \int S_{\alpha,\beta}(h) k \sin(kr)\, dr \tag{5.7}$$

and the partial structural factor by

$$F(k) = x_+^2 b_+^2 [S_{2+}(k) - 1] + x_-^2 b_-^2 [S_{2-}(k - 1)] + 2x_+ x_- b_+ b_- [S_{\pm}(k) - 1] \tag{5.8}$$

These equations (also undeduced) may seem pretty fearsome. However, the quantities present in Eq. (5.5), the partial factors, can all be determined from X-ray or neutron diffraction setups. Figures 5.8 and 5.9 show at a schematic level what one does to make diffraction measurements.

The material given here then shows how measurement of the diffraction of X-rays (also neutrons, see later discussion) gives the pair correlation function, $g_{\alpha,\beta}$. It can give much more. As shown in Section 3.11, the determination of $g_{\alpha,\beta}$ allows one to calculate a number of properties of the liquid or solution. A property calculated from pair correlation functions does not involve an assumed modeling theory. Instead, the experimentally determined pair correlation functions are the basis of the calculated properties. It is as though one had "worked out"[9] the structure first and then used the knowledge of that structure to calculate the properties. Is this a "higher level" approach

[9] "Working out the structure" means determining the $g_{\alpha,\beta}$s for the various entities (e.g., $\alpha$ and $\beta$) present in the liquid.

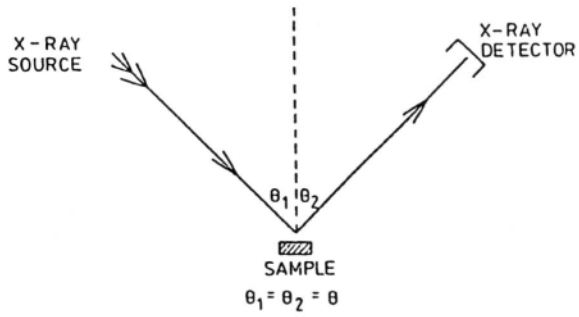


**Fig. 5.9.** Conventional arrangement for X-ray diffraction studies on liquids. (Reprinted from J. E. Enderby, in *Physics and Chemistry of Aqueous Ionic Solutions*, M. C. Bellisent-Fund and G. W. Nielson, eds., *NATO ASI Series C* **205**: 131, 1987.)

to the elucidation of the structure inside a liquid, rather than the alternative modeling one in which one sketches several possible pictures of the liquid and then applies uncontroversial theory to each to see the properties each model gives rise to, judging the validity of the hypothesized structure from the match of the calculated results with those of experiments?

### 5.2.5. Use of Neutrons in Place of X-rays in Diffraction Experiments

From the early years of this century, the only type of radiation used to find long-range order in solids and short-range order in liquids was X-rays. However, neutrons can also be used to carry out diffraction experiments, and with certain advantages, as will be seen. The trouble is that while it is fairly easy (hence, economically attractive) to use an X-ray source, one has to have a nuclear reactor handy to achieve a neutron stream. The advantages of using neutrons rather than X-rays in diffraction arise from a difference in how diffraction (i.e., interference) occurs for the two forms of radiation.

X-rays interact with matter because their electromagnetic oscillations are affected by the electrons of the material. Neutrons take no notice whatsoever of electrons when they pass through matter. They interact with the nuclei. Neutron diffraction is sensitive to the atomic number and atomic weight of the atoms constituting the substance. For example, it can distinguish easily between Fe and Co in alloys and between isotopes such as $^{35}Cl$ and $^{37}Cl$.

Thus, the $b$ terms in Eq. (5.6) are 11.7 for $^{35}Cl$ but 3.08 for $^{37}Cl$, a difference much greater than that intuitively expected. Such differences are helpful in using Eq. (5.7) to give $g_{\alpha,\beta}$ and to lead to the calculation of properties (Section 5.2.3.2). Variation in the concentration of the isotopes and measurements of the patterns for a series of such

**TABLE 5.11**

**Ratios of Ionic Radii ($r_+,r_-$), First Peak Positions of $g_{--}(r)$ and $g_{+-}(r)$, and Coordination Numbers ($n_{+-}$) for Some Molten Salts and Simple Geometrical Clusters**

| | $r_+/r_-$ | $r_{--}/r_{+-}$ | $n_{+-}$ | Structure |
|---|---|---|---|---|
| $ZnCl_2$ | 0.457 | 1.621 | 4.3 | T |
| $MgCl_2$ | 0.407 | 1.471 | 4.3 | S(?) |
| $CaCl_2$ | 0.611 | 1.342 | 5.4 | ? |
| $SrCl_2$ | 0.691 | 1.311 | 6.9 | O(?) |
| $BaCl_2$ | 0.833 | 1.245 | 7.7 | C(?) |
| $NiCl_2$ | 0.426 | 1.610 | 4.7 | T(?) |
| $NiBr_2$ | 0.354 | 1.608 | 4.7 | T(?) |
| $NiI_2$ | 0.319 | 1.577 | 4.2 | T(?) |
| Tetrahedron (T) | — | 1.633 | 4 | — |
| Octahedron (O) | — | 1.414 | 6 | — |
| Cube (C) | — | 1.155 | 8 | — |
| Square (S) | — | 1.414 | 4 | — |

Source: Reprinted from R. L. McGreevy and L. Pusztai, *Proc. Roy. Soc. Lond.* **A430**: 241, 1990.

changes provides added data for a given salt and improves finding the unknowns. All this being the case, one has to weigh the undeniable pros of neutron diffraction against the considerable cons of having to take a team of collaborators to a nuclear reactor to obtain the neutron stream and work there day and night[10] for some days.

What about the determination of *voids* in a liquid? Determination of the short-range order may not allow one to determine the distribution (number and size) of fluctuating voids in the liquid.[11] While such voids may play a vital part in the mechanism of transport, they *are* voids and hence would hardly make much impression upon the probing radiation.

Nevertheless, neutron diffraction work in molten salts gives rise to much new knowledge of the structure of these bodies; the only caveat is that it must be used in conjunction with other kinds of measurements; the data from these measurements are used to check on the structural concepts developed.

### 5.2.6. Simple Binary Molten Salts in the Light of the Results of X-ray and Neutron Diffraction Work

Table 5.11 contains typical results obtained from neutron diffraction, and the pair-correlation functions for $g_{Sr-Sr}(r)$, $g_{Sr-Cl}(r)$, and $g_{Cl-Cl}(r)$ are shown in Fig. 5.10.

[10]Channels on research reactors are let to research groups for a limited total time. The cost of even a small university teaching reactor ($10–20 million) is such that the amortization rate may be hundreds of dollars per hour.

[11]Such "volumes of nothingness" must be present to account for the large increase in volume upon fusion while at the same time the internuclear distance decreases (see Tables 5.9 and 5.10).

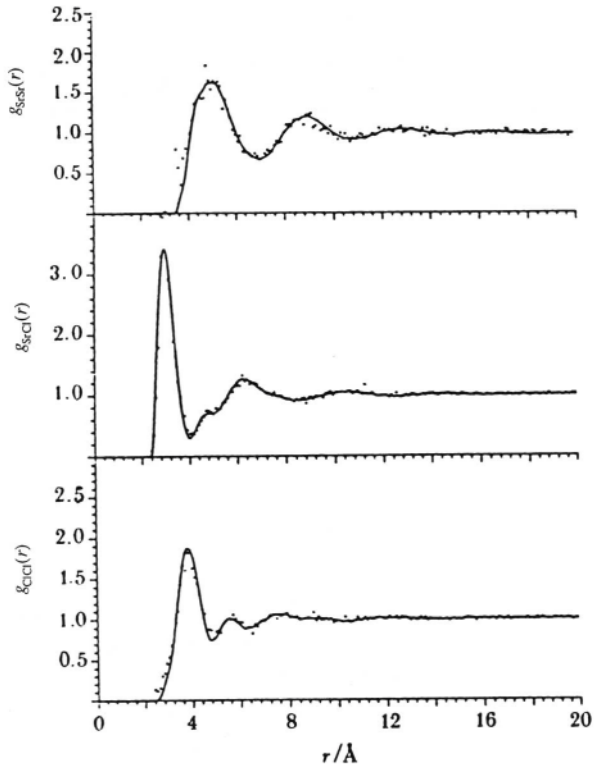


**Fig. 5.10.** Partial radial distribution functions for molten $SrCl_2$; solid line, experimental data; points, root mean cube fit. (Reprinted from R. L. McGreevy and L. Pusztai, *Proc. R. Soc. Lond. A* **430**: 241, 1990.)

Much neutron diffraction data of this kind are now available for molten salts. They are basic to structural knowledge of these pure electrolytes. However, the data do not play the same stellar role in determining the structure of liquid salts as they do for the solid salts because in the liquids the free space introduced on melting affects the dynamic movement of the ions and hence the liquid properties. In fact, this space is counterintuitive to the internuclear distances given by X-ray or neutron diffraction. The internuclear distances found in molten salts are smaller, not bigger, as might be thought from the increase in volume.

Data on simple molten salts can be interpreted without bringing in any orbital bond overlap; i.e., one can interpret the behavior of simple binary alkali halide molten salts in terms of ionic attraction and repulsion in a way similar to that used for the solid lattice. Molten salts containing complex anions—such as those consisting of $ZnCl_2$ and $AlCl_3$—need models that involve directed valence forces. Many results from different ways of modeling molten salts will be given in Section 5.2.8.

### 5.2.7. Molecular Dynamics Calculations of Molten Salt Structures

It has already been seen in Section 2.17 that computer simulation of structures in aqueous solution can give rise to calculations of some static (e.g., coordination numbers) and dynamic (e.g., diffusion coefficients) properties of ions in aqueous and nonaqueous solutions. One such computer approach is the Monte Carlo method. In this method, imaginary movements of the particles present are studied, but only those movements that *lower* the potential energy. Another technique is molecular dynamics. In this method, one takes a manageable number of atoms (only a few hundred because of the expense of the computer time) and works out their movements at femtosecond intervals by applying Newtonian mechanics to the particles under force laws in which it is imagined that only pairwise interactions count. The parameters needed to compute these movements numerically are obtained by assuming that the calculations are correct and that one needs to find the parameters that fit.

Now, these numerical simulation methods seem superior to the approaches that use alternative intuitive models. In the modeling approaches, one creates various imaginative hypotheses as to what the liquid salt might look like from inside it. Then, one calculates what one would expect from each intuited model in respect to its various properties, e.g., the diffusion coefficient. Models that predict nearest to the experimental result are taken as the best approximation to the real thing. In molecular dynamics calculations, on the other hand, one starts farther back by assuming a force law for interaction between the two kinds of particles present ( $K^+$ and $Cl^-$, say) and finding out by calculation what kind of arrangement among such particles is indicated by applying such laws to the particles' movements. In the end, which approach to apply—results of models or calculation of ionic movement—depends on which is cheaper.

Experimental determinations and bench-type research may continue for a generation or two, for both methods need experimental results as a standard to judge success. As the variety of available software grows and becomes more user friendly, the choice will move toward computer simulation.

Another factor that counts in the balance is the degree to which playing with a number of intuitive, imaginative models helps thinking new thoughts. Here one comes to the question of how knowledge will be advanced in the new century. Can computers imagine and create new ideas? Or must they always be supercalculating machines, using human-derived software that instructs the calculator to work out numerical equations written by intelligent beings? If the latter, is the intuitive perception of a number of alternative possible models more likely to enhance progress? Or will molecular dynamics simulation (computational chemistry) beckon on and spark the vital new fantasies from which new paradigms arise?

### 5.2.8. Modeling Molten Salts

Some typical radial distribution functions for molten salts (see Section 5.2.3.2) are shown in Fig. 5.11. Those plots are made by assuming pairwise interactions

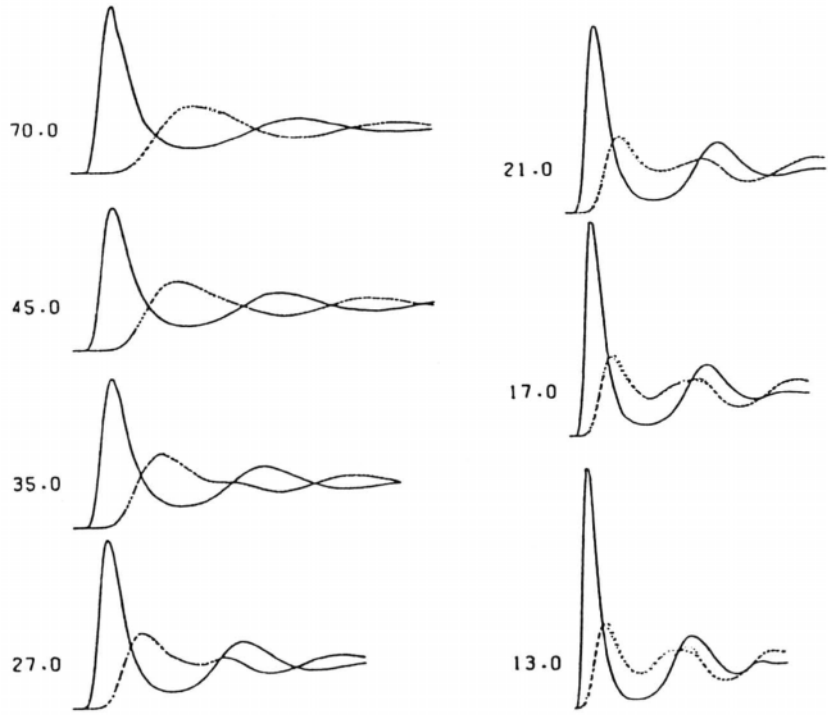


**Fig. 5.11**. Radial distribution functions of simulated KCl obtained by MC at $T = 1700$ K over a wide density range. The numbers are the molar volumes in $cm^3\ mol^{-1}$. The continuous line is $g_{+-}$, long dashes $g_{++}$, and short dashes $g_{--}$. (Reprinted from D. L. Price, M. L. Saboungi, W. S. Howells, and M. P. Tosi, *J. Electrochem. Soc.* **9**: 1, 1993.)

$$U_{ij} = \sum -\frac{e_i e_j}{r_{ij}} + \frac{B}{r_{ij}^{12}} \tag{5.9}$$

They naively assume that the *additivity* of such interactions (and nothing from ions outside the pairs) will allow a realistic calculation of physical properties.[12] However, a somewhat more mature view is to take into account the dipole moments induced among ions by nearest neighbors. Since this changes the ions' shapes (e.g., makes them spheroids and not spheres), the interaction equation usually assumed is not adequate.

[12]Why can patently wrong assumptions be made to give excellent agreement with experiment? Does the calibration of the parameters with experimental results in pairwise interaction equations introduce a degree of empiricism into computer simulation that suggests a lessened integrity in the calculation? Could pair potentials other than those used in Eq. (5.9) also give excellent results if their parameters were also calibrated on experimental data of a kind similar to that being calculated?

If the properties of one ion affect those of the other when they interact, an iterative approach has to be taken until constancy of intermolecular energy is obtained. This is because the dipoles induced in the ions exert counter fields upon the surrounding ions and the resulting change in shape modifies the values obtained for a system conceived as a sum of attractive and repulsive forces of unchanging spherical ions. If such a counter field can be calculated, then equations such as (5.9) can be used without the introduction of a dielectric constant in the Coulomb attractive term. Thus, dielectric constants are empirical devices that make an allowance for counter fields and forces in electrical systems.

## Further Reading

### *Seminal*

1. F. G. Edwards, J. E. Enderby, R. A. Howe, and D. I. Page, "Neutron Diffraction for Molten Salts," *J. Phys. Chem.* **8**: 3483 (1975).
2. J. Enderby, "The Structure of Molten Salts," *NATO ASI Series C* **202**: 1 (1987).
3. R. L. McGreevy and M. A. Howe, "Structure of Molten Salts," *J. Phys. Condens. Matt.* **1**: 9957 (1989).
4. R. L. McGreevy, "New Methods for Molten Electrolytes," *Nuovo Cimento* **12D**: 685 (1990).

### *Review*

1. B. Guillot and Y. Guissani, "Towards a Theory of Coexistence and Criticality in Real Molten Salts," *Mol. Phys.* **87**: 37 (1996).

### *Papers*

1. T. Kozlowski, *Int. J. Phys. Chem.* **100**: 95 (1996).
2. J. Ohno, A. C. Barnes, and J. E. Enderby, *J. Phys. Condens. Matt.* **8**: 3785 (1996).
3. Z. Akdeniz, G. Pastore, and H. P. Tosi, *Phys. Chem. Liq.* **32**: 191 (1996).
4. T. Koslowski, *Ber. Bunsen-Ges. Phys. Chem., Int. J. Phys. Chem.* **100**: 95 (1996).
5. L. Mouron, G. Roullet, J. J. Legendre, and G. Picard, *Computational Chemistry* **20**: 227 (1996).

## 5.3 MONTE CARLO SIMULATION OF MOLTEN POTASSIUM CHLORIDE

### 5.3.1. Introduction

The general principle behind a Monte Carlo procedure has already been described (Section 2.3.2). Woodcock and Singer were the first to make such a calculation for molten salts, and their work is the source of the following section.

In all simulations in which the interaction involves Coulomb's law, there is a difficulty in the extent to which the Coulombic terms can be summed because the number of particles used in the ensemble being considered (e.g., 216 in Woodcock and Singer's case) is too small. Thus, the Coulombic forces (which decline slowly with increasing distance) have not yet become negligible outside the "package." Some way of terminating them without spoiling the calculation had to be found. A solution to this problem, and the one that Woodcock and Singer used, is due to Ewald and lies in a purely mathematical technique by which one nonconverging series is converted into two converging series. One must bear with simplification here; a more quantitative description of Ewald's artifices would take precious space without significantly increasing the reader's comprehension of how ionic liquids work.

### 5.3.2. Woodcock and Singer's Model

Woodcock and Singer followed up on some considerations published earlier by Tosi and Fumi. The latter suggested that the potential that forms a suitable basis for the calculation of the pairwise addition potentials in a molten salt is suitably written as

$$U_{i,j(+)} = -\frac{z_i z_j e_0^2}{r_{i,j}} + b \exp B(\sigma_{i,j} - r) + \frac{c_{i,j}}{r^6} + \frac{d_{i,j}}{r^8} \tag{5.10}$$

This equation was first used by Born, Huggins, and Meyer and therefore bears their names. The first two terms represent, respectively, the attractive and repulsive potentials. The last two terms represent dipole-dipole and dipole-quadrupole potentials, respectively. In spite of allowing for the dipole interactions, the calculation is still a hard-sphere one, a mean spherical approximation, because the forces are not allowed to change the shape and the position of the particles. Later on, Saboungi et al.

**TABLE 5.12**

**Parameters Used in Eq. (5.10) for KCl**

| $\nu_{ij}$[a] ($cm^{-8}$) | $b$[b] ($10^{-12}$ erg) | $B$[c] ($10^{8}$ $cm^{-1}$) | $c_{i,j}$[d] ($10^{-60}$ erg $cm^{6}$) | $d_{i,j}$[d] ($10^{-76}$ erg $cm^{8}$) |
|---|---|---|---|---|
| ++2.926 | 0.423 | 2.97 | −24.3 | −24.0 |
| +−3.048 | 0.338 | 2.97 | −48.0 | −73.0 |
| −−3.170 | 0.253 | 2.97 | −124.5 | −250.0 |

Source: Reprinted from L. V. Woodcock and K. Singer, *Trans. Faraday Soc.* **67**: 12, 1971.
[a] Sum of ionic radii.
[b] Same value for all alkali halides.
[c] A common value for the three ion pairs in the salt.
[d] Calculated from spectroscopic data.

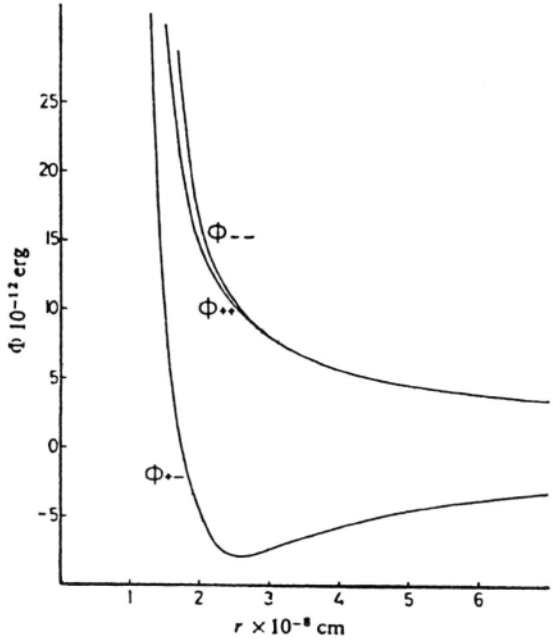


**Fig. 5.12.** Pair potentials for potassium chloride. (Reprinted from L. V. Woodcock and K. Singer, *Trans. Faraday Soc.* **67**:12, 1971.)

did take into account a mutual squeezing of the ions, and some of the work of this team will be described later.

The various parameters needed in these equations come from other work and are given in Table 5.12, taken from Woodcock and Singer. The pairwise potential for potassium chloride, first calculated by Tosi and Fumi in 1964, is reproduced in Fig. 5.12. Typical computational data for an MC calculation are given in Table 5.13. The software of the day generated only 80,000 steps per hour.

### 5.3.3. Results First Computed by Woodcock and Singer

Changes of volume upon fusion together with compressibilities, expansivities, and specific heats calculated by Woodcock and Singer are shown in Table 5.14. What is the uncertainty in these calculations? It is around $\pm 0.5$ cm$^3$ mol$^{-1}$ and within this error the agreement of simulated and experimental results is rather good. Thus, at 1045 K for the volumes

$$V = 41.48 \text{ cm}^3 \text{ mol}^{-1}, \text{ solid: } V_f^+ = 0.68 \pm 0.03, V_f^- = 0.73 \pm 0.04,$$

$$V = 51.24 \text{ cm}^3 \text{ mol}^{-1}, \text{ liquid: } V_f^+ = 1.14 \pm 0.06, V_f^- = 1.13 \pm 0.06.$$

**TABLE 5.13**
**Computational Data**

| Run | $V$ ($cm^3\ mol^{-1}$) | $T$ (K) | State | $\lambda/N$ | $100A/\lambda$ | $\Delta\phi$ ($10^3$ J $mol^{-1}$) | $\Delta p$ ($10^3$ bar) |
|---|---|---|---|---|---|---|---|
| 1 | 41.48 | 1045 | Solid | 741 | 32.2 | 0.15 | 0.08 |
| 2 | 42.70 | 1045 | Solid | 1481 | 33.4 | 0.15 | 0.05 |
| 3 | 43.92 | 1045 | Solid | 1296 | 35.0 | 0.40 | 0.11 |
| 4 | 48.80 | 1045 | Solid | 1296 | 38.2 | 0.20 | 0.11 |
| 5 | 46.36 | 1045 | Liquid | 1296 | 32.9 | 0.20 | 0.17 |
| 6 | 48.80 | 1045 | Liquid | 1852 | 33.7 | 0.25 | 0.19 |
| 7 | 51.24 | 1045 | Liquid | 1667 | 35.1 | 0.25 | 0.21 |
| 8 | 53.68 | 1045 | Liquid | 1667 | 36.5 | 0.20 | 0.11 |
| 9 | 58.56 | 1045 | Liquid | 1481 | 36.9 | 0.15 | 0.07 |
| 10 | 48.80 | 1306 | Liquid | 1852 | 38.7 | 0.25 | 0.20 |
| 11 | 51.24 | 1306 | Liquid | 1481 | 39.5 | 0.20 | 0.13 |
| 12 | 53.68 | 1306 | Liquid | 1667 | 40.8 | 0.20 | 0.17 |
| 13 | 54.66 | 1306 | Liquid | 2407 | 40.7 | 0.10 | 0.07 |
| 14 | 58.56 | 1306 | Liquid | 1667 | 41.0 | 0.35 | 0.18 |
| 15 | 63.44 | 1306 | Liquid | 1667 | 43.4 | 0.30 | 0.10 |
| 16 | 58.56 | 2090 | Liquid | 1296 | 50.8 | 0.55 | 0.22 |
| 17 | 63.44 | 2090 | Liquid | 1296 | 51.8 | 0.25 | 0.19 |
| 18 | 68.32 | 2090 | Liquid | 1667 | 53.7 | 0.20 | 0.15 |
| 19 | 73.20 | 2090 | Liquid | 1667 | 54.2 | 0.35 | 0.16 |
| 20 | 85.40 | 2090 | Liquid | 1481 | 54.6 | 0.40 | 0.14 |
| 21 | 63.44 | 2874 | Liquid | 926 | 57.9 | 0.20 | 0.13 |
| 22 | 72.30 | 2874 | Liquid | 1667 | 60.1 | 0.25 | 0.15 |
| 23 | 85.40 | 2874 | Liquid | 1667 | 60.9 | 0.45 | 0.15 |
| 24 | 97.60 | 2874 | Liquid | 1667 | 61.7 | 0.40 | 0.12 |

Source: Reprinted from V. Woodcock and K. Singer, *Trans Faraday Soc.* **67**: 12, 1971.

Radial distribution functions are characterized by the distance of closest approach $d$, the position $r^{max}$ and height $h$ of the main peak, the position $r^{min}$ of the minimum following the main peaks, and the coordination numbers $CN$, defined by

$$(CN)_m = (N-1)V^{-1}4\pi \int_0^{r_m^{min}} r^2 g_m(r)\, dr \tag{5.11}$$

$$(CN)_u = 1/2NV^{-1}4\pi \int_0^{r_u^{min}} r^2 g_u(r)\, dr \tag{5.12}$$

**TABLE 5.14**

**Changes in Fusion for KCl ($T_{m.p.}$ = 1045 K)**

| | Solid | Liquid | $\Delta_{MC}$ | $\Delta_{expt.}$ | % Changes (MC) |
|---|---|---|---|---|---|
| $<\phi^{DD}+\phi^{DQ}>$ $10^{3+}$ J mol$^{-1}$ | −30.4 | −25.9 | 4.5 | | −14.8 |
| $V$, cm$^3$ mol$^{-1}$ | 41.75 | 50.20 | 8.45 | 8.3<br>9.09<br>7.23 | 20.2 |
| $\kappa_T$, $10^{-6}$ bar$^{-1}$ | 10.1 | 36.1 | 26.0 | | 257 |
| $\alpha_p$, $10^{-4}$ K$^{-1}$ | 1.97 | 3.33 | 1.96 | | 99.5 |
| $\beta_v'$, bar K$^{-1}$ | 19.4 | 9.23 | −10.2 | | −52.4 |
| $C_v$, J K$^{-1}$ mol$^{-1}$ | 48.4 | 50.5 | 2.1 | | 4.3 |
| $C_p$, J K$^{-1}$ mol$^{-1}$ | 65.3 | 66.8 | 1.5 | 9.2<br>3.5 | 2.4 |

Source: Reprinted from L. V. Woodcock and K. Singer, *Trans. Faraday Soc.* **67**: 12, 1971.

$$(CN)_l = (1/2N - 1)V^{-1}4\pi \int_0^{r_l^{\min}} r^2 g_l(r)\, dr \tag{5.13}$$

On fusion, Woodcock and Singer's calculation found that the coordination number for molten KC1 decreases from 5.3 to 4 in accordance with experiment. The distance of closest approach rather unexpectedly decreases as the temperature increases, while the first peak (Fig. 5.13) becomes broader and lower (less order even in the first shell).

Bockris and Richards' experimental value of the free volume for KC1 ($V_f = 0.68$ cm$^3$ mol$^{-1}$) agrees well with that of Woodcock and Singer. The volume change on melting obtained experimentally, however, is 8.2 cm$^3$ mol$^{-1}$)which is only 3% less than the entirely acceptable calculated value obtained by Woodcock and Singer's Monte Carlo simulation. Their actual model for liquid KC1 is shown in Fig. 5.14 and appears to contain "hole volume" corresponding to modelistic concepts which feature this property (Section 5.5.1).

### 5.3.4. A Molecular Dynamics Study of Complexing

Saboungi et al. have carried out molecular dynamics studies in the 1990s that are a great improvement on those done in the pioneering Woodcock and Singer studies. They studied, for example, complexes between NaCl and $AlCl_3$ by means of a molecular dynamics program. These systems are well known from experimental work to form $AlCl_4^-$ and other, higher complex ions, such as $Al_2Cl_7^-$.

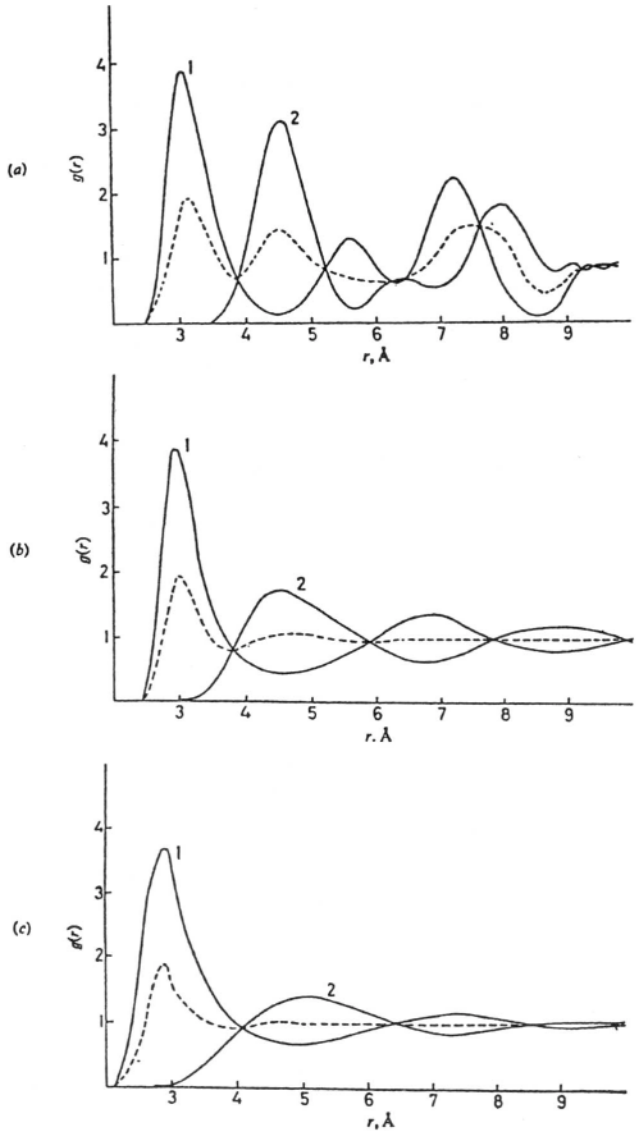


**Fig. 5.13.** Radial distribution functions for KCl. (a) Solid, $T$ = 1045 K, $V$ = 41.48 cm$^3$ mol$^{-1}$; 1, $g_u(r)$; 2, $g_1(r)$; ---, $g_e(r)$; (b) liquid, $T$ = 1045 K, $V$ = 48.80 cm$^3$ mol$^{-1}$; 1, $g_u(r)$; 2, $g_1(r)$; ---, $g_m(r)$; (c) liquid, $T$ = 2874 K, $V$ = 97.60 cm$^3$ mol$^{-1}$; 1, $g_u(r)$; 2, $g_1(r)$; ---, $g_m(r)$. (Reprinted from L. V. Woodcock and K. Singer, *Trans. Faraday Soc.* **67**: 12, 1971.)

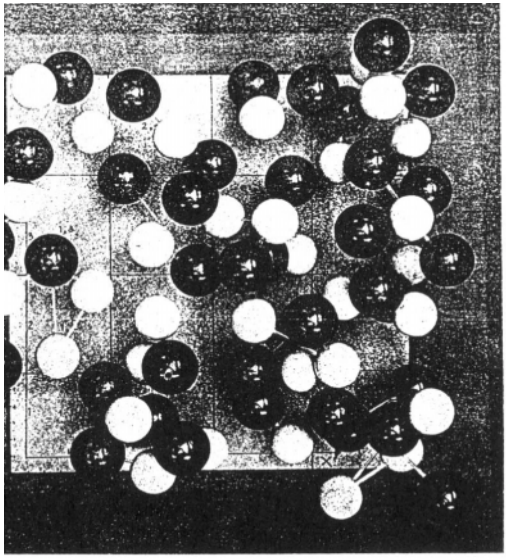

**Fig. 5.14.** Woodcock and Singer's representation of liquid KCl, the dark spheres representing chloride ions and white spheres representing potassium ions. (Reprinted from L. V. Woodcock and K. Singer, *Trans. Faraday Soc.* **67**: 12, 1971.)

In the molecular dynamics approaches to such systems, one of the principal novelties compared with the work on simpler systems such as KCl (Section 5.3.3) is the taking into account of anion polarizability, i.e., elimination of the hard-sphere approximation. Anions are by and large more polarizable than cations. The polarizability $\alpha$ is proportional to $r_i^3$. The radii of cations, formed by losing an outer electron, are smaller than those of the anions, which are formed by adding an electron. Hence, anions are mainly the ions affected when polarizability is to be accounted for.

When an anion feels the field of a cation $X$, a dipole moment is induced into the anion,

$$\mu_i = \alpha X \tag{5.14}$$

and this induced dipole moment will give rise to an additional energy of attraction between the monopole and the dipole (*cf.* the corresponding effect in the theory of hydration energy in Section 2.4.3). In addition, there will be dipole–dipole interactions.

The calculations of Saboungi et al. on these $NaCl\text{-}AlCl_3$ systems do not lack complexity. There are as many as ten terms of interaction. Thus,

$$U = u_{MM} + u_{MA} + u_{MX} + u_{AA} + u_{AX} + u_{XX^-} + u_{ddxx} + u_{mdmx} + u_{mdax} + u_{mdxx^+} \tag{5.15}$$

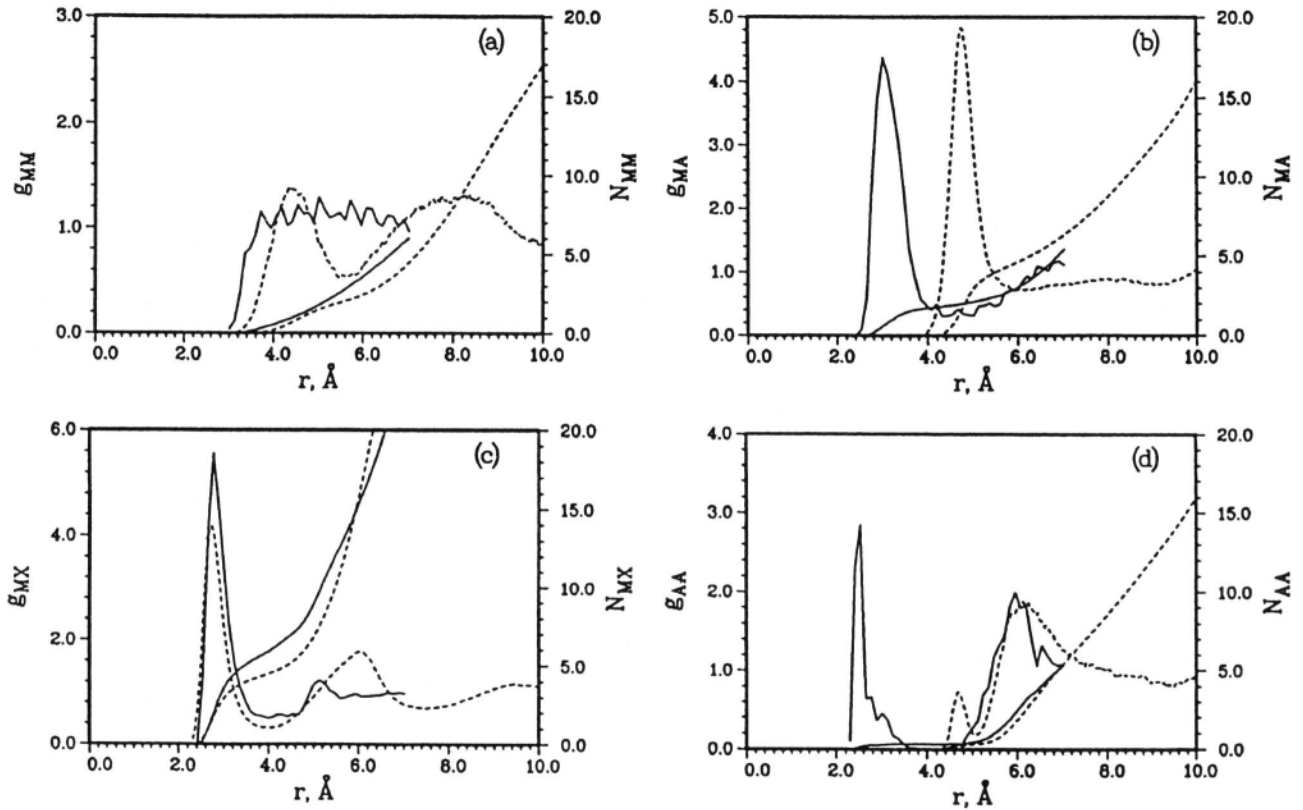


**Fig. 5.15.** Radial distribution functions $g_{ij}(r)$ and the radial dependence of the average coordination numbers $N_{ij}(r)$ for the molecule $MAX_4$. (Reprinted from M. L. Saboungi, D. L. Price, C. Scamehorn, and M. Tosi, *Europhys. Lett.* **15**: 281, 1991.)

Here, the first six terms refer to pair potential energies of interaction and the last four terms represent dipole–dipole or monopole–dipole interaction energies.

Taking the anion as polarizable not only introduces these last terms but also reduces the repulsive energies used compared with those of earlier calculations that took a "hard" anion according to the mean spherical approximation. By "hard" anion is meant one that doesn't respond to being squeezed, i.e., is not polarizable.

What do the calculated distribution coefficients look like? They are shown in Fig. 5.15. The positions of the first peaks show that the $Al^{3+}$ cations are largely coordinated with $Cl^-$ as $AlCl_4^-$. On the other hand, the parameter $b$ in the repulsive potential [see Eq. (5.10)] was given values so that the calculations would indeed show up $AlCl_4^-$ ions, so their appearance is not something that fills one with awe. According to the calculations, these anions are present to the extent of 92%. The empirically enlightened calculations show that there is some indication of doubly bridged A1-A1 pairs and these are assigned to $Al_2Cl_6$ molecules present in the melt (see Fig. 5.16). These molecular dynamics calculations (however much aided by information from prior experiments) allow many properties (e.g., the angles in entities such as NaAlCl) to be calculated (Fig. 5.16).

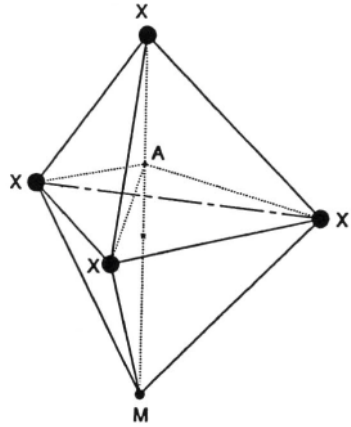


**Fig. 5.16.** Geometric relationship between $M^+$ and $AX_4^-$ tetrahedron. The $M^+$ cation sits perpendicular to the center of a face of the tetrahedron. Consequently, one M-A-X triplet exists at 180° for every three triplets at 64°. (Reprinted from M. L. Saboungi, D. L. Price, C. Scamehorn, and M. Tosi, *Europhys. Lett.* **15**: 281, 1991.)

Calculations taking into account the anion polarizability in $AlCl_4^-$ reduce the approximation associated with the simple additivity of pairwise potentials in computational modeling (hard-sphere approximation) of molten salts. They predict new entities (e.g., $Al_2Cl_6$) and in this respect have an advantage over earlier calculations.

## Further Reading

### *Seminal*


1. N. Metropolis, A. W. Rosenblath, M. W. Rosenblath, A. H. Teller, and E. J. Teller, "The Monte Carlo Method," *J. Chem. Phys.* **21**: 1087 (1953).
2. J. O'M. Bockris, A. Pilla, and J. L. Barton, "Change of Volume in the Fusion of Salts," *J. Phys. Chem.* **64**: 507 (1960).
3. M. P. Tosi and G. Fermi, "Computer Simulation Methods for Liquid Salts," *J. Phys. Chem. Solids* **25**: 31 (1964).
4. V. Woodcock and K. Singer, "Computer Simulation for Liquid KCl," *Trans. Faraday Soc.* **67**: 12(1971).


### *Reviews*


1. M. P. Allen and D. Tilderley, *Computer Simulation of Liquids,* Clarendon Press, Oxford (1986).
2. J. E. Enderby, in *The Structure of Molten Salts*, G. Mamantov and R. Marassi, eds., *NATO ASI Science Series*, *Series C* **202**: 2 (1988).


## Papers


1. H. T. J. Reijer and W. Van der Lugt, *Phys. Rev. B* **42**: 3395 (1990).
2. R. L. McGreevy and L. Pusztai, *Proc. Roy. Soc. Lond.* **A430:** 241 (1990).
3. M. L. Saboungi, D. L. Price, C. Scamehorn, and M. Tosi, *Europhys. Lett.* **15**: 281 (1991).
4. Z. Acadeniz and M. P. Tosi, *Proc. Roy. Soc. Lond.* **A437**: 75 (1992).
5. S. Itoh, I. Okada, and K. Takahashi, *Electrochemical Society, Molten Salts*, **92-16**: 88 (1992).
6. L. A. Curtiss, *Electrochemical Society, Molten Salts*, **93-9**: 30 (1993).


## 5.4. VARIOUS MODELING APPROACHES TO DERIVING CONCEPTUAL STRUCTURES FOR MOLTEN SALTS

### 5.4.1. The Hole Model: A Fused Salt Is Represented as Full of Holes as a Swiss Cheese

One of the models that can be used to approximately predict the properties of molten salts is called the *hole model.* The outstanding fact that led to this model is the large volume of fusion (10–20%) exhibited by simple salts on melting (Fig. 5.17). The basic idea of this rather artificial model is that within the liquid salt are tiny volume

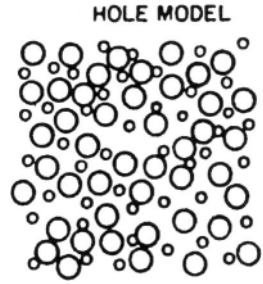


**Fig. 5.17.** The hole model with randomly located and variable-sized holes in the liquid.

elements, varying in size from the subatomic to about six ions, which are empty and constantly fluctuating in size. Such a model is a kind of liberation from the lattice concepts appropriate to solids and leads to equations that can explain liquid properties, some of them with reasonable numerical accuracy and without any of those "calibrating factors" that make the computer simulation approaches always agree with experiment.

How are the alleged holes in the molten salt produced? They are formed by a process analogous to the formation of a vacancy in a crystal, but in a less ordered fashion. The displacement of an ion from a lattice site in a solid produces a vacancy at its former site. In the case of the vacancy in a solid, however, the ion is removed so far from the original site that the displaced ion can be forgotten altogether. Suppose instead that at high temperatures in the course of thermal motion some of the ions constituting a cluster are displaced relative to each other but only by small amounts. Then a "hole" is produced between them (Fig. 5.18). Its size must vary in a random manner because the thermal motions that produce it are random. Further, since thermal motions occur everywhere in the liquid electrolyte, holes appear and disappear anywhere in this liquid. If one were able to label the holes with scintillating material and enlarge the signals so one could see them, the molten salt would look like a set of twinkling light sources, going on and off all over the melt.

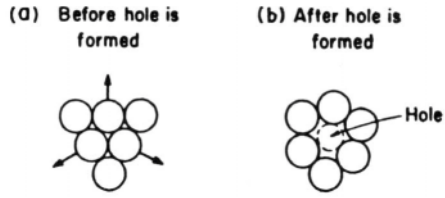


**Fig. 5.18.** The formation of a hole in a liquid by the relative displacement of ions in contact.

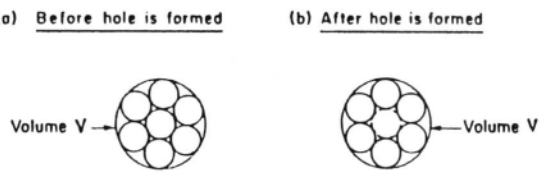


**Fig. 5.19.** The formation of a hole can also be looked at in terms of the number of ions occupying a volume *V*. In (a) seven particles occupy the volume *V* before the hole is formed, and, in (b), six particles occupy the same volume after hole formation.

If a liquid electrolyte (Fig. 5.19) could be sliced up and subjected to nanometer-scale photography with an exposure time of around $10^{-11}$ s, the photos would resemble those of cuts through a Swiss cheese. This is why, in the matter of randomness of size and location, the hole theory of liquids has been referred to in homely terms as the "Swiss cheese model." What the cheese represents, however, is the time-averaged picture of the holes. In the model, holes are continuously forming and disappearing, moving, coalescing to form larger holes, and diminishing into smaller ones.

Although this model of a liquid was suggested independently of the results obtained from computer modeling, the imagined picture of the hole model in Fig. 5.17 closely resembles the picture (Fig 5.14) from Woodcock and Singer's model derived from the Monte Carlo approach.

## 5.5. QUANTIFICATION OF THE HOLE MODEL FOR LIQUID ELECTROLYTES

### 5.5.1. An Expression for the Probability That a Hole Has a Radius between *r* and *r* + *dr*

To quantify the hole model, it is necessary to calculate a distribution function for the hole sizes. This is a plot of the number of holes per unit volume as a function of their size. As a first step toward this calculation, one can consider a particular hole in a liquid electrolyte and ask: What are the quantities (or variables) needed to describe this hole? This problem can be resolved by means of a formulation first published by Fürth in 1941.

Since a hole in a liquid can move about like an ion or other particle, the dynamic state of a hole is specified in the same way that one describes the dynamic state of a material particle. Thus, one must specify three position and three momentum coordinates: $x, y, z$ and $p_x, p_y, p_z$. There is, however, an extra feature of the motion of a hole that is not possessed by material particles. This feature concerns what is called its *breathing motion* (Fig. 5.20), i.e., the contraction and expansion of the hole as its size

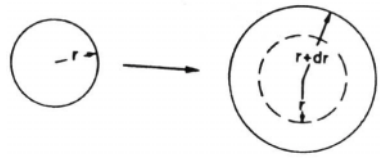


**Fig. 5.20.** The breathing motion of a hole involves its radial expansion.

fluctuates in the liquid. To characterize this breathing motion, it is sufficient to specify the hole radius $r$ and the radial momentum $p_r$ corresponding to the breathing motion. To characterize a hole completely, it is necessary to specify eight quantities: $x$, $y$, $z$, $p_x$, $p_y$, $p_z$, $r$, and $p_r$, whereas the first six only are adequate to describe the state of motion of a particle.

According to the normal equations of classical statistical mechanics, which are used to express velocities and momenta distributed in three dimensions, the probability $P_r$ that the location of a hole is between $x$ and $x + dx$, $y$ and $y + dy$, $z$ and $z + dz$; that its translational momenta lie between $p_x$ and $p_x + dp_x$, $p_y$ and $p_y + dp_y$, $p_z$ and $p_z + dp_z$; that its breathing momentum is between $p_r$ and $p_r + dp_r$; and, finally, that its radius is between $r$ and $r + dr$, is proportional to the Boltzmann probability factor,

$$P_r\,dx\,dy\,dz\,dp_x\,dp_y\,dp_z\,dp_r\,dr \propto e^{-E/kT} \times dx\,dy\,dz\,dp_x\,dp_y\,dp_z\,dp_r\,dr \qquad (5.16)$$

where $E$ is the total energy of the hole.

Since the desired distribution function only concerns the radii (or sizes) of holes, it is sufficient to have the probability that the hole radius is between $r$ and $r + dr$ irrespective of the location and the translational and breathing momentum of the hole. This probability $P_r\,dr$ of the hole's radius being between $r$ and $r + dr$ is obtained from Eq. (5.16) by integrating over all possible values of the location, and of the translational and breathing momentum of the hole, i.e.,

$$P_r\,dr \propto \left(\int\int\int\int\int\int\int e^{-E/kT} \times dp_x\,dp_y\,dp_z\,dp_r\,dx\,dy\,dz\right)dr \qquad (5.17)$$

However, the total energy of the hole on average does not depend upon its position; i.e., $E$ is independent of $x$, $y$, and $z$. Hence,

$$P_r\,dr \propto \left(\int\int\int\int e^{-E/kT} \times dp_x\,dp_y\,dp_z\,dp_r\right)\left(\int\int\int dx\,dy\,dz\right)dr \qquad (5.18)$$

Furthermore,

$$\int\int\int dx\,dy\,dz = V \qquad (5.19)$$

the volume of the liquid. Thus, by incorporating this $V$ into the proportionality constant implicitly associated with Eq. (5.18), one has

$$P_r dr \propto (\int\int\int\int e^{-E/kT} \times dp_x\, dp_y\, dp_z\, dp_r) dr \tag{5.20}$$

Now the total energy $E$ consists of the potential energy $W$ of the hole (i.e., the work required to form the hole) plus its kinetic energy. This kinetic energy is given by

$$\frac{p_x^2}{2m_1} + \frac{p_y^2}{2m_1} + \frac{p_z^2}{2m_1} + \frac{p_r^2}{2m_2} \tag{5.21}$$

where $m_1$ is the apparent mass[13] of the hole in its translational motions and $m_2$ is the apparent mass in its breathing motion. Hence,

$$E = W + \frac{p_x^2}{2m_1} + \frac{p_y^2}{2m_1} + \frac{p_z^2}{2m_1} + \frac{p_r^2}{2m_2} \tag{5.22}$$

Inserting this value of $E$ into the expression (5.20) for the probability of the hole's having a radius between $r$ and $r + dr$, one has

$$P_r\, dr \propto dr\, e^{-W/kT} \int_{-\infty}^{\infty} e^{-p_x^2/2m_1 kT} dp_x \int_{-\infty}^{\infty} e^{-p_y^2/2m_1 kT} dp_y \int_{-\infty}^{\infty} e^{-p_z^2/2m_1 kT} dp_z \int_{-\infty}^{\infty} e^{-p_r^2/2m_2 kT} dp_r \tag{5.23}$$

From the standard integral,

$$\int_{-\infty}^{\infty} e^{-ax^2} dx = \sqrt{\frac{\pi}{a}} \tag{5.24}$$

it is clear that

$$\int_{-\infty}^{\infty} e^{-p_x^2/2m_1 kT} dp_x = \int_{-\infty}^{\infty} e^{-p_y^2/2m_1 kT} dp_y = \int_{-\infty}^{\infty} e^{-p_z^2/2m_1 kT} dp_z = (2\pi m_1 kT)^{1/2} \tag{5.25}$$

[13] Any entity that moves displays the property of inertia, i.e., resistance to a change in its state of rest or uniform motion. That is, the entity has a mass. If the entity is not material (a hole is a region where in fact there is no material), one refers to an apparent mass. Holes in semiconductors have apparent masses like holes in liquids. The inertia of the hole arises as a result of the displacement of the liquid around the hole as it moves, which gives rise to dissipation of energy (Appendix 5.1).

and

$$\int_{-\infty}^{\infty} e^{-p_r^2/2m_2kT} dp_r = (2\pi m_2 kT)^{1/2} \tag{5.26}$$

By using these values of the integrals in Eq. (5.23), the result is

$$P_r\, dr \propto (2\pi kT)^2 m_1^{3/2} m_2^{1/2} e^{-W/kT} dr \tag{5.27}$$

It can be shown, however (see Appendix 5.1), that

$$m_1 = \frac{2}{3}\pi r^3 \rho \tag{5.28}$$

and

$$m_2 = 4\pi r^3 \rho \tag{5.29}$$

After taking all the quantities that are radius independent into the proportionality constant A, one has by combining Eqs. (5.27), (5.28), and (5.29) that

$$P_r\, dr = A r^6 e^{-W/kT}\, dr \tag{5.30}$$

The evaluation of the constant is achieved through the following plausible argument. The probability that a hole has some radius must be unity (i.e., is certain by definition). Equation (5.30) expresses the probability of the radius of the hole lying between $r$ and $r + dr$. Similarly, one can write down the probabilities of the radius' being between $r_1$ and $r_1 + dr$, between $r_2$ and $r_2 + dr$, etc. If all these probabilities for $r$ from zero to infinity are summed up (or integrated), then the sum must be unity, i.e.,

$$\int_0^{\infty} P_r\, d_r = \int_0^{\infty} A r^6 e^{-W/kT}\, dr \tag{5.31}$$

However, to carry out this integration, one must know whether the work of hole formation $W$ is a function of $r$; i.e., one must understand what determines the work of formation (or the potential energy) of a hole of radius $r$ (Fig. 5.21).

### 5.5.2. An Ingenious Approach to Determine the Work of Forming a Void of Any Size in a Liquid

A remarkably simple way of calculating the work of hole formation was found by Fürth, who treated holes in liquids, the sizes of which are thermally distributed, in an article published in the *Proceedings of the Cambridge Philosophical Society.* This is an erudite university journal whose readers are mainly members of the university's

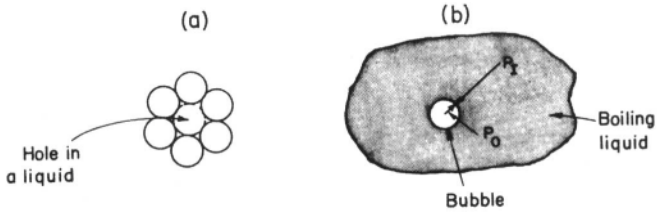


**Fig. 5.21.** The basis of the hole model of Fürth is the analogy between (a) a hole in a liquid and (b) a bubble in a liquid. An inward pressure $P_I$ and an outward pressure $P_O$ act on the bubble surface.

colleges, and this conservative choice of publication medium delayed recognition of the virtues of the model from 1941 until the 1970s, well after Monte Carlo calculations had begun. In Fürth's model, a hole in a fused salt is considered to simulate a bubble in a liquid (Fig. 5.21). The surrounding liquid exerts a hydrostatic pressure $P_I$ on the bubble surface. Inside the bubble, however, there is vapor, which exerts an outward pressure $P_O$ on the surface. The net pressure is therefore $P_I - P_O$. Furthermore, surface tension operates in the direction of reducing the surface area and therefore the surface energy of the bubble.

The total work required to increase the bubble size consists of two parts, the volume work $(P_I - P_O)V_H$ and the surface work $\gamma A$, where $P_I - P_O$, $V_O$, $\gamma$, and $A$ are the net pressure on the bubble surface, the increase of volume, the surface tension, and the increase of surface area of the bubble, respectively. Thus, the work done in making a bubble grow to a size having a radius $r$ is

$$W = (P_I - P_O)\frac{4}{3}\pi r^3 + 4\pi r^2\gamma \tag{5.32}$$

The first term, i.e., the volume term, is negligible compared to the second or surface term for bubbles of less than about $10^{-5}$ cm in diameter. The work of bubble formation reduces to

$$W = 4\pi r^2\gamma \tag{5.33}$$

This expression can also be obtained from the general equation (5.32) by setting $P_I = P_O$. This equality between $P_I$ and $P_O$ represents the condition that the liquid is boiling. The analogy between a hole and a bubble consists therefore in assuming that the work of hole formation is given by the expression for the work of bubble formation in a liquid. Let the ability of the model to replicate experimental results be the criterion of the acceptability of Eq. (5.33).

### 5.5.3. The Distribution Function for the Sizes of the Holes in a Liquid Electrolyte

Now that an expression for the work of hole formation has been obtained, it can be inserted into Eq. (5.31), which must be integrated to evaluate the constant $A$. One has

$$\int_0^\infty P_r\, dr = 1 = \int_0^\infty A r^6 e^{-ar^2} dr \tag{5.34}$$

where

$$a = \frac{4\pi\gamma}{kT} \tag{5.35}$$

To carry out the integration, the following standard formula is used

$$\int_0^\infty r^{2n} e^{-ar^2} dr = \frac{1 \times 3 \times 5 \ldots (2n-1)}{2^{n+1} a^n} \sqrt{\frac{\pi}{a}} \tag{5.36}$$

where $n$ is a positive integer. The integral in Eq. (5.34) is consistent with the standard formula if one substitutes $n = 3$, and therefore,

$$\int_0^\infty P_r dr = 1 = A \int_0^\infty r^{2\times 3} e^{-ar^2} dr = A \frac{1 \times 3 \times 5}{2^4 a^3} \frac{\pi^{1/2}}{a^{1/2}} = A \frac{15\pi^{1/2}}{16} \frac{1}{a^{7/2}} \tag{5.37}$$

The constant in Eq (5.34) is given by

$$A = \frac{16}{15\pi^{1/2}} a^{7/2} = \frac{16}{15\pi^{1/2}} \left(\frac{4\pi\gamma}{kT}\right)^{7/2} \tag{5.38}$$

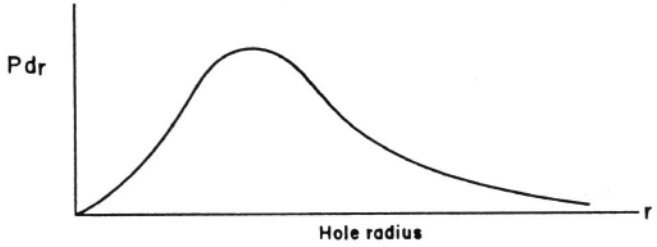


**Fig. 5.22.** How the probability $P_r\, dr$ that a hole has a radius between $r$ and $r +$ dr varies with $r$.

and the expression (5.30) for the probability of the existence of a hole of a radius between $r$ and $r + dr$ becomes

$$P_r\,dr = \frac{16}{15\pi^{1/2}}\,a^{7/2}r^6e^{-ar^2}\,dr \tag{5.39}$$

This is the distribution function which was said to be the goal at the beginning of Eq. (5.17). From it, the average hole volume and radius will shortly be seen to be obtainable (see Fig. 5.22).

### 5.5.4. What Is the Average Size of a Hole in the Fürth Model?

The average radius $\langle r\rangle$ of a hole can be obtained from Eq. (5.39) by multiplying the probability of the hole radius being between $r$ and $r + dr$ by the radius of the hole and integrating this product over all possible values of $r$. This is the general method of obtaining average values of a quantity of which the probability is known. Thus, the average hole radius is

$$\langle r\rangle = \int_0^\infty rP_r\,dr = \int_0^\infty r\,\frac{16}{15\pi^{1/2}}\,a^{7/2}r^6e^{-ar^2}\,dr = \frac{16}{15\pi^{1/2}}\,a^{7/2}\int_0^\infty r^7e^{-ar^2}\,dr \tag{5.40}$$

The integral in Eq. (5.40) can be evaluated by using the substitution $t = ar^2$,

$$\int_0^\infty r^7e^{-ar^2}\,dr \quad \underset{t^3/a^3 = r^6}{\overset{t = ar^2,\ dt/2a = r\,dr}{\longrightarrow}} \quad \frac{1}{2a^4}\int_0^\infty t^3e^{-t}\,dt \tag{5.41}$$

which leads to

$$\langle r\rangle = \frac{8}{15\pi^{1/2}}\,\frac{1}{a^{1/2}}\int_0^\infty t^3e^{-t}\,dt \tag{5.42}$$

The integral $\int_0^\infty t^3e^{-t}\,dt$ is the gamma function $\Gamma(3 + 1)$ (Appendix 5.2) and is equal to 3! from

$$\Gamma(x + 1) = \int_0^\infty t^xe^{-t}\,dt = x! \tag{5.43}$$

Hence, Eq. (5.42) becomes

$$\langle r\rangle = \frac{8}{15\pi^{1/2}}\left(\frac{kT}{\gamma}\right)^{1/2}\frac{1}{(4\pi)^{1/2}} \times 3 \times 2 \times 1$$

$$= \frac{8}{5\pi}\left(\frac{kT}{\gamma}\right)^{1/2}$$

$$= 0.51\left(\frac{kT}{\gamma}\right)^{1/2} \tag{5.44}$$

It follows that the average surface area of a hole calculated by this procedure is

$$4\pi\langle r\rangle^2 = 3.3\,\frac{kT}{\gamma} \tag{5.45}$$

Then from Eqs. (5.44) and (5.45), one obtains, clearly:

$$\frac{4\pi\langle r\rangle^2}{\langle r\rangle^2} \equiv \frac{3.5kT/\gamma}{[0.51(kT/\gamma)^{1/2}]^2} = 12.57 \tag{5.46}$$

What typical values of mean hole radius does Eq. (5.44) yield (Table 5.15)? By using the macroscopic surface-tension value, Eq. (5.44) shows that the average radius of a hole in molten KCl at 1173 K is 190 pm. The mean ionic radius, however, is 160 pm.

A typical hole therefore can accommodate an ion in a possible movement into a hole. This result is remarkable because of the process by which it has been attained. One began by considering that a liquid electrolyte was a liquid continuum interspersed by holes of random size and location imagined to be forming and collapsing as in a boiling liquid. Thus, the work of hole formation was taken to be equal to the work of expanding the surface area of a bubble in a boiling liquid. With the use of this expression and simple probability arguments, the average hole radius was calculated by taking the integral of Eq. (5.40) from zero to infinity.

**TABLE 5.15**

**Mean Hole Radius for Various Molten Salts at 1173 K**

| Molten Salt | Surface Tension, (dyn $cm^{-1}$) | Mean Hole Volume ($nm^3$) | Mean Hole Radius (nm) |
|---|---|---|---|
| NaCl | 107.1 | 0.032 | 0.170 |
| NaBr | 90.5 | 0.0417 | 0.190 |
| KCl | 89.5 | 0.0423 | 0.190 |
| KBr | 77.3 | 0.0527 | 0.210 |
| CsCl | 72.7 | 0.0518 | 0.220 |
| Nal | 66.4 | 0.0662 | 0.230 |
| KI | 60.3 | 0.0766 | 0.230 |

At a fixed temperature, the only parameter determining the mean hole size is the surface tension. Though one is aiming at a microscopic (structural) explanation of the behavior of ionic liquids, one goes ahead and uses the macroscopic value of surface tension. The mean hole radius then turns out to have the same order of magnitude as the mean radius of ions comprising the liquid.

A remarkable conclusion can be drawn by looking at Table 5.15. One sees that Fürth's theory of holes in liquids—liquids imagined to be nearly on the boil so that $(P_I - P_O) = 0$—indicates that the holes arising from the model are molecular in size. Why is this a remarkable conclusion? It is because no props (e.g., dependence on some measurement of volume increase on melting) which would ensure that the right hole size would turn up have been used. In fact, hitherto, nothing has been said about molecules, ions, or any structure. It might have been thought to be a long shot—taking the bubble in a boiling liquid and seeing in such a concept any molecular reality. Look back at Table 5.15. The molecular size of the holes arising from the theory is an established *fact.* The conclusion: the model is worth investigating further and seeing how its application works out when one comes to the interpretation of transport data (Section 4.5.2). At this stage, it is sufficient to be properly surprised: the idea of bubbles (holes) in liquids gives rise to the average size, which is that of the ions concerned. Later on (Section 5.6) it will be seen just how this result offers a possible mechanism for transport, e.g., viscous flow and diffusion.

The theory of an indication of molecular-sized holes supports the idea that the model reflects some aspects of reality in liquids. How can bubbles in liquids be used as the basis of a calculation of liquid properties? The answer is given by the degree to which such an approach predicts facts, for example, the compressibility (Table 5.16). The fact that it indicates the calculated size of holes seems to suggest a diffusion model in which critical acts may be the formation of the holes and the jumping into them of neighboring ions (but see Section 5.4.1).

These indications that one of the modeling approaches to molten salts looks remarkably promising does not mean that it is the final word in making models of molten salts. It is an imaginative portrayal, but there are some molten salts the properties of which are not covered at all by any theory of holes distributed like bubbles in boiling liquids. One of these undealt-with properties—the property of *supercooling liquids,* which continue to retain their properties below the normal melting point—must be looked into before one returns to a modeling interpretation of viscous flow, diffusion, and conductance (see Chapter 4).

### 5.5.5. Glass-Forming Molten Salts

A number of molten salt systems [e.g., the simple ionic system $Ca(NO_3)_2$-$KNO_3$], have the property of being able to be *supercooled*, i.e., to remain liquid at temperatures below the melting point down to a final temperature. This is called the *glass transition temperature*, and at this temperature the salts form what is called "a glass." This glass is only apparently solid. It is a highly disordered substance in which a liquid structure

**TABLE 5.16**

**Comparison of Calculated Isothermal Compressibilities with the Experimental Values (Hole Theory)**

| Salt | Temp. (K) | $10^{12}\beta$, calc. ($cm^2\ dyn^{-1}$) | $10^{12}\beta$, obs. ($cm^2\ dyn^{-1}$) |
|---|---|---|---|
| LiCl | 887 | 20.8 | 19.4 |
| | 1073 | 30.5 | 24.7 |
| | 1173 | 39.1 | 28.6 |
| | 1273 | 47.9 | 33.0 |
| NaCl | 1073 | 27.8 | 28.7 |
| | 1173 | 36.9 | 22.8 |
| | 1273 | 49.6 | 40.0 |
| KCl | 1045 | 27.6 | 36.2 |
| | 1073 | 30.2 | 38.4 |
| | 1173 | 42.3 | 45.7 |
| | 1273 | 56.7 | 54.7 |
| CsCl | 915 | 20.2 | 38.0 |
| | 1073 | 39.0 | 51.8 |
| | 1173 | 57.0 | 62.6 |
| | 1273 | 72.5 | 76.3 |
| $CdCl_2$ | 873 | 31.0 | 29.8 |
| | 973 | 37.3 | 33.1 |
| | 1073 | 46.9 | 36.9 |
| NaBr | 1020 | 32.8 | 31.6 |
| | 1073 | 40.1 | 33.6 |
| | 1173 | 47.4 | 38.6 |
| | 1273 | 59.5 | 44.9 |
| KBr | 1008 | 28.0 | 39.8 |
| | 1073 | 34.5 | 43.8 |
| | 1173 | 51.3 | 52.1 |
| | 1273 | 69.9 | 62.1 |
| CsBr | 909 | 56.3 | 49.1 |
| | 1073 | 76.0 | 67.1 |
| | 1173 | 97.5 | 82.7 |
| | 1273 | 130.5 | 103.1 |

—no long-range order—is *frozen* into what appears to be a solid. Although such systems were studied in the 1960s and earlier, they subsequently received a seminal and sustained contribution from the Australian physical chemist Angell, who has been the driving force behind the discovery of much of modern knowledge of the supercooled state.

Mathematical treatment of molten salts that supercool was first carried out by Cohen and Turnbull. The principal idea of the hole theory—that diffusion involves ions that wait for a void to turn up before jumping into it—is maintained. However, Cohen and Turnbull introduced into their model a property called the *free volume*, $V_f$. What is meant by this "free volume"? It is the amount of space in addition to that, $V_0$, filled by matter in a closely packed liquid. Cohen and Turnbull proposed that the free volume is linearly related to temperature

$$V_f = V - V_0 = V_m\alpha(T - T_0) \tag{5.47}$$

where $T_0$ is the temperature at which the free volume becomes zero. Cohen and Turnbull named the temperature at which a supercooled liquid becomes a glass the *glass transition temperature.*

To express the probability that the free volume occasionally opens up to form a hole, Cohen and Turnbull first defined a factor $\gamma$, which allows for the partial filling of the expanded free volume to the size of a hole. It can vary between $1/2 < \gamma < 1$. A value of $\gamma = 1$ means that the holes are empty, and a value of $\gamma = 1/2$ that they are half filled.

The authors rejected the normal thermal probability term, involving $e^{-E/RT}$. They used a statistical argument concerning the number of ways it is possible to mix free spaces with ions and found thereby the probability $P_r$ of finding a void volume $V^*$ as a fraction of the free volume. The expression for this probability comes to

$$P_r = e^{-\gamma V^*/V_f} \tag{5.48}$$

Then the most elementary expression for a diffusion coefficient would be:

$$D = lv \tag{5.49}$$

where $l$ is the distance covered in one jump and $v$ the velocity of the particle. This primitive expression would be true if there were a void always available and each jump were in the same direction. Since there are three distance coordinates, each having two directions (i.e., six directions), and since the coming-into-being of a hole has the probability given by Eq. (5.48), then,

$$D = \frac{1}{6} vle^{-\gamma V^*/V_f} \tag{5.50}$$

Substituting $V_f$ from Eq. (5.47),

$$D = \frac{1}{6} vle^{-\frac{\gamma V^*}{\alpha V_m(T - T_0)}} = Ae^{-\frac{B}{T - T_0}} \tag{5.51}$$

where

$$B = \frac{\gamma V^*}{\alpha V_m} \tag{5.52}$$

Cohen and Turnbull's model is oriented to liquids that form glasses. At the glass transition temperature (i.e., at $T = T_0$), the diffusion coefficient becomes zero, which is a rational consequence of what is thought to be going on: the supercooled liquid finally becomes a glass in which $D$ is effectively zero.

A difficulty might face the worker who wishes to apply Cohen and Turnbull's theory to transport phenomena in molten salts not only near the glass transition temperature but also above the normal melting point (see Section 5.6.2.2). Experimental evidence shows that the heat of activation of diffusion and of conductance for viscous flows is related to the normal melting point of the substance concerned

$$E_D^* = 3.74RT_{\text{m.p.}} \tag{5.53}$$

Accepting this on faith for the moment, then $B$ from Eq. (5.51) can be written as

$$B = \frac{\gamma}{\alpha}\frac{V^*}{V_m} = 3.74RT_{\text{m.p.}} \tag{5.54}$$

The order of magnitude of $V_f$ is $1\ \text{cm}^3\ \text{mol}^{-1}$. If one identifies $V^*$ with a void into which an ion jumps, then in transport phenomena this must be around $10\ \text{cm}^3\ \text{mol}^{-1}$, a typical molar volume for simple monatomic ions. Moreover, near to the melting point, $T = T_{\text{m.p.}}$ and $\gamma \propto 0.2$.

This result increases the credibility of the Cohen and Turnbull view: the meaning of $\gamma = 0.2$ is that the "hole" is 20% full, and this seems consistent with the picture of an ion-sized space filled 20% of the time with an ion.

## Further Reading

### *Seminal*

1. R. Fürth, "On the Theory of the Liquid State, I. The Statistical Treatment of the Thermodynamics of Liquids by the Theory of Holes," *Proc. Cambridge Phil. Soc.* **37**: 252 (1941).
2. R. Fürth, "On the Theory of the Liquid State, II. The Hole Theory of the Viscous Flow of Liquids," *Proc. Cambridge Phil. Soc.* **37**: 281 (1941).
3. M. H. Cohen and D. Turnbull, "Molecular Transport in Liquids and Glasses," *J. Chem. Phys.* **31**: 1164(1959).
4. A. F. M. Barton and R. J. Speedy, "Simultaneous Conductance and Volume Measurements on Molten Salts at High Pressure," *J. Chem. Soc. Faraday Trans.* **71**: 506 (1974).

### Reviews

1. C. A. Angell, "Transport and Relaxation Processes in Molten Salts," *NATO ASI Series C* **202**: 123 (1987).
2. G. Mamantov, C. Hussey, and R. Marassi, eds., *An Introduction to the Electrochemistry of Molten Salts*, Wiley, New York (1991).

### Papers

1. Y. Shirakawa, S. Tamaki, M. Saito, H. Masatoshi, and S. Harab, *J. Non-Cryst. Solids* **117**: 638 (1990).
2. W. Freyland, *J. Non-Cryst. Solids* **117**: 613 (1990).
3. R. L. McGreevy, *Nuovo Cimento* **12D** (4–5): 685 (1990).
4. T. Nakamura and M. Itoh, *J. Electrochem. Soc.* **137**: 1166 (1990).
5. M. L. Saboungi and D. L. Price, in *Proc. Int. Symp. Molten Salts*, Electrochemical Society, p. 8 (1990).
6. M. Abraham and I. Zloges, *J. Am. Chem. Soc.* **113**: 8583 (1991).
7. M. Noel, R. Allendoerfer, and R. A. Osteryoung, *J. Phys. Chem.* **96**: 239 (1992).
8. R. J. Speedy, F. X. Prielmeier, T. Vardag, E. W. Lang, and H. D. Ludemann, *J. Electrochem. Soc.* **139**: 2128 (1992).
9. C. A. Angell, C. Alba, A. Arzimanoglou, and R. Bohmer, *AIP Proc.* **256**: 3 (1992).
10. S. Deki, H. Twabuki, A. Kacinami, and Y. Kanagi, *Proc. Electrochem. Soc.* **93–9**: 252 (1993).
11. S. Itoh, Y. Hiwatari, and H. Miwagawa, *J. Non-Cryst. Solids* **156**: 159 (1993).
12. C. A. Angell, C. Lia, and E. Sanchez, *Nature* **362**: 137 (1993).
13. C. A. Angell, P. H. Poole, and J. Shao, *Nuovo Cimento* **16**: 993 (1994).
14. C. A. Angell, *Proc. Natl. Acad. Sci. U.S.A.* **92**: 6675 (1995).
15. C. A. Angell, *Science* **267**: 1924 (1995).
16. M. G. McClin and C. A. Angell, *J. Phys. Chem.* **100**: 1181 (1996).


## 5.6. MORE MODELING ASPECTS OF TRANSPORT PHENOMENA IN LIQUID ELECTROLYTES

### 5.6.1. Simplifying Features of Transport in Fused Salts

An important characteristic of liquid ionic systems is that they lack an inert solvent; they are *pure electrolytes*. Owing to this characteristic, some aspects of transport phenomena in pure molten salts are simpler than similar phenomena in aqueous solutions.

Thus, there is no concentration variable to be taken into account in the consideration of transport phenomena in a pure liquid electrolyte. Hence, there cannot be a concentration gradient in a *pure fused salt*, and [because of Fick's first law; see Eq. (4.16)] without a concentration gradient there cannot be pure diffusion. In an *aqueous*

*solution*, on the other hand, it is possible to have a concentration gradient for the solute and thus have diffusion in the normal sense.

Another consequence of the absence of a solvent in a pure liquid electrolyte is that the mean ion–ion interaction field as a function of distance within the liquid is constant. In solutions of ions in a solvent, however, the extent of ion–ion interaction is a variable quantity. It depends on the amount of solvent dissolving a given quantity of ionic solute, i.e., on the solute concentration.

## 5.6.2. Diffusion in Fused Salts

5.6.2.1. *Self-Diffusion in Pure Liquid Electrolytes May Be Revealed by Introducing Isotopes.* In the absence of a solvent, it is meaningless to consider a pure liquid electrolyte (e.g., NaCl) as having different amounts of NaCl in different regions. Let the possibility be momentarily considered that the system could be made to have more ions of one species (e.g., $Na^+$) in one region than in another. However, this is impossible over significant time spans because any attempt of a single ionic species to accumulate in one region and decrease in another is promptly stopped by the electric field that develops as a consequence of the separation of charges. Overall electroneutrality must prevail; i.e., there can be no congregation of an ionic species in one part of the liquid.

Fortunately, electroneutrality only requires that the total positive charge in a certain region be equal to the total negative charge. Suppose therefore that in a liquid sodium chloride electrolyte, a certain percentage of the $Na^+$ ions are replaced by a radioactive isotope of sodium. There is no difference between the $^{22}Na$ and $^{23}Na$ as far as the principle of electroneutrality is concerned; it is only required that the number of $Na^+$ ions plus the number of tagged $Na^{*+}$ ions are equal to the total number of $Cl^-$ ions (Fig. 5.23). However, the labeled $Na^{*+}$ ions and the nonradioactive $Na^+$ are completely different entities from the point of view of a counter; only the former produce the scintillations.

Herein lies a method of examining the diffusion of ions in pure ionic liquids that differs from the diffusion of ions in aqueous solution, which is governed by Fick's law. One takes a pure liquid electrolyte, say NaCl, and brings it into contact with a melt containing the same salt but with a certain proportion of radioactive ions, say, NaCl with radioactive $Na^{*+}$ ions. There is a negligible concentration gradient for $Na^+$ ions, but a concentration gradient for the tracer $Na^{*+}$ ions has been created. Diffusion of the tracer begins (Fig. 5.24).

If a capillary containing an inactive melt is suitably introduced into a large reservoir of tracer-containing melt at $t = 0$, then diffusion of the tracer into the capillary starts (Fig. 5.25). At time $t$, the experiment can be terminated by withdrawing the capillary from the reservoir. The total amount of tracer in the capillary can be measured by a detector of the radioactivity. From the study of the diffusion problem and the experimentally determined average tracer concentration in the capillary, the diffusion coefficient of the $Na^{*+}$ ions can then be calculated.

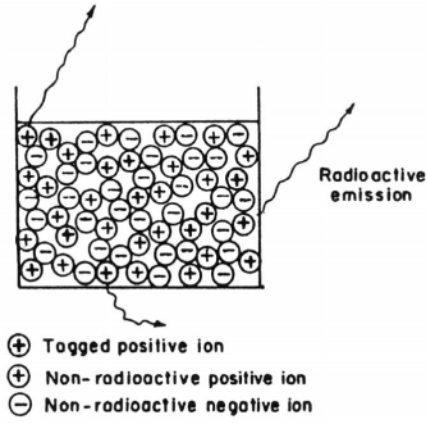


**Fig. 5.23.** The principle of electroneutrality is satisfied if the number of tagged positive ions plus the number of nonradioactive positive ions is equal to the total number of negative ions.

Since the tracer ions (e.g., $Na^{*+}$) diffuse among particles (e.g., $Na^{+}$) that are chemically just like themselves, one often refers to the phenomenon as *self*-diffusion (*tracer* diffusion is a more explanatory term) and to the diffusion coefficient thus determined as the *self*-diffusion coefficient.

5.6.2.2. *Results of Self-Diffusion Experiments.* Self-diffusion coefficient studies with fused salts really began to gather momentum after radioisotopes became

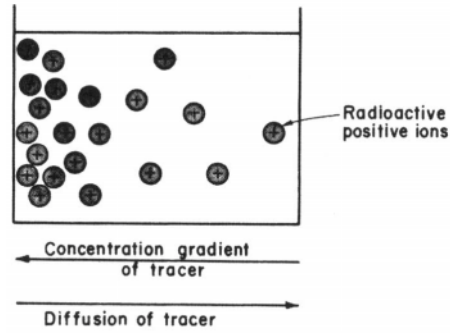


**Fig. 5.24.** The existence of a concentration gradient for tracer ions produces diffusion of the tracer, i.e., tracer diffusion.

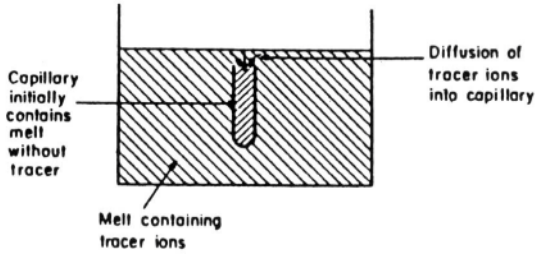


**Fig. 5.25.** A schematic of an experiment to study tracer diffusion. A capillary containing inactive melt is dipped into a reservoir of melt containing tracer ions. Tracer ions diffuse into the capillary.

widely available, i.e., after about 1950. Some of the data for comparing the diffusion coefficients of typical inert gases, room-temperature liquids, metals, and molten salts are presented in Tables 5.17, 5.18, and 5.19.

It can be seen that the diffusion coefficients of these liquid electrolytes (near their melting points) are of the same order of magnitude ($\sim 10^{-5}$ cm$^2$ s$^{-1}$) as for liquid inert gases, liquid metals, and normal room-temperature liquids. This fact suggests that the mechanism of diffusion is basically the same in all simple liquids, i.e., liquids in which the particles do not associate into pairs, triplets, or network structures (see Sections 3.8 and 4.8.8). The order of magnitude of the diffusion coefficient has evidently more to do with the liquid state than with the chemical nature of the liquid for in the case of the corresponding solid substances, the diffusion coefficient ranges (Table 5.19) over more than four orders of magnitude ($10^{-7}$ to $10^{-11}$ cm$^2$ s$^{-1}$).

An expected feature of the results on tracer diffusion is that the diffusion coefficient varies with temperature. The temperature dependence observed experimentally can be expressed in the type of equation exhibited by virtually all transport, or rate, phenomena.

**TABLE 5.17**

**Self-Diffusion Coefficients of Various Types of Substance**

| Type of Substance | Example | Temperature (K) | Diffusion Coefficient (cm$^2$ s$^{-1}$) |
|---|---|---|---|
| Liquid inert gas | Ar | 100 | $3.70 \times 10^{-5}$ |
| Room-temperature liquid | $CCl_4$ | 298 | $1.41 \times 10^{-5}$ |
| Liquid metal | Zn | 693 | $2.07 \times 10^{-5}$ |
| Molten salt | NaCl | 1113 | $D_{Na^+}$ $9.6 \times 10^{-5}$<br>$D_{Cl^-}$ $6.7 \times 10^{-5}$ |

**TABLE 5.18**

**Energies of Activation and Preexponential Factors for Self-Diffusion in Molten Group I and II Chlorides**

| Molten Salt/Tracer | $10^3 \times D_o^{\neq}$ ($cm^2\ s^{-1}$) | $E_D^{\neq}$ (kJ $mol^{-1}$) | Temp. Range (K) |
|---|---|---|---|
| $NaCl/^{22}Na$ | 2.1 | 29.87 ± 1.05 | 1093–1293 |
| $NaCl/^{36}Cl$ | 1.9 | 31.09 ± 3.51 | 1099–1308 |
| $KCl/^{42}K$ | 1.8 | 28.78 ± 2.13 | 1071–1256 |
| $KCl/^{36}Cl$ | 1.8 | 29.83 ± 2.05 | 1067–1260 |
| $CaCl_2/^{45}Ca$ | 0.38 | 25.65 ± 2.76 | 1056–1277 |
| $CaCl_2/^{36}Cl$ | 1.9 | 37.07 ± 4.02 | 1060–1292 |
| $SrCl_2/^{89}Sr$ | 0.21 | 22.51 ± 4.06 | 1194–1393 |
| $SrCl_2/^{36}Cl$ | 0.77 | 28.79 ± 3.01 | 1185–1430 |
| $BaCl_2/^{140}Ba$ | 0.64 | 37.49 ± 5.15 | 1267–1480 |
| $BaCl_2/^{36}Cl$ | 2.0 | 39.66 ± 4.27 | 1266–1476 |
| $CdCl_2/^{115}Cd$ | 1.1 | 28.62 ± 2.59 | 880–1079 |
| $CdCl_2/^{36}Cl$ | 1.1 | 28.45 ± 4.22 | 880–1075 |

$$D = D_0 \exp\left(-\frac{E_D^{\neq}}{RT}\right) \tag{5.55}$$

where $D_0$ is found to depend little on substance and temperature, and $E_D^{\neq}$ is the activation energy for self-diffusion (Fig. 5.26). Some preexponential factors and the corresponding energies of activation for diffusion are given in Table 5.18.

In some liquids, a deviation (Fig. 5.27) occurs from the straight-line log $D$ versus $1/T$ plots expected on the basis of the empirical exponential law for the diffusion coefficient (Eq. 5.55). An example of such a deviating liquid electrolyte is molten $ZnCl_2$, but in the case of this substance, structural changes have been noted with increasing temperature. This seems to be a reasonable explanation for the deviation from the straight-line log $D$ versus $1/T$ plot.

**TABLE 5.19**

**Tracer Diffusion Coefficients of Crystalline Substances near the Melting Point**

| Substance | Tracer | $D$ ($cm^2\ s^{-1}$) | Temperature (K) |
|---|---|---|---|
| Na | $^{22}Na$ | $1.7 \times 10^{-7}$ | 370 |
| Ag | $^{110}Ag$ | $2.8 \times 10^{-8}$ | 1173 |
| NaCl | $^{22}Na$ | $4.0 \times 10^{-9}$ | 1000 |
| PbS | ThB | $1.4 \times 10^{-9}$ | 1316 |
| Pb | ThB | $5.5 \times 10^{-10}$ | 597 |
| $PbI_2$ | ThB | $7.7 \times 10^{-11}$ | 588 |

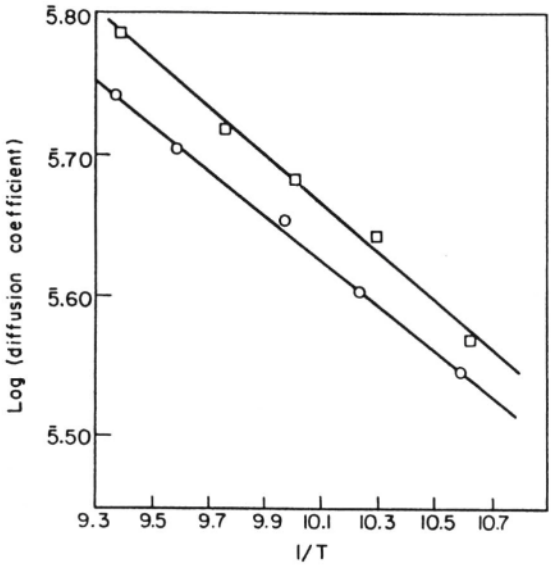


**Fig. 5.26.** The straight-line plot of log $D$ versus $1/T$ observed in the case of the diffusion of $^{134}Cs$ (○) and $^{36}Cl$ (□) in molten CsCl.

The activation energy for self-diffusion is usually a constant, independent of temperature. It is, however, characteristic of the particular liquid electrolyte. The dependence of the activation energy for self-diffusion on the nature of the fused salt was experimentally found by Nanis and Bockris in 1963 to be expressible in the simple relation of Fig. 5.28, given by the equation

$$E_D^{\neq} = 3.74RT_{\text{m.p.}} \tag{5.53}$$

where $T_{\text{m.p.}}$ is the melting point.

It is important to emphasize that this *same relation is valid for liquids in general*, including the liquid inert gases, organic liquids, and the liquid metals, a remarkable fact and one which some liquid theorists have had difficulty explaining (though see Section 5.7.5). Equation (5.53) does not apply, however, to associated liquids, or to those in which there is widespread intermolecular binding throughout the liquid, such as water or molten silicates, borates, and phosphates (Section 3.8).

### 5.6.3. Viscosity of Molten Salts

An examination of the properties of viscous flow of molten liquids shows that viscosity varies with temperature in a way quite similar to that of self-diffusion. For

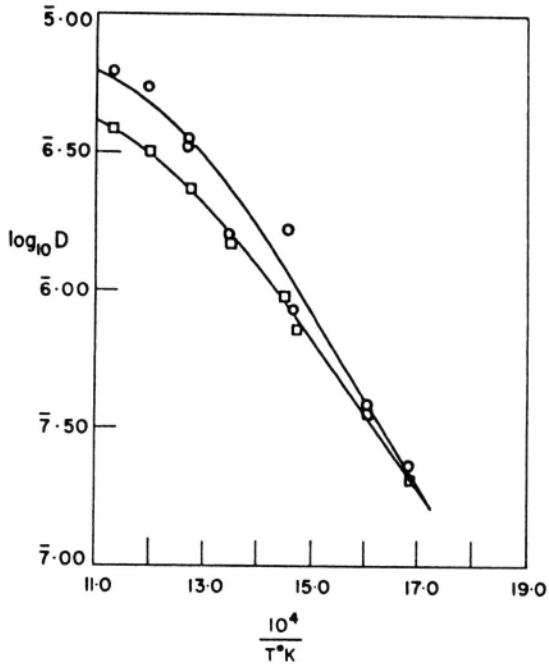


**Fig. 5.27.** An example of a log $D$ versus 1/T plot that is not a straight line. The curve is for the diffusion of $^{65}Zn$ (○) and $^{36}Cl$ (□) in molten $ZnCl_2$.

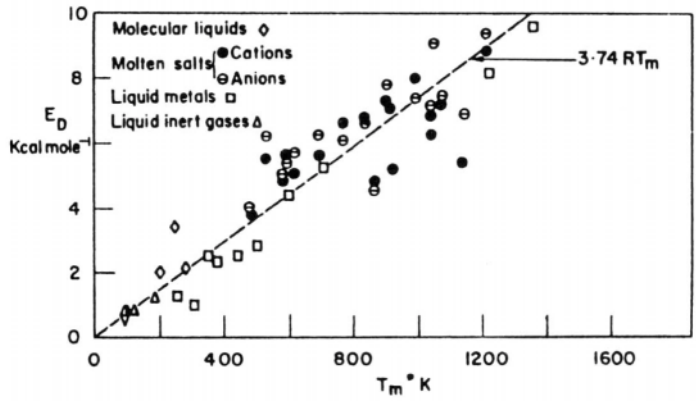


**Fig. 5.28.** The dependence of the experimental energy of activation for self-diffusion on the melting point (1 cal = 4.184 J).

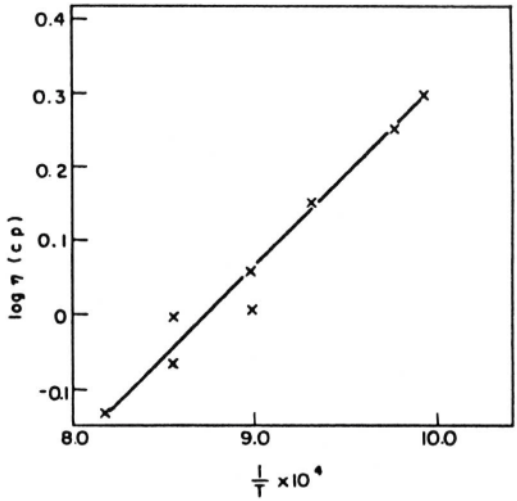


**Fig. 5.29.** The straight-line plot of log $\eta$ versus $1/T$ for viscosity of a molten salt.

simple, unassociated liquids, the temperature dependence is given by an empirical equation

$$\eta = \eta_0 e^{+E_\eta^*/RT} \tag{5.56}$$

where $\eta_0$ is a constant analogous to $D_0$, and $E_\eta^*$ is the energy of activation for viscous flow (Fig. 5.29 and Tables 5.20 and 5.21).

**TABLE 5.20**
**Viscosities of Fused Salts**

| Fused Salt | Temperature (K) | Viscosity (cP) |
|---|---|---|
| $CdCl_2$ | 873 | 2.31 |
| $CdBr_2$ | 873 | 2.61 |
| $PbBr_2$ | 823 | 2.98 |
| $PbCl_2$ | 873 | 2.75 |
| AgCl | 873 | 1.66 |
| AgBr | 873 | 2.27 |
| NaCl | 1173 | 1.05 |
| NaBr | 1028 | 1.43 |
| KCl | 1046 | 1.51 |
| KBr | 1003 | 1.57 |

**TABLE 5.21**
**Energies of Activation for Viscous Flow for Simple Molten Electrolytes**

| Molten Salt | $E_\eta^{\neq}$ (kJ mol$^{-1}$) | Molten Salt | $E_\eta^{\neq}$ (kJ mol$^{-1}$) |
|---|---|---|---|
| LiCl | 36.82 | KOH | 25.52 |
| LiBr | 25.10 | AgCl | 12.13 |
| LiI | 18.41 | AgBr | 12.97 |
| $LiNO_3$ | 17.57 | AgI | 24.27 |
| NaCl | 38.07 | $AgNO_3$ | 12.97 |
| NaBr | 33.43 | $TlNO_3$ | 15.06 |
| NaI | 30.96 | CuCl | 17.57 |
| $NaNO_3$ | 16.74 | $MgCl_2$ | 27.20 |
| $NaNO_2$ | 16.74 | $CaCl_2$ | 39.75 |
| NaOH | 23.01 | $BaCl_2$ | 37.66 |
| NaCNS | 24.27 | $PbCl_2$ | 28.03 |
| KCl | 32.64 | $PbBr_2$ | 25.94 |
| KBr | 31.38 | $CdCl_2$ | 16.74 |
| KI | 38.49 | $CdBr_2$ | 18.83 |
| $KNO_3$ | 15.48 | $NH_4NO_3$ | 19.25 |

This expression is formally analogous to Eq. (5.51) for the dependence of the self-diffusion coefficient upon temperature. For simple liquid electrolytes, the experimental activation energy for viscous flow is given by an expression (Fig. 5.30) identical to that for self-diffusion, i.e.,

$$E_\eta^{\neq} = 3.74RT_{\text{m.p.}} \tag{5.57}$$

The fact that this empirical law applies so widely clearly is trying to tell us something. It is that the basic factors determining viscous flow and self-diffusion are the same for all liquids that do not have to break bonds before they undergo transport.

Simple ionic liquids have viscosities in the range of 1 to 5 centipoises (cP). However, when there is an association of ions into aggregates, as, for example, in $ZnCl_2$ near the melting point, the viscous force-resisting flow of the melt increases above that noted for simple liquids. Such complex ionic liquids are discussed later (Section 5.8).

### 5.6.4. Validity of the Stokes–Einstein Relation in Ionic Liquids

All transport processes (viscous flow, diffusion, conduction of electricity) involve ionic movements and ionic drift in a preferred direction; they must therefore be interrelated. A relationship between the phenomena of diffusion and viscosity is contained in the Stokes–Einstein equation (4.179).

**TABLE 5.22**

**The $D\eta/T$ of Some Molten Salts for Testing the Stokes–Einstein Relation**

| Molten Salt | Tracer | Temperature (K) | $D_i \times 10^5$ ($cm^2\ s^{-1}$) | $\frac{D_i\eta}{T} \times 10^9$ (dyn $deg^{-1}$) |
|---|---|---|---|---|
| NaCl | $^{6}Li$ | 1180 | 13.2 | 1.09 |
| NaCl | $^{22}Na$ | 1180 | 10.2 | 0.85 |
| NaCl | $^{42}K$ | 1180 | 9.7 | 0.81 |
| NaCl | $^{86}Rb$ | 1180 | 9.2 | 0.76 |
| NaCl | $^{134}Cs$ | 1180 | 8.9 | 0.74 |
| KCl | $^{42}K$ | 1150 | 8.9 | 0.63 |
| NaI | $^{22}Na$ | 1026 | 9.5 | 1.20 |
| $CaCl_2$ | $^{45}Ca$ | 1154 | 2.6 | 0.79 |
| $SrCl_2$ | $^{89}Sr$ | 1260 | 2.4 | 0.70 |
| $BaCl_2$ | $^{140}Ba$ | 1356 | 2.4 | 0.69 |
| $CdCl_2$ | $^{115}Cd$ | 925 | 2.7 | 0.58 |
| $PbCl_2$ | $^{210}Pb$ | 851 | 1.5 | 0.59 |
| $LiNO_3$ | $^{6}Li$ | 581 | 2.1 | 1.77 |
| $NaNO_3$ | $^{22}Na$ | 638 | 2.6 | 0.88 |
| $KNO_3$ | $^{42}K$ | 667 | 2.1 | 0.68 |
| $AgNO_3$ | $^{110}Ag$ | 534 | 1.5 | 0.80 |

$$D = \frac{kT}{6\pi r\eta} \tag{5.58}$$

This equation was deduced in Section 4.4.8. It is of interest to inquire here about its degree of applicability to ionic liquids, i.e., fused salts. To make a test, the experimental values of the self-diffusion coefficient $D^*$ and the viscosity $\eta$ are used in conjunction with the known crystal radii of the ions. The product $D^*\eta/T$ has been tabulated in Table 5.22, and the plot of $D^*\eta/T$ versus $1/r$ is presented in Fig. 5.31, where the line of slope $k/6\pi$ corresponds to exact agreement with the Stokes–Einstein relation.[14]

Looking at Fig. 5.32, it can be seen that there is a fairly significant fit. The anions, particularly those of the group II halides, are not very consistent with the Stokes–Einstein relation. However, their poorer fit is offset by the better Stokes–Einstein behavior of the cations. The relatively good fit of the cations tempts one to conclude that there is a particular reason for the deviations of the anions. Some attempts have been made

[14]The essential applicability of this phenomenological equation is clearly shown by using the numerical comparison of $D\eta/T = k/6\pi r$. The right-hand side is $0.7 \times 10^9$ for $r$ = 300 pm, and the mean of the experimental values is $0.6 \times 10^9$, which is not bad!

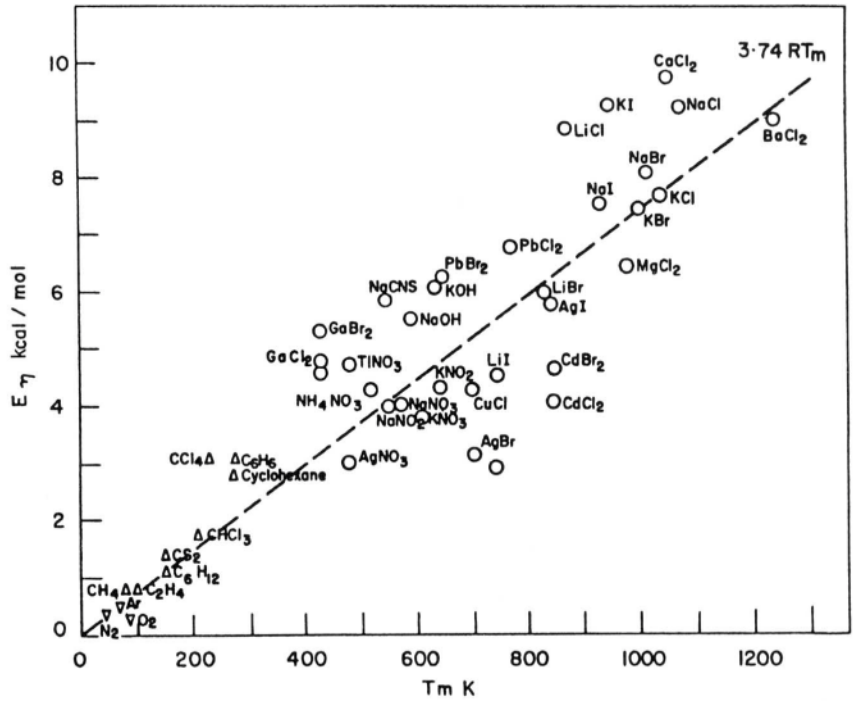


**Fig. 5.30.** The dependence of the experimental energy of activation for viscous flow on the melting point.

to elucidate this reason. For instance, it has been suggested that since anions are by and large larger than cations, they require greater local rearrangements at a site before they can jump into it, i.e., greater entropies of activation.

The Stokes–Einstein relation is based on Stokes' law in hydrodynamics according to which the viscous force experienced by a large sphere moving in an incompressible continuum is $6\pi r\eta v$. What Fig. 5.31 tells one is that, even though ions do not move in a continuum but among particles that are of approximately the same dimensions as the ions themselves, Stokes' law still holds! In view of the great dissimilarity of an ion in a structured medium and a sphere in an incompressible continuum, the rough applicability (in fused salts) of the Stokes–Einstein equation is somewhat unexpected and very useful. Of course, it is entirely consistent with the agreement between the heats of activation for viscous flow and self-diffusion. Each must evidently be concerned with the same rate-determining step, mechanism, and heat of activation.

### 5.6.5. Conductivity of Pure Liquid Electrolytes

The electrical conductance of molten salts is the easiest transport property to measure. In addition, knowledge of the order of magnitude of the equivalent conduc-

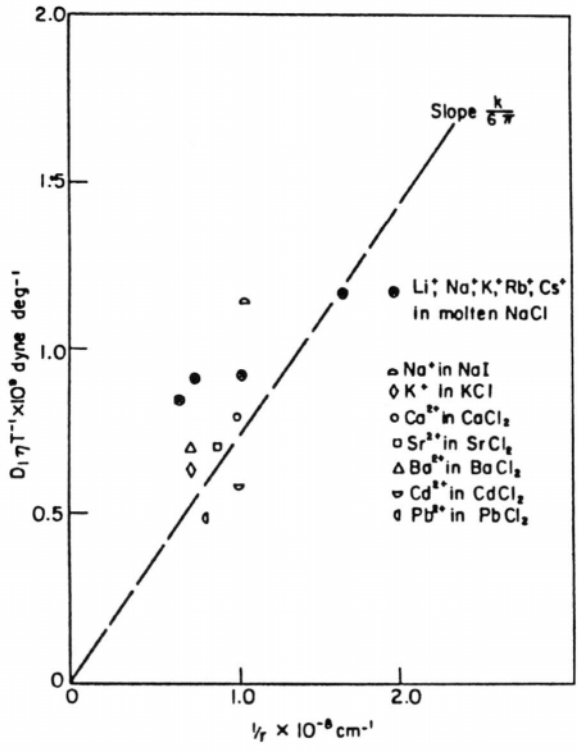


**Fig. 5.31.** When $D\eta/T$ is plotted against $1/r$, *a* straight-line of slope $k/6\pi$ should be obtained if the Stokes–Einstein relation is applicable to molten salts. The experimental points are indicated in the figure to show the degree of applicability of the Stokes–Einstein relation to molten salts.

tivity of a pure substance was used as a criterion for the nature of the bonding present. For these reasons, the electrical conductance of ionic liquids has been the subject of numerous studies.

The equivalent conductivities of some of the fused chlorides are given in Table 5.23, where the substances have been arranged according to the Periodic Table. The heavy line zigzagging across the table separates the ionic from the covalent chlorides. This structural difference is shown up sharply in the orders of magnitude of the equivalent conductivities.

Two further correlations emerge from Table 5.23. First, the equivalent conductivity decreases with increasing size of the cation (Table 5.24); second, there is a decrease in equivalent conductivity in going from the monovalent to the divalent and

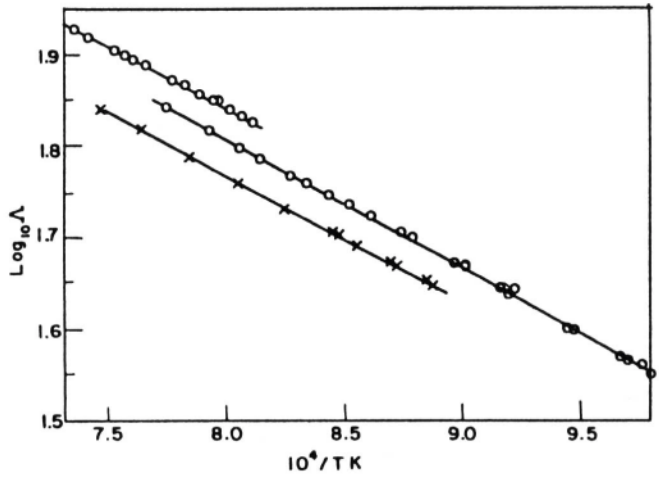


**Fig. 5.32.** The straight-line plot of log $\Lambda$ versus $1/T$.

then to the trivalent chlorides (Table 5.25), probably because of an increase in covalent character in this order.

As with the other transport properties, the specific (or equivalent) conductivity of fused salts varies with temperature.[15] For most pure liquid electrolytes, the experimental log $\Lambda$ versus $1/T$ plots are essentially linear (Fig. 5.32). This implies the usual exponential dependence of a transport property upon temperature

$$\Lambda = \Lambda_0 e^{-E^{\neq}_{\Lambda}/RT} \tag{5.59}$$

For some substances, the plots are slightly curved. In these cases, structural changes (e.g., the breaking up of polymer networks such as those observed with $SiO_2$) occur with change of temperature.

When the activation energies for conduction are computed from the log $\Lambda$ versus $1/T$ plots, it is seen (Table 5.26) that they are a little lower than the activation energies for viscous flow and self-diffusion, i.e.,

$$E^{\neq}_{\Lambda} < E^{\neq}_{D} \approx E^{\neq}_{\eta} \tag{5.60}$$

but follow the same pattern; they are proportional to the melting point temperature.

---

[15] A convenient means of comparing different salts is to use "corresponding temperatures"; usually 1.05 or 1.10 times the value of the melting point in kelvins is used for this purpose.

**TABLE 5.23**

**Equivalent Conductivities of Molten Chlorides ($Ohm^{-1}\ cm^2\ equiv.^{-1}$)**

| | | | | | |
|---|---|---|---|---|---|
| $HCl$<br>$\sim 10^{-6}$ | | | | | |
| $LiCl$<br>166 | $BeCl_2$<br>0.086 | $BCl_3$<br>0 | $CCl_4$<br>0 | | |
| $NaCl$<br>133.5 | $MgCl_2$<br>28.8 | $AlCl_3$<br>$15 \times 10^{-6}$ | $SiCl_4$<br>0 | $PCl_5$<br>0 | |
| $KCl$<br>103.5 | $CaCl_2$<br>51.9 | $ScCl_3$<br>15 | $TiCl_4$<br>0 | $VCl_4$<br>0 | |
| $RbCl$<br>78.2 | $SrCl_2$<br>55.7 | $YCl_3$<br>9.5 | $ZrCl_4$ | $NbCl_5$<br>$x = 2 \times 10^{-7}$ | $MoCl_5$<br>$x = 1.8 \times 10^{-6}$ |
| $CsCl$<br>66.7 | $BaCl_2$<br>64.6 | $LaCl_3$<br>29.0 | $HfCl_4$ | $TaCl_5$<br>$x = 3 \times 10^{-7}$ | $WCl_6$<br>$x = 2 \times 10^{-6}$ |
| | | | $ThCl_4$<br>16 | | $UCl_4$<br>$x = 0.34$ |

**TABLE 5.24**

**Dependence of Equivalent Conductivity upon Cationic Radius**

| Molten Salt | Radius of Cation (pm) | Equivalent Conductivity |
|---|---|---|
| $LiCl$ | 68 | 183 |
| $NaCl$ | 94 | 150 |
| $KCl$ | 133 | 120 |
| $RbCl$ | 147 | 94 |
| $CsCl$ | 167 | 86 |

**TABLE 5.25**

**Dependence of Equivalent Conductivity upon Valence of Cation**

| Molten Salt | Valence of Cation | Equivalent Conductivity |
|---|---|---|
| $NaCl$ | 1 | 150 |
| $MgCl_2$ | 2 | 35 |
| $AlCl_3$ | 3 | 15.1 |
| $SiCl_4$ | 4 | <0.1 |

**TABLE 5.26**
**Experimental Energies of Activation for Various Transport Process**

| Molten Salt | $E_{\Lambda}^{\neq}$ | $E_{D}^{\neq}$ (kJ mol$^{-1}$) | $E_{\eta}^{\neq}$ |
|---|---|---|---|
| LiCl | 8.62 | — | 36.4 |
| NaCl | 12.22 | 30.5 | 38.1 |
| $NaNO_3$ | 13.05 | 20.9 | 16.7 |
| KCl | 14.06 | 29.3 | 32.6 |
| $KNO_3$ | 13.18 | 23.4 | 15.1 |
| $CdCl_2$ | 9.20 | 28.5 | 16.7 |

### 5.6.6. The Nernst–Einstein Relation in Ionic Liquids

5.6.6.1. *Degree of Applicability.* Just as the Stokes–Einstein equation gives the relation between the transport of momentum (viscous flow) and the transport of matter (diffusion), the connection between the transport processes of diffusion and conduction leads to the Nernst–Einstein equation (see Section 4.4.9). For 1:1 electrolytes this is

$$\Lambda = \frac{F^2}{RT}(D_+ + D_-) \tag{5.61}$$

A more general expression of this same equation is

$$\Lambda = \frac{F^2}{RT}\sum_i z_i D_i \tag{5.62}$$

The Nernst–Einstein relation can be tested by using the experimentally determined tracer-diffusion coefficients $D_i$ to calculate the equivalent conductivity $\Lambda$ and then comparing this theoretical value with the experimentally observed $\Lambda$. It is found that the values of $\Lambda$ calculated by Eq. (5.61) are distinctly greater (by ~10 to 50%) than the measured values (see Table 5.27 and Fig. 5.33). Thus there *are* deviations from the Nernst–Einstein equation and this is strange because its deduction is phenomenological.[16]

[16] A phenomenological deduction is one that follows from general common sense or logic and involves only very general laws. It does not involve detailed models. So if experimental phenomena don't agree with predictions made on their basis, the only conclusion is that the conditions implied for the applicability of the laws do not apply to the case at hand. In this case, the expectation that the conductivity measured should agree with that obtained from diffusion data via the Nernst–Einstein equation requires that diffusion and conduction at least involve the *same particles* (e.g., $Na^+$ and $Cl^-$). If in diffusion an extra particle comes into the picture that is not effective in conduction, then the Nernst–Einstein law will not apply.

**TABLE 5.27**

**Test of the Nernst–Einstein Relation for Equivalent Conductivity of Molten NaCl**

| | Equivalent Conductivity | | | |
|---|---|---|---|---|
| | 1093 K | 1143 K | 1193 K | 1293 K |
| Observed | 138 | 147 | 155 | 171 |
| Calculated from Eq. (5.61) | 159 | 177 | 198 | 240 |

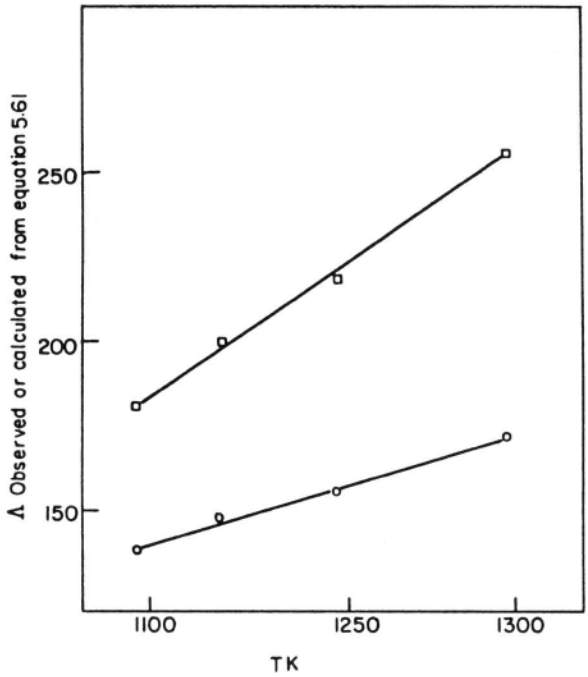


**Fig. 5.33.** Plot to show deviations from the Nernst–Einstein equation; (○) observed equivalent conductivity of molten NaCl and (□) calculated from Eq. (5.61).

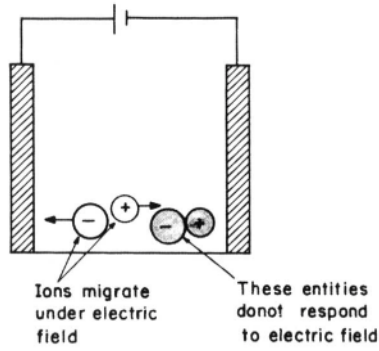


**Fig. 5.34.** An entity formed by the temporary or permanent association of a pair of oppositely charged ions is electrically neutral and therefore does not migrate under an electric field.

5.6.6.2. *Possible Molecular Mechanisms for Nernst–Einstein Deviations.* The observed conductivity is always found to be less than that calculated from the sum of the diffusion coefficients (Table 5.27), i.e., from the Nernst–Einstein relation [Eq. (5.61)]. Conductive transport depends only on the charged species because it is only *charged* particles that respond to an external field. If therefore two species of opposite charge unite, either permanently or temporarily, to give an uncharged entity, they will not contribute to the conduction flux (Fig. 5.34). They will, however, contribute to the diffusion flux. There will therefore be a certain amount of currentless diffusion, and the conductivity calculated from the sum of the diffusion coefficients will exceed the observed value. *Currentless diffusion will lead to a deviation from the Nernst–Einstein relation.*

It was suggested by Borucka et al. that a *permanent* association of positive and negative ions is not a necessary basis for a breakdown of the Nernst–Einstein equation. The only requirement is that diffusion should occur partly through the displacement of entities which have (momentarily, during jumps) a zero net charge and thus do not contribute to conduction. The entity may be, for instance, a pair of oppositely charged ions, in which case the diffusive displacement occurs by a coordinated movement of such a pair of ions into a paired vacancy (Fig. 5.35), i.e., a vacancy large enough to accept a positive and a negative ion at the same time. The pair of oppositely charged ions that jumps into a "paired vacancy" is neutral as a whole and therefore such coordinated jumps do not play a part in the conduction process, which is determined only by the separate, uncoordinated movements of single ions.

Thus, the experimentally observed diffusive flux of either of the ionic species is made up of two contributions—the diffusive flux occurring through the independent

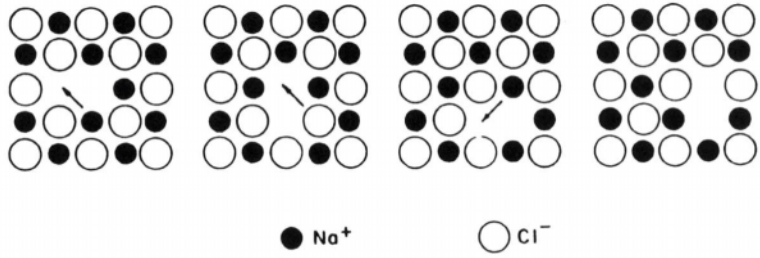


**Fig. 5.35.** Schematic diagrams to indicate how diffusive displacement can occur through a coordinated movement of a pair of ions into a paired vacancy.

jumps of ions and that occurring through paired jumps. Taking the example of the diffusion of $Na^+$ in an NaCl melt, one has[17]

$$J'_{Na^+} = J_{Na^+,ind} + J_{NaCl} \tag{5.63}$$

where $J'_{Na^+}$ is the experimentally observed flux of $Na^+$ (primes refer here to experimental quantities), $J_{Na^+,ind}$ is the diffusion of $Na^+$ by independent jumps, and $J_{NaCl}$ is the flux due to coordinated jumps of $Na^+$ and $Cl^-$ ions into paired vacancies

$$J'_{Na^+} = D'_{Na^+} \frac{dc_{Na^+}}{dx} \tag{5.64}$$

$$J_{Na^+,ind} = D_{Na^+,ind} \frac{dc_{Na^+}}{dx} \tag{5.65}$$

and

$$J_{NaCl} = D_{NaCl} \frac{dc_{Na^+}}{dx} \tag{5.66}$$

Adding Eqs. (5.65) and (5.66), one has

[17]The subscript NaCl must not be taken to mean that there are entities in the melt that might be considered "molecules" of sodium chloride. The NaCl does not refer to $Na^+$ and $Cl^-$ ions that are bound together like an ion pair in aqueous solution; rather, it refers to a pair of $Na^+$ and $Cl^-$ ions that undergo a coordinated jump into a paired vacancy during the short time for which they momentarily exist in contact. They do not contribute to the conductance because their jumps are directed not by the externally applied field but by the presence of a paired vacancy that exists before the ions jump as a pair.

$$J_{Na^+,ind} + J_{NaCl} = (D_{Na^+,ind} + D_{NaCl}) \frac{dc_{Na^+}}{dx} \tag{5.67}$$

However, from Eqs. (5.63) and (5.64)

$$J_{Na^+,ind} + J_{NaCl} = J'_{Na^+} = D'_{Na^+} \frac{dc_{Na^+}}{dx} \tag{5.68}$$

Hence,

$$D'_{Na^+} = D_{Na^+,ind} + D_{NaCl} \tag{5.69}$$

Similarly,

$$D_{Cl^-} = D_{Cl^-,ind} + D_{NaCl} \tag{5.70}$$

On adding, it is clear that

$$(D_{Na^+,ind} + D_{Cl^-,ind}) = (D_{Na^+} + D'_{Cl^-}) - 2D_{NaCl} \tag{5.71}$$

The $Na^+$ and $Cl^-$ ions that make coordinated jumps into paired vacancies, i.e., the NaCl species, contribute to diffusion but not to conduction since such a coordinated pair is effectively neutral. Hence, the Nernst–Einstein equation is only applicable to the ions that jump independently, i.e.,

$$D_{Na^+,ind} + D_{Cl^-,ind} = \frac{RT}{zF^2} \Lambda' \tag{5.72}$$

where $\Lambda'$ is the experimentally observed equivalent conductivity of molten NaCl. Making use of Eqs. (5.72) and (5.71), one has

$$\frac{RT}{zF^2} \Lambda' = (D'_{Na} + D'_{Cl^-}) - 2D_{NaCl} \tag{5.73}$$

or

$$\Lambda' = \frac{zF^2}{RT} (D'_{Na^+} + D'_{Cl^-}) - \frac{2zF^2}{RT} D_{NaCl} \tag{5.74}$$

The first term on the right-hand side corresponds to the value of the equivalent conductivity that would be calculated on the basis of the experimentally observed diffusion coefficients. Using the symbol $\Lambda_{calc}$ for this calculated value, i.e.,

$$\Lambda_{calc} = \frac{zF^2}{RT} (D'_{Na^+} + D'_{Cl^-}) \tag{5.75}$$

one has

$$\Lambda' = \Lambda_{\text{calc}} - \frac{2zF^2}{RT} D_{\text{NaCl}} \tag{5.76}$$

which shows that the experimental value of the equivalent conductivity is always less than that calculated from a Nernst–Einstein equation based on experimental diffusion coefficients. This is what is observed (Table 5.27).

## 5.6.7. Transport Numbers in Pure Liquid Electrolytes

5.6.7.1. *Transport Numbers in Fused Salts.* The concept and determination of transport numbers in pure liquid electrolytes is one of the most interesting, and most confusing, aspects of the electrochemistry of fused salts.

The concept has been referred to in Section 4.5.2. The transport number $t_i$ of an ionic species $i$ is the quantitative answer to the question: What fraction of the total current $I[= Ei_i]$ passing through an electrolyte is transported by the particular ionic species $i$? In symbols [see Eq. (4.234)]:

$$t_i = \frac{i_i}{I} = \frac{i_i}{\sum i_i} \tag{5.77}$$

In the case of $z{:}z$-valent salts, the transport number is simply given by

$$t_i = \frac{u_i}{\sum u_i} \tag{5.78}$$

where $u_i$ is the mobility of the ion concerned, e.g., that of $Li^+$ or $Br^-$. The coordinate system with which these mobilities are measured is considered later on. For a pure liquid electrolyte consisting of one cationic and one anionic species,

$$t_+ = \frac{u_+}{u_+ + u_-} \quad \text{and} \quad t_- = \frac{u_-}{u_+ + u_-} \tag{5.79}$$

It was seen (Section 2.4) that in aqueous solutions, the solvent could not be relegated to the status of an unobtrusive background. The solvent molecules, by entering into the solvation sheaths of ions, participated in their drift. Thus, in addition to the flows of the positive and negative ions, there was a flux of the solvent. This complication of solvent flux is absent in pure ionic liquids. There is, however, an interesting effect when a current is passed through a fused salt.

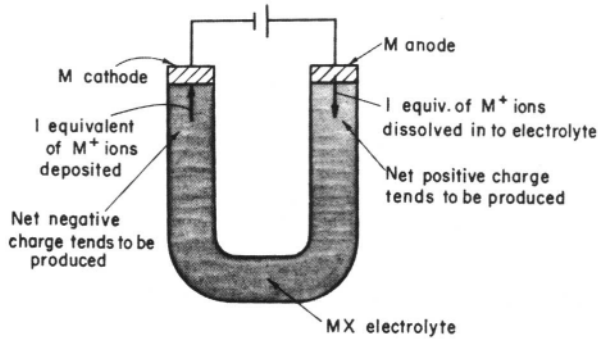


**Fig. 5.36.** Schematic U-tube setup with M electrodes and MX electrolyte. When 1 F of electricity is passed through the system, one equivalent of $M^+$ ions is deposited at the M cathode and one equivalent of ions is produced at the M anode. Hence, a negative charge tends to be produced near the cathode and a positive charge near the anode.

Consider that a fused salt MX is taken as the ionic conductor in a U tube and two M electrodes are introduced into the system as shown in Fig. 5.36. Let the consequences of the passage of 1 faraday (F) of electricity be analyzed. Near the cathode, one equivalent of $M^+$ ions will be removed from the system by deposition on the cathode, and near the anode one equivalent of $M^+$ ions will be "pumped" into the system. Since one equivalent of $M^+$ has been added and another equivalent has been removed, the total quantity of $M^+$ ions in the system is unchanged (Table 5.28).

Is the system perturbed by the passage of a faraday of charge? Yes, because near the cathode, one equivalent of $M^+$ ions has been removed, which has created a local excess of negative charge. This local unbalance of electroneutrality creates a local electric field.[18] A similar argument can be used for the anode region.

How do the ions of the liquid electrolyte respond to this perturbation, i.e., this creation of local fields? The ions start drifting under the influence of the fields so that the initial state of electroneutrality and zero field is restored. How do the positive and negative ions share this responsibility of moving to annul the unbalance of charges—more anions than cations near the cathode and vice versa? It should be noted (Fig. 5.37) that the original

[18]This unbalance of electroneutrality and creation of field should not be confused with that arising from the presence of the electrode, which causes an anisotropy in the forces on the particles in the electrode-electrolyte interphase region. That anisotropy *also* produces an unbalance of electroneutrality and an electric double layer (Chapter 6) with a field across the interface, but it occurs only within the first few tens of nanometers of the surface.

**TABLE 5.28**

**Changes in MX at Electrodes of Metal M in Transport Experiment**

| | Anode Compartment | Cathode Compartment |
|---|---|---|
| Electrode process per faraday passed | 1 g-eq $M^+$ dissolved | 1 g-eq $M^+$ deposited |
| Move out of compartment | $t_+$ g-eq $M^+$ | $t_-$ g-eq $X^-$ |
| Move into compartment | $t_-$ g-eq $X^-$ | $t_+$ g-eq $M^+$ |
| Net change of $M^+$ | $1 - t_+$ g-eq gained $= t_-$ | $1 - t_+$ g-eq lost $= t_-$ |
| Net change of MX | $t_-$ g-eq gained | $t_-$ g-eq lost |
| Mass change of MX in case of molten salt | $t_- M_{MX}$ g gained, where $M_{MX}$ is eq. wt. of MX | $t_- M_{MX}$ g lost, where $M_{MX}$ is eq. wt. of MX |
| Concentration change in case of aqueous solution | $t_-/V_A$ g-eq $dm^{-3}$ increase, where $V_A$ is vol. of anode compartment ($dm^{-3}$) | $t_-/V_C$ g-eq $dm^{-3}$ decrease, where $V_C$ is vol. of cathode compartment ($dm^{-3}$) |

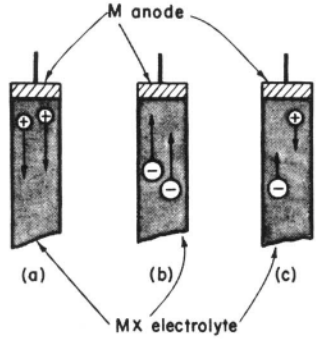


**Fig. 5.37.** The tendency for electroneutrality to be upset near electrodes is avoided in one of three ways. For example, near the anode, where positive charge tends to be produced, (a) positive ions can migrate away from the anode, (b) negative ions can migrate toward the anode, and (c) both (a) and (b) processes can occur to various extents.

electroneutral situation can be restored by (1) only cations moving in the anode-to-cathode direction; (2) only anions moving in the cathode-to-anode direction; and (3) both cations and anions moving in opposite directions to different extents. However, these possibilities represent different values of the transport numbers, which are the fractions of the total field-induced ionic drift arising from the various species.

5.6.7.2. *Measurement of Transport Numbers in Liquid Electrolytes.* Let $t_+$ and $t_-$ be the transport numbers of the $M^+$ and $X^-$ ions of the fused salt. The changes in the numbers of equivalents of $M^+$ and $X^-$ near the two electrodes are shown in Table 5.28, which is based on Fig. 5.36. The analysis of the changes leads to an interesting result. The passage of 1 F of charge is equivalent to transferring $t_-$ equivalents of the whole fused salt MX from the cathode region to the anode region (Fig. 5.38).

In the case of aqueous solutions, the ever-plentiful solvent could absorb this $t_-$ equivalents of MX and register the transfer as a concentration change of magnitude $t_-/V$ equivalents per liter, where $V$ is the volume of the compartment. On the other hand, a pure molten salt has no concentration variable. Hence, the transfer leads to an increase in mass near the anode.

In molten salts, therefore, it is the change in *mass* in a compartment that reveals transport numbers; in aqueous solutions, it was the change in *concentration.* However, unless it is performed properly, the experiment provides information only on the change in mass, not on the transport property.

What future has this mass increase? Left alone, the mass increase is short-lived and the transport experiment fails. This is because gravitational flow of the molten salt from the anode to cathode tends to equalize the amounts of MX in the two tubes (Fig. 5.39). It causes the liquid level in both tubes to be the same and wipes out the change in level that the ionic movements tend to make.

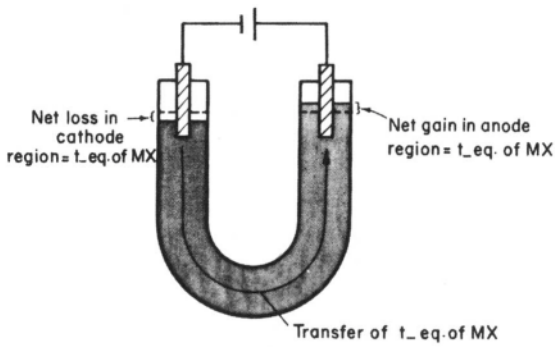


**Fig. 5.38.** As a result of the passage of 1 F of electricity, $t_-$ equivalents of MX electrolyte are transferred from the cathode region (where the electrolyte level falls) to the anode region (where the level rises).

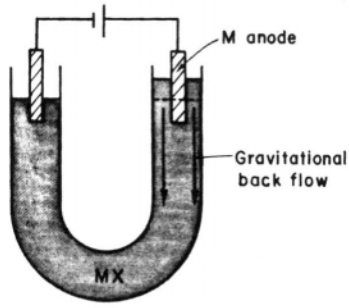


**Fig. 5.39.** The difference in electrolyte levels produced by the passage of 1 F of electricity leads to a gravitational flow of the electrolyte.

The first step in determining transport numbers in pure ionic liquids is to prevent the gravitational flow from masking the transfer of electrolyte. If the hydrodynamic backflow that gravity causes cannot be prevented, it must at least be taken into account. The general procedure is to minimize the gravitational flow by interposing a membrane between anode and cathode (Fig. 5.40). However, there are serious objections to the use of a membrane, owing to hydrodynamic interferences between this and the moving liquid.

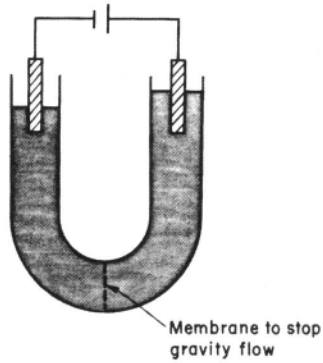


**Fig. 5.40.** The gravitational flow can be minimized by interposing a membrane between the anode and the cathode.

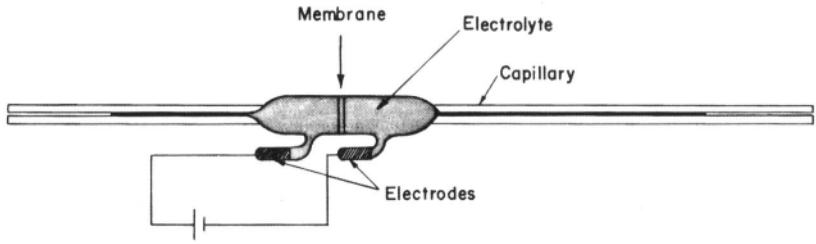


**Fig. 5.41.** A simple arrangement by which gravitational flow is avoided. The displacement of the electrolyte from the cathode to the anode region occurs at one level. The change in position of the melt in the capillary indicates the amount of electrolyte displaced.

It is also possible to open out the U tube and make the whole liquid "lie down" so that the movement of the fused salt occurs at one level and not against gravity. The amount of salt entering the anode region is then indicated, for example, by a sliver of molten metal pushed along by the movement of the salt in the capillary (Fig. 5.41). This method is also subject to difficulties, for the movement of salts in capillary tubes may not be smooth but is sometimes jerky.

This experiment directly demonstrates that *when electricity is passed through a fused salt, there is a movement of the salt as a whole.* In other words, the mass center of the liquid electrolyte moves. Now, the ions also are drifting with certain mobilities, i.e., velocities under unit field. But velocities with respect to what? One must define a coordinate system, or frame of reference, in relation to which the velocities (distances traversed in unit time) are reckoned. Though the laws of physics are independent of the choice of the coordinate system—the principle of relativity—all coordinate systems are not equally convenient. In fused salt it has been found convenient to use the mass center of the moving liquid electrolyte as the frame of reference, even though this choice, while providing a simple basis for computations, suffers from difficulties.

Even the elementary presentation given here makes it clear that transport-number measurements in fused salts are based on the transfer of the fused salt from the anode to the cathode compartment. The quantities measured are weight changes, the motion of indicator bubbles, the volume changes, etc. Some basic experimental setups shown in Fig. 5.42 include the apparatuses of Duke and Laity, Bloom, Hussey, and other pioneers in this field.

The migration of the electrolyte from the anode to the cathode compartment can also be followed by using radioactive tracers and tracking their drift. Since isotopic analysis methods are sensitive to trace concentrations, there is no need to wait for the electrolyte migration to be large enough for visual detection. The results of some transport-number measurements are given in Table 5.29.

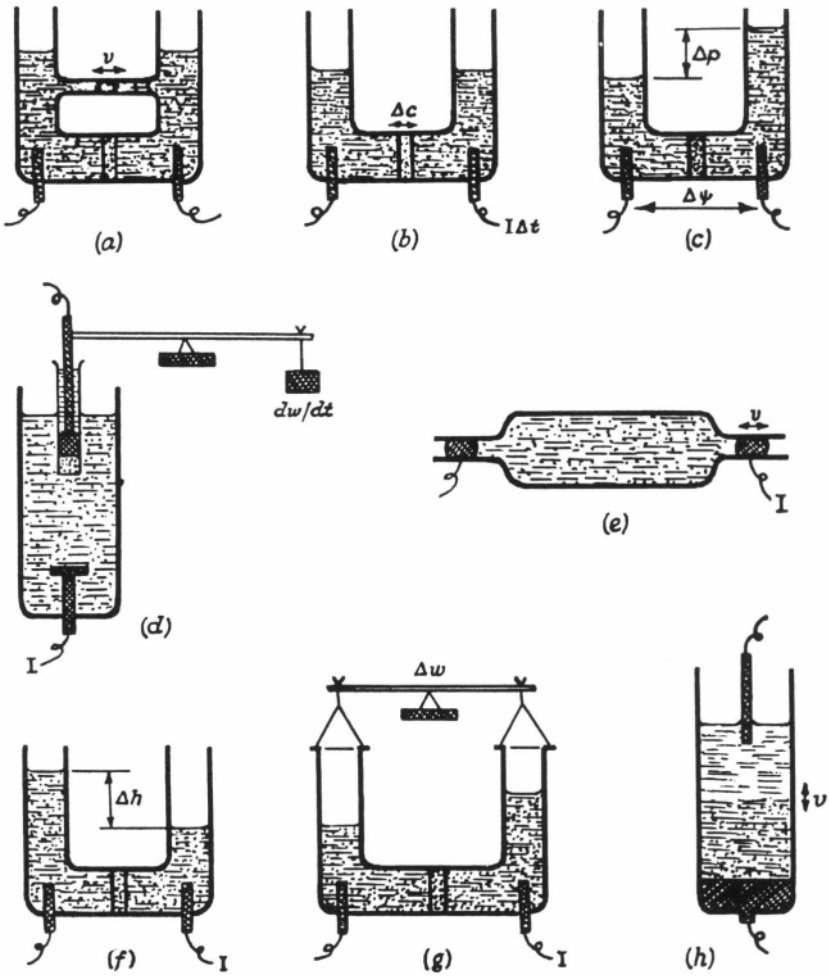


**Fig. 5.42.** Schematic diagrams of methods of determining transport numbers: (a) Measure velocity of the bubble; (b) measure transfer of the tracer; (c) measure the potential difference due to pressure difference; (d) measure the change in weight; (e) measure the transport of liquid metal electrodes; (f) measure the steady-state level; (g) measure the change in weight; (h) measure the moving boundary.

5.6.7.3. *Radiotracer Method of Calculating Transport Numbers in Molten Salts.* In the discussion of the applicability of the Nernst–Einstein equation to fused salts, it was pointed out that the deviations could be ascribed to the paired jump of ions resulting in a currentless diffusion. With fused NaCl as an example, it has been shown that there is a simple relation between the experimentally determined equivalent

**TABLE 5.29**
**Some Transport-Number Results for Fused Salts**

| Molten Salt | Transport Number of Cation |
|---|---|
| $LiNO_3$ | 0.84 |
| $NaNO_3$ | 0.71 |
| $AgNO_3$ | 0.72 |
| NaCl | 0.87 |
| KCl | 0.77 |
| AgCl | 0.54 |

conductivity $\Lambda'$ and the experimental diffusion coefficients of $Na^+$ and $Cl^-$ as indicated by radiotracer $Na^+$ and $Cl^-$. The relation is

$$\Lambda' = \frac{zF^2}{RT}(D'_{Na^+} + D'_{Cl^-}) - \frac{2zF^2}{RT} D_{NaCl} \tag{5.74}$$

From this expression, it is clear that one can determine $D_{NaCl}$. Knowing $D_{NaCl}$, one can obtain the diffusion coefficients $D_{Na^+,ind}$ and $D_{Cl^-,ind}$, of the independently jumping $Na^+$ and $Cl^-$ ions from the relations (5.69) and (5.70), i.e.,

$$D_{Na^+,ind} = D'_{Na^+} - D_{NaCl} \tag{5.80}$$

and

$$D_{Cl^-,ind} = D'_{Cl^-} - D_{NaCl} \tag{5.81}$$

Further, by using the Einstein relation [Eq. (4.172)] and the relation between absolute and conventional mobilities, one has

$$(u_{conv})_{Na^+} = z_{Na^+} e_0 (\bar{u}_{abs})_{Na^+} = z_{Na^+} e_0 \frac{D_{Na^+,ind}}{kT} = \frac{z_+ F}{RT} D_{Na^+,ind} \tag{5.82}$$

and similarly,

$$(u_{conv})_{Cl^-} = \frac{z_- F}{RT} D_{Cl^-,ind} \tag{5.83}$$

With these values of mobilities, the transport numbers can easily be calculated from the standard formulas

**TABLE 5.30**
**Comparison of the Transport Number of $Na^+$ in Molten NaCl Calculated from Equation (5.84) with Measured Values**

| | Transport Number of $Na^+$ in NaCl |
|---|---|
| Calculated from Eq. (5.84) | 0.71 |
| Measured values | 0.62 |
| | 0.87 |

$$t_+ = \frac{u_+}{u_+ + u_-} \quad \text{and} \quad t_- = \frac{u_-}{u_+ + u_-} \tag{5.79}$$

which, in the case of NaCl ($z_+ = z_- = 1$), reduces to

$$t_{Na^+} = \frac{D_{Na^+,ind}}{D_{Na^+,ind} + D_{Cl^-,ind}} \quad \text{and} \quad t_{Cl^-} = \frac{D_{Cl^-,ind}}{D_{Na^+,ind} + D_{Cl^-,ind}} \tag{5.84}$$

A comparison between transport numbers calculated in this way and those obtained by some of the experimental methods used is shown in Table 5.30.

## Further Reading

### *Seminal*


1. W. Klemm and W. Biltz, "Distribution of the Property of Ionic Conductance among Molten Salts on Liquid Halides in the Periodic Table," *J. Inorg. Chem.* **152**: 255 (1926).
2. F. R. Duke, R. W. Laity, and B. Owens, "Transport Numbers in Fused Salts," *J. Electrochem. Soc.* **104**: 299(1957).
3. A. Borucka, J. O'M. Bockris, and J. A. Kitchener, "The Nernst–Einstein Equation in Molten Salts," *Proc. Roy. Soc. Lond.* **A241**: 554 (1957).
4. G. J. Janz, C. Solomons, and H. J. Gardner, "Diffusion and Transport in Molten Salts," *Chem. Rev.* **58**: 241 (1958).
5. L. Nanis and J. O'M. Bockris, "Self-Diffusion: Heats of Activation as a Function of Melting Temperature," *J. Phys. Chem.* **67**: 2865 (1963).
6. H. Bloom, *The Chemistry of Molten Salts*, W. A. Benjamin, New York (1967).


### *Reviews*


1. C. L. Hussey, "Transport in and Transport Numbers in Molten Salts," in *Molten Salt Chemistry*, C. Mamantov and R. Marassi, eds., *NATO ASI Series C* **202**: 141 (1987).
2. C. A. Angell, "Transport and Relaxation Processes in Molten Salts," in *Molten Salt Chemistry*, G. Mamantov and R. Marassi, eds., *NATO ASI Series C* **202**: 123 (1987).
3. S. Smedley, *Interpretation of Ionic Conductivity in Liquids*, Plenum Press, New York (1990).

### *Papers*


1. S.I. Vavilov, *J. Non-Cryst. Solids* **123**: 34 (1990).
2. D. R. Chang, *Langmuir* **66**: 11332 (1990).
3. Y. Shirakawa and S. Tamaki, *J. Non-Cryst. Solids* **117**: 638 (1990).
4. D. G. Leaist, *Electrochim. Acta* **36**: 309 (1991).
5. K. Igarashi, *J. Electrochem. Soc.* **138**: 3588 (1991).
6. H. Rajabu, S. K. Ratke, and O. T. Furland, *Proc. Electrochem. Soc.* **16**: 595 (1992).
7. F. Lanlelme, A. Barhoun, and J. Chavelet, *J. Electrochem. Soc.* **140**: 324 (1993).
8. M. Poupait, C. S. Valesquez, and K. Hasseb, *J. Am. Chem. Soc.* **116**: 1165 (1994).
9. W. Wang and John Newman, *J. Electrochem. Soc.* **142**: 761 (1995).
10. C. Larive, M. Lin, and B. J. Piersma, *J. Phys. Chem.* **99**: 12409 (1995).
11. V. A. Payne, J. H. Xu, M. Fursyth, M. A. Ratner, D. F. Shriver, and S. W. Deleuw, *Electrochim. Acta* **40**: 2087 (1995).
12. C. Cametti, *J. Phys. Chem.* **100**: 7148 (1996).


## 5.7. USING A HOLE MODEL TO UNDERSTAND TRANSPORT PROCESSES IN SIMPLE IONIC LIQUIDS

### 5.7.1. A Simple Approach: Holes in Molten Salts and Transport Processes

Some facts about transport processes in molten salts have been mentioned (Section 5.6). Whether a hole model (Section 5.4) can provide an interpretation of these must now be examined. First it is necessary to cast the model into a form suitable for the prediction of transport properties. The starting point is the molecular-kinetic expression (Appendix 5.3) for the viscosity $\eta$ of a fluid, i.e.,

$$\eta = 2nm\langle v\rangle l \tag{5.85}$$

where $n$ and $m$ are the number per unit volume and the mass of the particles of the fluid, $\langle v\rangle$ is the mean velocity of the particles, and $l$ is their mean free path.

The quantity $l$ is linked to the model for viscous flow in fluids. According to this picture (Fig. 5.43), a fluid in motion is considered to consist of layers lying parallel to the direction of flow. (The slipping and sliding of these layers against each other provides the macroscopic explanation of viscosity.) When particles jump between neighboring layers, there is momentum transfer between these layers, the cause of viscous drag (Fig. 5.44). In this picture, the symbol $\langle v\rangle$ is taken to represent the component of the average velocity of the particles in a direction normal to the layers.

Irrespective of whether the fluid is in motion, the particles constituting the fluid continuously execute random motion. The particles of a *flowing* fluid have a drift superimposed upon this random walk. It is by means of the random walk of the particles from one layer to another that the momentum transfer between layers is

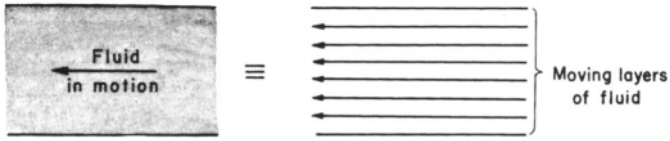


**Fig. 5.43.** A fluid in motion is considered equivalent to moving layers of fluid, the layers lying parallel to the flow direction.

carried on. This momentum transfer is visible to the observer as the *viscosity* of the fluid.

Holes also move. As argued earlier (Section 5.5.1), anything that moves at finite velocities must have an inertial resistance to motion, i.e., a mass (see Appendix 5.1). Although it may continue to be surprising, holes have masses and moving holes have momenta.

Thus, according to the hole theory, the random walk of holes between adjacent layers results in momentum transfer and therefore viscous drag in a moving fused salt (Fig. 5.45). On the basis of this model, the expression for the viscosity of an ionic liquid is

$$\eta = 2n_h m_h \langle v_h \rangle l_h \tag{5.86}$$

where $n_h$ and $m_h$ are the number per unit volume and the apparent mass for translational motion of the holes.

The velocity component $\langle v_h \rangle$ is given by the ratio of $l_h$, the mean distance between collisions (i.e., the mean free path), to $\tau$, the mean time between collisions,

$$\langle v_h \rangle = \frac{l_h}{\tau} \quad \text{or} \quad \langle v_h \rangle l_h = \langle v_h \rangle^2 \tau \tag{5.87}$$

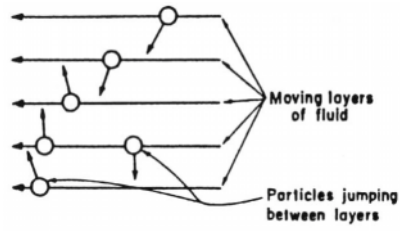


**Fig. 5.44.** Viscous forces are considered to arise from the momentum transferred between moving fluid layers when particles jump from one layer to another.

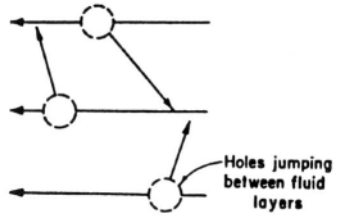


**Fig. 5.45.** According to the hole model, viscous drag arises from the momentum transferred between moving fluid layers when holes jump from one layer to another.

The viscosity can be written as follows

$$\eta = 2n_h\tau(m_h\langle v_h\rangle^2) \tag{5.88}$$

The theorem of the equipartition of energy can now be applied to the one-dimensional motion referred to by $\langle v_h \rangle$

$$\frac{1}{2} m_h\langle v_h\rangle^2 \approx \frac{1}{2} kT \tag{5.89}$$

and using this approximate relation, one has

$$\eta = 2n_h kT\tau \tag{5.90}$$

### 5.7.2. What is the Mean Lifetime of Holes in the Molten Salt Model?

The parameter $\tau$ now invites consideration. In the gas phase, $\tau$ is the mean time between collisions. What is the significance of $\tau$ in an ionic liquid?

In a liquid, in the present model, $\tau$ would be the mean lifetime of a hole, i.e., the average time between the creation and destruction of a hole through thermal fluctuation. To calculate this, one may use the formula for the number of particles escaping from the surface of a body per unit time per unit area into empty space, i.e.,

$$a = c\left(\frac{kT}{2\pi m}\right)^{1/2} e^{-A/RT} \tag{5.91}$$

where $c$ is the number of particles per unit volume, $m$ is the mass of a particle, and $A$ is the work necessary for a mole of particles lying on the surface of the hole to be released into its interior.

In a time $t$, $4\pi\langle r_h\rangle^2 at$ particles escape from the exterior into a spherical hole of radius $\langle r_h\rangle$. The hole will be filled by these particles if this number is equal to the number of particles in a sphere of radius $\langle r_h\rangle$, that is, $(4/3)\pi\langle r_h\rangle^3 c$. Then the time for destruction of the hole is

$$\tau = \frac{1}{3}\frac{\langle r_h\rangle c}{a} \tag{5.92}$$

Obviously, this is also the time for hole formation, and the lifetime, from Eqs. (5.91) and (5.92), is

$$\tau = \frac{\langle r_h\rangle}{3}\left(\frac{2\pi m}{kT}\right)^{1/2} e^{A/RT} \tag{5.93}$$

This is the mean lifetime of a hole. This expression is consistent with the idea that the hole theory represents a Swiss-cheese sort of model of a liquid with holes of different sizes [for $\langle r_h\rangle$ is the *mean* radius for holes varying in size according to Eq. (5.44)]. The holes keep on opening and shutting, and the mean time they are open is given by Eq. (5.93).

Before one leaves expression (5.93), it is well to note the innocent acceptance with which $A$ has been treated. It is the heat term associated with getting a hole "unmade," with collapsing the hole, the negative of the work of forming the hole. However, it has not yet been said how this will be calculated, and what terms go into this. Such a calculation will be one test that will be made of the hole theory in Section 5.7.6.

### 5.7.3. Viscosity in Terms of the "Flow of Holes"

By inserting the expression for the mean lifetime of a hole [Eq. (5.93)] into Eq. (5.90), one obtains the hole-theory expression for viscosity. Thus,

$$\eta = 2n_h kT\left[\frac{1}{3}\langle r_h\rangle\left(\frac{2\pi m}{kT}\right)^{1/2} e^{A/RT}\right]$$

$$= \frac{2}{3} n_h \langle r_h\rangle (2\pi m kT)^{1/2} e^{A/RT} \tag{5.94}$$

There are two quantities on the right-hand side of Eq. (5.94) which need discussion. They are $n_h$, the number of holes per unit volume of the liquid, and $A$, which occurs in the Boltzmann factor $\exp(-A/RT)$, for the probability of a successful filling of a hole. These quantities are discussed in terms of the closely related quantity of diffusion.

### 5.7.4. The Diffusion Coefficient from the Hole Model

Now that the viscous flow properties of an ionic liquid have been discussed, the next task is to derive an expression for the diffusion coefficient. The present modeling interpretation of the elementary act of a transport process consists of hole formation followed by a particle jumping into the hole. The focus in this elementary act has hitherto been the center of the hole.

What is the situation at the original site of the jumping ion? Alternatively stated: What has happened, as a consequence of the jump process, at the point where the ion was before it jumped? At this prejump site, there has been precisely that moving away of particles from a point that corresponds to hole formation (Fig. 5.46).

Thus, when a particle jumps, it leaves behind a hole. So then, instead of saying that a transport process occurs by particles hopping along, one could equally well say that the transport processes occur by *holes* moving. The concept is commonplace in semiconductor theory, where the movement of electrons in the conduction band is taken as being equivalent to a movement of so-called "holes" in the valence band. It has in fact already been assumed at the start of the viscosity treatment (Section 5.7.1) that the viscous flow of fused salts can be discussed in terms of the momentum transferred between liquid layers by moving holes.

Hence, when diffusion of particles occurs, there is a corresponding diffusion of holes. Instead of treating *ionic* diffusion as a separate subject, therefore, one can consider *hole* diffusion and write the Stokes–Einstein relation (Section 4.4.8) for the diffusion coefficient of holes

$$D = \frac{kT}{6\pi \langle r_h \rangle \eta} \tag{5.95}$$

The hole-theory expression for viscosity is known. It is Eq. (5.94). Let this be introduced into Stokes–Einstein relation [Eq. (5.95)]. Using Eq. (5.44) the result is

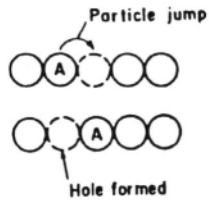


**Fig. 5.46.** When a particle jumps into a hole, there is the formation of a hole at the prejump site of the particle.

$$D = \frac{kT}{4\pi \langle r_h \rangle^2} \frac{(2\pi mkT)^{-1/2}}{n_h} e^{-A/RT}$$

$$= \frac{1}{4\pi(0.51)^2} \frac{\gamma}{n_h} (2\pi mkT)^{-1/2} e^{-A/RT}$$

$$= 0.31 \frac{\gamma}{n_h} (2\pi mkT)^{-1/2} e^{-A/RT} \tag{5.96}$$

The number of holes per unit volume can be expressed in terms of the known volume expansion of a mole of the liquid at the melting point $\Delta V_T$ divided by the mean hole volume $\langle V_h \rangle$ and reduced to the number per cubic centimeter by dividing by the molar volume of the liquid at $T$, $V_T$. Hence,

$$D = 0.31\gamma \frac{\langle V_h \rangle V_T}{\Delta V_T} (2\pi mkT)^{-1/2} e^{-A/RT} \tag{5.97}$$

Utilizing the value of the hole volume derived by substituting for $\langle r_h \rangle$ from Eq. (5.44) in $\langle V_h \rangle = (4/3)\pi \langle r_h \rangle^3$

$$D = \frac{0.17kTV_T}{(2\pi m)^{1/2} \Delta V \gamma^{1/2}} e^{-A/RT} \tag{5.98}$$

The assumed identity of the rates of hole diffusion and ionic diffusion is recalled. Thus, the final expression for the diffusion coefficient of ions in a fused salt is the same as that for holes, i.e., Eq. (5.98).

The first point to note about this expression, apart from the fact that it is of the form of the experimentally observed variation of $D$ with temperature (i.e., $D = D_0 e^{-E_D/RT}$), is that the energy of activation for self-diffusion of cations and anions should be the same. This is what is observed in Table 5.31.

What is meant by the term "Arrhenius activation energy?" This term arose from the work of the early gas kineticists, who wrote equations of the type

$$\text{Rate} = Ze^{-E/RT} \tag{5.99}$$

and considered $Z$ to have a negligible temperature dependence. Such an assumption would of course give

$$E = -R \frac{\partial \ln D}{\partial (1/T)} \tag{5.100}$$

**TABLE 5.31**

**Energies of Activation of Cation and Anion for Self-Diffusion in Simple Molten Electrolytes**

| | $E_D^{\neq}$ (kJ mol$^{-1}$) | |
|---|---|---|
| Molten Salt | Cation | Anion |
| NaCl | 30 ± 1 | 31 ± 3 |
| KCl | 29 ± 2 | 30 ± 2 |
| $CaCl_2$ | 26 ± 3 | 37 ± 4 |
| $SrCl_2$ | 23 ± 4 | 29 ± 3 |
| $BaCl_2$ | 38 ± 5 | 40 ± 4 |
| $CdCl_2$ | 28 ± 2 | 29 ± 3 |

and it is this coefficient that is often identified with the "energy of activation." Therefore, if one wants to calculate what a theory gives for this, one has to take into account whatever temperature dependence is possessed by the preexponential factor in the theory. If one knew (as one hopes to know later on in this chapter) a theoretical expression for $A$ of Eq. (5.98), one would have to calculate a theoretical value for $E$ from Eq. (5.100) (including the effect of the temperature dependence of the preexponential) and compare its theoretical value with the experimental value of $E$ calculated from Eq. (5.100). From Eq. (5.98),

$$-R\frac{\partial \ln D}{\partial(1/T)} = A + RT - RT^2\left(\frac{1}{\Delta V_T}\frac{d\Delta V_T}{dT} + \frac{1}{2\gamma}\frac{d\gamma}{dT} - \frac{1}{V_T}\frac{dV_T}{dT}\right) \tag{5.101}$$

In the following sections, a value of $A$ will be calculated. Used in the right-hand side of Eq. (5.101), it gives there the theoretical prediction of the experimental energy of activation, i.e., the left-hand side of Eq. (5.101) [*cf.* Eq. (5.100)].

### 5.7.5. Which Theoretical Representation of the Transport Process in Molten Salts Can Rationalize the Relation $E^{\neq} = 3.74RT_{m.p.}$?

It has been pointed out (Sections 5.6.2.2 and 5.6.3) that the heats of activation for viscous flow and for self-diffusion are given by the empirical generalization $E_\eta^{\neq} = E_D^{\neq} = 3.74RT_{m.p.}$, where $T_{m.p.}$ is the melting point in kelvins. Some of the data that support this statement are plotted in Figs. 5.28 and 5.30. The empirical law is applicable to all nonassociated liquids, not only ionic liquids. An empirical generalization that encompasses the rare gases, organic liquids, the molten salts, and the molten metals is indeed a challenge for theories of the liquid state, and hence also for fundamental electrochemists interested in pure liquid electrolytes.

Several approaches to the theory of liquids can be distinguished (see Section 5.2). One may express the properties of a liquid in terms of a distribution function (as given in Section 5.2.3.2), an expression that indicates the probability of finding particles at a distance $r$ from a central reference ion. One may be able to calculate the distribution function itself from molecular dynamics. Alternatively, one can make educated guesses about the scenarios inside the liquid, i.e., one agrees to temporarily assume a number of competing models of the structure, and goes on to develop the mathematical consequences of the various assumptions. The results of predictions from alternative models can then be compared with experiments and one may decide upon the most experiment-consistent model and use it as a working hypothesis to calculate other properties of the liquid model.

Several differing simple models of molten salts do indeed give reasonably close calculations of equilibrium properties, e.g., compressibility and surface tension. What these models do not do, however, is to quantitatively rationalize the data on the temperature dependence of conductance, viscous flow, and self-diffusion. The discovery by Nanis and Richards of the fact that simple liquids have heats of activation for all three properties given approximately by $3.74RT_{\text{m.p.}}$ presents a clear and challenging target for testing models of liquids.

### 5.7.6. An Attempt to Rationalize $E_D^{\neq} = E_\eta^{\neq} = 3.74RT_{\text{m.p.}}$

To find what Fürth's hole theory predicts for the heat of activation in viscous flow, it is necessary to attempt to use it to calculate the term $A$ in, e.g., Eq. (5.98). The meaning of $A$ has already been defined in Section 5.7.2. It is the work done in transferring a mole of particles from the surroundings of a hole into its interior.

An assumption will now be added to the model. It is that near or at the melting point, a hole is annihilated by the "evaporation" into it of *one* particle; i.e., just one particle fills it. There is no violation of physical sense in this assertion, for use of Eq. (5.44) shows that the size of the holes predicted by the hole theory is near that of the ions which are assumed in the model to jump into them. Correspondingly, the work done to annihilate a hole is numerically equal to the work done in forming a surface of radius $r$, namely, $4\pi\langle r\rangle^2\gamma$, where $\gamma$ is the surface tension. Hence, if $n_T$ particles must jump into a hole to annihilate it at temperature $T$

$$\frac{n_T A_T}{N_A} = 4\pi\langle r_T\rangle^2\gamma_T \tag{5.102}$$

where $A_T$ is the term $A$ (*per mole*, not molecule) at the temperature $T$. With the assumption made ($n_{\text{m.p.}} = 1$),

$$A_{\text{m.p.}} = N_A 4\pi\langle r_{\text{m.p.}}\rangle^2\gamma_{\text{m.p.}} \tag{5.103}$$

What of $n_T$ at $T$s other than the melting point, at which temperature $n_T$ has been assumed to be unity? From Eq. (5.44), the hole volume—and hence its surface area—should increase as $T$ increases (and $\gamma$ decreases, as it does with an increase in $T$). Of course, ions surround the hole and it seems reasonable to assume that as the hole volume increases, the number of ions that surround it will increase, and thus the number that is needed to fill it (thus causing the work $4\pi\langle r_T\rangle^2\gamma_T$) will also increase.

Let it be assumed that the difference ($\Delta V_T$) between the volume of the liquid salt and that of the corresponding solid is due only to holes. Then the number of holes per mole of salt at temperature $T$ is

$$\frac{\Delta V_T}{\langle v_{h,T}\rangle} \tag{5.104}$$

where $\langle v_{h,T}\rangle$ is obtained from Eq. (5.44).

Thus, the number of ions per hole at $T$ is

$$\frac{2N_A}{\Delta V_T/\langle v_{h,T}\rangle} \tag{5.105}$$

Hence,

$$\frac{\text{Ions per hole at } T}{\text{Ions per hole at m.p.}} = \frac{\Delta V_{\text{m.p.}}}{\Delta V_T}\,\frac{\langle v_{h,T}\rangle}{\langle v_{h,\text{m.p.}}\rangle} \tag{5.106}$$

Let it be assumed that the number of ions that will be needed to fill the hole at any temperature would be proportional to the number of ions per hole in the liquid. Thus,

$$\frac{n_T}{n_{\text{m.p.}}} = \frac{\Delta V_{\text{m.p.}} v_{h,T}}{\Delta V_T v_{h,\text{m.p.}}} \tag{5.107}$$

However,

$$n_T A_T = 4\pi N_A \langle r_T\rangle^2 \gamma_T \tag{5.108}$$

$$A_T = \frac{4\pi N_A \langle r_T\rangle^2 \gamma_T \Delta V_T v_{h,\text{m.p.}}}{\Delta V_{\text{m.p.}} v_{h,T}} \tag{5.109}$$

with $n_{\text{m.p.}} = 1$.

Thus [and with Eq. (5.44)]

$$\frac{A_T}{A_{\text{m.p.}}} = \frac{T_{\text{m.p.}}^{1/2}}{T_T^{1/2}} \frac{\Delta V_T}{\Delta V_{\text{m.p.}}} \frac{\gamma_T^{3/2}}{\gamma_{\text{m.p.}}^{3/2}} \tag{5.110}$$

One can obtain numerical values for the term on the right. It has been calculated from experimental data for some 14 simple molten salts, and if one restricts the range of experimental data used to about 200 K above the melting point, it is found that

$$\frac{T_{\text{m.p.}}^{1/2}}{T_T^{1/2}} \left( \frac{\gamma_T}{\gamma_{\text{m.p.}}} \right)^{3/2} \frac{\Delta V_T}{\Delta V_{\text{m.p.}}} \simeq 1 \tag{5.111}$$

Under such circumstances, from Eqs. (5.110) and (5.111),

$$A_T = A_{\text{m.p.}} \tag{5.112}$$

However,

$$A_{\text{m.p.}} = 4\pi \langle r_{\text{m.p.}} \rangle^2 \gamma_{\text{m.p.}} \tag{5.113}$$

From Eq. (5.44)

$$A_{\text{m.p.}} = 4\pi(0.51)^2 k T_{\text{m.p.}} = 3.3 k T_{\text{m.p.}} \text{ per ion} = 3.3 R T_{\text{m.p.}} \text{ per g-ion} \tag{5.114}$$

From Eq. (5.112),

$$A_T = A_{\text{m.p.}} = 3.3 R T_{\text{m.p.}} \tag{5.115}$$

This result may be compared with the empirical heat of activation by substituting it in Eq. (5.101). The term on the left of this equation, the experimental values, are found to be about $3.7RT_{\text{m.p.}}$. Using $A = 3.3RT_{\text{m.p.}}$, for which the derivation has been given here, on the right of Eq. (5.101), one obtains agreement between observed and calculated values of the heat of activation to within about 5–10%. The theory of holes is thus able to give some approximate, numerical account of the heat of activation in the transport of simple liquids above the melting point.

### 5.7.7. How Consistent with Experimental Values Is the Hole Model for Simple Molten Salts?

The Swiss-cheese model approach is consistent with the X-ray data, which show that the distance apart of ions remains constant or decreases on melting while the volume increases ~20%. In this respect, it is more consistent with experiment than

some other models which upon melting involve expansion of the "cell" in which each ion spends most of its life (so that the internuclear distance would increase).

An example of the ability of this Fürth hole model to reproduce experimental data numerically without previous appeal to experimental values of similar systems is shown in Table 5.32, which gives a comparison of experimental expansivities with the values that the hole theory yields. An interesting aspect of the evidence supporting the usefulness of this model is the relation of the (cell) free volume (Fig. 5.47) to the volume of the expansion of melting. This free volume, in the sense referred to here, is

**TABLE 5.32**

**Comparison of Calculated Expansivities with the Experimental Values**

| Salt | Temp. (°C) | $10^4\alpha$, Calc. ($°C^{-1}$) | $10^4\alpha$, Obs. ($°C^{-1}$) |
|---|---|---|---|
| LiCl | 614 | | |
| | 800 | 4.0 | 3.0 |
| | 900 | | |
| | 1000 | 4.0 | 3.3 |
| NaCl | 800 | 3.3 | 3.6 |
| | 900 | | |
| | 1000 | 3.6 | 3.9 |
| KCl | 772 | | |
| | 800 | 2.8 | 3.9 |
| | 900 | | |
| | 1000 | 3.2 | 4.2 |
| CsCl | 642 | | |
| | 800 | 4.2 | 4.1 |
| | 900 | | |
| | 1000 | 4.4 | 4.5 |
| $CdCl_2$ | 600 | 2.7 | 2.4 |
| | 700 | 2.7 | 2.4 |
| | 800 | 2.9 | 2.5 |
| NaBr | 747 | | |
| | 800 | 3.2 | 3.1 |
| | 900 | | |
| | 1000 | 4.0 | 3.4 |
| KBr | 735 | 2.5 | 3.7 |
| | 800 | 2.6 | 3.8 |
| | 900 | | |
| | 1000 | 3.0 | 4.1 |
| CsBr | 636 | 4.0 | 4.4 |
| | 800 | 4.2 | 4.6 |
| | 900 | | |
| | 1000 | 4.4 | 5.1 |

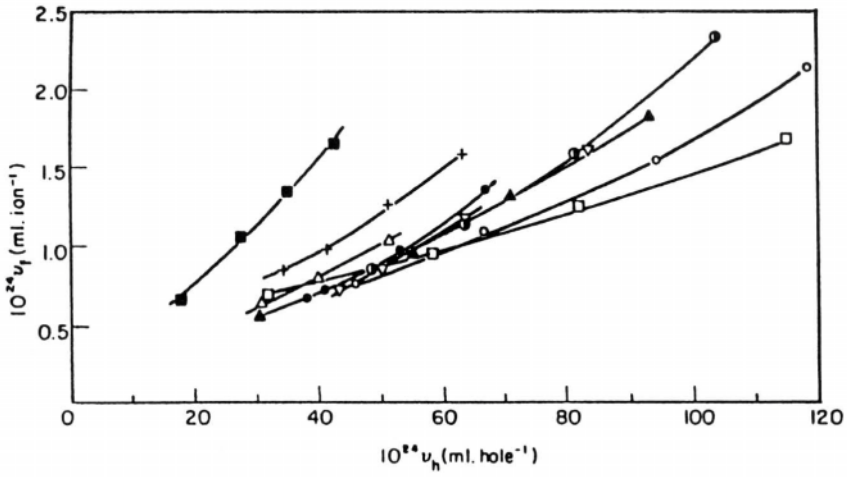


**Fig. 5.47.** Plot of the free volume per ion against the average hole volume; (■) LiCl, (△) NaCl, (●) KCl, (▲) CsCl, (+) NaBr, (▽) KBr, (◑) CsBr, (□) NaI, (○) KI.

the space that is free to each atom on the average. This relation is shown in Fig. 5.47. The continuous increase of the free volume with the hole volume is what would be expected with a model in which, for between one in five atoms, there is a neighboring hole, so that when a vibrating atom comes into contact with this space, its free volume (= cell free volume and part of the volume of the hole) is increased. Thus, the free volume due to the space within cells is related also to the hole volume, the volume injected on melting, because the average ion's freedom to move is increased by the presence of holes. This is just what Fig. 5.47 confirms.

One must not give the impression that Fürth's theory of holes in molten salts is more than an attempt to see what can be done in the matter of replicating experimental values without the use of experimental data relied on by competing models. It is the model that gives the greatest degree of numerical agreement for several properties, particularly those of transport. It is, on the other hand, a very crude model indeed. It attempts to deal with the problem in a curious, perhaps ingenious, way by using an analogy between holes in an actual molten salt and bubbles in a near-boiling liquid. One might at first not take it seriously, particularly when one finds that it eliminates the term $(P_I - P_O)V$ by assuming that the liquid is near boiling when $P_I = P_O$, but one should see merit in the ability of the model to predict experimental data without relying on values obtained from previous experimental determinations, as is done in Monte Carlo and molecular dynamics approaches. On the other hand, the theory involves some far-fetched imagery, for example, that *one* particle or thereabouts evaporates to annihilate a hole.

Further consideration shows that a liquid molten salt bears more than one resemblance to predictions of the hole theory. Ions do indeed tend to cling together in clusters so that the internuclear distance does not increase to allow for the observed large increase in volume on melting. Between these clusters of ions are gaps and cavities of varying sizes, undergoing rapid changes in size. Some models similar to the hole model seem unavoidable *if one is to attain consistency with the increase of volume on melting but lack of increase of the internuclear distance in the process.* No model of simple molten salts should be considered valid except a model that replicates such unbending facts, and after that it is largely a matter of how to describe the space introduced, varying in size and lifetime, in terms of physical chemistry, which is the challenge and the answer to the question: "Why is a liquid so fluid while a solid is so rigid?"

### 5.7.8. Ions May Jump into Holes to Transport Themselves: Can They Also Shuffle About?

*Constant-Volume Measurements: Big Jumps?* The theories representing trans- port in molten liquids which have been the subjects of Section 5.6 are all consistent with the one general idea as to how transport works in molten salts. This is that ions vibrate in their cells surrounded on all sides by counterions for a relatively long time, but when the opportunity arrives, they dart off into a nearby vacancy of some kind. Only Fürth's theory is clear about what they dart to—an opened-up neighboring cavity similar to those in the Woodcock and Singer model of Fig. 5.14, which then gets 90% filled up by the ion's arrival.

Then the rate at which transport, viscous flow, diffusion, and conduction occur is controlled by either the rate at which the opportunities for escape occur or the ease with which the ion jumps into the new "open structure." Of course, these statements apply only to molten salts such as sodium chloride, simple molten salts as they are called, and those for which the log $D$ versus $1/T$ line is straight (Fig. 5.49).[19] If the molten salt forms complexes (e.g., $ZnCl_4^{2-}$, which is formed in $NaCl\text{-}ZnCl_2$), then it is rather different; the control of transport rate in these substances will be discussed in a later section.

It is desirable to give some evidence that supports the idea that the ions await some rearrangement that allows the transporting ion to have a less coordinated existence for the brief moment of movement. If one determines the diffusion coefficient (or conductance, or viscosity) at constant pressure, then both these processes—the making of the cavity and the jumping into it—are components of the heat of activation (see Figs. 5.48 and 5.49). This can be written as

[19]Many molten salts apart from the archetypal NaCl show a straight line for log $D$ – $1/T$.

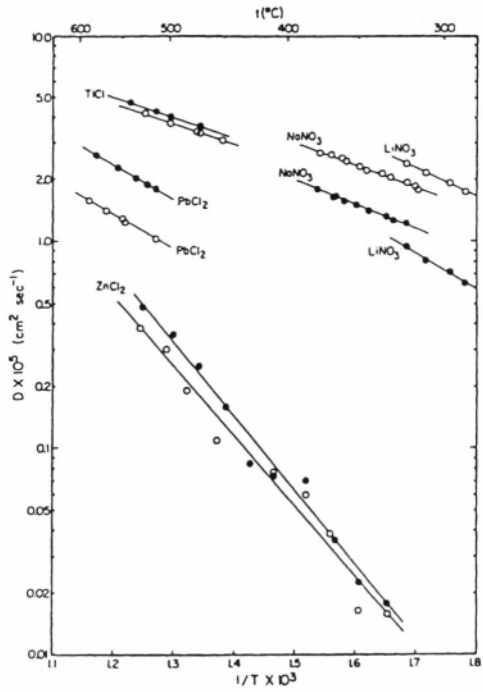


**Fig. 5.48.** Arrehnius plots of fused salt self-diffusion coefficients; (●) anions; (○) cations. [$LiNO_3$ and $NaNO_3$, Dworkin et al. (1960); TlCl and $PbCl_2$, Angell and Tomlinson (1965); $ZnCl_2$, Sjoblom and Behn (1968).]

$$-R\left(\frac{\partial \ln D}{\partial(1/T)}\right)_P = \Delta H_H^{\neq} + \Delta H_J^{\neq} \tag{5.116}$$

where the suffixes $H$ and $J$ represent, respectively, the process of hole formation and that for jumping into it.

One may also keep the temperature constant but vary the external hydrostatic pressure. Doing this at various temperatures, one obtains relations such as those shown in Fig. 5.50. Thus, knowing the expansivity and compressibility of the molten salt concerned, one can figure out what values of log $D$ have the same volume, though at different temperatures (see Figs. 5.51 and 5.52).

At constant volume there can be no change in volume as the temperature increases, a hypothetical and artificial state. Under these hypothetical conditions, changes of transport with temperature cannot be affected by any corresponding increase in the number of holes with temperature for if more holes were to increase with an increase of volume, the volume of the solution would increase. Hence, under such (hypotheti-

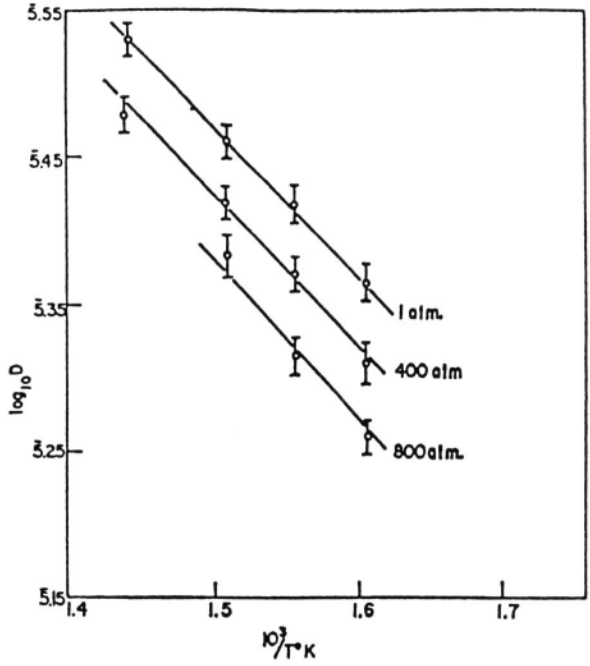


**Fig. 5.49.** Activation energy for diffusion at constant pressure ($^{134}$Cs ion in molten $NaNO_3$).

cal) conditions of constant volume, the energy for hole formation would no longer influence the rate of diffusion. For this reason, it is reasonable to write

$$-\left(\frac{\partial \ln D}{(1/T)}\right)_V = \Delta H_j^{\ddagger} \tag{5.117}$$

Knowing the values of $(\partial \ln D)/[\partial(1/T)]$ both at constant pressure but also at constant volume, one can separate out the heats of activation: the one for the formation of holes, and the one for jumping into holes. Some of the values obtained for ordinary liquids, molten metals, and molten salts are shown in Table 5.33.[20]

In rate theory terms, the rate constant for a happening is given by

$$\vec{k} = \frac{kT}{h} e^{-\Delta H^{\ddagger}/RT} e^{\Delta S^{\ddagger}/R} \tag{5.118}$$

[20]If $\Delta H_j^{\ddagger}/\Delta H_H^{\ddagger} < 0.3$, the "make hole, then jump in" model makes sense. It makes less sense if $\Delta H_j^{\ddagger}/\Delta H_H^{\ddagger} > 0.3$. Holes are there, all right, but they could be simply geographic features of the structure.

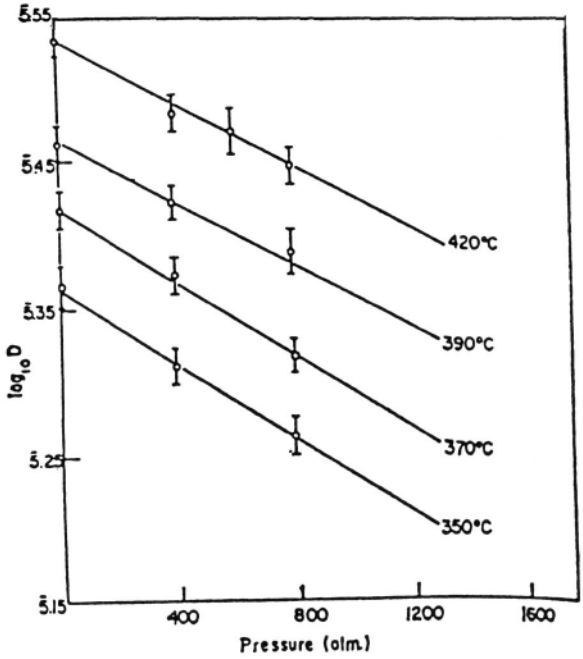


**Fig. 5.50.** Effect of pressure on the diffusion of $^{134}Cs$ ion in molten $NaNO_3$.

so that the lifetime of an event (e.g., the formation of a cavity) is

$$\tau = \frac{h}{kT} e^{\Delta H^{\neq}/RT} e^{-\Delta S^{\neq}/R} \tag{5.119}$$

Knowing $\Delta H^{\neq}$ and estimating $\Delta S^{\neq}$, the entropy of activation for its formation, one can calculate how long the hole will last.[21] Thus, the values experimentally found for $\Delta H_H^{\neq}$ and $\Delta H_J^{\neq}$ show that the hole lasts longer than the time for jumping

[21]There is a quantity referred to in transport calculations called the *velocity autocorrelation function* (see Section 4.2.19). When applied to the velocity of particles in liquids, it refers to the time needed for a particle to be free of the influence of the previous movement of particles (i.e., uncorrelated). For KCl at 1045 K, the value calculated by Smedley and Woodcock by means of a simulation gave $3 \times 10^{-13}$ s for the autocorrelation function—about one-tenth of the time for a jump calculated by a hole model (see Table 5.33) for $NaNO_3$.

This result is more consistent with a "shuffle-along" (Swallin) model than the "wait-for-a-cavity-and-leap-into-it" model. The weight of evidence (particularly the $E^{\neq} = 3.74\, RT_{m.p.}$ law) is in the other direction and one must then ask if neglect of the 20% volume increase on melting (with a decrease of internuclear distance) has invalidated the significance of the results in Smedley and Woodcock's calculation. To support this suggestion, one may point to the wrong sign arising from such models in calculating deviations from the Nernst-Einstein equation.

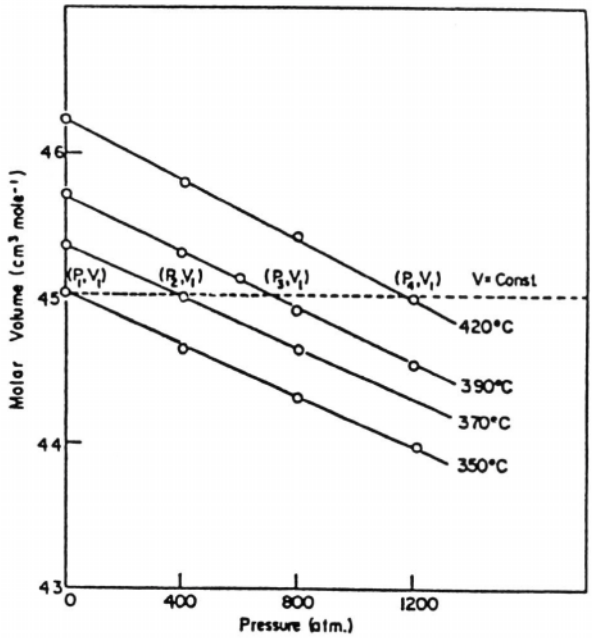


**Fig. 5.51.** Evaluation of constant-volume conditions (molten $NaNO_3$). Standard of reference: 1 atm, 623 K ($P_1$, $V_1$).

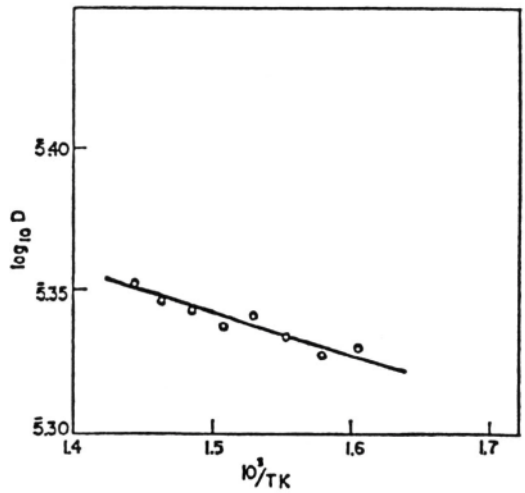


**Fig. 5.52.** Activation energy of "jumping" ($^{22}Na$ ion in molten $NaNO_3$).

**TABLE 5.33**

**Comparison of Heats of Activation at Constant Volume and Constant Pressure**

| Liquid | m.p. (K) | $\Delta H_H^{\neq}$ (kJ mol$^{-1}$) | $\Delta H_J^{\neq}$ (kJ mol$^{-1}$) | $\Delta H_J^{\neq}/\Delta H_H^{\neq}$ |
|---|---|---|---|---|
| $CCl_4$ | 250.3 | 13.8 | 4.6 | 0.33 |
| $C_6H_6$ | 278.6 | 16.7 | 2.9 | 0.25 |
| Hg | 234.2 | 4.2 | 4.0 | 0.96 |
| Ga | 302.9 | 4.6 | 4.1 | 0.89 |
| $NaNO_3$ | 580.0 | 18.0 | 3.3 | 0.18 |

($\Delta H_H^{\neq} >> \Delta H_J^{\neq}$). This is just a confirmatory calculation and it could not be any other way if the idea of an ion waiting for the right juxtaposition of things—so it has space to move elsewhere—represents microscopic reality, at least for the systems for which the above result holds.

### 5.7.9. Swallin's Model of Small Jumps

Many years ago, Swallin suggested another idea as a model for transport in molten metals and molten salts.[22] In his view, the free space that occurs when a liquid melts does not play a part in the mechanism of transport, diffusion, conductance, and viscous flow. This occurs, he suggested, by means of microjumps, a movement not unlike the gyrations of a person in a large football crowd trying to get out to his seat in the front row. Gaps in the crowd are too small to aid his motion, so that the only way is to shuffle slowly forward, pushing and being pushed. Swallin's[23] suggestion did not sit well with researchers studying molten salt at the time of its publication, however, because it was accompanied by the following equation

$$\Delta V^{\neq} = \frac{1}{6}\pi x_0^2 l \tag{5.120}$$

where $l$ is the jump distance and $x_0$ is the average distance between ion centers. This $\Delta V^{\neq}$ is the volume difference between the ion in its activated state—the quintessential situation of movement in the rate-determining happening—and the initial state, and it is determined easily at constant temperature from the equation

[22] The fact that (see Fig. 5.28) the temperature dependence of rare-gas liquids, ordinary liquids, liquid metals, and molten salts obeys the equation $E^{\neq} = 3.74\,RT_{\text{m.p.}}$ may mean they all have similar mechanisms for transport.

[23] Swallin's 1959 suggestion was made for metals. Here it may be more applicable than it seems to be to molten salts. Thus, in Table 5.33, it is seen that $\Delta H_H^{\neq}/\Delta H_J^{\neq} \approx 3$ for the ordinary liquids and molten salt quoted but is close to 1.1 for metals. This signifies that the transport rate in a metal is determined less by hole formation and influenced significantly by jumping.

$$\left(\frac{\partial \ln D}{\partial P}\right)_T = -\frac{\Delta V^{\neq}}{RT} \tag{5.121}$$

It can be seen that knowing $\Delta V^{\neq}$, one can calculate $l$, the jump distance. For $NaNO_3$ at 620 K, this is equal to 380 pm, which is too big by far to be called a microjump as required in Swellin's shuffling, though it is just the right kind of number for a jump into the conveniently opening neighboring cavity, hole, or vacant space.

On the other hand, Swallin's idea has not remained unused. One of the early simulation calculations on molten salt structures—that by Alder and Einwohner—found that a jump distance much smaller than the diameter of an ion fitted the simulation and therefore fitted Swallin's microjump model. However, this would not be consistent with the $\Delta V^{\neq}$ values, for if the microjump distance is $l$, then $\Delta V^{\neq} = (4/3)\pi\,(l/2)^3$ and as $l$ in the microjump model would be around 10-20 pm, $\Delta V^{\neq}$ would be about $2 \times 10^{-3}$ $cm^3$ $mol^{-1}$, compared with a measured $\Delta V^{\neq}$ of about 10 $cm^3$ $mol^{-1}$ (e.g., for $NaNO_3$ at 620 K).

Work by Rice and Allnutt[24] for molten salts posed another threat to the "making-holes-and-jumping-into-them" model. In fact, their work has been seen by some to pump life into the aging Swallin theory. The simulation they made was based on calculation of the distribution functions $g_{\pm}$ (see Section 5.5.3), but this could be its Achilles heel because the function thus calculated neglects the large change in volume that occurs in salts such as NaCl when they melt. This is like trying to play Hamlet with the Elsinore castle in the backdrop, but a large live African elephant walking across the stage—it takes no notice of the main point (internuclear distance decreases on melting but volume increases 11–28%). Tables 5.33 and 5.34 contain the values for $\Delta H_H^{\neq}$ and $\Delta H_J^{\neq}$ and Table 5.35 contains those of $\Delta V^{\neq}$.

At first it was thought that the work of hole making was as much as ten times greater than that of jumping, but later on the two values were found to be not so far apart, indicating that the difficulty of jumping can be competitive with that of hole making; the ion is less eager to avail itself of the conveniently opened up neighboring hole than had been thought.

So what of Swallin's shuffling and his idea of microjumps? There is no need to *abandon* microjumping even though the heat of activation for all nonassociated, noncomplexed liquids follows the law $E^{\neq} = 3.74RT_{m.p.}$, suggesting a unified mechanism of transport for metals, organic liquids, and molten salts. Perhaps in some liquids two kinds of steps contribute to transport in parallel.

It is only in the types of liquids that fit into the relation shown in Fig. 5.28 (i.e., the linear relation of $E_D^{\neq}$ to $T_{m.p.}$) that hole *formation* seems to be the rate-controlling

[24]The Rice–Allnutt model may be understood by taking the ions that move to be analogous to a man who enters a room full of partying people. His aim is to make it to the bar. There is no gap in the crowd present. He "dives in" and essentially *jiggles* his way forward. This is a similar picture to the "shuffling along" view presented in the 1950s by Swallin for diffusion in metals.

**TABLE 5.34**

**Diffusion Parameters at Constant Pressure and Constant Volume**

| Diffusion Parameters | $^{22}Na$ in $NaNO_3$ | $^{134}Cs$ in $NaNO_3$ | $^{134}Cs$ in $CaNO_3$ |
|---|---|---|---|
| | | Constant pressure | |
| $E$ (kcal mol$^{-1}$)[a] | 4.30 ± 0.30 | 4.69 ± 0.21 | 6.47 ± 0.32 |
| $D_0 \times 10^3$ [b] | 0.55 ± 0.13 | 1.24 ± 0.40 | 1.79 ± 0.25 |
| | | Constant volume | |
| $E$ (kcal mol$^{-1}$) | 0.78 ± 0.18 | 1.30 ± 0.17 | 1.83 ± 0.26 |
| $D_0 \times 10^5$ [b] | 3.9 ± 0.95 | 8.3 ± 2.3 | 6.9 ± 1.1 |
| $E$(constant volume)/$E$(constant pressure) | 0.18 | 0.27 | 0.28 |

[a] 1 cal = 4.184 J.
[b] $D_0$ is the preexponential factor.

event in transport. Take the case of the transport of protons in water (Section 4.11.6). They dart about, continuously jumping from water to water, tunneling through the barriers in between, with a slight tendency to go more in one direction than the other if there is an applied electric field or a concentration gradient. On the other hand, about one-fifth of the $H^+$ ions also move along as $H_3O^+$ moves along. Here, therefore, two mechanisms contribute to transport. There is nothing against assuming (according to Rice and Allnutt's calculations, which neglected the distributed cavities in liquids) that *some* movements of ions occur by a shoulder-to-shoulder pushing microjump shuffle. While the evidence for $E^{\neq} = 3.74RT_{\text{m.p.}}$ holds, and the $\Delta V^{\neq}$s are about the size calculated for a hole (if $\Delta H_H^{\neq} > \Delta H_J^{\neq}$), models involving cavity making and jumping into it seem more consistent with experiments than those that feature shuffling.

## Further Reading

### *Seminal*

1. H. Eyring, "A Hole Theory of Liquids," *J. Chem. Phys.* **4:** 283 (1936).

**TABLE 5.35**

**Activation Volumes for the Diffusion Process**

| | $^{22}Na$ in $NaNO_3$ | $^{134}Cs$ in $NaNO_3$ | $^{134}Ca$ in $CaNO_3$ |
|---|---|---|---|
| $\Delta V^{\neq}$ (cm$^3$ mol$^{-1}$) | 10.7 ± 1.7 | 14.9 ± 1.4 | 18.2 ± 2.2 |
| $V_h$ (cm$^3$ mol$^{-1}$) | 9.8 ± 1.0 | 9.8 ± 1.0 | 15.6 ± 1.6 |
| $\Delta V_J^{\neq}$ (cm$^3$ mol$^{-1}$) | 0.9 | 5.1 | 2.6 |

2. R. Fürth, "Transport Theory and Holes in Liquid," *Proc. Cambridge Phil. Soc.* **252:** 276, 281 (1941).
3. M. Nagarajan, L. Nanis, and J. O'M. Bockris, "Diffusion of Sodium 22 in Molten Sodium Nitrate," *J. Phys. Chem.* **68:** 2726 (1964).
4. S. R. Richards and J. O'M. Bockris, "Relation of Heats of Activation to the Melting Point in All Non-Associated Liquids," *J. Phys. Chem.* **69:** 671 (1965).

### *Papers*

1. Y. Tada, S. Hiraoka, and Y. Katsumura, *Ind. Eng. Chem. Res.* **31:** 2010 (1992).
2. C. K. Larive, M. F. Lin, B. J. Piersma, and W. R. Carper, *J. Phys. Chem.* **99:**12409 (1995).
3. M. Watanabe, S. Yamada, and N. Ogata, *Electrochim. Acta* **40:** 2285 (1995).
4. M. Ma and K. E. Johnson, *Can. J. Chem.* **73:** 593 (1995).
5. M. Abraham, M. C. Abraham, and I. Ziogas, *Electrochim. Acta* **41:** 903 (1996).

## 5.8. MIXTURES OF SIMPLE IONIC LIQUIDS: COMPLEX FORMATION

### 5.8.1. Nonideal Behavior of Mixtures

A measure of understanding has been gained on the structure and transport properties of simple ionic liquids. In practice, however, mixtures of simple liquid electrolytes are more important than pure systems such as liquid sodium chloride. One reason for their importance is that mixtures have lower melting points and hence provide the advantages of molten salts,[25] but with a lessening of the difficulties caused by high temperatures. What happens when two ionic liquids, for example, $CdCl_2$ and KCl, are mixed together?

Consider, for instance, the electrical conductance of fused $CdCl_2$ and KCl mixtures. If the equivalent conductivity of the mixtures (at a fixed temperature) were given by a simple additivity relation, then a linear variation of equivalent conductivity with the mole fraction of KCl should be observed (dashed line in Fig. 5.53). The straight line should run from the equivalent conductivity of pure liquid $CdCl_2$ at a particular temperature to that of pure liquid KCl at the same temperature. Some binary mixtures of single ionic liquids do indeed exhibit the simple additivity implied by the dashed line of Fig. 5.53.

[25] Advantages include no competing hydrogen or oxygen evolution during electrode reactions and an $e^{-E/RT}$ that gives a greater velocity in any rate process. The drawbacks are corrosion and the extra precautions that must be taken to avoid the breakdown of equipment. These threaten high-temperature experiments and make those above 2000 K extremely difficult to carry out. Such difficulties are greatly reduced by using the room temperature molten salts. However, their organic nature often leads to great dissymetry in ion size between cation and anion.

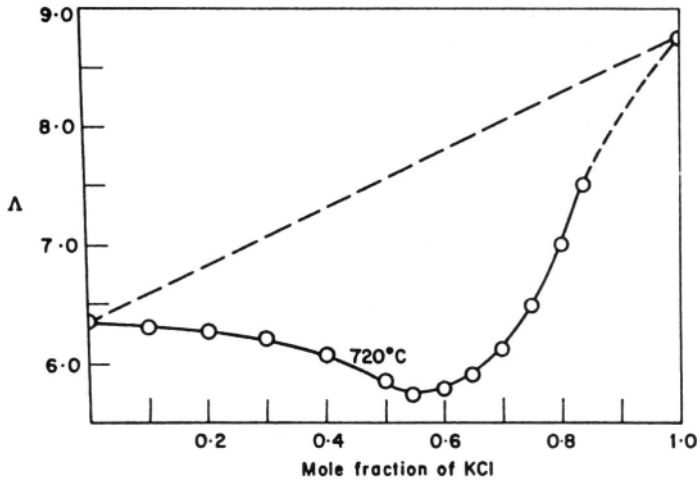


**Fig. 5.53.** The variation of the observed equivalent conductivity of $CdCl_2$–KCl mixtures as a function of the mole fraction of KCl. The dashed line corresponds to the variation that would be given by the additivity behavior.

There are, however, many systems in which deviations occur from a simple additive law for conductance. The system of $CdCl_2$ and KCl is a case in point (full line in Fig. 5.53). A minimum in the conductivity curve is observed. What is the significance of this minimum?

### 5.8.2. Interactions Lead to Nonideal Behavior

The situation is reminiscent of some happenings in aqueous solutions. At infinite dilution of, say KCl, the properties (e.g., equivalent conductivity) due to the $K^+$ and $Cl^-$ ions are additive (see Section 4.3.10). This is ideal behavior (see Section 3.4.1). With increasing concentration, however, there is a departure from ideality: the equivalent conductivities are not simply additive.

Nonideality in aqueous solutions (see Chapter 3) was ascribed to Coulombic attraction between $K^+$ and $Cl^-$ ions, and the ion-ion interaction theories were evolved for aqueous solutions. The electrostatic attraction between a pair of oppositely charged ions could overwhelm thermal jostling and result in the formation of ion pairs (see Section 3.8).

One can resort to similar explanations for departures from ideality in mixtures of simple ionic liquids. However, there are specific differences between the situation in fused salts and that in aqueous solutions. In pure liquid KCl, there is no concentration variable and therefore fused KCl has a single value of equivalent conductivity (at a particular temperature). The mean distance between the $K^+$ and $Cl^-$ ions cannot be altered, as it can be in aqueous solutions, by interposing varying amounts of solvent

because there is no solvent. Hence, the equivalent conductivity of pure liquid KCl embodies the effects of all the possible interactions for the temperature concerned. The thermodynamics of mixtures of molten salts has been intensively studied by Bloom, by Kleppa, and by Blander.

The interactions that one proposes to account for the deviations from ideality in mixtures of ionic liquids are interactions between the ions of one component of the mixture considered as a solvent and the ions of the other component that is added. In the case of KCl added to pure $CdCl_2$, one can consider, for example, the interactions between $Cd^{2+}$ ions and $Cl^-$ ions, and this interaction can be more than simply electrostatic, which is attraction without preferred direction. It may also involve *directed valence forces.*

### 5.8.3. Complex Ions in Fused Salts

It is intended here to discuss nonideality arising from complex ion formation. In the case of mixtures of pure liquid electrolytes, however, the idea of complex ion formation raises some conceptual problems.

Consider complex ion formation in the $CdCl_2$-KCl system, and let it be assumed for the moment that a $CdCl_3^-$ complex ion is formed. If such complex ions were formed in an aqueous solution of $CdCl_2$ and KC1, they would exist as little islands separated from other ions by large expanses of water. In fused salts, there are no oceans of solvent separating the ions. Thus, a $Cd^{2+}$ ion would constantly be coming into contact on all sides with chloride ions, and yet one singles out three of these $Cl^-$ ions and says that they are part of (or belong to) a $CdCl_3^-$ complex ion (Fig. 5.54). It appears that in the absence of the separateness possible in aqueous solutions, the concept of complex ions in molten salts is suspect. As will be argued later, however, what is dubious turns out to be not the concept but the comparison of complex formation in fused salts with complex formation in aqueous solutions.

It is more fruitful to compare complex formation in ionic liquids with the phenomenon of hydration of ions in aqueous solution (Chapter 2). It will be recalled that though an ion was seen as constantly nudged by the water molecules of the surrounding medium, a certain number of the water molecules—the "hydration

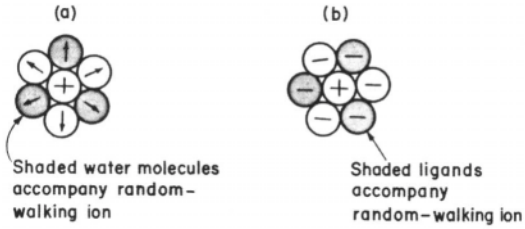


**Fig. 5.54.** The similarity between (a) a solvated ion in an aqueous solution and (b) a complexed ion in a mixture of ionic liquids.

number"—were considered to stay with the ion in its movement through the solution. The criterion by which the two kinds of water were distinguished was that all those water molecules that temporarily surrendered their translational degrees of freedom to the ion and participated in its random walk constituted its *solvation* sheath.

Similarly, a *completed* ion is an entity in which a certain number of ligand ions (e.g., three chloride ions in a $CdCl_3^-$ complex) participate in the random walk of the ion (i.e., the $Cd^{2+}$ ion in the $CdCl_3^-$ complex). The other $Cl^-$ ions only underg o promiscuous contacts with the $Cd^{2+}$ ion of the complex, not long-term affairs. The implication is that a complex ion (i.e., the ion and its ligands) is an entity with a lifetime that is at least several orders of magnitude longer than the time required for a single vibration.

From the standpoint of this comparison (Fig. 5.54), it is seen that the concept of a complex ion in a molten salt is at least as tenable as that of an ion with a primary solvation sheath (Section 2.4) in aqueous solutions. What experimental evidence exists for complex ions in fused salt mixtures? To anwer this question, one must discuss some results of investigating the structure of mixtures of simple ionic liquids.

### 5.8.4. An Electrochemical Approach to Evaluating the Identity of Complex Ions in Molten Salt Mixtures

Here one measures a quantity called the *transition time* at an electrode (see Chapter 7). One switches on a constant current through an electrode. This current is such that the electrode reactions occur fast enough and the activation overpotential is avoided. Under such conditions, an interval of time can be measured (the *transition time,* $\tau$) at which ions in the interfacial layer in contact with the electrode exhaust because they are being removed onto the electrode faster than the rate at which they are being supplied from the solution. Then the electrode potential undergoes a dramatic change in the electrode search for other ions to act as a sink for the electrons pouring into it, which corresponds to the constant current strength chosen.

Then it is easy to show (Inman and Bockris, 1961) that under these circumstances

$$E = E_{\tau/4} + \frac{RT}{nF} \ln \frac{\tau^{1/2} - t^{1/2}}{t^{1/2}} \tag{5.122}$$

Here $t$ is the time elapsed since the switch on of the current, and $E_{\tau/4}$ is the potential reached at one-fourth of the transition time $\tau$ described earlier.

The key point here is that $E_{\tau/4}$ is independent of the concentration of the species exchanging electrons at the electrode if there are no complexes formed. Conversely, it is empirically found that if complexes *are* present, $E_{\tau/4}$ varies with the concentration.

To illustrate how one might use this method to find the concentration of the complexes, consider a molten salt system such as $Cd(NO_3)_2$ dissolved in a eutectic of $NaNO_3$-$KNO_3$ at about 530 K. There are no complexes between $Cd^{2+}$ and $NO_3^-$ in the

system of $Cd(NO_3)_2$-$NaNO_3$-$KNO_3$. Correspondingly, it is found that, $E_{\tau/4}$ is independent of the concentration of $Cd^{2+}$ in this system.

What happens to $E_{\tau/4}$ when one adds to the nitrate system just described some ion that complexes Cd, e.g., $Cl^-$? Then it is found that $E_{\tau/4}$ changes with the concentration of added $Cl^-$, in contrast to its constancy in the absence of the $Cl^-$ ligand. Now, $\Delta E_{\tau/4} = E^0_{\tau/4} - E_{\tau/4}(c)$, where $E^0_{\tau/4}$ is the quarter-time potential under standard conditions, and $E_{\tau/4}(c)$ is the value of $E_{\tau/4}$ in the presence of $Cl^-$-containing complexes of Cd formed by adding, e.g., varying concentrations of KCl to the $Cd(NO_3)_2$-$NaNO_3$-$KNO_3$ eutectic.

DeFord and Hume derived expressions to treat the type of situations sketched above and a version of their equation is

$$F_0 = \left(\frac{\tau_0}{\tau_c}\right)^{1/2} \exp\left(\frac{nF}{RT}\Delta E_{\tau/4}\right) = \sum_{j=0}^{j=m} \beta_j c_{X^-}^j \tag{5.123}$$

Two symbols require definitions; $c_{X^-}$ is the ligand concentration (the $Cl^-$, for example) and $m$ is the maximum number of ligand ions associated with Cd, that is 3, as in $CdCl_3^-$; other terms have their usual meaning.

Further functions are defined as follows ($F_0$ is the experimentally determinable quantity):

$$F_1 = \frac{F_0 - \beta_0}{c_{X^-}} \sum_{j=1}^{j=m} \beta_j c_{X^-}^{j-1} \tag{5.124}$$

$$F_2 = \frac{F_1 - \beta_1}{c_{X^-}} \sum_{j=2}^{j=m} \beta_j c_{X^-}^{j-2} \tag{5.125}$$

$$F_3 = \frac{F_2 - \beta_2}{c_{X^-}} \sum_{j=3}^{j=m} \beta_j c_{X^-}^{j-3} \tag{5.126}$$

when $j = 0$, $\beta_0 = K_0$. $\beta_1$, $\beta_2$, etc., are related to the successive formation constants $K_1$, $K_2$, etc., by

$$\beta_1 = K_1 = \frac{[MX^{(n-1)+}]}{[M^{n+}]\,[X^-]} \tag{5.127}$$

**TABLE 5.36**

**Successive Formation Constants for Complexes of $Cd^{2+}$ with $X^-$ in $NaNO_3$ + $KNO_3$ (Eutectic at 530 K)**

| Ligand | $K_0 - \beta_0$ | $K_1 - \beta_1$ | $K_2$ | $K_3$ | $K_4$ | $C_{Cd(NO_3)_2}$ (mol $kg^{-1}$) |
|---|---|---|---|---|---|---|
| $Cl^-$ | 1 | $100 \pm 25$ | $7 \pm 3$ | $35 \pm 12$ | 0 | $0.98 \times 10^{-3}$ |
| $Br^-$ | 1 | $100 \pm 50$ | $65 \pm 33$ | $8 \pm 3$ | 0 | $0.92 \times 10^{-3}$ |
| $I^-$ | 1 | $500 \pm 250$ | $60 \pm 36$ | $53 \pm 22$ | $78 \pm 26$ | $0.82 \times 10^{-3}$ |

Source: Reprinted from D. Inman and J. O'M. Bockris, *Trans. Faraday Soc.* **57**: 2308, 1961.

$$\beta_2 = K_1 K_2 = \frac{[MX_2^{(n-2)+}]}{[M^{n+}]\,[X^-]^2} \tag{5.128}$$

$$\beta_3 = K_1 K_2 K_3 = \frac{[MX_3^{(n-3)+}]}{[M^{n+}]\,[X^-]^3} \tag{5.129}$$

By making suitable plots, it is possible to obtain the formation constants $K_1, K_2, \ldots$ of the complexes and then to calculate from the equations given above the formulas of the complexes present. For example, if $F_0$ is plotted against $c_{X^-}$ the extrapolation to $c_{X^-} = 0$ should equal $\beta_1$ $(= K_1)$ and the limiting slope at $c_{X^-} = 0$ should equal $\beta_2$, and so on, up the series. The $F$ against $c_{X^-}$ plot for the next-to-last complex present in the system should be a straight line with a slope equal to the overall formation constant for the complex of the highest coordination number, and the intercept at the $c_{X^-}$ plot for the last complex should be a straight line parallel to the $c_{X^-}$ axis. The calculated formation constants are given in Table 5.36.

The way this plots out is shown in Fig. 5.55. The figure illustrates a lesson that is easily understandable: the dominant complex changes with the concentration of the ligand.

### 5.8.5. Can One Determine the Lifetime of Complex Ions in Molten Salts?

Ideas on complex ions in molten salts tend to vary with the time at which they were published. In the first half of the century, there seemed no doubt that complex ions in molten salts were distinct entities and, it was implied, they were permanent. Later, there was doubt as to our ability to identify complex ions in molten salts. Thus, it was argued, there is no difficulty in accepting the existence of discrete ions in aqueous solutions because each ion is a separate entity, and there are many solvent

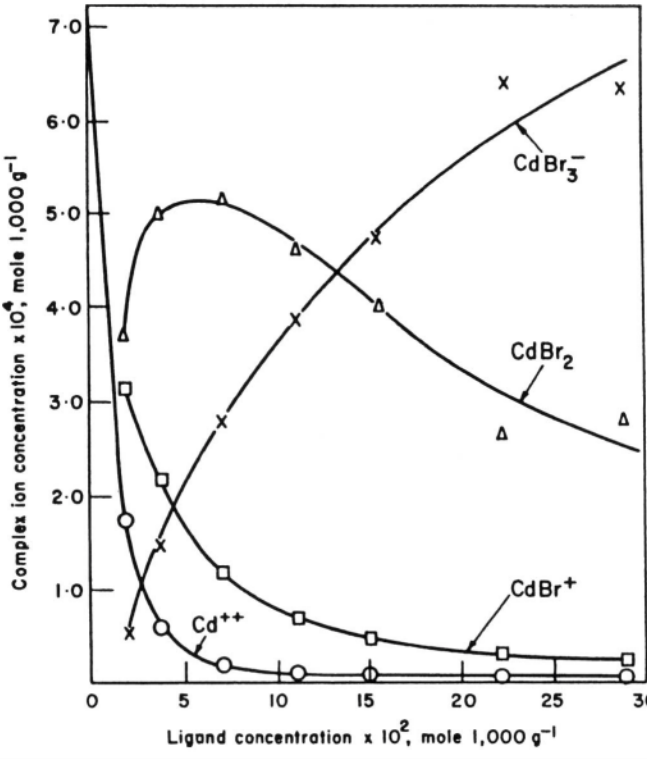


**Fig. 5.55.** Dependence of the concentration of various complex ions $Cd(Br)_x$ upon the addition of KBr.

molecules between each ion. In the molten salt, however, there is a continuum of ionic entities and whether complexed ionic species can be distinguished seems less certain; perhaps the $Br^-$ ligands in the imagined $CdBr_3^-$ are just shared equally among the solvated ions in a solvent such as $KNO_3$-$LiNO_3$.

These two views can be described in terms of a time $\tau$, representing the time an ion such as $Cd^{2+}$ remains bonded to a ligand, such as $Br^-$. In the two extreme views just given, $\tau$ would be minutes or even hours for long-lived complexes and zero for the concept that distinguishable complex ions in molten salts do not exist.

Such problems can be tackled by spectroscopic means, as shown later. Raman spectra, in particular, would indicate new lines having characteristic frequencies when $Br^-$ is added to $Cd(NO_3)_2$ in $KNO_3$-$LiNO_3$, and in the preceding section it has been shown that an analysis of the variations of the electrode potential of $Cd(NO_3)_2$ in $KNO_3$-$LiNO_3$ with $Cl^-$ addition has given reason to believe in complex ions in the cases quoted. However, there is a nifty electrochemical method that allows one to also obtain the *lifetime* of the individual ions and hence remove doubt as to the real existence of complex ions in molten salts.

If one applies a constant current density to an inert electrode such as Pt dipped into a molten salt consisting of a solvent (e.g., $KNO_3$-$LiNO_3$) with a solute of $Cd(NO_3)_2$, it is found that the transition time varies with the strength of the electric current passing across the electrode.

The "transition time" was described briefly in Section 5.8.4, but it is described in more detail in Chapter 7. When one switches on a cathodic current (electrons ejected from the electrode to the solution) at an electrode, at first there are plenty of ions in the region near the electrode and plenty of current can flow. However, there comes a time $\tau$, the transition time, when the solution near the electrode "runs out" of ions, and the electrode potential then undergoes a significant change.

The value of $\tau$ for simple situations (no complexing in solution) is given by

$$\tau^{1/2} = \frac{\pi n^2 F^2 D_i c_0^2}{4j^2} \tag{5.130}$$

where $j$ is the current density, $n$ is the number of electrons in the overall reaction, $F$ is the faraday, $D_i$ is the diffusion coefficient of the ion diffusing to the electrode, and $c_0$ is the concentration of, e.g., $Cd^{2+}$ ions in solution.

It can be readily seen from Eq. (5.130) that $j\tau^{1/2}$ should be a constant for $c_0$ independent of the applied current, and Fig. 5.56 shows that for the system indicated in the annotation to the figure, it is not. Why not?

Figure 5.56 contains two linear sections. Thus, $j\tau^{1/2}$ (which would be constant if all were simple) decreases as the current density increases. This is consistent with a homogeneous reaction occurring in the bulk of the solution. As the current strength increases, the dissociation of the complex becomes increasingly unable to keep up with the electrode's need for $Cd^{2+}$ ($c_0$ is kept constant). For this reason, $\tau$ sinks with an increase of current density and hence $j\tau^{1/2}$ decreases.

It is difficult to think of an interpretation consistent with these facts except some sequence of the kind:

$$CdBr_3^- \underset{\overleftarrow{k}_3}{\overset{\vec{k}_3}{\rightleftharpoons}} CdBr_2 \underset{\overleftarrow{k}_2}{\overset{\vec{k}_2}{\rightleftharpoons}} CdBr^+ \underset{\overleftarrow{k}_1}{\overset{\vec{k}_1}{\rightleftharpoons}} Cd^{2+} \tag{5.131}$$

One of these reactions must involve a slow, rate-determining step that prevents the complex from dissociating rapidly enough to make up the $Cd^{2+}$ quantities that the electrode removes from the interfacial region around it. Thus, in Fig. 5.56 for the lower line (with higher current densities) the story is qualitatively the same. However, the mathematical treatment goes into a different approximation at higher current densities with the slope change.

It is possible to show that a two-sloped graph such as that shown in Fig. 5.56 can be treated in such a way that the rate-controlling reaction in the above series can be identified as the slow dissociation of $CdBr_2$ and the corresponding lifetime of the entity involved evaluated, also. The lifetime determined for the $CdBr_2$ was 0.3 s in the nitrate

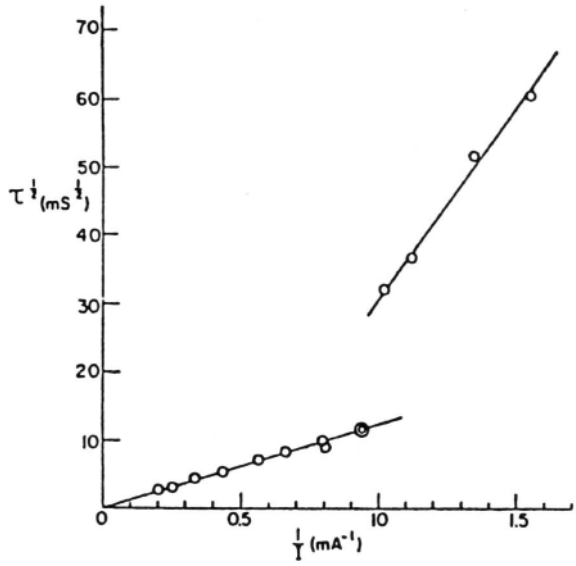


**Fig. 5.56.** $\tau^{1/2}$ against $1/I$ for $Cd^{2+} = 4.82 \times 10^{-3}$ mol kg$^{-1}$. KBr = $9.21 \times 10^{-2}$ mol kg$^{-1}$. (Reprinted from S. Srinivasan, D. Inman, A. K. N. Reddy, and J. O'M. Bockris, *J. Electroanal. Chem.* **5:** 476, 1965.)

eutectic considered. All this goes to show that there can be indeed complexed entities in molten salts and they live for quite long times,[26] although they are by no means permanent.

## 5.9. SPECTROSCOPIC METHODS APPLIED TO MOLTEN SALTS

Cryolite is $Na_3AlF_6$; in the process for the extraction of Al, $Al_2O_3$, which is obtained from the corresponding hydrate in the mineral bauxite,[27] is added to molten

[26] Long in comparison with some molecular complexes, which have lifetimes on the order of as little as $10^{-10}$ s.

[27] Bauxite is most easily available to U.S. companies from Venezuela and islands in the Caribbean; there is also a lot in Australia. When bauxite ceases to be economically obtainable from nearby sources (after the year 2000), Al will be extracted from clay (sodium aluminum silicate), which is one of the more abundant minerals on earth and occurs in all countries. $AlCl_3$ would be formed by chlorination of the clay and this compound would be added to a KCl-LiCl eutectic around 770 K. Electrolysis at this temperature would deposit solid Al. Because of the very large amount of Al available from clay, and because of its light weight, Al is tending to replace Fe even in automotive manufacture.

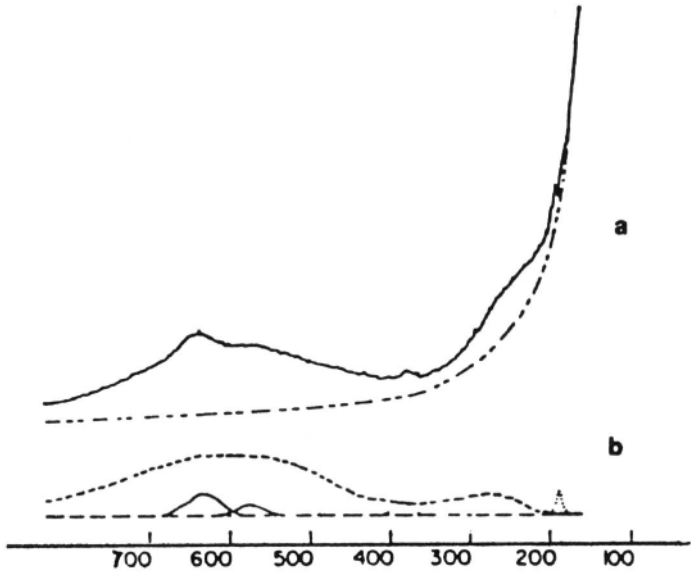


**Fig. 5.57.** (a) Spectrum of molten cryolite at 1380 K (— halation), (b) Analysis of the spectrum in Raman scattering (——), thermal radiation (- - - -), and instrumental background radiation (---). (Reprinted from C. Solomons, J. Clarke, and J. O'M. Bockris, *J. Chem. Phys.* **49:** 445, 1968.)

cryolite in such a way that Al deposits at the negative electrode of an electrolytic cell. This is the method by which Al is obtained throughout the world. It is the number one electrochemical process in terms of money invested.

In the study of this system, it is necessary to study the constitution of cryolite, what complex ions are present in it, if any. The work is difficult because the temperature is on the order of 1270 K, and cryolite is an aggressive substance, particularly after $Al_2O_3$ has been added; it attacks most materials, even refractory material such as $SiO_2$. Making up a cell that is both not attacked by the corrosive cryolite and has a transparent window for radiation to enter and leave is a challenge. The difficulty was first overcome in 1968 by Solomons et al., who used BN as a refractory not attacked by cryolite. In a typical Raman experiment, a focused laser beam enters into one hole in a BN crucible and the scattered light (see also Section 2.11), which carries information on the structure of the particles, emerges through another hole in the crucible. Surface tension keeps the liquid cryolite and alumina from escaping through the holes.

The Raman spectrum of cryolite is shown in Fig. 5.57. The features remaining after deconvolution are two peaks, one at a wavenumber of 633 and one at 577 $cm^{-1}$.

Both these peaks are polarized.[28] The relatively high frequency and polarized nature of these bands is consistent with the totally symmetric stretching frequency of Al–F in one of the two anions known to constitute cryolite—$AlF_4^-$ (tetrahedral) and $AlF_6^{3-}$ (octahedral).

In solid cryolite there is a band at 554 $cm^{-1}$ (wavenumbers)[29] that has been identified as originating in $AlF_6^{3-}$. Is the 575-$cm^{-1}$ band in the melt due to the same ion? The more intense band (see Fig. 5.57) at 633 $cm^{-1}$ would be expected to be from a complex of lesser coordination number and this fits $AlF_4^-$.[30]

What fits the observations reported is the equilibrium

$$AlF_6^{3-} \rightleftharpoons AlF_4^- + 2F^- \tag{5.132}$$

The mole fractions of $AlF_6^{3-}$ and $AlF_4^-$ are determined from the relative values of the peaks in the spectrum as 0.07 and 0.3, respectively; i.e., the $AlF_6^{3-}$ that dominates the solid at room temperature dissociates to a considerable extent in the liquid at 1270 K to the simpler complex.

When $Al_2O_3$ is added to molten cryolite, another ion, $AlOF_2^-$, also forms and may (surprisingly, because it is an anion) take part in the final reaction at the negative electrode[31] that produces Al.

---

[28] In Raman spectroscopy (see Section 2.11), one speaks of the polarization and depolarization of the scattered light. The depolarization ratio of a line is the ratio of the intensities within the scattered light polarized perpendicular ($\perp$) and parallel ($\parallel$) to the plane of polarization of the incident light. The depolarization ratio, $\rho$, is defined as $\rho \equiv I_\perp/I_\parallel$. There are several possibilities for the value of this ratio for the emergent light. It can be nonpolarized ($\rho = 1$), or retain its initial polarization ($I_\perp = 0$ and $\rho = 0$). In practice, a Raman line is counted as depolarized if $\rho = 0.75$ and polarized if $\rho < 0.75$. Of course, to observe this, one has to look at the Raman scattered light through a polarizing filter, which enables us to find the ratio of $\perp$ to $\parallel$ light. The importance of measuring the polarization of the scattered light is that its interpretation tells us about the symmetry of the scattering source, i.e., gives information on the nature of the ions present.

[29] *Wavenumber* is defined as $1/\lambda$, where $\lambda$ is the wavelength. However, $\nu\lambda = c$, where $\nu$ is frequency and $c$ is the velocity of light. A higher wavenumber means a lower $\lambda$ and a lower $\lambda$ means a higher frequency.

[30] Now for an oscillator, $\nu = (2\pi)^{-1}\sqrt{k/\mu}$, where $k$ is the force constant of the vibration and $\mu$ is the reduced mass of the oscillator, e.g., Al-F. A lower coordination number means a higher $k$, and hence $\nu$, because of lessened repulsion between the ligands and diminished screening of the nuclear charge on the cation.

[31] Readers should not be overly shocked at the idea that negatively charged anions such as $AlOF_2^-$ may react at cathodes, which are the *negative* electrodes in a cell. Electrodeposition at negative electrodes from negative anions is quite common (Cr plating of car bumpers occurs from $CrO_4^{2-}$). Although the anions are electrostatically repelled at a cathode, there may be a driving force as a result of a diffusion gradient.

This can be seen from the Nernst–Planck equation of Section 4.4.15. Here there are two terms. One contains a *potential* gradient, $\partial\psi/\partial x$, and the other a concentration gradient, $\partial c/\partial x$. For a negative anion approaching a negatively charged cathode, there is repulsion. However, transport *to* the electrode and deposition is still possible if the concentration gradient term (which tends to impel the anion *to* the cathode) dominates over the potential gradient term.

### 5.9.1. Raman Studies of Al Complexes in Low-Temperature "Molten" Systems

$AlCl_3$ complexes with inorganic ions such as $Cl^-$ to form $AlCl_4^-$ and $Al_2Cl_7^{2-}$, both of which register in Raman spectra. $SnCl_2$ might be considered a fruitful partner for $AlCl_3$. Solomons and Clarke found pure $SnCl_2$ to be polymerized when liquid, and it is highly viscous. The obvious question is: What happens when $AlCl_3$is added to $SnCl_2$ (both being in the liquid state)? This seems an ideal sort of question for study by a Raman spectroscopist since Al–Cl and Sn–Cl both show Raman-active bands.

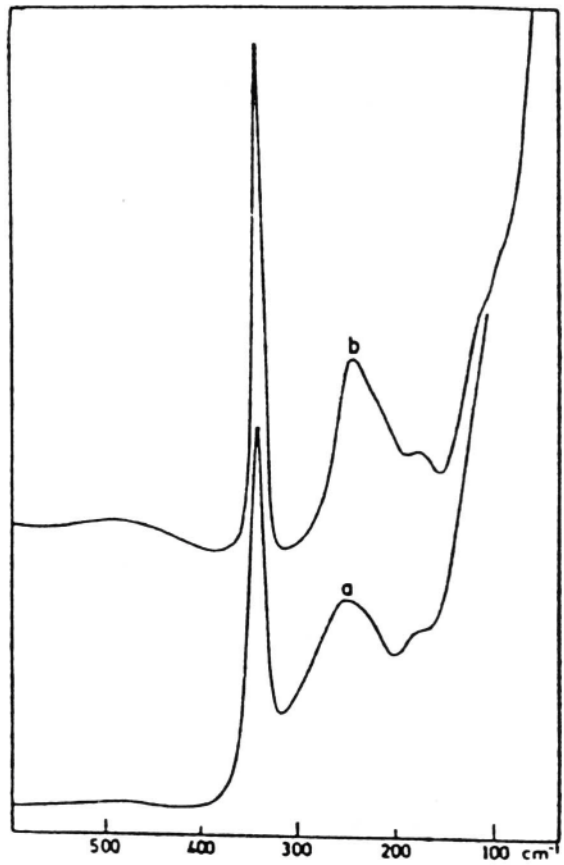


**Fig. 5.58.** Raman spectra of equimolar $SnCl_2$–$AlC_{l3}$ mixtures: (a) spectrum of the liquid ($T$= 500 K) and (b) spectrum of the glass ($T$= 298 K). (Reprinted from B. P. Gilbert, F. Taulelle, and B. Tremillon, *J. Raman Spectros.* **19:** 1,1988.)

Figure 5.58 shows the spectra for the equimolar liquid and the corresponding glass. Features that are not in the spectrum of either $SnCl_2$ or liquid $AlCl_3$ before they are brought together are observed at ~250 $cm^{-1}$. This wavenumber is known to be characteristic of Sn-Cl bonds. When the melt is cooled to form a glass, the 250-$cm^{-1}$ band breaks up to show a band at 248 $cm^{-1}$ and one at 219 $cm^{-1}$. The 248-$cm^{-1}$ band is probably partly depolymerized $SnCl_2$,

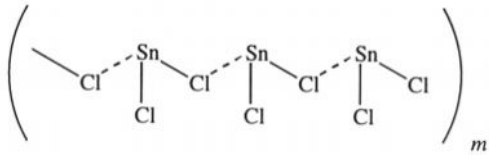


The other band at 219 $cm^{-1}$ will be characteristic of a new Sn-Cl bond and this could come from the breakdown of the $SnCl_2$ polymer, perhaps in a new complex, $Sn(AlCl_4)_2$, either as

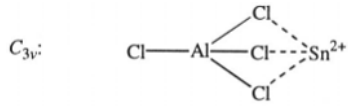


or as


The second structure is preferred because it brings about a lesser symmetry in the complex ion and this decreased symmetry is found to lead to an explanation of one of the characteristics of the spectra, the fact that they exhibit polarization, i.e., have differences in the spectra when the polarized light incident on the sample is in either the parallel or the vertical plane, respectively. Thus, polarization of the scattered Raman radiation is expected from the $C_{2v}$ but not from the $C_{3v}$ complex ion.

### 5.9.2. Other Raman Studies of Molten Salts

Some idea of how Raman spectroscopy works—how light from nonelastic scattering on molecules contains information on the vibratory state of the bonds therein—has been given in Section 2.11. Raman spectroscopy can be used to obtain information on the structure of ions in molten salts, as has been shown in the last three sections. Here, two further molten salt systems that contain complexes and that have been subjected to Raman spectroscopy are described. The first one concerns melts of zinc chloride hydrate.

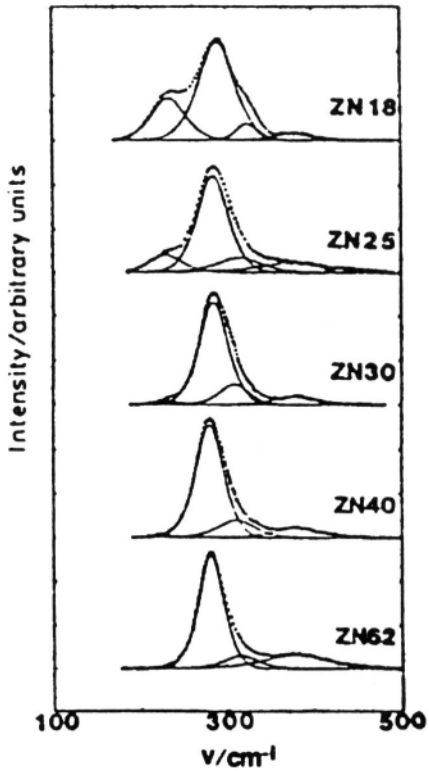


**Fig. 5.59.** Background-corrected Raman spectra for $ZnCl_2$ hydrate at 298 K. Solid lines show the peak components obtained by the least-squares fits. (Reprinted from T. Pom, T. Yamaguchi, S. Hayaschi, and H. Ohtaki, *J. Am. Chem. Soc.* **93:**2620,1989.)

The associated spectra and Raman frequencies are shown in Fig. 5.59 from the work of Yamaguchi et al. The predominant band at 280–289 $cm^{-1}$ is attributable to the Zn–Cl vibration in $(ZnCl_4)^{2-}$. There is also a peak at 227–234 $cm^{-1}$ for solutions containing less than 40% Zn. The same peak is found in anhydrous $ZnCl_2$ melts and is probably due to $(ZnCl_4)^{2-}$ in aggregates (i.e., a number of ions joined together by Cl atoms). Polarized light studies on the symmetry and structure do not seem to have been done.

Another system studied by Raman spectroscopy concerns molten salts at room temperature, which usually involve organic compounds. The system consists of

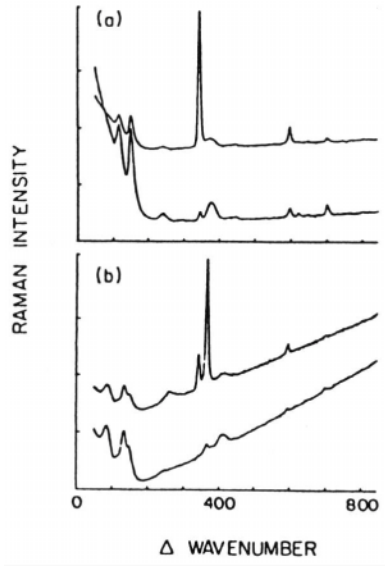


**Fig. 5.60.** Raman spectra for $GaCl_3$:MEIC melts at room temperature: (a) $n$=0.35 molar fraction $GaCl_3$ and (b) $n$=0.64 molar fraction $GaCl_3$. For both, the upper spectrum is vertically polarized, $I_{\parallel}$, and the lower one is horizontally polarized $I_{\perp}$. The intensity scales are different for the two polarizations. (Reprinted from S. P. Wicelinski, R. J. Gale, S. D. Williams, and G. Mamantov, *Spectrochim. Acta* **45A:** 759,1989.)

gallium chloride in 1-methyl-3-ethylimidazolium chloride (MEIC) at ambient temperatures. This system was examined by Mamantov et al. using an exciting wavelength of 514.5 nm and some spectra are shown in Fig. 5.60.

Table 5.37 contains data on the chlorogallates. The peak at 376 $cm^{-1}$ corresponds to $GaCl_4^-$ but when the molar fraction of $GaCl_3 > 0.5$, one would expect

$$GaCl_4^- + GaCl_3 \rightleftharpoons GaCl_7^- \tag{5.133}$$

The latter ion would have peaks as shown in the table; there is a weak peak at ~365 $cm^{-1}$ that may indicate the presence of $Ga_2Cl_7^-$.

**TABLE 5.37**

**Raman Vibrational Frequencies of Known Chlorogallate Species**

| $(GaCl_4^-)$ | $(Ga_2Cl_7^-)$ | $(Ga_2Cl_7^-)$ | $(Ga_2Cl_6)$ | $(Ga_2Cl_6)$ |
|---|---|---|---|---|
| | 120 s | 90 s | 63 vs | 98 vs |
| 153 s | 140 s | 96 s | 110 sh, w | 115 w |
| 343 s, p | 266 w, p | 107 m | 166 m | 168 m |
| 370 sh, w | 316 w, p | 141 m | 267 w | 244 m |
| | 366 s, p | 284 m | 320 m | 330 m |
| | 393 sh, m | 365 vs | 340 s | 345 m |
| | | 407 m | 411 s, p | 405 s |
| | | | 464 w | 456 m |
| $(GaCl_3$:CsCl melt) | $(GaCl_3$:CsCl melt) | $(KGa_2Cl_7$, solid) | $(GaCl_3$, 275 °C) | $(GaCl_3$, solid) |
| 45 mol% $GaCl_3$ | 70 mol% $GaCl_3$ | | | |
| 460 °C | 275 °C | | | |

Source: From S. P. Wicelinski, R. Z. Gale, S. D. Willams, and G. Mamantov, *Spectrochim. Acta* **45A**: 759, 1989.

Notes: s, strong; m, medium; w, weak; sh, shoulder; v, very strong; p, polarized.

### 5.9.3. Raman Spectra in Molten $CdCl_2$-KCl

Tanaka et al. investigated liquid $CdCl_2$-KCl with special reference to the complexes formed in the liquid state at from 750–980°. They used Hg blue light ($\lambda$ = 435.8 nm) and green light ($\lambda$ = 546.1 nm) as exciting sources. Four peaks were recorded and the strongest ones are shown in Table 5.38.

The interpretation of what these peaks mean in terms of structure was made by Tanaka et al. by comparing the numerical values of peaks shown in Table 5.38 with values obtained for the corresponding solids where the structure is known by means of the interpretation of X-ray diffraction patterns. Polarized light in the exciting source was used in the investigation and indicated the degree of symmetry in the structure of the ion being observed.

Over the range of compositions of 33–66 mol% $CdCl_2$ in $CdCl_2$-KCl, no change was observed in the Raman results; i.e., over this midrange of compositions there is a stable complex. The peaks and polarization data were compatible with the complex $CdCl_3^-$ in pyramidal structure (tetrahedral and planar structures had also been possibilities).

### 5.9.4. Nuclear Magnetic Resonance and Other Spectroscopic Methods Applied to Molten Salts

When a certain radio frequency ($\simeq 10^7$ $s^{-1}$) is applied to substances which themselves have been placed in magnetic field of about $10^4$ G (or 1 T), absorption of the applied frequency occurs. The origin of this absorption lies in the spin of the protons

**TABLE 5.38**

**Frequency of Raman Peak with Strong Intensity Observed from the Molten $CdCl_2$-KCl System**

| Salt | Mol% KCl | Temperature (°C) (Max. Deviation ±8) | Frequency [$\Delta\nu$ ($cm^{-1}$)] | Intensity[a] | Exciting Radiation $Hg_e$ – 4358 Å $Hg_c$ – 5461 Å |
|---|---|---|---|---|---|
| $2CdCl_2$-KCl | 33·3 | 482–548 | 255 ± 5 | M | e, c |
| | | 482–548 | 257 ± 2 | M | |
| $3CdCl_2$-2KCl | 40·0 | 605–708 | 260 ± 2 | M | e, c |
| | | 455 | 254 ± 2 | S | |
| $CdCl_2$-KCl | 50·0 | 482–708 | 262 ± 2 | S | e, c |
| | | 482–548 | 257 ± 2 | S | |
| $2CdCl_2$-3KCl | 60·0 | 605–708 | 260 ± 2 | S | e, c |
| $CdCl_2$-2KCl | 66·6 | 482–660 | 259 ± 2 | S | e, c |

Source: M. Tanaka, K. Balasubramanyam, and J. O'M. Bockris, *Electrochim. Acta* **8**: 621, 1964.
[a]M, medium; S, strong.

and neutrons in the nucleus of the atoms of the material. Contrary to the dogma of an earlier physics, the properties of nuclei are not immune to their surroundings, i.e., to the doings of electrons outside the nucleus, and hence to the chemical properties of the substance and to the environment. Thus, a study of these frequencies of nuclear magnetic resonance can give information on the properties of the systems being irradiated.

Instead of varying the frequency of the exciting radiation, as in other kinds of spectroscopies, and finding maxima at which absorption occurs, the usual thing with NMR is to keep the frequency of the incident radiation applied to the substance the same and vary the strength of the magnetic field $H$ applied to it. The entity being measured is the *absorption* ($A$) of the applied radiation as a function of the magnetic field strength. Maxima and submaxima are observed, and the values of these (which measure absorption in the nucleus) as well as the width of the spectral band can be analyzed in a way that gives rise to information on the chemical structure of the substance being irradiated.

As an example, in liquid $BeF_2$-LiF, one can interpret the characteristics of the NMR absorption as being due to the existence of $BeF_4^-$. The ion is stable to 820 K. However, no evidence of the ion's rotation is seen, and a probable interpretation of this is that $BeF_4^-$ groups are bonded into bigger structures, which prevent rotation of individual units in the structure.

The radiation applied to materials induces an oscillatory extra magnetic field in the nucleus and one thing which this does is alter the energy distribution among the protons there. The change is not much but it reestablishes itself to the earlier equilibrium values when the incident radiation is removed. It turns out that the time taken for

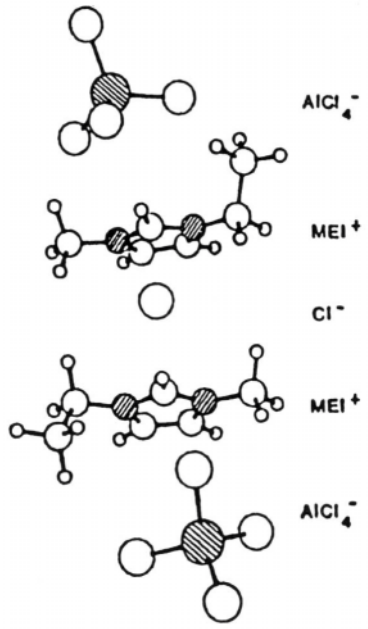


**Fig. 5.61.** Fully optimized configuration of the $AlCl_4^-$-$MEI^+$-$Cl^-$-$MEI^+$-$AlCl_4^-$ system. (Reprinted from D. Dymek, N. E. Heimer, J. W. Rowang, and J. S. Wilkes, *J. Am. Chem. Soc.* **110:** 2722,1988.)

what is named the *spin–lattice relaxation* ($\tau$) is between 1 and 100 s and this is a convenient sort of time to measure. Study of $\tau$ can give information, e.g., on the time of relaxation in diffusional movements in salts containing $^7Li$, $^{23}Na$, and $^{87}Pb$.

The study of ions containing aluminum in the liquid state can be done via NMR very conveniently, particularly since their complexes with certain large organic molecules are stable at room temperature. One may bring $AlCl_3$ into contact with, e.g., pyridine or imidazoline and the result is a number of new materials that melt at or near room temperature to form true solvent-free liquid electrolytes (see Section 5.12). The cation may be pyridinium or imidazolonium, and analysis of the degree of absorption in the Al nucleus as a function of the applied magnetic field strength can be used to determine the structure, e.g., of the Al-containing ion. $^{27}Al$ is the atom for which nuclear resonance is being observed, and it turns out that it gives two signals. The positions of these peaks are consistent with one peak being due to isolated $AlCl_4^-$ groups and the other to $Al_2Cl_7^-$ dimers (Fig. 5.61).

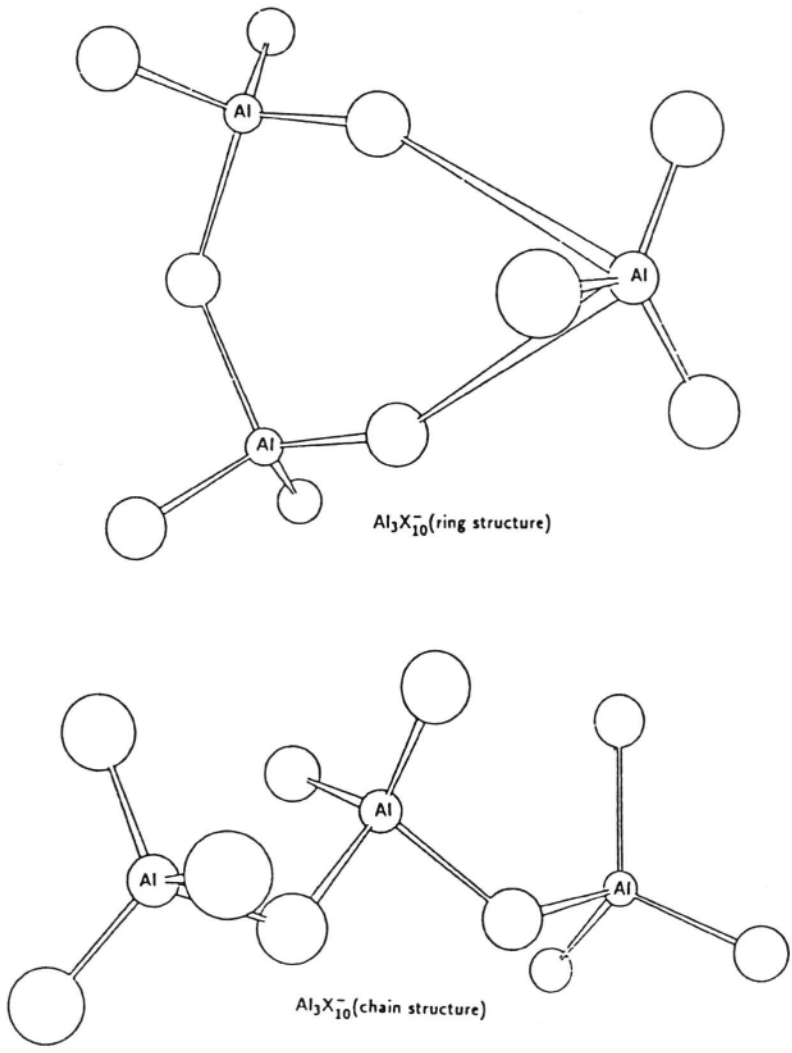


**Fig. 5.62.** Ring and chain structures of $Al_3X_{10}^-$. (Reprinted from M. Blander, E. Bierwagen, K. G. Calkin, L. A. Curtiss, D. L. Price, and M. L. Saboungi, *J. Chem. Phys.* **97:** 2733, 1992.)

Electron paramagnetic resonance (EPR) and neutron diffraction can also be used to study molten salts. An example of the former is a study of the motion of large organics [2,2,6,6-tetramethylpiperidine-l-oxyl (tempo) and 4-amino tempo, or tempamine] dissolved in room-temperature molten salts, e.g., 1-ethyl-3-methylimidazalo-

nium chloride (ImCl) and $AlCl_3$. One can learn about the dynamics of movement in these systems from such studies.

Neutron diffraction has been applied to the chloroaluminate melts to determine the shape and structure of a number of anions there. They turn out to have chain and ring structures in the higher members similar to those in liquid silicates and borates (Fig. 5.62).

## Further Reading

### *Seminal*


1. D. DeFord and D. N. Hume, "The Determination of Consecutive Formation Constants of Complex Ions from Polarographic Data," *J. Am. Chem. Sot:* **73**: 5321 (1951).
2. D. Inman and J. O'M. Bockris, "Complex Ions in Molten Salts: A Galvanostatic Study," *Trans. Faraday Soc.* **57**: 2308 (1961).
3. S. Srinivasan, D. Inman, A. K. N. Reddy, and J. O'M. Bockris, "The Lifetime of Complex Ions in Ionic Liquids: an Electrode Kinetic Study," *J. Electroanal. Chem.* **5**: 476 (1963).
4. M. Tanaka, K. Balasubramanyam, and J. O'M. Bockris, "Raman Spectrum of the $CdCl_2$-KC1 System," *Electrochim. Acta* **8**: 621 (1963).
5. C. Solomons, J. Clarke, and J. O'M. Bockris, "Identification of the Complex Ions in Liquid Cryolite," *J. Chem. Phys.* **49:** 445 (1968).


### *Review*


1. J. F. Stebbins, "Nuclear Magnetic Resonance at High Temperatures," *Chem. Rev.* **91**:1353 (1991).


### *Papers*


1. C. L. Hussey, I-Wen Sun, S. Strubinger, and P. A. Bernard, *J. Electrochem. Soc.* **137**: 2515 (1990).
2. C. L. Hussey, I-Wen Sun, S. Strubiner, and P. A. Bernard, *J. Electrochem. Soc.* **137**: 2515 (1990).
3. M. Blander, E. Bierwagen, K. G. Calkin, L. A. Curtiss, D. L. Price, and B. L. Saboungi, *J. Chem. Phys.* **97**: 2733 (1992).
4. S. Takahashi, M. L. Saboungi, R. J. Klinger, M. J. Chen, and J. W. Rathke, *Electrochem. Soc. Proc.* **92-16:** 345 (1992).
5. E. A. Pavlatou and G. N. Papatheodorou, *Electrochem. Soc. Proc.* **92-16**: 72 (1992).
6. D. L. Price, M. L. Saboungi, S. Hashimito, and S. C. Moss, *Electrochem. Soc. Proc.* **92-16**: 14 (1992).
7. M. Oki, K. Fukushima, Y. Iwadata, and J. Mochinaga, *Electrochemical Society*, *Molten Salts* **93-9**: 9(1993).
8. D. L. Price, M. L. Saboungi, W. S. Howell, and M. P. Tosi, *Electrochemical Society*, *Molten Salts* **93-9**: 1 (1993).
9. J. F. Stebbins, S. Sen, and A. M. George, *J. Non-Cryst. Solids* **193**: 298 (1995).

10. S. Das, G. M. Bejun, J. P. Young, and G. Mamantov, *J. Raman Spectrosc.* **26**: 929 (1995).

## 5.10. ELECTRONIC CONDUCTANCE OF ALKALI METALS DISSOLVED IN ALKALI HALIDES

### 5.10.1. Facts and a Mild Amount of Theory

Bronstein and Bredig were the discoverers (1958) of the unexpected fact that 1% concentrations of alkali metals dissolved in molten salts show electronic conductivity. In the K-KC1 system, the conductance was found to increase more than linearly with concentration while in the Na-NaCl system, it increases less than linearly.

The equation for the specific conductivity (see Section 4.3.6) is

$$\kappa = FN_e u_e \tag{5.134}$$

where $N_e$ is the number of moles of electrons per cubic centimeter, $u_e$ is the mobility in $cm^2 V^{-1} s^{-1}$, and $F$ is the electrical charge on 1 g-ion (96,500 C). Equation (5.134) yields values for the mobilities. In the Na system, the mobility was found to be equal to 0.4 $cm^2 V^{-1} s^{-1}$, and in the K system, 0.1 $cm^2 V^{-1} s^{-1}$. When the Na is 0.01 $M$ in the Na system, the concentration of electrons is about $10^{19}$ electrons $cm^{-3}$.

These values of mobilities of 0.1 and 0.4 $cm^2 V^{-1} s^{-1}$ obtained at 1070 K at first appear to be 250 times more than those for the corresponding ions in aqueous solution at 300 K ($\sim 5 \times 10^{-4}$ $cm^2 V^{-1} s^{-1}$). It would hardly be reasonable to compare mobilities at different temperatures. If one recalculates the ionic mobility for a hypothetical situation of an alkali ion in an aqueous solution at 1070 K, the value for the mobility in aqueous solution should increase from about $5 \times 10^{-4}$ to about 0.2 $cm^2 V^{-1} s^{-1}$. Hence, when the correction for the temperature difference *is* accounted for, the electron's mobility in the molten salt is not very different from that of an ion in the corresponding ion in an aqueous solution.

What about the lifetime of the electrons that conduct? One can find the lifetime from a simple phenomenological theory of conductivity. Thus, the equation of motion for the electron's movement under an electric field in the molten salt is

$$m_e \frac{du}{dt} = -Xe_0 - Cu \tag{5.135}$$

Here $e_0$ is taken as negative. The field $X$ accelerates the electron and there is a retarding force $Cu$ which, because of the Stokes–Einstein equation (Section 4.4.8), one assumes to be proportional to velocity.

Integrating Eq. (5.135), and taking $u$ at $t = 0$ to be equal to zero, one gets

$$u_e = -\frac{Xe_0\tau}{m_e}(1 - e^{-t/\tau}) \tag{5.136}$$

where $t$ is the time after the last collision and $\tau$ is the time at which the mobility is $[1 - (1/e)] = 1 - (1/2.7183) = 0.64$ of the final value (as the electron accelerates). Thus, the value at $t = \infty$, the steady-state value, is

$$u = -\frac{Xe_0\tau}{m_e} \tag{5.137}$$

In order to obtain some idea of the order of magnitude of $\tau$, it is reasonable to take $u$ as the mean of the values for the two salts described, i.e., $\frac{1}{2}(0.1 + 0.4) = 0.25$. $X$ is 1 V $cm^{-1}$, $m_e = 9 \times 10^{-28}$ g, and $e_0 = 1.6 \times 10^{-19}$ C.

Thus,

$$\tau = 1.5 \times 10^{-9} \text{ s} \tag{5.138}$$

which is a typical lifetime for an electron in a solid.

The meaning of $\tau$ is the average time the electron has to move from one ion before interacting again with another one. Hence, the distance traveled in one direction between collisions when the applied field is 1 V $cm^{-1}$ is only $\sim 0.25 \times 1.50 \times 10^{-9} = 4 \times 10^{-10}$ cm = 0.004 nm, a surprisingly small distance, although it is consistent with the short tunneling distance found in the following model analysis.

### 5.10.2. A Model for Electronic Conductance in Molten Salts

The fact that a concentration of about 1 mol% of an alkali metal in a molten salt system can cause a considerable specific conductance demands some kind of explanation. At 1 %, the electrons are about 2 nm apart, on the limit for tunneling site to site. What is the mechanism of their easy passage through the molten salt?

Emi and Bockris suggested a model for this phenomenon that bears some resemblance to the Conway–Bockris–Linton (CBL) theory of the mobility of protons in solution. Here (Section 4.11.6), protons tunnel from their positions attached to a given water to another water when—under the influence of the proton's field—this latter has rotated sufficiently to offer an orbital in which to receive a jumping proton.

There are three steps in the corresponding calculation for electrons. In the first, one finds the energy of an electron with respect to its zero potential energy *in vacuo*, both the energy in the filled state in the atom and in the empty state on a cation (each at equilibrium, i.e., having an energy at a minimum of the potential-energy–displacement relations). The next step is to allow the atom and ion to be displaced from their equilibrium positions to such an extent that the potential energy of the filled and empty electronic states in the atom and ion, respectively, become equal, which is the condition for radiationless transfer.

**TABLE 5.39**
**Mobility of Electrons**[a]

| Na-NaCl | | | | | | K-KCl | | | | | |
|---|---|---|---|---|---|---|---|---|---|---|---|
| 1121 K | | | 1166 K | | | 1091 K | | | 1133 K | | |
| $X_M$ | $\mu_{obs}$ | $\mu_{calc}$ | $X_M$ | $\mu_{obs}$ | $\mu_{calc}$ | $X_M$ | $\mu_{obs}$ | $\mu_{calc}$ | $X_M$ | $\mu_{obs}$ | $\mu_{calc}$ |
| 1.10 | 34 | 45 | 0.81 | 34 | 50 | 1.03 | 31 | 32 | — | — | — |
| 1.47 | 43 | 45 | 1.87 | 40 | 50 | 2.65 | 34 | 32 | — | — | — |
| 2.93 | 29 | 45 | 3.84 | 28 | 50 | 3.61 | 55 | 32 | — | — | — |
| 3.16 | 32 | 45 | 4.25 | 33 | 50 | 7.24 | 87 | 32 | 4.23 | 58 | 36 |

[a]Unit of mobility: $(cm^2\ V^{-1}\ s^{-1}) \times 10^3$; $X_M$ = mol% of metal atoms.

Gamow-type expressions (see Section 4.11.5) can be used for the calculations of the probability of tunneling (from atom to cation) and thereafter it is relatively simple to calculate the electron mobility. This is given by the concentration times the vibration frequency times the probability of tunneling from atom to ion.

According to this theory (Table 5.39), the mobility is not affected by the concentration of electrons, because at 1% they are too far apart to interact. No change in

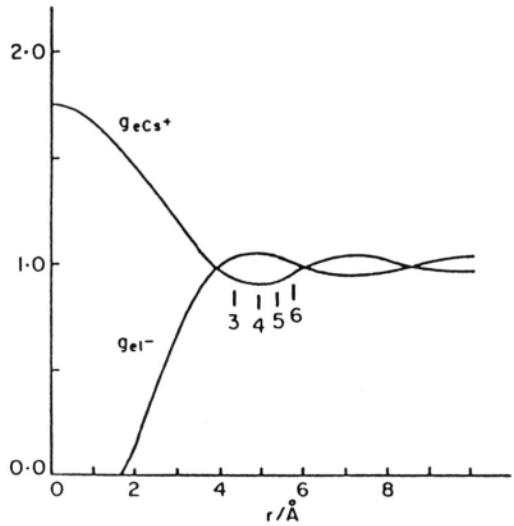


**Fig. 5.63. Electron–$Cs^+$ and electron–$I^-$** radial pair correlation functions. (Reprinted from C. Malescio, *Mol. Phys.* 69: 895,1990.)

mobility was detected as a result of a temperature change of 40 degrees for Na-NaCl (experimental; Table 5.39).

The radial distribution function of electrons in Cs has been calculated and is shown in Fig. 5.63. The numbers given on the figure are the coordination numbers of the electron by $Cs^+$ in terms of the distances from the center of the $Cs^+$ ion. They are calculated from

$$N(r) = 4\pi \int_0^r g_r r^2 \, dr \tag{5.139}$$

where $g_r$ is the distribution function for the electron in Cs and $r$ is the radius of the electron orbit in the outermost shell. Values ranging from 3 to 6 agree with those from corresponding neutron diffraction evidence.

Molecular dynamics calculations in metal–molten salt systems which could lead to diffusion and conduction values were first made by Parinello and Rahman in 1984. They have been used particularly by Malescio to examine the degree of delocalization of the electrons, which increases with the radii of the metal atoms.

## Further Reading

### *Seminal*

1. H. R. Bronstein and M. A. Bredig, "The Electrical Conductivity of Solutions of Alkali Metals in Their Molten Halides," *J. Am. Chem. Soc.* **82**: 2077 (1958).
2. T. Emi and J. O' M. Bockris, "Electronic Conductivity in Ionic Liquids," *Electrochim. Acta* **16**: 2081(1971).

### *Papers*

1. G. Malescio, *Mol. Phys.* **69**: 895 (1990).
2. G. Malescio, *Nuovo Cimento* **13D**: 1031 (1991).
3. G. M, Harberg and J. J. Egan, *Proc. Electrochem. Soc.* **16**: 22 (1992).
4. J. Lin and J. C. Poignet, *J. Appl. Electrochem.* **22**: 1111 (1992).
5. J. Bouteillon, M. Jaferian, J. C. Poignet, and A. Reydat, *J. Electrochem. Soc.* **139**: 1 (1992).
6. D. Naltland, T. Reuj, and W. Freyland, *J. Chem. Phys.* **98**: 4429 (1993).
7. J. C. Gabriel, J. Bouteillon, and J. C. Poignet, *J. Electrochem. Soc.* **141**: 2286 (1994).
8. L. Arurault, J. Bouteillon, and J. C. Poignet, *J. Electrochem. Soc.* **142**: 16 (1994).

## 5.11. MOLTEN SALTS AS REACTION MEDIA

Molten salts can be good media in which to carry out chemical reactions. The rate of all reactions increases exponentially with temperature. A *liquid* medium causes a higher rate of reaction to occur in a solute compared with that in a gas at the same temperature. Why is this? The situation needs thought. In the gaseous state, reactants

experience only a fleeting contact when they collide, which is often too brief a contact to reach thermal activation and a successful product formation. Thus, gas molecules fly around at about $10^5$ cm $s^{-1}$ at room temperature. When they collide, the actual time of contact is less than $10^{-12}$ s.

A different situation is observed in liquids. Here, the time one reactant spends next to another is much longer than that in the gas phase. For this reason, the two particles can enlarge the possibilities from those of fleeting acquaintance to the more productive ones of prolonged contact, leading much more often to permanent association. One can determine the order of magnitude of the time of contact (see Section 4.2.18) as

$$D = kl^2 \tag{5.140}$$

where $D$ is the diffusion coefficient, $k$ is the rate constant for diffusion, and $l$ is the distance a particle covers in one jump of its movement in diffusion. From the above equation,

$$\frac{1}{k} = \tau = \frac{l^2}{D} \tag{5.141}$$

Thus, $\tau$ is the residence time, the time between "hops," the time the two reactant particles have to decide whether to react. Near the melting point of a molten salt, the diffusion coefficient in solutes is on the order of $10^{-5}$ $cm^2$ $s^{-1}$. With $l$ chosen as $3 \times 10^{-8}$ cm (a typical value of the distance between sites within the molten salt structure), one obtains $\sim 10^{-10}$ s for the residence time, which is about 100 times longer than that in the gas phase at the same temperature and hence there is a hundredfold greater chance to react.

However, there is another reason why the molten salt is often a more effective medium for carrying out a reaction quickly. Reaction rates are proportional to $e^{-E_a/RT}$, where $E_a$ is the energy of activation of the reaction. Assume $E_a = 10^5$ J $mol^{-1}$. Then, if one compares the rates at 300 and 600 K, the reaction rate is $10^8$ higher at the higher temperature if the rate-determining step in the reaction remains the same.

Consider, for example, a dissolved organic molecule, RH, reacting with dissolved $O_2$ to give $CO_2$ and $H_2O$. If the reaction at 300 K occurs at a rate $v_1$, that at 600 K should occur at a greatly increased rate. Could this be achieved by heating the dissolved materials in an aqueous solution? Of course not! For unless one uses a pressure vessel (with the added expense of having one made), the aqueous solution cannot be heated much above 373 K before the solution boils. On the other hand, molten salts are available over the whole temperature range—from room temperatures with the $AlCl_3$ complexes in organics such as imidazoline—to molten silicates at 2000 K.

A good example of the success of a molten salt reactor is the work carried out by Guang H. Lin at Texas A&M University in 1997. This has led to a new method for the complete consumption of carbonaceous material at low cost. Lin introduced a mixture of paper, wood, and grass in pellets into a molten salt eutectic of $KNO_3$, and

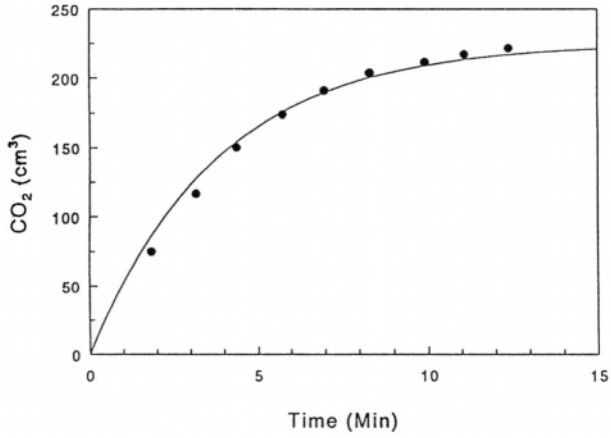


**Fig. 5.64.** Production of $CO_2$ as a function of time in a molten salt reactor of $KNO_3$ and $LiNO_3$.

$LiNO_3$ at temperatures that ranged from 670 to 870 K. At the same time, he contrived to have a stream of minute bubbles of $O_2$ at 670 K flow through the liquid electrolyte. The organic material (incompletely dissolved) reacts very rapidly to give $CO_2$ and $H_2O$. A plot of some of Lin's results[32] is shown in Fig. 5.64.

The oxygen stream can be merely air. Lin showed that the method can be extended to consume rubber. Scaled up, Lin's work *could be the solution to most waste disposal problems* (including consumption of the solid sludge left over from the modern treatment of sewage; rubber tire disposal; and that of superdangerous organics such as Agent Orange). The point is that the combustion is so complete and so quick that there are no noxious effluents to reach the air.

## Further Reading

### *Seminal*

1. J. E. Gordon, *Application of Fused Salts in Organic Chemistry,* in *Techniques and Methods of Organic Chemistry,* Vol. 1, Marcel Dekker, New York (1969).
2. L. Lessing, "Sewage Disposal in Molten Salts," *Fortune* 138 (July 1973).
3. J. W. Tomlinson, "High-Temperature Electrolytes," in *Electrochemistry: The Past Thirty and the Next Thirty Years,* H. Bloom and F. Gutmann, eds., Plenum Press, New York (1977).

### *Papers*

1. L. Kaba, D. Hitchens, and J. O'M. Bockris, *J. Electrochem. Soc.* 137: 5 (1990).

[32]The key to success is to keep the pellets from rising to the top of the molten salt and floating there. Lin contrived to inject the pellets beneath a cage of metal gauze where they remain trapped—keeping them in contact with the molten salt and $O_2$ until consumed.

2. A. Berrukov, O. Deryabina, L. Maharinsky, N. Halterinsky, and A. Berlin, *Int. J. Polym. Mater.* **14**: 101 (1990).
3. E. Sada, H. Kumazawa, and M. Kudsy, *Ind. Ghem. Res.* **31**: 612 (1992).
4. U. Gat, J. R. Engel, and H. L. Dodds, *Nuc. Technol.* **100:** 390 (1992).
5. C. Tennakoon, R. Bhardwaj, and J. O'M. Bockris, *J. Appl. Electrochem.* **26**: 18 (1996).

## 5.12. THE NEW ROOM-TEMPERATURE LIQUID ELECTROLYTES

At the beginning of this chapter it was pointed out that aqueous and many nonaqueous electrochemical systems suffer from the small size of the potential range in which solutes dissolved in them can be examined. This is because (for pH = 0, say) if the potential of an electrode immersed therein is more *negative* than 0.00 V on the normal hydrogen scale (see Section 4.8.3), the water itself in the solution begins to decompose to form $H_2$. On the other hand, at a potential more *positive* than 1.23 V on the same scale, the aqueous solvent tends to decompose to form $O_2$.

It is true that this small window of 1.2 V is extendable in both potential directions, particularly on the positive side because the phenomenon of overpotential (Chapter 7) is especially strong there and the potential that has to be applied to the positive electrode to get a significant current density may be as high as 1.8 V. Nevertheless, it has been felt for decades that systems were needed in which one could make the potential of electrodes more positive (thus releasing a greater power in oxidation) and also more negative (greater power of reduction) than is currently possible because of the solvent decomposition problem in aqueous solutions.

Indeed, the possibility of using molten salts to extend the potential window in which electrochemical reactions can occur has been one of the driving forces behind the need to know about the liquid electrolytes described in this chapter. Thus, for liquid NaCl, significant decomposition does not occur till c. 3.0 V have been applied across an electrochemical cell containing liquid NaCl. This gives twice the electrochemical window, which in aqueous systems is as low as 1.2 V. However, the sacrifice has been that one had to work at more than 1120 K, with all the attendant experimental difficulties that work at high temperatures brings.[33]

It has long been known that liquid electrolyte systems that melted in the low hundreds of degrees were available in systems of metal chlorides and $AlCl_3$, and that some tetraalkylammonium salts melted at < 373 K. Hurley and Wier in 1951 showed that a 2:1 mixture of some complex organic chlorides with $AlCl_3$ gave liquid electrolytes at room temperatures. The discovery remained undeveloped for more than 25

[33]There are a good many of these, although they are less at temperatures below, say 770 K, when glass vessels can still be used, and they increase exponentially as the temperature is increased. They include the difficulty that the containing vessels tend to dissolve in the liquid electrolyte solvent, the evaporation and decomposition thereof, the need to take precautions in experimental design to achieve a uniform temperature, the troubles of extensive thermal insulation, cracking of the refractory vessels, etc.

years. However, in 1977, Halena Chum, writing with Koch and Osteryoung,[†] found that such systems (to be precise: 1-Methyl-3-ethylimidazolonium chloride in union with $AlCl_3$) could be made into liquid electrolyte solvents, and that many such systems had melting points near room temperature. Such systems have been under intensive examination in the '80s and '90s, largely by American electrochemists, among whom Osteryoung, Wilkes, and Hussey have—each with his own team—led most of the contributions. Although the chemistries (including the redox properties) of many of these systems have been researched, their applications (e.g., to energy storage systems) are in the early development stage and promise rich yields. The electrochemical windows are often above 3 V and occasionally extend even to 6 V!

### 5.12.1. Reaction Equilibria in Low-Melting Point Liquid Electrolytes

Redox reactions are subject to examination in solvent systems such as 1-butylpyridinium chloride with $AlCl_3$, which melts at 308 K (correspondingly, 1-3-dialklyimidazolonium chloride). These molecules are

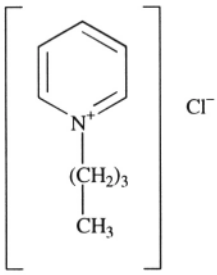


1-butylpyridinium chloride

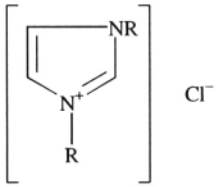


1,3-dialkylimidazolonium chloride

Many treatments of these solvent systems are in terms of acid–base equilibria, and the basis is to regard $Cl^-$ as a Lewis base.[34] In these terms, the heptachloroaluminate is a strong Lewis acid.

---

[†]Robert Osteryoung is picked out here for recognition because—apart from his pioneering work on low temperature molten salts—he is well known for his early work on pulse techniques (Chap. 8). He was the first to develop computers to control electrochemical experiments. Professor Osteryoung is a Head of Chemistry at North Carolina State University where unlike some great researchers, he is well known for his success as an able administrator.

[34]In Lewis's view, a base *donated* an electron pair and an acid accepted an electron pair. For example, consider the reaction

$$R_3N + BF_3 \rightarrow R_3N - BF_3$$

The $R_3N$ is the base and the $BF_3$ the acid.

This definition of acids and bases is broader than that of Brønsted, which had an acid as something that *gave* protons and a base as something that *accepted* protons. Thus, Lewis's definition includes reactions involving $H^+$ ions, oxide ions, and solvent interactions.

In one of the low-melting liquid electrolyte systems containing $AlCl_3$ one has a changing acid/base character, depending on the ratio of $AlCl_3$ to the organic partner.

| BASE | ACID |
|---|---|
| $AlCl_3/RCl < 1$ | $AlCl_3/RCl > 1$ |
| $R^+$, $Cl^-$ and $AlCl_4^-$ | $Al_2Cl_7^-$ |

In systems of organic chlorides such as R–Cl with $AlCl_3$, when the $AlCl_3$ is first added (in low concentrations), the Al is largely in the form of $AlCl_4^-$, but as the $AlCl_3$ increases in relative concentration, the system becomes acid in the Lewis sense, and the dominating constituent is the ion $Al_2Cl_7^-$:

$$2\,AlCl_4^- \rightleftharpoons Al_2Cl_7^- + Cl^- \tag{5.142}$$

To obtain the equilibrium constant in these systems, one can use electrochemical cells such as those described in Section 3.4.8. For example, measurements that involve Al electrodes have a $K$ value of $3.8 \times 10^{-13}$ at 308 K and the reaction is displaced to the right in a system formed with butylpyridinium chloride.

Attractive interactions occur between acids such as $R^+$, $Al_2Cl_7^-$, $AlCl_4^-$, and $Cl^-$. A sign of this is the increase in viscosity.

Among the kind of probable structures are ($Im^+$= imidazolonium),

$$Cl^- - Im^+ - Cl^-$$

$$Cl^- - Im^+ - AlCl_4^-$$

$$AlCl_4^- - Im^+ - Al_2Cl_7^-$$

and NMR measurements are consistent with these structures.

### 5.12.2. Electrochemical Windows In Low-Temperature Liquid Electrolytes

Whereas 1.2 V is the fundamental electrochemical window in aqueous solutions, more than 3 V is available in some of the currently discussed systems. As a concrete example, Al can be electrochemically deposited from $Al_2Cl_7^-$ at –0.4 V with an Al electrode taken as reference. The evolution of $Cl_2$ occurs at +2.5 V against the same reference electrode. Thus, the window is 2.5 – (–0.4) = 2.9 V.

### 5.12.3. Organic Solutes in Liquid Electrolytes at Low Temperatures

A number of organic solutes undergo reaction with $AlCl_3$. For example, aromatic amines dissolve in the room-temperature molten electrolyte butylpyridinium chloride. Triphenylamine (TPA) shows two stages of oxidation upon polarographic examina-

tion. The first reaction involves the formation of the radical cation. On the other hand, in a neutral or acid melt, the behavior is different and probably

$$TPA \rightarrow TPA^{+} + e$$

followed by

$$TPA^{+} \rightleftharpoons TPB + H^{+}$$

$$TPB \rightarrow TPB^{2+} + 2\,e^{-} \qquad (5.143)$$

### 5.12.4. Aryl and Alkyl Quaternary Onium Salts

Although researches on room-temperature systems of $AlCl_3$ and butylpyridinium chloride have contributed a new vista to the physical chemistry and electrochemistry of molten salts, the systems carry with them the disadvantage that few of the materials mentioned are commercially available. Correspondingly, molten systems containing the easily available pyridinium cation have to pay a penalty in that pyridinium is easy to reduce.

On the other hand, *onium* salts based in N (or S or P) are commercially available in abundance. Extended by introducing a variety of alkyl and aryl groups, they present a large variety of properties, being all liquid electrolytes.

**TABLE 5.40**
**Sources of Quaternary and Ternary Onium Compounds**

| Compound | Source | Purity (%) |
|---|---|---|
| Trimethylphenylammonium chloride | Kodak | 98 |
| Triethylphenylammonium iodide | Kodak | 99 |
| Trimethylbenzylammonium chloride | Sherex (in water) | 60–65 |
| Triethylbenzylammonium chloride | Kodak | 99 |
| Dimethylethylbenzylammonium chloride | Sherex | N.A. |
| Dimethylphenylbenzylammonium chloride | Pfaltz and Bauer | N.A. |
| Methyldiphenylsulfonium tetrafluoroborate | Lancaster Synthesis | 98 |
| Ethyldiphenylsulfonium tetrafluoroborate | Lancaster Synthesis | 98 |
| Trimethylphenylphosphonium iodide | K and K | N.A. |
| Tetraethylammonium chloride | Kodak | 98 |
| Tetrabutylammonium chloride | Kodak | 92 |
| Tetrapentylammonium chloride | Kodak | 97 |
| Tetrahexylammonium chloride | Kodak | — |
| Tetraheptylammonium chloride | Kodak | 99 |
| Trioctylpropylammonium chloride | Kodak | 90 |
| Tetrabutylammonium perchlorate | Kodak | 99 |

Source: Reprinted from S. D. Jones and G. E. Blomgren, *J. Electrochem. Soc.* **136**: 424, 1989.
[a]N.A. = not available

**TABLE 5.41**

**Melting Points of Various Ammonium Chlorides**

| Chloride | Melting Point (K) |
|---|---|
| Tetramethylammonium chloride | 693 |
| Tetrapentylammonium chloride | 414 |
| Tetrahexylammonium chloride | 385 |
| Tetraheptylammonium chloride | 264 |
| Trimethylphenylammonium chloride | 510(subl.) |

Source: Reprinted from S. D. Jones and G. E. Blomgren, *J. Electrochem. Soc.* **136**: 424, 1989.

**TABLE 5.42**

**Room-Temperature Conductivities of Mixtures of Various Ammonium Chlorides and Aluminum Chloride in a 1:2 Mole Ratio**

| Chloride | Conductivity (mS $cm^{-1}$) |
|---|---|
| Trimethylphenylammonium chloride | 3.40 |
| Triethylphenylammonium chloride | 1.29 |
| Trimethylbenzylammonium chloride | 1.46 |
| Triethylbenzylammonium chloride | 0.32 |
| Dimethylethylbenzylammonium chloride | 0.63 |
| Dimethylphenylbenzylammonium chloride | Very low |

Source: Reprinted from S. D. Jones and G. E. Blomgren, *J. Electrochem. Soc.* **136**: 424, 1989.

**TABLE 5.43**

**Behavior of Sulfonium and Phosphonium Compounds with Aluminum Chloride at a 1:2 Mole Ratio**

| Compound | Observation |
|---|---|
| Methyldiphenylsulfonium tetrafluoroborate | Liquid at room temperature; conductivity = 0.76 mS $cm^{-1}$ at 300 K |
| Ethyldiphenylsulfonium tetrafluoroborate | Melting point slightly above room temperature; conductivity = 2.1 mS $cm^{-1}$ at 308 K |
| Trimethylphenylphosphonium iodide | Melting point slightly above room temperature; conductivity = 3.0 mS $cm^{-1}$ at 308 K |

Source: Reprinted from S. D. Jones and G. E. Blomgren, *J. Electrochem. Soc.* **136**: 424, 1989.

The breadth of the compounds available can be gauged from Table 5.40. Some of the remarkable properties of these compounds are exhibited in Tables 5.41 to 5.43, taken here from the pioneering work of Jones and Blomgren in 1989. Melting points go down as the complexity increases. Tetraheptylammonium chloride melts at 264 K! However, the more complex salts have high viscosity and low conductivity. Conductivity is reduced by the presence of aryl groups. Mixed with $AlCl_3$, liquid eutectics at 198 K can be obtained.

There is probably an interaction between the $\pi$ electrons of the arylammonium cations and the $Al_2Cl_7^-$ anions. This would account for the lowering of the melting point by these salts. Furthermore, these $\pi$ bonds may well be *delocalized*, again helping to lower the melting point. The smaller organic groups provoke lower viscosity and hence (Walden's rule) a higher conductance.

The electrochemical window obtainable with the low-temperature liquid onium systems is about 3 V, which is about the same as that with high-temperature liquid NaCl. NMR measurements of these low-temperature electrolytes can be informative. For example, $EtAlCl_2$-containing melts can be examined by registering the NMR characteristics of probe groups (e.g., $^{13}C$ and $^{47}Al$). The NMR relaxation provides information on interactions in systems such as $MEI^+$ groups and various properties of $EtAlCl_2$. It is found that $MEICl\text{-}AlCl_3$ exhibits interaction of the $MEI^+$ ring and $EtAlCl_2$. Even greater electrochemical windows, up to 4 V, are available, for example, with an alkyl-substituted aromatic heterocyclic cation and trifluoromethane sulfonate.

### 5.12.5. The Proton in Low-Temperature Molten Salts

$H^+$ is regarded as a contaminant in molten salt work. It arises from the pervasive presence of water vapor. It can be studied, e.g., with $AlCl_3$-1-ethyl-3-methylimidazolonium chloride (ImCl). The methods used have been Fourier transform infrared (FTIR) and NMR spectroscopies and standard electrochemical techniques.

The proton is found to exist in these melts as HCl and $HCl_2^-$. The equilibrium between these two forms can be studied by the methods stated (particularly NMR) and turns out to be much in favor of the anion. If the concentration of HCl is above 0.5 in mole fraction, various complex ions ($H_nCl_{n+1}^-$, $n > 2$) begin to form. Thus, it turns out that $H^+$ can be taken up in these salts, but only in the form of complex anions.

## Further Reading

### *Seminal*

1. F. Hurley and J. P. Wier, "Electrodeposition of Metals from Fused Quaternary Ammonium Salts," *J. Electrochem. Soc.* **98**: 203 (1951).
2. H. L. Chum, V. R. Koch, L. L. Miller, and R. A. Osteryoung, "An Electrochemical Scrutinity of Organometallic Iron Complexes and Hexamethylbenzene in a Room Temperature Molten Salt," *J. Am. Chem. Soc.* **97**: 3265 (1975).

### *Review*

1. R. A. Osteryoung, "Organic Chloraluminates Ambient Temperature," in *Molten Salts*, G. Mamantov, ed, *NATO ASI Series C* **202**: 329 (1987).

### *Papers*

1. J. Jeng, R. D. Allendorfer, and R. A. Osteryoung, *J. Phys. Chem.* **96**: 3531 (1992).
2. J. L. E. Campbell and K. E. Johnson, *Proc. Electrochem. Soc.* **92-16**: 317 (1992).
3. P. C. Truelove and R. A. Osteryoung, *Proc. Electrochem. Soc.* **92-16**: 303 (1992).
4. P. C. Truelove and R. T. Carlin, *Proc. Electrochem. Soc.* **93-9**: 62 (1993).
5. R. T. Carlin and T. Sullivan, *J. Electrochem. Soc.* **139**:144 (1992).
6. T. L. Riechel and J. S. Wilkes, *Proc. Electrochem. Soc.* **92-16**: 351 (1992).
7. T. L. Riechel and J. S. Wilkes, *J. Electrochem. Soc.* **140**: 3104 (1993).
8. R. A. Mantz, R. C. Truelove, K. T. Carlin, and R. A. Osteryoung, *Inorg. Chem.* **34**: 3846 (1995).
9. W. J. Gau and I. W. Sun, *J. Electrochem. Soc.* **143**: 914 (1996).
10. E. Hondrogiannis, *J. Electrochem. Soc.* **142**:1758 (1995).
11. W. R. Carper, *Inorg. Chim. Acta* **238**: 115 (1995).
12. K. E. Johnson, *Can. J. Chem.* **73**: 593 (1995).

## 5.13. MIXTURES OF LIQUID OXIDE ELECTROLYTES

### 5.13.1. The Liquid Oxides

Fused salts (and mixtures of fused salts) are not the only type of liquid electrolytes. Mention has already been made of *fused oxides* and in particular mixtures of fused oxides. A typical fused oxide system is the result of intimately mixing a nonmetallic oxide ($SiO_2$, $GeO_2$, $B_2O_3$, $P_2O_5$, etc.) and a metallic oxide ($Li_2O$, $Na_2O$, $K_2O$, MgO, CaO, SrO, BaO, $Al_2O_3$, etc.) and then melting the mixture. The system can be represented by the general formula $M_xO_y - R_pO_q$, where M is the metallic element and R is the nonmetallic element.

Why give these liquids special consideration? Are not the concepts developed for understanding molten salts adequate for understanding molten oxides? The essential features of fused salts emerge from models of the liquid state. There is no doubt that the fluidity of molten salts demands a model with plenty of free space, and a model based on density fluctuations that are constantly occurring in all parts of the liquid seems about the best way to think of the inside of a molten liquid. Is the same dependence on the opening up of temporary vacancies an adequate basis for explaining the behavior of the fused oxides?

### 5.13.2. Pure Fused Nonmetallic Oxides Form Network Structures Like Liquid Water

Some of the special features of molten oxides must now be described for it is these features that do not permit the hole model of ionic liquids to be applied to fused oxides

**TABLE 5.44**

**Specific Conductivity of Water and Molten $SiO_2$ and NaCl near the Melting Point**

| Substance | $\kappa$ (S cm$^{-1}$) | Temp (K) |
|---|---|---|
| $SiO_2$ | $7.7 \times 10^{-4}$ | 2073 |
| NaCl | 3.6 | 1074 |
| $H_2O$ | $4 \times 10^{-8}$ | 291 |

in the same way it is applied to molten salts. The first interesting feature of molten silica, is that its conductivity is more like that of water (i.e., molten ice) than that of fused NaCl (Table 5.44).

The dissimilarity in the conductivities of liquid NaCl, on the one hand, and liquid water and liquid silica, on the other, is of fundamental importance. When NaCl is fused, the ionic lattice (the three-dimensional periodic arrangement of ions) is broken down (see Section 5.1.2) and one obtains an *ionic liquid.* When ice is melted, the tetrahedrally directed hydrogen bonding involved in the crystal structure of ice is partially retained. Thus, water is not a collection of separate water molecules but an association (based on hydrogen bonding) of water molecules in a three-dimensional network. The network, however, does not extend indefinitely. There is a periodicity and only short-range order, implying a certain degree of bond breaking. It is this network structure that is responsible for the small mole fraction of free ions ($H^+$ and $OH^-$) in water, in contrast to the almost total absence of any ion association (into pairs, complexes, etc.) in liquid NaCl. This great difference in the concentration of charge carriers is responsible for a difference in the specific conductivities of liquid NaCl (high charge carrier concentration) and liquid water (very low charge carrier concentration) that is several orders of magnitude.

The specific conductivities of water and of fused silica are both very low. This suggests that the structures of crystalline water [Fig. 5.65(a)] and crystalline silica [Fig. 5.65(b)] have much in common. Each oxygen atom in ice is surrounded tetrahedrally by four other oxygens, the oxygen–oxygen bonding occurring by a hydrogen bridge (the hydrogen bond). In crystalline silica, there are $SiO_4$ tetrahedra occurring through an oxygen bridge. The different forms of ice and the different forms of silica (Fig. 5.66) correspond to different arrangements of the tetrahedra in space.

It is reasonable therefore to consider that fused silica resembles liquid water. Just as liquid water retains from the parent structure (ice) the three-dimensional network but not the long-range periodicity of the network, one would expect that liquid silica also retains the continuity of the tetrahedra, i.e., the space network, but loses much of the periodicity and long-range order that are the essence of the crystalline state. This model of fused silica, based on keeping the extension of the network but losing the translational symmetry of crystalline silica, implies a low concentration of charge

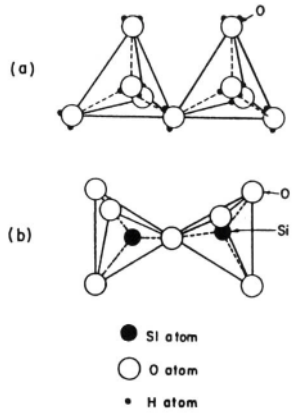


**Fig. 5.65.** The similarity between the basic building blocks of (a) ice and (b) crystalline silica structures.

carriers in pure liquid silica and therefore low conductivity in comparison with a molten salt (see Tables 5.44 and 5.45).

### 5.13.3. Why Does Fused Silica Have a Much Higher Viscosity Than Do Liquid Water and the Fused Salts?

It has just been argued that the conductivities of simple ionic liquids, on the one hand, and liquid silica and water, on the other, are vastly different because a fused salt is an unassociated liquid (it consists of individual particles) whereas both molten silica and water are associated liquids with network structures. What is the situation with regard to the viscosities of fused salts, water, and fused silica? Experiments indicate that whereas water and fused NaCl have similar viscosities not far above the melting points of ice and solid salt, respectively, fused silica is a highly viscous liquid (Table 5.46). Here then is an interesting problem.

One successful theory of transport processes in liquids are based on elementary acts, each act consisting of two steps: (1) holes are formed and (2) particles jump into these holes (see Section 5.7.4). For fused salts and other nonassociated liquids, this theory was successful in explaining the movements and drift of particles although it clashed with molecular dynamics calculations that seemed to favor a shuffle-along mechanism for transport. The *mean* volume of a hole is determined by the surface tension as follows [*cf.* Eq. (5.44)]:

$$\langle v_h \rangle = 1.6 \left( \frac{kT}{\gamma} \right)^{3/2} \tag{5.144}$$

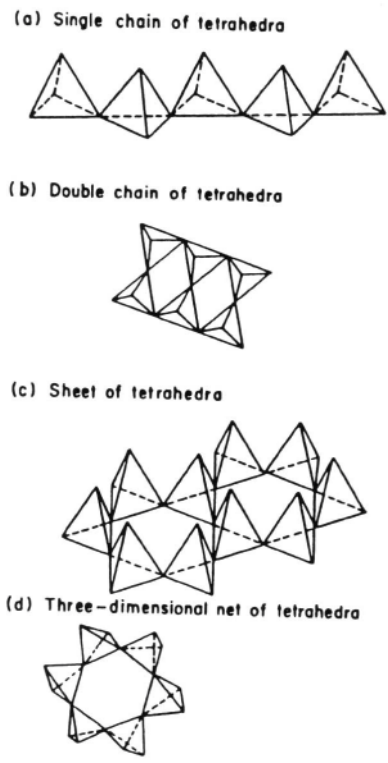


**Fig. 5.66.** Forms of silicates resulting from different ways of linking up $SiO_4$ tetrahedra: (a) single chain of tetrahedra; (b) double chain of tetrahedra, as in asbestos; (c) sheets of tetrahedra, as in clay, mica, and talc; and (d) networks of tetrahedra, as in ultramarine.

from which it turns out that in *unassociated fused salts*, the size of the holes is roughly equal to the size of individual ions. In those simple liquids, holes can receive ions of the fused salt which jump into them. Furthermore, in simple ionic liquids, the free energy of activation for the jumping of ions into holes is much less than that of the free energy for forming the holes. Once the hole is formed in a fused salt, the jump into the hole is three to ten times easier than forming the hole.

The surface tension of fused silica is only about three times that of fused sodium chloride. Hence [see Eq. (5.144)] in fused silica also there would be many holes of atomic dimensions, as for fused ionic liquids.

**TABLE 5.45**

**Electric Conductance in the Liquid Silicates**

| Cation | Composition $XM_xO - YSiO_2$, $X:Y$ | $\kappa_{1750\,°C}$ (S $cm^{-1}$) | $\Lambda_{1750\,°C}$ | $\Delta H^*$ (kcal $g^{-1}$ $ion^{-1}$)[a] |
|---|---|---|---|---|
| $K^+$ | 1:2 | 1.5 | 71.8 | 8.2 |
| | 1:1 | 2.4 | 82.7 | 8.0 |
| $Na^+$ | 1:2 | 2.1 | 83.3 | 12.0 |
| | 1:1 | 4.8 | 126.0 | 13.5 |
| $Li^+$ | 1:2 | 2.5 | 77.8 | 11.6 |
| | 1:1 | 5.5 | 109.0 | 10.6 |
| | 2:1 | 23.2 | 332.0 | 9.6 |
| $Ba^{2+}$ | 1:2 | 0.18 | 6.4 | 33.2 |
| | 1:1 | 0.60 | 16.2 | 17.5 |
| | 2:1 | 1.32 | 29.9 | 9.0 |
| $Sr^{2+}$ | 1:2 | 0.21 | 7.7 | 36.0 |
| | 1:1 | 0.63 | 15.7 | 26.7 |
| | 2:1 | 1.4 | 26.8 | 17.0 |
| $Ca^{2+}$ | 1:2 | 0.31 | 11.4 | 30.0 |
| | 1:1 | 0.83 | 18.4 | 20.0 |
| | 2:1 | 1.15 | 18.8 | 20.0 |
| $Mn^{2+}$ | 1:2 | 0.55 | 18.2 | 24.0 |
| | 1:1 | 1.8 | 35.1 | 16.0 |
| | 2:1 | 6.3 | 85.5 | 12.0 |
| $Fe^{2+}$ | 1:1 | 1.82 | 44.0 | 15.0 |
| $Mg^{2+}$ | 1:2 | 0.23 | 6.5 | 34.0 |
| $Mg^{2+}$ | 1:1 | 0.72 | 12.2 | 24.0 |
| | 2:1 | 2.15 | 24.7 | 17.0 |
| $Al^{3+}$ | 10 wt% | $3.10^{-3}$ | 0.20 | 22.0 |
| $Ti^{4+}$ | 10 wt% | $6.10^{-4}$ | 0.05 | 35.7 |

[a] 1 cal = 4.184 J

**TABLE 5.46**

**Viscosities of Fused Silica, Water, and Fused NaCl**

| Substance | Temp. (K) | Viscosity (poise) |
|---|---|---|
| Liquid $SiO_2$ | 1993 | $3 \times 10^6$ |
| Water | 298 | $9 \times 10^{-3}$ |
| Fused NaCl | 1123 | $13 \times 10^{-3}$ |

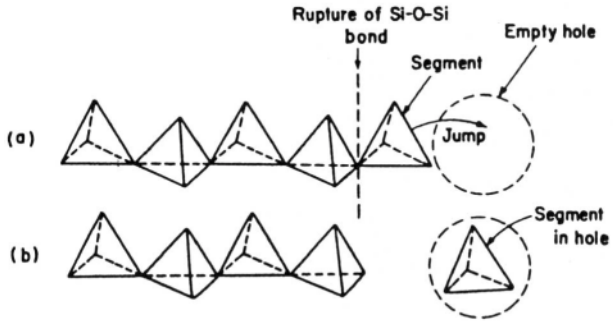


**Fig. 5.67.** Schematic diagram to show a segment of an $SiO_4$ chain breaking off and jumping into an empty hole: (a) before jump and (b) after jump.

In simple ionic liquids (e.g., NaCl), the holes are atom sized; *so are the jumping ions.* Jumping is easier than making holes. What particles can jump into holes in fused silica? Obviously, large chunks of a silicate network (for suggestions, see later discussion) cannot jump into holes that are about the same size as those that receive $Na^+$ and $Cl^-$, etc. How then can jump-dependent transport processes occur? There may be a way. Small segments (one to a few atoms in size) can break off from the network and these pieces (segments) can do the jumping (Fig. 5.67).

A comparison between transport processes in simple fused salts and in fused $SiO_2$ is interesting. In molten salts, the jump was easier than making the hole but nevertheless many voids of different sizes were shown to form in the liquid. The rate of the process was controlled more by the rate of hole formation than the easier jumping. However, with molten silica, the balance of influences is different. Holes are as easily formed as in the ionic liquids because the rate of hole formation is controlled by the vibrations of the atoms relative to each other, but it is difficult to produce individual small particles because this would involve rupturing strong Si–O–Si bonds holding the network together (Table 5.47). Therefore, in the silicates, the rate-determining process is the bond-rupture step. While in simple ionic liquids the experimental activation energy[35] for a transport process, such as a viscous flow, is determined predominantly by the enthalpy of hole formation, in associated liquids with network structures it is determined entirely by the energy required to break the bonds of the network to produce a "flow unit" sufficiently small to jump into the relatively easily made hole.

[35]It will be recalled that it was decided that the quantity obtained from the slope of the log $\eta$ versus $1/T$ curve would be termed an *energy* of activation irrespective of whether it pertains to constant-pressure or constant-volume conditions, though under the former it is an enthalpy and under the latter, it is an energy.

**TABLE 5.47**

**Comparison between Transport Processes in Simple Fused Salts and in Liquid Silica**

| | System | |
|---|---|---|
| | Fused Salt | Liquid Silica |
| Essence of situation | Particles waiting to jump into holes | Holes waiting for small enough segments of networks |
| Rate-determining step | Hole formation | Rupture of bonds between segments and network |
| Energy of activation for transport process (approx.) | $\Delta H_{\text{hole formation}}$ | $\Delta H_{\text{bond rupture}}$ |

In this difference of the rate-controlling mechanism for flow lies the answer to the next question. Why is the viscosity of associated water similar to that of molten NaCl, which has no network? The difference in the viscosity behavior of water and of fused silica lies in the ease with which segments can be broken off the two networks. The Si–O–Si chemical bonds are much more difficult to rupture than the O–H–O hydrogen bonds (Table 5.48). Thus, flow units—probably individual $\mathbf{H_2O}$ molecules—are so easily produced in water that the holes do not have much of a wait; an ease of flow, high fluidity or low viscosity, results. This is not the case with fused silica because of the much higher bond-breaking energy, and a high viscosity results.

Some support for the idea that the viscous-flow properties of associated liquids such as liquid silica and water are determined by the step of bond breaking rather than that of hole formation comes from the experimental plots of log $\eta$ versus $1/T$. These plots suggest a slight trend away from linearity (Fig. 5.68), which is not the case for fused salts (Fig. 5.29). For water also, the plot is curved slightly, with the experimental energy of activation for viscous flow $E_{\eta,p}$ decreasing with increasing temperature. The explanation for this phenomenon is as follows. Because the energy of activation for viscous flow depends upon the breaking of bonds and because, according to the Boltzmann distribution, the fraction of broken bonds increases with temperature, the

**TABLE 5.48**

**Heat of Dissociation of Si–O and O–H Bonds**

| Bond | Heat of dissociation (kcal $mol^{-1}$)[a] |
|---|---|
| Si–O–Si | 104 |
| O–H–O, hydrogen bond | 5 |

[a] 1 cal = 4.184 J.

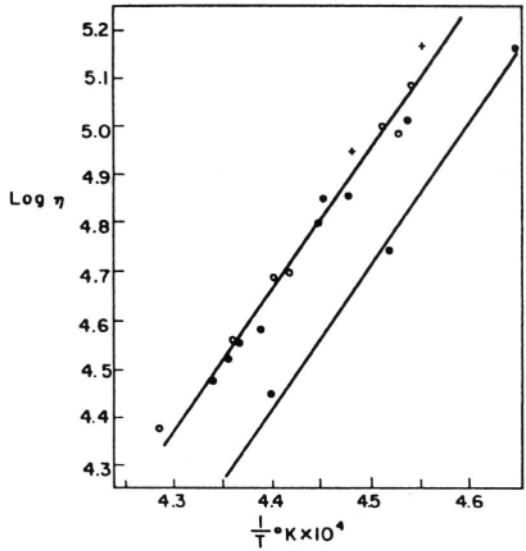


**Fig. 5.68.** Two independent sets of data for the difficultly determinable viscosity $\eta$ of liquid $SiO_2$. Both suggest a slight tendency to curve in the sense that the energy of activation becomes higher at the lower temperatures.

fraction required to be broken by the shearing force in viscous flow decreases with an increase in temperature and, correspondingly, there is a decreasing energy of activation with increasing temperature.

To summarize: Unlike fused salts, mixtures of fused oxides are *associated liquids*, with extensive bonding between the individual molecules or ions. In fused oxides, hole formation occurs but it is not the step that determines the rate of transport processes. It is the rate of production of individual small jumping units that controls them. This conclusion makes it essential to know what (possibly different) entities are present in fused oxides and what are the *kinetic* entities. In simple fused salts, the jumping particles are already present (they are the ions themselves); the principal problem is the structure of the empty space or free volume or holes, and the properties of these holes. In molten oxides, the main problem is to understand the structure of the macrolattices or particle assemblies from which small particles break off as the flow units of transport.

### 5.13.4. Solvent Properties of Fused Nonmetallic Oxides

If fused silica is a three-dimensional, aperiodic network, all the atoms are to some extent joined together, i.e., the liquid is a giant molecule. Can ions dissolve in such a

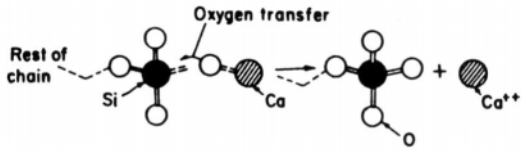


**Fig. 5.69.** The interaction between a metal oxide and a silicon atom of the silica network.

structure? Water also is a network structure like $SiO_2$, and ions dissolve in water. Hence, liquid $SiO_2$ may well be expected to have solvent properties leading to the production of ionic solutions.

Water, it may be recalled (Chapters 2 and 4), has two modes of solvent action, depending on the nature of the added electrolyte. The water can contact an ionic crystal (e.g., NaCl), detach the ions from the lattice through the operation of ion–dipole (or ion–quadrupole) forces, and convert them to hydrated ions (Chapter 2).

The water can also interact *chemically* with a potential electrolyte (e.g., $CH_3COOH$). The hydrogen atom forming part of the hydroxyl group of the organic acid does not differentiate between the oxygen atoms of the water network and that of the OH group. The hydrogen of the OH group detaches itself from the organic acid. Two ions are thus formed: a hydrogen bonded to a water molecule from the solvent and an organic anion. This mode of solvent action is a proton-transfer or acid–base reaction.

The type of solvent action that fused nonmetallic oxides have on metallic oxides may be likened to the second type of dissolution process, i.e., proton-transfer reactions. The process may be pictured as follows. The oxygens cannot discriminate between the metal ions $M^+$ (of the metallic oxide), with which they have been associated in the lattice of a metal oxide before dissolution, and the oxygen atoms of the $SiO_4$ tetrahedra contained in the solvent—fused silica. The oxygen atoms sometimes therefore leave the metal ions and associate with those of the tetrahedra. Dissolution has occurred with a type of oxygen-transfer reaction (see Fig. 5.69).

There is a further analogy between the solvent actions exercised by water and a fused nonmetallic oxide. Just as water dissolves an electrolyte at the price of having its structure disturbed, so also the reaction resulting from the addition of a metallic oxide to a fused nonmetallic oxide like silica is equivalent to a bond rupture between the $SiO_4$ tetrahedra (Fig. 5.70). Solvent action occurs in fused oxide systems along with a certain breakdown of the network structures present in the pure liquid solvent (e.g., in pure liquid silica).

### 5.13.5. Ionic Additions to the Liquid-Silica Network: Glasses

An interesting aspect of molten oxide electrolytes may be mentioned at this point. Some liquids can appear to be solids, i.e., some solids are really liquids of such high

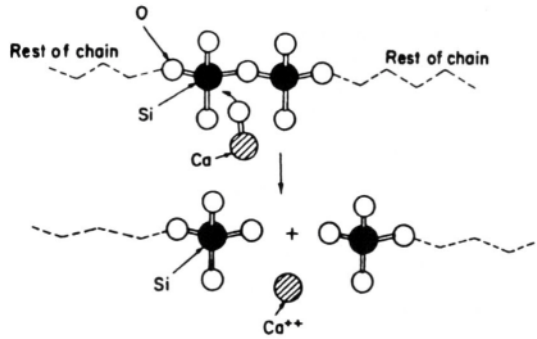


**Fig. 5.70.** The oxygen-transfer reaction leads to a rupture between the $SiO_4$ tetrahedra.

viscosity that no significant flow occurs over tens or hundreds of years. These solidlike liquids are called *glasses.* The structure breaking that has just been described is an aspect of the basic mechanism behind the formation of glasses, which might be regarded as "cold molten silicates."

When ions with a relatively large radius and small peripheral field are added to liquid silica, they produce structure breaking in the network. This is shown in a one-dimensional way in Figs. 5.69 and 5.70. With an increase in the number of ruptures in the network, there is an increase in the number of "free" or "dangling" ends of the ruptured network. The network becomes increasingly *distorted* with an increase in the mole fraction of the metallic oxide present.

If the "broken-down network" is at a sufficiently high temperature, it is known as a *liquid silicate.* Such a system results, for example, from adding an alkali oxide (e.g., $Na_2O$) in low concentration to $SiO_2$. At these temperatures the system can be distinctly a *liquid*, though the viscosity near the melting point may be, for example, 427 poises (P) (at 1820 K), whereas that of water at its melting point is about 0.01 P. When the temperature is dropped, the liquid silicate attempts to "freeze," but, to do this, the long-range order of the crystalline silicate has to be reestablished. The establishment of order, however, requires rearrangement of the structure; i.e., the kinetic units of the broken-down network must move into the sites corresponding to order. Were these particles, or kinetic units, simple, they would be agile, i.e., their movements would be easy, the viscosity would be low, and the restoration of crystalline order would be accomplished almost immediately. A crystalline solid with a sharp melting point would result.

However, this reorganization is precisely what is not quickly accomplished by the entities in the broken-down networks in liquid silicates. The entities[36] resulting from

[36]The nature of these large anionic entities that exist in glass-forming silicates is discussed in Section 5.13.8.

the rupturing of three-dimensional networks when metal oxides are added are large and sluggish. They cannot get into line in time; the viscosity is too high. The loss of thermal energy during cooling catches them still out of position as far as the regular three-dimensional arrangement of the crystalline silicate is concerned. Then it is too late, for as the temperature drops still further, they are still less likely to be able to get back into line before the structure forming about them is too inhibiting to allow further movement. The loss of thermal energy freezes the structure of the liquid silicate—a glass is formed. It is a "frozen liquid," i.e., a liquid that has been supercooled to such a high viscosity that it seems to have the essential requirement of a solid—absence of flow. A beam of X-rays, however, would reveal an essential characteristic of the liquid state, namely, the absence of long-range periodicity.

If, however, sufficient time is allowed (e.g., a few hundred years), a sufficient number of the units of the broken-down network will get back into line. Long-range order will be partly reestablished; the glass will "deglassify" or devitrify, as it is called, and will often split up and break.

How is the liquid-silicate network affected by the addition of various types of ions in the production of the peculiar and complicated kind of pure electrolyte, a glass? It is the answer to this structural question that provides the basis for the understanding of the *glassy* state.

### 5.13.6. The Extent of Structure Breaking of Three-Dimensional Network Lattices and Its Dependence on the Concentration of Metal Ions Added to the Oxide

The extent of breakdown of the network structures present in a pure liquid solvent can be viewed in the following way. The $SiO_4$ tetrahedron is accepted as the basic structural unit in a mixture of metallic oxide and fused silica. However, are the tetrahedra linked together at all and, if so, how are they linked together? What is the number of links per silicon? Water molecules are the basic structural unit in an aqueous solution, but extensive linkage and intermolecular bonding occurs in pure water. How is this linkage in molten $SiO_2$ affected by the presence of new ions dissolved in it (Section 5.1)?

In a fused-oxide system, the metal oxide (e.g., $Na_2O$) is the structure breaker; in aqueous solutions, the electrolyte (e.g., NaCl) is the structure breaker. Does the extent of structural breakdown of the continuous Si–O network present in pure silica before the addition of MO depend on the concentration of MO? The extent of breakdown must indeed depend on the concentration of the structure breaker; then one would expect that properties that depend on the size and nature of the structures present would also be concentration dependent.

In fused-oxide systems, a simple way of expressing the concentration of the metal oxide $M_xO_y$ in the fused nonmetallic oxide $R_pO_q$ is sometimes used. This involves the so-called "O/R ratio." The O/R ratio is related to the mole fraction of the metallic

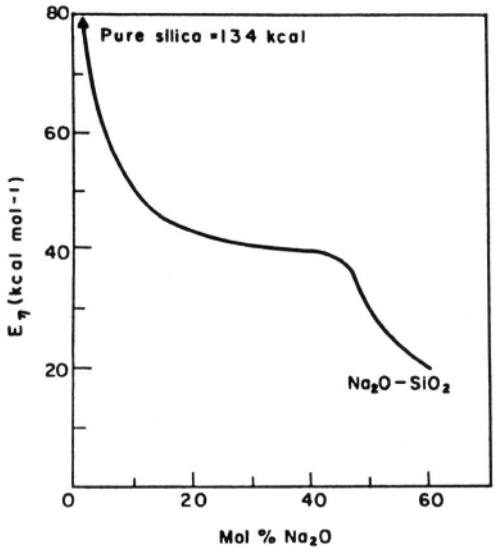


**Fig. 5.71.** The variation of the energy of activation for viscous flow in an $Na_2O + SiO_2$ melt as a function of the mole percent of $Na_2O$. (1 cal = 4.184 J)

oxide. For example, an O/Si ratio of 4 in a system of $Li_2O$ and $SiO_2$ is obtained when the $Li_2O$ has a mole fraction of 66% (i.e., $2Li_2O + SiO_2$ has four Os to one Si).

One way of probing the sizes of structures present in fused-oxide systems and their variation with the mole fraction of MO added to the nonmetallic oxide is through the variation of the ease of flow with composition. The viscosity of the system must be keenly sensitive to the size and nature of the kinetic entities present because it is these entities that must make the jumps from site to site involved in viscous flow.

Experimental results on the variation of the energy of activation for viscous flow, $E_\eta$, as a function of the mole percent of the metal oxide are shown in Fig. 5.71. The basic feature of the results appears to be a very high ($\sim$630 kJ mol$^{-1}$ or 150 kcal mol$^{-1}$) energy of activation for viscous flow of the pure nonmetallic oxide and then a rapid fall with addition of the metallic oxide, whereupon there is a leveling off to a value of about 167 kJ mol$^{-1}$ (40 kcal mol$^{-1}$), which remains relatively unchanged between about 10 and 50 mol% of $Na_2O$ in $SiO_2$. This behavior can be used (Section 5.13.7) as a touchstone in deciding between alternative models for the structural changes accompanying changes in metal-ion concentration.

The structural theories presented will be in terms of the liquid silicates because most research on molten oxides has been done with them, but one can extend the basic structural ideas to fused-oxide systems involving metal oxides dissolved in $B_2O_3$ and

$P_2O_5$ and probably to most liquid electrolytes in which there are largely continuous network structures at very low concentrations of $M_xO_y$.

## 5.13.7. Molecular and Network Models of Liquid Silicates

A naive view of events after the addition of metallic oxides to molten silica is to think of different uncharged molecular species, the species changing with the mole fraction of the metallic oxide. This view has to be given up quickly because studies of *mixtures* of $M_xO_y$ and $SiO_2$ show that these systems are highly conducting and therefore are rich in charge carriers (Table 5.45). One has to suggest ionic, rather than molecular, structures.

A second attempt at interpreting the structure of liquid silicates starts with a consideration of the curve of $E_\eta$ versus the mol% of $M_xO_y$ (Fig. 5.71). It is in terms of the gradual breakdown of the three-dimensional network of fused silica. Just as there is *thermal* bond breaking on going from crystalline to fused silica, one can consider that with the addition of, say, $Na_2O$, the additional O atoms cause Si–O–Si bonds in the originally continuous network of $SiO_2$ to break. This produces structure breaking to various composition-dependent degrees. A mole fraction of 66% for $M_2O$ implies, as already stated, an O/Si ratio of 4 and must therefore be considered a composition at which the only anions are $SiO_4^{4-}$ ions;[37]

What model can be suggested for the corresponding structural changes "inside" the fused-oxide system for the $M_2O$ mole-fraction range from 0 to 66%? From the fact that there is such a sharp fall in the energy of activation for viscous flow between zero and about 10 mol% of $M_2O$ (Fig. 5.71), one must think of a radical change (over this composition range) in the difficulty of causing a kinetic entity or flow unit to break off from the rest of the structure and jump from site to site in the random walk that is the basis of diffusion (Section 5.7.4). The model must of course contain the explanation of the generation of more free ions to account for an increase in conductivity with an increasing amount of MO. The anions postulated as dominant for a given O/R ratio must meet some exacting requirements. Thus (1) they must have formulas consistent with the overall O/R ratio; (2) they must have a total charge that compensates for the total charge of the cations and thereby ensures overall electroneutrality; and (3) they must be shaped in a way consistent with the bond angles, particularly the R–O–R angle, shown from X-ray data in the corresponding solids.

The broad approach used by Zachariasen in the *network* model of liquid silicates is to break down the network present in the pure fused nonmetallic oxide thus

---

[37]Correspondingly, for $M_2O > 66$ mol%, there are oxygen atoms in excess of the ability of the Si atoms present to coordinate them (O/Si ratio > 4). Hence, liquids with such compositions probably contain $SiO_4^{4-}$ and $O^{2-}$ entities in addition to the $M^+$ cations present.

**TABLE 5.49**

**Network Theory of Liquid Silicate Structure**

| Range of Composition (mol% $M_2O$) | Silicate Entities Present |
|---|---|
| 0 | Continuous 3-D network of $SiO_4$ tetrahedra with small degree of thermal bond breaking |
| 0–33 | Essential 3-D network of $SiO_4$ tetrahedra with number of broken bonds equal to number of added O atoms from $M_2O$; end of 3-D boundary at 33% |
| 33 | "Infinite" 2-D sheets of $SiO_4$ tetrahedra; $M^+$ ions and $O^-$ ions between sheets |
| 33–50 | Region of sheets and some chains of tetrahedra |
| 50 | Chains of infinite length |
| 50–60 | Chains of decreasing length |
| 66 | $SiO_4^{4-}$ |

Three-dimensional network with some thermal bond breaking (e.g., $SiO_2$) $\xrightarrow[\text{added}]{M_2O}$ two-dimensional sheets

$\xrightarrow[\text{added}]{\text{more } M_2O}$ one-dimensional chains $\xrightarrow[\text{more } M_2O]{\text{still}}$ simple $SiO_4^{4-}$ monomers

The details of the network theory of liquid-silicate structures, which was first suggested to explain the glassy state, are presented in Table 5.49. The chief defect of this model is that it argues for very large changes in the heat of activation for viscous flow in the composition range of 33 to 66%. However, this is not what is indicated in Fig. 5.71, where the large change comes after 10% oxide. This is because in the network model the size and shape of the kinetic unit—the jumping entity—is supposed to undergo a radical change in the composition range of 33 to 66%. Thus (Table 5.49), sheets are being broken up into chains. The kinetic unit of flow would therefore be expected, in this model, to change radically in size over *this* composition range, and this diminution in size of the flowing unit would be expected to make the heat of activation for viscous flow strongly dependent on composition in *this* composition range (33 to 66% $M_2O$). In contrast to the expectation, however, the $E_\eta$ changes by only 25% over the composition range of 10 to 50% $M_xO_y$ (Fig. 5.71), whereas from 0 to 10% the change in energy of activation is about 200% (Fig. 5.71).

Another inconsistency of the earlier network model concerns the implications that it has for phenomena in the composition region around 10% $M_xO_y$. This is an important composition region. Experimentally, whether one measures the composition dependence of the heat of activation for viscous flow, of expansivity, of compressibility, or

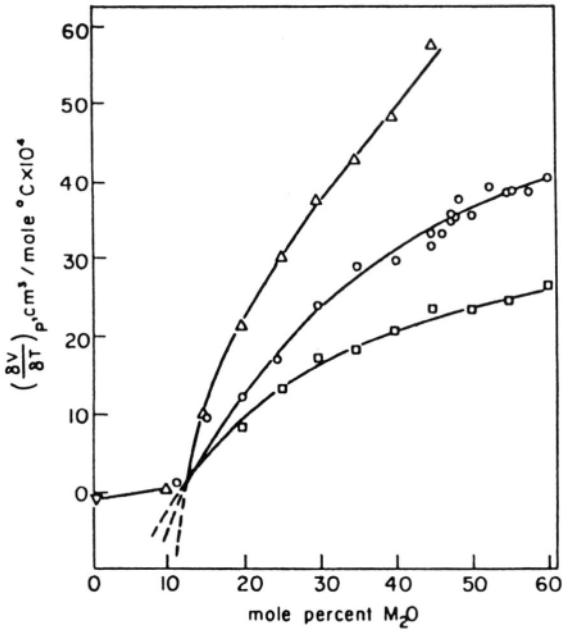


**Fig. 5.72.** The sharp change in the expansivity of $M_2O$-$SiO_2$ melts around the 10 mol% of $M_2O$ composition; (△) $K_2O + SiO_2$, (○) $Na_2O + SiO_2$, (□) $Li_2O + SiO_2$, (▽) $SiO_2$.

of other properties, in all cases there is always a sharp and significant change (Fig. 5.72) around the 10% $M_xO_y$ composition, which indicates a radical structural change at this point. However, this composition has no special significance at all, according to the former network model. Thus, although the network model served well in an earlier stage of the development of the theory of glasses, one must reconsider the situation and develop a model that corresponds more closely, in the expectations it produces, to the experimental facts.

### 5.13.8. Liquid Silicates Contain Large Discrete Polyanions

Consider the situation as one *decreases* the O/R ratio, i.e., decreases the mole percent of the metallic oxide $M_xO_y$. Between 100 and 66% there is little need for special modeling because the quadrivalency of silicon and the requirements of stoichiometry demand that the ionic species present be monomers of $SiO_4^{4-}$ tetrahedra. It is in the composition range of 66 to 10% $M_xO_y$ that the network model fails (see Section 5.13.7) in the face of facts.

What are the requirements of a satisfactory structural model for ionic liquids in this composition range? First, since transport-number determinations show that the

conduction is essentially cationic, the anions must be large in size compared with the cations (see Sections 4.4.8 and 4.5). Second, the marked change in properties (e.g., expansivity) occurring at 10% $M_xO_y$ indicates radical structural changes in the liquid in the region of this composition. From the sharp rise of the heat of activation for the flow process to such high values (toward $420\ kJ\ mol^{-1}$ at compositions below 10 mol% $M_xO_y$) with decreasing mole percent of $M_xO_y$ in this composition region, one suspects that the structural change that is the origin of all the sudden changes near 10 mol% $M_2O$ must involve sudden aggregation of the Si-containing structural units into networks. The difficulty of breaking bonds to get a flowing entity out of the network and into another site explains the very sluggish character of the liquid at 10 or less mol% of $M_xO_y$. The potential flow unit (perhaps here $SiO_2$ itself) has to break off four bonds to flow. Finally, from 66 to 10% *there must be no major changes in the type of structure*, except some increase in the *size* of the entities, because there is only a small increase in the heat of activation for viscous flow over this composition region (*cf.* Fig. 5.71). This relative constancy of the heat of activation for flow over this composition region means that the various structural units present can become the kinetic entities of flow over this region without great change of the energy involved; i.e., the flow units present over the composition range must be similar.

The construction of a model (Table 5.50) can therefore start from the $SiO_4^{4-}$ ions present in the *orthosilicate* composition (66% $M_xO_y$). With a decrease in the molar fraction of $M_xO_y$, the size of the anions must increase to maintain the stoichiometry. One can consider that there is a joining up, or polymerization, of the tetrahedral $SiO_4^{4-}$ monomers. For example, the dimer $Si_2O_7^{6-}$ (Fig. 5.73) could be obtained thus

**TABLE 5.50**

**Discrete-Polyanion Model of Liquid Silicates**

| Range of Composition (mol% $M_2O$) | Type of Silicate Entities Present |
|---|---|
| 0 | Continuous 3-dimensional networks of $SiO_4$ tetrahedra with some thermal bond breaking and a fraction of $SiO_2$ molecules |
| 0–10 | Essentially $SiO_4$ network with number of broken bonds approximately equal to number of added O atoms from $M_2O$, having fraction of $SiO_2$ molecules and radicals containing $M^+$ |
| 10–33 | Discrete silicate polyanions based upon a six-membered ring ($Si_6O_{15}^{6-}$) |
| 33–55 | Mixture of discrete polyanions based on $Si_3O_9^{6-}$ and $Si_6O_{15}^{6-}$ or $Si_4O_{12}^{8-}$ and $Si_8O_{20}^{8-}$ |
| ~55–66 | Chains of general form $Si_nO_{3n+1}^{(2n+2)-}$, e.g., $Si_2O_7^{6-}$ |
| 66–100 | $SiO_4^{4-} + O^{2-}$ ions |

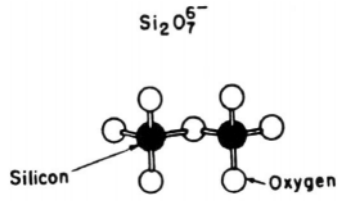


**Fig. 5.73.** The dimer ion $Si_2O_7^{6-}$.

$$SiO_4^{4-} + SiO_4^{4-} \xrightarrow{-O} O_3^{3-}Si - O - SiO_3^{3-}$$

This chemical change into polyanions is the concept of the *discrete-polyanion* model (Bockris and Lowe, 1954) for the structure of mixtures of liquid oxides corresponding to compositions greater than 10% $M_xO_y$ and less than 66%.

At the outset, it does not seem easy to derive the structure of the polyanions predominant for each composition of the liquid oxides. However, several criteria can be used to suggest their structure. Electroneutrality must be maintained for all compositions; i.e., the total charge on the polyanion group per mole must equal the total cationic charge per mole for a given composition. Since the cationic charge per mole must decrease with decreasing $M_xO_y$ mole percent, the negative charge on the polyanions per mole equivalent of silica must also decrease. It follows that the size of the polymerized anions must increase as the molar fraction of $M_xO_y$ decreases.

After a dimer, i.e., $Si_2O_7^{6-}$, is formed, the next likely anionic entity to appear as the $M_xO_y/SiO_2$ ratio falls might be expected to be the trimer

$$O_3^{3-}Si - O - SiO_3^{3-} + SiO_4^{4-} \rightarrow O_3^{3-}Si - O - Si(O^-)_2 - O - SiO_3^{3-}$$

Following the trimer, a polymeric anion with four units may be invoked to satisfy the requirements of electroneutrality and stoichiometry, etc., the general formula being $Si_nO_{3n+1}^{(2n+2)-}$. On this basis, however, when a composition of 50% $M_xO_y$ is reached, i.e., when the mole fraction of $M_xO_y$ is equal to that of $SiO_2$, the Si/O ratio is 1:3. However, from the general formula for the chain anion, i.e., $Si_nO_{3n+1}^{(2n+2)-}$, it is clear that O/Si = 3 when $(3n + 1)/n = 3$, i.e., when $n \rightarrow \infty$. Near 50% $M_xO_y$, an attempt to satisfy electroneutrality and stoichiometry by assuming that linear chain anions (extensions of the dimers and trimers) are formed would imply a large increase in the energy of activation for viscous flow in the composition range of 55 to 50 mol% of $M_xO_y$ because here the linear polymer would rapidly approach a great length. However, no such sharp increase in the heat of activation for viscous flow is observed experimentally in the range of 55 to 50 mol% of $M_xO_y$ (see Fig. 5.71). Hence, the composition range in the liquid oxides in which linear anions can be made consistent with the flow data is relatively small—between 66 and somewhat greater than 50 mol% of $M_xO_y$. The linear

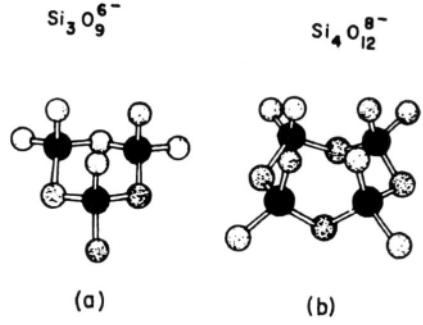


**Fig. 5.74.** The proposed ring anions: (a) $Si_3O_9^{6-}$ and (b) $Si_4O_{12}^{8-}$.

anion must be given up as a dominant anionic constituent before the metal oxide composition has dropped to 50 mol%.

An alternative anionic structure near a 50% composition that satisfies stoichiometric and electroneutrality considerations is provided by *ring formation.* If, in the composition range of 55 to 50% $M_xO_y$, the linear anionic chains (which are assumed to exist at compositions between some 50 and 60 mol% $M_xO_y$) link up their ends to form rings such as $Si_3O_9^{6-}$ or $Si_4O_{12}^{8-}$ (Fig. 5.74), then such ring anions satisfy the criteria of the O/Si ratio, electroneutrality, and also the Si–O–Si valence angle that X-ray data leads one to expect. Thus, the $Si_3O_9^{6-}$ anion corresponds to an O/Si ratio of 3, and if one is considering a 50% CaO system, the charge per ring anion is 6–, and the charge on the three calcium ions required to give $3CaO/3SiO_2$ is 6+. Further, the $Si_3O_9^{6-}$ anion is not very much larger than the $Si_2O_7^{6-}$ dimer and hence there would not be any large increase in the heat of activation for viscous flow. With regard to the Si–O–Si bond angle, in the $Si_3O_9^{6-}$ and $Si_4O_{12}^{8-}$ ions, it is near that observed for the corresponding solids, i.e., the minerals wollastonite and poryphrite, respectively, which are known to contain $Si_6O_9^{6-}$ and $Si_4O_{12}^{8-}$.

Further structural changes between 50 and 30% $M_xO_y$ are based on the $Si_3O_9^{6-}$ and $Si_4O_{12}^{8-}$ ring system. At the 33% compositions, polymers $Si_6O_{15}^{6-}$ and $Si_8O_{20}^{8-}$ (Fig. 5.75) can be postulated as arising from dimerization of the ring anions $Si_3O_9^{6-}$ and $Si_4O_{12}^{8-}$ (Fig. 5.74). As the $M_xO_y$ concentration is continuously reduced, further polymerization of the rings can be speculatively assumed. For example, at $M_xO_y/3SiO_2$ when $M_xO_y$ is 25%, the six-membered ring would have the formula $Si_9O_{21}^{6-}$ and would consist of three rings polymerized together (Fig. 5.76) (Table 5.50).

Ring stability might be expected to lessen with increase in size and increasing proportion of $SiO_2$ because the silicate polyanions that correspond to compositions approaching 10 mol% of $M_xO_y$ would be very long. The critical 10% composition at which there is a radical change in many properties may be explained as that composition in the region of which a *discrete* polymerized anion type of structure becomes

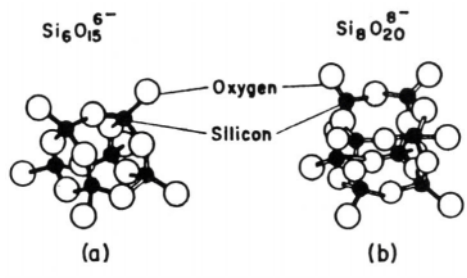


**Fig. 5.75.** The proposed large ring anions: (a) $Si_6O_{15}^{6-}$ and (b) $Si_8O_{20}^{8-}$.

unstable (because of size) and rearrangement to the random three-dimensional network of silica occurs. That is, a changeover in structural type occurs to what is fundamentally the $SiO_2$ network, with some bond rupture due to the metal cations. The very large increase in the heat of activation for flow that takes place at this composition (Fig. 5.71) would be consistent with this suggestion, as would also the sudden fall in expansivity.

These ideas about the discrete-polyanion model for liquid-silicate structures are summarized in Table 5.50. As in most models, the description is highly idealized. Thus, all the silicate anions may not have the Si–O–Si angle of the crystalline state; only the *mean* angle may have the crystalline value. Furthermore, the discrete anion suggested for a particular composition is intended to be that which is *dominant*, though not exclusive. Mixtures of polymerized anions may be present at a given composition, the proportions of which vary with composition.

The discrete-polyanion model is a speculative one because no direct proof of the existence of its ring-polymeric anions, for example, is available. It provides a much more consistent qualitative account of facts concerning the behavior of liquid silicates than does the network model. It predicts the observed marked changes in properties near 10% $M_2O$ (Fig. 5.72), the relatively small variation in $E_\eta$ over the concentration range of 10 to 50% (Fig. 5.71), etc. The suggestions for the structure of the anions

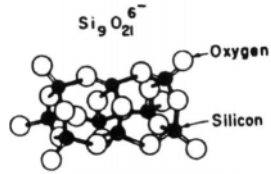


**Fig. 5.76.** The proposed six-membered ring anion $Si_9O_{21}^{6-}$.

receive some indirect support from solid-state structural analyses of certain mineral silicates.

### 5.13.9. The "Iceberg" Model

There are some facts, however, which cannot be easily explained in terms of the discrete-polyanion model. First, the partial molar volume of $SiO_2$, which is related to the size of the $SiO_2$-containing entities, is relatively constant from 0 to 33 mol% $M_2O$ (Fig. 5.77). On the basis of the discrete-polyanion model, the critical change at 10% $M_xO_y$ involving the breakdown of three-dimensional networks and the formation of discrete polyanions would require a decrease in molar volume of $SiO_2$ at about 10% $M_xO_y$ for the following reasons. The $SiO_2$ structure is a particularly open one and has a large molar volume; in contrast, a structure with discrete polyanions would involve a closing up of some of the open $SiO_2$ volume and a decrease in partial molar volume compared with the $SiO_2$ networks. Second, it is a fact that in certain ranges of composition (e.g., 12 to 33% $M_2O$) $M_2O$ and $SiO_2$ are not completely *miscible.* The two liquids consist of an $SiO_2$ phase and a metal-rich phase. The discrete-polyanion model cannot accommodate this phenomenon.

It was suggested by Tomlinson, White, and Bockris (1958) that in the composition range of 12 to 33% $M_2O$, two structures are present. One is similar to that which exists at 33% in the discrete-polyanion model. The other is a structure corresponding to glassy or vitreous silica, i.e., fused silica with the randomized three-dimensional

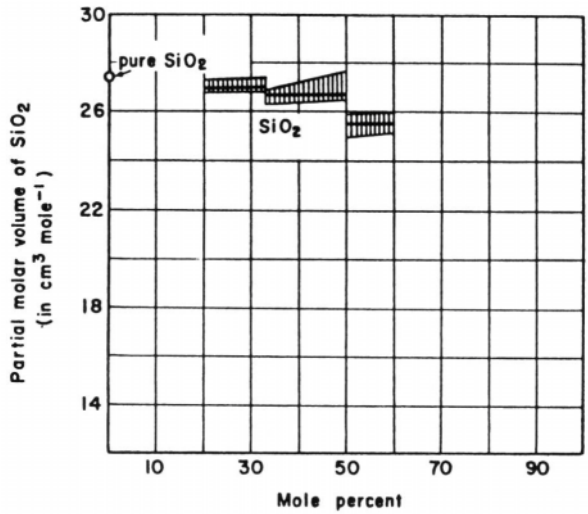


**Fig. 5.77.** The negligible change in the partial molar volume of an $Li_2O$-$SiO_2$ melt over the range of 0 to 33 mol% of $Li_2O$.

networks frozen in. The vitreous silica is in the form of "islets" or "icebergs"—hence the name, the *iceberg model* of liquid-silicate structure. These icebergs are similar to the clusters that occur in liquid water (Section 5.13.2). The submicroscopic networks may be pictured as continually breaking down and re-forming. Microphase regions of $M_xO_y/2SiO_2$ (the 33% structure) occur in the form of thin films separating the $SiO_2$-rich icebergs; hence there is the possibility of a separation of the liquid into two phases, one rich in $SiO_2$ and the other rich in $M_xO_y$. Since most of the $SiO_2$ is present in the icebergs, the almost constant partial molar volume of $SiO_2$ is rationalized.

An estimate of the order of magnitude of the iceberg size can be made. For 12% $M_2O$, the radius of an (assumed spherical) iceberg is about 1.9 nm, and at 33% $M_2O$, the iceberg of the iceberg model becomes identical in size with the discrete polyanion of the discrete-polyanion model, which has a radius of about 0.6 nm.

### 5.13.10. Icebergs As Well as Polyanions

In the iceberg model, the structure of the medium on a microscale is heterogeneous. Flow processes would involve slip between the iceberg and the film. No Si–O–Si bonds need be broken. At present, it seems that both the discrete-polyanion model and the iceberg model probably contribute to the structure of liquid silicates. In a sense, the iceberg model is the most complete model because it involves the discrete polyanions as well as the $SiO_2$ entities called icebergs.

### 5.13.11. Spectroscopic Evidence for the Existence of Various Groups, Including Anionic Polymers, in Liquid Silicates and Aluminates

The structure of liquid silicates suggested in the last few sections was presented as a reasonable *interpretation* of conductance, viscous flow, and density measurements and the variation of the heats of activation with composition, for example. What evidence for the chains, rings, and icebergs is given from spectral approaches such as Roman and NMR? If all is well in the earlier interpretation, it should be possible to see evidence of the structures in the spectral peaks.

The earliest workers to obtain this evidence were Furokawa et al., and then a little later, work was carried out by McMillan. These researchers found that in systems based on $Na_2O$-$SiO_2$, the metasilicate and the disilicate had two peaks, one that showed up at $950\ cm^{-1}$ and one at $1150\ cm^{-1}$, respectively. What molecular entities should these peaks represent? This kind of question is grist for the mill among spectroscopists, who often argue a great deal about the significance of the blips and "shoulders" on their curves. In this system they have come up with a decisive but unambitious answer—each peak represents the vibrations of the Si–O bond and the peak for this varies with composition. Such a conclusion, of course, does not indicate the structural units present.

Evidence of various structures of the silicate anions shows up from these Raman and IR studies. The results are shown with the attendant peaks in Table 5.51.

Although these anions are simpler than the structures deduced on the basis of transport measurements, they agree with the structure (see Section 5.6). Chains are present, as are $O^{2-}$ and $SiO_2$. However, up to 1997, no peaks have yet been registered that are characteristic of the ring structures known to exist in the corresponding solids, the suggested presence of which in the liquid silicates fits stoichiometry, bond angles, and the behavior of the heat of activation for viscous flow as a function of composition (Fig. 5.71).

Farnan and Stebbins performed NMR measurements on simple molten silicates in 1990 and managed to pull more out of their data than other workers in this area.

**TABLE 5.51**

**Compositional Ranges (Expressed as Bulk Melt Nonbridging Oxygens/Si) of Coexisting Structural Units (within Analytical Uncertainty) for Melts on Metal Oxide–Silica Systems**

| Nonbridging Oxygens/Si Range | Coexisting Anionic Structural Units |
|---|---|
| | $Na_2O$-$SiO_2$ |
| >0–0.05 | $SiO_2$, $Si_2O_5^{2-}$ |
| 0.05–1.0 | $SiO_2$, $Si_2O_5^{2-}$, $SiO_3^{2-}$ |
| 1.0–1.4 | $Si_2O_5^{2-}$, $SiO_3^{2-}$, $SiO_4^{4-}$ |
| 1.4–2.0 | $Si_2O_5^{2-}$, $SiO_3^{2-}$, $Si_2O_7^{6-}$, $SiO_4^{4-}$ |
| | $BaO$-$SiO_2$ |
| >0–0.2[2] | $SiO_2$, $Si_2O_5^{2-}$ |
| 0.2–1.0 | $SiO_2$, $Si_2O_5^{2-}$, $SiO_3^{2-}$ |
| 1.0–1.1 | $SiO_2$, $Si_2O_5^{2-}$, $SiO_3^{2-}$, $SiO_4^{4-}$ |
| 1.1–2.4[2] | $Si_2O_5^{2-}$, $SiO_3^{2-}$, $Si_2O_7^{6-}$, $SiO_4^{4-}$ |
| >2.4[2] | $SiO_3^{2-}$, $Si_2O_7^{6-}$, $SiO_4^{4-}$ |
| | $CaO$-$SiO_2$ |
| >0–0.3[2] | $SiO_2$, $Si_2O_5^{2-}$ |
| 0.3–1.0 | $SiO_2$, $Si_2O_5^{2-}$, $SiO_3^{2-}$ |
| 1.0–2.2 | $Si_2O_5^{2-}$, $SiO_3^{2-}$, $SiO_4^{4-}$ |
| 2.2–3.0 | $SiO_3^{2-}$, $Si_2O_7^{6-}$, $SiO_4^{4-}$ |
| >3.0[3] | $SiO_3^{2-}$, $Si_2O_7^{6-}$, $SiO_4^{4-}$, $O^{2-}$ |

Source: From B. O. Mysen, *Structure and Properties of the Silicate Melts*, New York, Elsevier (1988).

They measured the lifetime of the $SiO_4^{4-}$ tetrahedra and found it to be $\sim 10^{-6}$ s. What happens after an ion dies? Lifetime implies an exchange (perhaps by means of $O^-$) between $SiO_4^{4-}$ and another ion. By making such measurements on quenched samples as a function of temperature, it is possible to get the heat of activation for the critical step in viscous flow. Remarkably, the values for $Li_2O\text{-}SiO_2$ turn out to be 176 kJ mol$^{-1}$, which is within 8–13 kJ mol$^{-1}$ of those measured earlier for viscous flow in $K_2O\text{-}SiO_2$. This fits well with the model for viscous flow (see Fig. 5.71). According to this model, an entity has to break off from the silicate anion (i.e., exchange to another structure) before the critical unit (which must be the size of a hole) can move into the cavity, thus giving consistency to the idea of ions of limited lifetime. The dependence on temperature of the NMR peaks for $2Li_2O\text{-}SiO_2$ is shown in Fig. 5.78.

Up until the late 1990s the spectroscopic confirmation of the liquid silicates of the model suggested in Sections 5.13.7 and 5.13.9 was limited to the ions

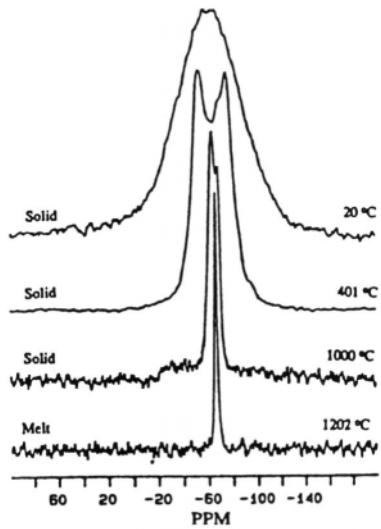


**Fig. 5.78.** Variable-temperature $^{29}Si$ NMR spectra of the lithium orthosilicate/metasilicate mixture. Typically, narrow spectra required 64 pulses and broader spectra 500 pulses. The line broadening used in processing each spectrum was less than 10% of the total line width. (Reprinted from I. Farnan and J. F. Stebbins, *J. Am. Chem. Soc.* **112**: 32,1990.)

$SiO_4^{4-}$, $SiO_3^{2-}$, $Si_2O_5^{2-}$, and $Si_2O_7^{6-}$, etc. However, the ring anions also suggested are well confirmed in the corresponding solid silicates.

The degree of certainty in the structures deduced as a result of modeling reasoning from the facts of transport, partial molar volumes, etc., are better than one might think. However, one needs to consider two important facts to be able to pick up the proper structures; these are the necessity for electroneutrality and the fixed O–Si–O angle. Thus, for a certain O/Si ratio, there must be a certain number of charges per ion to match the concentration of cations that the ratio determines. The other matter concerns the O–Si–O bond angle, which is fixed at 120°.

Taking these two facts into account effectively decreases the number of structures possible at a given O/Si value. They are those given in Table 5.50. Now, if there is molecular silica present ($H_2O$ molecules in the complex water structure), as seems to be indicated by the small change of $\bar{V}_{SiO_2}$ over the composition range 0–33 mol% $Li_2O$ in the $Li_2O$-$SiO_2$ system, molecular $SiO_2$ may indeed be added to the structure present in the range of 12-33 mol% in $M_xO_y$–$SiO_2$, and this would decrease the size of the corresponding polyanion, probably to $Si_4O_{12}^{6-}$.

A system of interest among the silicates is $Al_2O_3$-$SiO_2$, partly because of the relevance of knowledge of the structure of the corresponding glasses and liquids to geochemistry and materials science. Using $^{27}$A1 and $^{29}$Si, Poe et al. found it possible to obtain the coordination number of O for the molecules cited above. Using IR spectra, they were able to get information on the structure, leading to the idea of considering polyhedra involving Al, which tends to replace Si as the main ion to which O coordinates in $Al_2O_3$-$SiO_2$ structures. Poe et al. identified $AlO_4$, $AlO_5$, and $AlO_6$ (polyhedra) with peaks at 700–900, 600–700, and 500–600 $cm^{-1}$, respectively. How are these polyhedra related to each other? It seems likely that exchange of O is the active process:

$$AlO_4 \rightleftharpoons AlO_5 \rightleftharpoons AlO_6$$

The critical variables are the O/Al ratio and the molecular size, and hence the representative anion formulated must depend on these parameters just as it does for the $M_xO_y$–$SiO_2$ systems (see Section 5.13.8).

The change in composition with the ions presented was determined by shifts of the NMR peaks. The liquid samples were splat-quenched—dropped into a cold body in such a way that rapid solidification occurred, easing the measurements which then could be made at room temperature. There is a danger in this method since the quenching may not be fast enough, so that some change in structure from that at a given composition and temperature may occur before the quenching ends.

## 5.13.12. Fused Oxide Systems and the Structure of Planet Earth

We live on an apparently solid earth, but the solidified crust is only some 60 km thick. As one moves down into it, the temperature increases from about 300 K on the

surface toward about 1000 K at the bottom of the solid crust where the magma begins. From here, for the next 6000 km (i.e., to the center of the earth) the temperature is thought to remain in the 1000–2000 K range but the *pressure* increases linearly. The mantle down to the iron core is made up of silicates of varying kinds which are liquefied from the solid rock not only by the high temperatures but also by the increasing pressure. Do the structures presented in the last few sections exist in the earth's interior? What is the effect of pressure upon the structure of liquid silicates?

These questions cannot be answered unless one knows the pressure inside the earth as the depth increases. Knowledge of this is incomplete and it clearly must be obtained somewhat indirectly (e.g., from the study of the pattern of seismic distur-

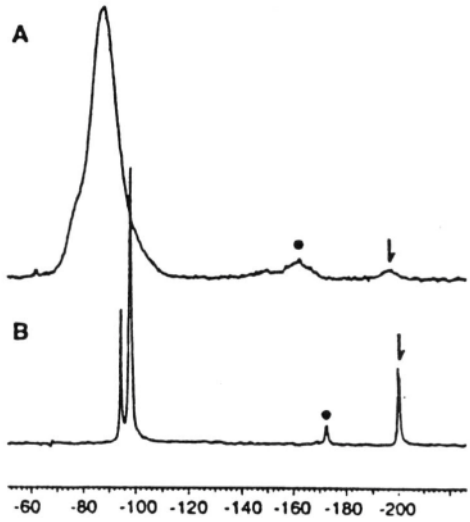


**Fig. 5.79.** $^{29}$**Si NMR** spectra of $Na_2Si_2O_3$ samples quenched from 8 GPa: (a) 1700 K, glassy and (b) 1420 K, crystalline. Peaks marked with dots are spinning side bands; peaks marked with arrows are attributed to $^{29}$Si. Exponential line broadenings of about 20% of the peak widths (20 and 100 Hz) were applied to enhance signal-to-noise ratios. Scales for all spectra are in parts per million relative to tetramethylsilane (TMS). (Reprinted from X. Sue, J. F. Stebbins, M. Kanzaki, and R. D. Tronnes, *Science* **245**: 963, 1993.)

bances, etc.). However, one can also use the average density of the earth (6.7) and ask what is the force per unit area at the bottom of a vertical column 1000 km deep. This force per unit area turns out to be on the order of $6 \times 10^{10}$ Pa.

Making a physiochemical measurement at $\sim 10^{11}$ Pa and ~2000 K is clearly very difficult indeed. How could it be achieved? One approach is to pressurize a silicate such as $Na_2Si_2O_5$ at 1700 K (glassy state) and then freeze it very rapidly so that the structure corresponding to the high pressure and temperature remains frozen in the sample. Then NMR measurements can be made at room pressure and temperature while the structure from the high pressure and temperature remains present. What can be seen (Fig. 5.79)?

The main difference that occurs at these high pressures (like those deep in the earth) is that the coordination number of Si begins to change. Throughout the material described in this chapter so far, the central assumption has been that Si is four-coordinated with O, as in $SiO_4^{2-}$ but also in the polymer ions assumed for O/Si < 4. Now, as seen from the arrow points in Fig. 5.79, some amount of six-coordinated Si exists as well as a trace of octahedral structures.

Does this mean that deep in the magma liquid silicates would have a different structure from that described on the basis of measurements at atmospheric pressure? Probably! We are far from knowing what the detailed changes are, or being able to say, for example, that the polymer ions in Fig. 5.75 are now smaller in size. However, at least according to Xue et al. (1992), deep in the earth there is a more random distribution of bridging and nonbridging oxygens than that observed in solid and liquid silicates under conditions at the earth's surface.

### 5.13.13. Fused Oxide Systems in Metallurgy: Slags

Knowledge of what goes on inside fused oxide systems is important not only as a basis for future advances in glass technology but also for metallurgical processes. Consider, for example, one of the most basic processes in industry, the manufacture of iron in a blast furnace (Fig. 5.80). Iron ore, coke, and flux (essentially limestone and dolomite) are fed into the top of the furance. Compressed air fed in through openings in the bottom of the furnace converts the carbon in coke to carbon monoxide, which reduces the iron oxide to iron. Molten iron collects at the bottom. On top of the molten metal is a layer of molten material called *slag*.

What is slag? A typical chemical analysis (Table 5.52) shows that it consists mainly of silica ($SiO_2$), alumina ($Al_2O_3$), lime (CaO), and magnesia (MgO)—in fact, precisely the kinds of substances (i.e., nonmetallic oxides such as $SiO_2$ and metallic oxides such as CaO) the structure of which is being discussed here. (Slags, in fact, can be regarded as molten glasses.) The constituents of the slags are present in the ores and in coke.

Successful operation of the furnace and production of an iron with the desired composition (and hence metallurgical properties) depend so much on making the slag

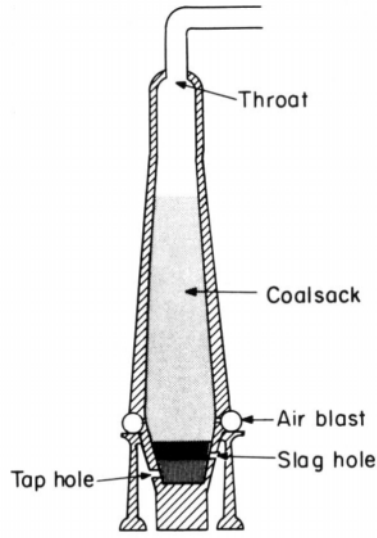


**Fig. 5.80.** Schematic of a blast furnace.

with the right composition by controlling the raw materials fed into the furnace that it is sometimes said: "You don't make iron in the blast furnace, you make slag!"

Can one explain this importance of the slag? Measurements of conductance as a function of temperature and of transport number indicate that the slag is an ionic conductor (liquid electrolyte). In the metal–slag interface, one has the classic situation (Fig. 5.81) of a metal (i.e., iron) in contact with an electrolyte (i.e., the molten oxide electrolyte, slag), with all the attendant possibilities of corrosion of the metal. Corrosion of metals is usually a wasteful process, but here the current-balancing partial electrodic reactions that make up a corrosion situation are indeed the very factors that control the equilibrium of various components (e.g., $S^{2-}$) between slag and metal and hence the properties of the metal, which depend greatly on its trace impurities. For example,

**TABLE 5.52**
**Analysis of a Typical Slag**

| Constituents | Fe | Mn | $SiO_2$ | $Al_2O_3$ | CaO | MgO | S |
|---|---|---|---|---|---|---|---|
| Percentage | 0.34 | 1.18 | 34.67 | 14.58 | 44.78 | 3.21 | 1.36 |

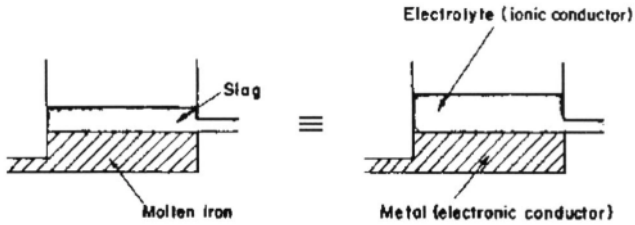


**Fig. 5.81.** Molten metal in contact with slag is electrochemically equivalent to a metal in contact with an electrolyte.

$$S[\text{in metal}] + 2\,e \rightarrow S^{2-}[\text{in slag}]$$

$$Fe \rightarrow Fe^{2+} + 2\,e$$

The quality of the metal in a blast furnace is thus determined largely by electrochemical reactions at the slag–metal interface. Making good steel and varying its properties at will depends on making good slag first. Future developments in steel making depend on having electrochemists controlling the electrical potential at the slag–metal interface.

## Further Reading

### *Seminal*

1. W. Zachariasen, "Chain and Sheet Structure of Glasses," *J. Am. Chem. Soc.* **54**: 3841 (1932).
2. J. O'M. Bockris and D. C. Lowe, "Viscosity and the Structure of Liquid Silicates," *Proc. Roy. Soc. Lond.* **A226**: 423 (1954).
3. J. O'M. Bockris, J. D. MacKenzie, and J. A. Kitchener, "Viscous Flow in Silica and Binary Liquid Silicates," *Trans. Faraday Soc.* **51**: 1734 (1955).
4. J. W. Tomlinson, J. L. White, and J. O'M. Bockris, "The Structure of the Liquid Silicates; Partial Molar Volumes and Expansivities," *Trans. Faraday Soc.* **52**: 299 (1956).

### *Review*

1. B. O. Mysen, *Structure and Properties of the Silicate Melts*, Elsevier, New York (1988).

### *Papers*

1. J. E. Stebbins and I. Farnan, *Science* **255**: 586 (1992).
2. B. T. Poe, P. E. McMillan, C. A. Angell, and R. K. Sato, *Chem. Geol.* **96**: 333 (1992).
3. Y. Kawasita, J. Dong, T. Tsuzuki, Y. Ohmassi, M. Yao, H. Endo, H. Hoshimo, and M. Inni, *J. Non-Cryst. Solids* **156**: 756 (1993).
4. C. Scamehorn and C. A. Angell, *Geochim. Cosmochim. Acta* **55**: 721 (1991).
5. X. Xui, J. F. Stebbins, M. Kenza, and R. G. Tronnes, *Science* **245**: 962 (1996).

## APPENDIX 5.1. THE EFFECTIVE MASS OF A HOLE

The pressure gradient in a fluid in the direction $x$ as a result of an instantaneous velocity $u$ in that direction can be expressed as

$$\frac{dP}{dx} = \rho X - \rho \frac{du}{dt} - \left( u \frac{du}{dx} + v \frac{du}{dy} + w \frac{du}{dz} \right) + \eta \left( \frac{d^2u}{dx^2} + \frac{d^2u}{dy^2} + \frac{d^2u}{dz^2} \right) + \frac{\eta}{3} \frac{d}{dx} \left( \frac{du}{dx} + \frac{dv}{dy} + \frac{dw}{dz} \right) \tag{A5.1.1}$$

Similar equations exist for the pressure gradients along the other two mutually perpendicular axes, $y$ and $z$. In these equations, $P$ is pressure; $\rho$ is the density of the fluid, and $\eta$ is its viscosity; $u$, v, and $w$ are the instantaneous fluid velocities at the points $x$, $y$, and $z$ in the directions of the three coordinate axes; and $X$ is the component of the accelerating force in the $x$ direction.

Stokes has shown that in cases where the motion is small and the fluid is incompressible and homogeneous, etc., these equations can be simplified to a set of three equations of the form

$$\frac{dP}{dx} = \eta \left( \frac{d^2u}{dx^2} + \frac{d^2u}{dy^2} + \frac{d^2u}{dz^2} \right) - \rho \frac{du}{dt} \tag{A5.1.2}$$

plus an equation of continuity

$$\frac{du}{dx} + \frac{dv}{dy} + \frac{dw}{dz} = 0 \tag{A5.1.3}$$

Solution of Eqs. (A5.1.2) and (A5.1.3) in spherical coordinates leads to a general expression of the form

$$\text{Force} = 2\pi a \int_0^{\pi} (-P_r \cos\theta + T_\theta \sin\theta)_a \sin\theta \times d\theta \tag{A5.1.4}$$

for the force of the fluid acting on the surface ($r = a$) of a hollow sphere oscillating in it with a velocity $v$ given by $ce^{i\omega t}$, where $P_r$ and $T_\theta$ are the instantaneous normal and tangential pressures at the points $r$ and $\theta$, $c$ is the velocity at time $t = 0$, and $\omega$ is the frequency of oscillation. The term in $T_\theta$ can be ignored for present purposes since it corresponds to a viscous force acting on the sphere owing to its motion through the liquid.

Inserting the appropriate expressions for $P_r$, ignoring the terms arising from the viscosity of the liquid since there can be no viscous slip between a liquid and a hole, and proceeding through a number of algebraic stages yields

$$\text{Force} = -\left(\frac{2}{3}\pi a^3 \rho\right) c\omega i e^{i\omega t} \tag{A5.1.5}$$

where $\rho$ is the density of the fluid. Writing now

$$m' = \frac{4}{3}\pi a^3 \rho \tag{A5.1.6}$$

for the mass of fluid displaced by the sphere gives

$$\text{Force} = -\left(\frac{m'}{2}\right) c\omega i e^{i\omega t} \tag{A5.1.7}$$

However, from the equation

$$\frac{dv}{dt} = \ddot{x} = ci\omega e^{i\omega t} \tag{A5.1.8}$$

and on remembering that, by Newton's law of motion, action and reaction are equal and opposite, it follows that

$$\text{Effective force due to spherical hole} = \left(\frac{m'}{2}\right)\ddot{x} \tag{A5.1.9}$$

This force thus corresponds to the force $(m'/2)\ddot{x}$ that would be produced by a solid body of mass $m'/2$ operating under conditions where the fluid is absent; it is thus produced by a hole of *effective* mass $m'/2$ or $\frac{2}{3}\pi a^3 \rho_{\text{liquid}}$.

## APPENDIX 5.2. SOME PROPERTIES OF THE GAMMA FUNCTION

The gamma function $\Gamma(n)$ is defined thus

$$\Gamma(n) = \int_0^\infty e^{-t} t^{n-1}\, dt$$

Some of its properties are as follows:

1. When $n = 1$,

$$\Gamma(1) = \int_0^\infty e^{-t}\, dt = 1$$

2. When $n = \frac{1}{2}$,

$$\Gamma\left(\frac{1}{2}\right)=\int_0^\infty e^{-t}t^{-1/2}\,dt$$

Put $t = x^2$, in which case

$$dt = 2x\,dx$$

$$t^{-1/2}\,dt = 2\,dx$$

and

$$\Gamma\left(\frac{1}{2}\right)=2\int_0^\infty e^{-x^2}\,dx$$

Using Eq. (5.24), i.e.,

$$\int_0^\infty e^{-ax^2}\,dx=\frac{1}{2}\sqrt{\frac{\pi}{a}}$$

one has

$$\Gamma\left(\frac{1}{2}\right)=\sqrt{\pi}$$

3. $$\Gamma(n+1)=\int_0^\infty e^{-t}t^n\,dt$$

Integrating by parts,

$$\int_0^\infty \underset{u}{t^n}\underset{dv}{e^{-t}}\,dt = -[\underset{u}{t^n}\underset{v}{e^{-t}}]_0^\infty + n\int_0^\infty \underset{v}{e^{-t}}\,\underset{du}{t^{n-1}}\,dt$$

$$= n\Gamma(n)$$

Hence,

$$\Gamma(n+1) = n\Gamma(n)$$

## APPENDIX 5.3. THE KINETIC THEORY EXPRESSION FOR THE VISCOSITY OF A FLUID

Consider three parallel layers of fluid, $T$, $M$, $B$ (Fig. 5.82), moving with velocities $v + (\partial v/\partial z)\lambda$, $v$, and $v - (\partial v/\partial z)\lambda$, respectively, where $z$ is the direction normal to the

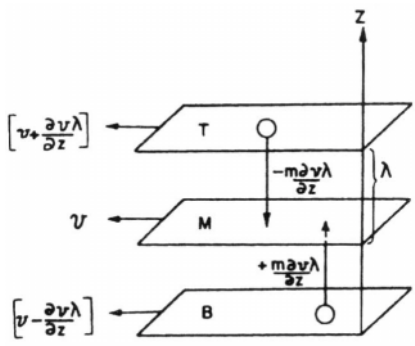


**Fig. 5.82.** Viscous forces arise from the transfer of momentum between adjacent layers in fluid.

planes and $\lambda$ is the mean free path of the particles populating the layers, i.e., the mean distance traveled by the particles without undergoing collisions. In the direction of motion of the moving layers, the momenta of the particles traveling in the *T*, *M*, and *B* layers is $m[v + (\partial v/\partial z)\lambda]$, $mv$, and $m[v - (\partial v/\partial z)\lambda]$, respectively.

When a particle jumps from the *T* to the *M* layer, the net momentum gained by the *M* layer is $mv - m(v + (\partial v/\partial z)\lambda) = -m(\partial v/\partial z)\lambda$. If $\langle\omega\rangle$ is the mean velocity of particles in the direction normal to the layers, then, in 1 s, all particles within a distance $\langle\omega\rangle$ will reach the *M* plane. If one considers that there are *n* particles per cubic centimeter of the fluid and the area of the *M* layer is *A* $cm^2$, then $n\langle\omega\rangle A$ particles make the $T \rightarrow M$ crossing per second, transporting a momentum per second of $-[n\langle\omega\rangle Am(\partial v/\partial z)\lambda]$ in the downward direction.

When a particle jumps from the *B* to the *M* layer, the net momentum gained by the *M* layer is $mv - m[v - (\partial v/\partial z)\lambda] = +m(\partial v/\partial z)\lambda$, i.e., the momentum transported per particle in the *downward* direction is $-m(\partial v/\partial z)\lambda$. Hence, the momentum transferred per second in the downward direction owing to $B \rightarrow M$ jumps is $-[n\langle\omega\rangle Am(\partial v/\partial z)\lambda]$.

Adding the momentum transferred owing to $T \rightarrow M$ and $B \rightarrow M$ jumps, it is clear that the momentum transferred per second in the downward direction, i.e., the rate of change of momentum, is $-2n\langle\omega\rangle m\lambda[A(\partial v/\partial z)]$. This rate of change of momentum is equal to a force (Newton's second law of motion). Thus, the viscous force $F_\eta$ is given by

$$F_\eta = -(2n\langle\omega\rangle m\lambda)A\frac{\partial v}{\partial z} \qquad \text{(A5.3.1)}$$

However, according to Newton's law of viscosity, the viscous force is proportional to the area of the layers and to the velocity gradient, and the proportionality constant is the viscosity, i.e.,

$$F_\eta = -\eta A \frac{\partial v}{\partial z} \tag{A5.3.2}$$

From Eqs. (A5.3.1) and (A5.3.2), it is clear that

$$\eta = 2nm\langle\omega\rangle\lambda \tag{A5.3.3}$$

## EXERCISES

1. From different tables in the text, determine the average change of internuclear distance upon melting for group IA and IIA halides. Then, tabulate the change of volume for the same act. Comment on any contradictions you see when comparing these two sets of data.

2. Draw the potential-energy vs. distance curves for the pair potentials in a molten salt.

3. Calculate the mean hole size in CsBr for which the surface tension is 60.7 dyn $cm^{-1}$ at 1170 K.

4. It is possible by measuring the velocity of sound to determine the "free volume" of a liquid. Reference to the corresponding free volume for a solid shows that there this concept describes the solid volume in a cell of the crystalline solid, diminished by the volume of an atom in it.

   In a molten salt (as shown by a diagram in the text), the free volume increases with the hole volume in a roughly proportional way. Consider this correlation and make deductions as to what kind of structure in a molten salt would be consistent with the observation quoted.

   To what degree and in what way do the data on heats of activation at constant volume and constant pressure contribute to these deductions?

5. Explain the meaning of *refraction* and *diffraction.* What does a diffraction pattern look like? Write down expressions for the radial distribution function. What is the physical significance of the decline in value of the maximum with increasing distance from the reference point?

6. Explain the difference between diffraction measurements with X-rays and with neutrons. Determine which method you would use in examining a molten salt.

7. Determine and explain the terms *radial distribution function*, *pair correlation function*, and *partial structural factors.*

8. By using the pair potentials of one of the pioneer works in the modeling of molten salts (Woodcock and Singer) as well as the corresponding parameters in this work, calculate the equilibrium distance for $Li^+$ and $Cl^-$ ions just above the

melting point. In what way is the much later work of Saboungi et al. considered to be an improvement on the pioneer calculations of Woodcock and Singer?

9. In Fürth's theory of cavities in liquids, there is a distribution function for the probability of the hole size. It is

$$P\,dr = \frac{16}{15\pi^{1/2}}\,a^{7/2}r^6e^{-ar^2}\,dr$$

Deduce an expression for the mean hole size from this function. Work out the mean radius of holes for molten KCl near the melting point if the surface tension is 89.5 dyn $\mathbf{cm}^{-1}$ and the melting point is 1040 K.

10. Calculate the work of hole formation in molten sodium chloride, using the Fürth approach. The surface tension of NaCl, molten salt at 1170 K, is 107.1 dyn $\mathbf{cm}^{-1}$ and the mean hole radius of NaCl is $\mathbf{1.7 \times 10^{-8}}$ cm. (Contractor)

11. Describe the physical meaning of the glass transition temperature.

12. Explain the idea of a glass-forming liquid electrolyte and the glass transition temperature. Cohen and Turnbull were the first to formulate a quantitative theory of diffusion in a glass-forming liquid. Using equations from their theory, show how it leads to an abrupt change of the diffusion coefficient from a value continuous with that of the liquid above its melting point to zero at the glass transition temperature.

13. (a) Assess the total number of individual Si–O bonds in a mole of $\mathbf{SiO_2}$.

    (b) Give a chemical explanation of why the addition of $\mathbf{Na_2O}$ to silicate causes the breaking up of the tetrahedral network.

    (c) Assuming three coordination exclusively for B in borate glasses, calculate the moles of base needed to form a chain structure. What is the formula of the glass? (Xu)

14. Frozen liquids can also flow. Research has found that the window glass of many medieval churches in Europe has a thicker bottom than top (by as much as a millimeter), and this deformation is evidently caused by the flowing of the silicate under the effect of gravity. Calculate how far the moving species in the glass can travel in a millennium at room temperature. [Hint: The glass produced in ancient Europe is very similar to the so-called "soda-glass" today, which contains about 20 mol% $\mathbf{Na_2O}$.] (Xu)

15. From data in the text, work out a measure of the degree to which $E^{\neq} = 3.74RT_{\text{m.p.}}$ measures the activation energy for *transport* in molten salts. Does this equation apply to other liquids?

16. Explain the value of constant-volume and constant-pressure measurements of transport rates. What can one conclude from utilizing the values of each?

17. The determination of transport numbers in aqueous electrolytes is relatively easy (Chapter 3), but in molten salts it poses difficulties of concept, which in turn demand specialized apparatus. Explain why direct determination is difficult. Would it not be better to abandon the direct approach and use the approximate applicability of the Nernst–Einstein equation, relying on self-diffusion determinations? Any counter considerations?

18. Calculate the transport numbers of the cation and the anion in molten CsCl at 943 K. The experimental equivalent conductivity of the fused salt is $67.7\ \text{ohms}^{-1}\ \text{cm}^2$ equiv. The observed diffusion coefficients of $Cs^+$ and $Cl^-$ ions in molten CsCl are $3.5 \times 10^{-5}$ and $3.8 \times 10^{-5}\ \text{cm}^2\ \text{s}^{-1}$, respectively. (Contractor)

19. Use the text to find an equation giving the "lifetime" of a hole in a molten salt. Calculate it for KC1 using data in the text.

20. Calculate the relaxation time for an electron conducting in a metal–molten salt mixture. (The mobility for such systems is about $0.2\ \text{cm}^2\ \text{V}^{-1}\ \text{s}^{-1}$.)

21. For a molten salt mixture in which the reaction at an electrode involves one electron, $D_{\text{solute}} = 5.4 \times 10^{-5}\ \text{cm}^2\ \text{s}^{-1}$ and $c_0 = 0.1\ \text{mol dm}^{-3}$. Electrolysis is occurring in constant-current pulses of 4 A $\text{cm}^{-2}$. Calculate the time at which the reactant in the interface is exhausted.

22. In Raman spectroscopy of cryolite, a higher value of $\nu$ favors a lower coordination number. Why?

23. In the text of Chapter 5, there are X-ray data on the internuclear distance in the solid and liquid forms of the alkali halides. In all cases, the internuclear distance *contracts* on melting. Find the mean contraction in percent. What kind of structure in the liquid could be consistent with your finding?

24. In Chapter 5, there are data on the increase in volume of the solid lattice when it becomes liquid. Work out the average increase in volume in percent and compare it with the average contraction of the internuclear distance on melting (see the previous problem). What kind of structure of molten salts does this suggest?

25. Why is it that neutrons are preferred to X-rays in carrying out diffraction experiments with, e.g., molten salts? What is the disadvantage (in practice) of using neutrons compared with X-rays?

26. Sketch a few of the typical anionic polymer ions likely to be present at each composition range in molten oxides. What new ions are formed if O/Si > 4? Which ions have been confirmed to be present by spectroscopic methods?

27. State, in less than 50 words, the essential principles behind the Monte Carlo and molecular dynamics methods of calculating the numerical values of phenomena in liquids. Why is it that such methods need prior experimental determinations in nearby systems?

28. Some of the ambient-temperature molten salts are made up from certain alkyl ammonium salts or, alternatively, a mixture of $AlCl_3$ with organics such as imidazolonium chloride. They have two strong advantages over traditional molten salts with melting points several hundred degrees above room temperature: their great ease of handling and the very large electrochemical window that they allow.

    From the information given in the chapter, suggest up to six solvents (systems) that would allow the electrochemical oxidation of complex organics such as polymerized isoprene (rubber) or even Teflon (polymerized tetrafluoroethylene) at less than 373 K.

29. From the Cohen-Turnbull configurational entropy model, prove that the temperature dependence of relaxation time $\tau$ and viscosity $\eta$ of super-cooled liquids are both non-Arrhenius, i.e., of the $\exp[BT_0/(T - T_0)]$ type, where $T_0$ is a characteristic temperature. (Xu)

30. $Ca(NO_3)_2$-$KNO_3$ (CKN) is a well-known molten salt that easily vitrifies upon cooling. An attempt to ascertain the fragility of this system was made on a CKN sample with a glass transition temperature of 350 K. This sample was heated up to 390 K and its dielectric relaxation time measured by an impedance bridge as $10^{-2}$ s. Classify this ionic liquid. (Xu)

31. Assume that the electrical conductivity of CaO is determined primarily by the diffusion of $Ca^{2+}$ ions. Estimate the mobility of cations at 2070 K. The diffusion coefficient of $Ca^{2+}$ ions in CaO at this temperature is $10^{-14}$ $m^2$ $s^{-1}$. CaO has an NaCl structure with $a = 0.452$ nm. Account for your observation. (Contractor)

32. The equivalent conductivity of molten salts depends upon the cationic radius. Plot the equivalent conductivities of molten salts of monovalent cations against the corresponding cationic radii. Comment on this linear dependence. (Contractor)

33. The diffusion coefficient of tracer $Cl^-$ ion in molten NaCl is $4.2 \times 10^{-5}$ $cm^2$ $s^{-1}$ at 1290 K and $6.7 \times 10^{-5}$ $cm^2$ $s^{-1}$ at 1110 K. Calculate the values of the activation energy and the preexponential factor. (Contractor)

34. Given that the equivalent conductivity of molten NaCl is 153 $ohm^{-1}$ $cm^2$ $equiv^{-1}$ at 1193 K and that the self-diffusion coefficients of $Na^+$ and $Cl^-$ ions in molten NaCl are $9.6 \times 10^{-5}$ and $6.7 \times 10^{-5}$ $cm^2$ $s^{-1}$, respectively, evaluate the Faraday constant. (Contractor)

## PROBLEMS

1. In the text, data are given on the changes of volume on melting for certain molten salts. Find out the free space per ion (use a standard compilation of ionic radii). In the text will also be found a table showing some changes of internuclear distances on melting. What is your conclusion in respect to the type of structure for molten salts?

2. In deviations from the Nernst–Einstein equation in a molten salt, one hypothesis involved paired-vacancy diffusion. Such a model implies that holes of about twice the average size are available at about one-fifth the frequency of average-sized holes. Use the equation in the text for the distribution of hole size to test this model.

3. Based on the results of the hole model of ionic liquids, derive the average surface area $\langle S \rangle$ and volume $\langle V \rangle$ of the holes. Compare $\langle S \rangle$ and $\langle V \rangle$ with the area and volume calculated from the average hole radius. Calculate the work needed to be done in making a hole of the average size at 1170 K in any molten salt if Fürth's "nearly boiling" assumption holds. [Hint: $\Gamma$-function $\Gamma(n) = \int_0^\infty e^{-t} t^{n-1}\, dt$, has the following properties: (1) $\Gamma(0.5) = \pi^{1/2}$; (2) $\Gamma(n + 1) = n!$ when $n$ is a positive integer; or (3) $\Gamma(n + 1) = n\Gamma(n)$ when $n$ is positive real. (See Xu)

4. Use the Woodcock and Singer results in the text to calculate the coordination number of $K^+$ by $Cl^-$ using the equations recorded and the radial distribution functions shown.

5. The radial distribution function is the principal entity in the use of X-ray and neutron diffraction data to determine a structure. Write an expression for the number of particles, $B$, in a spherical shell of radius $r$ with respect to a reference particle. Calculate the number of particles in that shell, assuming that the material concerned has a density of 1.6; that the first shell outside the reference atom $S$ is at least a distance of 0.20 nm from the latter (internuclear distance); and that the $g_r - r$ relation is idealized to a square box, height 2.0 and width 0.10 nm.

6. Fürth's model for liquids pictures the liquid as if the vacant spaces in it behave like bubbles in a boiling liquid. Several other versions of liquids as disturbed solids with vacancies exist. The Woodcock and Singer Monte Carlo simulation of KC1 shows a structure for liquid KC1 similar to that of Fürth's proposition. However, the most important point in favor of the model is this: a contradiction to competing theories, in particular those arising from molecular dynamics, is that it allows an explanation of the heat of activation exhibited for diffusion and viscous flow for all nonassociated liquids, $E^{\neq} = 3.74RT_{\text{m.p.}}$.

   Comment on the following:

(1) The expression for the hole size in Fürth's theory uses the surface tension of the liquid and then gives a remarkable fit to ion size.

(2) The calculated compressibility and expansivity of typical sample molten salts are ±~20% of the actual values.

(3) There is a linear relation between the free volume from sound velocity measurements and the hole volume (from volume of fusion data).

7. Several diagrams given in the text for transport properties attest to the validity of the empirical expression $E^{\neq} = 3.74RT_{\text{m.p.}}$. It appears that from liquid $H_2$, through liquid organics, to molten salts and metals, the activation energy when plotted against $T_{\text{m.p.}}$ has a slope of 3.74*R*. Discuss the significance of this. How is this uniformity of behavior to be seen as consistent with two mechanisms of transport, that in which the occurrence of vacancies is the key element and that in which "pushing through the crowd" is a more fitting description of the movement in transport?

8. Take the data in the text on transport (unassociated molten salt data only) and work out $E^{\neq}_{\text{jump}} + E^{\neq}_{\text{hole formation}}$. Discuss whether this conforms more to a "jump into a hole" (Fürth) or "shuffle along" model of transport (Swallin). Make a similar comparison for the activation volume.

9. (a) Use data in Chapter 5 to calculate the transport number in molten NaCl and find out the temperature dependence of the coordinated diffusion coefficient, $D_{\text{NaCl}}$.

   (b) If the difference between calculated and observed equivalent conductivity in the table in this chapter is phenomenologically attributed to the association (either permanent or transient) between cations and anions in molten salt, what is the temperature dependence of this "association degree" and how would you explain the seeming contradiction with our knowledge about cation–anion interaction? (See Xu)

10. The conductance calculated from the Nernst–Einstein equation is several tens of percentages more than that measured. An interpretation is that the diffusion coefficient includes contributions from jumps into paired vacancies and these (having no net charge) would contribute nothing to the conductance while counting fully for the diffusion.

    Assume one takes a 1:1 molten salt for which the increase of volume on melting is 20%, while the internuclear distance shrinks by 5%. Calculate on the basis of simple statistics the fraction of paired vacancies. For simplicity, assume the radii of the cation and the anion are equal (as in KF) and use the Stokes–Einstein equation to calculate the diffusion coefficient of the ions and that of the paired vacancies. (The viscosity of KF at 1000 K is 1.41 centipoise; the mean radius

of $K^+$ and $F^-$ is 0.131 nm.) Then calculate the contribution of the paired vacancies to the diffusion and find out how much greater the Nernst–Einstein equation would indicate the conductance to be than it really is.

11. When a metal such as Na is dissolved in a molten salt such as NaCl, it is found that 1 mol% of the metal gives rise to significant electronic conductance. Utilize the equation $\kappa = FNu$, where $N$ is the number of moles of Na per cubic centimeter and $u$ is the mobility ($0.4\ cm^2\ V^{-1}\ s^{-1}$). What would be the average distance apart of the Na atoms? On the basis of this distance and an approximation square-well model, calculate the probability of electron tunneling between a K atom and a $K^+$ ion in molten KC1 and thereby the mobility.

    Is the order of magnitude of your result consistent with the observed mobility? If not, suggest an alternative model for electronic conductance of alkali metals in alkali metal salts.

12. Using the distribution function, make a plot of probability that a hole has a radius $\langle r_h \rangle$ in molten sodium chloride at 1170 K. The surface tension of molten sodium chloride at 1170 K is $107.1\ dyn\ cm^{-1}$, and the mean hole radius is $1.7 \times 10^{-8}$ cm. (Contractor)

13. In the Fürth hole model for molten salts, the primary attraction is that it allows a rationalization of the empirical expression $E^{\neq} = 3.74RT_{m.p.}$. In this model, fluctuations of the structure allow openings (holes) to occur and to exist for a short time. The mean hole size turns out to be about the size of ions in the molten salt. For the distribution function of the theory (the probability of having a hole of any size), calculate the probability of finding a hole two times the average (thereby allowing paired-vacancy diffusion), compared with that of finding the most probable hole size.

14. In the liquid oxides of the type $M_xO_y$–$SiO_2$, there are certain limitations on the absolute structures. The O–Si–O angle may be assumed to be between 90° and 120°; the saturated valence of Si is 4 and that of O is 2. Electroneutrality means that the total charges on the metal ions (e.g., $Na^+$, $Ca^{2+}$, and $Al^{3+}$) must be equal in number to the corresponding charges on the silicate anions. Finally, it is always possible from the known composition, in mol%, to determine the value of O/Si, e.g., 4 in $Ca_2SiO_4$. On the basis of these "givens," calculate the likely structure of a liquid oxide for which O/Si is 2, 3, 4, and 5.

15. The heats of activation for flow in simple molten salts are generally <40 kJ $mol^{-1}$. In the liquid silicates, the corresponding heat of activation is 5 to 10 times higher than that for $CaO_2$, $Na_2O$ <50% in $SiO_2$. Why is there this very significant difference? Is there evidence that connects transport properties in NaCl-type molten salts—the movement into gaps or vacancies in the struc-

ture—to a probable rate-determining step in the flow of liquid oxides (i.e., liquid silicates, borates, and phosphates)?

16. There are several ways by which the structure of pure liquid electrolytes may be examined. A leading way currently is by means of neutron diffraction, a method that acts by registering the interferences caused by the reflection of neutrons and gives the internuclear distance. Examine this method with respect to its ability to contribute to conclusions stimulated by the two most outstanding facts relevant to the structure of molten salts. These are that when the salt melts and expands, the ions get nearer together rather than farther apart, and that the degree of expansion on melting, particularly for the alkali halides, is about 20% of their volume in the solid. To what kind of structures do these striking facts point? Can neutron diffraction measure empty space?

17. Ring and chain structures of $Al_3X_{10}^-$ were deduced by Blander and Saboungi in 1992 and are given in diagrams in the text. Compare the structure shown there ($Al^{3+}$ the coordinating ion) with those deduced by MacKenzie and Lowe for the liquid silicates in 1955 (also given in the text). Differences? Similarities? Why is the working temperature range for the liquid silicates (>1600 K) different from the room-temperature systems studied by Blander and Saboungi?

18. A pairwise potential widely used in both Monte Carlo and molecular dynamics computations is given as

$$\phi_{ij}(r) = A_{ij}\frac{z_i z_j}{r} + B_{ij}\exp[C_{ij}(\sigma_{ij} - r)] + D_{ij}r^{-6} + E_{ij}r^{-8}$$

which describes the potential as a function of distance between two ions $i$ and $j$; $z_i$ and $z_j$ are charges on $i$ and $j$, respectively, while $\sigma_{ij}$ is the size parameter of the ion pair (normally the sum of the crystallographic radii of $i$ and $j$). $A_{ij}$, $B_{ij}$, $C_{ij}$, $D_{ij}$, and $E_{ij}$ are constants estimated from the studies on the crystal of the corresponding salt.

(a) Identify the term that dominates the attraction between a pair of oppositely charged ions in long range and the term that prevents these two ions from "falling into each other."

(b) Which parameter in the second term determines the steepness of the repulsion felt by these two ions once their size parameters and center-to-center distances have been fixed?

(c) In molten silicate, the Si–Si equilibrium distance is ca. 0.32 nm. Determine by calculation whether the force due to the second term or the Coulombic-like charge repulsion dominates. What does the result suggest concerning the stability of the silicate network? ($B_{ij} = 0.19 \times 10^{-19}$ J; $C_{ij} = 3.44 \times 10^{10}$ m$^{-1}$; $r_{Si} = 1.31 \times 10^{-10}$ m.)

(d) For simple molten salts such as KC1, the various parameters are given as follows:

| $\sigma_{ij}$, $10^{-10}$ m | $B_{ij}$, $10^{-19}$ J | $C_{ij}$, $10^{10}$ $m^{-1}$ | $D_{ij}$, $10^{-79}$ J $m^6$ | $E_{ij}$, $10^{-99}$ J $m^8$ |
|---|---|---|---|---|
| ++ 2.926 | 0.423 | 2.97 | −24.3 | −24.0 |
| +− 3.048 | 0.338 | 2.97 | −48 | −73.0 |
| −− 3.170 | 0.253 | 2.97 | −124.5 | −250.0 |

$$A_{ij} = 2.307 \times 10^{-28} \text{ J m}$$

Plot the distance dependence of interaction potentials for the pairs $K^+ - K^+$, $K^+ - Cl^-$ and $Cl^- - Cl^-$, respectively. (Xu)

19. When a liquid supercools (i.e., does not crystallize when its temperature drops below the thermodynamic melting point), the liquidlike structure is frozen due to the high viscosity of the system. The supercooled liquid is in a so-called *viscoelastic state.* If the crystallization can be further avoided as the temperature continues to drop, a glass transition will happen at a certain temperature, where the "frozen liquid" turns into a brittle, rigid state known as a "glassy state." A well-accepted definition for glass transition is that the relaxation time $\tau$ of the system is $2 \times 10^2$ s or the viscosity $\eta$ is $10^{12}$ Pa s (an arbitrary standard, of course).

(a) Calculate the average distance an ion can travel during the period of a single relaxation time in a substance with a room-temperature glass transition.

(b) A simple relation between relaxation time and viscosity exists in all liquids down to the glass transition temperature: $\tau = K\eta$, where $K$ has a very small temperature dependence and can be regarded as a constant independent of temperature. Obtain this constant and calculate the theoretical upper limit of the viscosity of liquids, using the fact that the electronic relaxation time measured in the far infrared region is $10^{-13}$ s. (Xu)

20. In the equation $\eta = A \exp[BT_0/(T - T_0)]$ and $\tau = A' \exp[BT_0/(T - T_0)]$, the constant $B$ is an important characteristic of the structure of the liquid; its inverse is known as the "fragility" of the liquid, i.e., the greater $B$, the stronger (or the less fragile) the liquid.

(a) Explain how the value of $B$ influences the non-Arrhenius behavior of both the relaxation time $\tau$ and viscosity $\eta$.

(b) According to the value of B, liquids can be classed into categories of "strong" (large value of $B$), "intermediate" (medium value of $B$), and "fragile" (small value of $B$). Pure silicate belongs to "strong" with a $B$ value of ca. 100; as $Na_2O$ is added, the fragility increases and the resultant glass passes via intermediate ($B < 50$) into fragile ($B < 10$). Interpret this transformation on a structural level. (Xu)

## MICRO RESEARCH PROBLEMS

1. Using references cited in the text, research the history and development of room-temperature molten salts. The first publication was by Hurley and Weir in 1951. Why was there silence for a quarter century? What contribution was made by Halena Chum in the pioneering 1977 work?

   Make a 250–500 word summary of the contributions of teams led, respectively, by Osteryoung, Wilkes, and Hussey. Aluminum is often involved in this chemistry. It has very advantageous properties for storing energy because of the combination of the low molecular weight and 3-electron transfer reactions to form $Al^{3+}$. Because of the availability of $O_2$, an advantageous electricity storage device would consist of a room-temperature molten salt involving $Al^{3+}$ (which would deposit in a cathodic charging reaction and dissolve during discharge) and a redox coupling involving $O_2$.

   Devise a cathodic reduction reaction to occur during discharge of a cell that would reduce $O_2$ in the melt and be comparable with the Al organic type of solution.

2. What is the difference between "average hole radius $<r>$" and "radius of the most populous hole $r_{max}$?" Calculate the "most popular" hole radius $r_{max}$ and compare it with $<r>$.

   If the answer in the above question is no, what parameter is needed to describe the distribution of the hole size? Is there validity to the statement that "all holes are of the same size in molten salts?" Using data in Table 5.15, find the above distribution for KC1 molten salt at 1170 K.

   [Hint: numerical integration may be needed to solve the last question.] (Xu)

*This page intentionally left blank*

## SUPPLEMENTARY REFERENCES HELPFUL IN THE SOLUTION OF THE PROBLEMS


Adler, B. J., and Wainwright, T. E., *J. Chem. Phys.* **27**: 1208 (1959).
Angell, C. A., Cheesman, P. A., and Tamaddon, S., **218**: 885 (1982).
Bernal, J. D., and Fowler, R. H., *J. Chem. Phys.* **1**: 515 (1933).
Bjerrum, N., *Kgl. Danske Videnskab. Selskab.* **7**: 9 (1926).
Blum, E. L., *Inorg. Chem.* **24**: 139 (1977).
Bockris, J. O'M., *Quart. Rev. Chem. Soc.* **44**: 151 (1948).
Bockris, J. O'M., *Trans. Faraday Soc.* **45**: 989 (1949).
Bockris, J. O'M., and Lowe, D., *J. Electrochem. Soc.* **102**: 609 (1954).
Böhmer, R., Sanchez, E., and Angell, C. A., *J. Phys. Chem.* **96**: 9090 (1992).
Card, D. N., and Valleau, J. P., *J. Chem. Phys.* **52**: 6232 (1970).
Conway, B. E., *J. Electrochem. Soc.* **129**: 138 (1982).
Davies, C. W., *Ionic Association,* Butterworth, London (1962).
Fajans, K., and Johnson, O., *J. Am. Chem. Soc.* **64**: 668 (1942).
Fawcett, W. R., and Tikanen, A. C., *J. Phys. Chem.* **100**: 4251 (1996).
Frank, B., and Wen, J., *J. Electrochem. Soc.* **129**: 138 (1982).
Friedman, H. L., *Ionic Solution,* Interscience, New York (1962).
Friedman, H. L., *NATO ASI Series C: Mathematical and Physical Sciences* **205**: 61 (1987).
Friedman, H. L., Raineri, E. O., and Wodd, O. M. D., *Chem. Scr.* **29A**: 49 (1989).
Gurney, R., *J. Chem. Phys.* **19**: 1499 (1953).
Inman, D., and Bockris, J. O'M., *Trans. Faraday Soc.* **57**: 2308 (1961).
Kebarle, P., and Godbole, E. W., *J. Chem. Phys.* **39**: 1131 (1968).
Ling, C. S., and Drost-Hansen, W., *Adv. Chem. Soc.* **129**: 75 (1975).
Metropolis, N., *J. Chem. Phys.* **21**: 1087 (1953).
Ramanathan, K. V., and Pinto, R., *J. Electrochem. Soc.* **134**: 165 (1987).
Rasaiah, J. C., *NATO ASI Series B: Physics* **193**: 135 (1987).
Rasaiah, J. C., and Friedman, H. L., *J. Chem. Phys.* **48**: 2742 (1968).
Rossky, P. J., and Friedman, H. L., *J. Chem. Phys.* **72**: 5694 (1980).
Soper, A. K., Nielson, G. W., Enderby, J. E., and Howe, R. A., *J. Phys. Soc.* **10**: 1793 (1977).
Tanaka, M., Tanaka, J., and Nagakura, S., *Bull. Chem. Soc. Japan* **39**: 766 (1965).
Tomlinson, J. W., White, A., and Bockris, J. O'M., *Trans. Faraday Soc.* **54**: 1822 (1958).
Wertheim, G. K., *Phys. Rev.* **30**: 4343 (1984).
Xue, X., Stebbins, J. F., Kanzaki, M., and Tronnes, R. G., *Science* **245**: 963 (1990).

*This page intentionally left blank*

# INDEX